Characterisation of metabotropic glutamate receptor 4 as a therapeutic target in Parkinson's disease

Mann, Elizabeth Caroline

Awarding institution:
King's College London

Characterisation of metabotropic glutamate receptor 4 as a therapeutic target for Parkinson's disease.

Elizabeth C. Mann

2018

Submitted for the degree of Doctor of Philosophy

Wolfson Centre for Age-Related Diseases
King's College London

Abstract

Parkinson's disease (PD) is a progressive, neurodegenerative disease with limited symptomatic treatment options and no currently licensed, disease-modifying therapies. This thesis sets out to examine the neuroprotective, therapeutic potential of systemically-administered compounds acting on metabotropic glutamate receptor 4 (mGluR4) in a rat 6-hydroxydopamine model of early-stage PD. Additionally, the rat model is explored for its ability to reflect the non-motor, in addition to motor, symptoms of PD.

A positive allosteric modulator (PAM) and an agonist of mGluR4 were examined for their neuroprotective efficacy in the early stage model of PD. Although the PAM failed to provide neuroprotection, animals treated with the mGluR4 agonist show improved performance in motor tests and also significant protection of dopaminergic cells in the substantia nigra pars compacta. Furthermore, the mGluR4 agonist caused a significant reduction of motor disability without inducing any dyskinesia side-effects in a marmoset model of PD but failed to reduce existing dyskinesia.

This mGluR4-mediated neuroprotection was hypothesised to arise from a number of different mechanisms including a reduction of excitotoxicity due to moderation of subthalamic nucleus (STN) overactivity (not explored here) and a reduction in inflammatory activity. The results presented here show that, although there may be some effect of systemic mGluR4 agonism on reducing inflammation, many other pathways may also be implicated as shown through a microarray highlighting gene expression significantly altered following agonist administration.

In addition to studies on mGluR4, some model characterisation work was also carried out. Anxiety and craving, non-motor symptoms commonly seen in PD patients, were observed in the bilateral version of the early stage rat model of PD. This could indicate that the model is useful for examining mGluR4 agonists and other potential treatments of PD more fully, in a holistic sense, rather than the traditional methods of separating out the treatment of motor and non-motor symptoms.

In conclusion, a systemically-administered agonist of mGluR4 showed promise in the treatment of neurodegeneration in an early-stage model of PD in rats. This appears to have a number of underlying mechanisms including some modulation of inflammation and also transcriptional changes to genes which have been shown to affect neurodegeneration and neuroprotection. Furthermore, this agonist also has anti-Parkinsonian potential without causing dyskinesia - mGluR4 is therefore a suitable and promising target for further research in PD.

Acknowledgements

"Science is nothing but a series of questions that lead to more questions, which is just as well, or it wouldn't be much of a career path, would it?"

- Terry Pratchett and Stephen Baxter - The Long Earth

My primary supervisor, Dr Susan Duty, must get the lion's share of my thanks for the completion of this work. Throughout, she has been generous with her time and knowledge and willing to entertain just enough of my many avant-garde ideas - thanks for okaying the non-motor work and the poster colour schemes, and for not bringing up my obsession with the cerebellum *too* often. Dr Pete Atkinson, my second supervisor, also deserves many thanks for his constructive feedback; it has always been valuable to have a different point of view on my work. Thanks to both him and Eisai for adding to my PhD experience.

A number of people have made the technicalities of my research possible through advice, demonstration, and patient tuition. I would like to thank Tom Pitcher for his assistance with behaviour and dissection and his great generosity of spirit; Carl Hobbs for his time, enthusiasm and encyclopædic knowledge of almost everything (but most of all immunohistochemistry, music and film); Dave Chambers for his patience in taking me through every single mix and wash of the microarray protocol and his willingness to listen to all of my science grousing; Sonia Talma for making me feel so welcome at Eisai and taking the time to figure out all of my arrays with me; Dr Sarah Salvage and her group for their expertise in the marmoset study, and especially Louise for all of her patient advice on tail veins so early in the morning; and finally the BSU team, especially Claire and Garry, for their time and care, and their wealth of strange snacks, given so freely.

The rest of the Duty lab have also played an enormously important role in the formation of this thesis. I would like to thank all of the previous members of the Duty mGluR projects; although in many cases I have never met them, they have supported this project through their own data and their, in some cases legendary, scientific thoroughness. In particular in this group I would like to thank Martin for his memorable words of encouragement and inspiration at the start of my project. I would like to thank Ed for providing me with a role model of PhD and post-doc life of patience and enthusiasm. I'm not sure whether it was fate or planning that we got on so well in our little lab but we shared so many interests and laughs that it's now impossible to imagine my time otherwise - how do you do a PhD? You just do a PhD. I also should not (and could not)

forget Yaz, who was a hurricane of fresh air in the last year of my PhD - hold on to some of that enthusiasm and you will go far.

Thank you also to the many people with whom I have shared an office over the years, in particular: Em, who has been my rock when research was suboptimal and I hope, for science's sake, that someone gives her some money to carry on; brother $\Sigma\omega\tau\acute{\eta}\rho\eta\varsigma$, who is an optimal human with a wonderful interest in everything and whose company is ever-uplifting; Ariana, who does every single thing with a brilliantly fiery (sassy?) Maltese passion and Book, who is incredibly generous and ever curious. Thanks to all the other PhDs and post-docs of the Wolfson who made my time there fun, especially: Merrick (tinkety tonk old fruit), Emily (thanks for the football and pop culture knowledge) and Christina (thanks for being exceptionally well-adjusted and reasonable at all times).

These people may never know that they have been thanked, but have made such a significant contribution to my life that I feel I must do so anyway. Dr Humphries and Mr Snell (nobody could have had more inspiring teachers) showed me that it is valuable to work hard at things that don't necessarily come naturally and, in doing so, showed me that I could achieve this. I will always remember them both. To everyone who came next at the Pharmacology department at the University of Bath - and even Paul Mitchell - thanks for all the science and beers, it was great.

Last but by no means least I would like to thank my family. My Mum, who has been so much a part of my life the whole way through that she could probably make her own contribution to this thesis, and my Dad, who sciened with me from my earliest days, have supported me in every decision. I literally would not be here without them, of course, but I want to thank them for being my amongst best friends too. Rob - I fell in love with him, grew up with him and am lucky enough to spend my future with him. Knowing that we have each other's backs through all that has happened and will happen makes everything, including writing this, doable. And thanks for persuading me to write in LaTeX. ⌣̈

··-· --- ·-·

-·· --- - , -·· ·- ··· ····

·- -· -·· - ···· · --- - ···· · ·-· ···

Acronyms

5-HT 5-hydroxytryptamine.

6-OHDA 6-hydroxydopamine.

AD Alzheimer's disease.

ADX88178 5-Methyl-N-(4-methylpyrimidin-2-yl)-4-(1H-pyrazol-4-yl)thiazol-2-amine.

AIMs abnormal involuntary movements.

AMPA α-amino-3-hydroxy-5-methyl-4-isoxazolepropionic acid.

ATP adenosine triphosphate.

BCA bicinchoninic acid.

BDNF brain-derived neurotropic factor.

BLA basolateral amygdala.

BSA bovine serum albumin.

cAMP cyclic adenosine monophosphate.

CNS central nervous system.

COMT catechol-o-methyl transferase.

DAB 3,3'-diaminobenzidine.

DAT dopamine active transporter.

DLB dementia with Lewy bodies.

DMSO dimethyl sulfoxide.

DRN dorsal raphe nucleus.

ELISA enzyme-linked immunosorbent assay.

GABA gamma-aminobutyric acid.

GDNF glial cell-derived neurotrophic factor.

GFAP glial fibrillary acidic protein.

GFP green fluorescent protein.

GI gastrointestinal.

GPCR G-protein coupled receptor.

GPe external globus pallidus.

GPi internal globus pallidus.

HRP horseradish peroxidase.

i.p. intraperitoneal.

Iba1 ionized calcium-binding adaptor molecule 1.

IFNγ interferon-γ.

IMS industrial methylated spirits.

iNOS inducible nitric oxide synthase.

IP10 Interferon γ-induced protein 10.

L-SOP L-serine-O-phosphate.

L-AP4 L-2-amino-4-phosphonobutyrate.

L-DOPA L-3,4-dihydroxyphenylalanine.

LID levodopa-induced dyskinesia.

LPS lipopolysaccharide.

LSP1-2111 (2S)-2-amino-4-(hydroxy(hydroxy(4-hydroxy-3-methoxy-5-nitrophenyl)methyl)phosphoryl)butanoic acid.

LTD long-term depression.

LTP long-term potentiation.

Lu AF21934 (1S, 2R)-N1-(3,4-dichlorophenyl)-cyclohexane-1,2-dicarboxamide.

MAO-B monoamine oxidase B.

MCI mild cognitive impairment.

MFB medial forebrain bundle.

mGluR metabotropic glutamate receptor.

mGluR4 metabotropic glutamate receptor 4.

MHCII major histocompatibility complex class II.

MIP1α Macrophage Inflammatory Protein 1α.

mPFC medial prefrontal cortex.

MPP$^+$ 1-methyl-4-phenylpyridinium.

MPTP 1-methyl-4-phenyl-1,2,3,6-tetrahydropyridine.

MSOP methylserine-O-phosphate.

NA noradrenaline.

NAc nucleus accumbens.

NAM negative allosteric modulatior.

NBQX 2,3-dihydroxy-6-nitro-7-sulphamoyl-benzo(F)quinoxaline.

NFκB nuclear factor-κB.

NMDA N-Methyl-D-aspartate.

NSAID non-steroidal, anti-inflammatory.

p.o. *per os*.

PAM positive allosteric modulator.

PBS phosphate-buffered saline.

PD Parkinson's disease.

PDD Parkinson's disease dementia.

PEG400 polyethylene glycol 400.

PET positron emission tomography.

PHCCC N-phenyl-7-(hydroxyimino)cyclopropa[b]chromen-1a-carboxamide.

PNS periperal nervous system.

RBD REM sleep behaviour disorder.

REM rapid eye movement.

RIPA radioimmunoprecipitation assay.

ROS reactive oxygen species.

RRF retrorubral field.

s.c. subcutaneous.

S.E.M. standard error of the mean.

SDS sodium dodecyl sulfate.

SERT serotonin transporter.

SNc substantia nigra pars compacta.

SNr substantia nigra pars reticulata.

SSRI selective serotonin reuptake inhibitor.

STN subthalamic nucleus.

TBS tris-buffered saline.

TCA tricyclic antidepressant.

TH tyrosine hydroxylase.

TNFα tumour necrosis factor α.

VM ventral mesencephalon.

VMAT2 vesicular monoamine transporter 2.

VTA ventral tegmental area.

VU0155041 (+/-)-cis-2-(3,5-dichlorphenylcarbamoyl)cyclohexanecarboxylic acid.

Contents

List of Figures

List of Tables

1 Introduction

1.1 What is Parkinson's disease

Parkinson's disease (PD) is a neurodegenerative disease which was originally characterised by James Parkinson over 200 years ago in 'An Essay on the Shaking Palsy' (more recently republished as Parkinson (2002)). In his essay, Parkinson characterised the shaking palsy primarily as a motor disorder comprising tremor, muscular weakness and abnormal posture (Parkinson 2002). In individual case studies, Parkinson shows awareness of other, non-motor, symptoms that are, today, known to result from PD itself - such as excessive production of saliva, urinary incontinence, constipation, depression and daytime sleepiness. Our present understanding of PD encompasses a great many more symptoms. Each person with PD is likely to experience different sets of these symptoms, which will change over the course of the disease.

The symptoms of PD can nominally be split into two groups: the motor symptoms, by which the disease is commonly recognised, and the non-motor symptoms which may emerge in the 'prodromal' phase (prior to the onset of motor symptoms) or during or after diagnosis. Whenever their onset relative to diagnosis, in many cases, the non-motor symptoms of PD are only firmly linked to the disease following recognition of the motor symptoms. This is likely due to the fact that the non-motor symptoms (e.g. gastrointestinal problems and depression) can also appear alone or may be linked to other disorders. The motor symptoms are therefore key for diagnosis of PD. The cardinal motor symptoms of PD often begin unilaterally, but spread bilaterally over time. They are:

- Tremor - often described as 'pill rolling'. This manifests as a high-frequency tremor in the extremeties.
- Bradykinesia - literally 'slow movement'. This often presents as a an apparent difficulty in initiating intended motions or a loss of spontaneous motion.
- Rigidity - a muscular resistance of the affected limbs to being moved, either consciously by the patient or by an external force.
- Postural instability - a difficulty in balancing during everyday tasks such as walking.

The category of non-motor symptoms of PD has expanded to encompass all symptoms of PD not included in the list of caridnal motor symptoms. Thus, the group of non-motor symptoms in-

clude psychiatric, gastrointestinal and cognitive signs - amongst others. The spectra of non-motor symptoms of PD are discussed in detail in Chapter 5 of this thesis.

The estimates for prevalence of PD vary widely between studies. This is likely a factor of the chosen method of data collection (e.g. survey or medical record) (de Rijk et al. 1997) and the precise population captured (e.g. genetic, environmental or age differences). One group found that the overall prevalence of PD in Europeans over the age of 65 was 1.8% and that this figure did not vary between sexes or between countries (de Rijk et al. 2000). Using a survey, de Rijk et al. (1997) found that this incidence strictly increased with each 5 year age bracket from 65-70 up to 85-90. When Parkinsonism (presence of at least two of the cardinal motor symptoms outlined above) was included in the inclusion criteria, the European incidence rose to 2.3%. Indeed, the inclusion of undiagnosed Parkinsonian symptoms (tremor, rigidity, bradykinesia or postural instability) as a criterion in their study led to the recognition of a substantial number of people with previously undiagnosed PD (de Rijk et al. 1997).

This serves to highlight the difficulty in establishing a firm definition of PD with which to study a PD population for any research purpose. Nevertheless, it can be agreed that PD is highly detrimental to the quality of life of those who suffer from it, and poses a significant burden on healthcare systems worldwide. For these reasons, a great body of work has been undertaken to improve the understanding of the mechanisms and pathology underlying PD symptoms and the ways in which the resulting illness might be treated or arrested.

1.1.1 Aetiology

James Parkinson speculates upon the cause of PD in his essay, suggesting that it may arise from a disease of the spinal cord (*'medulla spinalis'*) (Parkinson 2002). Today, although we are not closer to defining a single causative factor, it is recognised that PD may be defined in terms of two aspects of its pathology: the progressive degeneration of a number of nuclei in the brain; and the appearance of Lewy bodies - intracellular aggregates of misfolded α-synuclein and other proteins.

Braak et al. (2003) tie these two processes together in a suggested progression of PD through the brain which is now known as Braak staging. They suggest that the advancement of symptoms and neurodegeneration can be traced through neuronal pathways by observing the presence of Lewy bodies. As Lewy bodies advance through the nuclei of the brain which are known to be affected by Parkinson's, cell death and symptoms arise. Braak et al. (2003) map the course of Lewy body

pathology through the brains of people with PD who died at varying intervals after diagnosis and also in the brains of people who died with no diagnosis of PD or any recorded Parkinsonisms, but nevertheless show signs of Lewy bodies in brain stem nuclei. These cases were considered to be prodromal PD. By grading the disease severity in these cases, Braak et al. (2003) find that, in the potential prodromal cases, pathology is apparent in the brain stem and olfactory tubercules, and has, by later stages (post diagnosis), spread through the midbrain and affects the cortex (Figure 1.1). It is, however, very difficult to be sure that any or all of the cases labelled prodromal in this study would have gone on to develop PD, rather than remaining asymptomatic or developing an alternative Lewy body disorder such as Lewy body dementia (reviewed in Galasko (2017).

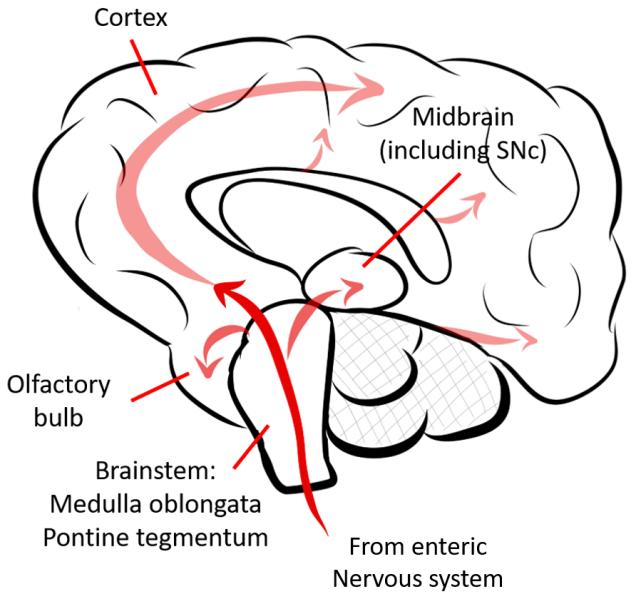

Figure 1.1: A diagram of a human brain in sagittal profile with arrows representing the spread of Lewy body pathology over time with PD. Darkest red arrow colour represents earliest affected areas and lighter colours represent areas affected later in the disease. Diagram design adapted from Braak et al. (2003).

The Braak staging theory has since been expanded to accommodate an additional 'second hit' theory. This states that Parkinson's may also originate in the enteric nervous system as a result of environmental (perhaps more specifically, consumed) triggers. At present, it is not known whether the gut stages of pathogenesis precede or succeed the olfactory and brain stem phases of disease development, or indeed whether the order of these events is consistent between PD sufferers.

The gut hypothesis is backed by two important pieces of evidence: gastrointestinal symptoms of PD (chiefly, constipation) normally precede motor symptoms by a number of years (Savica et al. 2009) and Lewy body pathology has been found in the enteric nervous system of people with

all stages of PD (Braak et al. 2006). These pieces of evidence both indicate a strong involvement of the gut and the enteric nervous system in PD. It should also be noted, however, that Lewy body pathology has been observed in the enteric nervous system of those who experienced late-life constipation without developing symptoms of PD (Abbott et al. 2007). Furthermore, the frequency of bowel movements has been significantly correlated with nigral neuron density in an elderly population without Lewy body pathology or a diagnosis of PD (Petrovitch et al. 2009). This suggests that the relationship between PD, Lewy bodies and gastrointestinal symptoms may be more complex than initially thought.

1.1.1.1 Environmental factors

The vast majority of PD cases are described as idiopathic - of no known cause. In these cases, it is likely that a number of factors predict the onset of the disease. The most difficult to test of these potential causes is the environmental component. A number of seemingly disparate environmental factors shown to increase the risk of developing PD have been examined in recent years including caffeine and nicotine consumption, rural living, head injury, drinking of well water, exposure to pesticides and some types of infection. These will be examined individually within this section. Clearly few of these factors lead with any certainty to the development of neurodegeneration in any form - showing how incomplete our understanding of PD aetiology is at present. Below, each of the environmental factors that have been proposed to impact considerably upon the risk of Parkinson's are detailed.

Consumption of caffeine and nicotine are negatively correlated with incidence of PD - that is to say that those who smoke tobacco (and find quitting difficult) and/or regularly consume coffee or black tea appear to be at less risk of developing PD than those who do not (reviewed by Ross & Petrovitch (2001). There are three hypotheses for why this might be the case:

1. Those who will go on to develop PD have prodromal traits associated with an indifference to traditionally addictive substances (Evans et al. 2005).
2. Caffeine and nicotine are neuroprotective (Maggio et al. 1998, Chen et al. 2001).
3. Consumption of caffeine and/or nicotine alters the gut microbiota in such a way as to reduce inflammation and/or α-synuclein accumulation and misfolding (thus, the formation and spread of Lewy bodies) (Derkinderen et al. 2014).

Whatever the underlying mechanism, meta-analyses have found that 'ever-smokers' (those who have smoked at any time in their lives) have a relative risk of developing PD of between 0.55 and

0.59 (Kiyohara & Kusuhara 2011, Li et al. 2015). This relative risk decreases further for those who have not quit smoking to approximately 0.31 (Kiyohara & Kusuhara 2011). However, there is some evidence in an animal model of PD that nicotine-free tobacco and decaffeinated coffee may also provide neuroprotection, through an antioxidant mechanism unrelated to caffeine or nicotine (Trinh et al. 2010).

Studies have shown that people who experience repeated blows to the head or spine, such as may occur in contact sports like boxing or American football, are predisposed towards chronic traumatic encephalopathy later in life (Solomon 2018). The symptoms of chronic traumatic encephalopathy vary, but may involve aspects of dementia and Parkinsonism (Solomon 2018). For these reasons, it can be difficult to differentiate chronic traumatic encephalopathy from Parkinson's itself unless a post-mortem examination of the brain tissue is undertaken. This difficulty in diagnosis may be the root of reports that head injuries are a risk for later life development of PD. Case-control and population studies have found evidence both in support of (Harris et al. 2013, Jafari et al. 2013), and against (Fang et al. 2012, Savica et al. 2012, Kenborg et al. 2015), this hypothesis.

Another, better established, risk for the development of PD is exposure to pesticides. Many studies have examined the impact of exposure to pesticides on the incidence of PD through various means including examining the percentage of PD patients who live rurally or regularly drink well-water from wells located on or near to farms using pesticides (Freire & Koifman 2012). The body of evidence correlating PD to pesticide exposure by any means is growing rapidly. Although there is not yet any definitive evidence showing that pesticide exposure causes PD, there appears to be a strong link between the two. Furthermore, a number of the more commonly used animal models of PD in preclinical research involve the exposure of organisms to pesticides such as rotenone, paraquat and maneb. These will be discussed in more detail in the animal models section of this introduction.

Higher incidence of PD development has been recorded in populations of those addicted to drugs of abuse. A population-based assessment by Curtin et al. (2015) shows that users of methamphetamine or amphetamine were almost 3 times more likely than the general population to develop PD. Although this appears to be at odds with the hypothesis that pro-dromal PD patients may be less likely to show signs of addiction, three mechanisms by which methamphetamine could cause PD have been proposed. Firstly, methamphetamine has been shown to bind to, and cause misfolding in, α-synuclein which may potentially lead to the appearance of Lewy body pathology

(Tavassoly & Lee 2012). Secondly, methamphetamine has been shown to cause alterations to firing of dopaminergic neurons by alterering the activity of dopamine active transporter (DAT) (Saha et al. 2014). Finally, methamphetamine has been shown to have neurotoxic effects independent of dopamine and α-synuclein: through inhibition of mitochondrial complex I and generation of reactive oxygen species (ROS) (Thrash et al. 2010).

Some infections have also been associated with an increased risk of the development of PD. For example, there is a significant association between infection with hepatitis C (Wu et al. 2015) or *Helicobacter pylori* (Nielsen et al. 2012) and increased risk of developing Parkinson's. This may be due to the creation of an inflammatory environment by these pathogens, which may cause neuroinflammation via cytokines able to cross a disrupted blood-brain barrier, such as is seen in PD (Kortekaas et al. 2005). Autoantibodies have also been shown to play a potential role in PD pathogenesis (Dahlström et al. 1990). Helicobacter pylori infection has been shown to induce such autoantibodies against gastric mucosa, thereby producing further inflammation which can outlast the infection (Appelmelk et al. 1997).

Despite this evidence behind the multitude of potential environmental causes of PD, the strongest risk factor for development of the disease in later life is still a family history of PD or tremor (Noyce et al. 2012).

1.1.1.2 Genetic factors

Approximately 5% of cases of PD are recognised as familial - caused by a gene mutation which, when inherited, reliably gives rise to PD (Klein & Westenberger 2012). These genetic causes allow some insight into the mechanisms underlying PD in the general population. For example, certain genes with a role in synaptic transmission (LRRK2, SNCA (Gómez-Suaga et al. 2014, Wang et al. 2014)) or mitochondrial function (SNCA, LRRK2, PINK1, Parkin, DJ-1, VPS35 (Dias et al. 2013, Wang et al. 2016)) can reliably give rise to PD in early adulthood.

Of the genes giving rise to familial PD which are listed in Table 1.1, the 5 best studied are SNCA, Parkin, PINK1, DJ-1 and LRRK2. Their function in health and disease will be discussed in more detail below.

SNCA

SNCA encodes α-synuclein. A number of missense mutations within SNCA, along with mulipi-

Table 1.1: Genes in Parkinson's disease					
Symbol	Gene	Inheritance	Symbol	Gene	Inheritance
PARK 1	*SNCA*	AD	PARK 8	*LRRK2*	AD
PARK 2	*Parkin*	AR	PARK 14	*PLA2G6*	AR
PARK 6	*PINK1*	AR	PARK 15	*FBX07*	AR
PARK 7	*DJ-1*	AR	PARK 17	*VPS35*	AD

Table 1.1: A summary of the confirmed, known genes in which mutations give rise to familial PD. Adapted from Klein & Westenberger (2012). AD, autosomal dominant; AR, autosomal recessive.

cations of the SNCA gene, have been identified as causal for PD (Nuytemans et al. 2010). The first discovered and most well known of these missense mutations is Ala53Thr (Polymeropoulos et al. 1996, 1997). Taken together, these mutations and multiplications of SNCA are thought to be responsible for approximately 6% of familial PD cases in a Caucasian population, though much lower numbers in other populations (Nuytemans et al. 2010).

In the healthy population, α-synuclein is thought to play a role in synaptic transmission and membrane remodelling (reviewed in Bendor et al. (2013)). In the population with SNCA mutant-PD, misfolded α-synuclein oligomerises and spreads through the nervous system through prion-like propagation mechanisms (Masuda-Suzukake et al. 2013). These pathogenic α-synuclein oligomers form the intracellular masses known as Lewy bodies. The question of whether Lewy bodies cause cell death or represent a 'coping mechanism' for the detoxification of intracellular α-synuclein oligomers has not yet been answered with any certainty.

It has been shown that Lewy body load in patients with mild or early stage PD is lower than in patients with severe PD (Wakabayashi et al. 2007). Initially, this was taken as evidence that neurons with Lewy bodies were preferentially dying and so Lewy bodies were seen as a cause of cell death. Conversely, Milber et al. (2012) show that Lewy pathology is preceded by neurodegeneration in a study comparing tissue from patients with either incidental Lewy body disease or PD. More objectively, though in only 3 cases, Tompkins & Hill (1997) show that Lewy body-containing neurons were not more likely to show signs of apoptosis than neurons without Lewy bodies in the substantia nigra pars compacta (SNc) of PD patients. Lewy bodies have also been demonstrated to accumulate with age in non-Parkinson's populations (Jellinger 2004).

Regardless of the true role of Lewy bodies in PD, given the severity of PD in those with SNCA

mutations or duplications it is hard to believe that α-synuclein is purely incidental to PD. It is likely that the accumulation of misfolded α-synuclein within neurons interferes with the normal functioning of the cell and eventually causes apoptosis (reviewed in Schulz-Schaeffer (2015)). Those with SNCA mutations or multiplications may develop early onset PD, with a higher load of α-synuclein being correlated with a greater severity or an earlier onset of disease (Miller et al. 2004, Olgiati et al. 2015).

LRRK2

Leucine-rich repeat kinase 2 (LRRK2) comprises a number of functional binding domains, the substrates of which are only recently being discovered (Steger et al. 2016). Missense mutations in LRRK2 are traditionally considered to be causative for PD and have been found in over 50% of familial PD patients, making LRRK2 by far the most common PD gene (Nuytemans et al. 2010). The 80 missense mutations characterised in LRRK2 thus far occur along the length of the protein and in all functional domains. Perhaps surprisingly given its autosomal dominant status in PD, LRRK2 mutations have been observed in late onset, sporadic cases of PD in addition to the earlier onset, familial PD (Di Fonzo et al. 2006). Not only this, but LRRK2 mutations have also been recorded in a healthy control population (Carmine Belin et al. 2006). The complexity of these findings and the current lack of understanding about the function of each domain of LRRK2 make the pathogenicity of 'umbrella' LRRK2 mutations difficult to pin down. It is likely that the severity of LRRK2-associated PD depends upon the specific location and form of mutation.

Parkin

The function of Parkin in a healthy population is in the ubiquitin proteasome system, in tagging misfolded and dysfunctional proteins for degradation, and in mitochondrial function. When expressed homozygously, loss of function mutations result in juvenile onset PD (Kitada et al. 1998). Those with heterozygous Parkin mutations may still go on to develop PD at an older age, though some heterozygous mutations have also been observed in healthy individuals (Brüggemann et al. 2009, Thompson et al. 2013). Thus, it may be considered that heterozygosity of a Parkin mutation is a risk factor for development of sporadic PD, but homozygosity is causative.

PINK1

PINK1, or P-TEN-induced putative kinase 1, was discovered by Valente et al. (2001) when Parkin mutations were ruled out as a causative factor in autosomal recessive juvenile onset Parkinsonism in a Sicilian family. Like Parkin and many other genes implicated in PD, PINK1 is involved in the mitochondrial response to oxidative stress (Chien et al. 2013). In PD, homozygous PINK1

missense mutations represent the PD-causing mutation in approximately 6.5% of the familial PD population (Nuytemans et al. 2010). Heterozygous expression of mutated PINK1 has been observed in patients with sporadic PD and healthy controls (Brooks et al. 2009). This, again, indicates a gene which causes a spectrum of severity of PD phenotypes, with heterozygosity conferring a higher risk of developing PD but not a necessary progression.

DJ-1

DJ-1 is a third autosomal recessive PD gene which was originally identified by van Duijn et al. (2001) in a Dutch family. The likely function of intact DJ-1 is as an oxidative stress sensor and antioxidant (Mitsumoto & Nakagawa 2001). Xiong et al. (2009) also show that DJ-1 may function in a complex with Parkin and PINK1. As such, it seems that missense mutations in DJ-1 may cause similar effects to those better characterised in Parkin and PINK1, and confer similar susceptibility to disease.

In addition to these autosomal dominant and autosomal recessive genes which predict early-onset PD, there are likely to be a multitude of genes affecting similar functions which increase the risk of developing PD fractionally. The most common of these risk factor gene mutations is in the β-glucocerebrosidase gene (GBA) associated with Gaucher's disease. Unmutated β-glucocerebrosidase is involved in the production of glucocerebroside and necessary for the normal functioning of the lysosome (Rijnboutt et al. 1991), thus Gaucher's disease is characterised by an inability to degrade glucocerebroside. Neudorfer et al. (1996) observed that Gaucher's disease patients and, importantly, their close family members, seemed to develop PD with a higher-than-normal frequency. Larger scale studies confirmed this association by examining the frequency of GBA mutation in PD patients (Neumann et al. 2009, Nichols et al. 2009). A number of hypotheses about the role of glucocerebroside in PD exist, including reduced removal (and therefore accumulation) of α-synuclein (Murphy et al. 2014) and increased α-synuclein aggregation (Goldin 2010).

In reality, the most likely scenario is that most cases of PD which are currently described as idiopathic or sporadic arise from a mixture of these hypothesised low-risk gene variants and environmental factors which each confer predisposition towards development of the disease.

1.1.1.3 Mechanisms underlying death of nigrostriatal neurons

As suggested by the varied list of environmental and genetic risk factors presented previously, there are a number of components to PD-induced neurodegeneration and theories about why the

SNc is specifically affected. These are discussed, in turn, below.

α-synuclein and Lewy pathology

As previously mentioned, the theory of spreading Lewy body pathology underlying the expression of PD symptomatology was proposed by Braak et al. (2003). This use of Braak staging implies that Lewy bodies mirror the progression of PD and may even underlie it. However, there is some debate about whether Lewy bodies are a cause or an effect of the neurodegeneration seen in PD (Schulz-Schaeffer 2015).

Rather than Lewy bodies being directly responsible, or even a reliable marker for, nigral, PD-related apoptosis, an alternative hypothesis has been proposed. Aggregation of α-synuclein in the neuron interferes with proteins involved in synaptic function, thereby reducing synaptic activity (Nemani et al. 2010, Spinelli et al. 2014). This disruption to function may cause a gradual reduction of postsynaptic spines and eventually result in measurable neurodegeneration (Schulz-Schaeffer 2015). Lewy bodies might therefore be formed as an attempt to detoxify these problematic α-synuclein aggregates, rather than being a causative feature of degeneration (Schulz-Schaeffer 2015).

Nevertheless, the intracellular buildup of misfolded α-synuclein can cause endoplasmic reticulum stress and, through this, prolonged activation of the unfolded protein response (Ryu et al. 2002, Hoozemans et al. 2007). While acute activation of the unfolded protein response is considered to be neuroprotective (Wu & Kaufman 2006), it is believed that the chronic activation seen in neurodegenerative diseases such as PD is detrimental to cell survival (Urra et al. 2013). This is reinforced by the key roles that some of the causative PARK genes have in the unfolded protein response process (Imai et al. 2000).

Innate sensitivity of SNc neurons

The dopaminergic neurons originating in the SNc are notable for a few reasons. They have exceptionally complex axonal structures with a high degree of arborisation (Parent & Parent 2006); a high density of axonal mitochondria (Pacelli et al. 2015) and also a high basal metabolic requirement (Matsuda et al. 2009, Surmeier et al. 2011). These increased energetic demands may set the neurons of the SNc apart from even the neighboring ventral tegmental area (VTA) and mark them out as vulnerable to apoptosis following oxidative stress.

The higher levels of mitochondrial function in the SNc also give rise to higher concentrations of

ROS (Pacelli et al. 2015) - damaging oxygen radicals produced as a byproduct of the electron transport chain function. Not only this, but intracellular dopamine has been shown to undergo spontaneous oxidation, leading to further production of ROS (Alagarsamy et al. 1997). This means that, while dopaminergic neurons may be more prone to oxidative stress than cells containing other neurotransmitters, the physiology of the SNc cells makes them even more so. This may help to explain why the cells of the SNc appear to specifically affected by PD compared to surrounding nuclei.

In addition, the cells of the SNc characteristically contain neuromelanin - a dark pigment with a structure based on catecholamines. There has been some suggestion that neuromelanin may be a trigger for α-synuclein aggregation in the SNc (Li et al. 2012).

Inflammation

Neuroinflammation is a key feature of PD and other neurodegenerative diseases. Activated microglia and astrocytes, elevated levels of pro-inflammatory chemokines (Mogi et al. 1994) and activation of the complement system (Yamada et al. 1992) have all been recorded in PD patients and models (McGeer, Itagaki, Akiyama & McGeer 1988, Tansey et al. 2007) and this will be discussed in more detail in Chapter 4. This inflammation may arise, in part, from immune activation by the build-up of misfolded α-synuclein (Klegeris et al. 2008). Dopamine itself has been shown in *in vitro* experiments to provide a modulatory effect on both astrocytes and microglia through its oxidative products and action on D2 receptors on glial cells (Yoshioka et al. 2016, Dominguez-Meijide et al. 2017). These findings suggest that a loss of dopamine as seen in PD may itself provide an inflammatory cue.

Injection of non-specific inflammatory agents such as lipopolysaccharide (LPS) into the ventral mesencephalon (VM) causes specific degeneration of the SNc (Herrera et al. 2000, Iravani et al. 2005, 2008) - showing that these neurons are particularly vulnerable to cell death in inflammatory conditions. The same effect has also been shown following systemic administration of LPS (Qin et al. 2007). This may, again, be related to the susceptibility of the SNc to oxidative stress which may, in the case of inflammation, be provided by activated microglia (Peterson & Flood 2012, Iravani et al. 2014).

It seems likely that neuroinflammation in PD may be cyclical - with misfolded α-synuclein and cell death causing inflammation, and inflammation contributing to protein misfolding and cell death in return (Kurkowska-Jastrzębska et al. 1999). However, there may be a way to harness

inflammation to provide neuroprotection (Iravani et al. 2012). This will be discussed further in the treatments section of this introduction (p. 50).

Glutamate

Excitotoxicity is a pathological process arising from excess glutamate causing an increase intracellular Ca^{2+} and leading eventually to cell death. Excitotoxicty is considered to be a secondary effect in PD, but nevertheless may be a considerable addition to the multiple neurotoxic simuli in the disease (Ambrosi et al. 2014). Altered roles of glutamate in the PD brain are proposed to underlie a vicious cycle of cell death via a number of mechanisms:

- Altered basal ganglia signalling - The reduced dopamine output of the SNc which occurs in PD gives rise to altered signalling throughout the basal ganglia. As a result of this, a glutamatergic nucleus called the subthalamic nucleus (STN) becomes hyperactive (Remple et al. 2011). This results in a change in the glutamatergic input to the SNc and a increase in the activity for these at-risk cells (Shimo & Wichmann 2009) and an increase in extracellular glutamate with the potential to cause excitotoxicity (Rodriguez et al. 1998). When added to the strain caused by the cell morphology, inflammatory environment and oxidative stress, this may increase the risk of apoptosis or autophagy.

- Neuroinflammation - Under normal circumstances, astrocytes take up excess glutamate from the extracellular space in order to reduce the risk of excitotoxicity (Anderson & Swanson 2000). In neuroinflammatory settings such as PD, this process is impaired (Hoekstra et al. 2015). Extracellular glutamate has been shown to accumulate following activation of cultured astrocytes which were treated with an inhibitor of complex 1 of the electron transport chain in order to model PD (McNaught & Jenner 2000).

- Altered excitatory post-synaptic potentials - aggregation of α-synuclein has been shown to increase excitatory transmission via α-amino-3-hydroxy-5-methyl-4-isoxazolepropionic acid (AMPA) receptors (Hüls et al. 2011). This leads to the accumulation of Ca^{2+} in these cells (Hüls et al. 2011), though only certain AMPA receptors allow passage of Ca^{2+}.

The roles of glutamate in PD will also be discussed further in Chapter 3.

1.2 The basal ganglia

Many regions of the central nervous system (CNS) are affected by the spread and progression of Parkinson's. As each area is affected, so the relative function declines and symptoms become apparent. The motor symptoms of PD are characteristic of the disease, and arise from the decline in function of circuitry controlling movement known collectively as the basal ganglia. The key driver of this circuitry, the SNc, is highly affected in PD. As neurons in the SNc are lost over the course of the disease, so the basal ganglia signalling becomes imbalanced and motor symptoms develop. In order to fully understand the changes which occur in the basal ganglia during PD, it is first important to understand the normal connectivity and functioning of the individual nuclei in a healthy organism.

1.2.1 Anatomy and functioning of the basal ganglia

The basal ganglia is made up of a number of communicating nuclei in the brain which, together, co-ordinate motor processes. The connectivity of the basal ganglia is extremely complex, comprising many interconnected nuclei and feedback loops. However, these connections may be simplified into three major 'pathways', known as the indirect, direct and hyperdirect motor pathways. Traditionally, the indirect and direct pathways are thought to arise from distinct neuronal populations within the striatum and exert opposing effects on motor function (Albin et al. 1989, DeLong 1990), while the hyperdirect pathway bypasses the striatum altogether. The direct and indirect pathways, the classical pathways of the basal ganglia, originate from activation of dopamine receptors in the striatum (Figure 1.2).

1.2.1.1 Nigrostriatal pathway

The SNc is a dopaminergic nucleus in the VM. The cell bodies located in the SNc project to the striatum via the medial forebrain bundle (MFB). It is the degeneration of the SNc cell bodies that underpin the motor symptoms which are characteristic of PD.

The SNc is innervated by a number of different regions and neurotransmitters. The striatum and globus pallidus have been shown to provide inhibitory, gamma-aminobutyric acid (GABA)-ergic input and the STN and prefrontal cortex input excitatory, glutamatergic stimuli (Kanazawa et al. 1976). In a healthy basal ganglia, the balance of these opposing inputs to the SNc dictates the rate of firing of the efferent neurons. The major efferent neurons from the SNc comprise the

nigrostriatal tract and innervate GABA-ergic medium spiny neurons, a type of projection neuron which represents around 95% of the cells of the striatum Smith et al. (2002).

Most medium spiny neurons express dopamine receptors, either D_1R or D_2R, though a small subpopulation express both (Le Moine & Bloch 1995, Aizman et al. 2000). The D_1R-expressing medium spiny neurons have also been shown to co-express substance P and dynorphin. D_1R is Gαs coupled, meaning that agonism at this receptor causes an increase in intracellular cyclic adenosine monophosphate (cAMP) and an overall increase in neuronal excitability (Nishi et al. 2011). In general, the medium spiny neurons expressing D_1R lie at the head of the direct motor pathway. Therefore, activation of these neurons by nigrostriatal dopamine activates the direct motor pathway - the pathway which drives voluntary movement. The indirect pathway works to inhibit unwanted (involuntary) movement though, if overactive, can reduce the output of the direct pathway. Thus the combined activity of these pathways in a healthy individual produces voluntary movement alone, while their dysregulation can result in involuntary movement or akinesia.

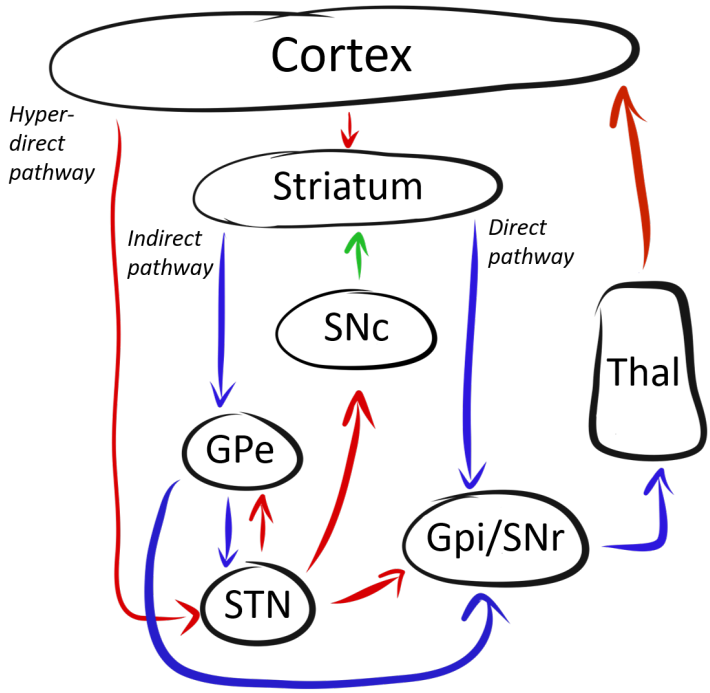

Figure 1.2: A diagram depicting simplified pathways of the intact basal ganglia. The green arrow represents dopaminergic signalling, blue arrows represent GABA-ergic signalling and red are glutamatergic. SNc, substantia nigra pars compacta; GPe, external globus pallidus; STN, subthalamic nucleus; GPi, internal globus pallidus; SNr, substantia nigra pars reticulata. Diagram adapted from Galvan & Wichmann (2008).

In contrast to D_1R, D_2R is Gαi coupled, meaning that agonism leads to the inibition of adenylyl cyclase, a reduction in cAMP and a reduction in neuronal excitability (Hernandez-Lopez et al. 2000). D_2R-expressing medium spiny neurons have been shown to co-express enkephalin and control the indirect pathway (Hernandez-Lopez et al. 2000). This means that, with a consistant supply of dopamine from the SNc, activity in the indirect pathway in inhibited. Together, these two pathways link the remaining nuclei of the basal ganglia and control motor function in opposition to each other.

1.2.1.2 Corticostriatal pathway

In addition to the dopaminergic afferents, the striatum is also activated by glutamatergic afferents originating in the cortical laminae III and V (McGeorge & Faull 1989). These gluatamatergic neurons synapse onto the GABA-ergic medium spiny neurons, expressing D_1R or D_2R and representing 95% of the striatal neurons, and are therefore directly involved in the motor circuitry. The cortical glutamatergic efferents can also synapse onto the remaining 5% of striatal neurons -GABA-ergic and cholinergic interneurons. These then influence the activity of medium spiny neurons and form an indirect inhibitory control on medium spiny neuron activity which may be associated with the motor execution of choices (Gage et al. 2010).

1.2.1.3 Direct pathway

The direct pathway is formed through a monosynaptic link between the D_1R-expressing medium spiny neurons of the striatum and the internal globus pallidus (GPi)-substantia nigra pars reticulata (SNr) structure (Figure 1.2). As this link is primarily GABAergic, the main role of the direct pathway is to inhibit the GPi-SNr, thus disinhibiting the thalamic nuclei and reducing activation of the motor cortex.

1.2.1.4 Indirect pathway

The indirect pathway is more complex than the direct pathway, involving a greater number of nuclei, despite ultimately ending at the same point (the GPi-SNr). The D_2R and enkephalin-expressing GABAergic medium spiny neurons of the indirect pathway synapse onto the external globus pallidus (GPe) which is, itself, GABA-ergic. As dopamine is released from the SNc onto the D_2R-expressing neurons, the GPe is disinhibited, leading to an increase in GABA-ergic inhibitory tone at the synapse from the GPe to the STN - a nucleus in the indirect pathway and the main

glutamatergic body within the basal ganglia (Parent & Hazrati 1995). The STN outputs to the GPi-SNr complex, activating the GABA-ergic output nuclei of the basal ganglia and inhibiting the thalamus, thereby disinhibiting the motor cortex. The GPe has been also shown to have efferent projections directly to the GPi-SNr, in addition to other basal ganglia nuclei (Parent & Hazrati 1995).

In addition, the STN and the GPe form a negative feedback loop wherein overactivation of the STN by a reduction in activity of the GPe causes activation of the GPe through the STN's glutamatergic output and therefore a reduction in activity of the STN by an increase in the GABAergic activity of the GPe (Parent & Hazrati 1995). This feedback loop should ensure that activity of the indirect pathway of the basal ganglia is controlled at all times.

By these means, the direct and indirect pathways would work in opposite directions if activated simultaneously, providing inibition and excitation, respectively, to the GPi-SNr complex. However, in reality, the presence (Figure 1.2) or absence (Figure 1.3) of dopamine dictates the differential activation of these pathways.

1.2.1.5 Hyperdirect pathway

The hyperdirect pathway is so called because it bypasses the striatum altogether, connecting cortical glutamatergic efferents to the STN and, subseqeuntly, exciting the GPi-SNr complex (Bosch et al. 2012). This pathway may play a role in switching between involuntary and voluntary movements (Nambu et al. 2002).

1.2.1.6 Thalamocortical pathway

The thalamocortical pathway acts as the final pathway within the basal ganglia before the initiation of movement. It is inhibited by activation of the indirect pathway, and therefore activation of the GPi-SNr complex. As a result of the activation of the GABA-ergic efferents from the GPi-SNr, the thalamic nuclei are inhibited from supplying feedback to the cortex (in cingulate, premotor and motor areas) via glutamatergic efferents (Schell & Strick 1984, McFarland & Haber 2002). Conversely, when the GPi-SNr are inhibited through activation of the direct pathway, the thalamocortical neurons are disinhibited, leading to increased activity in the cortex and increased motor function.

1.2.2 Degeneration of the nigrostriatal pathway

1.2.2.1 Alterations in basal ganglia signalling

In PD, the degeneration of the SNc has major effects on all three motor pathways, initiated by the loss of dopaminergic innervation of the striatum.

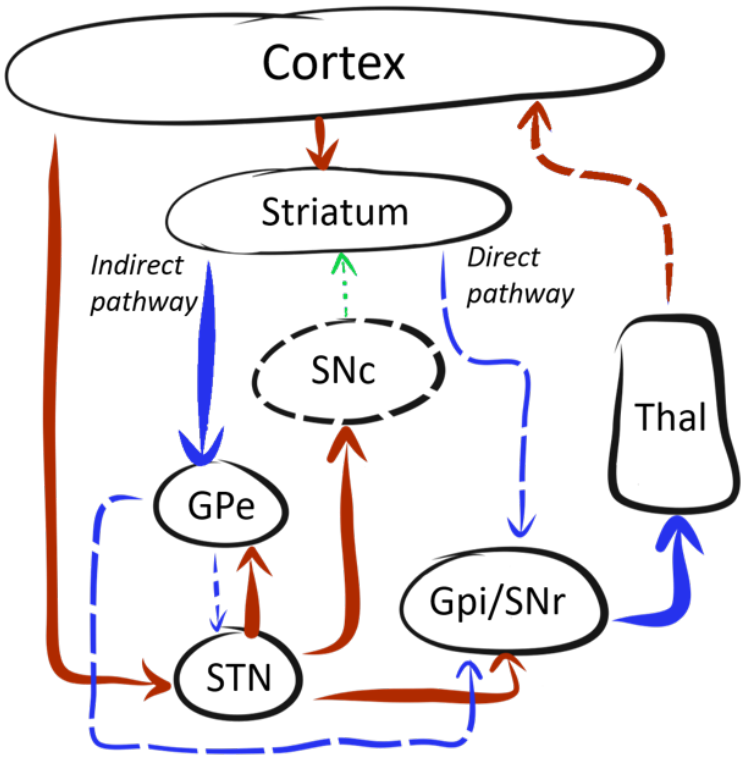

Figure 1.3: A diagram of the basal ganglia in PD. Thick lines indicate pathways which become overactive, dotted lines indicate a reduction in activity compared to a healthy basal ganglia. Blue arrows denote GABA-ergic transmission, red arrows denote glutamatergic transmission and the green arrow shows the dopaminergic projection from the SNc to the striatum. SNc, substantia nigra pars compacta; GPe, external globus pallidus; STN, subthalamic nucleus; GPi, internal globus pallidus; SNr, substantia nigra pars reticulata. Diagram adapted from Galvan & Wichmann (2008).

Under normal circumstances, activation of D_1R-containing neurons and inhibition of D_2R-containing neurons by dopamine from nigral neurons promotes the direct pathway and dampens activity of the indirect pathway. Animal models have provided evidence that, following a nigrostriatal lesion, the indirect pathway becomes hyperactive (Galeffi et al. 2003) and the activity of the direct pathway is reduced. At the same time, it seems likely that the reduced activity at D_1R, caused by a reduction in dopamine in the striatum, causes a reduction in activity of the direct pathway (Mallet et al. 2006). The hyperdirect pathway is also affected in low dopamine conditions, though,

in PD, the impact of this may be less than the impact of alterations in the direct and indirect pathways (Nambu et al. 2002, Chu et al. 2017).

Overall, these changes lead to overactivation of the GPi-SNr output nuclei, inhibition of the thalamus and a reduction of thalamocortical feedback, causing bradykinesia. Aside from alterations in signalling arising from low striatal dopamine, other changes within the basal ganglia are likely to contribute to the generation of symptoms in PD.

1.2.2.2 Additional considerations

Beta oscillations

Beta oscillations are neural oscillations with a frequency between 12.5 and 30Hz which are, in a healthy population, suppressed prior to and during conscious movement (Baker et al. 1997). Oscillations within these frequencies may therefore be described as akinetic. Higher-than-normal levels of beta oscillatory activity have been associated with striatal dopamine depletion. This phenomenon has been recorded in the basal ganglia of PD patients, 1-methyl-4-phenyl-1,2,3,6-tetrahydropyridine (MPTP)-treated marmosets and 6-hydroxydopamine (6-OHDA)-lesioned rats (Little & Brown 2014).

Synaptic dysfunction

Long-term potentiation (LTP) and long-term depression (LTD) are modes of synaptic plasticity essential for learning and adaptation in the brain. In PD models, both LTP and LTD are altered in the corticostriatal pathway (Calabresi et al. 1992, Quik et al. 2006). These changes in the plasticity of striatal neurons are likely influenced by changes in neuronal excitability through reduction in nigrostriatal dopamine (Calabresi et al. 1992, Quik et al. 2006). This, in turn, is thought to be driven by alterations in subunit composition of the postsynaptic N-Methyl-D-aspartate (NMDA) receptors in striatal spiny neurons (Gardoni et al. 2006, Paille et al. 2010). These aberrant forms of synaptic plasticity also play an important role in the development of levodopa-induced dyskinesia (LID), discussed fully in a later section of this chapter (section 1.4.2.1, p.53).

The net result of the alterations in signalling, oscillations and plasticity is impairment of the functioning of the basal ganglia and, consequently, the motor symptoms of PD.

1.3 Modelling Parkinson's disease

In order to investigate the cause, pathology and treatment of PD, a diverse battery of preclinical models are used. These models of PD are highly varied and range from immortalised cell lines used in culture, through rodent models to non-human primates. Research has even been conducted to characterise and treat Parkinsonism in humans who, as a result of the use of impure illegal substances (Langston et al. 1983), or through side effects of medication (Shin & Chung 2012), became depleted of dopamine. All models hold value in examining different aspects of PD using different techniques. Nevertheless, care must be taken when identifying the most suitable model for any individual situation. For the purposes of this thesis, a model with the potential for neurodegeneration (and therefore neuroprotection) is necessary.

In determining the suitability of PD models for use with this project, three broad criteria were considered: the feasibility of supporting the model given the facilities and materials available, the validity of the model itself and the suitability of the model in attempting to address the research hypothesis. In terms of the ability to maintain a model, it is evident that the equipment and expertise available limits, to a large extent, which models of PD which may be utilised by any one research group. For example, supporting a colony of Parkinsonian non-human primates requires a far different pool of resources than does the maintenance of immortalised, dopaminergic cells.

Picking a model which satisfies the second and third criteria is more difficult but essential to being able to correctly interpret results of the research conducted. In terms of assessing the validity of a model, physical disease models, in particular *in vivo* models, should be assessed against 3 criteria of validity (Willner 1986).

- Face validity - does the model display aspects which seem to relate to the disease being modelled and furthermore, are these aspects measurable? This type of validity must be applied differently to *in vitro* and *in vivo* models - while a rat may display bradykinesia or levodopa-induced dyskinesia, an isolated neuron may become apoptotic or show altered responses to stimuli.

- Construct validity - does the model have the same underlying features as the disease being modelled? For example, in the case of PD, does the model feature cell death/neuronal loss and proteinaceous aggregates/Lewy bodies in the same way as the brains of PD patients?

- Predictive validity - is it possible to 'treat' the model using compounds or methods which are efficacious in treating the disease? Similarly, it should not be possible to 'treat' the models using treatments which have been tested and proved ineffective in the disease itself. This reduces the potential for false negative and false positive discoveries when using the model to research new treatments or understand the mechanism of existing ones.

Finally, taking the validities of the potentially available models into account, a model is selected on the basis of whether it features aspects important to the hypothesis. If the hypothesis addresses one aspect of the disease then it is important that the model exhibits this feature, even if at the expense of other features which may be considered essential to the disease.

Below, the most commonly used models of PD will be considered in terms of their validity and their potential utility in exploring potential neuroprotection. In this section, discussion of these models in terms of their face and predictive validity will focus on assessment of motor symptoms. The ability of each model to represent the non-motor symptoms of PD will instead be covered in Chapter 5.

1.3.1 *In vitro* models of Parkinson's disease

In exploring potential therapeutics or mechanisms within PD, agents may be added to cultured cells in order to induce a PD-like phenotype. The most commonly applied agents are the toxins 1-methyl-4-phenylpyridinium (MPP^+), 6-OHDA and rotenone - which cause mitochondrial dysfunction through inhibition of complex I and IV (Figure 1.4) (Heikkila et al. 1985, Glinka & Youdim 1995). The resulting impairment of the electron transport chain leads to the generation of reactive oxygen species and the reduction of adenosine triphosphate (ATP) production, and a degenerative phenotype similar to that seen in PD. In addition, 6-OHDA may also auto-oxidise, generating hydrogen peroxide and a superoxide radical (Sachs & Jonsson 1975) and rotenone has been documented to cause proteasome inhibition and activation of the unfolded protein response (Shamoto-Nagai et al. 2003), both of which are implicated in PD.

Cells may also be genetically manipulated in order to display some of the mutations which underlie familial Parkinson's. The effects of these mutations are often similar to those of the toxins and may interfere with the unfolded protein response (GBA (Schapira 2015)) or synaptic transmission (LRRK2, SNCA (Gómez-Suaga et al. 2014, Wang et al. 2014)) or cause oxidative stress (SNCA,

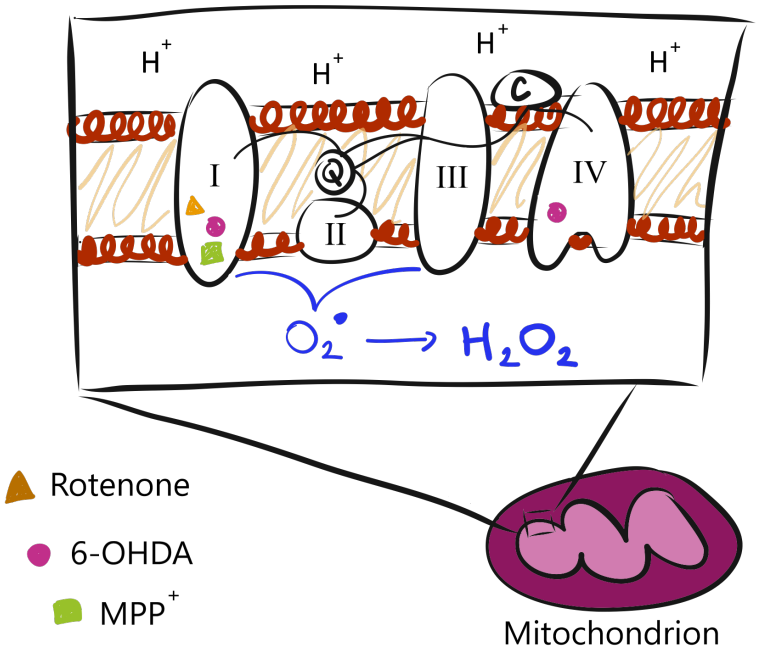

Figure 1.4: Diagram of the electron transport chain within the phospholipid bilayer separating the mitochondrial matrix from the intermembrane space. Electrons are generated through a series of reduction-oxidation reactions from complexes I and II, through coenzyme Q, complex III and cytochrome C to complex IV (electron-generating reactions follow the flow of the arrows through the diagram). Under normal conditions, these reactions produce H_2O and ATP. In models of PD however, the listed toxins act within the electron transport chain at the points indicated to inhibit the healthy production of ATP and cause excessive generation of oxygen radicals and hydrogen peroxide. Q, coenzyme Q; C, cytochrome C. Adapted from Osellame et al. (2012).

LRRK2, PINK1, Parkin, DJ-1, VPS35 (Dias et al. 2013, Wang et al. 2016)).

Assessing the predictive validity of *in vitro* models of PD is difficult, as no neuroprotective treatments are currently licensed for Parkinson's and symptomatic efficacy is impossible to judge in single cells. Lai & Yu (1997), amongst others, show that dopamine and L-3,4-dihydroxyphenylalanine (L-DOPA) can, themselves, cause cytotoxicity through oxidative stress when added to cultured SH-SY5Y cells, and that the addition of antioxidants such as N-acetyl-L-cysteine can protect against this effect. Indeed, there is prelimary evidence that antioxidants may be of use in the treatment of PD (Monti et al. 2016), so this may be considered in favour of the predictive validity of cell lines. Conversely, however, a great many potential neuroprotective treatments are discovered *in vitro* but very few eventually prove successful in humans.

1.3.1.1 SH-SY5Y cells

SH-SY5Y cells are a derivative of the SK-N-SH cell line, which itself was derived from metastasized human neuroblastoma cells (Biedler et al. 1978). Being derived from a cancer cell line, SH-SY5Y cells are immortalised and show a number of genetic alterations commensurate with this. However, Krishna et al. (2014) find that most genes found in major pathways relating to PD have at least one complete copy. Initial characterisation of SH-SY5Ys by Biedler et al. (1978) found that they contained dopamine-β-hydroxylase, necessary for the conversion of dopamine to noradrenaline. Further exploration revealed the presence of tyrosine hydroxylase (the rate-limiting enzyme in the production of catecholamines - Figure 1.5), marking SH-SY5Y cells out as catecholaminergic, if not purely dopaminergic.

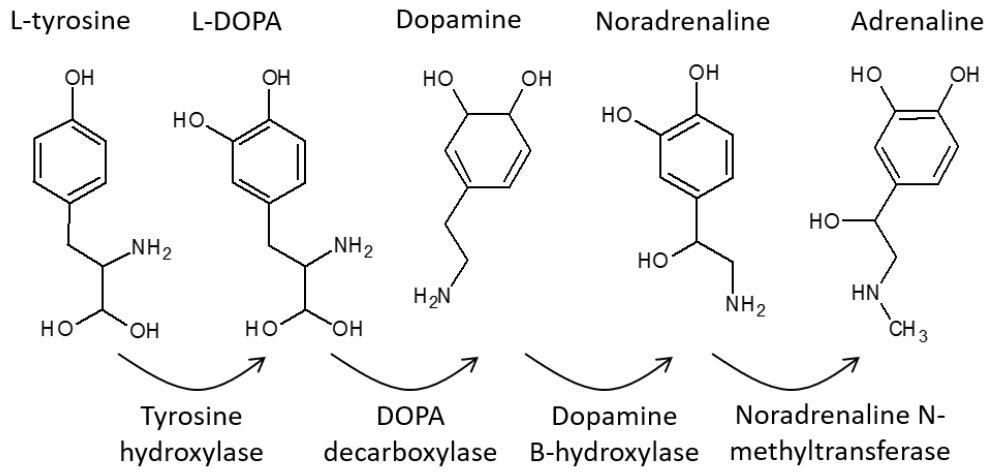

Figure 1.5: The catecholamine synthetic pathway.

1.3.1.2 PC12 cells

PC12 cells are a rat cell line derived from the adrenal medulla and can be differentiated through addition of growth factors to 'adult' neurons with different phenotypes. PC12 cells are dopaminergic, cholinergic and noradrenergic in nature (Hirsch et al. 1993), making them suitable for studying neurotransmission in a wide variety of neurological models. In PD research, PC12 cells are subjected to toxins or genetic manipulations as outlined above, and the deleterious effects of these operations offset by potential neuroprotective therapeutics.

Although there is little difference between the PC12 and SH-SY5Y cells in terms of their relative expression of neurotransmitters, their reponse to stimuli - including neurotoxic pesticides such as

rotenone - is quite disparate (Heusinkveld & Westerink 2017). These differences in response are important considerations when deciding which immortalised cell line is appropriate for a given research hypothesis, if at all.

1.3.1.3 Primary ventral mesencephalon cultures

Though primary cultures are here classed alongside immortalised cell cultures, their methodology and potential as a model of PD is very different. In contrast to immortalised cell lines, primary cultures are taken directly from the developing brains of embryonic or foetal animals. Typically, VM cultures may then be grown with the addition of potential neuroprotective treatments or toxins in order to examine survival or changes in the protein or gene expression profile. Although VM cultures are taken from the developing brain, they may be considered better models of the whole midbrain than immortalised cells as they form more complex networks, being comprised of different cell types (neuronal and glial) (Popova et al. 2017).

1.3.2 Non-mammalian, *in vivo* models of Parkinson's disease

1.3.2.1 *Caenorhabditis elegans*

C. elegans is a nematode worm increasingly used for modelling developmental and degenerative disorders on a whole-organism level. The advantages of using *C. elegans* over larger, more traditional organisms are plain - their small size and high turnover makes them cheap to keep and efficient for modelling genetic disorders. Nematode worms can also be characterised and sorted in a similar manner to cells, providing a high-throughput option for drug screening in whole organisms - albeit simple ones (Yan et al. 2014).

In terms of their ability to provide a model of human diseases, *C. elegans* exhibit the basic biology necessary for replicating a PD phenotype. They have analogues of necessary ion channels, neurotransmitters, receptors and synaptic mechanisms on 302 neurons, including 8 dopaminergic neurons (Sulston et al. 1975, Bargmann 1998). The nematodes display very basic behaviours, such as food foraging, which may be examined and interpreted for 'symptoms' of Parkinsonism. Worms may be mutated to overexpress α-synuclein or other mutated forms of PARK genes in order to provide models of PD (Table 1.1). These worms display reduced rates of locomotor activity and reduced dopamine levels which are dependent on the age of the worm and the level of mutant gene expression (Hamamichi et al. 2008). Similarly, exposure to toxins such as 6-OHDA (Cao et al.

2005) and MPP^+ (Braungart et al. 2004) also result in dopaminergic neuronal loss and motor deficits. In this respect, the face validity of the *C. elegans* model is clearly higher than for *in vitro* models as symptoms can be demonstrated, if only at a basic level.

C. elegans has also been used to explore the function of certain genes and gene mutations within PD pathways. Mitochondrial dysfunction, oxidative stress (Ray et al. 2014) and impairment of the unfolded protein response (Martinez et al. 2017) all feature in PD models in *C. elegans*. This mirrors processes underlying degeneration both in 'higher order' mammalian PD models and in what we understand of PD itself, bolstering the construct validity of the *C. elegans* model.

The predictive validity of *C. elegans* models is more difficult to assess. In *C. elegans*, as in other animal models, neuroprotective treatments have been proposed and characterised but not carried through to clinical trials (Shi et al. 2013, Fu et al. 2014, Liu et al. 2015). However, there have been reports that L-DOPA may both provide symptomatic relief (restoration of motor capacity) (Zheng et al. 2012) and cause dyskinesia (increased thrashing without increased distance travelled) (Gupta et al. 2016).

1.3.2.2 *Drosophila melanogaster*

The fruit fly (*D. melanogaster*) is another small organism with a high turnover which is cheap to keep and has reasonable conservation of genes with humans and other model animals (Pienaar et al. 2010), making it ideal for fast-paced genetics experiments. Understanding of *D. melanogaster* genetics is relatively advanced, and so mutations in PD genes may be made organ-specific in order to provide a visible phenotype without risking larval lethality, as in the rough-eye phenotype for Unkempt mutants (Avet-Rochex et al. 2014). This is key to aid sorting of live flies for reproduction while also affording the opportunity to study the function of genes critical to survival in an otherwise healthy organism (Iyer et al. 2016). Unsurprisingly, given the availability of such techniques, the fruit fly is primarily used in order to understand signalling pathways in health, disease and treatments (Guo 2012). However, it may also be used as a model in which to test potential therapeutics in a high-throughput manner (Willoughby et al. 2013).

With respect to its utility as a PD model, the fruit fly has a number of dopaminergic neurons (which degenerate with age or the accumulation of Lewy bodies in flies expressing mutated α-synuclein (Feany & Bender 2000)) and a drive to climb upwards on a vertical surface which may reliably be used in order to quantify motor ability. Despite many promising findings that such

genetic manipulations or neurotoxin administrations may cause a reliable PD phenotype (Feany & Bender 2000, Coulom & Birman 2004, Wang et al. 2007, Kim et al. 2012) follow-up studies have found conflicting results. Navarro et al. (2014) find that, in attempting to replicate results obtained with 5 different models of PD in *D. melanogaster* (mutation in α-synuclein, PINK1 or Parkin, or administration of rotenone or paraquat), no neuronal loss occurred in any - though a reduction of motor ability and a reduction in dopaminergic neuron-associated green fluorescent protein (GFP) was observed.

L-DOPA has been shown to reduce motor impairment in PINK1 mutant flies, alongside a number of other compounds which anecdotally improve motor function in PD (though not proven clinically) (Jansen et al. 2014).

1.3.2.3 *Danio rerio*

In addition to the small size and fast life-cycle which mark other non-traditional organisms out as useful in research, *D. rerio*, or zebrafish, have the advantage that their embryos are transparent. This means that, with the addition of GFP, developmental changes are extremely easy to observe and to image. Zebrafish genetics and neuronal connectivity are well recorded and an area of neurons expressing tyrosine hydroxylase (TH) has been observed and found to be analagous in function to the human SNc and VTA (Son et al. 2003), with an additional region characterised as the striatum of the zebrafish (Rink & Wullimann 2001). Furthermore, many of the key genes whose dysfunction gives rise to familial Parkinson's (Table 1.1) are conserved in *D. rerio* and expressed appropriately in dopaminergic neurons (Flinn et al. 2008).

In zebrafish, knockout or dysfunction of PINK1 gives rise to a Parkinsonian phenotype of dopaminergic cell death and locomotor impairment accompanied by an increase in ROS which may be rescued through administration of antioxidants or expression of wild-type PINK1 (Anichtchik et al. 2008, Xi et al. 2010). Toxins, including MPP^+, 6-OHDA and rotenone, are also able to induce dopamine-specific degeneration in zebrafish (Anichtchik et al. 2004, Bretaud et al. 2004, Lam et al. 2005). The motor symptoms (impaired swimming) of the degeneration caused by these compounds may be treated with L-DOPA or antioxidants (Feng et al. 2014).

In summary, despite our increasing knowledge of all of these non-mammalian models, and their utility in picking apart the genetics underlying PD, their lack of fine motor readouts makes them

unsuitable for use with the present research. Furthermore, this exposition will go on to detail non-motor symptoms which may be observed in animal models (Chapter 5) and, in this arena, cell models, invertebrates and fish have little to offer.

1.3.3 Pharmacological, mammalian models of Parkinson's disease

Despite the chronic, progressive nature of PD, acute animal models exist which, for a period of time, mirror the reduction in monoaminergic transmission seen in late stages of the disease. While these models fail to mimic the neurodegeneration or progressive disability, they are still used to examine the efficacy of symptomatic treatments. They have advantages over many of the other mammalian models in that surgery or breeding programmes are not required for their use.

1.3.3.1 Reserpine

Reserpine is an old antipsychotic and antihypertensive drug which prevents uptake of monoamines (dopamine, serotonin and noradrenaline) into the presynaptic terminal by blocking vesicular monoamine transporter 2 (VMAT2) (Schuldiner et al. 1993). Monoamines remaining in the synapse are broken down by monoamine oxidase B (MAO-B) and, with the loss of storage capacity induced by reserpine, the nervous system is effectively depleted of monoamines. Despite its transient nature and lack of nigral cell loss, the reserpine model retains acceptable construct validity due to the depletion of serotonin and noradrenaline in parallel with the much focused-upon dopamine loss. This more accurately models the complex deficits seen in Parkinson's than many other dopamine-centric models (Jellinger 1991). In addition to this, PD changes can be seen throughout the basal ganglia of reserpinised animals as a direct response to the monoamine loss - the rate of STN firing increases (Robledo & Feger 1991) causing an increase in extracellular glutamate in the GPi and other basal ganglia nuclei (Biggs et al. 1997).

Reserpinised animals display akinesia and rigidity, in line with typical motor symptoms of PD, which may be treated with potential therapeutics (Valenti et al. 2005). Dopamine agonists, L-DOPA, MAO-B and catechol-o-methyl transferase (COMT) inhibitors and amantadine are all able to reverse reserpine-induced akinesia in rodents (Goldstein et al. 1975, Colpaert 1987). This highlights the good face validity of the model and and predictive validity (Table 1.2, p.47) for symptomatic treatments.

1.3.3.2 Haloperidol

Similarly to reserpine, haloperidol is an antipsychotic drug which may be used to transiently induce a state of Parkinsonism in animals characterised by catalepsy (muscular rigidity accompanied by a loss of response to external stimuli). Unlike reserpine, however, haloperidol acts as an antagonist at D1 and D2 receptors at the head of the direct and indirect motor circuits from the striatum (Creese et al. 1975). This causes a reduction of input to the basal ganglia in the same manner as dopaminergic cell death and results in similar motor symptoms - akinesia and muscle rigidity. The construct underlying haloperidol-induced catalepsy is therefore quite dissimilar to that of human PD, however some few similarities have been noted. Chiefly, administration of haloperidol may result in acutely reduced striatal content of multiple catecholamines (Kulkarni et al. 2009) and the resulting signalling imbalance within the basal ganglia causes an increase in extracellular glutamate at the GPi (Biggs et al. 1997).

The haloperidol catalepsy model has also shown good predictive validity in dopamine agonists and L-DOPA (Kobayashi et al. 1997), and is commonly used as a dose-finding tool when examining potential new therapeutics (Bennouar et al. 2013, Iderberg et al. 2015). When determining the therapeutic efficacy of potential neuroprotective treatments, however, some degree of cell death is necessary for understanding efficacy. This is not present in either of the above acute models of PD, which instead feature reversible changes to neurochemistry and are therefore also unsuitable for observing changes to Parkinsonian symptomatology following chronic treatments.

1.3.4 Neurodegenerative, mammalian models of Parkinson's

To this end, some more permanent lesion models are needed. The classical lesion models consist either of intracranial administration of 6-OHDA in rats or mice, or systemic administration of MPTP in mice or non-human primates. The pesticide rotenone is also becoming increasingly well used and characterised as an agent capable of inducing Parkinsonism in mammals.

1.3.4.1 6-OHDA

The potential of 6-OHDA for use in PD models was first realised by Ungerstedt (1968), who was the first to inject it into the SNc and striatum. When injected intracranially, 6-OHDA is uptaken into monoaminergic neurons, causing oxidative stress through inhibition of complexes I and IV

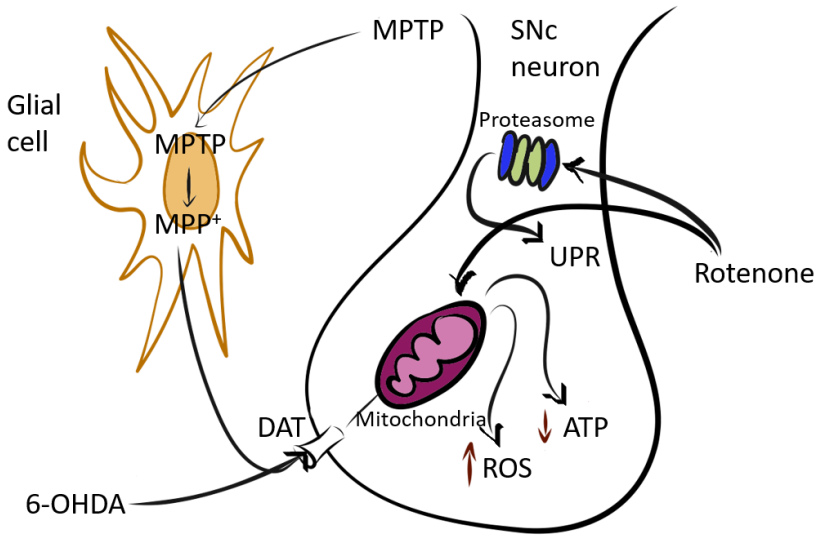

Figure 1.6: A summary of the mechanisms of action of neurotoxins used to develop animal models of Parkinson's. The diagram shows a glial cell and a dopaminergic nigral neuron. 6-OHDA is administered intracranially and enters cells through DAT channels whereupon it may auto-oxidise to produce ROS, or inhibit complexes I and IV of the mitochondrial electron transport chain and reduce the supply of ATP. This alters the metabolic rate of the cell and predisposes it to apoptosis (Lu et al. 2018). MPTP and rotenone cross the blood-brain barrier and are administered systemically. MPTP is processed by MAO-B within glial cells to MPP^+ and is uptaken by DAT (Melamed et al. 1985, Gainetdinov et al. 1997) to inhibit complex I of the electron transport chain with results similar to those caused by 6-OHDA. Rotenone enters the cell across the cell membrane. It causes damage to the cell both by inhibiting complex I of the electron transport chain (Li et al. 2003) and by inhibiting proteasome activity. This causes a buildup of damaged and misfolded proteins which trigger the unfolded protein response (Wang et al. 2006). ROS, reactive oxygen species; UPR, unfolded protein response.

of the mitochondrial electron transport chain (Glinka & Youdim 1995) (Figures 1.4 and 1.6) and producing ROS by auto-oxidation (Hanrott et al. 2006). This leads to apoptosis of monoaminergic neurons and activation of glial cells (Walsh et al. 2011). These processes mirror those which occur in human PD and so, in that respect, 6-OHDA has good construct validity. However, 6-OHDA animals do not display Lewy body pathology, a hallmark of PD in humans. Furthermore, dopaminergic cell death develops very quickly following lesioning; unlike the slow process of degeneration which occurs in human PD. The predictive validity of the 6-OHDA rodent model is outlined in Table 1.2, p.47.

The spectrum of 6-OHDA models is fully detailed in the introduction to Chapter 2, during which the development of the 6-OHDA model used for the current work is discussed.

1.3.4.2 MPTP

The ability of MPTP to cause specific dopaminergic deficits following systemic administration was discovered following accidental exposure of a number of laboratory workers and drug addicts to the compound (by intravenous injection, inhalation or cutaneous absorption) in separate incidents (Davis et al. 1979, Langston et al. 1983, Pakkenberg & Pakkenberg 1996). Those affected by exposure developed chronic Parkinsonism which involved akinesia, slurred speech, excessive salivation and a 'pill-rolling' tremor (Langston et al. 1983). Following the death of one of the patients, selective nigral cell death and the appearance of Lewy body-like inclusions were observed (Davis et al. 1979), confirming the similarities of MPTP-associated Parkinsonism in humans and PD itself.

Studies have shown that metabolism and clearance of MPTP is much faster in rodents than in primates, leading to some species being seemingly unaffected by MPP^+ toxicity (Chiueh et al. 1984, Johannessen et al. 1985). These findings mean that, *in vivo*, MPTP is most commonly used with mice and non-human primates, and that mice require a much higher dose of MPTP in order to achieve the same effect as in primates (Burns et al. 1983, Heikkila, Hess & Duvoisin 1984). This leads to some potential risk to experimenters - as exposure of mouse-level doses of MPTP could cause severe disability to a human. For this reason, special measures such as an isolated holding room, personal protective equipment and careful training must be put in place before MPTP work can be considered (Jackson-Lewis & Przedborski 2007). Furthermore, the large doses of MPTP needed to induce Parkinsonism in mice can result in a high lethality rate due to off-target cardiovascular effects (Jackson-Lewis & Przedborski 2007).

As in humans exposed to MPTP, mice develop bradykinesia and selective and bilateral loss of dopaminergic midbrain cells and striatal terminals (Heikkila, Hess & Duvoisin 1984, Ogawa et al. 1985). Although Lewy body-like inclusions have been reported by some groups (Meredith et al. 2002), others have been unable to replicate the finding (Shimoji et al. 2005). When considered alongside the mitochondrial and lysosomal dysfunction which occur following administration of MPTP, these data suggest that the face and construct validities of the mouse MPTP model are high. It must be noted, however, that degeneration is still a rapid occurrence, as with 6-OHDA, rather than the slow decline seen in PD. Furthermore, variability in the MPTP mouse model is high and relies on the constancy of a number of factors (including mouse strain, supplier, age, gender and weight), which suggests that findings from the MPTP mouse model may be challenging to fully replicate in a different environment (Miller et al. 1998, Jackson-Lewis & Przedborski 2007).

Assessing the predictive validity of the MPTP mouse model is more challenging than in 6-OHDA models. This is because the toxicity of MPTP must occur via a broad, two-step process: the conversion of MPTP to MPP^+ in glial cells and the action of MPP^+ within the neuron to cause cell death (Figure 1.6). Some compounds which appear to be neuroprotective in the MPTP model act to prevent the formation of MPP^+ - an intervention which would not be of benefit to Parkinson's patients - rather than to prevent cell damage by oxidative stress or metabolic change. For example, Heikkila, Manzino, Cabbat & Duvoisin (1984) find that MAO-B is responsible for the conversion of MPTP to MPP^+ and, consequently, administration of MAO-B inhibitors prior to MPTP can prevent the formation of MPP^+ and thereby prevent neurodegeneration. However, in support of the predictive validity of the murine MPTP model, the gold standard of symptomatic PD treatment - L-DOPA - does improve motor deficits (Ogawa et al. 1985).

The non-human primate MPTP model has a similar profile to the murine version, but with increased face validity. As a result of the greater intelligence and dexterity of primates, it is possible to test non-motor symptoms of Parkinsonism with more accuracy and confidence. The motor and non-motor profile of MPTP-treated non-human primates will be discussed further in Chapters 3 and 5.

1.3.4.3 Rotenone

Rotenone is a lipophilic pesticide which, like MPTP, is able to diffuse across the blood-brain barrier following systemic administration and cause mitochondrial dysfunction (Heinz et al. 2017) (Figures 1.4 and 1.6). In addition, rotenone is thought to cause inhibition of the proteasome which leads to the accumulation of ubiquitinated protein aggregates within the cell (Wang et al. 2006). This mirrors genetic mutations in familal PD which also cause a breakdown of the ubiquitin-proteasome system (McNaught & Olanow 2003). Rotenone has also been reported to cause gastrointestinal symptoms and Lewy-like pathology within the mesenteric nervous system (Drolet et al. 2009). In these respects then, construct validity for rotenone rodent models of PD is high.

However, rotenone also has a significant cardiovascular toxicity which may cause a high mortality rate when used in rodents (Betarbet et al. 2000). Additionally, some animals seem unaffected by neurodegeneration following rotenone administration, though the reason for this is not yet known (Betarbet et al. 2000). Thus, variability of rotenone-based models can be high and results difficult to replicate. Reports of motor symptoms arising from rotenone administration are likewise

inconsistent (Alam & Schmidt 2002, Cannon et al. 2009, von Wrangel et al. 2015) and so face validity varies between experiments.

Clearly, variability in model outcome is a drawback when assessing drugs for potential symptomatic or neuroprotective effects. Nevertheless, groups have shown that L-DOPA and apomorphine are of use in treating Parkinson's symptoms arising in rotenone-treated animals (Alam & Schmidt 2002, Cannon et al. 2009) (Table 1.2).

Table 1.2: Predictive validity of mammalian PD models

	Reserpine	Haloperidol	6-OHDA	MPTP	Rotenone
L-DOPA	✓	✓	✓	✓	✓
Dopamine agonists	✓	⇜⇝	✓	✓	⇜⇝
MAO-B inhibitors	✓	✓	✓	✓	
COMT inhibitors	⇜⇝	⇜⇝	✓	✓	
Anti-cholinergic		✓		✓	
Amantadine	✓	✓	✓	✓	

Table 1.2: Table adapted from Duty & Jenner (2011) showing the predictive validities of animal models of PD against the classes of drugs used to treat PD. ✓denotes a model which has good predictive validity for the majority of drugs in a given category. ⇜⇝ denotes a model which appears to have good predictive validity for less than half of the drugs in a given category. Blanks are left where predictive validity has not been recorded.

1.3.4.4 Genetic manipulations in mice

The genetics of PD are increasingly well documented and characterised in models like *C. elegans* and *D. melanogaster*. These easily genetically manipulable models have homologues of human genes, the dysfunction of which has been shown to lead to familial PD (Table 1.1). There have been many attempts to use these genes to create a reliable mouse model of PD which shows construct, face and predictive validity of PD. Here, each gene is briefly discussed in terms of its mouse models.

- *SNCA* - Synuclein-based mouse models vary in their initiation of pathology. Synuclein oligomers may be injected directly into the brain (Paumier et al. 2015), pathology initiated through injection of viral vectors expressing the A53T mutant synuclein gene (Oliveras-Salvá et al. 2014) or the mice may be engineered to overexpress mutant synuclein globally or in a

promoter-specific manner (Giasson et al. 2002). Unsurprisingly, the properties of the model depend heavily on which of these are utilised. In some models, no degeneration is seen and in others there is degeneration but only in one target area (Chesselet 2008). Perhaps the most promising of the murine synuclein models is a mouse overexpressing mutant (A53T) synuclein driven by a prion promoter. These mice suffer from progressive motor disability, Lewy body-like inclusions throughout the brain (Giasson et al. 2002) and also progressive neurodegeneration - however the SNc appears unaffected while instead, neurons in other regions, including the motor cortex, are depleted (Martin et al. 2006).

- *LRRK* - On its own, LRRK2 deletion or mutation does not cause any accumulation of α-synuclein, dopaminergic degeneration or motor phenotypes (Andres-Mateos et al. 2009). However, combining a LRRK2 mutation with A53T α-synuclein overexpression may exaggerate the phenotype (Lin et al. 2009).

- *Parkin* - Parkin-deficient mice do not display degeneration of the nigrostriatal pathway and are not more susceptible to the degenerative effects of MPTP than wild type mice (Aguiar et al. 2013, Rial et al. 2014). There are conflicting reports of Parkin knockout strains developing motor or non-motor symptoms independent of the lack of PD pathology (Perez & Palmiter 2005, Rial et al. 2014).

- *PINK1* - As is the case in Parkin and LRRK2 mice, PINK1-knockout does not cause α-synuclein pathology or neurodegeneration on its own. When combined with α-synuclein overexpression, however, the model retains a higher construct validity, displaying both more severe nigral degeneration and synuclein phosphorylation than in α-synuclein overexpressing mice (Oliveras-Salvá et al. 2014).

- *VPS35* - Although one of the less studied PD genes, there is evidence that expression of a mutated form of VPS35 by a viral vector induces nigral degeneration and axonal synuclein pathology in rats (Tsika et al. 2014).

- Mitopark - The mitopark model differs from the others listed here in that is is not a direct attempt to replicate a mutation which underlies PD but, instead, to replicate the effects. The mitopark model is constructed through a conditional knockout of the mitochondrial

transcription factor Tfam in midbrain dopaminergic neurons. Mitopark mice display an age-related decline in motor functions and a decrease in dopamine levels in midbrain nuclei (Galter et al. 2010). Despite the apparently good face and construct validity of this model, its use and popularity remain limited.

1.4 Current treatments

James Parkinson, in keeping with the medical wisdom of the 1800s, suggests that regular letting of blood may help to relieve some of the symptoms of PD (Parkinson 2002). Perhaps more logically, he also suggests that a cure, if at all possible, would be best implemented in the early stages of the disease, prior to major disability and the accompanying reduction in quality of life of PD patients. As yet, the clinical treatment of PD has not reached the stage of a cure or reliable neuroprotection, though a range of symptomatic treatments for PD exist. Below, each of the potential treatments for the motor symptoms of PD are discussed in detail. Treatments for non-motor symptoms currently tend to be non-specific for PD and are, instead, specific to the symptom (*e.g.* antidepressants for PD-depression, laxatives for constipation etc.), but those that are specific will be discussed in the 'Unmet medical needs' section (p.53).

1.4.1 Symptomatic treatments

1.4.1.1 Dopamine replacement

The gold standard treatment for PD is L-DOPA, a precursor of dopamine which is able to cross the blood brain barrier. L-DOPA was first discovered as a treatment for PD in 1961 following the observation that there was a great reduction of dopamine in post-mortem brains from PD patients (Birkmayer & Hornykiewicz 1961). L-DOPA is capable of crossing the blood-brain barrier following peripheral administration and, once there, is uptaken by catecholaminergic neurons through DAT or serotonin transporter (SERT). Once inside the cells, L-DOPA is acted on processed by DOPA decarboxylase (Figure 1.5, p.38) to produce dopamine, thus replenishing the intracellular supply reduced by SNc cell death. The simplicity of this solution to PD akinesia is remarkable, as is its efficacy in the early stages of treatment.

L-DOPA is often co-administered with a DOPA decarboxylase inhibitor which cannot cross the blood brain barrier. This prevents peripheral DOPA decarboxylase from metabolising L-DOPA before it reaches the CNS and therefore reduces the peripheral effects of dopamine such as hypotension. Other enzymes which metabolise L-DOPA and dopamine, such as COMT and MAO-B may also be inhibited in order to prolong the therapeutic effects of L-DOPA administration. Indeed, inhibitors of these enzymes (commonly used drugs include selegiline and rasagiline for MAO-B inhibition and entacapone and tolcapone for COMT inhibition) are effective monotherapies for reducing the severity of motor symptoms in the early stages of PD (Talati et al. 2009).

Despite being the most widely used and effective treatment for the motor symptoms of PD, L-DOPA can cause severe side effects, termed LID, which worsen over time with continued treatment. LID encompasses a spectrum of involuntary drug-induced movements including painful muscle contractions and involuntary writhing. This will be discussed in more detail in the 'Unmet medical needs' section of this introduction (p.53). In addition to LID, L-DOPA treatment has been associated with arrhythmia, emotional disturbance, confusion and hallucinations (Foster & Hoffer 2004).

1.4.1.2 Dopamine agonists

The theory behind the use of dopamine agonists is very similar to that of L-DOPA - they are used in an effort to replace the lost dopaminergic tone in the PD basal ganglia. In accordance with this aim, the dopamine agonists prescribed for PD, such as pramipexole, bromocriptine and ropinirole, primarily act at D_2R in order to target downregulation of the overactive striatopallidal neurons of the indirect pathway. In this way, the glutamatergic output of the STN onto the GPi-SNr is reduced and the thalamus is disinhibited (the composition of the indirect pathway was detailed on p.31). Some mixed D_1/D_2 receptor agonists, such as pergolide and apomorphine, may also be prescribed - boosting the activity of the direct pathway at the same time as inhibiting the indirect pathway.

Dopamine agonists may be used in earlier stages of treatment in an attempt to delay prescription of L-DOPA and the resulting LID. Indeed, dopamine agonists themselves may present a lesser risk of inducing dyskinesia (Rascol et al. 2000, Holloway et al. 2004). Nevertheless, dopamine agonists increase the risk of other side effects such as hallucinations (Kataoka et al. 2014), somnolence and impulse control disorders (Nissen et al. 2012, Valença et al. 2013) - making choosing between between L-DOPA and dopamine agonist treatment for each patient challenging.

1.4.1.3 Non-dopaminergic pharmacological strategies

Although deterioration of the dopaminergic nigrostriatal tract, and the subsequent effects on the basal ganglia, is perhaps the most discussed effect of PD, other neurotransmitter systems and nuclei are heavily affected by the disease. The damage to glutamatergic, noradrenergic and cholinergic systems can underlie also motor symptoms, meaning that treatments altering these other neurotransmitter systems may also result in functional improvements.

- Amantadine is a partial NMDA receptor antagonist. Although its primary use in PD is against LID (Fox et al. 2011, Pahwa et al. 2017), it has also been shown to have some antiparkinsonian potential of its own (Schwab et al. 1969).

- Safinamide is an MAO-B inhibitor with multiple other targets, such as DAT and glutamate release inhibition. It has shown some efficacy in the symptomatic treatment of motor deficits and LID in clinical trials (Borgohain et al. 2014, Deeks 2015) and has recently been licensed by the EMA and FDA (Teixeira et al. 2018). Safinamide has also been shown to provide an anti-inflammatory effect and neuroprotection in a 6-OHDA rat model (Sadeghian et al. 2016).

- Adenosine 2A receptor antagonists, Istradefylline and Tozadenant, have been approved in certain territories for the treatment of motor symptoms and wearing off after L-DOPA (Mizuno et al. 2013).

Despite these potentially promising non-dopaminergic therapies, the most reliable symptomatic treatments for PD still rely on dopamine agonism or replacement.

1.4.1.4 Surgical strategies

Surgical interventions have also been shown to be effective in the symptomatic treatment of PD. However, due to the risks involved in such invasive surgery and the poor health of the average PD patient, such treatment options have a very limited utility.

The primary targets of surgical interventions for PD are the overactive nuclei in the basal ganglia - STN and GPi. Initially, such interventions focussed on creating lesions within these nuclei: creating a subthalamotomy or pallidotomy and reducing all motor symptoms of PD (Baron et al. 1996, Alvarez et al. 2009, Çoban et al. 2009). More advanced forms of these surgeries instead take advantage of the finding that high frequency electrical stimulation of the same nuclei reversibly reduce signalling (Klassen et al. 2011, Limousin et al. 1995). This technique, known as deep brain stimulation, has shown to be reliably effective in reducing all of the motor symptoms of PD, even allowing L-DOPA treatment to be reduced without negative consequences (Anderson et al. 2005). Deep brain stimulation has also been shown to reduce subthalamic beta-oscillations, thereby providing additional evidence of antiparkinsonian efficacy (Quinn et al. 2015).

1.4.2 Unmet medical needs

Clearly, the current treatments of PD are imperfect; they give temporary relief from motor symptoms at the cost of reducing efficacy over time and the development of potentially debilitating side effects. Furthermore, they do not affect the non-motor symptoms which are as much a part of life with PD as bradykinesia. Perhaps most importantly however, the treatments currently licensed for PD are not disease modifying - they do not halt (or even slow) the course of the disease, nor promote neuronal repair in areas affected by neurodegeneration. These key areas of unmet need in the treatment of PD are not neglected however, and progress is being made towards addressing each one.

1.4.2.1 L-DOPA-induced dyskinesia (LID)

As discussed previously in this introduction, L-DOPA is the gold standard treatment for PD and the vast majority of PD patients eventually require L-DOPA to control their motor symptoms. Nevertheless, L-DOPA is far from a perfect solution in PD, carrying a high risk of severe side effects.

LID is a side effect of prolonged L-DOPA treatment in PD patients whereby patients suffer involuntary, non-purposeful movements of the limbs and upper body. These movements are classified as either choreic (spasming or twitching) or dystonic (sustained and often painful muscular contractions causing twisting of the body). LID may occur when L-DOPA plasma concentrations are at their highest, lowest or changing between doses. The prevalence of all types of LID rises from 0% in the first year of treatment to approximately 40% by 4-6 years (Ahlskog & Muenter 2001) and 95% by 15 years of treatment (Hely et al. 2005).

Current evidence suggests that LID develops as a result of pulsatile dopaminergic stimulation in the otherwise dopamine-depleted brain, arising from inconsistent release of dopamine over time (Stocchi & Olanow 2004). Under the circumstances of dopamine denervation, L-DOPA appears to be taken up by noradrenergic and serotonergic neurons and converted to dopamine in these cells by amino acid decarboxylase (Tanaka et al. 1999). As these cells have no feedback mechanism to regulate dopamine release, synaptic levels of dopamine can change remarkably over short periods (Carta et al. 2007) and, consequently, the pulsatile dopaminergic stimulation thought to underlie development of LID. Indeed, PD patients with an intact serotonergic system are at higher risk of developing LID earlier on than those with serotonergic deficits (Carta et al. 2007, Politis et al.

2014). Zeng et al. (2010) found that, in the brains of marmosets with LID, there was considerable hypertrophy of serotonergic varicosities in the striatum - suggesting further that plasticity of this system plays a role in LID induction. In addition, aberrant pathological plasticity of corticostriatal neurons has also been implicated in the development of LID (Zhang et al. 2013).

Treatments for LID often comprise altered formulation of L-DOPA. For example, extended release forms of L-DOPA are thought to reduce fluctuations in dopamine levels and therefore reduce the corticostriatal compensations (Stocchi & Olanow 2004). In addition, the NMDA receptor antagonist Amantadine has shown mixed efficacy against LID (Crosby et al. 2003), again demonstrating a role for glutamatergic signalling such as that in the corticostriatal pathway.

1.4.2.2 Non-motor symptoms

The non-motor symptoms of PD are increasingly understood to be no less a burden of PD than the motor symptoms, and often affect the quality of life of the patient to the same, or even a greater degree (Shulman et al. 2002). The non-motor symptoms experienced by any one individual with PD may differ almost entirely from another PD patient. Some researchers are seeking to group symptoms together to distinguish different clinical subtypes of PD (Sauerbier et al. 2016). In the future, this approach may enable personalised treatment of an individual's PD based on their likelihood of developing particular symptoms over the future course of their disease.

Non-motor symptoms of PD may be split into a number of different groups:

- Sensory features involve distortion to sensory perceptions, including olfactory deficits, visual alterations and chronic or neuropathic pain.

- Neuropsychiatric disturbances are common features of PD with anxiety or depression occurring in approximately 35% of the PD population (Reijnders et al. 2008). Cognitive decline is often a feature of later stage PD, though other Parkinson's spectrum disorders, such as Parkinson's disease dementia (PDD), are characterised by the earlier appearance of dementia in the disease process.

- Sleep disturbances, most often in the form of REM sleep behaviour disorder (RBD) are recorded in a high proportion of newly diagnosed PD patients (Sixel-Döring et al. 2014).

Likewise, those who are diagnosed with RBD have a higher likelihood of a subsequent diagnosis of PD than do the general population (Schenck et al. 1996).

- Autonomic features of PD may also appear before the onset of the motor features, with constipation as one of the earliest recorded symptoms of those who go on to develop PD (Adams-Carr et al. 2016).

The non-motor symptoms will be discussed in much greater detail in Chapter 5 of this thesis.

Holistic treatment of PD as both a motor and non-motor disorder is not currently possible due to our limited understanding of the similarities in pathophysiology underlying the production of both sets of symptoms. As a result, each non-motor symptom is traditionally treated as though it were an exception in an otherwise healthy individual, with varying degrees of success. Nevertheless, progress is being made towards treating each symptom as a part of PD and clinical trials are underway for drugs in a number of different PD indications:

- 5HT2A inverse agonist, Pimavanserin, has been approved for the treatment of PD psychosis in the USA (Sahli & Tarazi 2018).
- Anticholinesterases such as donepezil, galantamine and rivastigmine have undergone clinical trials for PD dementia (Ishikawa et al. 2014, Kandiah et al. 2017).
- Antidepressants of the selective serotonin/noradrenaline reuptake inhibitor class are being trialled for pain syndromes and depression in PD (Djaldetti et al. 2007). Opioids such as oxycodone are also being trialled for pain syndromes (Trenkwalder et al. 2015).

1.4.2.3 Progressive neurodegeneration

It is generally accepted that, at the point of diagnosis of PD, considerable damage to the SNc (between 30 and 50% neuronal loss by some estimates (Fearnley & Lees 1991)) has already taken place (Figure 1.7).

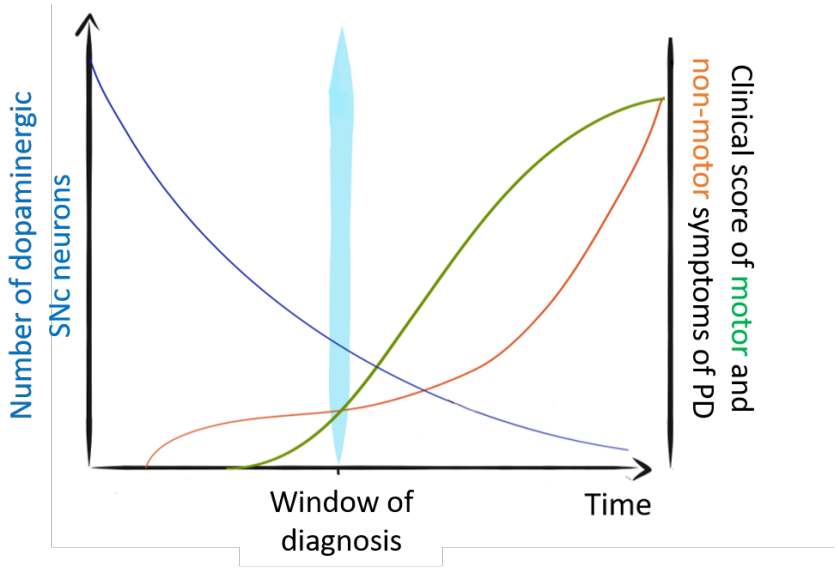

Figure 1.7: A diagram showing the clinical progression of PD over time, adapted from Lebouvier et al. (2010).

Arresting or slowing the development of PD at the earliest possible point (likely that of diagnosis) would reduce the evolution of PD symptomatology and help to preserve quality of life for PD patients. There are currently no neuroprotective therapies licensed to protect against further neurodegeneration, however a number of different avenues of potential neuroprotective treatments are being explored.

- Anti-inflammatory strategies

  Anti-inflammatory treatments in PD aim to break the detrimental cycle of cell death and neuroinflammation. Non-steroidal, anti-inflammatory (NSAID) drugs have been shown, *in vitro* and *in vivo*, to provide protection in models of PD (Aubin et al. 1998, Ferger et al. 1999, Carrasco & Werner 2002). Indeed, some studies found that regular users of ibuprofen, a widely used NSAID, had a lower incidence of PD than the general population (Chen et al. 2003, Gao et al. 2011), though this is not universally agreed upon (Becker et al. 2011).

  However, inflammation is not necessarily neurodegenerative. Some studies have found that

immune activation by administration of inflammatory compounds is able to drive expression of neurotrophic factors such as glial cell-derived neurotrophic factor (GDNF) (Iravani et al. 2012). Similarly, activation of astrocytes has been shown to rescue dopaminergic neurons *in vivo* from MPP^+-mediated neurotoxicity (Nam et al. 2015).

In *in vivo* experiments, neuroprotection often goes hand-in-hand with an anti-inflammatory effect (Chan et al. 2010, Betts et al. 2012, Sadeghian et al. 2016). Hiowever, in such studies it can be difficult to tell with certainty whether the inflammation results from the neurodegeneration or vice versa - and likewise whether an anti-inflammatory effect is responsible for the neuroprotection or vice versa. For the reasons described here, the link between immune activation and neuroprotection or neurodegeneration has proven complex and challenging to untangle, and will be further explored in Chapter 4.

- Antioxidants

  Evidence of high levels of ROS as a result of mitochondrial dysfunction are apparent in PD (Perry & Yong 1986, Sofic et al. 1992). The ROS, or oxygen free radicals, can interfere with normal cellular function and ultimately lead to neurodegeneration. Dietary intake of antioxidants such as vitamin E and β-carotene has been shown to decrease the risk of developing PD (Miyake et al. 2011).

  Treatment of those who already have PD with antioxidants aims to remove the oxygen free radicals before they can increase damage to intracellular molecules. This approach has shown some measure of promise in preclinical models (Oyagi et al. 2008, Jin et al. 2014), but has not yet shown to be effective in clinical trials (Beal et al. 2014).

- Neurotrophins

  Neurotrophic factors such as brain-derived neurotropic factor (BDNF) and GDNF have been shown to be reduced in the brains of PD patients (Mogi et al. 1999, Chauhan et al. 2001). Adding or stimulating production of growth factors in preclinical models of PD has been shown to be neuroprotective (Eslamboli et al. 2005, Boshoff et al. 2018). However, evidence from clinical trials using similar approaches has been mixed (Gill et al. 2003, Lang et al. 2006).

- Anti-α synuclein strategies

  α-synuclein is a hallmark of PD. Accumulated, misfolded α-synuclein has been shown to interfere with synaptic function and cause neuroinflammation. Approaches which have shown some promise in combatting α-synuclein accumulation in preclinical trials have included immunisation against α-synuclein (reviewed in Schneeberger et al. (2012)), boosting clearance of α-synuclein in the CNS (Roy et al. 2012) and reducing aggregation of misfolded α-synuclein (reviewed in (Török et al. 2016)).

- Glutamatergic strategies

  Amantadine is not the only glutamate receptor targeting drug to be considered for use in PD. Compounds targeting all of the major groups of glutamate receptors: AMPA, NMDA and all 3 groups of metabotropic glutamate receptor (mGluR) have been studied for their neuroprotective potential in preclinical models of PD. In particular, the location of mGluRs throughout the basal ganglia and their potential to reduce transmission across overactive synapses is of interest in the treatment of PD. The remaining section of this Introduction will cover the rationale behind this approach in full (Section 1.5 from p.59).

1.5 Glutamate in PD

As noted previously in this introduction, aberrant glutamatergic signalling is a major feature of the Parkinsonian and dyskinetic basal ganglia (Ambrosi et al. 2014, Picconi & Calabresi 2014). Initial efforts focussing on correcting these glutamatergic changes focussed on the ionotropic glutamate receptors (Graham et al. 1990).

1.5.1 Ionotropic glutamate receptors

Ionotropic glutamate receptors are a class of fast-conducting cation channels, comprised of AMPA, NMDA and kainate receptors, whose primary roles are to mediate excitatory potentials and synaptic plasticity. Given these physiological roles, the interest in these receptors as therapeutic targets for PD, where glutamatergic signalling is increased and aberrant synaptic plasticity occurs, is self-evident.

As kainate receptors are relatively poorly characterised compared to the other ionotropic glutamate receptors, with few compounds available that specifically and solely target them, the focus of this section will be on AMPA and NMDA receptors.

1.5.1.1 AMPA receptors

AMPA receptors are the first receptor to undergo changes during synaptic plasticity. Primarily located on the postsynaptic membrane, altered numbers, sensitivity (via subunit composition or phosphorylation) or location of AMPA receptors dictate the firing of the postsynaptic neuron at a glutamatergic synapse (reviewed in Huganir & Nicoll (2013)) and, therefore, the continued strength of the synaptic connection.

The structure of AMPA receptors is a homo- or hetero-tetramer, with 4 individual subunits known as GluA1 - 4. Each subunit has slightly different properties regarding kinetics, ion permeability and receptor trafficking and so the subunit composition ultimately describes the functional properties of the receptor. The majority of AMPA receptors contain the subunit GluA2 and have low calcium permeability or are calcium-impermeable. Nevertheless, an important minority of AMPA receptors without GluA2 are calcium-permeable and are important in aspects of synaptic function, plasticity and excitotoxicity.

In PD and PD models, evidence for AMPA receptors as a symptomatic or neuroprotective therapeutic target is poor. 2,3-dihydroxy-6-nitro-7-sulphamoyl-benzo(F)quinoxaline (NBQX), an AMPA receptor antagonist, has variously been found effective (Klockgether et al. 1991, Konitsiotis et al. 2000) and ineffective (Luquin et al. 1993) in alleviating the motor symptoms of PD in MPTP-treated marmosets. Additionally, Turski et al. (1991) found that NBQX was unable to provide neuroprotection in MPP^+ and 6-OHDA rat models of PD following local or systemic administration. In the ionotropic class of glutamate receptors, by far the most evidence points to NMDA receptors as being the more suitable therapeutic target.

1.5.1.2 NMDA receptors

Like AMPA receptors, NMDA receptors comprise a number of subunits whose properties dictate the properties of the completed receptor and ion channel. In the case of NMDA receptors, there are seven subunits, split into three subfamilies by sequency homology: GluN1, GluN2 (A, B, C and D) and GluN3 (A and B). The subunits are combined to form a complete, heterotetrameric NMDA receptor, with the majority of NMDA receptors being composed from GluN1 and GluN2 subtype subunits.

NMDA receptor channel opening depends upon the binding of both glutamate and glycine to the extracellular binding sites on GluN2 and GluN1 respectively. Even so, the cell must first be depolarised by the actions of other ion channels such as AMPA in order to dislodge the Mg^{2+} block from the channel of the NMDA receptor before cations can pass through the pore. Once the pore is open, the channel permits non-selective and volatge-dependent passage of Na^+, K^+ and Ca^{2+}.

In treating the symptoms of PD in preclinical models, antagonists of NMDA receptors have made sufficient impact to be progressed to clinical trials. These preclinical studies found antiparkinsonian potential of NMDA antagonists when injected into the GPi of MPTP-treated non-human primates (Graham et al. 1990) or reserpinised rats (Klockgether & Turski 1990), though this could not be replicated following systemic administration (Graham et al. 1990, Klockgether & Turski 1990). Similarly positive results were obtained in preclinical models when using subtype-specific compounds (Nash et al. 1999, Steece-Collier et al. 2000, Löschmann et al. 2004) though this was not reflected when an antagonist of GluN2 subunit-containing NMDA receptors was trialled in the clinic (Addy et al. 2009). Despite this, clinical trials for NMDA antagonists as symptomatic treatments in PD continue (Moreau et al. 2013).

Further evidence shows a number of different mechanisms for potential neuroprotection with NMDA receptor antagonists, spanning reduced excitotoxicity or neuroinflammation and promoted production of neurotrophic factors (Armentero et al. 2006, Wu et al. 2009, Ossola et al. 2011). Based on this evidence, NMDA antagonists have shown mixed promise as neuroprotective agents in preclinical PD studies. While some groups reported total protection in rat and mouse models (Turski et al. 1991, Kanthasamy et al. 1997), others reported no effect of antagonist treatment (Kupsch et al. 1992, Zuddas et al. 1992). This mixed evidence, and the potential of severe adverse effects on cognition and drowsiness, has so far restricted the further exploration of NMDA antagonists in clinical trials (Hallett & Standaert 2004). With this in mind, targeting mGluRs, which are capable of more subtle alterations to intracellular signalling pathways, is a natural next step.

1.5.2 Metabotropic glutamate receptors

mGluRs are a family of class C G-protein coupled receptors (GPCRs) which modulate both excitatory and inhibitory transmission through regulation of neuronal excitability and neurotransmitter release. Like all GPCRs, mGluRs are composed of 7 α-helical transmembrane domains. The orthosteric binding site is located on the extracellular N-terminus, while the α, β and γ G protein subunits bind intracellularly between the 3rd and 4th transmembrane domains (Gomeza et al. 1996). This binding causes a conformational change in the receptor structure which promotes the exchange of Gα-bound guanoside diphosphate for guanosine triphosphate. This causes the release of the intracellular Gα and β-γ subunits and the activation of their respective signalling cascades (mechanisms of nucleotide exchange, conformational change and G protein subunit release are reviewed in Oldham & Hamm (2008)).

The mGluRs discovered thus far comprise eight individual members, which may be split into three subgroups based on second messenger coupling, pharmacological profile and structural similarity. These subgroups are group 1 (mGluR1 and 5), group II (mGluR2 and 3) and group III (mGluR4, 6, 7 and 8). mGluRs naturally exist as homo- or heterodimers within and between subgroups (Doumazane et al. 2011). Some hints about the differing properties of dimer combinations have been reported (Kammermeier 2012) though, due to the lack of compounds targeting specific dimer combinations, the full implications of this discovery are yet to be realised.

GPCRs in general make popular drug targets due to the ease of targeting and potential for allosteric modulation. Allosteric modulators are compounds which bind to a site on a receptor other than the orthosteric site and modulate, rather than turn on or off, the receptor signalling pathway. mGluRs in particular have been examined for their therapeutic potential in a range of indications including schizophrenia, drug addiction and autism spectrum disorders (Nicoletti et al. 2015). As potential therapeutic targets for PD, mGluRs were first identified in the 1990s, when they were found to have a distribution throughout the basal ganglia and the potential to reduce activity of the indirect motor pathway (Testa et al. 1994, Rouse et al. 2000). Each subgroup will be discussed in turn in terms of receptor pharmacology and potential for therapeutic targeting.

1.5.2.1 Group I mGluRs

Group I mGluRs consist of mGluR1 and mGluR5. These receptors are located primarily postsynaptically (Shigemoto et al. 1997) and couple to Gαq - meaning that, upon activation, they ac-

tivate phospholipase C. Phospholipase C hydrolyses phosphatidylinositol-4,5-bisphosphate bound to the intracellular membrane, resulting in diacyl glycerol and inositol 1,4,5-trisphosphate. 1,4,5-trisphosphate mediates the release of Ca^{2+} from the intracellular store within the endoplasmic reticulum. The Ca^{2+} influx causes the release of the Mg^{2+} block from NMDA receptor channels, increasing neuronal excitability and also, along with diacyl glycerol, causes the activation of protein kinase C. Typically, the increase in intracellular Ca^{2+} and activation of protein kinase C may then promote a range of processes and functions through phosphorylation on serine or threonine residues (Kennelly & Krebs 1991).

Distribution of the group I mGluRs in brain regions associated with motor function is shown in Table 1.3 (p.65).

Due to the excitatory potential of group I mGluRs, the emphasis for antiparkinsonian potential has been on examining group I antagonists and negative allosteric modulators. In preclinical testing, compounds targeting mGluR5 showed greater potential in reducing the symptoms of PD than did those targeting mGluR1 (Ossowska et al. 2001, Breysse et al. 2002, Ambrosi et al. 2010). Many preclinical studies have also been conducted to establish the effect of group I mGluR antagonists on L-DOPA-induced abnormal involuntary movements (AIMs) in rodent models (Dekundy et al. 2006, Mela et al. 2007, Gravius et al. 2008, Rylander et al. 2009). Again, it was also established that mGluR5 antagonists were more effective at reducing dyskinesias than mGluR1 antagonists (Dekundy et al. 2006).

In addition to efficacy against the symptoms of PD, the neuroprotective potential of compounds targeting group I mGluRs has also been examined. MPEP and MTEP, mGluR5 antagonists, have shown the ability to reduce activity of the STN and microglia in PD models (Armentero et al. 2006, Hsieh et al. 2012). Further to this, these compounds have also shown the potential to provide neuroprotection in rodent (Battaglia et al. 2004, Aguirre et al. 2005, Vernon et al. 2005, Armentero et al. 2006) and non-human primate (Masilamoni et al. 2011) preclinical models of PD, though this finding was not universal (Ambrosi et al. 2010).

Based on this wealth of evidence in preclinical models, it is not surprising that mGluR5 has made the most headway into clinical trials, albeit primarily for LID, of any of the mGluR members:

- Dipraglurant is a negative allosteric modulator of mGluR5 developed by Addex Therapeutics and The Michael J. Fox Foundation. It has been shown to be safe and effective in the treatment of LID in phase II clinical trials (Tison et al. 2016).

- Mavoglurant, an allosteric antagonist developed by Novartis, reached phase II of clinical trials for LID. Further studies with Mavoglurant were discontinued due to lack of efficacy (and also increased adverse events compared to placebo).

It is generally considered that Mavoglurant failed due to the compound formulation and study designs rather than issues with mGluR5 as a target in LID (Rascol et al. 2014).

1.5.2.2 Group II mGluRs

Group II consists of mGluR2 and 3. These receptors are primarily located presynaptically (though have also been found postsynaptically) (Shigemoto et al. 1997) and couple to Gαi. When activated, the α subunit inhibits adenylyl cyclase, thus preventing the conversion of ATP to cAMP. This, in turn, reduces the activity of protein kinase A and the activity of ion channels requiring phosphorylation by this kinase. Additionally, the β-γ subunit can inhibit the activity of Ca^{2+} channels. In this way, the overall excitability of the cell is reduced. Alternatively, group II mGluR may also couple through Gαo (Kammermeier et al. 2003). In this instance, the β-γ subunit works to open inwardly-rectifying K^+ channels, thereby stabilising the resting potential of the cell and preventing increased excitability (Lei et al. 2000).

The group II mGluRs have been recorded as presynaptic autoreceptors at glutamatergic synapses (Xi et al. 2002) and also as heteroreceptors at other synapses, working to regulate release of neurotransmitter in the synaptic cleft (Salt & Eaton 1995, Lorrain et al. 2003). The distribution of these receptors within the motor areas of the CNS can be found in Table 1.3.

Preclinically, pan-group II agonists or postive allosteric modulators (PAMs) have shown promise in a number of models. When administered intracranially, Dawson et al. (2000) and Murray et al. (2002) found that group II agonists could reverse akinesia associated with the administration of reserpine. Murray et al. (2002) also found that systemic administration of the same compound could provide a neuroprotective effect in 6-OHDA lesioned animals. This finding was replicated by Vernon et al. (2005). Group II mGluR agonists have also been found to provide neuroprotection in a MPTP mouse model of PD (Battaglia et al. 2003). Knockout studies have suggested that mGluR3 is primarily responsible for this potential neuroprotective effect (Corti et al. 2007) and this has been confirmed in follow-up studies (Battaglia et al. 2009, Caraci et al. 2011). At the time of writing, however, no group II mGluR compounds have entered clinical trials for PD or related conditions.

Table 1.3: Distribution of mGluR in rodent CNS motor nuclei							
	Group I		Group II		Group III		
	mGlu1	mGlu5	mGlu2	mGlu3	mGlu4	mGlu7	mGlu8
Striatum	+	++	-	+	++	++	+
NAcc	+	+++	-	++	++	+++	++
GPe	+	+	-	+	+	+	+
EPN (GPi)	+	+	-	+	+	+	+
STN	+	+	+	+	+	+	+
SNc	++	+	-	+	+	+	+
SNr	+	+	-	+	+	+	+
Cortex	-	+	+	+	+	+++	++
VThal	+	+	-	+	+++	++	+
Cerebellum	++	-	+	+	+++	+	+
Astrocytes	?	✓	✓		✓	✓	✓
Microglia	?	✓	✓	✓	✓	*X*	✓

Table 1.3: mGluR expression in regions relevant to motor function according to Saugstad et al. (1997), Testa et al. (1994), Messenger et al. (2002). Astrocyte expression data were gathered from Vanzulli & Butt (2015), Lin et al. (2014), Geurts et al. (2005), Wroblewska et al. (1998). Microglia expression data were gathered from Byrnes et al. (2009), Taylor et al. (2002, 2003). NAcc, nucleus accumbens; GPe, external globus pallidus; EPN, entopeduncular nucleus; GPi, internal globus pallidus; STN, subthalamic nucleus; SNc, subtantia nigra pars compacta; SNr, substantia nigra pars reticulata; VThal, ventral thalamic nuclei. Graph legend: - indicates no expression beyond background staining and + to +++ indicates increasing strength of expression in brain regions. In glial cells, ✓indicates presence while *X* indicates absence.

1.5.2.3 Group III mGluRs

Group III contains metabotropic glutamate receptor 4 (mGluR4), 6 (which is expressed mainly in the retina), 7 and 8. These receptors are primarily located presynaptically (Shigemoto et al. 1997) and, like group II, couple to Gαi/o. The distribution of these receptors within the CNS can be found in Table 1.3.

As in group II mGluR research, subtype-selective group III mGluR compounds are fairly new and much of the preliminary research has been conducted with compounds acting on all members of group III. Using brain slice preparations or *in vivo* microdialysis, group III mGluR agonists like L-2-amino-4-phosphonobutyrate (L-AP4) and L-serine-O-phosphate (L-SOP) have been found to inhibit GABA release or inhibitory post-synaptic potentials evoked at the corticostriatal synapse (Pisani et al. 1997) and the striatopallidal synapse (Valenti et al. 2003, MacInnes & Duty 2008). Likewse, excitatory post-synaptic potentials or glutamate release have been shown to be reduced by the same compounds at the subthalamonigral synapses (Valenti et al. 2005, Austin et al. 2010, Broadstock et al. 2012, Lopez et al. 2012). As the group III mGluRs have been shown to be located presynaptically, these effects must arise from an mGluR-mediated reduction of exocytosis of neurotransmitter at the synapse. The effects on the range of synapses discussed above show that the group III mGluRs may act both as heteroreceptors and autoreceptors depending upon the location (Corti et al. 2002, Messenger et al. 2002).

In intact organisms, L-AP4 and L-SOP have been found to reduce akinesia in haloperidol and reserpine models (Valenti et al. 2003, MacInnes et al. 2004, Austin et al. 2010). Pan-group III agonists have also displayed neuroprotective efficacy in lesion models of PD. Austin et al. (2010) found that supranigral infusion of L-AP4 into 6-OHDA lesioned animals was able to provide both functional preservation and neuroprotection. The promising effects of pan-group III agonists have been shown to be most likely reliant on the modulation of mGluR4 activity. Initially, Valenti et al. (2003) showed that effects of L-AP4 on striatopallidal inhibitory post-synaptic potentials were absent in mGluR4 knockout mice. To investigate this effect further, studies were conducted using mGluR4-specific compounds as they became available. The results of these studies are detailed in the introduction to Chapters 3 and 4.

1.6 General hypotheses and aims for this thesis

Previous work in this lab has aimed to fulfil one of the key unment needs in the treatment of PD - a lack of neuroprotective therapeutics. Over time, these studies have shown a strong potential of group III mGluR, and particularly mGluR4, activating compounds to provide neuroprotection in preclinical models of PD (Austin et al. 2010, Betts et al. 2012, Broadstock et al. 2012). This work was primarily conducted through intracerebral administration of mGluR agonists and PAMs and so does not represent a therapeutic option which can directly translate to the clinic. With the development of systemically active mGluR compounds, more recent studies have explored the efficacy of systemically administered compounds. To date, systemically-administered compounds have been unable to provide neuroprotective benefit in models of late stage PD (Finlay 2014). In this thesis, the main focus remains on investigating the therapeutic potential of these systemically-administered compounds, though in an earlier stage model of PD.

1.6.1 Broad aims of this thesis

To fully characterise unilateral and bilateral partial 6-OHDA lesion rat models of PD for motor and non-motor symptoms of early stage Parkinson's.
Characterisation of motor symptoms of PD and degeneration of dopaminergic midbrain neurons in undertaken in a unilateral, partial lesion rat model in Chapter 2. A bilateral version of the partial lesion model characterised in Chapter 2 is explored for both motor and non-motor signs in Chapter 5.

Using the unilateral, partial lesion model of early PD, to explore the neuroprotective potential of systemically administered mGluR4 activating compounds and the potential underlying protective mechanisms.
The neuroprotective potential of a PAM and an agonist is examined in Chapter 3, and the potential underlying mechanisms of protection are explored in Chapter 4.

To briefly characterise the L-DOPA-sparing and antiparkinsonian efficacy of targeting mGluR4 in an MPTP marmoset model of PD and LID through a collaborative study with Dr Sarah Salvage (KCL).
This study is detailed in Chapter 3.

1.6.2 Hypotheses

Unilateral injection of 6-OHDA into the dorsal striatum will create a model of early stage PD with measurable asymmetrical motor deficits and nigrostriatal cell death as measured through simple behavioural tests and immunohistochemistry.

Implementing such an early-stage model bilaterally will demonstrate both motor and non-motor symptoms of PD which will be measurable with simple behavioural tests.

The use of an early stage model of PD through the formation of a terminal, partial rather than axonal, full lesion will provide an ideal platform to demonstrate neuroprotective efficacy of systemically administered compounds.

Activation of mGluR4 via systemically administered compounds will provide neuroprotection in a mild, partial lesion rat model of early stage Parkinson's.

Any neuroprotection provided by mGluR4 activating compounds in the aforementioned model will have some anti-inflammatory component.

Systemic administration of an mGluR4 agonist, alongside administration of L-DOPA, in an MPTP marmoset model of PD and LID will be L-DOPA-sparing and reduce the incidence of LID. In addition, mGluR4 agonism in the absence of L-DOPA will have antiparkinsonian efficacy in the same model without causing dyskinesia.

2 Development of a unilateral partial lesion rat model

2.1 Introduction

Amongst all of the models detailed in the introduction to this thesis, the 6-hydroxydopamine (6-OHDA) model was chosen to underpin the current project. This choice was made as a result of the good reproducibility, construct and predictive validity of the 6-OHDA models, in addition to the potential for tests of fine and gross motor skill and non-motor symptoms as discussed below.

Within the category of mammalian 6-OHDA models, there exist many variants which display a range of symptoms and so may be differentiated based on face validity. These may be categorised by the size of the lesion and location of injection. Lesions may be created through stereotaxic injection of 6-OHDA into the substantia nigra pars compacta (SNc) directly, the medial forebrain bundle (MFB) or the striatum. The choice of where to inject may be made based on which areas will be studied *ex vivo* with the aim of minimising mechanical damage in those areas. Alternatively, if potential therapeutic compounds are to be delivered through an intracranial cannula, it may be most efficient to deliver 6-OHDA in the same location in order to minimise the need for repetitive invasive surgery. Full lesions ($> 95\%$ nigral, dopaminergic cells lost) aim to replicate Parkinson's disease (PD) in its final stages, though the 6-OHDA full lesion models typically overshoot as nigral cell losses in severe PD in humans have been estimated at 66-84% (Pakkenberg et al. 1991, Damier et al. 1999) - to this end, partial lesions may be more representative of the human disorder.

Lesions created in the striatum are often smaller in size (known as partial lesions). This occurs because, following intrastriatal administration, 6-OHDA is uptaken by a subset of the dopaminergic nerve terminals located there to have the final effect of causing apoptosis in a corresponding subset of cells in the SNc (Przedborski et al. 1995). For this reason, it is easier to attain a range of lesion sizes from injections of varying concentrations of 6-OHDA when delivered intrastriatally than the limited range of lesions originating from injections into the SNc or MFB. Partial lesions can vary considerably in size and different studies have aimed for between 30-70% reduction in striatal tyrosine hydroxylase (TH) and TH-positive cells in the SNc (Przedborski et al. 1995, Sauer & Oertel 1994) and may exist in the dorsal or ventral, rostral or caudal striatum depending upon the site of injection. Partially lesioned animals may also have a motor phenotype (Tadaiesky et al. 2008), but it is likely to be more subtle than in a fully-lesioned animal and so typically-used motor tests may find no impairment.

Unilateral lesions are useful in that each animal provides its own, innate control: for each lesioned hemisphere there exists an intact SNc and striatum to provide a direct comparison for TH content or cell number and, for each paw with a motor deficit, there exists a paw undertaking the same motions but unaffected by Parkinsonism. The weakness of this model however, is that although Parkinson's is primarily an asymmetrical disease, both hemispheres are affected (Barrett et al. 2011, Wang, Yang, Sun, Vesek, Mosher, Vasavada, Chu, Kanekar, Shivkumar, Venkiteswaran & Subramanian 2015). Furthermore, left and right brain function are not analogous in all structures (Sullivan et al. 2009, 2014, Carriere et al. 2014) and so a left lesion may perform differently from a right lesion (Sullivan & Szechtman 1994, Marin et al. 2015). Bilateral lesions, on the other hand, provide no innate control, potentially necessitating larger n numbers to account for variability between animals. In addition, a different set of motor tests must be applied to bilaterally lesioned animals than are used for unilaterals, as tests of unilateral differences (e.g. cylinder test, stepping test and drug-induced rotations - all detailed below) tend to rely on motor asymmetry. This makes studies undertaken with bilaterally lesioned animals difficult to compare directly to unilateral lesion studies.

- Bilateral, full lesion - Bilateral full lesions cause very severe disabilities in animals which may require tube feeding to remedy the resulting aphagia and dehydration (Sakai & Gash 1994). As a result, the bilateral, full lesion 6-OHDA model is not very commonly used.

  Sakai & Gash (1994) show that overt motor deficits occur in animals with a bilateral lesion of $> 80\%$, and that these deficits manifest as significant decreases in vertical and horizontal activity in an open field arena. The symptoms of bilateral, full lesions may be relieved by L-3,4-dihydroxyphenylalanine (L-DOPA) treatment (Sakai & Gash 1994) although such animals also experience more severe abnormal involuntary movements (AIMs) than unilaterally lesioned animals following chronic exposure to L-DOPA (Marin et al. 2015).

- Unilateral, full lesion - Unilateral, full lesions are probably the most commonly used of the 6-OHDA models. Although unilateral, fully-lesioned animals may lose weight following surgery, they are usually capable of feeding themselves and so have a higher survival rate compared to bilateral, fully lesioned animals (Marin et al. 2015). Unilaterally, fully lesioned animals display quantifiable forelimb akinesia (Olsson et al. 1995, Schallert et al. 2000) and can be provoked to perform circling behaviours by administration of apomorphine, amphetamine or L-DOPA (Hudson et al. 1993). L-DOPA may also be used to induce AIMs in

unilaterally lesioned animals, which may be displayed to a greater extent in animals lesioned in the right hemisphere (Marin et al. 2015).

Full lesion models are more suited to the examination of symptomatic treatments and transplantation procedures than for neuroprotective treatments (Przedborski et al. 1995). Partial lesion models are more likely to provide useful models for characterisation of neuroprotective compounds, as they provide a model of earlier stages of PD - when a large percentage of vulnerable, dopaminergic neurons remain and such treatments would likely be provided.

- Bilateral, partial lesion - Bilateral partial lesions are increasingly being studied in respect to their ability to model both motor and non-motor aspects of PD (Tadaiesky et al. 2008, Silva et al. 2016). In the experience from this lab, bilaterally partially lesioned animals do not lose more weight following lesioning than unilaterally lesioned animals, making them a more robust and easy-to-use model than bilateral fully lesioned animals. This type of lesion will be described in further detail in Chapter 5 where it has been used to examine the non-motor symptoms of PD.

- Unilateral, partial lesion - Unilateral, partial 6-OHDA lesions may be the most suitable way to assess neuroprotective efficacy of a compound whilst still being able to use well-published tests of motor asymmetry such as those detailed in this chapter. With these animals, as with partial bilaterals, weight loss following lesioning is subtle and the animals recover quickly. They do not appear impaired in everyday tasks such as eating or drinking, but animals with differently sized partial lesions may still be differentiated using traditional motor tests (unpublished observation).

Variations on the 6-OHDA lesion model have previously been used to good effect by members of this group to explore effects and mechanisms of compounds affecting glutamate and gamma-aminobutyric acid (GABA) receptors in addition to other targets (Austin et al. 2010, Betts et al. 2012, Broadstock et al. 2012, Boshoff et al. 2018).

Given the need for a reliable but mild lesion effect, and the advantages gained by the ability to contrast lesioned and intact hemispheres, a unilateral partial lesion was chosen for the majority of the studies performed in this thesis. The partial lesion model was also hypothesised to provide a hospitable background against which to test systemically-administered neuroprotective thera-

peutics - in that degeneration would be less rapid and inflammation potentially less severe than in full lesion counterparts. In summary, the 6-OHDA unilateral, partial lesion model was chosen due to:

- Good predictive and face validity with fair construct validity (including neurodegeneration and neuroinflammation) despite the relatively rapid progression of neurodegeneration.
- Rapid surgical lesioning procedure which results in a lesion that is highly reliable within and between studies.
- Ability to produce a partial lesion which mimics the early stages of Parkinson's and produces a measurable motor phenotype.
- Previous experience with stereotaxic surgery within the group.

2.2 Aims and objectives

As discussed in the introduction to this thesis, many of the older animal models of Parkinson's disease are underpinned by either an acute, pharmacological effect which wears off over time, or a rapid and complete destruction of the nigrostriatal pathway. These states have low construct validity when compared with the slow and progressive deterioration seen in PD and, though they have been well utilised in examining potential symptomatic treatments, may therefore also prove to have low predictive validity in finding disease-modifying treatments.

The objective of this study was to find a reliable unilateral, partial 6-OHDA lesion in rats to model the early stages of Parkinson's. The model would ideally have approximately the same loss of TH-positive cells in the SNc as many patients display at the point of diagnosis (30-50% loss (Fearnley & Lees 1991)) in order to best mimic the disease at the point when treatments are likely to be initiated. The ideal model would also display some measurable and quantifiable motor deficit using easily-implemented and minimally invasive motor tests.

The starting point for the design of this model was taken from Przedborski et al. (1995), who began characterisation of a partial lesion model of varying sizes at the same location. Two different doses of 6-OHDA were compared in order to find the most appropriate dose for subsequent studies. The doses chosen were 8.75μg, taken directly from Przedborski et al. (1995), and 12μg as an intermediate dose between the 8.75 and 17.5μg doses characterised by Przedborski et al. (1995).

2.3 Materials and Methods

All procedures were performed in accordance with the U.K. Animals (Scientific Procedures) Act, 1986.

2.3.1 Implementation of lesion

26 male Sprague-Dawley (SD) rats (225-275g, Harlan, UK) were maintained on a 12 hour light-dark cycle in a temperature and humidity controlled room with *ad libitum* access to dry chow and tap water. Rats were given at least 7 days to acclimatise to the unit prior to lesioning. The conditions were randomised such that the experimenter was aware of which animals were in the same group, but not which group represented which condition.

Animals were subject to induction of anaesthesia using 5% isoflurane and the top of the head shaved and swabbed with 0.4% w/v chlorhexidine gluconate (dilution of Hibiscrub, Mölnlycke UK). Viscotears liquid gel (Alcon, Switzerland) was applied to the eyes to prevent drying or damage. Stereotaxic lesioning took place with the animals under inhaled isofluorane anaesthesia (2% maintenance, adjusted for individuals based on respiration). Once the animal was appropriately situated within the ear bars and maintenance nose cone, the skull surface was exposed. Lesions were made using 8.75μg 6-OHDA in 3.5μl 0.2% sodium ascorbate (n=8), 12μg 6-OHDA in 3μl 0.2% sodium ascorbate (n = 8) or 0.2% sodium ascorbate alone (sham condition, n=10), at AP +0.2mm, ML -3mm from bregma and -5.5mm from skull surface with the incisor bar set at -3.3mm (adapted from Przedborski et al. (1995) (Figure 2.1). The infusions took place at a speed of 1μl/minute and the needle was left in place for a further 3 minutes following infusion to prevent reflux of 6-OHDA. Following withdrawal of the needle, the incision was cleaned with sterile gauze swabs and sutured using coated Vicryl sutures with a 3-0 gauge needle (Ethicon Inc, USA). Animals were given 0.01mg/kg buprenorphine (Vetergesic, Ceva Health Care Ltd, France) via subcutaneous (s.c.) injection with 5ml/kg sterile saline for management of post-operative pain and rehydration, and housed in a heating cabinet at 25°C overnight. All animals were then weighed daily and rehydrated with subcutaneous saline as necessary until their pre-surgery weight was regained. Rats were allowed to recover for a minimum of 5 days prior to behavioural testing.

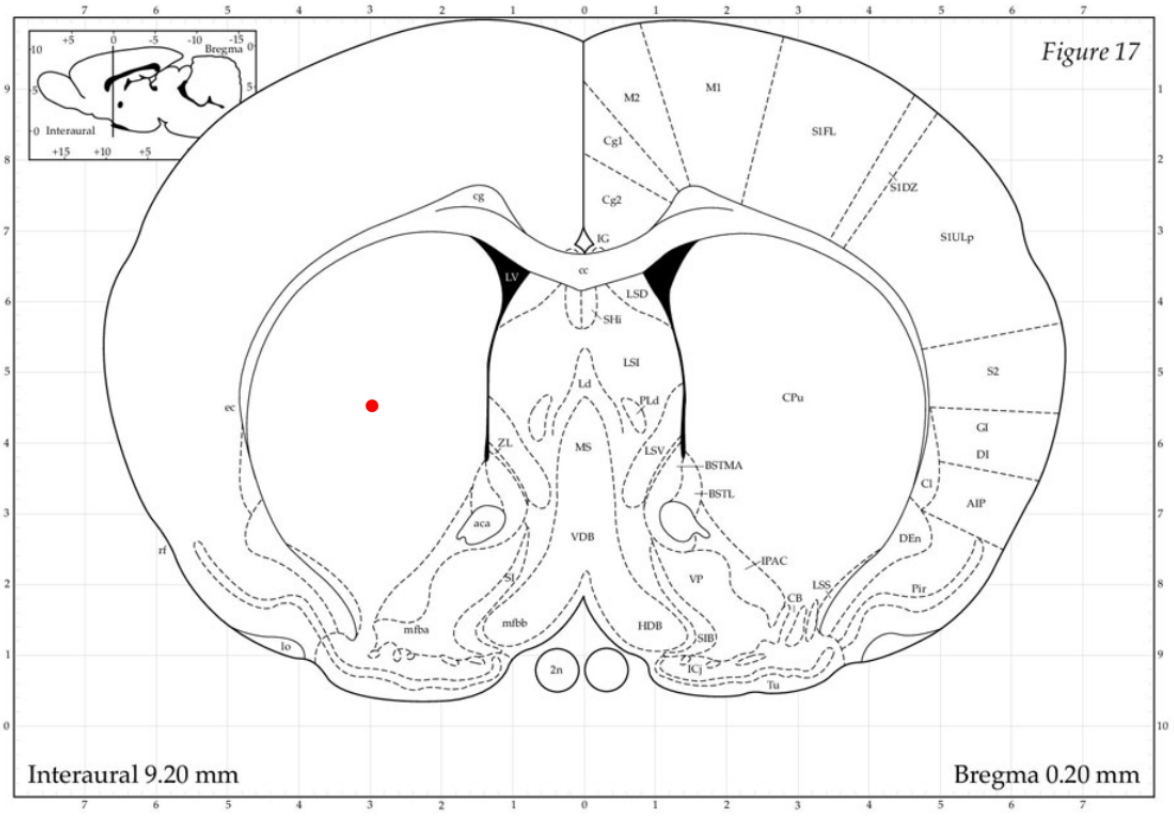

Figure 2.1: A diagram of the lesion site. This image depicts the brain as though the reader were face to face with the rat, with the lesion made in the rat's right striatum. Figure is adapted from Paxinos & Watson (1986).

2.3.2 Behavioural characterisation of lesion

Lesion development was tracked using behavioural tests which were carried out by an experimenter blinded to which group of animals had undergone which lesion condition. The schedule of behavioural tests for the partial lesion characterisation is shown in Figure 2.2.

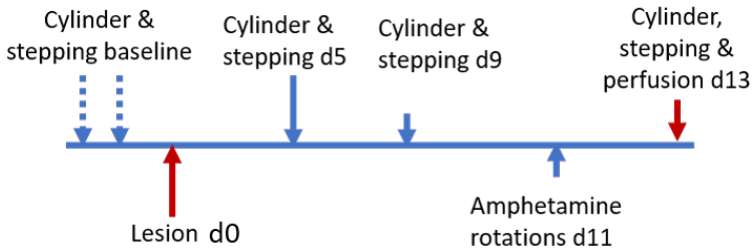

Figure 2.2: Timeline of surgical procedures and behavioural tests for characterisation of the partial lesion model.

2.3.2.1 Cylinder test

The cylinder test examines asymmetry in the use of the forepaws for exploration of a novel environment (Schallert et al. 2000). It has become a commonly used test of impairment or preservation in models which impose unilateral central nervous system (CNS) damage, such as stroke, spinal cord injury, or unilateral 6-OHDA. The animal will rely less on its impaired forepaw to bear weight during exploration and so the ratio of right and left forepaw weight-bearing touches to the side of the cylinder will alter when a unilateral CNS lesion is present. Previously in this lab, the cylinder test has been used with fully-lesioned (i.e. $\geq 90\%$ nigral cell loss) rats (Betts et al. 2012). Here, we characterise its utility in partially lesioned rats.

Rats were placed inside a clear perspex cylinder (21cm diameter, 34cm height) set up with a mirror placed at an approximate 85° angle behind to enable the scorer to see behaviours performed anywhere within the cylinder. The test was recorded using a JVC Everio camcorder mounted on a tripod, and videos were scored at a later date. The test lasted for a minimum of 5 and maximum of 10 minutes depending on the activity of the rats.

A weight-bearing touch was judged by the position of the paw on contact - the 'palm' must have contacted and the fingers spread for a touch to count as weight-bearing. Each touch with left (impaired, contralateral to, or on the opposite side to the lesion site) and right (unimpaired, ipsilateral to, or on the same side as the lesion site) paw or both paws together was counted and recorded. A single paw touch received a score of 1 corresponding to its side, and a touch with both paws simultaneously received a score of 0.5 to each side. Any rat which scored < 10 within the testing period was disqualified from the analysis.

2.3.2.2 Adjusted step test

The adjusted step test was first described by Olsson et al. (1995), and is designed to measure a proxy of postural instability in rats. The experimenter supported the animal by holding the hindquarters and one of the forepaws, and allowing the free forepaw to rest on a horizontal surface. The animal was then moved along the surface for 5 seconds over a 90cm distance, and the number of steps taken to adjust balance were counted. This test was repeated 3 times for each forepaw in both the 'forehand' and 'backhand' direction and the number of steps in each condition averaged across the 3 trials.

2.3.2.3 Amphetamine-induced rotations

Dopamine release at the nigrostriatal synapse leading to motor responses can be stimulated by peripheral injection of amphetamine. Where a nigrostriatal lesion is in place and there is cell loss in the SNc, dopamine release at the striatal synapse is reduced. This leads to an asymmetry of motor output between the lesioned and intact hemispheres and, consequently, the impaired and unimpaired limbs. Hefti et al. (1980) and Hudson et al. (1993) find that if the lesion is $> 50\%$, this dopamine asymmetry will lead to measurable ipsiversive turning behaviour as a direct result of the lesion.

In these studies, turning behaviour was measured automatically using a tethered rotometer system connected to RotoRat software (MedAssociates Inc.). Rats were tethered to the rotometer and their spontaneous circling behaviour was recorded for 30 minutes prior to injection with amphetamine in order to establish baseline activity. D-amphetamine sulfate (Tocris, Bio-Techne, UK) was administered peripherally (5mg/kg intraperitoneal (i.p.)) and the rats immediately replaced in the rotometers for a further 120 minutes. Circling behaviour was measured in 5 minute time bins and is expressed as net ipsiversive rotations (ipsiversive - contraversive) for each time bin or in total.

2.3.3 Histological characterisation of lesion

Rats were culled in order to examine the size of the lesion using histology at 2 weeks post-lesion. Rats were given an overdose (200mg via i.p. injection) of sodium pentobarbital (Euthatal. Merial Animal Health Ltd, UK) and, when no pedal reflex was seen, but before cessation of life, the chest cavity was exposed. The animal was then transcardially perfused via the left ventricle with phosphate-buffered saline (PBS) until blood was replaced, followed by 10% buffered formalin solution (Sigma Aldrich, Dorset, UK) until limbs and head resisted manipulation. The whole brain was then removed and placed into fresh 10% formalin for additional fixation on a rocker for $\geq$48 hours then stored, in formalin, at 2-5°C.

After fixation, brains were cut into sections between -6.3 to -3.14mm from bregma, containing the midbrain and SNc, and -3.14 to +2.52mm from bregma, containing the striatum (Paxinos & Watson 1986). These sections were then dehydrated and de-fatted using a TP1020 tissue processor (Leica). Tissue was progressed through 90% industrial methylated spirits (IMS) for 1×4h, 100% IMS for 3×4h, xylene for 3×4h and 60°C paraffin wax for 3×4h. The processed tissue was then

embedded into paraffin wax blocks for sagittal sectioning at 7μm on a microtome (RM2135 Leica, Germany). Three consecutive sections in every 8 were taken and mounted on glass SuperFrost Plus adhesion slides (Thermo Fisher Scientific, Massachusetts, US and VWR, Pennsylvania, US) with the use of a paraffin section flotation bath heated to 40°C (Electrothermal, Cole-Parmer UK) and allowed to dry at room temperature overnight.

Before the start of the staining procedure, air dried slides were incubated at 60°C for $\geq$ 30 minutes, then immediately transferred to xylene (2×5 min) followed by IMS (4×2 min) for total dewaxing. Dewaxed slides were then incubated for 10 minutes in 3% hydrogen peroxide solution and washed in cold tap water.

Antigen retrieval solution comprised 10mM citric acid solution, buffered to pH6.4 and preheated prior to use. Slides were then placed into preheated citric acid solution and heated under pressure for 7 minutes. The pressure cooker was removed from the microwave once the pressure normalised (according to the pressure valve position) and slides were washed in cold, running tap water until cool (approximately 5 minutes).

Following this, each section was incubated with blocking buffer (1% bovine serum albumin (BSA) in 0.1M tris-buffered saline (TBS) and 0.1% NaN3, pH 7.6) in a humidity chamber, then for 2 hours in primary anti-TH solution (Tyrosine hydroxylase rabbit polyclonal antibody, AB152 Merck Millipore, Canada) at a dilution of 1:750 in blocking buffer. Biotinylated goat anti-rabbit IgG antibody at 1:300 (Vector laboratories, USA) was then applied for 1 hour following a wash in TBS, then StreptABC/horseradish peroxidase (HRP) conjugate for 30 minutes, before developing in 0.05% 3,3'-diaminobenzidine (DAB) in TBS for ten minutes, or until well developed.

Slides were coverslipped using DPX (Sigma Aldrich, Dorset, UK) and left to dry overnight before cleaning off the excess. Each section was imaged at 10x using an Axioskop camera and Nikon microscope for nigral cell counts or a Canon DSLR camera with a macro lens for densitometry. Cell counts and densitometry image analysis were both conducted using ImageJ image processing software.

Densitometries were performed on images converted to 8-bit black and white following calibration to a standard calibration image file. For the purposes of densitometric analysis, a background reading was taken for each image in order to control for subtle differences in lighting conditions between slides. The background reading was taken in unstained areas of tissue, such as white mat-

ter tracts or cortex, that appeared in the same image. In order to fully characterise the size and position of the lesion within the striatum, each level (caudal, mid and rostral) was split into quadrants (represented DM, DL, VM, VM - Figure 2.8, p.89). Each level and quadrant underwent densitometry and the figures recorded separately, using three consecutive sections to represent each level. Similarly, in the SNc, TH-positive cell numbers were counted and recorded at caudal, mid and rostral levels using three consecutive sections to represent each level. Caudal, mid and rsotral levels of striatum were taken at -0.96 to -0.12mm, -0.12 to 0.96mm and 0.96 to 1.92mm from bregma respectively (Paxinos & Watson 1986). Caudal, mid and rostral levels of the SNc were taken at -6.12 to -5.52mm, -5.52 to -5.04mm and -5.04 to -4.56mm from bregma respectively (Paxinos & Watson 1986). Statistical tests were conducted using GraphPad Prism 7.

2.3.4 Statistical analysis

All data were tested for normality using the D'Agostino and Pearson omnibus normality test (or Shapiro-Wilk for groups with $n < 8$) prior to undergoing any tests for significant differences between groups.

Where 8.75μg and 12μg lesioned and sham groups were compared over time in behavioural tests, a repeated measures 2-way ANOVA was used, followed by Sidak's multiple comparisons test, Tukey's test (simple effects between lesion conditions) or Dunnett's test (where values were compared to a control value) if significance was seen in the ANOVA. Where the performance of lesioned animals was compared to their own baseline (as in the adjusted step test), a repeated measures 1-way ANOVA was used with a Dunnett's post-test if the initial ANOVA reached significance. Where values representing lesion conditions at a single time point were compared, as in the histological comparisons, a 1-way ANOVA was used with a Dunnett's post-test.

2.4 Results

This study compared animals with a lesion created using 8.75μg or 12μg 6-OHDA and sham-lesioned animals. One animal from the 8.75μg 6-OHDA group died during surgery, meaning that the final group sizes were $n = 10$ in the sham group, $n = 8$ in the 12μg 6-OHDA group and $n = 7$ in the 8.75μg 6-OHDA group.

2.4.1 Behavioural characterisation of lesioned animals

2.4.1.1 Cylinder test

The cylinder test was able to differentiate between 8.75μg or 12μg lesion groups and sham (Figure 2.3). There was a significant effect of lesion on the number of touches made with the contralateral paw ($p = 0.0068$), a significant effect of time ($p < 0.0001$) and also a significant interaction between variables ($p = 0.0168$) in the initial 2-way ANOVA. A Dunnett's multiple comparisons test revealed a significant reduction of contralateral paw uses between lesioned and sham groups at day 5 for both 8.75μg and 12μg 6-OHDA groups and at day 9 for the 12μg group.

In both lesion groups, there was a reduction of use of the contralateral paw by day 5 post lesion. In animals lesioned with 8.75μg 6-OHDA, paw use fell to 35.3%±3.5 of total but had recovered to 47.3% ± 4.1 by 9 days. In animals lesioned with 12μg 6-OHDA, paw use fell to 29.1% ± 3.0 of total touches by day 5 ($p < 0.001$) and remained relatively stable at this level. At days 5 and 9 post-surgery, sham animals did not show any deficit in the cylinder test, however there was some reduction in contralateral paw use by day 13 ($p < 0.05$ compared to baseline).

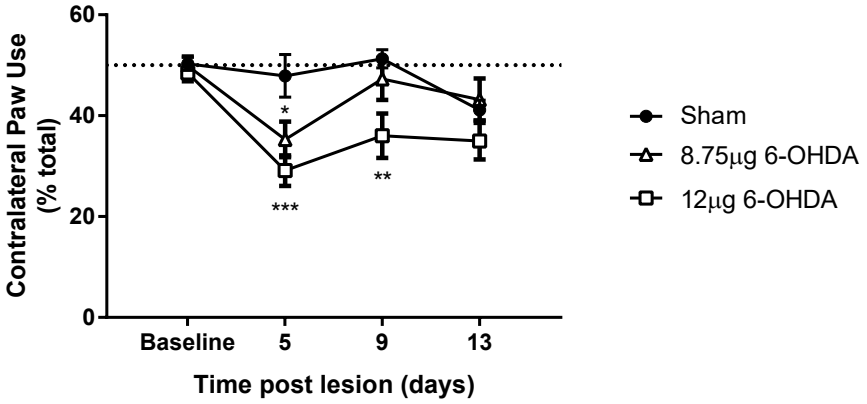

Figure 2.3: Measurement of weight-bearing, exploratory touches made with the contralateral paw by lesioned and sham animals in the cylinder test. * = $p < 0.05$, ** = $p < 0.01$, *** = $p < 0.001$ compared to sham at same time point. 2 way-ANOVA with Dunnett's post-test. Data are mean ± standard error of the mean (S.E.M.) and n=7-10 per group.

2.4.1.2 Adjusted step test

Sham animals were not tested in the adjusted step test as an oversight due to inexperience. Instead, the performance of animals in both lesion conditions following surgery is compared to their baseline performance.

In the 12μg 6-OHDA lesion animals, there was a significant effect of lesion on the contralateral forehand condition of the step test ($p = 0.0007$ in 1-way ANOVA with repeated measures). Dunnett's multiple comparisons test revealed a significant reduction in number of forehand contralateral steps compared to baseline at 5 days ($p < 0.01$) and 9 days post-lesion ($p < 0.01$). The 12μg group performed an average of 11 ± 0 steps at baseline which reduced to a minimum of 6 ± 1 by day 5. The 8.75μg group did not have a significantly impaired performance post-lesion compared to baseline. Animals lesioned with 8.75μg 6-OHDA performed an average of 11 ± 1 steps at baseline, which reduced to a minimum of 9 ± 0 by 13 days (Figure 2.4a).

In the contralateral backhand adjusted step test (Figure 2.4b), as in both conditions using the ipsilateral paw, 8.75μg and 12μg 6-OHDA-lesioned animals' performance did not fall below baseline (Figure 2.4c and 2.4d).

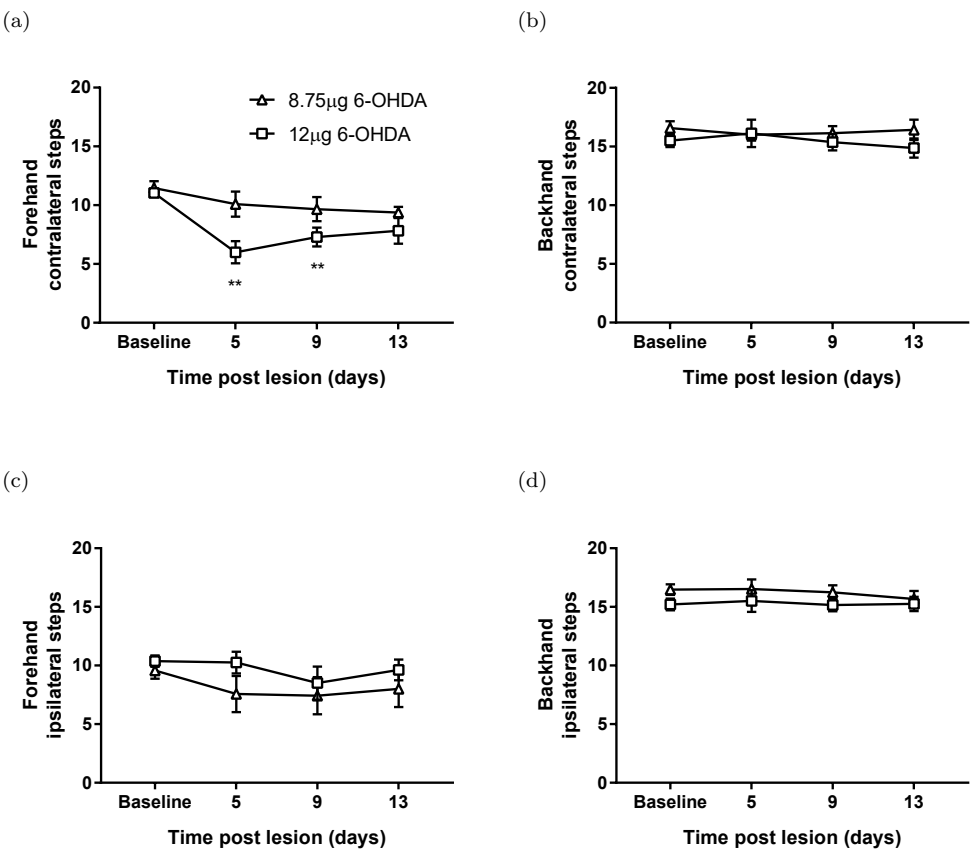

Figure 2.4: Number of adjusting steps taken in the step test in animals lesioned with either 8.75 or 12μg 6-OHDA. The number of steps taken are shown in four conditions: using the contralateral paw in the a) forehand and b) backhand directions, and using the ipsilateral paw in the c) forehand and d) backhand directions. ** = $p < 0.01$ in 12μg 6-OHDA compared with baseline. Repeated measures 1-way ANOVA with Dunnett's post-test. Data are mean ± S.E.M. and n=7-8 per group.

2.4.1.3 Amphetamine-induced rotations

When considering the data in Figure 2.5a, the amphetamine-induced rotation test was able to differentiate between 12μg and sham groups between 25 and 50 minutes after amphetamine administration (2-way ANOVA with Bonferroni post-test, Figure 2.5a). In addition, compared to their pre-amphetamine baseline, the 12μg 6-OHDA group also achieved significantly higher rotations between 20-50 and 65-80 minutes ($p < 0.05$ at each point, following $p < 0.0001$ for effect of lesion in 1-way repeated measures ANOVA with Dunnett's post-test). Conversely, the net number of ipsiversive rotations following amphetamine in the 8.75μg 6-OHDA group was not significantly different to their pre-amphetamine baseline or to the sham group ($p = 0.67$, 1-way repeated measures ANOVA).

In total, the 8.75μg performed an average of 85 ± 23 rotations in the 120 minute period following administration of amphetamine, while the 12μg performed 460 ± 203 rotations overall. Both lesion condition groups performed significantly more net ipsiversive rotations than sham animals overall. Sham rats performed an average of 6 ± 5 rotations in the 120 minute duration of the test (Figure 2.5b).

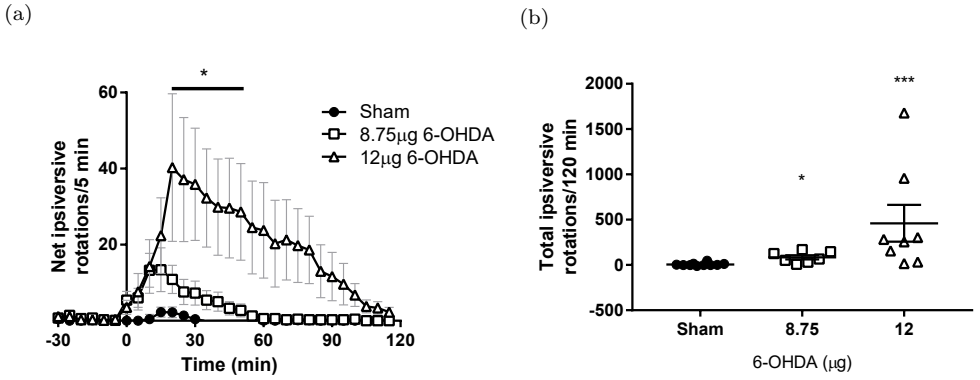

Figure 2.5: Net ipsiversive rotations produced in lesioned and sham rats following administration of 5mg/kg amphetamine. a) The number of net ipsiversive rotations produced per 5 minute time bin over 30 minutes pre- and 120 minutes post-amphetamine. * = $p < 0.05$ for 12μg over indicated time points against sham at the same times, 1-way ANOVA with Dunnett's post-test. b) Total net ipsiversive rotations produced over the 120 minutes post-amphetamine. * = $p < 0.05$, *** = $p < 0.001$ compared to sham. For all, data are mean ± S.E.M. and n = 7-10 per group.

2.4.2 Histological characterisation of lesion

Figure 2.6 shows representative images of TH-stained SNc from animals in different lesion groups. Some subtle loss of staining is evident in lesion groups when compared to the intensity of colour in the sham SNc. TH-stained fibres reamining in the lesioned SNc may disguise the cell loss in these images until cell counts are performed. The 40x previews at the bottom of the figure make this cell loss within the stained fibres more apparent.

When all levels of the SNc are averaged, there was significant cell loss in the 12μg, but not the 8.75μg, 6-OHDA-lesioned group compared to the sham group ($p < 0.001$ in a 1-way ANOVA with Dunnett's post-test, Figure 2.7a). When each caudal-rostral level was examined separately, there was significant TH positive cell loss compared to sham-lesioned tissue at caudal ($p < 0.01$), mid ($p < 0.001$) and rostral ($p < 0.05$) levels of the SNc in the 12μg lesion condition, but not in the 8.75μg 6-OHDA group (2-way ANOVA with Dunnett's post-test, Figure 2.7b).

When raw cell counts were examined (Figure 2.7c), there was no significant loss of TH-positive cells in either lesion group in the caudal SNc. In mid SNc, there was a significant reduction in TH-positive cells in the lesioned SNc of 12μg-lesioned animals, with 94 ± 8 cells per section of the intact, and 58 ± 7 in the lesioned SNc ($p < 0.05$ in 2-way ANOVA). At the rostral level, animals lesioned with 12μg 6-OHDA had a significant reduction from 86 ± 9 cells per section in the intact SNc to 59 ± 7 cells in the lesioned SNc ($p < 0.05$ in a 2-way ANOVA).

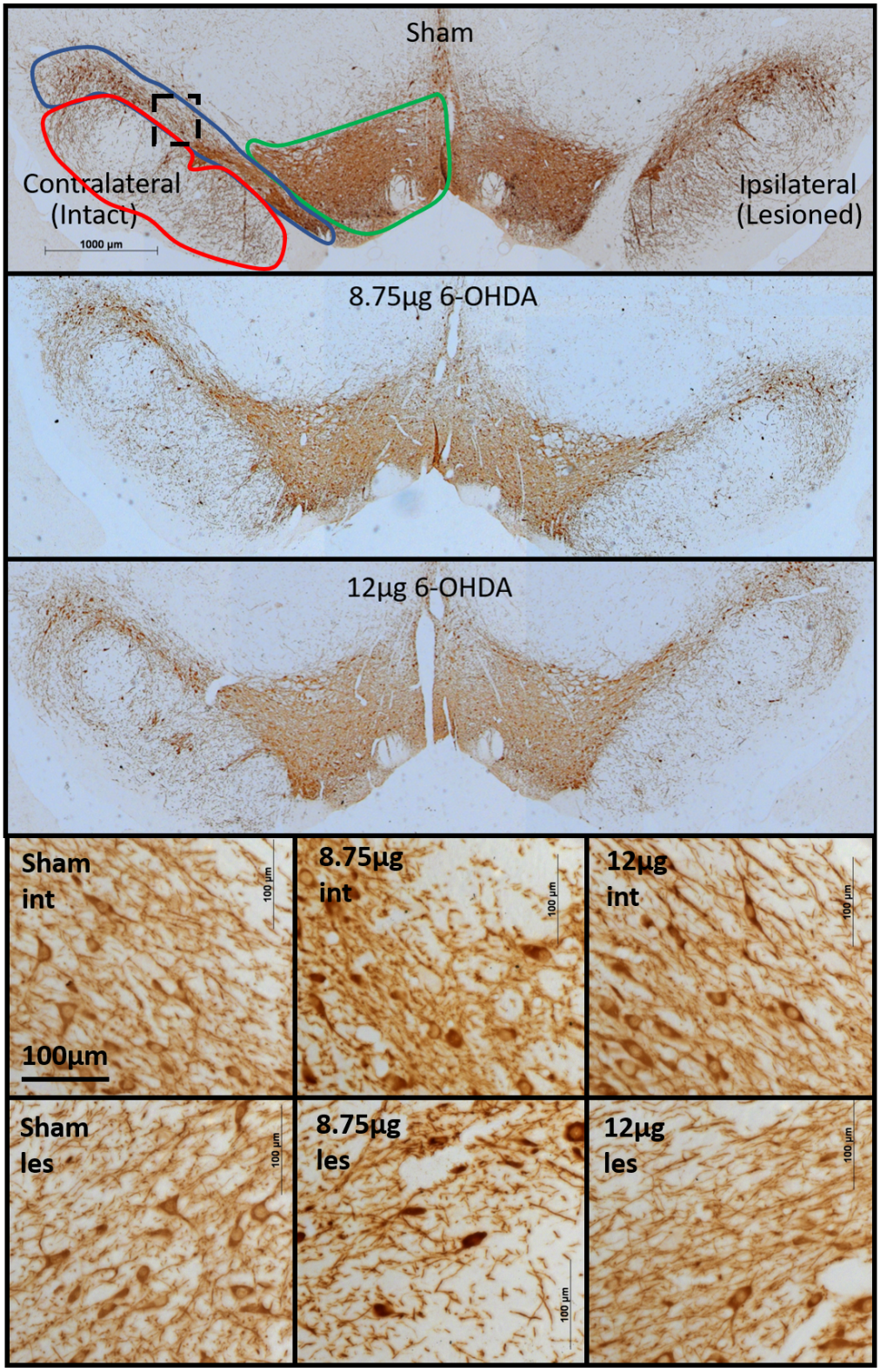

Figure 2.6: Representative images of TH-positive cells and fibres remaining in the nuclei of the ventral midbrain in lesioned and sham animals. In the intact hemisphere, the SNc is ringed in blue, the ventral tegmental area (VTA) in green and the substantia nigra pars reticulata (SNr) in red. The black box represents area expanded for 40x previews of cell loss at bottom of figure.

(a)

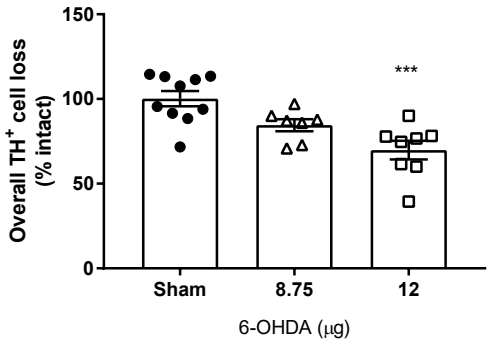

(b)

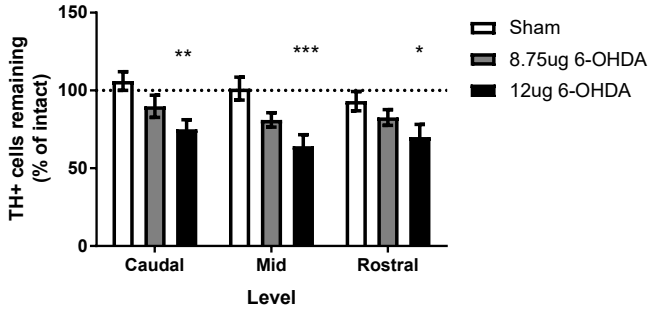

(c)

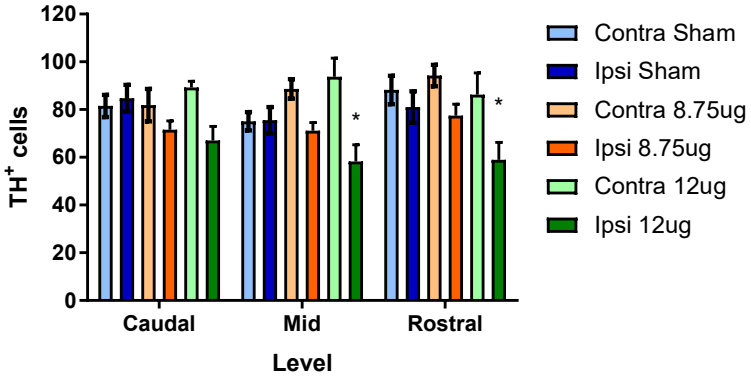

Figure 2.7: TH-positive cells remaining in the SNc in lesioned and sham animals. a) Cells in lesioned SNc section expressed as a percentage of intact SNc cell numbers averaged throughout the SNc. *** = $p < 0.05$ compared to sham values in a 1-way ANOVA with Dunnett's post-test. b) Average cells in the lesioned SNc as a percentage of intact SNc per section. * = $p < 0.05$, ** = $p < 0.01$, *** = $p < 0.001$ in 2-way ANOVA lesion groups compared to sham with Dunnett's post-test. c) Raw numbers of TH-positive cells remaining in each section of intact and lesioned SNc * = $p < 0.05$ compared to intact SNc in a 2-way ANOVA wiith Tukey's post-test. Data are mean ± S.E.M. and n=7-10 per group.

In the striatum, the representative images shown in Figure 2.8 depict TH-positive staining in fibres, with the 6-OHDA groups showing lesions that were primarily located dorsally-centrally within the structure. Quantification showed that there was also some mild but significant loss of ventral TH stain density in two locations following lesions with 12μg 6-OHDA (Figure 2.9b and 2.9d).

There was a significant reduction in TH in both groups when the overall average TH reduction was examined (mean average of all quadrants and all levels per animal), $p < 0.05$ for the 8.75μg lesion condition and $p < 0.001$ for 12μg lesions in 1-way ANOVA with Dunnett's post-test (Figure 2.9a).

Caudally, there was a significant effect of lesion group ($p < 0.0001$), a significant effect of quadrant ($p < 0.0001$) and a significant interaction between variables ($p = 0.0006$, Figure 2.9b. In the DM quadrant, where the loss of TH was most pronounced, 8.75μg 6-OHDA decreased TH stain to $70.1\% \pm 8$ of the intact striatum and 12μg reduced TH to $47.1\% \pm 6$ of the intact striatum.

In mid striatum, there was a significant effect of lesion group ($p < 0.0001$), a significant effect of quadrant ($p < 0.0001$) and a significant interaction between variables ($p = 0.0004$). In the DL quadrant, where the loss of TH was most pronounced, 8.75μg 6-OHDA decreased TH stain to $81.2\% \pm 8$ of the intact striatum and 12μg decreased TH to $44.9\% \pm 7$ of the intact striatum (Figure 2.9c).

In rostral striatum, there was a significant effect of lesion group ($p < 0.0001$), a significant effect of quadrant ($p < 0.0001$) and a significant interaction between variables ($p = 0.0014$). In the DL quadrant, where the loss of TH was most pronounced, 8.75μg 6-OHDA decreased TH stain to $79.3\% \pm 9$ of the intact striatum and 12μg decreased TH by $46.5\% \pm 10$ of intact (Figure 2.9d).

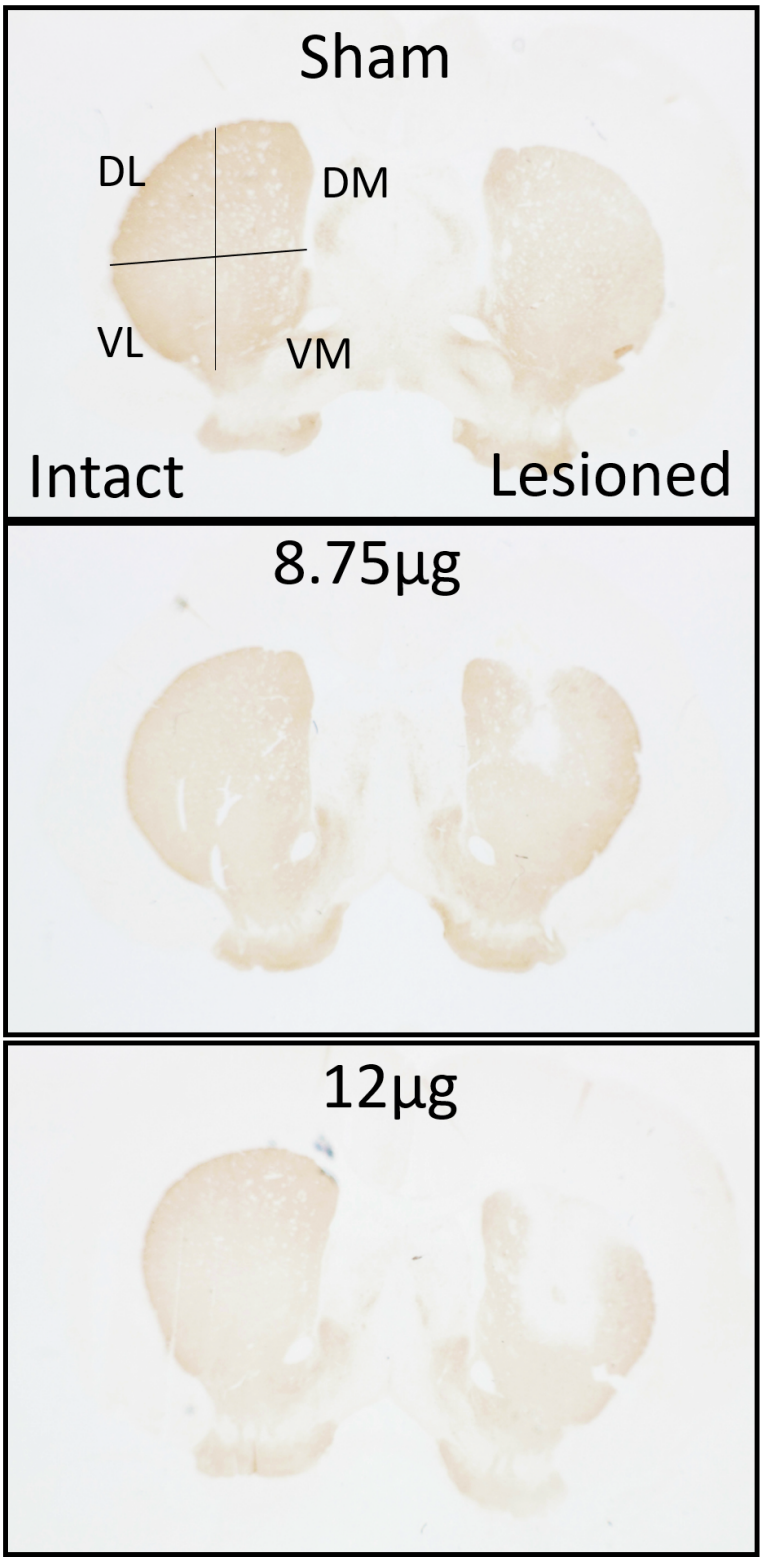

Figure 2.8: Representative images of striatal TH-staining. DM dorsomedial striatum, DL dorsolateral striatum, VM ventromedial striatum, VL ventrolateral striatum.

(a)

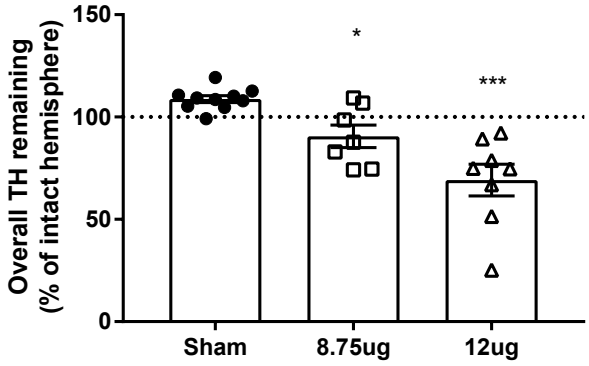

(b)

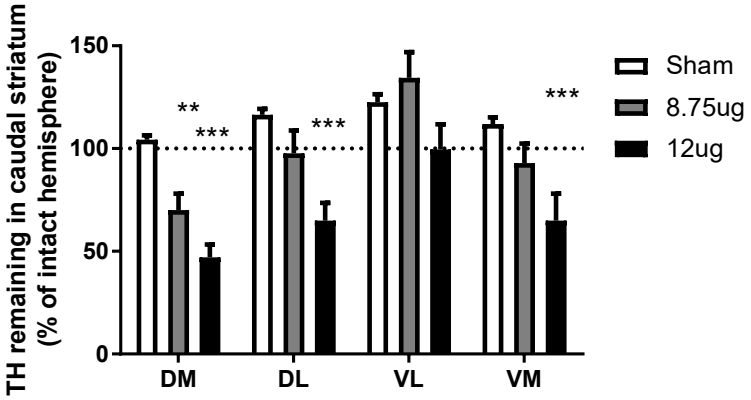

(c)

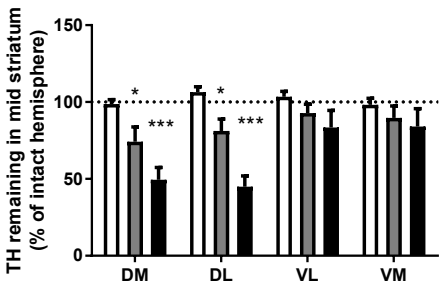

(d)

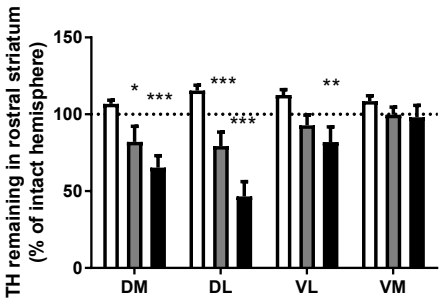

Figure 2.9: Densitometry of TH stain throughout the striatum of lesioned and sham animals. a) TH density averaged throughout all levels and quadrants of the striatum in lesioned and sham animals. * = $p < 0.05$, *** = $p < 0.001$ compared to sham. 1-way ANOVA with Dunnett's post-test. Figures b - d represent % TH remaining in caudal, mid and rostral striatum respectively. * = $p < 0.05$, ** = $p < 0.01$, *** = $p < 0.001$ compared to sham. 2-way ANOVA with Dunnett's post-test. For all, data are mean ± S.E.M. and n=7-10 per group. DM dorsomedial striatum, DL dorsolateral striatum, VM ventromedial striatum, VL ventrolateral striatum.

2.5 Discussion

This study sought to characterise a partial lesion model of Parkinson's in rats which mimics the early stages of PD and could be adopted for neuroprotection studies (detailed in Chapter 3). This model would therefore ideally display measurable but modest degeneration of dopaminergic neurons in the SNc and terminals in the striatum (between 30-50% in each region), accompanied by a quantifiable motor deficit.

The two different concentrations of intrastriatal 6-OHDA were chosen on the basis of studies in the literature. The lesion created by 8.75μg 6-OHDA was characterised by Przedborski et al. (1995) to produce a partial lesion of around 65% in the SNc. In other studies, Kirik et al. (1998), Roedter et al. (2001), Hernandez-Baltazar et al. (2013) concentrations of 20μg 6-OHDA injected intrastriatally were variously found to cause partial and full lesions in a range of protocols including single and multi-site injections. The 12μg 6-OHDA single-site injection was therefore intended as a midpoint between the 8.75μg and 17.5μg doses.

The motor deficit of lesioned animals was examined over the 2 weeks following administration of 6-OHDA. The motor phenotype of the model proved to be subtle using the tests normally applied to fully, unilaterally lesioned animals. This mirrors well what is seen at the point of diagnosis in PD, when motor symptoms have started to emerge but are not yet severe. Histological observation of cell loss in the SNc and terminal loss in the striatum shows that the model gives a reliable, partial lesion at the time point of 13 days post-lesion, used in previous neuroprotection studies by this lab (Betts et al. 2012).

2.5.1 Histological confirmation of lesion

In this initial characterisation of the lesion there was a significant loss of TH-positive cells only in the 12μg 6-OHDA lesion condition. In real terms, this was a loss of 30% of the cells in the lesioned hemisphere SNc compared to the unlesioned SNc, and was fairly consistent along the rostral-caudal plane. It is generally accepted that, at the onset of motor symptoms in PD patients, approximately 30-50% of the SNc dopaminergic neurons have been lost (Fearnley & Lees 1991, Kordower et al. 2013, Noyce et al. 2016). The cell loss in this lesion lies at the low end of estimates for diagnosis-stage PD, and this is perhaps in keeping with the subtle motor deficit observed in the lesioned animals.

In the striatum, although areas of significant terminal loss were present in the 8.75μg lesion model, the 12μg model proved to have a much more consistent lesion which was reliably present in the dorsal, mid and lateral striatum along the whole rostral-caudal axis, with some ventral presence. When the striatum was taken as a whole, the lesion caused with 12μg of 6-OHDA was a reduction of 30.9% of the TH density compared to the intact striatum. This compares favourably to a whole-striatum reduction in binding of a dopamine active transporter (DAT) ligand (an alternative measure of dopamine system dysfunction and degeneration) of 35% in patients at Hoehn and Yahr Stage 1 ("Unilateral involvement only usually with minimal or no functional disability" - Hoehn & Yahr (1967)) (Brücke et al. 1997). The figure of a 30.9% reduction in striatal TH seen here is also similar to the loss of TH density in the striatum from 1-3 years after diagnosis (Kordower et al. 2013, Fearnley & Lees 1991). In addition, Kordower et al. (2013) find that the dorsal striatum is most affected throughout PD and the ventral striatum left intact for longer - this information validates both the use of a lesion of this size and also a lesion in this location.

Given that the aim of the present study was to find a model suitable for preclinical, neuroprotection studies, which require both reliable neurodegeneration and a measurable phenotype, the 8.75μg 6-OHDA study was deemed unsuitable. It will, however, be discussed below for completeness.

2.5.2 Behavioural characterisation of lesioned animals

2.5.2.1 Cylinder test

The cylinder test showed that animals in the 12μg 6-OHDA lesion group showed a significant deficit in contralateral paw use by day 5 post-lesion, which remained fairly stable over the course of the experiment. Animals in the 8.75μg 6-OHDA group shared the initial motor deficit at day 5 but seemed to 'rebound' and, by day 9, showed considerable recovery of function. That the sham group also show a contralateral paw deficit by day 13 cannot be ignored. The sham group behavioural tests were conducted prior to the lesion group tests and, in examining these data thoroughly, it seems evident that factors other than the lesion may have been a strong influence on performance in the cylinder test. Noise from nearby building work and lack of experience in conducting behavioural tests are the best candidates to explain the unexpected performance of the sham animals.

Although sham animals' decline in participation over the course of the study was evident during analysis, lesioned animals also appeared less motivated to participate in repeated tests than base-

line ones. This raises the possibility that the animals become bored with the test when repeatedly exposed to it. The primary source of motivation for animals to participate in the cylinder test is exploration of a novel environment - and so the measurements obtained arise purely from spontaneous behaviour rather than externally motivated behaviours (such as fear of some aspect of the test as in the forced swim test and learned avoidance tests, or reward as in operant conditioning paradigms) (Hånell & Marklund 2014). It follows that frequent exposure to a test which relies on novelty may reduce motivation, and therefore participation. Although it is not anticipated that a reduced number of touches due to boredom would alter the asymmetry of the animals' exploration, it is certainly true that the more behaviours that are available to measure, the more accurate the average will be. For this reason, in later studies, methods were employed to keep animals engaged in the cylinder test upon re-exposure. These methods included turning off lights for a short period of time and making noises in order to provoke further exploratory behaviour.

That the motor deficit observed in the cylinder test is at its most profound on day 5 and lessens at subsequent time points is also an item of interest in the present study. A spontaneous recovery of motor function following 6-OHDA lesion has been observed by other groups characterising similar unilateral, partial (terminal) lesion models in both mice (Alvarez-Fischer et al. 2008) and rats (Monville et al. 2006), and using variations on a rotorod protocol to characterise motor deficits. Luthman et al. (1987) find that, following 6-OHDA lesioning in newborn rats, significant serotonergic compensation takes place. If this same compensatory mechanisms exist into adulthood, this may provide an explanation of motor recovery following lesioning as serotonin has been shown to play a role in motor function (Brocco et al. 2002, Mizoguchi et al. 2002).

It is, perhaps, a leap to assume that the CNS of adult rats is capable of the same plasticity as that of a newborn. The mechanisms which mask the effects of SNc cell loss in PD prior to the point of diagnosis may provide alternative clues to the source of functional recovery following a partial lesion. Bezard et al. (2003) highlight the possibility of D_2 receptor up-regulation or alterations in subthalamic nucleus (STN) or internal globus pallidus (GPi) electrical activity as compensatory changes following nigral cell loss in early PD, and these have also been observed in animal models of PD (Hollerman & Grace 1992, Choi et al. 2012, Lintas et al. 2012) but would not be evident through TH or DAT immunohistochemistry.

Overall, in terms of reflecting the progression of TH loss in the striatum and SNc, the cylinder test seems appropriate - demonstrating measurable deficits with the 30% striatal TH loss seen in 12μg lesioned animals which is differentiable from the lesser deficit seen in the 8.75μg lesioned

animals with 10% striatal TH loss.

2.5.2.2 Adjusted step test

Sham animals were not tested in the adjusted step test during this study. This was an oversight due to inexperience. The addition of sham data to this test would have enabled a stronger interpretation of the effects of lesion by improving the understanding of the potential effects of test repetition boredom on this test. Nevertheless, post-lesion comparisons to the pre-lesion baseline of each group still allowed interpretation of these data.

As in the cylinder test, the adjusted step test was able to differentiate animals with different sizes of lesion (12μg 6-OHDA-lesioned animals from 8.75μg lesioned animals) until day 13 post-lesion. At this point, the gradual decline in performance of 8.75μg animals came level with the sharper, but more stable, decline in performance of the 12μg animals. The contralateral forehand direction of the stepping test proved to be the only condition in which lesioned animals (in the 12μg 6-OHDA group) performed significantly fewer steps at any time point than at baseline, and provides another indicator of the subtlety of the early-stage model motor phenotype. In the present study, there was no decline in backhand contralateral steps following the lesion in either lesion group. Whether or why the number of backhand steps with the contralateral paw is a less sensitive measure of a lesion than forehand steps with the same paw is not widely discussed in the literature. The minimised lesion effect on backhand contralateral stepping has been observed in one study (Roedter et al. 2001) and not in others (Olsson et al. 1995, Betts et al. 2012) and may due to the size or positioning of the lesion.

The lack of a reduction in the number of steps produced over time by either group in the ipsilateral paw conditions suggests that animals did not have reduced participation in this test over time as in the cylinder test. This ties in with the hypothesis that the reduction in participation in the cylinder test resulted from a reduced interest in exploring a decreasingly novel environment. By comparison, in the stepping test, a considerable proportion of the motivation is external (provided by the experimenter in manoeuvering the animal) while the motivation of the animal is in taking adjusting steps in order to provide postural stability for itself.

2.5.2.3 Amphetamine-induced rotations

While a subtle amphetamine-induced rotation phenotype was seen in animals lesioned with 8.75μg 6-OHDA, a much more robust rotational response was seen in 12μg animals, which was significantly larger than that seen in sham animals.

A few studies have correlated the number of rotations produced by a given dose of amphetamine with the loss of TH in either the striatum and SNc, including Hefti et al. (1980), Hudson et al. (1993) and Olds et al. (2006). Hudson et al. (1993) estimate that a striatal lesion size of 60-80% or a nigral lesion size of 50% are necessary for the reliable production of rotations with 5mg/kg d-amphetamine. Olds et al. (2006) predicts more reliable rotational behaviour with a smaller lesion of 30% striatal TH loss or 60% nigral cell loss producing approximately 250 rotations in 60 minutes following amphetamine. One reason for this inconsistency is likely that Olds et al. (2006) and Hudson et al. (1993) do not consider the dorsal-ventral placement of their lesion within the striatum. Olds et al. (2006) also find that 'very low rotators' (animals producing few ipsiversive rotations following administration of amphetamine) have great TH cell loss in the lateral SNc but little in the central SNc, while 'high rotators' have a uniform loss. This suggests the possibility that medial-lateral placement of the lesion within the SNc may affect rotations in addition to the dorsal-lateral placement in the striatum.

Broadly speaking, the dorsal striatum is strongly involved in sensorimotor co-ordination and the ventral striatum in motivation and reward (Robbins & Everitt 1992). A 30% lesion which is entirely in the ventral striatum results in few amphetamine-induced rotations compared to a similarly sized lesion which is entirely dorsal (Joyce et al. 1981). Given this, it seems very possible that a smaller, dorsal lesion as used in the present study can result in an ampetamine-rotation phenotype stronger than that caused by a larger, central or ventral lesion. As the Olds et al. (2006) study injects into the SNc and the Hudson et al. (1993) into the medial forebrain bundle, it is likely that the resulting lesions in the striatum are not specifically dorsally located.

As to the medial-lateral placement of the lesion - in the present study, the SNc was not subdivided into medial and lateral sections and so the lesion placement within the SNc is difficult to judge. Deniau et al. (1996) suggests that cell bodies in the lateral SNc project preferentially to the lateral striatum. Here, the striatum was subdivided into layers and quadrants, with no remarkable differences between cell loss in the lateral and medial quadrants in either the ventral or dorsal sections. If these areas do indeed map faithfully onto the respective regions of the SNc then it

follows that cell loss within the medial-lateral axis of the SNc was uniform in the current study. By the findings of Olds et al. (2006), this would suggest that the rats in this dose finding study might be 'high rotators' - producing high numbers of ipsilateral rotations despite their modest cell and terminal loss.

2.6 Summary and conclusions

Given the appropriate location and size of the nigrostriatal lesion caused by intrastriatal injection of 6-OHDA detailed in this study, and the emergence of a measurable motor phenotype, the 12μg 6-OHDA striatal infusion seems a plausible model of early stage Parkinson's. These qualities show that the model has face validity and, as discussed in the introduction to this chapter in relation to the spectrum of 6-OHDA models, this model also has a degree of underlying construct and predictive validity whilst still being easy to implement.

In summary, a unilateral, partial lesion model was created in rats which showed reliable nigral cell death and striatal terminal loss. This lesion was accompanied by subtle, but measurable, motor symptoms which may be quantified through asymmetry in the cylinder and adjusted stepping tests or amphetamine-induced rotations. This model is therefore suitable for use in assays to assess the neuroprotective efficacy of agents when delivered at the early stages of PD.

3 Targeting mGluR4 as a potential therapeutic approach in animal models of PD and LID

3.1 Introduction

As discussed in the general introduction, agonists of group III metabotropic glutamate receptors (mGluRs) have been shown to have good efficacy in providing neuroprotection in animal models of Parkinson's disease (PD). Further to this discovery, a convincing narrative for the use of metabotropic glutamate receptor 4 (mGluR4)-specific activating compounds as a neuroprotective treatment for PD has developed.

3.1.1 Neuroprotective potential of targeting mGluR4

Betts et al. (2012) showed that (+/-)-cis-2-(3,5-dichlorphenylcarbamoyl)cyclohexanecarboxylic-acid (VU0155041), an 'agoPAM' (allosteric agonist and positive allosteric modulator) (Niswender et al. 2008), when infused above the substantia nigra pars compacta (SNc) in 6-hydroxydopamine (6-OHDA)-lesioned animals, was capable of providing neuroprotection. This was measurable in terms of motor preservation in behavioural tests and also counts of tyrosine hydroxylase (TH)-positive cells in the SNc. However, this neuroprotective effect was not replicated when VU0155041 was substituted with a systemically available mGluR4 positive allosteric modulator (PAM) ((1S, 2R)-N1-(3,4-dichlorophenyl)-cyclohexane-1,2-dicarboxamide (Lu AF21934)), delivered orally (Finlay 2014).

On the other hand, Battaglia et al. (2006) found that systemic injection of N-phenyl-7-(hydroxyimino)cyclopropa[b]chromen-1a-carboxamide (PHCCC), another mGluR4 PAM, prior to administration of 1-methyl-4-phenyl-1,2,3,6-tetrahydropyridine (MPTP) reduced the resulting cell loss in wild-type mice and not in mGluR4 knockout animals. Although this lends further support to the notion that mGluR4 activation may result in neuroprotection, it appears to be at odds with the finding by Finlay (2014) that a systemically delivered mGluR4 PAM does not provide neuroprotection in models of PD. These two studies differed in a number of important aspects, however, and these may provide the key to understanding the alternative outcomes. These studies used different mGluR4 PAM compounds, methods of delivery, dosing regimens and, perhaps most importantly, animal models. The study by Battaglia et al. (2006) utilised an MPTP-treated marmoset model with a partial lesion while the Finlay (2014) study utilised a rat 6-OHDA full

lesion model. It seems likely that this difference in lesion severity was a large contributor to the success of the PAM in the hands of Battaglia et al. (2006) and not in Finlay (2014).

Rodriguez et al. (1998) hypothesised that cell loss in the SNc leads to aberrant activity in the basal ganglia. This pathological change in signalling causes disinhibition of the subthalamic nucleus (STN) which in turn causes excitotoxicity in the SNc, and perhaps also the external globus pallidus (GPe) and substantia nigra pars reticulata (SNr) - leading to a viscious cycle of degeneration.

As discussed in the general introduction, when activated, mGluR4 reduces the amount of neurotransmitter released into the synaptic cleft. Acting at each of the synapses discussed above, whether gamma-aminobutyric acid (GABA)-ergic or glutamatergic, mGluR4 agonists and PAMs normalise activity of the local synapse and ultimately the basal ganglia as a whole. This action may then serve to reduce the excitotoxic (cell death mediated by excessive glutamate causing widespread calcium release and apoptosis) exposure of the SNc cells from the overactive, glutamatergic STN and thereby cause neuroprotection (Rodriguez et al. 1998).

However, not all sources agree that STN-mediated excitotoxicity is a leading cause of neurodegeneration either in PD or in PD models (Hilker et al. 2005, Luquin et al. 2006, Finlay 2014) and alternative putative hypotheses for the neuroprotective efficacy of group III mGluR agonists and PAMs also exist. One such leading hypothesis is that the activation of mGluRs on glial cells can lead to a reduction of neuroinflammation - this will be discussed further in Chapter 4. It has also been hypothesised that the neuroprotective and symptomatic effects of mGluR4 compounds may arise from their actions to normalise pathological activity at various synapses throughout the basal ganglia.

3.1.2 Normalisation of basal ganglia activity

In PD and PD models such as the 6-OHDA-lesioned rodent, various studies have shown that the indirect motor pathway becomes hyperactive due to the lack of dopamine input into the striatum and subsequently reduced activation of the D_1 and D_2 receptors (Albin et al. 1989, Kravitz et al. 2010) (Figure 3.1). Both symptomatic treatments, like L-3,4-dihydroxyphenylalanine (L-DOPA), and potential neuroprotective treatments, such as mGluR4 agonists, aim to normalise activity within the basal ganglia. While symptomatic treatments modify synaptic activity in the basal ganglia acutely, the aim of neuroprotective treatment might be to normalise the activity on a

longer term basis.

mGluR4 activation has been reported to modify activity at various synapses which become overactive in PD and PD models, each discussed in turn below. In some cases, such normalisation of activity through mGluR4 activation following the induction of a lesion has led to neuroprotection.

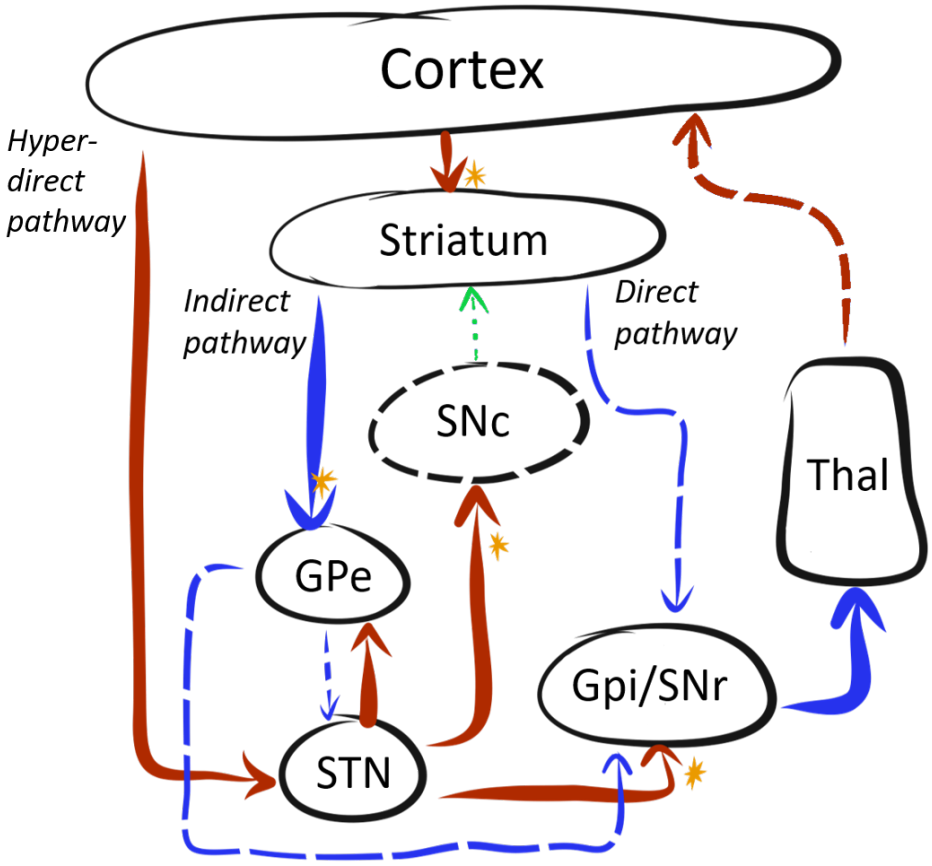

Figure 3.1: A diagram of the basal ganglia in Parkinson's. Overactive pathways are indicated with wide arrows, underactive pathways are indicated with narrow, dashed lines. Glutamatergic synapses are highlighted in red, GABA-ergic pathways in blue and dopaminergic pathways in green. Synapses where mGluR4 is shown to be presynaptically expressed are labelled with a yellow star (Messenger et al. 2002, Corti et al. 2002, Battaglia et al. 2006, Iskhakova & Smith 2016). SNc, substantia nigra pars compacta; GPe, external globus pallidus; STN, subthalamic nucleus; GPi, internal globus pallidus; SNr, substantia nigra pars reticulata. Diagram adapted from Galvan & Wichmann (2008).

3.1.2.1 Subthalamonigral synapse

Broadstock et al. (2012) found that, following co-application of PHCCC and a group III mGluR agonist (L-2-amino-4-phosphonobutyrate (L-AP4)), glutamate release from the STN was reduced.

This translated to a reduction of akinesia in reserpinised rats when PHCCC was infused above the SNr. Valenti et al. (2005) also showed that application of L-AP4 reduced excitatory post-synaptic potentials from the STN to the rat SNc, and that this was potentiated by application of PHCCC. Furthermore, the L-AP4-mediated inhibition of excitatory postsynaptic potentials was reduced in slice preparations from mGluR4-knockout mice, further defining the role of mGluR4 in regulation of the activity of the subthalamonigral pathway. This demonstrates the potential function of mGluR4 at the subthalamonigral synapse, which is overactive in both Parkinsonian animals and PD patients (Robledo & Feger 1991, Limousin et al. 1998).

3.1.2.2 Striatopallidal synpase

Through the use of electrophysiology, Marino et al. (2003) and Valenti et al. (2003) showed that PHCCC and L-AP4 were able to inhibit transmission across the striatopallidal synapse. Translating this evidence, Battaglia et al. (2006) found that systemic PHCCC was able to reduce MPTP-mediated neurodegeneration through a focus on normalising activity across the striatopallidal synapse. In this study by Battaglia et al. (2006), infusion of PHCCC into the GPe was found to provide almost the same level of neuroprotection as systemically administered PHCCC (Battaglia et al. 2006). This suggests that mGluR4 activity at the striatopallidal synapse may be key to mGluR4-mediated neuroprotection.

3.1.2.3 Corticostriatal synapse

Iskhakova & Smith (2016) studied expression of mGluR4 in the mouse striatum using electron microscopy. They found that 73% of glutamatergic terminals expressing vGluT1 (a vesicular glutamate transporter used here to demarkate corticostriatal terminals) co-expressed mGluR4 - showing that the majority of corticostriatal synapses in the mouse may be controlled by mGluR4 activity. Furthermore, Iskhakova & Smith (2016) show that 70% of those synpases do not match with D_1 receptor-positive spines, suggesting that, instead, they target the D_2 receptor-controlled indirect pathway. This evidence hints that, by targeting the mGluR4 receptor within the striatum, the D_2-mediated, overactive indirect pathway can be preferentially moderated while the underactive, D1-mediated direct pathway can be left functionally intact. In support of this, Bennouar et al. (2013) show that Lu AF21934 can inhibit transmission across the corticostriatal synapse and find that such modulation can provide antiparkinsonian effects in animal models.

Overactivity of the glutamatergic corticostriatal pathway is additionally implicated in the gener-

ation of levodopa-induced dyskinesia (LID), and there is some evidence that mGluR4 may be of efficacy in the treatment of this side effect of L-DOPA treatment, in addition to the treatment of PD itself.

3.1.3 L-DOPA-sparing strategies and dyskinesia

mGluRs in all 3 groups have also been studied with respect to their potential as combination therapies for bradykinesia in PD alongside L-DOPA, or their ability to moderate the dyskineisa side effects induced by long-term treatment with L-DOPA. Respectively, these potential roles of mGluRs are known as L-DOPA-sparing efficacy and antidyskinetic efficacy. Although these two roles require very different actions of a drug, in the treatment of PD they go hand-in-hand. Where a drug is found to be L-DOPA-sparing, the dose of L-DOPA given to treat PD can be reduced at a point early on in treatment. This may delay the onset of LID, one of the most severe side effects of L-DOPA. Where a drug can moderate the dyskinesia caused by long term usage of L-DOPA, it may do so either by reducing the development of LID or by reducing the severity or incidence of already developed LID.

3.1.3.1 mGluR4 as an L-DOPA-sparing target

There exists strong evidence to suggest that mGluR4 represents a viable target for L-DOPA-sparing treatment.

Using the mGluR4 PAM 5-Methyl-N-(4-methylpyrimidin-2-yl)-4-(1H-pyrazol-4-yl)thiazol-2-amine-(ADX88178), Le Poul et al. (2012) show a therapeutic potential of mGluR4 in reducing the dose of L-DOPA needed to combat akinesia in bilteral, 6-OHDA-lesioned rats and also in MitoPark mice. Similarly, Iderberg et al. (2015) showed an L-DOPA-sparing effect of the PAM, VU0364770, in unilaterally 6-OHDA-lesioned rats. However, the same was not true of the mGluR4 agonist (2S)-2-amino-4-(hydroxy(hydroxy(4-hydroxy-3-methoxy-5-nitrophenyl)methyl)phosphoryl)-butanoic acid (LSP1-2111) (Iderberg et al. 2015). Finally, Bennouar et al. (2013) found that a reduced dose of L-DOPA was needed to combat akinesia when given alongside the mGluR4 PAM, Lu AF21934, in unilateral, 6-OHDA-lesioned rats. Whether the results of these studies reflect a neuroprotective potential of mGluR4 compounds or a true L-DOPA-sparing potential remains to be seen.

3.1.3.2 mGluR4 as a target in LID

Evidence to support mGluR4 as a target for LID is much more mixed than that of the L-DOPA-sparing efficacy of mGluR4 activation.

Le Poul et al. (2012) found no evidence that a single administration of ADX88178 could modulate established L-DOPA-induced abnormal involuntary movements (AIMs) (the rodent correlate of LID). Similarly, Iderberg et al. (2015) showed that neither LSP1-2111 (an mGluR4 agonist), nor VU0364770 (an mGluR4 PAM) could reduce the expression of established AIMs in 6-OHDA-lesioned rats. Furthermore, neither of these compounds were capable of modifying the development of L-DOPA-induced AIMs when given alongside L-DOPA.

In direct contrast to this evidence, Lopez et al. (2011) found that, when 6-OHDA-lesioned mice were co-administered LSP1-2111 alongside L-DOPA, the development of AIMs was significantly attenuated. Nevertheless, a single administration of LSP1-2111 was not able to affect AIMs that had already developed (Lopez et al. 2011). Likewise, Bennouar et al. (2013) found that administration of the mGluR4-specific PAM, Lu AF21934, alongside L-DOPA was able to reduce the incidence of development of AIMs in 6-OHDA-lesioned rats. However, when the Bennouar et al. (2013) study was reproduced by Finlay (2014), Lu AF21934 appeared to have no effect on either the development of AIMs or the expression of established AIMs.

The evidence for the antidyskinetic efficacy of mGluR4, however mixed, has been sufficient to support the development, and submission to clinical trials, of an mGluR4 PAM, Foliglurax (Prexton Pharmaceuticals), for the treatment of established LID in PD (Charvin et al. 2017).

LID is also often studied in non-human primates, likely due to the more accurate reproduction of the range of human movements in this model than in rodent models. It is much easier to characterise LID in primates than in rodents due to the wide range of human-like movements available to study in the primate, and also the improved similarity to the human disorder (Iderberg et al. 2012). Despite this, as of yet there is only one publication detailing the efficacy of mGluR4 compounds (a PAM) on dyskinesia in primates (Charvin et al. 2018). The study by Charvin et al. (2018) shows a significant effect of mGluR4 PAM Foliglurax (PXT002331) on Parkinsonism in macaques with an apparent partial lesion induced by MPTP and an effect on LID in macaques which appear to have a full lesion. In contrast to this, unpublished observations from work in the present lab found no effect of an alternative mGluR4 PAM, Lu AF21934, on Parkinsonism or LID

in MPTP-treated marmosets.

While data on mGluR4 for the treatment of AIMs in rodent and primate models appears mixed, we were fortunate to have access to some MPTP-treated marmosets with established dyskinesia. We used this opportunity to be the first to explore the antidyskinetic and L-DOPA-sparing efficacy of an mGluR4 agonist in non-human primates.

3.2 Hypotheses and aims

Multiple hypotheses are tested by studies presented in this chapter, and each evolved in sequence from the findings of the last:

1. (Betts et al. 2012) found that VU0155041 (an mGluR4 agoPAM) had a neuroprotective effect when delivered intracranially to 6-OHDA, fully-lesioned rats. This effect was not replicated when VU0155041 was substituted with the systemically available mGluR4 PAM (Lu AF21934) and administered via oral gavage. **We hypothesised that Lu AF21934, when orally administered in partially lesioned 6-OHDA-lesioned rats (characterised in Chapter 2), would provide a neuroprotective effect**. This effect would be measurable by histology to assess TH staining in the striatum and SNc. **The aim of this study was to examine whether a 6-OHDA partial lesion rat model would be more sympathetic to neuroprotective effects of mGluR4 compounds than the full lesion model used in Finlay (2014)**.

   The reasoning behind this hypothesis was that systemic delivery of the drug may provide insufficient levels of compound at the necessary sites of action in the brain to provide protection in a fully-lesioned animal when compared to intracranial administration. Therefore, the use of a partial lesion may provide a more suitable environment for this proof-of-concept study. This hypothesis was tested here in a protocol used previously in the group and adapted from that used in the Betts et al. (2012) study in which neuroprotection arose from the administration of an mGluR4 agoPAM.

2. Given the lack of neuroprotective efficacy of systemically administered PAMs subsequently revealed in partially-lesioned animals (study 1, above), **we hypothesised that, in the Betts et al. (2012) study, the mGluR4 agonist activity of VU0155041 was more important for the provision of neuroprotection than was the PAM activity**; and that it was for this reason that Lu AF21934 provided no neuroprotection. Therefore, in order to test this hypothesis, the method of systemic administration in a partial lesion model was repeated but an mGluR4 orthosteric agonist, LSP1-2111, was substituted for the PAM that was used to test hypothesis 1. **The aim of this study was therefore to discover whether a systemically active, selective, mGluR4 agonist, LSP1-2111, could provide neuroprotection in the 6-OHDA partial lesion rat model of PD.**

3. mGluR4 compounds have been variously found to have L-DOPA-sparing activity, the capacity to reduce established LID or the capacity to reduce the development of LID. **We hypothesised that the systemically available mGluR4 agonist, LSP1-2111, would reduce the severity of LID in MPTP-treated marmosets**.

   This work was undertaken at King's College London in collaboration with Dr. Sarah Salvage's group.

   The aims of this study were to:

   (a) Determine whether LSP1-2111 can be used to boost the antiparkinsonian effect of a submaximal dose of L-DOPA (L-DOPA sparing).

   (b) Determine whether LSP1-2111 can reduce LID in primed, Parkinsonian marmosets.

   (c) Determine whether LSP1-2111 alone has an antiparkinsonian effect and/or causes dyskinesia in primed, Parkinsonian marmosets.

3.3 Materials and Methods

All procedures were performed in accordance with the U.K. Animals (Scientific Procedures) Act, 1986.

3.3.1 Compounds tested

Table 3.1 shows the structure and classification of the two compounds, (Lu AF21934 and LSP1-2111) tested for neuroprotective efficacy in the partial lesion rat model detailed in 'Development of a Unilateral Partial Lesion Rat Model'. Both compounds were synthesised and provided by Lundbeck (Denmark), and additional LSP1-2111 was synthesised and provided by Eisai (UK).

Table 3.1: Compounds tested

Structure	Name	Classification
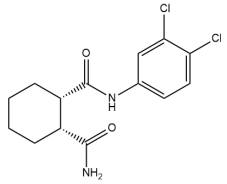	**Lu AF21934** (1S, 2R)-N1- (3,4-dichlorophenyl)-cyclohexane- 1,2-dicarboxamide	mGluR4 positive allosteric modulator
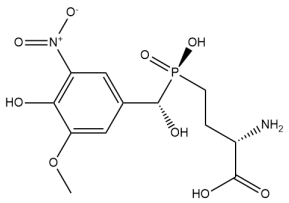	**LSP1-2111** (2S)-2-amino-4- (hydroxy(hydroxy(4-hydroxy- 3-methoxy-nitrophenyl)methyl) phosphoryl)butanoic acid	mGluR4 orthosteric agonist

Table 3.1: Details of compounds studied for neuroprotective efficacy in a partial, 6-OHDA lesion rat model of PD.

3.3.2 Choosing appropriate doses

Lu AF21934 has an EC_{50} at human mGluR4 of 500±200nM (Bennouar et al. 2013), and LSP1-2111 has an EC_{50} at human mGluR4 of 1.5μM (Cajina et al. 2014). Given this, the timings and routes of compound administration were further informed by pharmacokinetic data gathered from naïve rats, dosed acutely, previously in this lab (Finlay 2014) and by Cajina et al. (2014). These data are outlined in Table 3.2. The pharmacokinetics and pharmacodynamics of these compounds in non-human primates are not currently available in the literature.

Table 3.2: Compound PK data

Compound	Dose	Route	$T_{1/2}$ (hours)	plasma C_{max} (ng/ml)	time of C_{max} (hours)	plasma:brain
Lu AF21934	10mg/kg	p.o.	1.4±0.1	869±202	1	
Lu AF21934	30mg/kg	p.o.	0.8±0.1	4733±758	1	0.65
LSP1-2111	10mg/kg	s.c.	0.3	11000±3700	0.5	0.02

Table 3.2: Pharmacokinetic data on compounds examined for neuroprotective efficacy.

For the 30mg/kg *per os* (p.o.) dose of Lu AF21934, the plasma C_{max} was 4733ng/ml, or 15μM, almost ten times the EC_{50} at human mGluR4. The brain C_{max} was found to be approximately 4000ng/ml - around 8 times the EC_{50} (Finlay 2014). However, the free brain concentration is believed to be around 3% of the total, and therefore around 0.38μM - slightly under the EC_{50} (Bennouar et al. 2013, Finlay 2014). Nevertheless, Bennouar et al. (2013) show that Lu AF21934 at 10 or 30mg/kg is capable of reducing haloperidol-induced catalepsy in rats and that, when given alongside L-DOPA, can reduce LID. The neuroprotective potential of Lu AF21934 (at 10 and 30mg/kg) was previously examined in a full-lesion rat model by this group and no effects were seen (Finlay 2014), possibly due to the severity of the lesion.

Following the 10mg/kg dose of LSP1-2111, the plasma C_{max} was 11μg/ml (31μM) (Cajina et al. 2014). Cajina et al. (2014) also measured the concentration in cerebrospinal fluid at 1.7μg/ml and judged this to be close to the unbound fraction, giving 4.6μM LSP1-2111 or 3 times the EC_{50}. LSP1-2111 concentration in brain tissue was measured at 360ng/ml (0.989μM), approximately one third of the EC_{50} at human mGluR4 (Cajina et al. 2014). In support of these doses being efficacious, Iderberg et al. (2015) show that LSP1-2111 (at 1, 3, 10, 15 and 30mg/kg intraperitoneal (i.p.)) has efficacy in reducing catalepsy following administration of haloperidol.

3.3.3 Lu AF21934 neuroprotection study

37 male Sprague-Dawley rats (200-250g on arrival, Harlan, UK) were maintained on a 12 hour light-dark cycle (7am - 7pm light) in a temperature and humidity controlled room with *ad libitum* access to dry chow and tap water. Rats were given at least 7 days to acclimatise to the unit prior to lesioning.

Animals were randomised to treatment groups using a random number generator (Haahr 1998) and the dosing, lesioning, behavioural tests and immunohistochemistry for both studies were carried out by a single experimenter blinded to treatments received by each group by a third party. As the groups in the Lu AF21934 study were to contain unequal numbers (as a result of a shortage of compound), animals were allocated in groups of 5, with all conditions except the highest dose receiving two groups of animals.

Animals were dosed with Lu AF21934 (an mGluR4 PAM) or vehicle twice daily from 1 day prior to lesioning to 7 days post-lesion (a total of 9 days' dosing). For the purposes of this study, Lu AF21934 was formulated in polyethylene glycol 400 (PEG400) and administered p.o., at 7am and 6pm, in a volume of 2ml/kg at 1mg/kg ($n = 10$), 10mg/kg ($n = 10$) or 30mg/kg ($n = 5$), with a vehicle group receiving PEG400 alone ($n = 10$). Sonication and gentle heating were used in order to dissolve Lu AF21934 at the highest concentration of 15mg/ml. Lu AF21934 is known to be stable in solution for $\geq$7 days (C. Bundgaard, personal communication) and so Lu AF21934 solution was formulated every 6 days during the study in order to maximise consistency between animals and minimise wastage. Lu AF21934 was initially administered using metal oral administration gavages, but these were swapped for flexible plastic gavages (Instech, USA) due to poor tolerance of repeated dosing with metal gavages in a minority of animals resulting in the early terminations of 2 animals from the Lu AF21934 study. These animals were replaced, joining a later treatment group in order to keep group sizes as originally planned.

Lesioning protocol, behavioural tests and perfusion took place as described in Chapter 2. Briefly, all animals were given partial lesions using 12μg 6-OHDA in 3μl 0.2% sodium ascorbate injected at 1μl/minute into the right, dorsal striatum (AP +0.2mm, ML -3mm from bregma and -5.5mm from skull surface with the incisor bar set at -3.3mm) under inhaled isoflurane anaesthesia. 0.01mg/kg buprenorphine (Vetergesic, Ceva Health Care Ltd, France) was given for post-operative pain management and the wound was sutured once the injection needle was withdrawn. Cylinder, adjusted

step and amphetamine-induced rotation tests were used to track development of the lesion over time and assess motor preservation *in vivo*. These tests were performed exactly as described in Chapter 2. The timeline of these interventions is shown in Figure 3.2 and was based on previous neuroprotection studies undertaken with Lu AF21934 in this lab using a 6-OHDA full-lesion model (Finlay 2014).

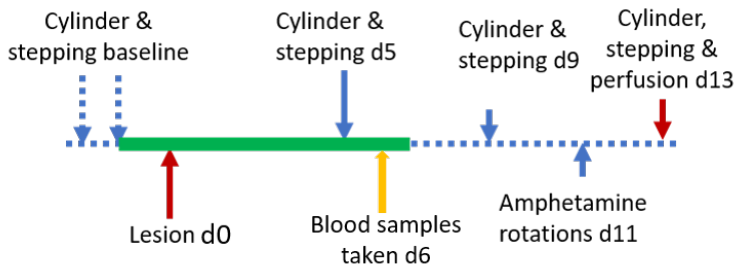

Figure 3.2: A diagram of the timeline for neuroprotection studies. The green bar along the timeline indicates duration of dosing from 1 day prior, to 7 days post-lesion - 9 days total.

One day prior to the end of compound administration, blood was taken for pharmacokinetic analysis. 1 hour after the 7am administration of Lu AF21934 or vehicle, 0.25 - 0.5ml of blood was withdrawn from the tail vein using a 23G 3/4" butterfly needle (Becton, Dickinson and Company, USA) and deposited into a heparinised collection tube (Sarstedt, Germany). The tube was kept on ice for $<$ 1hr during the collection procedure, then immediately centrifuged at 5000RPM at -10°C for 15 minutes. Plasma was then withdrawn from the tube and frozen at -80°C to be used for offsite pharmacokinetic analysis. Plasma samples were further prepared for analysis at Lundbeck (Copenhagen, Denmark) and analysed by ultra performance liquid chromatography - tandem mass spectrometry (UPLC-MS/MS) there.

As in Chapter 2, at the point of sacrifice (2 weeks post-lesion), rats were given an overdose (200mg via i.p. injection) of sodium pentobarbital (Euthatal - Merial Animal Health Ltd, UK) and perfused with phosphate-buffered saline (PBS) followed by 10% formalin. Brains were removed and large coronal blocks each containing either the midbrain or striatum were excised and post-fixed in 10% formalin for a further 48 hours. Brain sections were then then processed using a TP1020 tissue processor (Leica) and embedded in paraffin wax. Immunohistochemical staining for TH was undertaken and images taken and analysed as detailed in section 2.3.3, p.77. Briefly, in the SNc, the number of TH-positive cell bodies were counted in the lesioned and intact hemispheres. In the striatum, densitometry was used in order to ascertain the density of TH-positive terminals in the lesioned striatum and this was expressed as a percentage of the density of stain in the contralateral

striatum. ImageJ was used to measure the density of stain in these areas. The density of TH stain in the cortex of the same hemisphere was designated as 'background' and subtracted from the striatal readings. For each area of interest, 3 consecutive sections per animal were stained and the data obtained from them averaged.

3.3.3.1 Statistical analysis

All data were tested for normality using the Shapiro-Wilk test as the 30mg/kg Lu AF21934 group had a low n ($n = 5$). Normality tests were undertaken prior to the data undergoing any tests for significant differences between groups.

Where treatment groups were compared over time in behavioural tests, a repeated measures 2-way ANOVA was used, followed by Sidak's multiple comparisons test (all conditions compared) or Dunnett's test (where values were compared to a control value) if significance was seen in the ANOVA. Where data were compared between regions and between treatment groups, a 2-way ANOVA was used. Where values representing lesion conditions at a single time point were compared as in the overall histological comparisons, a 1-way ANOVA was used with a Dunnett's post-test.

3.3.4 LSP1-2111 neuroprotection study

30 male Sprague-Dawley rats (200-250g on arrival, Harlan, UK) were held and acclimatised in the same manner as in the Lu AF21934 study. Randomisation to treatment groups took place with the used of a random number generator (Haahr 1998) and all treatments, behaviour and immunohistochemistry was carried out by an experimenter blinded to the treatment groups by a third party.

LSP1-2111 (an mGluR4 orthosteric agonist) is known to be stable in solution for $\geq$8 days at room temperature (C. Bundgaard, personal communication) so LSP1-2111 solution was formulated every 6 days during the study in order to improve consistency of doses and minimise wastage.

As in the Lu AF21934 neuroprotection study, the compound (in this case, LSP1-2111) was administered twice daily from 1 day prior to, to 7 days post-lesion. In this study, LSP1-2111 was formulated in sterile 0.9% saline and adjusted to pH7.4 using 1M NaOH. LSP1-2111 was administered with a subcutaneous (s.c.) injection, twice daily (at 7am and 6pm) in a volume of 5ml/kg at either 1mg/kg ($n = 10$) or 10mg/kg LSP1-2111 ($n = 10$) or saline vehicle alone as a control ($n = 10$). S.c. administration was well tolerated but the site of injection was varied in order to reduce irritation.

Lesion surgeries and behavioural tests took place at the same time points and in the same manner as described in the methods of the Lu AF21934 neuroprotection study (Figure 3.2, p.110). As in the Lu AF21934 study, blood was withdrawn from the tail vein 1 hour following the 7am dose of LSP1-2111 or vehicle on the final day of dosing. Plasma was removed from the whole blood sample following the centrifugation procedure detailed in the Lu AF21934 neuroprotection study methods and sent to Lundbeck for UPLC-MS/MS analysis to determine the plasma drug concentration.

Animals were sacrificed and perfused at two weeks post-lesion as in Chapter 2 and the brain removed and further fixed in 10% formalin for 48 hours. Large coronal blocks each containing the midbrain or the striatum were removed and processed using a Leica TP1020 for the Lu AF21934 study. Coronal sectioning and TH histology took place as in Chapter 2.

For each area of interest, 3 consecutive sections of tissue were stained, imaged and analysed, and the outcome was averaged. For TH staining, this was undertaken as in Chapter 2. Briefly, in the SNc, the number of TH-positive cell bodies were counted in the lesioned and intact hemispheres.

In the striatum, densitometry was used in order to ascertain the density of TH-positive terminals in the ipsilateral striatum and this was expressed as a percentage of the density of stain in the contralateral striatum. ImageJ was used to ascertain the density of stain in these areas. The density of TH stain in the cortex of the same hemisphere was designated as 'background' and subtracted from the striatal readings.

3.3.4.1 Statistical analysis

All data were tested for normality using the D'Agostino and Pearson omnibus normality test prior to undergoing any tests for significant differences between groups.

Where treatment groups were compared over time in behavioural tests, a repeated measures 2-way ANOVA was used, followed by Sidak's multiple comparisons test, Bonferroni (simple effects between lesion conditions at a given time point) or Dunnett's test (where values were compared to a control value) if significance was seen in the ANOVA. Where data were compared between regions and between treatment groups, a 2-way ANOVA with Sidak's or Dunnett's post-test was used. Where average values representing treatment conditions at a single time point were compared, as in the histological comparisons, a 1-way ANOVA was used with a Dunnett's post-test.

3.3.5 MPTP primate study

The effects of LSP1-2111 on LID in MPTP-treated marmosets was assessed in collaboration with Dr Sarah Salvage's group. The study was planned by Dr Sarah Salvage, Dr Susan Duty and Elizabeth Mann, the dosing and behavioural work was undertaken by Louise Lincoln and Ria Fisher (observed by Elizabeth Mann), data analysis was undertaken by Dr Sarah Salvage, Mike Jackson and Elizabeth Mann.

Approximately 3-5 years prior to the described study, marmosets underwent administration of MPTP at 2.0mg/kg daily for 5 days (precise protocol according to Smith et al. (2002)). This resulted in the animals showing symptoms of Parkinsonism including bradykinesia, rigidity and tremor. All animals were also pre-primed to express dyskinesia on exposure to L-DOPA through repeated (up to 28 days) oral administration of 8-12.5mg/kg L-DOPA and 10mg/kg benserazide in 10% sucrose solution. None of the animals in this study were test-drug naïve, but all had undergone a 'washout' period of several weeks following the previous study.

Animals were selected for the study from a pool of MPTP-treated marmosets based on locomotor activity following L-DOPA treatment. Briefly, 10 MPTP-treated marmosets were given L-DOPA (at 4, 6 and 8mg/kg) with 10mg/kg benserazide p.o. and locomotor activity was recorded (as detailed below) for 5 hours. Animals with similar locomotor scores were selected for the present study and the dose of L-DOPA which gave rise to submaximal motor response was recorded.

A modified latin square was used to randomise treatments whilst keeping administration of LSP1-2111 in an escalating manner - such that any severe side effects could be ascertained at low doses and before higher doses were given. In this fashion, all animals received all treatments (with an interval of $\geq$ 48 hours between doses) for a final group size of $n = 6$. LSP1-2111 was administered s.c. in 0.9% saline at 1, 3 or 6mg/kg in a volume of 1ml/kg. Immediately following administration of LSP1-2111, 8mg/kg L-DOPA and 10mg/kg benserazide were given in a combined p.o. administration of 2ml/kg. Behaviour was also recorded from animals given both vehicles, only L-DOPA or only 6mg/kg LSP1-2111 to form the following treatment groups:

- Vehicle (saline) + vehicle (10% sucrose)
- Vehicle (saline) + L-DOPA (8mg/kg p.o. + 10mg/kg benserazide)
- LSP1-2111(1 mg/kg s.c.) + L-DOPA (8 mg/kg p.o. + 10mg/kg benserazide)
- LSP1-2111 (3 mg/kg s.c.) + L-DOPA (8 mg/kg p.o. + 10mg/kg benserazide)

- LSP1-2111 (6 mg/kg s.c.) + L-DOPA (8 mg/kg p.o. + 10mg/kg benserazide)
- LSP1-2111 (6 mg/kg s.c.) + vehicle (10% sucrose)

On the day of the study, animals were acclimated to locomotor measurement cages ($50cm \times 60cm \times 90cm$) housing 8 horizontal infrared beams (and an additional 3 across the floor) for 60 minutes. During this time, baseline locomotor activity was recorded automatically. Following the baseline period, LSP1-2111 and L-DOPA (or respective vehicle) were administered according to the aforementioned randomisation protocol and the marmosets replaced in the cages. Measurements of dyskinesia and motor disability were then recorded every 30 minutes for 5 hours by trained observers. Locomotor activity was recorded automatically as the number of breaks of infrared beams in the cages in 30 minute time bins.

When rating the animals for disability, a number of criteria were considered (Table 3.3), giving a maximum possible score of 18.

Table 3.3: Marmoset disability scoring

	+0	+1	+2	+3	+4
Alertness	Alert	Sleepy	Sleepier		
Reaction	Present	Reduced	Slow	Absent	
Checking	Present	Reduced	Absent		
Attention	Normal	Abnormal			
posture	Normal	Abnormal trunk +1 Abnormal limbs +1 Abnormal tail +1			Grossly abnormal
Balance and co-ordination	Normal	Impaired	Unstable	Spontaneous falls	
Vocalisation	Present	Reduced	Absent		
motility	Normal	Bradykinesia Hyperkinesia	Akinesia Hyperkinesia		

Table 3.3: Scoring scales for all categories of disability in MPTP-treated marmosets.

Dyskinesia measurements were counted from choreic (defined as rapid, random flicking movements of the limbs) and dystonic (defined as a sustained abnormal posture) dyskinesia and ranked from 0-4 as follows:

- 0 = absent
- 1 = mild, fleeting dyskinesia
- 2 = more prominent abnormal movements, but not significantly affecting normal behaviour
- 3 = frequent and at times continuous dyskinesia affecting normal activity
- 4 = severe, virtually continuous dyskinetic activity, disabling to the animal and replacing normal behaviour

3.3.5.1 Statistical analysis

Prior to analysis, data were transformed by $Y = \sqrt{Y}$ in order to normalise distribution (Fisher et al. 2018).

This transformation allowed the application of parametric tests to scored data and so repeated measures 1-way ANOVAs were applied to area under the curve (AUC) data, with Sidak's multiple comparisons test comparing each group to its respective vehicle condition if the initial ANOVA showed a significant effect of treatment (L-DOPA alone and LSP1-2111 alone compared to the vehicle/vehicle condition and L-DOPA with 1, 3 or 6mg/kg LSP1-2111 compared to L-DOPA alone). Data displayed over time as a curve were tested with a repeated measures 2-way ANOVA with a Sidak's multiple comparisons post-test comparing each time point of a group's performance to the baseline point if a significant effect of treatment was seen in the initial ANOVA.

3.4 Results

3.4.1 Lu AF21934 neuroprotection study

One animal was eliminated from the vehicle group of the Lu AF21934 neuroprotection study due to lack of a visible lesion. This animal displayed a TH density of stain in the lesioned striatum which was > 2 standard deviations from the mean value for the group.

3.4.1.1 Cylinder test

There was no difference in performance between vehicle or Lu AF21934 groups in the cylinder test (Figure 3.3). When comparing the raw numbers of contralateral paw touches using a 2-way ANOVA, there was a main effect of time ($p < 0.0001$), but not of treatment group ($p = 0.47$). All groups had similar a baseline performance and displayed reduced use of the contralateral paw following lesioning, with the greatest deficits seen on day 5 post lesion. The use of the contralateral paw by vehicle-treated group decreased to 25.0% by day 5 post lesion from an average of 32 ± 4 touches at baseline to 11 ± 2 by day 5. Animals treated with 1mg/kg Lu AF21934 showed a reduction in contralateral paw use 17.6% of total touches by day 5. At the same time point, contralateral forepaw use in animals in the 10mg/kg Lu AF21934 group fell to 19.4% of total touches, and animals dosed with 30mg/kg Lu AF21934 to 11.6%. All groups showed a measure of functional recovery by day 9, as seen in the characterisation of the model in Chapter 2.

(a)

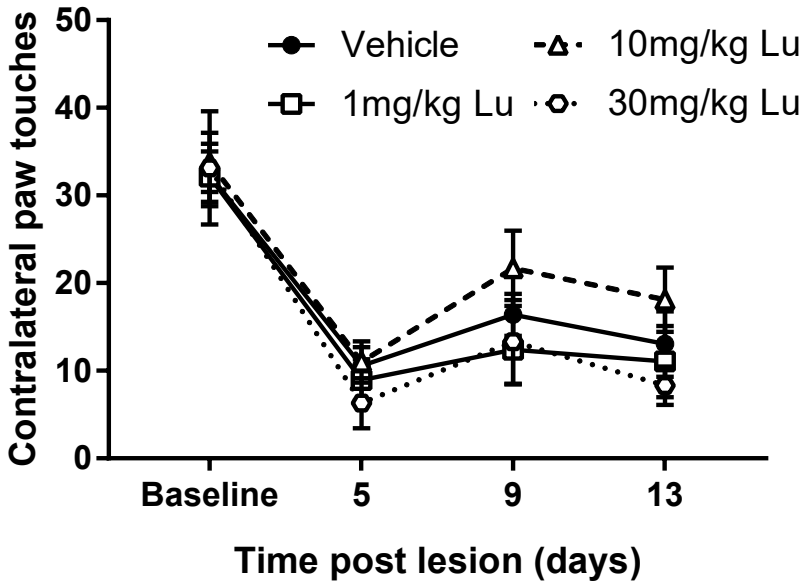

(b)

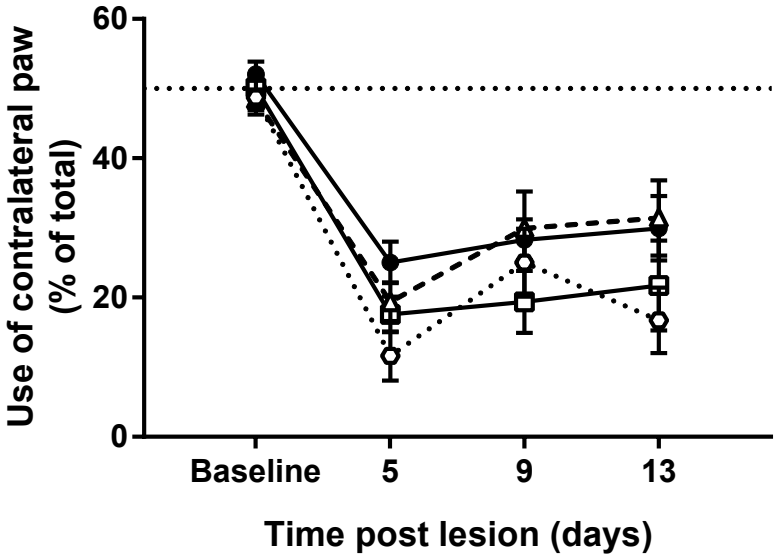

Figure 3.3: Number of weight-bearing exploratory touches made in the cylinder test by lesioned animals dosed with Lu AF21934 or vehicle. a) Number of touches made with contralateral paw b) Contralateral touches expressed as a % of total. For all, data are mean ± standard error of the mean (S.E.M.) and n=5-10 per group.

3.4.1.2 Adjusted step test

The adjusted step test was not able to differentiate between animals in different treatment groups in any condition. In the contralateral forehand condition, there was no significant effect of treatment group ($p = 0.17$), but an effect of time ($p < 0.0001$) and no interaction between variables ($p = 0.31$) in a repeated measures 2-way ANOVA (Figure 3.4a). In this condition, a Dunnett's post-test showed that animals in all groups were significantly impaired at all time points compared with their average baseline performance ($p < 0.0001$). In the vehicle treatment group, forehand contralateral steps fell to 6 ± 1 steps at day 5, from 13 ± 0 at baseline. This was relatively consistent throughout the remaining time points and all other groups followed this trend.

In the backhand contralateral condition, there was much less of a deficit compared to baseline, but still a significant effect of time ($p < 0.0001$) and not of treatment group ($p = 0.15$) and no interaction between variables ($p = 0.47$) in a repeated measures 2-way ANOVA (Figure 3.4b). A Dunnett's post-test showed that vehicle-treated animals and animals in the 1mg/kg Lu AF21934 group showed a significant reduction in backhand contralateral steps at days 9 and 13 ($p < 0.05$) post lesion. Rats in the 10mg/kg group were only significantly poorer than baseline at 5 days post lesion ($p < 0.05$) and rats in the 30mg/kg group performed significantly worse than baseline at all time points ($p < 0.05$).

The ipsilateral conditions of the stepping test also found significant effects of time on performance ($p < 0.0001$ in forehand and backhand conditions) in a 2-way ANOVA (Figures 3.4c and 3.4d). Dunnett's post-tests revealed that vehicle treated animals performed significantly fewer steps at day 13 post-lesion than at baseline ($p < 0.05$) in both the forehand and backhand conditions and, in the backhand condition alone, animals treated with 10mg/kg Lu AF21934 performed significantly fewer steps at day 13 than at baseline ($p < 0.001$).

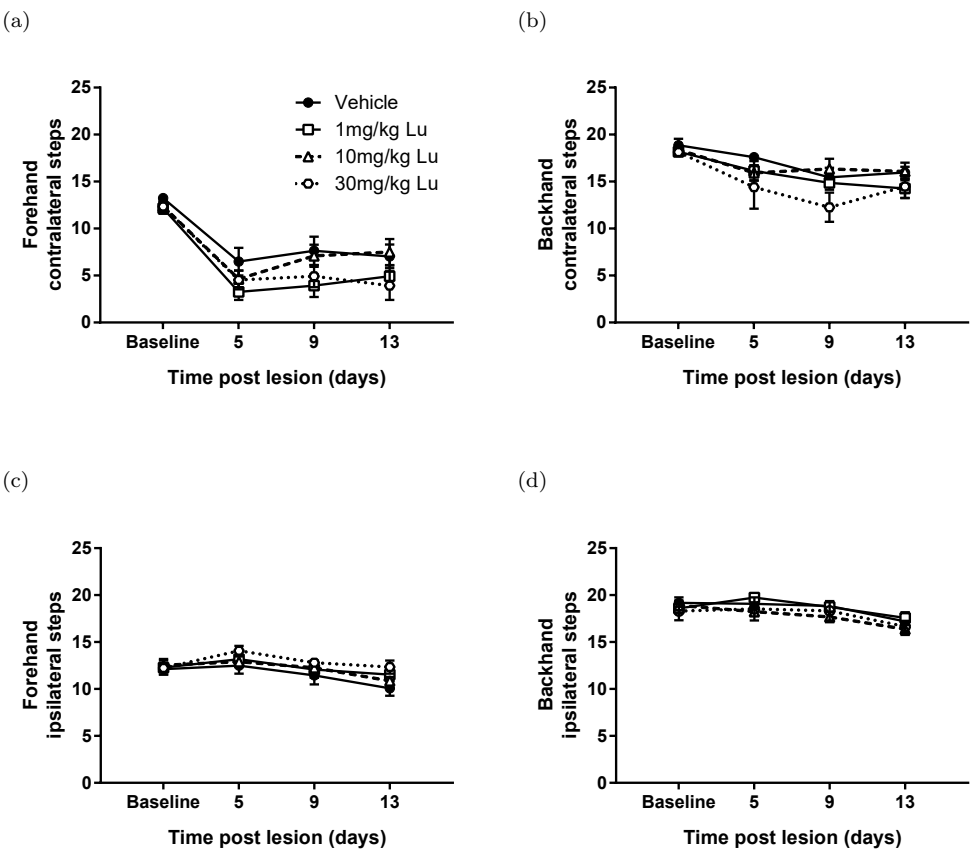

Figure 3.4: Number of adjusting steps taken using ipsilateral and contralateral forepaws in lesioned animals dosed with Lu AF21934 or vehicle. Stepping test outcomes in Lu AF21934 neuroprotection study. Steps taken with the contralateral paw in the a) forehand and b) backhand direction or with the ipsilateral paw in the c) forehand and d) backhand direction. For all, data are mean ± S.E.M. and n=5-10 per group.

3.4.1.3 Amphetamine-induced rotations

Amphetamine-induced rotations were measured on day 11 post-lesion, 4 days following the end of Lu AF21934 dosing. Despite a considerable trend towards a dose-dependent reduction in net ipsiversive rotations, a Kruskal-Wallis test revealed no significant difference in total rotations between the vehicle-treated group and any of the Lu AF21934 groups ($p = 0.19$) (Figure 3.5a). This did not change when only the peak of rotational activity was analysed (Figure 3.5b). On average, over the total time of 120 minutes post-amphetamine, the vehicle-treated animals performed 873 ± 161 net ipsiversive rotations, the 1mg/kg Lu AF21934 treated animals performed 610 ± 177, the 10mg/kg group 672 ± 221 and the 30mg/kg group 314 ± 115.

When examining the data over time as presented in Figure 3.5c, there was a significant effect of time ($p < 0.0001$) but not of treatment group ($p = 0.359$) and no interaction between variables ($p = 0.92$) in a repeated measures 2-way ANOVA. A Dunnett's post-test revealed that vehicle-treated animals performed significantly more rotations ($p < 0.05$) compared to their average pre-amphetamine baseline from 15 - 85 minutes post-injection. Animals in the 1mg/kg and 10mg/kg Lu AF21934 treatment groups performed significantly more rotations ($p < 0.05$) compared to their average pre-amphetamine baseline from 15 - 60 minutes. In contrast, animals in the 30mg/kg Lu AF21934 treatment group did not rotate significantly more than their pre-amphetamine baseline at any point following amphetamine. This therefore shows some evidence of treatment effects.

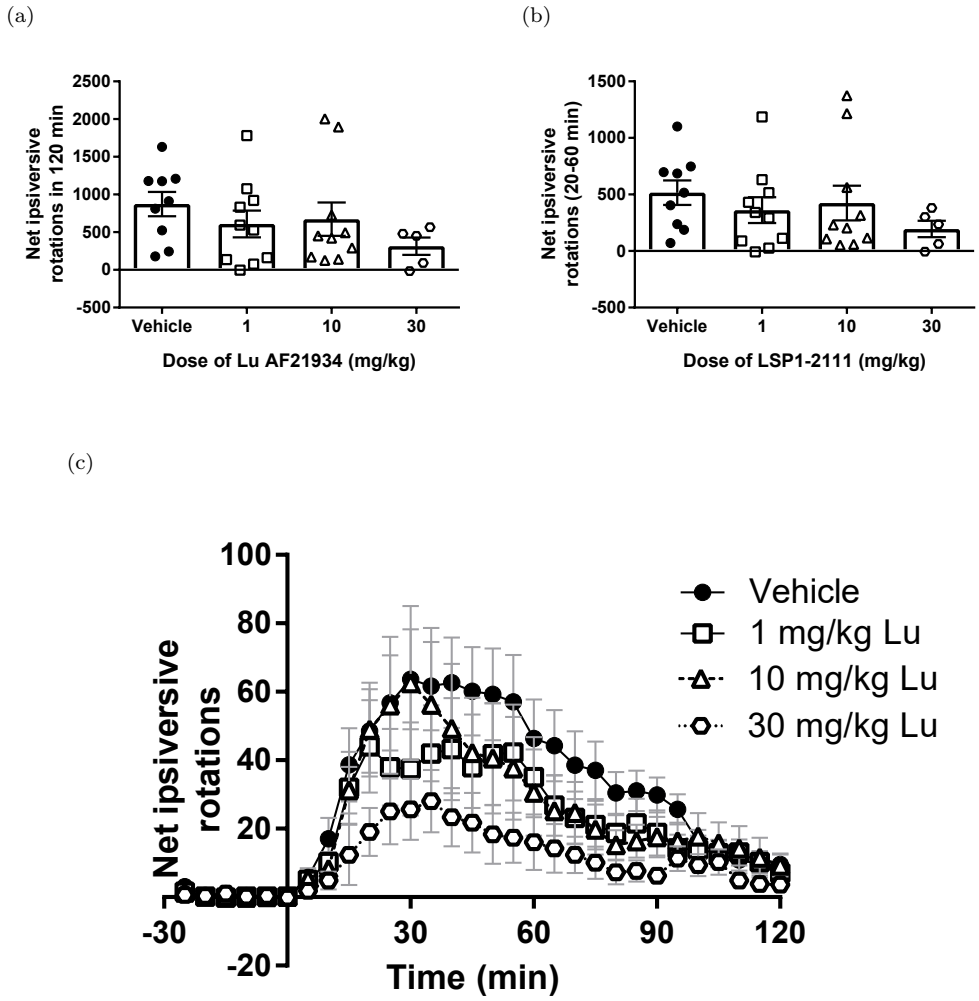

Figure 3.5: Number of amphetamine-induced net ipsiversive rotations over time in lesioned animals dosed with Lu AF21934 or vehicle. a) Net ipsiversive rotations in 120 minutes and b) between 20-60 minutes (the peak of rotational activity) following injection with 5mg/kg amphetamine. c) Net ipsiversive rotations (ipsiversive rotations - contraversive rotations) in 5 minute time bins for 30 minutes prior to and 120 minutes post injection with 5mg/kg amphetamine. Standard error bars are rendered in light grey for ease of data visualisation. * = $p < 0.05$ against average baseline rotations across time points indicated by horizontal bar. Solid bar shows time points with significantly more rotations than baseline for vehicle treated animals, while the dotted bar indicates time points with significantly more rotations than baseline for 1 and 10mg/kg Lu AF21934-treated animals. Animals treated with 30mg/kg Lu AF21934 did not rotate significantly more than baseline at any point. For all graphs, data are mean ± S.E.M. and n=5-10 per group.

3.4.1.4 Histological characterisation of lesion

Figure 3.6 shows representative images of the SNc stained for TH from animals in each treatment group. Although the subtle lesion is evident in the right-hand side of the image (and more clearly in the magnified inserts), there does not appear to be a visible effect of Lu AF21934 treatment. Indeed, there was no significant effect of Lu AF21934 treatment ($p = 0.91$) on the number of TH-positive cells remaining in the SNc in the lesioned hemisphere compared to vehicle treatment in a 1-way ANOVA (Figure 3.7a). This did not change when the cell loss in the SNc of animals in different treatment groups was compared at different levels of the SNc quantified as a % of the intact SNc (Figure 3.7b) and expressed as absolute numbers for both sides (Figure 3.7c).

Across all levels, there was an average of 52 ± 2 cells remaining per section in the lesioned SNc of vehicle-treated animals ($58.7\% \pm 2.6$ of the intact side). In the lesioned SNc of animals in the 1, 10 and 30mg/kg Lu AF21934 groups, there were an average of 50 ± 4, 51 ± 2 and 45 ± 3 cells per section of lesioned SNc respectively.

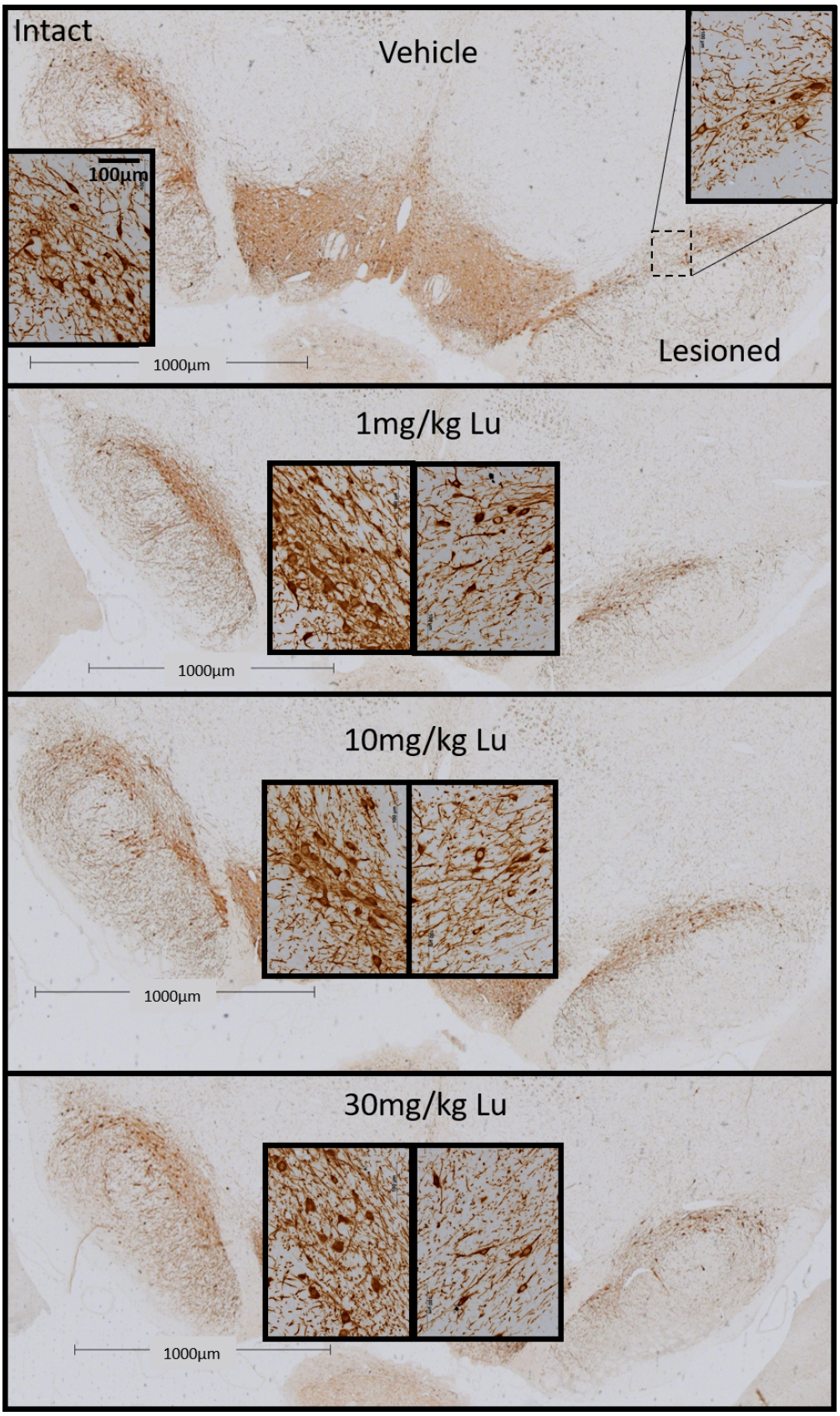

Figure 3.6: Representative images of TH-stained cells in the mid SNc with the unilateral lesion on the right hand side. Inserts are 40x magnification of a region of the SNc indicated on the image from vehicle-treated animal tissue in order to better visualise cell loss.

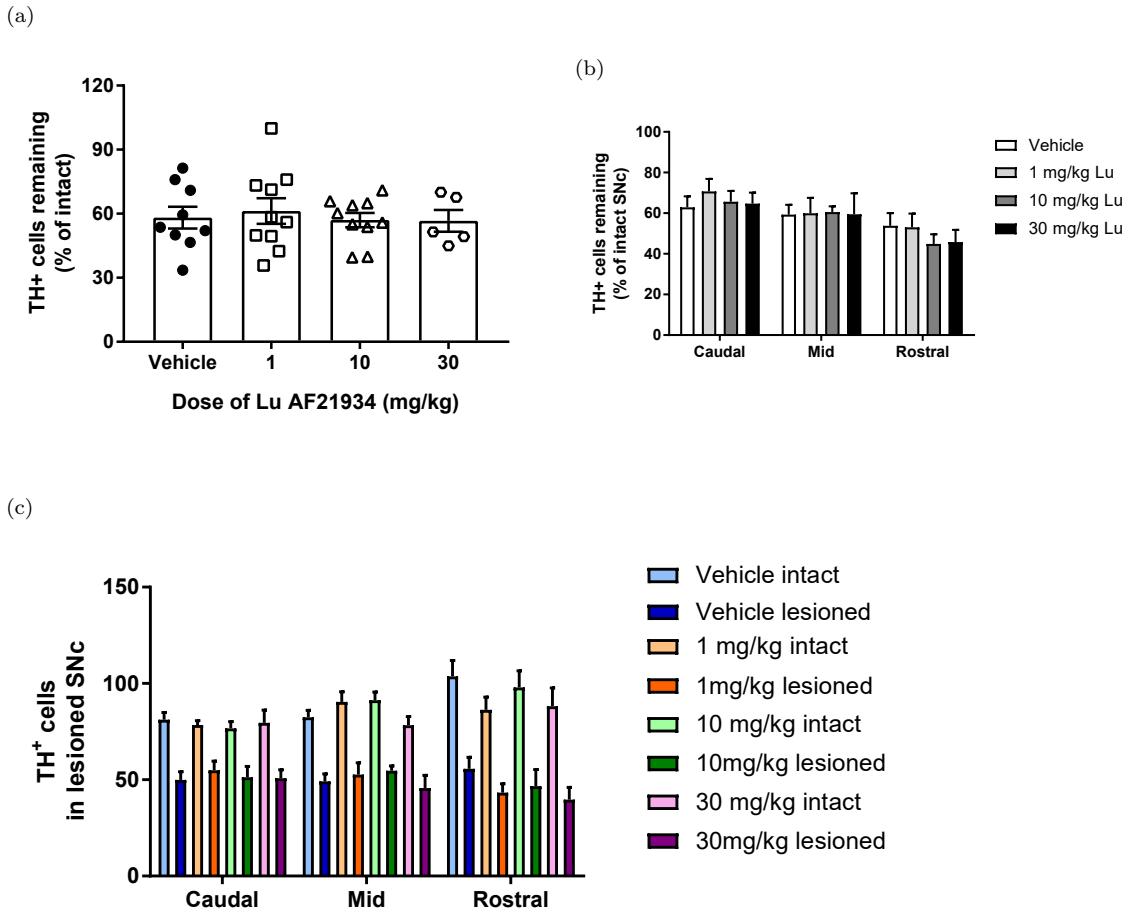

Figure 3.7: Characterisation of TH-positive cells in the lesioned and intact SNc. a) TH-positive cells remaining in leisoned SNc as a percentage of intact SNc (averaged over caudal, mid and rostral levels). b) Counts of TH-positive cells in each section of the SNc in the lesioned hemisphere as a percentage of intact. c) Average numbers of TH-positive cells in intact and lesioned SNc at all levels and in all treatment groups. Data are mean ± S.E.M. and n=5-10 per group.

Figure 3.8 shows representative images of TH-staining in the caudal striatum of animals from each treatment group. The effects of lesioning are clearly visible in reduced staining in the dorsal-mid striatum of right hemisphere.

There was no effect of treatment group on the density of TH stain when averaged across all levels and quadrants of the striatum ($p = 0.88$, Figure 3.9a). In vehicle-treated animals there was an average of $37.0\% \pm 5.3$ TH remaining in the lesioned striatum as compared with the intact hemisphere. In animals in the 1, 10 and 30mg/kg treatment groups there was an average of $43.2\% \pm 6.6$, $42.0\% \pm 4.8$ and $39.0\% \pm 9.2$ TH remaining in the lesioned striatum compared to the intact. Taking into account that the lesion was primarily dorsal in nature, it may be true that averaging across the entire striatum may lose finer changes in TH expression which occur in the dorsal striatum. Nevertheless, when only the dorsal quadrants are taken into account, there was still no significant effect of treatment ($p = 0.90$).

Striatal lesion size did not differ significantly in animals from different treatment groups at any level (Figures 3.9b, 3.9c and 3.9d) in a 2-way ANOVA.

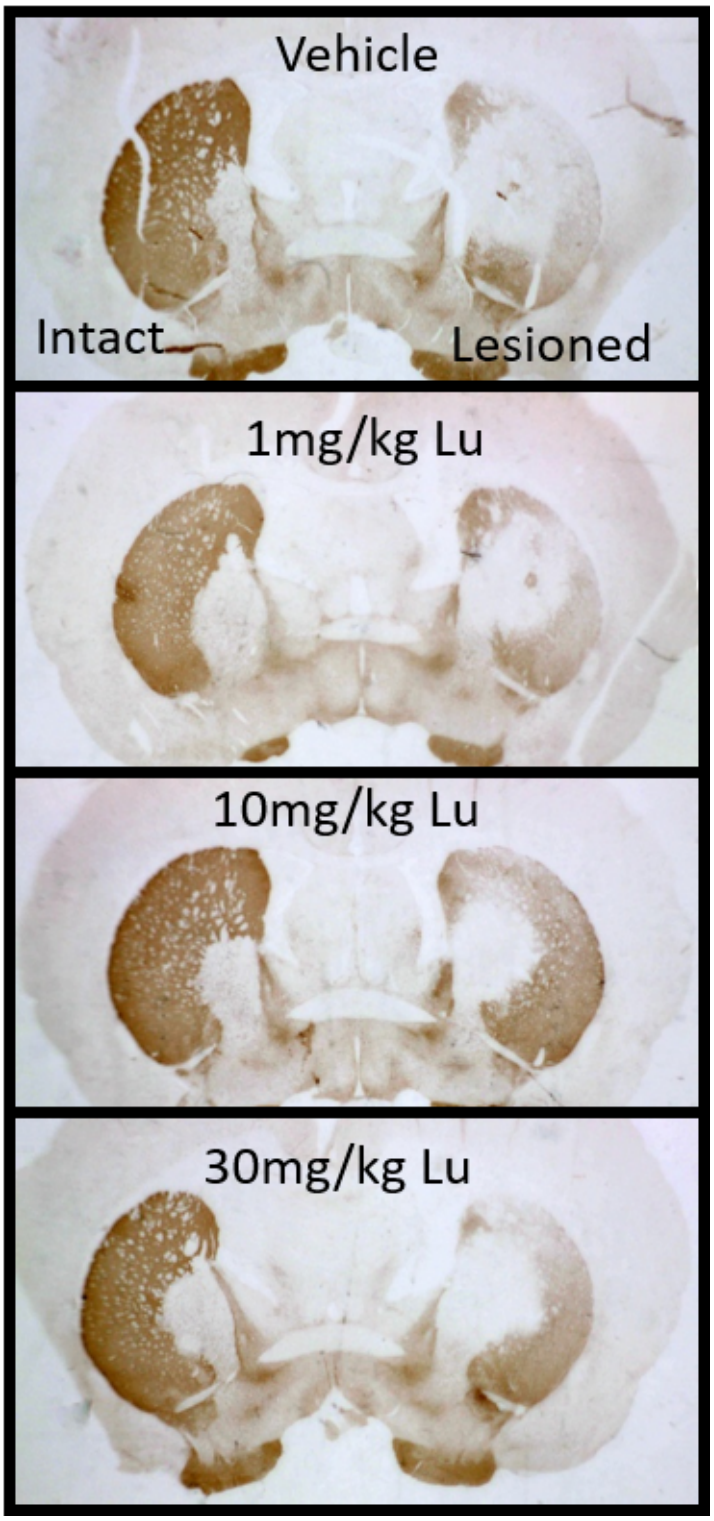

Figure 3.8: Representative images of TH-stained cells in the SNc. Unilateral lesion on the right hand side.

(a)

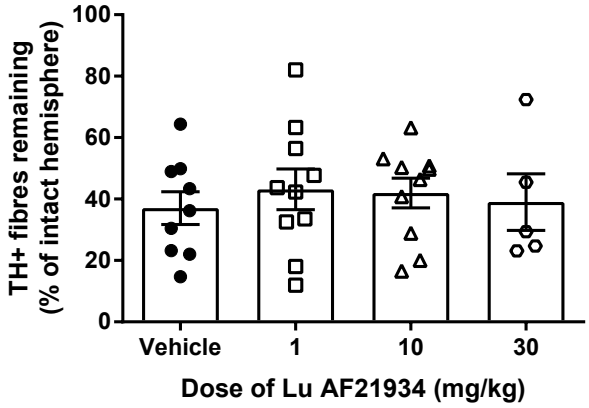

(b) Caudal striatum

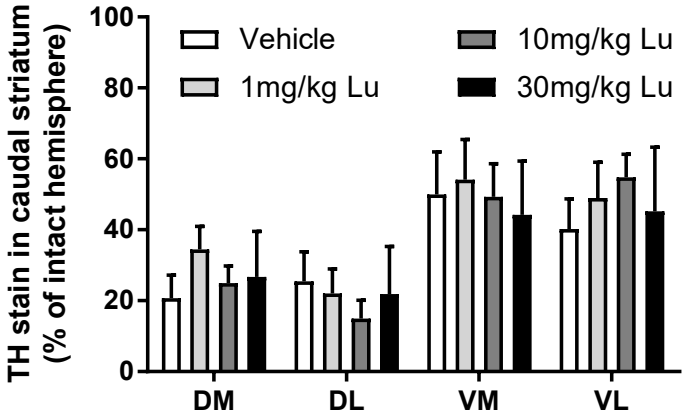

(c) Mid striatum

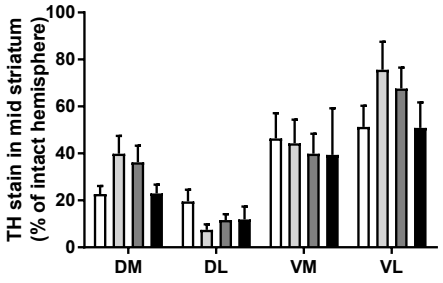

(d) Rostral striatum

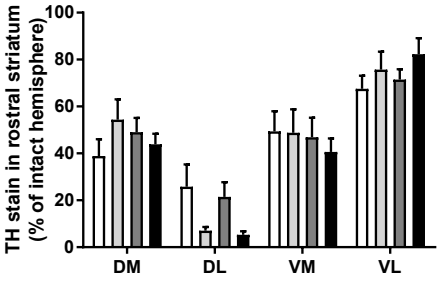

Figure 3.9: Characterisation of TH loss via stain densitometry in lesioned and intact striatum of lesioned animals dosed with Lu AF21934 or vehicle. a) Loss of TH throughout the lesioned striatum measured by reduction of TH stain densitometry. TH densitometry in b) caudal, c) mid and d) rostral striatum as a percentage of densitometry in the intact striatum. For all, data are mean ± S.E.M. and n=5-10 per group. DM, dorsomedial; DL, dorsolateral; VL, ventrolateral; VM, ventromedial.

3.4.1.5 Pharmacokinetics

Pharmacokinetic testing on plasma from Lu AF21934-treated animals revealed a drug presence of 925 ± 299ng/ml for animals dosed with 10mg/kg and 2014 ± 652ng/ml for animals in the 30mg/kg group 1 hour after oral administration of the compound. In previous studies conducted with Lu AF21934, the plasma concentration 1 hour after oral administration of 10mg/kg was found to be 869 ± 202ng/ml and 4733 ± 758ng/ml following administration of 30mg/kg Lu AF21934. The plasma concentration of Lu AF21934 following the 30mg/kg dose was therefore decreased considerably from the initial PK studies.

3.4.2 LSP1-2111 neuroprotection study

One animal in the 1mg/kg LSP1-2111 group was eliminated from analysis due to the lack of a lesion visible in TH histology. The optical density of TH stain in the lesioned striatum of this animal was > 2 standard deviations from the mean value of the group.

3.4.2.1 Cylinder test

There was no difference in performance between LSP1-2111 groups and the vehicle group in the cylinder test. When comparing the raw numbers of contralateral paw touches using a 2-way ANOVA (Figure 3.10a), there was no effect of LSP1-2111 treatment ($p = 0.51$), a main effect of time ($p < 0.0001$) and no interaction between variables ($p = 0.45$). Sidak's post-test revealed that, in vehicle-treated animals, there was a significant reduction in use of the contralateral paw compared to baseline (32 ± 3) at day 5 (7 ± 2) and 13 post lesion (20 ± 3, $p < 0.01$). Animals in the 1 and 10mg/kg LSP1-2111 treatment groups also showed significant declines of similar magnitude in use of the contralateral paw in the cylinder test at days 5, 9 and 13 ($p < 0.05$) and days 5 and 13 ($p < 0.05$) respectively.

(a)

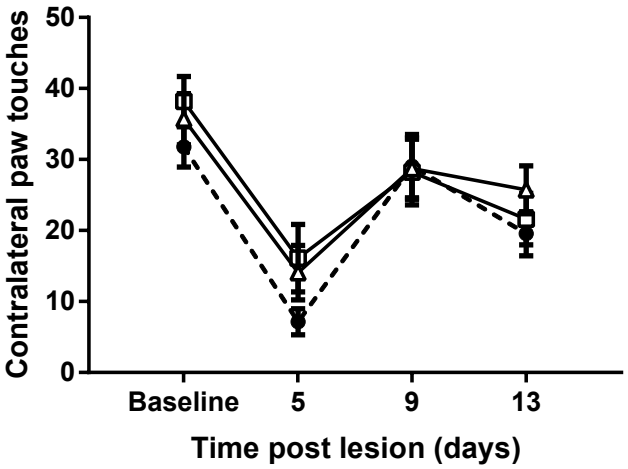

(b)

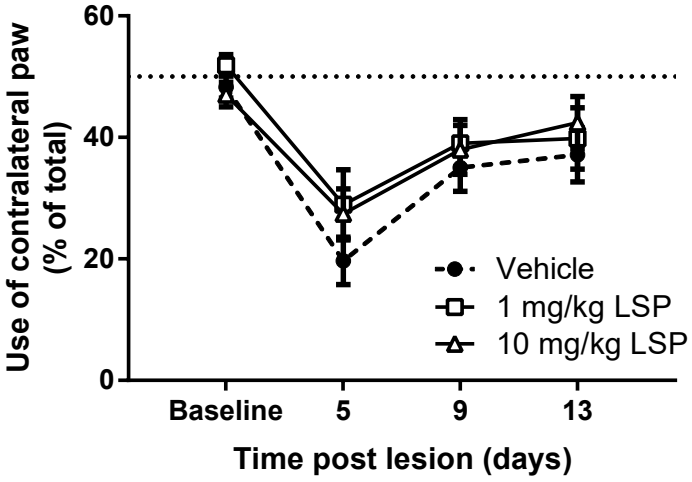

Figure 3.10: Numbers of weight-bearing touches made in the exploration of a novel environment (the cylinder test) over time by lesioned animals dosed with LSP1-2111 or vehicle. a) The average number of weight-bearing touches made with the contralateral paw by animals in each treatment group over time. b) The average number of contralateral weight-bearing touches expressed as a percentage of the total number of weight-bearing touches. For all, data are mean ± S.E.M. and n=9-10 per group.

3.4.2.2 Adjusted step test

The results of the adjusted step test here mirror those seen in the Lu AF21934 study. The forehand contralateral stepping condition was the most able to show the deficit resulting from the 6-OHDA lesion and other conditions showed a slow decline over time.

The adjusted step test was not able to differentiate between animals in different treatment groups in any condition. In the contralateral forehand condition, there was a significant effect of time ($p < 0.0001$) but not of treatment group ($p = 0.74$), and no interaction between variables ($p = 0.30$) in a repeated measures 2-way ANOVA (Figure 3.11a). In this condition, a Dunnett's post-test showed that animals in all groups were significantly impaired at all time points compared with their average baseline performance ($p < 0.05$). In the vehicle treatment group, forehand contralateral steps fell to 6 ± 1 steps from 12 ± 0 steps at baseline by day 5, and remained relatively stable at this level.

In the backhand contralateral condition, there was much less of a deficit compared to baseline, but still a significant effect of time ($p < 0.0001$) though not of treatment group ($p = 0.17$) and no interaction between variables ($p = 0.14$) in a repeated measures 2-way ANOVA (Figure 3.11b). However, a Dunnett's post-test showed that vehicle-treated animals performed a significantly reduced number of backhand contralateral steps at all time points post lesion ($p < 0.01$). Meanwhile, rats in the 1mg/kg treatment group did not significantly decline in performance after baseline and rats in the 10mg/kg group were only significantly poorer than baseline at 5 days post lesion ($p < 0.0001$) and 13 days post lesion ($p < 0.01$).

The ipsilateral conditions of the stepping test also found significant effects of time on performance in a 2-way ANOVA (Figures 3.11c and 3.11d). Dunnett's post-tests revealed that only the vehicle treated animals performed significantly fewer steps at days 9 and 13 post-lesion than at baseline ($p < 0.05$) in the forehand condition. In the backhand condition, vehicle-treated animals performed significantly fewer steps at days 9 and 13 ($p < 0.001$), animals in the 1mg/kg LSP1-2111 group performed significantly fewer steps only at 13 days post-lesion ($p < 0.0001$) and animals treated with 10mg/kg LSP1-2111 performed significantly fewer steps at days 9 ($p < 0.05$) and 13 ($p < 0.0001$) than at baseline.

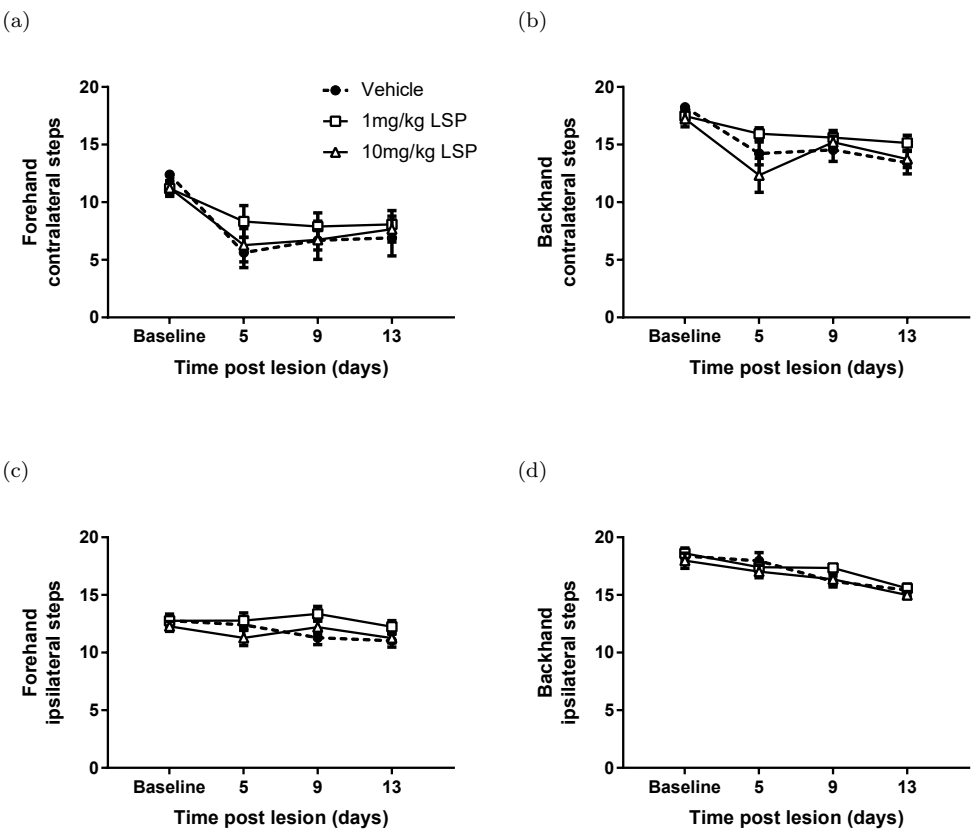

Figure 3.11: Numbers of adjusting steps taken by animals with their contralateral and ipsilateral paws before and at 3 time points following a unilateral, partial 6-OHDA lesion. Steps taken with the contralateral paw in the a) forehand and b) backhand direction. Steps taken with the ipsilateral paw in the c) forehand and b) backhand direction. For all, data are mean ± S.E.M. and n=9-10 per group.

3.4.2.3 Amphetamine-induced rotations

The amphetamine-induced rotation test was implemented on day 11 post-lesion, 3 days following the last administration of LSP1-2111 or vehicle. There was no significant effect of treatment ($p = 0.080$) but a significant effect of time ($p < 0.0001$) and a significant interaction between variables ($p < 0.0001$) in a repeated measures 2-way ANOVA (Figure 3.12a). A Bonferroni post-test revealed that vehicle-treated animals rotated significantly more than their pre-amphetamine baseline from 20-75 minutes ($p < 0.01$). Animals in the 1mg/kg LSP1-2111 group produced significantly more rotations than baseline for a shorter length of time (20-55 minutes, $p < 0.05$) and animals in the 10mg/kg LSP1-2111 group did not rotate significantly more than baseline during any of the recorded 5 minute time bins. If the same analysis is performed over only the peak rotational period (which, here, is between 20-60 minutes post-amphetamine) as is used in Betts et al. (2012), a significant effect of treatment becomes apparent ($p < 0.05$). Specifically, at 35 and 40 minutes post-amphetamine, animals in the 10mg/kg LSP1-2111 group rotate significantly less than animals in the vehicle group.

Despite an obvious trend towards a dose-dependent reduction in rotations performed by animals in LSP1-2111 groups, there was no significant difference between total numbers of rotations performed by animals in different treatment groups in a 1-way ANOVA ($p = 0.079$, Figure 3.12b). However, if the same analysis is performed over the peak activity period of 20-60 minutes, animals treated with 10mg/kg LSP1-2111 are shown to produce significantly fewer ipsiversive rotations than vehicle-treated animals (Figure 3.12c).

(a)

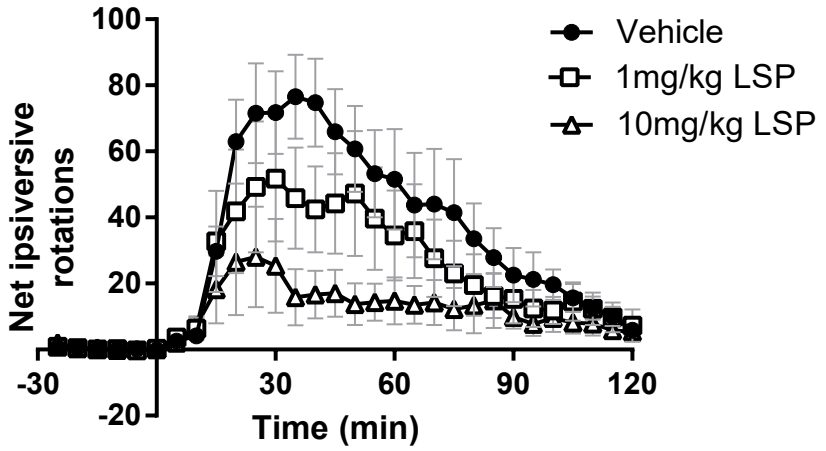

(b)

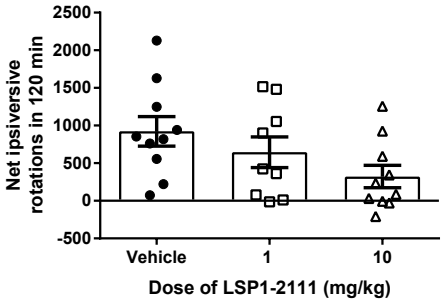

(c)

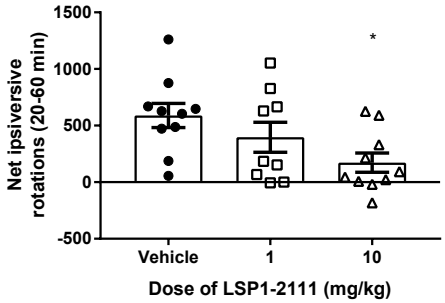

Figure 3.12: Net numbers of amphetamine-induced ipsiversive rotations in lesioned animals dosed with LSP1-2111 or vehicle. a) Net ipsiversive rotations (ipsiversive - contraversive) for each treatment group in 5 minute time bins prior to and following administration of 5mg/kg amphetamine. Standard error bars are rendered in light grey for ease of data visualisation. * = $p < 0.05$, ** = $p < 0.01$ against average baseline rotations across time points indicated by horizontal bar in 2-way repeated measures ANOVA witn Bonferroni post-test. Solid bar shows time points with significantly more rotations than baseline for vehicle treated animals, while the dotted bar indicates time points with significantly more rotations than baseline for 1mg/kg LSP1-2111-treated animals. Animals treated with 10mg/kg LSP1-2111 did not rotate significantly more than baseline at any point. b) Total number of net ipsiversive rotations over the 120 or c) 20-60 minutes post-amphetamine, * = $p < 0.05$ vs vehicle controls in a 1-way ANOVA with Dunnett's post-test. For all, data are mean ± S.E.M. and n=9-10 per group.

3.4.2.4 Histological characterisation of lesion

Figure 3.13 shows representative images of TH-stained SNc from animals in each of the treatment groups in the LSP1-2111 neuroprotection study. There appears a subtle lesion, as before, in the right hemisphere SNc. From the images, it is difficult to ascertain whether there are a greater number of cells in the lesioned SNc of LSP1-2111-treated animals. When examining the number of TH-positive cells in the lesioned SNc through cell counts however, it was found that there was a significant preservation overall in the SNc in animals treated with 10mg/kg LSP1-2111 compared to vehicle ($p < 0.05$, Figure 3.14a).

When each level of the SNc was considered, there was a significant effect of treatment group ($p = 0.019$) and a significant effect of nigral level ($p = 0.0002$) but no significant interaction between variables ($p = 0.68$) in a 2-way ANOVA (Figure 3.14b). Sidak's post-test revealed that, in the caudal, lesioned SNc, there was an average of preservation of $72.1\% \pm 4.5$ cells in the lesioned SNc in vehicle-treated animals, $82.9\% \pm 5.8$ in animals treated with 1mg/kg LSP1-2111 and $87.3\% \pm 6.7$ in animals treated with 10mg/kg LSP1-2111. This trend towards a dose-dependent preservation of cells was retained in mid SNc, and also in the rostral SNc where the animals treated with 10mg/kg had significant preservation of TH-positive cells in the SNc compared to vehicle-treated animals ($87.2\% \pm 8.0$ of intact compared with $56.9\% \pm 5.7$ in the vehicle-treated group).

When examining raw numbers of TH positive cells (Figure 3.14c), there was evidence of significant cell loss only in the rostral level of the SNc and only in vehicle or 1mg/kg SNc-treated animals, and not in animals treated with 10mg/kg LSP1-2111 ($p < 0.0001$ for effect of level and treatment in a 2-way ANOVA, with further results through Sidak's post-test).

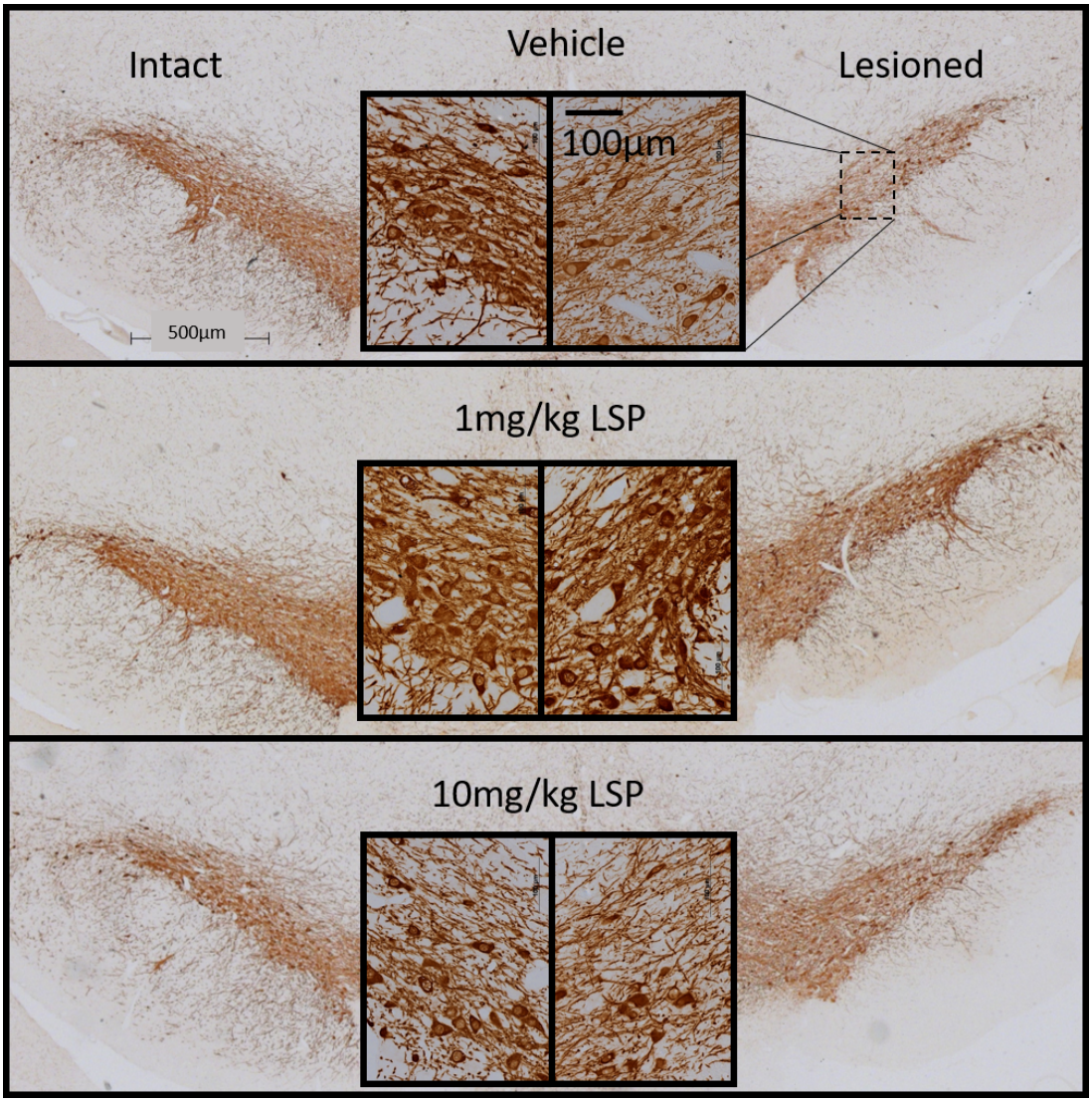

Figure 3.13: Representative images of TH stain in the rostral SNc (approximately -5mm from bregma) of animals from each treatment group.

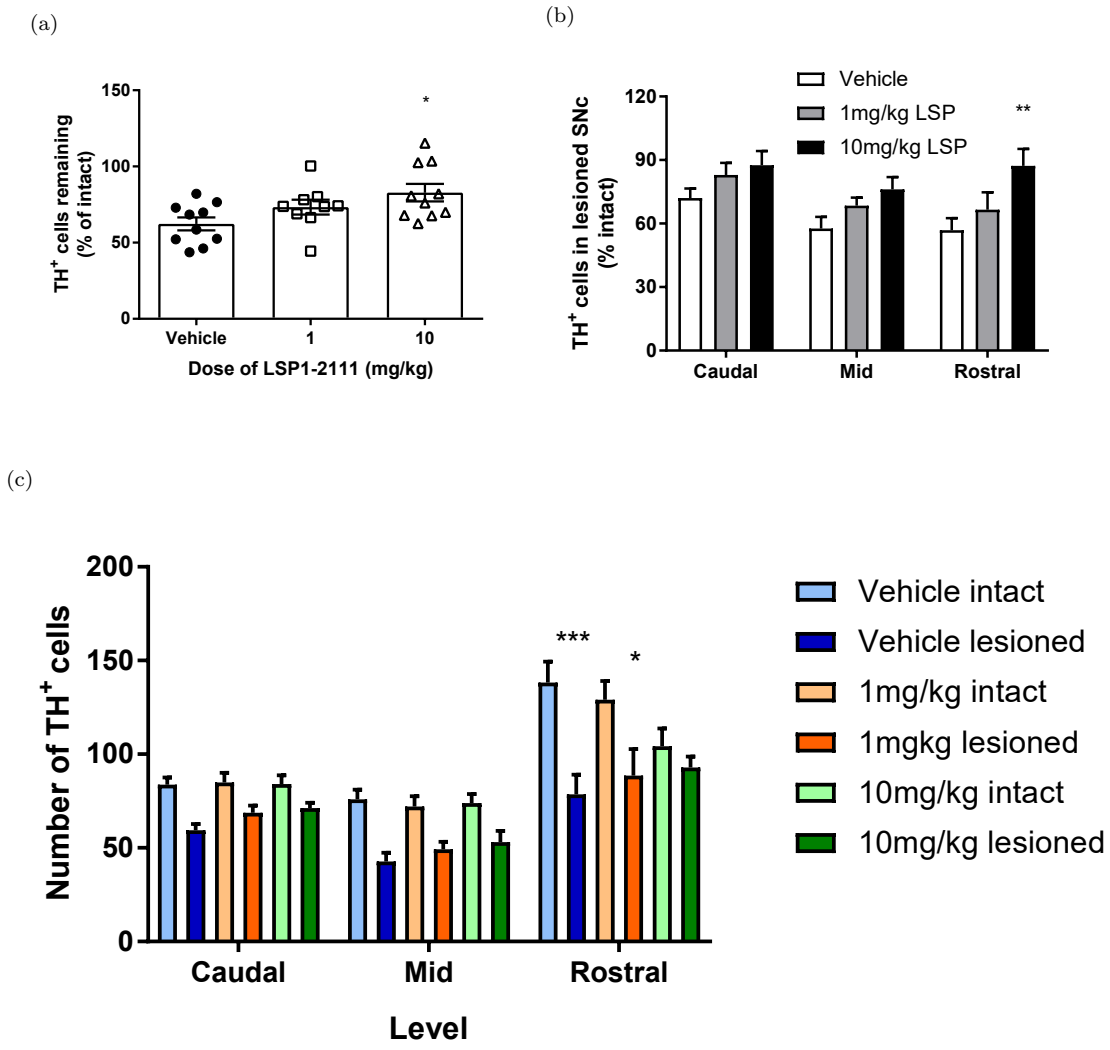

Figure 3.14: Counts of TH-positive cells in lesioned and intact SNc following LSP1-2111 or vehicle treatment. a) Overall average TH cells remaining in the SNc (as a percentage of intact) * = $p < 0.05$ compared to vehicle group in 1-way ANOVA with Dunnett's post-test. b) Average TH-positive cells remaining in each level of the SNc for each treatment group as a percentage of the intact SNc. ** = $p < 0.01$ compared to vehicle group in 2-way ANOVA with Sidak's post-test. c) Overall raw cell counts for each level of the SNc in each treatment group. * = $p < 0.05$ and *** = $p < 0.001$ compared to contralateral side in 2-way ANOVA with Sidak's post-test. For all, data are mean ± S.E.M. and n=9-10 per group.

Figure 3.15 shows representative images of the TH-stained striatum of animals from each treatment group. Lesions are visible as a reduced density of TH stain in the right-side, dorsal striatum all animals, but there appears to be a dose-dependent reduction of lesion in sections from LSP1-2111-treated animals.

There was a non-statistically significant trend towards a dose-dependent effect of LSP1-2111 treatment on the density of TH stain when averaged across all levels and quadrants of the striatum ($p = 0.099$, Figure 3.16a). In vehicle-treated animals there was an average of $42.6\% \pm 5.4$ TH stain remaining in the lesioned striatum as compared with the intact hemisphere. In animals in the 1mg/kg LSP1-2111 treatment group there was an average of $49.7\% \pm 8.4$ TH remaining in the lesioned striatum and in the 10mg/kg group there was $63.2\% \pm 6.2$ remaining.

There was, however, a significant effect of treatment on striatal TH stain density at both caudal and mid levels ($p < 0.01$), a significant effect of quadrant on the analysis at all levels ($p < 0.0001$) and no interaction at any level ($p = 0.8$) in 2-way ANOVAs (Figures 3.16b, 3.16c, 3.16d). Dunnett's multiple comparisons tests revealed that striatal lesion size was significantly lower in animals in the 10mg/kg LSP1-2111 group than vehicle-treated animals in the dorsolateral and ventrolateral quadrants of the mid striatum only ($p < 0.05$ Figure 3.16c).

As in the consideration of the data in the Lu AF21934 neuroprotection study, it may be of value to consider that the lesion is dorsal in nature. When only the dorsal quadrants are taken into account, there remains no significant effect of treatment ($p = 0.12$). In order to verify the reliability of TH as a marker of true striatal terminal loss, the pattern of dopamine active transporter (DAT) loss within the mid striatum was examined. There was found to be a similar trend towards preservation of stain with the lesioned striatum of vehicle-treated animals containing a level of DAT staining equivalent to $31.5\% \pm 3.1$ of the intact striatum, animals in the 1mg/kg LSP1-2111 group showing levels of $38.6\% \pm 21.2$ that of intact and 10mg/kg animals showing $43.8\% \pm 6.3$ that of the intact striatum (data not shown).

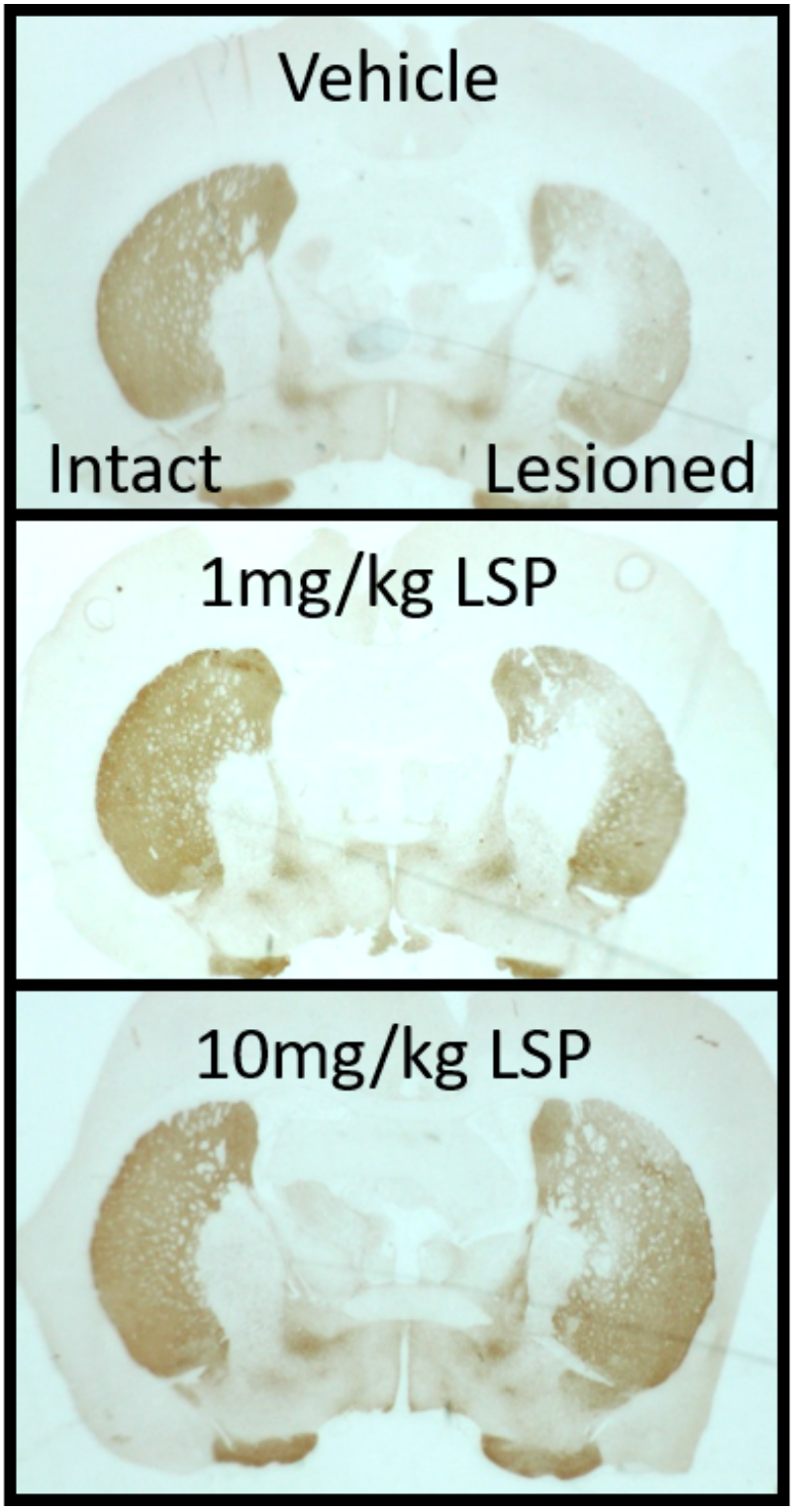

Figure 3.15: Representative images of TH stain in caudal striata from animals in each treatment group

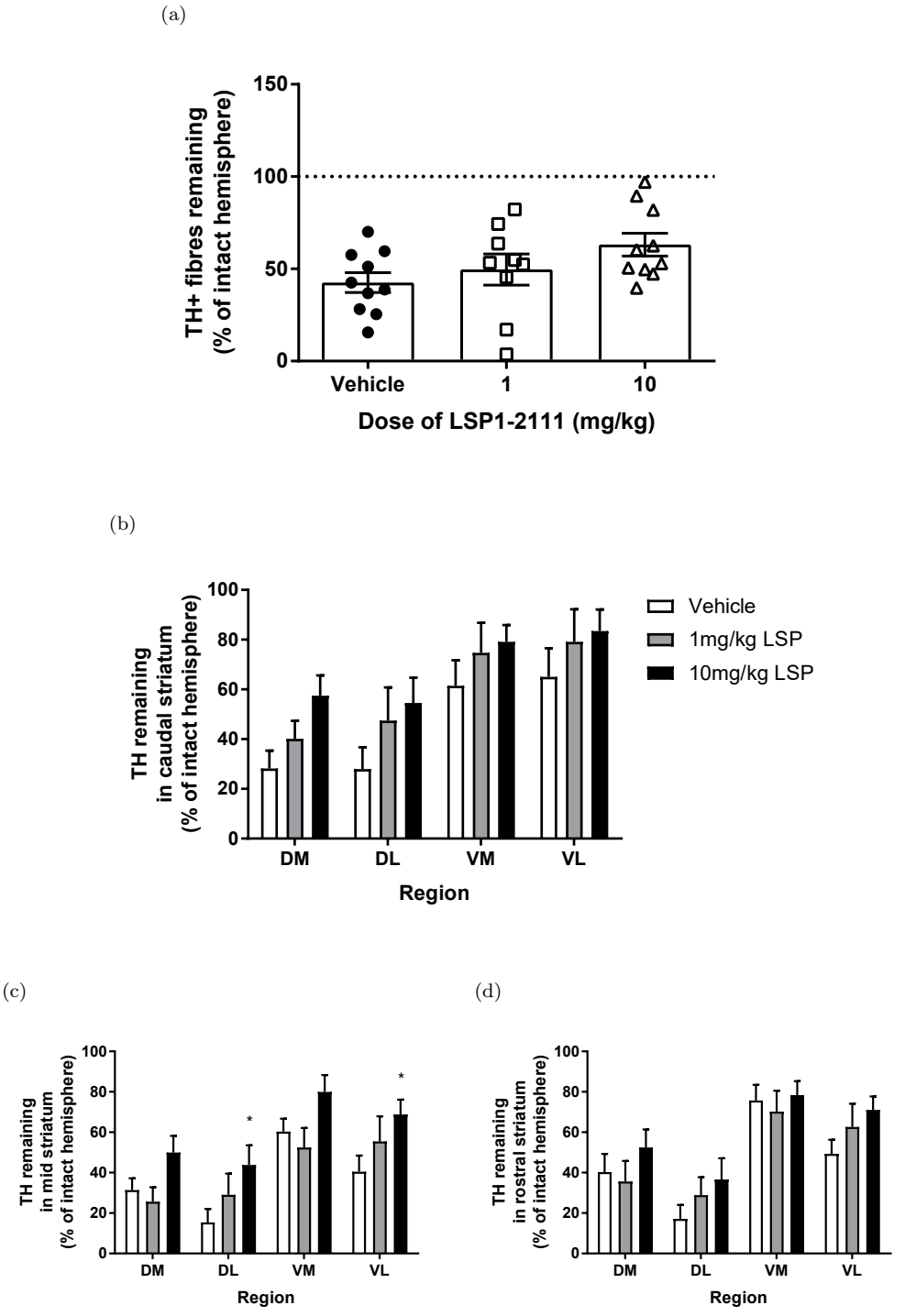

Figure 3.16: TH stain density was examined in quadrants of lesioned and intact striatum of animals in vehicle or LSP1-2111 treatment groups. a) Striatal TH remaining across all levels and quadrants of the striata averaged and expressed as a percentage of the densitometry of the contralateral striatum. b-d) A break down of the TH levels in each quadrant of the striatum at the caudal, mid and rostral levels, as a percentage of the equivalent quadrant of the intact hemisphere. * = $p < 0.05$ against vehicle in a 2-way ANOVA with Dunnett's post-test. For all, data are mean ± S.E.M. and n=9-10 per group. DM, dorsomedial; DL, dorsolateral; VL, ventrolateral; VM, ventromedial.

3.4.2.5 Pharmacokinetics

Pharmacokinetic testing on plasma samples from LSP1-2111-treated animals revealed a drug presence of 897±237ng/ml for animals dosed with 1mg/kg and 10546±2725ng/ml for animals in the 10mg/kg group 1 hour after s.c. administration of the compound. In previous studies conducted with LSP1-2111, the plasma concentration 1 hour after a single s.c. administration of 10mg/kg was found to be 11000±1000ng/ml, with a corresponding concentration of 700±400 ng/ml in brain extracellular fluid Cajina et al. (2014).

3.4.3 LSP1-2111 in MPTP-treated primates

3.4.3.1 Locomotor activity

Locomotor activity was measured in MPTP-treated marmosets from 30 minutes prior to administration of LSP1-2111 and L-DOPA to 5 hours (300 minutes) post administration. These measurements were taken in an automated fashion through infrared beam breaks. In accordance with previously conducted pharmacokinetic analysis (Cajina et al. 2014, Iderberg et al. 2015) and observations, the peak behavioural response to both compounds was 30-60 minutes following administration.

Movement patterns of the hyperkinetic animals was characterised by periods of inactivity on the floor or perch of the cage followed by outbursts of frantic movement often involving quick series' of leaps between walls and perches.

Data were transformed by $y = \sqrt{y}$ in order to normalise distribution of data points and enable parametric tests (Fisher et al. 2018). Although locomotor activity theoretically in not bounded and therefore may not require normalisation, in this case, animals reaching a high point of hyperkinesis are likely to become severely dyskinetic - thereby limiting the locomotor activity scale. Therefore this data normalisation procedure was applied to account for 'abnormality' of the driven activity such as that following administration of L-DOPA.

A repeated measures 2-way ANOVA showed that there was a significant effect of time following administration ($p < 0.0001$) and of treatment ($p < 0.0001$) on locomotor activity, and a significant interaction between the two variables ($p < 0.0001$, Figure 3.17a). Sidak's multiple comparisons post-test examining the difference between locomotor activity produced by each treatment to their respective baseline point (30 min prior to administration) found significant increases in activity following L-DOPA (30-90 minutes post-administration, $p < 0.001$) and all combinations of L-DOPA and LSP1-2111 (at 60 minutes post-administration for 1mg/kg, $p < 0.01$, 30-90 minutes for 3mg/kg, $p < 0.001$ and from 30-160 minutes for 6mg/kg, $p < 0.001$).

A repeated measures 1-way ANOVA on the area under the curve of the locomotor activity over time (Figure 3.17c) found there to be a significant effect of treatment ($p = 0.0049$), though Sidak's multiple comparisons post-test was not able to find any further differences between treatments and their relative vehicle control (vehicle/vehicle for either L-DOPA or LSP1-2111 alone and L-DOPA alone as a control for L-DOPA with LSP1-2111).

(a)

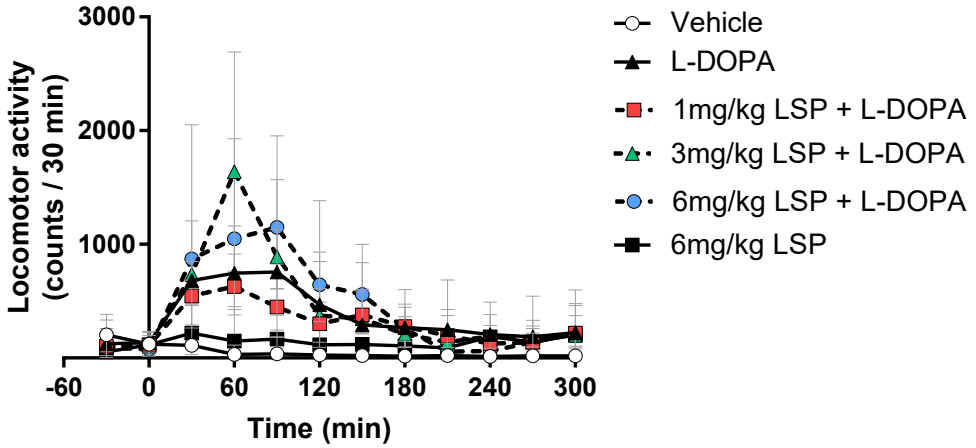

(b)

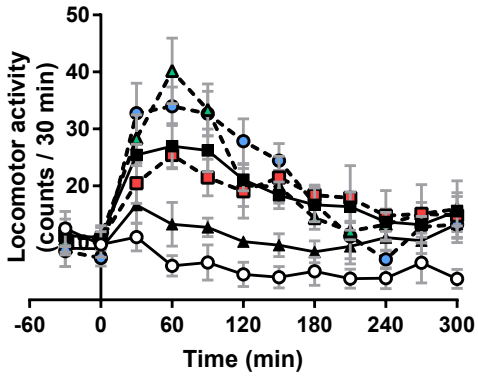

(c)

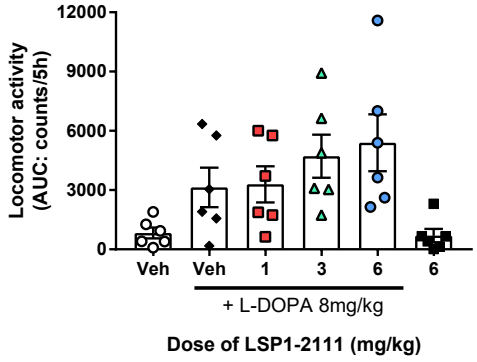

Figure 3.17: Efficacy of LSP1-2111 treatment, with or without L-DOPA, in improving locomotor activity in MPTP-treated marmosets as measured by infrared beam breaks over time. a) Change in locomotor activity in MPTP-treated marmosets over time following treatment with L-DOPA and/or varying concentrations of LSP1-2111. b) A graph of $y = \sqrt{y}$ from subfigure a. c) Graph displaying the area under the curve of the data displayed in graph a. Data are median ± interquartile range and n=6 per group.

3.4.3.2 Disability

Disability of MPTP-treated marmosets was examined by trained observers using a 19-point scale comprising 8 different measures of ability (detailed on p.115) and the data transformed in the same $y = \sqrt{y}$ method for analysis. When examined over time, motor disability was significantly impacted by the time post administration ($p < 0.0001$) and by treatment ($p < 0.0001$), with some small interaction between variables ($p < 0.0001$) in a repeated measures 2-way ANOVA (Figure 3.18a). A Sidak's multiple comparisons test revealed that when animals were given vehicle/vehicle, no significant reduction in motor disability was seen at any time point compared to the baseline (0 minutes post-administration). In contrast, when animals were given L-DOPA with 3mg/kg LSP1-2111, they had significantly reduced disability from 30 - 300 minutes following administration ($p < 0.001$). When given L-DOPA alone or with 1mg/kg LSP1-2111, animals showed significant reduction in disability from 30 - 270 minutes ($p < 0.001$). Following administration of 6mg/kg LSP1-2111 with LSP1-2111, marmosets had significantly reduced disability from 30 - 210 minutes and again at 270 minutes following administration ($p < 0.001$). Importantly, LSP1-2111 alone was also capable of reducing motor disability in these animals, with a significant reduction from 30 - 180 minutes ($p < 0.001$) compared with their baseline measure.

In Figure 3.18b, the data from the vehicle/vehicle, L-DOPA/vehicle and vehicle/LSP1-2111 conditions are presented alone for ease of visualisation. In this figure, both LSP1-2111 and L-DOPA groups are compared to the vehicle/vehicle group and show highly significant improvements in motor disability.

There was also a significant difference between treatment groups and their respective control when the data were examined in the area under the curve format (Figure 3.19b) and tested using a repeated measures 1-way ANOVA ($p < 0.0001$). Sidak's multiple comparisons post-test further showed a significant decrease in motor disability in animals treated with LSP1-2111 or L-DOPA alone ($p = 0.0004$ and $p = 0.0014$ respectively) compared to double vehicle condition animals. Although LSP1-2111 and L-DOPA combination groups also show significantly improved motor disability compared with the double vehicle condition, they are not significantly different from their L-DOPA/vehicle control.

(a)

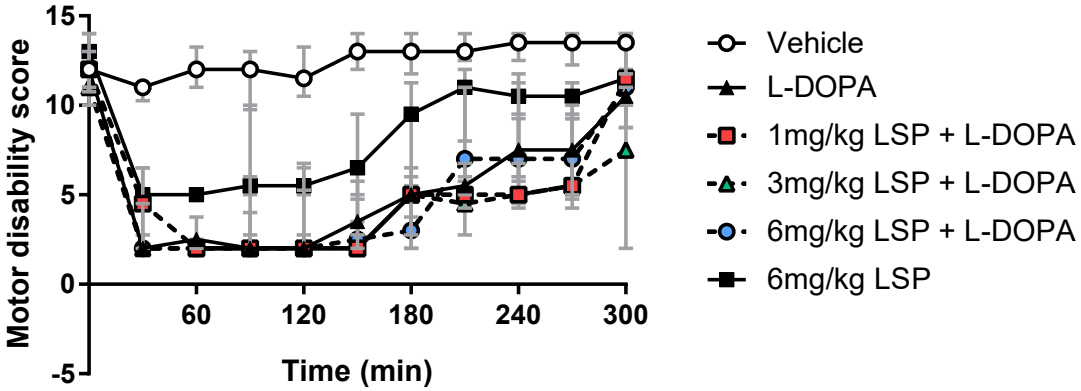

(b)

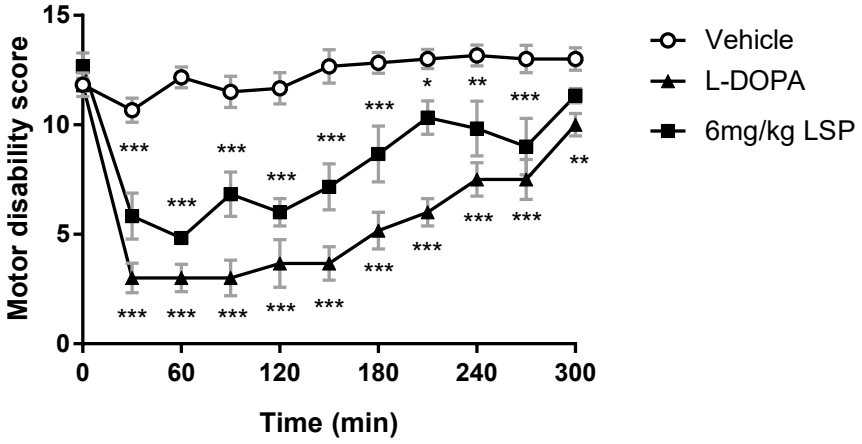

Figure 3.18: Efficacy of LSP1-2111 treatment, with or without L-DOPA, in reducing scored disability in MPTP-treated marmosets. a) Change in motor disability score in MPTP-treated marmosets over time following treatment with L-DOPA and/or varying concentrations of LSP1-2111. b) Simplification of the graph shown in a comparing the efficacy of LSP1-2111 alone and L-DOPA alone to vehicle/vehicle in the relief of motor disability. * = $p < 0.05$, ** = $p < 0.01$ and *** = $p < 0.001$ against vehicle condition in a 2-way repreated measures ANOVA with Sidak's post-test. Data are median ± interquartile range and n=6 per group.

(a)

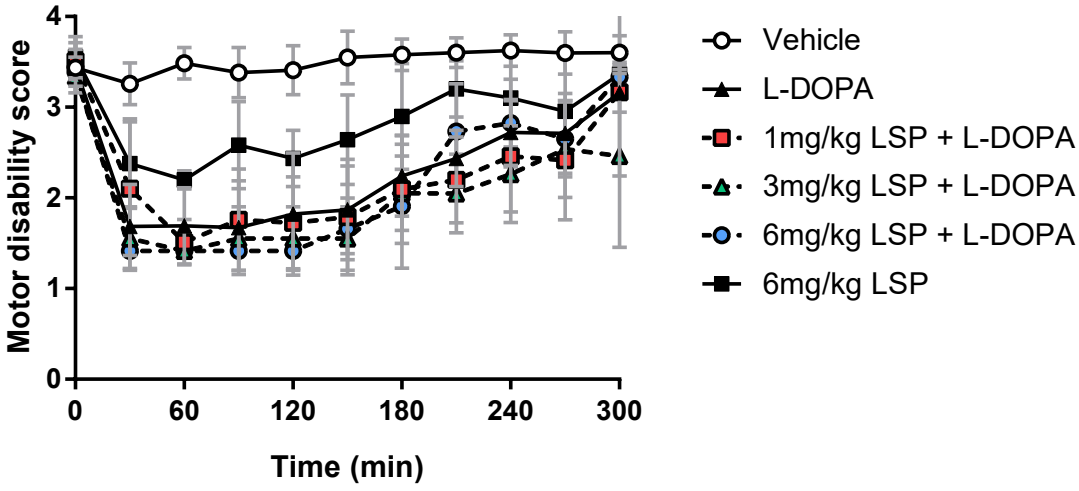

(b)

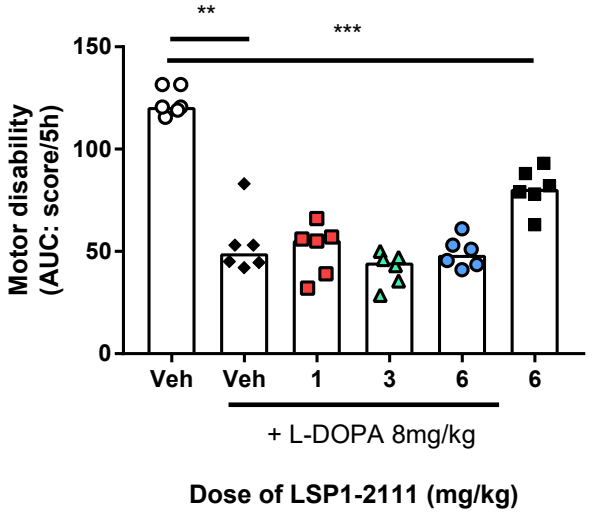

Figure 3.19: Transformed data indicating efficacy of LSP1-2111 treatment, with or without L-DOPA, in reducing scored disability in MPTP-treated marmosets. a) A graph of $y = \sqrt{y}$ from 3.18a. b) Graph displaying area under the curve data from 3.18a. ** $= p < 0.01$, *** $= p < 0.001$ in a RM 1-way ANOVA with Sidak's post-test comparing groups to relevant vehicle. Data are median ± interquartile range and n=6 per group.

3.4.3.3 Dyskinesia

Dyskinesia (encompassing choreic and dystonic types) was measured on a 4-point scale by trained observers and the data transformed by $y = \sqrt{y}$ for analysis. In a repeated measures 2-way ANOVA (Figure 3.20a), there was found to be a significant effect of time ($p < 0.0001$) and treatment ($p < 0.0001$) and an interaction between the two ($p < 0.0001$). In a Sidak's post-test, it was found that the administration of 6mg/kg LSP1-2111 alone did not cause significant dyskinesia compared to the baseline measure taken at 0 minutes post-administration. When marmosets were administered L-DOPA alone, they showed significant dyskinesia from 30-120 minutes post administration. When 1, 3 or 6mg/kg LSP1-2111 was given in addition, dyskinesias were visible from 60 - 120 minutes ($p < 0.001$), 30 - 120 minutes ($p < 0.001$) and 30 - 150 minutes ($p < 0.001$) respectively.

When these data are presented in the format of area under the curve (Figure 3.20c), a 1-way repeated measures ANOVA finds a significant effect of treatment ($p = 0.0002$). Sidak's multiple comparisons post-test further revealed that, as expected, L-DOPA alone caused significant dyskinesia compared to the double vehicle condition ($p < 0.05$). Key to the aims of this experiment, Figure 3.20c shows that there was no significant increase in expression of dyskinesia following administration of LSP1-2111 than following vehicle alone - meaning that LSP1-2111 alone does not cause dyskinesia. Secondly, LSP1-2111 does not significantly reduce or increase dyskinesia when given in combination with L-DOPA compared with L-DOPA alone.

(a)

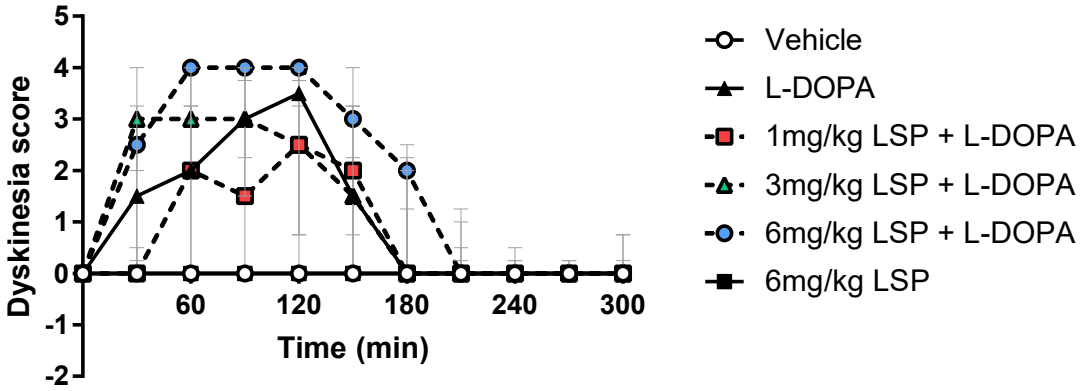

(b)

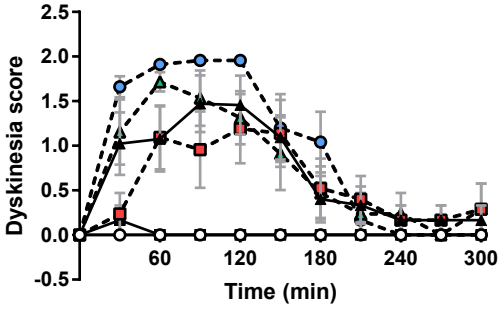

(c)

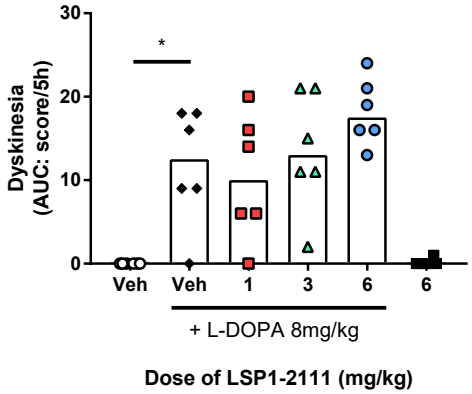

Figure 3.20: Efficacy of LSP1-2111 treatment, with or without L-DOPA, in reducing scored dyskinesia in MPTP-treated marmosets. a) Change in dyskinesia in MPTP-treated marmosets over time following treatment with L-DOPA and/or varying concentrations of LSP1-2111. b) Transformed data by $y = \sqrt{y}$ from subfigure a. c) Efficacy of LSP1-2111 treatment in reducing dyskinesia in MPTP-treated marmosets. * = $p < 0.05$ in a RM 1-way ANOVA with Sidak's post-test comparing groups to relevant vehicle. Dunn's multiple comparisons. Data are median ± interquartile range and n=6 per group.

3.5 Discussion

These studies sought to examine the neuroprotective efficacy of an mGluR4 PAM (Lu AF21934) and an mGluR4 agonist (LSP1-2111) in a rat partial lesion model of Parkinson's disease. In addition, the potential antiparkinsonian and L-DOPA-sparing abilities of LSP1-2111 were tested in MPTP-treated marmosets. In brief, the studies revealed a lack of neuroprotective efficacy with Lu AF21934 and a modest neuroprotective effect of LSP1-2111 in the 6-OHDA rat model. Further tests revealed an antiparkinsonian effect of LSP1-2111 but no antidyskinetic effect in MPTP-treated marmosets.

3.5.1 Lu AF21934 neuroprotective study

The Lu AF21934 neuroprotection study followed from a previous study completed in this group examining the ability of Lu AF21934 to provide neuroprotection in a full-lesion rat model of PD. This, in turn, arose from the observation that VU0155041, a compound with both mGluR4 agonist and PAM activity, could provide a neuroprotective effect when injected intracranially. The aims of these subsequent studies were to replicate these effects with systemically bioavailable mGluR4 compounds.

The previous full-lesion Lu AF21934 study failed to find a neuroprotective effect of treatment (Finlay 2014) however, it was hypothesised at the time that this may be due to the rapid and severe development of a full lesion impeding any potential for systemically administered pharmacological intervention. The implementation of a partial lesion with a slower rate of degeneration and lesser dopaminergic cell and terminal loss, as described in Chapter 2, was hypothesised to combat this barrier to protection.

Here, it is apparent that the employment of a partial lesion has not improved the neuroprotective efficacy of orally-administered Lu AF21934. No neuroprotection was observed through the examination of nigral dopaminergic cells or striatal terminals and no significant functional preservation was seen in any of the behavioural tests implemented in the study.

Two factors may have had some confounding effect on the data gathered during this study, though it is difficult to imagine that either could mask a robust protective effect completely:

- The small group size of animals in the 30mg/kg Lu AF21934 cohort ($n = 5$ compared with

$n = 10$ in other groups). Ideally groups to be compared will comprise the same number of individuals. In this case, however, limited availability of Lu AF21934 itself forced a smaller size of the highest dose group. Both unequal group sizes and small group sizes predispose towards a higher likelihood of type 2 statistical errors (false negative - incorrect acceptance of the null hypothesis). However, if this were the case in the present study, it might still reasonably be expected that hints of a dose-dependent protective effect could be seen in the 1mg/kg or 10mg/kg Lu AF21934 groups which was certainly not the case here.

- The plasma drug concentration of animals from the present study was 925 ± 299ng/ml for animals dosed with 10mg/kg and 2014 ± 652ng/ml for animals in the 30mg/kg group. In a previous study, the plasma concentration at the same time point was found to be 869 ± 202ng/ml in animals dosed with 10mg/kg and 4733 ± 758ng/ml following administration of 30mg/kg Lu AF21934. Although plasma concentrations between the two studies match for the 10mg/kg dose, the 30mg/kg is less than half in the present study than was was observed in the past. It is important to remember that, in the previous PK study, naïve animals were given a single, acute dose of Lu AF21934 prior to sampling. In contrast, the PK in the present study was on plasma taken from lesioned animals following almost 9 days of twice-daily dosing with Lu AF21934. These key differences in protocol may be responsible for the difference between PK values, perhaps due to enzyme induction following chronic exposure (reviewed in Barry & Feely (1990)).

  Although the process of Lu AF21934 metabolism has not been detailed in the published literature, it seems sensible to suspect that cytochrome P450 enzymes, typically located in the liver and resposible for the majority of phase I drug metabolism reactions, may be involved. Individual CYP450 enzymes have been shown to be differentially induced and inhibited depending on acute or chronic dosing regimens with a diverse array of compounds in different models (Alsaad et al. 2012, Fukushima et al. 2013, Ledesma et al. 2014). If Lu AF21934 can also have effects such as these on the induction or inhibition of the enzyme responsible for its metabolism, then this may explain why the PK values following a single dose differ from those obtained after 9 days of twice-daily dosing - particularly at high concentrations.

The final point to be addressed in regard to the Lu AF21934 study is the apparent trend towards a dose-dependent reduction in amphetamine-induced rotations. The test detailed here occurs 3 days after the end of regular dosing with Lu AF21934 and so is unlikely to result from an acute pharmacological effect of the drug as, with a plasma half life of approximately 1 hour, Lu AF21934

will not be present in the brain by this time point. The separation instead implies that there may be some longer term effect of Lu AF21934 which reduces the rotational response following amphetamine administration. This effect was also observed in the Lu AF21934 full-lesion study.

The reduction in net ipsiversive rotations was not due to a significant increase in contralateral rotations but rather reflective of reduced ipsiversive rotations. This alteration in behavioural response to amphetamine may be in response to an as-yet-unidentified neurochemical adaptation to the lesion as was observed by (Lynch & Carey 1989). This adaptation may underlie some finer changes in the activity of neurons within the basal ganglia which are not evident in TH histology. For example, Slawinska et al. (2013) propose that Lu AF21934 can alter the activity and firing rates of neurons in healthy mice. Gubellini et al. (2014) show that Lu AF21934 can significantly inhibit transmission across the striatopallidal synapse using an *in vitro* slice electrophyisology preparation and Wieronska et al. (2015) show, using *in vivo* microdialysis, that Lu AF21934 administration can inhibit release of dopamine and serotonin in the rat frontal cortex.

Further to this, PAMs have been shown, in some cases, to alter the rates of desensitization or deactivation of their target receptors (Weeks et al. 2014). In many cases, PAMs slow these events, opening the cells expressing the target receptor up to overactivation from the normal level of agonism by prolonging the effect of receptor binding (Quirk & Nisenbaum 2002, Sun et al. 2002, Weeks et al. 2014). In theory, it is possible that long term application of Lu AF21934 caused alterations in the functioning of the lesioned basal ganglia through excessive action of glutamate upon mGluR4 mediated by slow desensitization of the receptor. It has been suggested previously that, in the Parkinsonian basal ganglia, there are elevated levels of glutamate due to hyperactivation of the STN. Coupled with this, an increase in mGluR4 activity as may be driven by PAM-mediated slow desensitisation would likely result in a reduction in activity of the internal globus pallidus (GPi)-SNr complex. This, in turn, would disinhibit the thalamic nuclei and increase thalamocortical firing, thereby increasing locomotor activity. Such an effect would cause an apparent reduction of lesion effect in motor tests without necessarily providing protection.

Regardless of the uncertainty surrounding the generation of the behavioural data, it remains clear that the mGluR4 PAM, Lu AF21934, does not provide a neuroprotective effect in this model despite evidence from Battaglia et al. (2006) that a partial lesion may be protected by a systemically administered mGluR4 PAM. As mentioned previously, even with the use of a partial lesion model in the Lu AF21934 study presented here, there are a number of key differences remaining between the present study and the study of Battaglia et al. (2006) which make direct

comparison difficult. Chiefly:

- Methodological differences - The dosing regimen employed by Battaglia et al. (2006) involved a single administration of PHCCC prior to a single administration of MPTP, with immunhistochemical evaluation of the lesion taking place 7 days later. This a seemingly unlikely model of PD neuroprotective treatment - where treatment is given once and solely prior to development of measurable degeneration. In the present study, a more translatable model is used, wherein the potential neuroprotective compound is administered throughout the duration of lesion development.

- The potential neuroprotective compound is different - Although PHCCC and Lu AF21934 have never been directly compared, the pharmacokinetic properties of the two compounds are likely quite different. Certainly solubility, and therefore administration, is an issue for both compounds. While Battaglia et al. (2006) administer PHCCC in cremaphor EL or saline with 50% dimethyl sulfoxide (DMSO), the present study used PEG400. These vehicles are all known for having biological effects in their own right and indeed Battaglia et al. (2006) show a stark difference in immunohistochemical outcome of animals dosed with 50% DMSO or cremaphor EL alone.

- Different animal models of degeneration - Although terminal administration of 6-OHDA results in a partial lesion comparable to the lesion resulting from the application of a single dose of MPTP as in Battaglia et al. (2006), the use of an intracerebral injection in the present study may result in other model aspects not discussed by Battaglia et al. (2006). For example, neuroinflammation seen in the 6-OHDA model as a result of mechanical damage during the injection process would not be present in the systemic MPTP model. Although Battaglia et al. (2006) display staining for glial fibrillary acidic protein (GFAP) in their study, they do not show any quantification, making the inflammatory aspects of these two models difficult to compare. Neuroinflammation in the 6-OHDA model used in this study is discussed in detail in Chapter 4.

- Methods of measurement are different - In Battaglia et al. (2006), the quantification of neuroprotection via histology was undertaken in a different manner to that used here. In Battaglia et al. (2006), cells were counted in 10 sections which were taken to be representative of the the whole SNc and the total number of cells in the structure extrapolated using an estimated area size. In the present study, cells were counted in different areas of the SNc but no attempt was made to extrapolate to the whole structure. This difference in quantification may account for some differences in results between the studies due to the heterogeneity of cell loss and neuroprotection as characterised in the LSP1-2111 study detailed here.

- Behavioural measurement of neuroprotection - In Battaglia et al. (2006) no behavioural tests appear to have been conducted to examine the functionality of the neuroprotection. This additional information would have been useful in the characterisation of the observed neuroprotection and, further, would have provided a further point of comparison between the studies.

Thus, to conclude, although Battaglia et al. (2006) have achieved neuroprotection following systemic administration of an mGluR4 PAM in contrast to the present study, it is difficult to compare the two thoroughly in order to understand exactly why this difference in outcome has arisen.

3.5.2 LSP1-2111 neuroprotective study

Having failed to replicate the neuroprotective efficacy of the VU0155041 ago-PAM with Lu AF21934 - a systemically available mGluR4 PAM - this led us to propose that it was the agonist activity of VU0155041, rather than the PAM activity, that was important for neuroprotection. Thus, the next step was to examine the neuroprotective potential of LSP1-2111 - a systemically available agonist of mGluR4.

3.5.2.1 LSP1-2111-mediated neuroprotection

In the present study, the plasma concentration of LSP1-2111 1 hour after dosing with 10mg/kg LSP1-2111 s.c. in a lesioned animal treated twice daily for 9 days was found to be almost identical to that found in previous studies examining PK after a single dose in a naïve animal. Here, the value was measured at $10.6 \pm 2.7\mu$g/ml (29.12μM) while in naïve animals the concentration was measured at 11μg/ml (31μM) (Cajina et al. 2014). With an estimated plasma:brain ratio of 0.02 (Cajina et al. 2014), this suggests that a brain concentration of LSP1-2111 of 582nM would have been achieved in the present study - around one third of the EC_{50} at human mGluR4 of 1.5μM. Although the EC_{50} of LSP1-2111 at rodent mGluR4 is not published, LSP1-2111 has been shown to have functional effects at these doses (Wierońska et al. 2013, Iderberg et al. 2015). This may suggest that:

1. The EC_{50} of LSP1-2111 is lower in rats and mice than in humans, as has been documented for other substances (Hibell et al. 2000, Jemnitz et al. 2008).
2. *In vivo*, functional effects may be achieved at concentrations lower than the *in vitro* EC_{50}.
3. That neuronal excitability or functioning may be affected by long-term, 'low-dose' LSP1-2111.

In the present study, LSP1-2111 mediates a dose-dependent, significant preservation of the SNc overall. Although this protection is evident overall in animals following administration of 10mg/kg LSP1-2111, it appears to be driven in large part by the significant protection in the rostral SNc. This rostral effect may, in part, be due to there being seemingly fewer cells in the contralateral SNc of 10mg/kg LSP1-2111 animals than vehicle-treated animals (104 ± 9 compared to 138 ± 11) and thus a larger percentage of cells in the lesioned SNc. It is important to note that this difference in cells in the contralateral, rostral SNc is not significant. Accounting for the difference, it may be the case that rostral SNc sections in animals from the 10mg/kg group were cut at a slightly

different level than those from vehicle group. If this were the case, however, it would still be expected that the ratio of lesion-related cell loss would be maintained throughout the SNc - making the possibility of sections being from slightly different levels unlikely to skew the findings of this study. Furthermore, the average cell number in the rostral level of the contralateral SNc from the 10mg/kg group (104 cells) is more in line with cell numbers from the equivalent locations in vehicle-treated animals of the Lu AF21934 study (105 cells) and the time course study of Chapter 4 (107 cells) than is the vehicle group average in the present study (138 cells). These favourable comparisons with other studies further emphasise the reliability of the data and provide confidence in the protective effect seen with 10mg/kg LSP1-2111.

Dose-dependent preservation of TH terminals is also evident in the striatum. Although, when averaged, TH preservation in overall striatum is not significant, when each level and quadrant is individually examined, significant protection is evident in the lateral quadrants of the mid layer in the 10mg/kg LSP1-2111 group. This area of the striatum has been tied to sensorimotor function in rodents and broadly encompasses hindlimb, forelimb and vibrissae sensorimotor feedback via the sensorimotor cortex (Brown et al. 1998).

Whether the striatal functional topography may be mapped back to specific areas of nigral cell bodies has been a widely debated topic (Beckstead et al. 1979, Redgrave & Mitchell 1982, Deniau et al. 1996, Maurin et al. 1999) though it is now generally accepted that this is the case. Maurin et al. (1999) suggest that cell bodies in the rostral SNc may preferentially innervate sensorimotor areas of the striatum (mid level, dorsal striatum). This finding supports the significant preservation of dorsal areas on the striatum giving rise to significant preservation of the rostral SNc (or *vice versa*) as is seen here. It has also been suggested that lateral SNc cell bodies may preferentially project to lateral striatal areas (Deniau et al. 1996). In the present study, the SNc was not divided into medial and lateral areas but it is nevertheless interesting to speculate that medial-lateral differences in cell preservation within the SNc might mirror the slightly more lateral lesion within the striatum here too.

The reason for the specific preservation of these sites is not immediately apparent. The dorsal striatum in rats, or caudate as it is known in higher organisms, has been shown to have no expression gradient for D_1R (Piggott et al. 1999) but a caudal-rostral low-high gradient for D_2R (Levey et al. 1993, Alakurtti et al. 2013), though other groups have found exceptions to this finding (Piggott et al. 1999, Gangarossa et al. 2013). The SNc is thought to be more heterogeneous in composition, with Hanaway et al. (1970) noting that cells in the rostral SNc appear darker

in colour (perhaps indicating higher neuromelanin content) and larger in size in the rat than cells in the caudal SNc. The differences in cell composition and receptor expression observed in these studies suggest that differential expression of mGluR4 within these structures is feasible. If mGluR4 expression varied in such a way throughout the striatum or SNc then this may be one explanation for the preferential preservation in the rostral SNc. However, a well detailed topography of striatal or nigral mGluR4 is not yet known.

3.5.2.2 Functional preservation

The dopaminergic neuroprotection observed in the SNc and striatum showed some signs of functional relevance in terms of improving motor outcomes - though only in tests of 'driven' movement and not in spontaneous motor tests.

In all treatment groups in the LSP1-2111 neuroprotection study, the cylinder test appears to show that the motor deficit is at its most profound on day 5 post-lesion, followed by a degree of functional recovery in all groups. This effect was observed to a lesser degree in the characterisation of the model in Chapter 2 but was muddied by a reduction in participation of the animals upon repeated exposure to the test. In the present study, participation was retained through the application of a greater number of stimuli in order to provoke exploratory behaviour and so a reduction of participation cannot be used to explain the apparent functional recovery by day 9 post-lesion.

Further to the observation of spontaneous improvements to motor function, LSP1-2111 appears to drive a very subtle improvement in the cylinder test, however this does not approach significance. The subtlety of this functional improvement following neuroprotection, compared with the amount of spontaneous recovery in all groups, suggests that crude measurements of weight-bearing touches in the cylinder test may not be optimal for picking out fine motor changes such as those which occur with the partial lesion model. Variations on the cylinder test have been used for assessing finer motor changes following various types of central nervous system damage (Roome & Vanderluit 2015). Footage from the tests detailed in the present study may be re-assessed by these alternative methodologies in the hope of finding further differences between animals in different treatment groups.

Similarly, there is no obvious effect of LSP1-2111 on the adjusted step test. With the contralateral paw, the 1mg/kg LSP1-2111 group appears to perform slightly better than the 10mg/kg or vehicle groups, with a more gradual decline in performance post-lesion in both the forehand and

backhand directions. This may, again, provide evidence that behavioural tests of a different type are required for this size of lesion.

In the amphetamine-induced rotation test, a clear separation between groups is evident, reflecting the significant reduction of lesion size following LSP1-2111 treatment. The 10mg/kg LSP1-2111 group performed significantly fewer rotations then the vehicle group when the most active period of the test was assessed. There may, again, be some underlying alterations to neuronal activity based on the long-term activation states of the mGluR4 receptor as was hypothesised for the Lu AF21934-mediated reduction in amphetamine-induced rotations. However, the overall difference in nigral lesion size seen between vehicle and 10mg/kg LSP1-2111-treated animals was approximately 20% (from 62.3% TH cells remaining in vehicle animals to 82.8% in LSP1-2111 animals). Such a substantial preservation of the SNc has been shown to impact measurably upon the number of rotations produced following amphetamine administration (Hudson et al. 1993) so the present data are consistent with this idea.

Finally, it may have been illuminating to apply some additional behavioural tests with these animals. Further tests could be specific for hindlimb, forelimb or vibrissae function and sensitivity in order to aid understanding of regional effects of the lesion or of protection in the striatum rather than broader tests of global motor circuitry used here (Brown et al. 1998).

The difference in efficacy between Lu AF21934 and LSP1-2111 in this paradigm is startling, particularly when considering that these two compounds share a target. The difference in their mechanism of action is likely the key to illuminating their difference in functional outcome. The PAM must necessarily rely on sufficient presence of an endogenous agonist (in this case, glutamate) in order to display a functional outcome of receptor binding. Should there be an insufficiency of such a ligand, for example at a GABA-ergic synapse such as the striatopallidal synapse, then a PAM with no intrinsic agonist activity, such as Lu AF21934, binding to mGluR4 will have no efficacy, while compounds with intrinsic agonist activity such as VU0155041 or LSP1-2111 will activate a signalling event.

It was originally theorised that in the PD or parkinsonian brain (as in the 6-OHDA-lesioned rat), overactivity of the STN would increase glutamate levels to such an extent that allosteric agonism at non-glutamatergic synapses would become a useful tool. However, using *in vivo* microdialysis, Finlay (2014) showed that glutamate levels are not significantly elevated in 6-OHDA-lesioned rat, at least at the SNc and SNr. Given this evidence, it may well be the case that Lu AF21934

failed to provide neuroprotection due to insufficient levels of endogenous glutamate to provide receptor activation at key GABA-ergic synapses within the basal ganglia (such as the striatopallidal synapse), while LSP1-2111 was effective in providing neuroprotection since the presence of glutamate was not necessary due to its orthosteric agonist properties.

Overall, these studies have revealed some neuroprotective efficacy of a systemically administered mGluR4 agonist, but not a PAM. MGluR4 agonists may therefore have a good future as neuroprotective treatments and are certainly worthy of further investigation.

3.5.3 LSP1-2111 in MPTP-treated marmosets

LSP1-2111 also showed promising antiparkinsonian activity in an established marmoset model of PD. In this model, LSP1-2111 was shown to be capable of reducing motor disability in Parkinsonian animals without causing dyskinesia. However, LSP1-2111 was not shown to be capable of reducing established LID when co-administered with L-DOPA.

One aim of this study was to examine the potential of LSP1-2111 to reduce LID in MPTP-treated marmosets. In this respect, the findings were clear: LSP1-2111 had no antidyskinetic effect. At all doses tested there was no real change in LID compared with L-DOPA alone - at 1mg/kg, the time of significant dyskinesia expression was slightly reduced and at 6mg/kg it was slightly increased. This finding is in agreement with rodent studies which find no L-DOPA sparing effects of a single administration of mGluR4 agonists to animals with established dyskinesia (Lopez et al. 2011, Iderberg et al. 2015). Furthermore, administration of 6mg/kg LSP1-2111 on its own did not cause any expression of dyskinesia in primed animals.

A second aim was to examine the potential antiparkinsonian efficacy of LSP1-2111. The additional readouts of disability and locomotor activity need some further interpretation before their meaning is clear. For example - one category of disability contributing to the score is motility, where a low score indicates normal activity but a high score may indicate either severe hyperkinesia or hypokinesia (either of which would reflect highly abnormal motility). Clearly, if the disability score is high due to hyperkinetic activity then this may also greatly contribute to high counts of locomotor activity. The use of beam breaks for quantification of locomotor activity provides valuable information but does not contain a readout of quality of movement - an important consideration in this case. The vehicle/vehicle condition shows that untreated Parkinsonian animals show very little motor activity in this test. Studies by other groups comparing healthy, untreated marmosets to drug treatment groups show that marmosets naturally do not move much once inside these unstimulating cages (Costall et al. 1987, Cagni et al. 2014). This therefore suggests that the extremely high levels of locomotor activity provoked by L-DOPA in this study are unnatural rather than therapeutic (Löschmann et al. 1992) - when these animals are given L-DOPA, it does not restore them to 'normal' levels of activity but instead makes them hyperkinetic. Using this comparison, the limited effect of LSP1-2111 alone on motility is put into perspective perhaps as a more healthy restoration of motor function despite the apparently low levels of movement in the cages over time.

This comparison of the performance of animals treated with LSP1-2111 alone to those same an-

imals treated with vehicle alone shows that the average locomotor count of LSP1-2111-treated animals at their peak of activity, 30 minutes post-administration (329 ± 135 beam breaks in half an hour), is considerably higher than a vehicle-treated MPTP marmoset produced (48 ± 25) (Johnston et al. 2010, Fisher et al. 2018). It is interesting to note that, in vehicle-treated animals, the peak of activity occurs immediately after their entrance into the test cage and, thereafter, almost strictly diminishes - as though driven by novelty alone. In contrast, even in animals treated with LSP1-2111 alone, the highest peak of activity occurs after the compound administration - perhaps showing an effect of drug overcoming the 'wearing off' of the novelty and the drive for exploration.

Further to this improvement in locomotor activity following LSP1-2111 alone, there appears a potentiation of L-DOPA-induced locomotor activity with with 6mg/kg LSP1-2111, with this condition causing a trend towards higher counts of locomotor activity than when animals were given LSP1-2111 alone. Conversely, the addition of 1mg/kg LSP1-2111 caused a reduction in the number of time points at which locomotor activity of these animals was significantly higher than at baseline compared with L-DOPA alone (though these data presented as area under the curve suggest no difference between these two conditions). These measurements may reflect the non-significant increase and decrease, respectively, in dyskinesia seen following the 1mg/kg and 6mg/kg combination treatment in comparison to L-DOPA alone, with the different incidences and severity of dyskinesia causing changes in movement and, consequently, beam breaks.

Motor disability was significantly improved for a long duration in animals after all treatments compared to vehicle/vehicle, including LSP1-2111 alone - and this measure gives the strongest evidence in this study that LSP1-2111 has antiparkinsonian activity in its own right. The motor disability score was composed of a number of different factors. The precise breakdown of which categories of motor disability scored what for each treatment would be of use in fully understanding the impact and mechanism of LSP1-2111 in treating symptomatic Parkinsonism in these animals.

The reduction in disability seen in these marmosets may mirror the effect underlying the mGluR4-mediated reduction in haloperidol-induced catalepsy seen in rodents by other groups (Bennouar et al. 2013, Iderberg et al. 2015) - reflecting a modulation of the indirect pathway of the basal ganglia. This effect has been shown to take place due to agonism of mGluR4 on the striatopallidal pathway (Marino et al. 2003, Valenti et al. 2003, Gubellini et al. 2014). Such an effect would reduce the concentration of GABA in the striatopallidal synapse, reducing the inhibition of the GPe and thereby increasing the downstream inhibition of the STN. This would have the end result

of correcting the functioning of the basal ganglia in order to restore normal motor function for a period. Indeed, this is reinforced by the findings of Bogenpohl et al. (2013), who found significant increases in the firing rate of striatal and pallidal neurons following microinjection of L-AP4 in awake, MPTP-treated rhesus macaques. This suggests normalisation of the basal ganglia function in Parkinsonian animals - compatible with the potential explanation of the findings of the present study. However, Bogenpohl et al. (2013) also investigated the ability of VU0155041 to modify firing rates in this same paradigm and found no effect - suggesting either that the improvement in firing rate is driven by a group III mGluR other than mGluR4, or that an agoPAM such as VU0155041 is incapable of proving the same functional alterations that an orthosertic agonist (such as LSP1-2111 and L-AP4) can.

This interpretation that an mGluR4 agonist has superior antiparkinsonian effect to an mGluR4 PAM appears at odds with the very recent finding of Charvin et al. (2018). In fact, the study by Charvin et al. (2018) finds that PXT002331, an mGluR4 PAM, provides a robust antiparkinsonian effect when given alongside L-DOPA but almost no effect when given alone. In the same study, Charvin et al. (2018) find an LID-reducing effect of PXT002331. This is in contrast to the present study which found no L-DOPA boosting or sparing property of the mGluR4 agonist but found that it served well in reducing Parkinsonism when given alone. This disparity in results between these two studies hints at a considerable difference between marmoset and macaque models (incorporating different MPTP dosing regimens for a different resulting lesion) and/or a difference in mechanism of action of the compounds.

- Macaques and marmosets are different in a number of key aspects. While marmosets are classed as new world monkeys, macaques are classed as old world monkeys - they are considerably larger in size, closer evolutionary relatives to humans and display more highly developed cognitive behaviours and facility to learn than marmosets (Spinelli et al. 2004, Wilson et al. 2013, Miller et al. 2016). The differences underlying this distinction in classification may include some key divergence in brain or neurochemical structure between these animals which limits their comparison in PD studies. However, Hardman et al. (2002) compared the basal ganglia of marmosets and macaques, alongside those of rats, baboons and humans, and found only subtle structural and neurochemical differences between the non-human primates. These differences within the group of primates were much smaller than the differences between the groups of rats, humans and the collection of primates. This evidence may suggest that the differences between marmoset and macaque, while considerable, may not affect the functioning of the basal ganglia and its response to drug treatment.

- In the present study, marmosets were dosed with MPTP at 2mg/kg daily for 5 days. Putting aside any potential differences in reaction to MPTP between marmosets and macaques, this is still a considerably different protocol for induction of Parkinsonism than Charvin et al. (2018) use for their macaque model. To provoke an early stage PD model, Charvin et al. (2018) use $0.05 - 0.25$ mg/kg MPTP intravenously, 2-3 times per week for up to 15 months. Their late stage model utilises a regimen of s.c. infusion of MPTP via an osmotic minipump for around 6 months (Charvin et al. 2018). As neither the present study nor the study by Charvin et al. (2018) examine the size of lesion which results from the lesioning protocol, and as activity of different species is difficult to compare usefully, it is hard to judge whether either of the lesioning protocols used by Charvin et al. (2018) map well onto the lesioning protocol used in the present study. If the lesions created are considerably different in size or location, this stark difference in method of induction of Parkinsonism may be a key factor underlying differences in response to mGluR4 compounds.

- One reason why PXT002331 might only provide therapeutic activity in the presence of L-DOPA may be that L-DOPA-mediates a change in glutamate availability throughout the basal ganglia, which may allow activity of the PAM through increased availability of endogenous agonist (Morin et al. 2013). As an orthosteric agonist, LSP1-2111 would not require such an increase in endogenous glutamate in order to cause an effect and so is capable of producing a therapeutic effect without L-DOPA. This may prove to be a more useful effect in the long term as it may delay (or remove) the need for L-DOPA treatment and the associated development of dyskinesia.

Overall, the present study shows the ability of LSP1-2111 to reduce disability in Parkinsonian animals without inducing dyskinesia. Although not undertaken as part of this thesis, Lu AF21934 was also examined in a similar study with MPTP-treated marmosets and found to have neither a positive nor a negative effect on dyskinesia or on disability (unpublished observation).

3.6 Summary and conclusions

Sub-chronic Lu AF21934 administered during lesion development was unable to provide functional improvement or neuroprotection in a partial lesion rat model of Parkinson's. In the same paradigm, LSP1-2111 provided modest but significant protection to TH-positive SNc cells and protection of TH terminals in the striatum and functional improvement. Furthermore, acute LSP1-2111 alone reduced motor disability in MPTP-treated marmosets and did not cause dyskinesia. The difference in efficacy between Lu AF21934 and LSP1-2111 in both the rat neuroprotection paradigm and the marmoset dyskinesia paradigm (PAM and agonist) is hypothesised to be due to insufficient levels of glutamate in the basal ganglia to facilitate activity of Lu AF21934, while LSP1-2111, as an orthosteric agonist, has activity at mGluR4 in its own right.

Modest but significant neuroprotection is conferred by 10mg/kg LSP1-2111 which is most evident in the rostral SNc. Although there appeared to be a disappointing lack of LSP1-2111-mediated functional recovery in these animals when examined using tests of spontaneous motor function, this may be a factor of the use of motor tests better suited to a more overt, full lesion than a subtle partial lesion. Nevertheless, the amphetamine-induced rotation test showed a significant reduction in rotational behaviour even off drug for animals which had been treated during lesion development with 10mg/kg LSP1-2111. The differences shown by this test reinforce the immunohistochemical evidence of neuroprotection and may point to a strong motor phenotype in these animals when motor behaviour is driven rather than spontaneous.

LSP1-2111 also showed potential for symptomatic treatment of PD by reducing motor impairment in Parkinsonian marmosets without causing dyskinesia. This result shows that mGluR4-based therapies may also hold promise for PD patients with late stage disease in addition to their potential for neuroprotection in earlier stage disease.

Previous studies by other members of the group and also in other groups suggest that mGluR4 activating compounds can reduce activity of the indirect pathway of the basal ganglia and excitotoxic activity of the STN (Cuomo et al. 2009, Austin et al. 2010, Gubellini et al. 2014) and, although this was not measured in the present studies, these factors may well have played a role in the effects described. A potential anti-inflammatory component to mGluR4-mediated neuroprotection is also supported by previous studies (Betts et al. 2012) and will be examined in Chapter 4.

4 Mechanistic insight into the partial lesion model and mGluR4-mediated neuroprotection

4.1 Introduction

In Chapter 3 of this thesis, the metabotropic glutamate receptor 4 (mGluR4) agonist (2S)-2-amino-4-(hydroxy(hydroxy(4-hydroxy-3-methoxy-5-nitrophenyl)methyl)phosphoryl)butanoic acid (LSP1-2111) was found to provide neuroprotection in a rat 6-hydroxydopamine (6-OHDA) partial lesion model of Parkinson's disease (PD). In this chapter, the potential mechanisms underlying this neuroprotection are subject to scrutiny. In particular, the neuroinflammatory component of the model itself is examined and any potential anti-inflammatory component to the neuroprotection (as was shown in (+/-)-cis-2-(3,5-dichlorphenylcarbamoyl)cyclohexanecarboxylic acid (VU0155041) by Betts et al. (2012)) is examined.

4.1.1 Neuroinflammation

The central nervous system (CNS) hosts an immune system which is separate from that of the periphery. Activation of this immune response can be difficult to measure, since it does not give rise to the same visible symptoms as activation of the peripheral nervous system such as pain or swelling. However, despite its low visiblity, the CNS immune response is still extremely important, especially in neurodegenerative disorders where a chronic inflammatory environment may become detrimental to neuronal survival.

As in the peripheral immune system, the CNS immune response is based around production of pro- or anti-inflammatory mediators by specialist immune cells. In the case of the CNS, these cells are mostly grouped together under the umbrella term, glia. Microglia are an important member of the glial cell family, constituting around 10% of all of the glial cells. They are phagocytic in nature and mirror the function of peripheral macrophages - indeed, microglia express many of the same cell surface markers as macrophages including CD68 and ionized calcium-binding adaptor molecule 1 (Iba1), which are upregulated upon activation in both cell types.

In a healthy CNS, microglia play a role in maintaining homeostasis; phagocytosing damaged cells or cellular debris. These functions also serve well in a disease state, where activated microglia phagocytose infectious agents and can act as antigen presenting cells, thus preventing CNS damage. Microglia have been shown to be activated by other components of the CNS immune response

such as the complement cascade (discussed below) (Lui et al. 2016), inflammatory cytokines (small proteins involved in autocrine, paracrine and endocrine signalling) (Papageorgiou et al. 2016) or even, according to one report, neuromelanin found in the substantia nigra pars compacta (SNc) cells (Wilms et al. 2003). When activated, microglia have been shown to produce pro- or anti-inflammatory cytokines in addition to potential neurotoxins such as superoxide ions (Michelucci et al. 2009, Mead et al. 2012).

Another type of glial cell is the astrocyte, which is estimated to make up between 20-40% of all glial cells (Pelvig et al. 2008). Like microglia, astrocytes have an important role in supporting homeostasis in the CNS, providing trophic support to neurons (Patel & Gray 1993) and ensuring the maintenance of physiological, rather than pathological, concentrations of ions and neurotransmitters at synapses (Moidunny et al. 2016). However, astrocytes also play an important role in inflammation and can respond to activation by producing pro- or anti-inflammatory chemokines (Meeuwsen et al. 2003) and altering the environment at the synapse to change the excitability of the post-synaptic neuron (reviewed in Perea et al. (2009)).

In addition to cytokine signalling, there are other systems in the body with the capacity to promote inflammation. The complement system is a collection of proteins which are cleaved in a cascade. The protein fragments resulting from the complement cascade trigger phagocytosis via opsonisation in dendritic cells (Ellegård et al. 2014), inflammation by increasing chemokines from monocytes (An et al. 2014) and membrane attack on the surface of pathogenic cells (Triantafilou et al. 2013).

Finally, oligodendrocytes represent a third type of glial cell whose purpose is to myelinate the axons of neurons, though they also have the capacity to produce and secrete neurotrophic factors (Philips & Rothstein 2017). In this respect, oligodendrocytes appear less likely to play a key role in the inflammatory process, and their link to PD is presently unclear.

4.1.2 Inflammation in Parkinson's

Inflammation and oxidative stress are key players in the pathophysiology of PD and, in the CNS, both are processes which are heavily mediated by glial cells (Niranjan 2014). This indicates a potentially critical function of glia, particularly microglia and astrocytes, in the pathogenesis of PD.

4.1.2.1 Microglia

The first evidence in support of a large neuroinflammatory component to PD was the finding that large numbers of microglia were present in the SNc of the brains of people with PD (McGeer, Itagaki, Boyes & McGeer 1988). This finding was paralleled by Imamura et al. (2003), who saw increased numbers of major histocompatibility complex class II (MHCII)-positive microglia in both the substantia nigra and the putamen when compared to age-matched, healthy controls. Indeed, Imamura et al. (2003) showed that there was also a significantly higher number of MHCII-positive microglia throughout the cortex in the brains of PD patients.

This microglial activation has also been associated with enhanced expression of cytokines and reduced expression of neurotrophic factors in the cerebrospinal fluid and post-mortem brain tissue from PD patients (Nagatsu & Sawada 2005). However, it is unclear as to whether these changes represent a cause or an effect of other important events in PD such as neuronal degeneration.

4.1.2.2 Astrocytes

Astrocytes are also implicated in the PD process, though perhaps more due to their conspicuous absence in and around the SNc in PD post-mortem brains (Mena & García de Yébenes 2008). This absence implies that astrocytes may otherwise be providing neuroprotective support to the dopaminergic midbrain neurons; perhaps through the absorbance of dopamine-derived free radicals (Takuma et al. 2004). Those dopaminergic neurons displaying an astrocyte presence seem to survive for longer in PD brains than those without (Damier et al. 1993) - again demonstrating an astrocyte-mediated survival mechanism. These nigral astrocytes were discovered using immunohistochemical staining for glutathione peroxidase - an enzyme which is protective against oxidative stress induced by hydrogen peroxide - supporting, in particular, a role for astrocytes in scavenging of free radicals in PD (Damier et al. 1993).

Further linking glial dysfunction to PD pathogenesis are studies examining the impact of PINK1 dysfunction. These studies have shown that loss of function of PINK1 (PARK6), a gene affected in some forms of familial PD, affects innate immune function in glial cells through interfering with proliferation and enhancing a pro-inflammatory phenotype through nitric oxide release (Choi et al. 2013, Sun et al. 2018).

Although the above groups have reported a reduced number of astrocytes in the PD brain, others

have shown an increased number of highly glial fibrillary acidic protein (GFAP)-positive, reactive astrocytes in brain areas related to PD (Mythri et al. 2011). As astrocytes it has been shown that astrocytes may secrete trophic factors and scavenge free radicals, functions which support neuronal survival (Engele & Bohn 1991, Damier et al. 1993, Makar et al. 1994), so this proliferation of astrocytes in PD is believed to be a compensatory, protective response to oxidative stress (Mythri et al. 2011).

4.1.2.3 Inflammatory mediators

Simple counting of inflammatory cell types is of limited use in characterising the neuroinflammatory environment of a brain. This is because both microglia and astrocytes have been shown to possess the ability to change phenotype and may promote either an inflammatory or an anti-inflammatory environment or, more likely, some middle ground between the two (Michelucci et al. 2009, Simpson et al. 2010, Nash et al. 2011). To this end, analysing the inflammatory mediators, such as cytokines, expressed by these cell types promises to show a more detailed and informative picture of the inflammatory climate within the brain. Demonstrating this, analysis of post-mortem brain tissue from PD patients has shown increases in tumour necrosis factor α (TNFα), interferon-γ (IFNγ) and nuclear factor-κB (NFκB); all of which are key regulators of the inflammatory response (Mogi et al. 1994, 2007). In addition to this, brain-derived neurotropic factor (BDNF) and nerve growth factor (NGF), neurotrophic factors which support survival of neurons, were found to be downregulated in the SNc of PD patients (Mogi et al. 1999).

Examination of the cerebrospinal fluid of PD patients has revealed elevated levels of cytokines including the pro-inflammatory IL-1β and IL-6, which can act either in a pro- or anti-inflammatory manner (Blum-Degen et al. 1995). In a later study the same authors found that, although IL-6 was elevated in the cerebrospinal fluid of PD patients, the concentration was inversely correlated with the severity of the disease (Müller et al. 1998), demonstrating that IL-6 in PD may be acting in an anti-inflammatory, neuroprotective capacity which is lost at later stages of the disease.

This link between PD and inflammation has been further strengthened by the acknowledgement that polymorphisms in genes coding for cytokines may predispose towards development of PD. Such polymorphisms have been observed in a number of cytokine genes, including TNFα (Wilson et al. 1997), IL-1β (McGeer et al. 2002), IL-6 (Håkansson et al. 2005), IL-8 (Ross et al. 2004) and IL-18 (Xu et al. 2011).

Expression of complement proteins has been shown to be significantly reduced in the cerebrospinal fluid of PD patients (Finehout et al. 2005). However, this was hypothesised to be as a result of depletion through over-activation of the system - especially since other groups have found a significant upregulation of complement mRNA in the PD brain (McGeer & McGeer 2004).

4.1.3 Inflammation in mammalian models of Parkinson's

Many of the neuroinflammatory changes that have been recorded in PD patients have also been recaptiulated in animal models of PD. These changes are discussed below and summarised in Table 4.1, p.171.

4.1.3.1 Microglia

An increase in the number and reactivity (through expression of MHCII or CD11b) of microglia has been measured at the site of injection and connected brain regions in rodent models of PD using 6-OHDA (Akiyama & McGeer 1989, Walsh et al. 2011, Stott & Barker 2014). Similar increases were also seen in the brains of primates (McGeer et al. 2003) and mice which had undergone 1-methyl-4-phenyl-1,2,3,6-tetrahydropyridine (MPTP) treatment to cause a lesion, though the precise inflammatory effects of lesioning were found to be strain-specific (Yasuda et al. 2008). Furthermore, microglial activation following MPTP-treatment was found to be higher in aged mice than young mice. As PD is primarily a disorder of the elderly, and neuroinflammation is correlated with age (reviewed in Godbout & Johnson (2006)), the MPTP-treated, aged mouse therefore shows good potential as a model of microglial activation in PD.

Some groups have reported increased microglial activation following rotenone administration (Gao et al. 2002, Sherer et al. 2003, Emmrich et al. 2013), though in line with all reported rotenone effects, this has not been seen by all groups (Klintworth et al. 2009).

In genetic models of PD, α-synuclein transgenic mice are the only model to reliably report microglial activation (Tofaris et al. 2006, Su et al. 2008).

4.1.3.2 Astrocytes

Similar patterns of astrocytosis have been reported as for microgliosis. Significant increases in astroglial activation have been observed in the brains of rodents lesioned using 6-OHDA (Gomide

et al. 2005, Walsh et al. 2011, Stott & Barker 2014). Yasuda et al. (2008) found astrocytosis, like microgliosis, to be strain-specific in MPTP-treated mice, affecting B6 but not BALB/c mice. MPTP-treated rhesus monkeys also displayed signs of astrocyte activation (upregulation of ICAM-1) many years after MPTP exposure (Miklossy et al. 2006).

Astrogliosis was only observed in rotenone-induced Parkinsonism following a direct infusion into the medial forebrain bundle (MFB), and not after subcutaneous infusion (Sherer et al. 2003, Norazit et al. 2010).

As with microglial activation, increased astrocyte number was only observed in the α-synuclein overexpression model of all of the murine genetic models of PD (Giasson et al. 2002, Rockenstein et al. 2002).

4.1.3.3 Inflammatory mediators

Inflammatory mediators present in the brain or cerebrospinal fluid of 6-OHDA-lesioned animals seem surprisingly sparsely recorded considering the model is so well used in the PD field. Nevertheless, higher levels of TNFα and complement protein 1q (Park et al. 2010, Harms et al. 2011) have been recorded in 6-OHDA-lesioned rat brain.

By comparison, altered inflammatory mediators are widely characterised in MPTP models. Grünblatt et al. (2001) showed that IL-1β, IL-6, IL-7, IL-10 and NFκB were all upregulated in the ventral mesencephalon (VM) and striatum of MPTP-treated mice. In addition, Il-10, IL-12, IL-13, IFNγ and TNFα were shown to be upregulated in the cerebrospinal fluid of MPTP-treated mice in a different study (Yasuda et al. 2008). Similarly, Ohnuki et al. (2010) found that elements of the complement system and IL-11 were upregulated in the brains of primates treated with MPTP.

Treatment with rotenone was shown to cause upregulation of COX-2, NFκB, TNFα, IL-1β and IL-6 in the midbrain of rats, though neurodegeneration was not measured (Thakur & Nehru 2015). Likewise, the VM of α-synuclein overexpressing mice showed elevated levels of IL-1α, IL-6 and TNFα but did not display signs of degeneration (Su et al. 2008, Theodore et al. 2008).

Table 4.1: Activation of neuroinflammation in animal models of PD				
Model	Microglia	Astrocytes	Cytokines	Complement
6-OHDA	✓	✓	✓	✓
MPTP	✓	✓	✓	✓
Rotenone	⇜⇝	⇜⇝	✓	*X*
α-synuclein transgenic mouse	✓	✓	✓	*X*

Table 4.1: A summary of neuroinflammatory changes seen in animal models of PD. ✓shows that a neuroinflammatory component has been found to be activated in a model similarly to its activation in tissues from PD patients. ⇜⇝ indicates that some evidence exists to show a neuroinflammatory feature in that particular model, but that evidence is contested by other papers. *X* shows that a feature does not appear to have been investigated in that model. Microglia: Akiyama & McGeer (1989), McGeer et al. (2003), Yasuda et al. (2008), Liu et al. (2010), Sherer et al. (2003), Tofaris et al. (2006), Su et al. (2008). Astrocytes: Gomide et al. (2005), Yasuda et al. (2008), Sherer et al. (2003), Giasson et al. (2002), Rockenstein et al. (2002). Mediators: Park et al. (2010), Harms et al. (2011), Grünblatt et al. (2001), Yasuda et al. (2008), Ohnuki et al. (2010), Thakur & Nehru (2015), Su et al. (2008), Theodore et al. (2008).

4.1.4 Effects of mGluR4 on inflammation

Neuroinflammation is a highly relevant aspect of PD which is present in a number of the most popular animal models, and may be affected significantly by neuroprotective treatment (Betts et al. 2012), again suggesting an important role for neuroinflammation in neurodegeneration and neuroprotection. As the target of LSP1-2111, the neuroprotective therapy examined in the previous chapter, is mGluR4, it is important to understand the potential effects of mGluR4 agonism on neuroinflammatory processes. Any anti-inflammatory effect of this compound may well relate to its neuroprotective efficacy, as was discovered for the ago-PAM VU0155041 by Betts et al. (2012).

McNaught & Jenner (1999) found that co-culturing VM neurons with astrocytes that had previously been activated by lipopolysaccharide (LPS) increased the neuronal death caused by application of 6-OHDA or 1-methyl-4-phenylpyridinium (MPP^+). Furthermore, Zhou et al. (2006) show that adding LPS directly to VM neuronal cultures does not cause cell death, but that adding LPS to astrocytic cultures, then adding the conditioned media from those astrocyte cultures to VM cultures causes significant neuronal death. This LPS-mediated astrocyte activation is likely mediated via toll-like receptor 4 (TLR4) or CD14 (Tarassishin et al. 2014). These findings show in a very simple cell system that glial dysfunction may play a role in neurodegeneration of the forms seen in PD and PD animal models.

When astrocyte cultures were incubated with the group III agonist L-2-amino-4-phosphonobutyrate (L-AP4) shortly before addition of LPS, neuronal death on addition of the conditioned media was significantly reduced (Zhou et al. 2006). This neuroprotective effect was not present when methylserine-O-phosphate (MSOP), a group III antagonist, was added prior to L-AP4, or when L-AP4 was added directly to the neuronal culture rather than the astrocytic culture. This finding serves to demonstrate further that the environment created by reactive astrocytes can be damaging to VM neurons, but also that the neurodegenerative activity of activated astrocytes may be reduced by group III metabotropic glutamate receptor (mGluR)-activating compounds.

Similar studies have been conducted to observe the neurodegenerative and neuroprotective potential of microglia. Taylor et al. (2002) show that cerebellar granule neurons subjected to conditioned media from microglia activated with chromogranin A undergo significant apoptosis. This apoptotic effect of activated microglia is also apparent when microglia and neurons are co-cultured. In a later study, Taylor et al. (2003) show that addition of L-AP4 to microglia activated with chromogranin A or LPS and co-cultured with cerebellar granule neurons causes significant preser-

vation of those neurons. This neuroprotective effect of L-AP4 is blocked by a group III antagonist (Taylor et al. 2003), showing again the potential anti-inflammatory and neuroprotective effect of group III activators.

More recently, an anti-inflammatory effect of an mGluR4-specific positive allosteric modulator (PAM) has been recorded in primary microglia (Ponnazhagan et al. 2016). 5-Methyl-N-(4-methylpyrimidin-2-yl)-4-(1H-pyrazol-4-yl)thiazol-2-amine (ADX88178), was added to microglial cultures prior to addition of LPS. Following a 24 hour incubation, levels of the inflammatory markers TNFα, inducible nitric oxide synthase (iNOS) and MHCII were found to be significantly lower in cultures treated with ADX88178 or L-AP4. This effect was not seen in microglia isolated from mGluR4 knockout mice, showing that the anti-inflammatory effect is mGluR4-specific, even when perpetrated by a pan-group III PAM or agonist.

This anti-inflammatory potential of mGluR4 has also been seen *in vivo*. Previously in this group, a neuroprotective effect of VU0155041, an mGluR4 agoPAM, has been found in 6-OHDA-lesioned rats. Alongside, and potentially underlying, this neuroprotection, reductions in inflammatory markers were observed in the SNc - the site of lesion and administration of VU0155041. Levels of Iba1 were significantly reduced in the SNc following subchronic administration of VU0155041, and numbers of GFAP-positive astrocytes were also reduced, albeit non-significantly (Betts et al. 2012).

4.1.5 Gene transcription

An alternative approach to understanding a variety of mechanisms underlying the LSP1-2111, or mGluR4, mediated neuroprotection seen in the previous chapter is by transcriptomic analysis. This whole-genome technique allows a view of all changes in RNA expression which were brought about by an intervention (pharmacological, surgical, environmental etc.) in any given sample. In a typical transcriptomic study, the transcriptome (the sum of all mRNA) of a particular tissue from an intervention or a disease group is compared against the transcriptome of that same tissue from a healthy or vehicle control population. The comparison allows visualisation of the genes which are significantly more or less transcribed in the disease or following the intervention than in the control population and thereby gives hints about which proteins may be differently expressed.

This type of study is useful for finding changes in RNA transcription which may indicate mechanisms of a disease process or treatment which are hitherto uncharacterised, and may lead to a change in direction of investigation. For example, if an anti-inflammatory effect was not a sig-

nificant component of the neuroprotective action of LSP1-2111, then a transcriptomic study may suggest alternative routes of investigation through alterations in expression of mRNA suggesting alternative mechanisms (e.g. mitochondrial function). Findings from these type of large scale microarray studies are typically followed up with more focussed investigations of specific data suggested by the transcriptomic array.

4.1.5.1 Transcriptional changes in PD

Transcriptional changes in post-mortem tissue from PD patients have been widely examined with varying concordance (Sutherland et al. 2009, Oerton & Bender 2017). This variability can be traced to a number of factors detailed below.

- Tissue heterogeneity and regional differences: Many cell types can be found within one tissue sample, meaning that transcriptomic analysis is likely to be profiling a number of different cells within a region following a straight dissection without differentiation between cells. Not only this, but many such transcriptomic analyses attempt to compare tissue from different brain regions; whether medial and lateral SNc or cortex and caudate. The transcriptional profile of these different cell types and tissue from different regions are likely to be highly heterogeneous due to their different roles in health and disease. Attempting to pool or compare samples with such different transcriptional profiles may well muddy the results and hide important transcriptional changes while making incidental changes seem prominent.

- Disease heterogeneity: PD patients may be stratified by disease phenotype; the observance of different symptoms or an alternative route for the spread of Lewy pathology. These different types of PD may cause, or arise from, different transcriptional changes within the same regions of the brain so grouping them together for a transcriptional study may cause a lot of variation within and between studies (Riess et al. 2002).

- Different genetic backgrounds of patients from which samples are taken: transcriptional profile may vary significantly between people from different genetic backgrounds, regardless of their disease state (Stranger et al. 2007). This may also confound transcriptomic analysis.

- Difference in probe design within and between different arrays/platforms: microarrays from different manufacturers and even different iterations of the same array may utilise different

probe designs and probe sets making a direct comparison difficult.

- Differences in data analytical technique: Concordance between transcriptomic studies may also differ depending on the method of data analysis. Currently, where individual gene expression changes are compared between studies, concordance is low (0.15 (Oerton & Bender 2017)), but this figure is increased when biological pathways are compared instead (0.3 (Oerton & Bender 2017)).

Another important consideration for the interpretation of transcriptomic studies in PD is the understanding of cause and effect. From examining the transcriptional changes in post-mortem brain tissue, it is impossible to understand which changes are brought about as an effect of PD and which are underlying causes.

Despite these considerations, a number of PD transcriptomic studies have been published. Oerton & Bender (2017) reported 33 such studies including 15 conducted on human PD samples and 13 on rodent models of PD. Some key findings of the human transcriptomic studies examined include altered expression of transcripts relating to pathways such as: electron transport chain complex impairment, induction of heat shock proteins (Zhang et al. 2005), downregulation of dopamine signalling and growth factor pathways (Sutherland et al. 2009), molecular chaperones, ubiquitination, vesicle trafficking (Hauser et al. 2005), pro-inflammatory cytokines and glial specific genes (Duke et al. 2007) (as noted in section 4.1.2), copper-binding and Wnt signalling (Cantuti-Castelvetri et al. 2007).

For individual genes, the most common hits in top 50 upregulated hits of all human studies were HSPA1A (a heat shock protein which mediates protein folding) , RELN (Reelin, an extracellular matrix protein), SLCO4A1 (a solute carrier for organic anions) and HSPA1B (another heat shock protein). The most commonly downregulated genes were RGS4 (a negative regulator of $G_{i/o}$ and G_q-protein signalling), TAC1 (preprotachykinin, which can be modified to produce substance P, neurokinin A and neuropeptide K and γ) and AGTR1 (an angiotensin II receptor).

These alterations bear little similarity to changes seen in animal models and the animal models bear little similarity to each other, with concordance between mouse models at 0.03 and concordance between rat models at -0.04 (Oerton & Bender 2017). These values improve when studies are compared within model type, with murine MPTP studies showing a concordance of 0.1 and

genetic models of 0.12 but 6-OHDA models remaining low at -0.03 (Oerton & Bender 2017). Likewise Burns et al. (2015) found no correlation between gene regulation in MPTP, PINK1 or α-synuclein mouse models and human PD.

Miller & Federoff (2005) found 6 genes which were significantly regulated in common between human PD, MPTP-treated mice and α-synuclein over-expressing mice, though not all in the same direction - dopamine active transporter (DAT), EN-1 (which regulates expression of FGF8), HK-1 (a glycolytic enzyme), DSCR1L1 (inhibitor of calcineurin), ZFP162 (a signal transducer and activator of RNA protein) and SLC25A14 (a mitochondrial solute carrier). Of these, only DSCR1L1, HK-1 and ZFP162 were regulated the same way in all 3 groups (down, down and up respectively). Transcriptomic studies on tissue from 6-OHDA-lesioned rats, the model used throughout this thesis, found significant upregulation of pathways involved in extracellular matrix modification, signal transduction, inflammation, synaptic transmission and regeneration-associated genes (Kanaan et al. 2015).

In contrast to this reported lack of correlation within and between animal models, an in-house comparison rendered by Dr Gareth Williams suggests a good correlation between transcriptomic signatures from the SNc of the 6-OHDA-lesioned rat (Kanaan et al. 2015) and the SNc of PD patients (Moran et al. 2006, Lesnick et al. 2007). Kanaan et al. (2015) examined transcription in the VM of striatally-lesioned rats at weeks 1, 2, 4, 6 and 16 post-lesion and the correlation with post-mortem PD brains varies over this time period. Nevertheless, correlation between rat data gathered by Kanaan et al. (2015) and the post-mortem study by Lesnick et al. (2007) remains high throughout. It is at its lowest at week 1 post-lesion in the lateral SNc (0.38) and at its highest on week 6 in the medial SNc (0.80). Correlation between the rat data (Kanaan et al. 2015) and human data gathered by Moran et al. (2006) is at its lowest on week 4 post-lesion (0.49) and highest on week 2 (0.70). Even at the points of lowest correlation between these studies, the similarity between data sets seems to far outstrip the correlations reported by Oerton & Bender (2017).

These differences in reported correlations between transcriptomic profiles of animal models is likely due to methodological differences in model application and dissection - which can make significant differences in the transcriptomic profile of a sample. Further differences in the methodology of comparison may also play a role in the differences in these findings.

4.2 Hypotheses and aims

The aims of studies presented in this chapter were to characterise the inflammatory response to a partial 6-OHDA lesion and the anti-inflammatory capabilities of LSP1-2111, a mGluR4 agonist. Each study formed a logical progression from the last:

- **We hypothesised that neuroprotection provided by LSP1-2111 would be underpinned by an anti-inflammatory effect.** In order to assess this, inflammatory markers were assessed by histology on tissue generated in Chapter 3 from 6-OHDA-leisoned, LSP1-2111-treated animals. **The aim of this study was to examine whether anti-inflammatory efficacy was a key underlying factor of the neuroprotective capability of LSP1-2111 seen in Chapter 3.**

- The anti-inflammatory effect of VU0155041 in the Betts et al. (2012) study was observed at 7 days post-lesion and immediately after the cessation of regular VU0155041 administration. The anti-inflammatory effect of systemic LSP1-2111 observed here was less potent, however the window of observation was 14 days post-lesion and after 7 days' washout of LSP1-2111. **We hypothesised that the peak of inflammatory activity induced by 6-OHDA lesioning may have passed by 14 days post-lesion**. If true, this would imply that one possible reason why no anti-inflammatory effect of LSP1-2111 was seen in study 1, above, may be that mGluR4-mediated separation between groups at 7 days post-lesion was lost by 14 days. To test this hypothesis, a time course of inflammatory activity was observed at 2, 3, 4 and 7 days following a unilateral, partial 6-OHDA lesion. This was then compared to inflammatory cell levels at 14 days in vehicle and LSP1-2111-treated animals in the LSP1-2111 neuroprotection study. **The aim of this study was to examine the acute inflammatory activity of the partial, striatal 6-OHDA lesion in order to better understand the results of the previous study examining anti-inflammatory efficacy of LSP1-2111.**

- The presence of inflammatory cells at 7 days was shown to be less than at 14 days, and only a modest effect of inflammation found by rudimentary histological cell counts. **We hypothesised that chemoattractant cytokines at 7 days post-lesion might be responsible for the increase in inflammatory cells by 14 days, and that the profile of these chemokines would differ between tissues from LSP1-2111-treated and**

vehicle-treated animals. In order to test this hypothesis, a series of cytokines arrays and enzyme-linked immunosorbent assays (ELISAs) were carried out to examine the presence of pro-inflammatory cytokines in lesioned and intact tissue from the striatum and midbrain of LSP1-2111-treated and control animals.

- Evidence for an anti-inflammatory effect of LSP1-2111 in the previous studies was mild. **We hypothesised that LSP1-2111 may provide neuroprotection by means other than an anti-inflammatory effect.** In order to identify other potential neuroprotective mechanisms of LSP1-2111, a GeneChip assay was used to provide information about the transcriptional changes manufactured by a single administration of LSP1-2111 in otherwise naïve animals.

4.3 Materials and Methods

4.3.1 Inflammation in 6-OHDA-lesioned, LSP1-2111-treated rats

Paraffin-embedded sections of brain containing striatum and SNc were taken from the lesioned animals dosed with LSP1-2111 from the neuroprotection study detailed in Chapter 3. Briefly, 30 animals underwent a 6-OHDA partial lesion and 9 days of twice-daily dosing with saline vehicle (n = 10), 1mg/kg (n = 10) or 10mg/kg LSP1-2111 (n = 10) from 1 day prior- to lesion to 7 days post-lesion. Animals were deeply anaesthetised and perfused at day 13 post-lesion, when the brain was removed and processed as per the details in Chapter 2.

7μm tissue sections were dewaxed and processed through antigen retrieval as in previous studies in Chapter 2. Immunohistochemistry was undertaken with the antibodies detailed in Table 4.2, using the protocol described in section 2.3.3, p.77.

Table 4.2: Antibodies used for immunohistochemistry

Target	Primary antibody	Dil	Secondary antibody	Dil
Iba-1	goat polyclonal ab5076 Abcam, UK	1:750	biotinylated horse anti-goat IgG	1:300
GFAP	rabbit polyclonal ab7260 Abcam, UK	1:1500	biotinylated goat anti-rabbit IgG	1:300

Table 4.2: Information on antibodies used to characterise inflammatory changes in paraffin-embedded rat brain sections using immunohistochemistry.

In the case of Iba1 stains, representative images were taken at high magnification (using a 20x objective on a Nikon microscope with an Axioskop camera). In the striatum, these images were taken in each quadrant of the lesioned and intact striatum. In the SNc, images were taken from the central and lateral SNc. No difference was found in the number of Iba1-stained cells between these regions and so one image central to the two areas was taken to be representative of the whole SNc at each level of rostral, mid and caudal regions using the co-ordinates described on p.77). This field of view covered approximately half the length of the SNc, leaving the most central and most lateral quarters out. In each of these images, the number of Iba1-positive cells was counted and the total averaged across the 3 consecutive sections.

For GFAP, images were taken of striatal sections exactly as described for tyrosine hydroxylase (TH)-stained striatum (p.77). Density of the GFAP stain was recorded in the same way in all four quadrants of both lesioned and intact striatum, and in each cortex. In the lesioned striatum, the densitometric analysis was taken around, and not including, the glial scar at the needle tract and injection site. The background values of the cortex were subtracted from the density values of the quadrants in the same hemisphere and the lesioned GFAP values expressed as a percentage of the intact.

For GFAP stains in the SNc, images were taken from the central and lateral SNc at 20x magnification, as in Iba1 analysis. Again, there was found to be no difference in stain density between these two regions and so one image was taken to represent the GFAP staining in the SNc at any each rostral-caudal level. Densitometry was undertaken as for GFAP in the striatum, with areas of no staining used to provide background values. At each level, data from 3 consecutive sections were averaged and used to represent GFAP densitometry for each animal.

4.3.1.1 Statistical analysis

All data were tested for normality using the D'Agostino and Pearson omnibus normality test prior to undergoing any tests for significant differences between groups. Where data were compared between regions and between treatment groups, a 2-way ANOVA with Sidak's or Dunnett's post-test was used. Where average values representing treatment conditions at a single time point were compared, as in the histological comparisons, a 1-way ANOVA was used with a Dunnett's post-test.

4.3.2 Time course of inflammation following 6-OHDA lesion

It was hypothesised that the 2 week time point used for immunohistochemical analysis in the neuroprotection studies may have been too late to capture the peak of inflammatory activity following the lesion. The time course study was carried out in order to test this hypothesis. TH, Iba1 and GFAP were measured at days 2, 3, 4 and 7 following the lesion in order to characterise degeneration and inflammation in the acute period following lesion, with the knowledge of the changes which have occurred by 14 days gained from the LSP1-2111 neuroprotection study.

For the purpose of better understanding these acute changes, 40 male SD rats (225-275g, Harlan, UK) were injected at AP +0.2mm, ML -3mm from bregma and -5.5mm from skull surface

with either 12μg 6-OHDA to create a lesion ($n = 20$) or 0.2% sodium ascorbate in sham animals ($n = 20$) as described in section 2.3.1, p.74. No behavioural tests were undertaken with this cohort of animals.

Animals were killed by an overdose (200mg via intraperitoneal (i.p.) injection) of sodium pentobarbital (Euthatal - Merial Animal Health Ltd, UK) at 48, 72, 96 hours or 7 days post-lesion (n=5 per time point). When no pedal reflex was seen but before cessation of life, the animal was decapitated. The brain was rapidly removed and a 4mm section containing the midbrain placed into 10% formalin for post fixing for $\geq$ 72 hours on a rocker. The striata were dissected out of the remaining forebrain sections and each was individually frozen on dry ice and stored at -80°C to be used for western blotting. The midbrain tissue was then processed and embedded in paraffin wax as described in on p.77 for immunohistochemistry.

Following the observation that cell loss and neuroprotection were both greatest in the rostral SNc during the LSP1-2111 neuroprotection study, the rostral SNc was used as the region of interest for this study. Antibodies used in this characterisation are detailed in Table 4.2 on p.179. Brain tissue was sectioned and stained using the 3,3'-diaminobenzidine (DAB) protocol as described on p.77.

For the imaging of TH DAB staining, the procedure described in the Chapter 2 methods was used. For Iba1 and GFAP-positive cells, characteristic images taken using a 20x magnification objective from central, rostral SNc were used. Images were imported into ImageJ for analysis and converted to 8-bit greyscale. A reference image with a set scale bar was used to import the image scale into analysis and density of DAB, stain density was calibrated using a greyscale calibration image. Iba1 staining was analysed by a number of different methods. Manual counting in a representative field of view in the central, rostral SNc was carried out in 3 sections per animal. Optical density was undertaken for the whole field of view image and for individual cells counted within the field of view by manual circling of the cell body of Iba1-positive cells. Using this method alongside the imported image scale, the cell body area of circled cells was also calculated.

For analysis of GFAP images, the images were then binarised, despeckled twice in order to remove noise and skeletonised. The skeleton image was analysed using the lowest intensity branch prune cycle method with elimination of end points and end pruning in order to effect Strahler analysis of branch points. Similar methods have been developed by Mong et al. (1996), Koh et al. (2002), Salois & Smith (2016), from which the current method was adapted for use with ImageJ. Data

were produced from three consecutive sections and analysed to give an average value.

4.3.2.1 Western blotting

Western blotting was chosen for quantification of proteins in the striatum in order to measure expression throughout the tissue, rather than restricting quantification to specific regions as is necessary with immunohistochemical techniques. In addition, this was considered to be a valuable opportunity to become familiar with the use of an additional molecular biology analytical technique.

Frozen samples were each homogenised on ice using a glass mortar and pestle in 500μl pH7.4 radioimmunoprecipitation assay (RIPA) buffer containing protease and phosphatase inhibitors. The composition of RIPA buffer is listed in Table 4.3.

Table 4.3: Composition of RIPA buffer (per 10ml)

Reagent	Conc.	Supplier
NaCl	150mM	Sigma-Aldrich
Tris HCl	50mM	Sigma-Aldrich
EDTA	0.1mM	Sigma-Aldrich
NP-40	1%	Sigma-Aldrich
Sodium deoxycholate	0.5%	Sigma-Aldrich
SDS	0.1%	Sigma-Aldrich
Protease cocktail inhibitor	1 tab	Sigma-Aldrich
Phosphatase cocktail inhibitor	1 tab	Merck

Table 4.3: Composition of RIPA buffer used for tissue homogenisation.

A bicinchoninic acid (BCA) assay (Sigma-Aldrich, USA) was performed on each homogenate in order to ascertain the protein content of each sample and enable standardisation before Western blotting. 5μl of sample was added at 1:2, 1:4 and 1:8 dilutions to BCA reagents A and B (50:1) in a 96-well plate (Nunc A/S, Denmark) in triplicate. Bovine serum albumin (BSA) was used to form a standard curve in each plate in the range: 2, 1.5, 1, 0.75, 0.5, 0.25, 0.125, 0.0625 and 0mg/ml. The plate was then incubated at 37°C for 30 minutes before reading. Absorbance at 562nm was recorded using a plate reader (Molecular Devices, Spectramax) for the standards and

samples and the standard curve used to determine concentration of protein in each sample.

Using this information, neat samples were then diluted in deionised water and Laemmli sample buffer (GenScript, USA) to make 100μl solution containing 1mg/ml protein and heated at 95°C for 5 minutes before freezing at -20°C for storage.

24-well 10% sodium dodecyl sulfate (SDS)-polyacrylamide gels were made according to ProtoGel kit instructions (National Diagnostics, USA). Briefly, the resolving gel mixture was combined, poured between the glass plates used in elecrophoresis and allowed to set for 30 minutes. Following this, the stacking buffer was mixed, poured on top of the set resolving gel and a comb added to for the 24-wells. The stacking buffer was left to set for a further 30 minutes before the gels were ready for use. Pooled, naïve striata obtained from rats used in other studies were used in all gels to provide an inter-blot control, next to a full-range molecular weight marker (RPN800E; Amersham). 20μl of each sample with Laemmli buffer was loaded and gels were run at 120V for approximately 2.5 hours, or until the dye front had reached the bottom of the gel.

Table 4.4: Antibodies used for Western blotting

Target	Primary antibody	Conc	Secondary antibody	Conc
β-tubulin	rabbit polyclonal ab18207 Abcam, UK	1:10,000	goat anti-rabbit IR 800 ab216773 Abcam, UK	1:10,000
Tyrosine Hydroxylase	rabbit polyclonal AB152 Merck Millipore, Canada	1:10,000	goat anti-rabbit IR 800 ab216773 Abcam, UK	1:10,000
GFAP	rabbit polyclonal ab7260 Abcam, UK	1:10,000	goat anti-rabbit IR 650 ab96886 Abcam, UK	1:10,0000

Table 4.4: Information on antibodies used to characterise lesions in Western blots.

Proteins were then transferred to nitrocellulose membranes (Amersham Biosciences) at 60V for 90 minutes and blocked with 5% milk solution in 0.1% tween-20/PBS (PBST-milk). After blocking, membranes were incubated in the desired primary antibody in blocking solution overnight at 4°C (antibodies listed in Table 4.4. Iba1 was also investigated in western blots but trials with the

antibody were not successful - no protein band was seen either at the expected molecular weight or elsewhere). Following washes, secondary antibody in blocking solution was added to the membranes for 1 hour. The membrane was then washed in phosphate-buffered saline (PBS) before imaging.

Membranes were imaged using an Odyssey infrared scanner (Li-cor, USA) set to analyse images at wavelengths of 700nm and 800nm (depending upon the emission wavelength of the secondary antibody used). ImageJ was used to determine band intensities. Markers of interest for each sample were expressed relative to β-tubulin, used here as a housekeeping marker. Values from each gel were adjusted based on the difference in intensity of the inter-blot control in order that between-gel differences were controlled.

4.3.2.2 Statistical analysis

All data were tested for normality using the Shapiro-Wilk normality test (for groups with a low n) prior to undergoing any tests for significant differences between groups.

Where data were not normally distributed and more than two conditions were compared (as in the cytokine array membranes) the Kruskal Wallis test was used followed by a Dunn's test if the initial test showed significance.

Where data were normally distributed and are given as lesioned hemisphere as a percentage of the intact, animals in the lesion group were compared to their sham counterparts at the same time point using unpaired t-tests. Where raw data are presented (intact and lesioned hemispheres of both groups at all time points are represented on one graph), a 2-way ANOVA was used. If the initial ANOVA showed significance in both variables, Sidak's multiple comparisons post-test was used to compare each condition with all other conditions.

4.3.3 Cytokines in inflammatory responses

4.3.3.1 Generation of tissue for use in inflammatory mechanistic assays

For the generation of tissue for the cytokine array and subsequent ELISAs, lesioning protocol, LSP1-2111 treatment with the optimal dose (10mg/kg) and the cylinder test took place as described in Chapter 2. Briefly, all animals were given partial lesions using 12μg 6-OHDA injected at

1μl/minute into the dorsal striatum (AP +0.2mm, ML -3mm from bregma and -5.5mm from skull surface with the incisor bar set at -3.3mm) under inhaled isoflurane anaesthesia. LSP1-2111 in 0.9% saline (10mg/kg, n=10) or 0.9% saline (n=10) was administered subcutaneously to animals twice daily at 7am and 6pm for 1 day prior to and 7 days post lesion, as in Chapter 3.

On day 7 post-lesion, prior to the 7am dose, the cylinder test was used in order to confirm the presence of a lesion in all animals. 3 hours after the final 7am administration (7 days post-lesion), animals were culled by cervical dislocation without the use of anaesthetics and brains were rapidly dissected out. For each animal, cerebellum; right and left cortex; right and left striatum and right and left VM (containing the SNc) were dissected out and snap frozen using isopentane (Thermo Fisher Scientific, USA) cooled with dry ice before individual storage at -80°C prior to homogenisation. The use of a unilateral lesion in all animals alongside the administration of vehicle and LSP1-2111 treatment gave the following groups of tissue in each of the striatum and VM regions:

- Intact (contralateral), vehicle-treated.
- Lesioned (ipsilateral), vehicle-treated.
- Intact (contralateral), LSP1-2111-treated.
- Lesioned (ipsilateral), LSP1-2111-treated.

Tissue from 5 animals from each group (vehicle-treated or LSP1-2111-treated) was designated for testing of inflammatory markers and cytokines, and the remaining tissue was reserved for a future multiplex assay.

4.3.3.2 Cytokine arrays

Cytokine arrays and cytokine ELISAs took place at Eisai Ltd, Hatfield. Tissue was removed from storage at -80°C and weighed. Homogenisation bufffer (PBS with 1x HALT phosphatase and protease inhibitors and 1% Triton-X) was added at a volume of 1ml per 100mg of tissue. Tissue was first withdrawn multiple times through a 21G hypodermic needle for approximately 90 seconds, then through a 23G needle for a further 90 seconds, or until no further reduction in particle size was achieved. Homogenates were then centrifuged at $12,000 \times g$ for 30 minutes at 4°C in order to remove cellular debris. Supernatant was removed and retained for cytokine quantification.

A BSA assay was carried out on 2μl neat supernatant in triplicate with the method detailed in Chapter 2 in order to ascertain the protein concentration of each sample. Samples were then diluted to a concentration of 2mg of protein/ml and 80μl each of the 5 samples in each group were pooled in equal ratio to give a stock sample which was representative of the group.

The cytokine array was carried out according to the protocol supplied with the array kits (Rat Cytokine Antibody Array Kit: ARY008, R&D Systems, USA) and adapted for use with a fluorescence imager. Briefly, Array Buffer 6 (blocking buffer) was added to each well of the supplied 4-well dish along with one cytokine array membrane per well. Cytokine array membranes contained antibody spots for 29 different cytokines in duplicate. A representative image of one of the arrays is shown in Figure 4.1. Membranes were carefully removed from between protective sheets and placed into the multi-dish (1 per well). Arrays were then incubated in the blocking solution for 1 hour at room temperature on a rocker. 100μl pooled supernatant samples were added to 500μl of Array Buffer 4 and the final volume adjusted to 1.5ml with Array buffer 6 and 15μl of reconstituted Detection Antibody Cocktail added to each preparation. This mixture was then incubated for 1 hour at room temperature before being added to the membranes following aspiration of the blocking solution. Membranes were incubated with the prepared samples overnight at 4°C on a rocker.

On the following day, membranes were washed three times with 1x Wash Buffer for 10 minutes each before 4ml IRDye 800CW Streptavidin (LI-COR, USA) diluted 1:5000 in Array Buffer 4 was added and the membranes incubated in the dark for 1 hour. Membranes were then washed as before and scanned at 800nm using an Odyssey CLx (LI-COR Biosciences, USA).

Intensities for each 'dot' were recorded using Image Studio Lite (LI-COR Biosciences, USA) and the local background values for each 'dot' subtracted from the intensity. Intensity values for duplicate 'dots' were averaged and normalised between arrays using reference dots from striatal or VM intact, vehicle-treated tissue arrays. 3 arrays were run per sample pool in order to ensure accuracy. Array data were analysed though in this case it is recognised that each n comprises a technical replicate rather than a different sample, as all samples from individual animals were pooled for the purpose of these arrays.

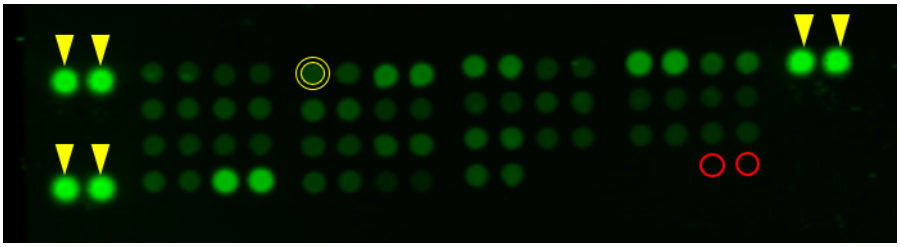

Figure 4.1: A representative image of a cytokine array adapted for use with a fluorescence imager as detailed above. Yellow arrowheads show the location of positive control spots and red circles show the approximate location of negative control spots. All spots are printed in duplicate, with the duplicate spots as neighbours on the array. Here, one spot is shown outlined in order to demarcate the approximate boundary of fluorescent intensity analysis. The outer ring around this same spot shows the approximate area of local background intensity values.

4.3.3.3 ELISAs

Using the data from the cytokine arrays, 3 targets were chosen which displayed an apparent lesion effect and drug effect, and their regulation between groups was consistent with an inflammatory event occuring due to lesioning (Macrophage Inflammatory Protein 1α (MIP1α), Interferon γ-induced protein 10 (IP10) and CXCL7). These targets were chosen from observation of the VM inflammatory data which seemed to have a larger effect of LSP1-2111 treatment. Additionally, one target with a high expression and a significant lesion effect was chosen in order to validate the array approach (CXCL7 in the VM). ELISAs against these chosen targets were purchased and run as per the accompanying protocol. Prior to running the samples in full, 2 samples (1 each of vehicle-treated animal intact and lesioned hemisphere tissue) were diluted to 1:2, 1:4, 1:10 and 1:50. These single-sample dilutions were run against the standard curve in order to ascertain the most appropriate dilutions at which to run the samples. A further TH ELISA was performed in order to confirm the presence of a lesion.

TH

The rat TH ELISA was purchased from 2BScientific, UK (SEB438Ra-96T). A standard curve was created in duplicate, with final concentrations ranging from 10ng/ml to 0.156ng/ml by factors of two, and two additional wells with only 100μl sample diluent buffer to give 0pg/ml. Striatal tissue supernatant was added to the plate in duplicate at at dilution of 1:2 in PBS to a volume of 100μl. The plate was then covered and incubated at 37°C for 1 hour. Following the incubation, plate contents were removed and replaced immediately with 100μl per well of detection reagent A (likely biotinylated anti-TH antibody) at a dilution of 1:100 with assay diluent A, then re-covered and incubated for a further 60 minutes at 37°C. The wells were then washed 3 times with wash buffer in 0.1M PBS and blotted on fibre-free paper. 100μl of detection reagent B (likely to form

an avidin-biotin complex) at a dilution of 1:100 with assay diluent B was added to each well before a further 30 minute incubation at 37°C. 5 washes were then carried out with wash buffer before adding 90μl of 3,3',5,5'-tetramethylbenzidine (TMB) colour developing agent and returning to the incubator for 15 minutes. At the end of this time, 50μl stop solution (0.16M sulphuric acid) was added to each well and the optical density of absorbance for each well immediately read in a microplate reader at wavelength of 450nm and 540nm for the purpose of wavelength correction.

MIP1α

The rat MIP1α ELISA was purchased from Abcam, UK (ab213916). A standard curve was created in duplicate, with final concentrations ranging from 500pg/ml to 7.8125pg/ml by factors of two, and two additional wells with only 100μl sample diluent buffer to give 0pg/ml. Centrifuged VM tissue homogenate was added to the plate in duplicate at at dilution of 1:2 in sample diluent buffer to a volume of 100μl. The plate was then covered and incubated at 37°C for 90 minutes. Following the incubation, plate contents were removed and replaced immediately with 100μl per well of biotinylated anti-MIP1α antibody diluted 1:100 in antibody diluent buffer then re-covered and incubated for a further 60 minutes at 37°C. The wells were then washed 3 times with 0.1M PBS and blotted on fibre-free paper. 100μl of avidin-biotin complex was added to each well at 1:100 dilution in ABC dilution buffer before a further 30 minute incubation at 37°C. 5 washes were then carried out with PBS before adding 90μl of 3,3',5,5'-tetramethylbenzidine (TMB) colour developing agent and returning to the incubator for 25 minutes. At the end of this time, 100μl stop solution (0.16M sulphuric acid) was added to each well and the optical density of absorbance for each well immediately read in a microplate reader at wavelength of 450nm and 540nm for the purpose of wavelength correction.

IP10

The rat IP10 ELISA was purchased from Abnova, Taiwan (KA2203). A standard curve was created in duplicate, with final concentrations ranging from 1000pg/ml to 15.625pg/ml by factors of two, and two additional wells with only 100μl assay diluent buffer to give 0pg/ml. Centrifuged VM tissue homogenate was added to the plate in duplicate at at dilution of 1:2 in sample diluent buffer to a volume of 100μl. The plate was then covered and incubated at room temperature for 2 hours. Following the incubation, plate contents were removed and the wells washed 4 times with 1x wash buffer from the 15x buffer supplied with the kit. Each wash consisted of the addition of 300μl wash buffer to all wells and placing the plate on a rocker for 5 minutes before evacuating the wells. Detection anti-IP10 antibody was then diluted 1:100 in assay diluent to a final concentation of 0.83μg/ml and added to each well at a volume of 100μl. The plate was then incubated at room

temperature for a further 2 hours before repeating the wash steps. 100μl of streptavidin-HRP, diluted 1:400 with assay diluent, was added to each well and incubated for 30 minutes at room temperature. Following 4 more wash steps, 100μl of substrate solution was added to each well and the plate was incubated for 15 minutes in the dark while the colourimetric change took place. 100μl stop solution was immediately added to each well and the plate read in a microplate reader at 450 and 540nm as before.

CXCL7

This ELISA was run on both striatal and VM tissue homogenate. The VM ELISA was undertaken in order to provide evidence for the utility of the cytokine array approach due to the apparently large lesion effect seen in the VM with this cytokine. The striatal tissue was run in order to further explore a potential effect of LSP1-2111 on cytokine expression.

The rat CXCL7 ELISA was purchased from Abcam, UK (ab100781). A standard curve was created in duplicate, with final concentrations ranging from 50,000pg/ml to 68.59pg/ml by factors of three, and two additional wells with only 100μl sample diluent buffer to give 0pg/ml. Centrifuged VM or striatal tissue homogenate was added to the plate in duplicate at at dilution of 1:20 or 1:5 respectively in assay diluent buffer to a volume of 100μl. The plate was then covered and incubated at 4°C overnight. The following day, plate contents were removed and the wells washed 4 times with 1x wash buffer from the 5x buffer supplied with the kit. Wash buffer was evacuated from the wells immediately following addition and the plate was blotted dry between each addition. Detection anti-CXCL7 antibody was then diluted 1:80 in assay diluent and added to each well at a volume of 100μl. The plate was then incubated at room temperature for 1 hour before repeating the wash steps. 100μl of streptavidin-HRP, diluted 1:400 with assay diluent, was added to each well and incubated for 45 minutes at room temperature. Following 4 more wash steps, 100μl of substrate solution was added to each well and the plate was incubated for 30 minutes in the dark while the colourimetric change took place. 50μl stop solution was immediately added to each well and the plate read in a microplate reader at 450 and 540nm as before.

In all ELISAs, all duplicate wells' absorbance was averaged and the samples' absorbance mapped to the standard curve for each cytokine using the equation of the line of standard curve. In cases where the samples' cytokine concentration fell in the lower end of the standard curve (MIP1α, IP10), the lower half of the curve was plotted which formed a straight line - giving rise to a linear equation. In the case of CXCL7, sample concentration was in the mid regions of the standard curve and so a log-log graph was plotted using the full standard curve to generate a straight line

and descriptive equation. These methods allowed accurate calculation of the concentration of each cytokine in the sample homogenates. The sample absorbance values mapped to their respective standard curve using the line equation generated values which were then multiplied by the dilution factor used when the samples were plated in the ELISA. Finally, readings were normalised to the results of the BSA assay performed in connection with the earlier cytokine arrays in order to normalise the levels of cytokine to the levels of total protein for each sample.

4.3.4 LSP1-2111-mediated transcriptional changes

4.3.4.1 Generation of tissue

For generation of the VM and striatal tissue used in the GeneChip array, naïve animals were given a single, subcutaneous dose of LSP1-2111 (10mg/kg) or saline (n=4 per group). 3 hours after administrations, rats were culled via cervical dislocation and the brain removed. Right and left VM and striata were rapidly dissected and mechanically dissociated in 1ml lysis buffer (400711-13, Agilent Technologies, USA) with 7μl β-mercaptoethanol. Samples were then repeatedly vortexed and agitated until fully homogenised. At this point, 200μl of homogenate was removed for further preparation and the remainder stored at -20°C.

4.3.4.2 RNA elution and purification

200μl of fresh 70% ethanol was added to the homogenised tissue sample and mixed thoroughly. The mixture was then tranferred to a RNA-binding spin cup (Agilent Technologies, USA) in a collection tube and spun in a microcentrifuge for 30 seconds before discarding the filtrate and retaining the spin cup with bound RNA. DNAase (Agilent Technologies, USA) was added in order to improve the purity of the final product and incubated at 37°C for 15 minutes. The RNA, still bound to the spin cup, was then washed once with a high-salt wash buffer and twice with a low-salt wash buffer before elution. 30μl of elution buffer was added to the matrix inside the spin-cup, incubated at 25°C for 2 minutes and then microcentrifuged. This step was repeated in order to improve the RNA yield. The elution buffer-RNA mixture was then stored at 20°C overnight.

An RNA 6000 Pico kit (Agilent Technologies, USA) was used in order to measure the yield and purity of the RNA extracted from the tissue homogenates. A gel-dye mix was prepared as per the supplied protocol and loaded into an Agilent RNA chip through the loading well. Pressure was

applied for 30 seconds in order to ensure the gel mix had spread evenly. Green RNA Pico marker was added to the ladder and sample wells to enable visualisation of sample. 1μl Pico ladder was added to the ladder well and 1μl of each sample to the other wells. The chip was then vortexed and loaded into a Bioanalyser (Aglient Technologies, USA). The run was judged successful if the ladder showed 7 well resolved peaks and each sample showed 1 marker peak and 2 ribosomal RNA peaks atop a broader mRNA 'hump' as in Figure 4.2. Striatum and VM samples with highest mRNA yield were chosen for genomic analysis. These corresponded to 3 animals from each initial group of 4. The chosen samples were normalised to the sample with the lowest yield prior to cDNA amplification from RNA.

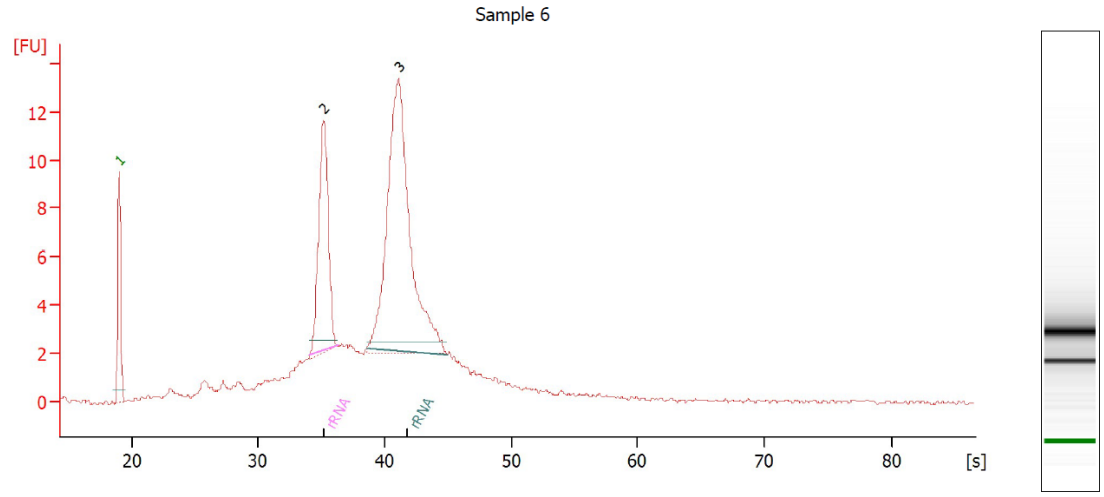

Figure 4.2: A representative graph of the yield and purity of RNA extracted from tissue from LSP1-2111-treated rats. The graph displays the characteristic single marker peak (1) and broad mRNA hump with 2 rRNA peaks overlaid (2 and 3) showing successful extraction without contamination.

4.3.4.3 Manufacture of cDNA

To convert RNA to cDNA, first strand primers were annealed at 65°C for 2 minutes and a first strand master mix prepared. The master mix was added to each tube of sample with annealed primers and run through the termal cycler on a program of gradual heating (4°C - 2 minutes, 25°C - 30 minutes, 42°C - 15 minutes, 70°C - 15 minutes). A second strand master mix was then added and the mixture cycled (4°C - 1 minute, 25°C - 10 minutes, 50°C - 30 minutes, 80°C - 20 minutes). The tubes were briefly centrifuged prior to cDNA purification.

cDNA was cleaned and purified using Agencourt beads - polystyrene beads which reversibly bind DNA and can be magnetised when exposed to a magnetic field. Agencourt beads were washed,

resuspended, added to each sample and incubated for 10 minutes. Following this, the bead-cDNA mixture was placed on a magnet, washed using fresh 70% ethanol and then air dried prior to single primer isothermal amplification (SPIA). A SPIA master mix was prepared and added to the cDNA-bead mixture. The tubes were then placed in a thermal cycler and gradually heated (4°C - 1 minute, 47°C - 75 minutes, 95°C - 5 minutes). The beads were then re-magnetised and the cleared SPIA cDNA transferred to a new tube. SPIA cDNA was then purified through a spin column (QIAquick PCR purification kit, QIAGEN, Germany) multiple times in 80% ethanol.

SPIA cDNA was next fragmented into sections of around 80bp and labelled with biotin. A fragmentation master mix was prepared and added to each SPIA cDNA sample and tubes placed in a thermal cycler (37°C - 30 minutes, 95°C - 2 minutes). Biotin labelling master mix was then added to the fragmented SPIA cDNA and the tubes replaced in the cycler (37°C - 60 minutes, 70°C - 10 minutes). Each labelled sample was then added to a Rat230 2.0 GeneChip (Affymetrix/Thermo Fisher Scientific, USA) and left to hybridise overnight.

4.3.4.4 GeneChip scanning

Following wash steps, the chips were loaded into a GeneChip Scanner 3000 7G and scanned for relative fluorescent intensity against a grid of the known positions of sequences within the chip. Areas of consistent low intensity where bubbles had prevented full hybridisation were automatically excluded from subsequent analysis. In order to control for this, multiple sequences relating to the same gene were distributed widely around the chip such that excluding one region from analysis was not likely to prevent the regulation of any one gene from being characterised.

4.3.4.5 Data handling and analysis

As each chip was scanned, an .ARR file was generated which contained information on the relative intensity of all sequences within the chip. This file was then compared against a freely available annotation file (Rat230-2.na36.annot.csv) using Transcriptome Analysis Console software (Thermo Fisher Scientific, USA). The annotation file contained information on the sequences used in the array, such as the location of each sequence within the genome and the name of the gene containing each sequence (if known).

The overall signal data for each sample was subject to principal component analysis in order to examine the profile similarity between and within groups of the same type of samples. A list of

gene expression was generated for each sample (3×3 saline SNc, saline striatum, LSP1-2111 SNc and LSP1-2111 striatum). Within groups, the regulation of genes was averaged to give a figure representative of the effect of LSP1-2111 or saline within that tissue sample. The gene regulation for saline was then compared to that of LSP1-2111 in SNc and striatum samples in order to give figures representing the relative up- or downregulation of each gene by LSP1-2111 compared to saline controls.

Multiple sequences relating to expressed sequence tags (ESTs) were present on both SNc and striatum gene lists. These represented regions of the genome which have not yet been confirmed to relate to specific, well-characterised genes. Given the provision of the position of the sequence within the genome, it is possible to make a 'best guess' as to which gene in the vicinity of the sequence is represented - but this is a time consuming and uncertain process. Therefore, only named sequences were used in the analysis.

903 sequences representative of genes in the VM and 624 in the striatum were up or downregulated ≥ 2 fold by a single administration of LSP1-2111 and these were all observed to be significant changes (< 0.05) by the Transcriptome Analysis Console software (Thermo Fisher Scientific, USA). Of these sequences, 495 in the SNc and 398 in the striatum have been well characterised and could be linked to a named gene with a known function by the Transcriptome Analysis Console analysis software. Data which remained significant following application of a false discovery rate correction through the Trancriptome Analysis Console has also been noted, though this likely represents a high false negative rate and so all gene regulation passing the $p < 0.05$ significance rate are still considered. Due to the large amount of data generated through this approach, the simplest way to ascertain the function of each gene was determined to be cluster analysis. Volcano plots were also generated to show regulation of individual genes in each tissue (LSP1-2111 compared to saline).

Pathway analysis was performed through the Transcriptome Analysis Console software. Pathway analysis was found to provide better concordance between data sets in PD than individual gene expression changes when examining microarray data (Sutherland et al. 2009). Results of the GeneChip analysis data were compared, by the software, to WikiPathways - an open-source, online signalling pathway resource (Slenter et al. 2018). A list of pathways involving one or more of the significantly regulated genes was output. The list featured the number of LSP1-2111-regulated genes involved in the pathway, in which direction each regulated the pathway and the significance of the overall pathway regulation by LSP1-2111. The pathway list was then mapped to the cluster analysis, allowing an overview of the functions of each gene cluster to be formed. This analysis

was undertaken independently for the hits from the VM and striatum.

4.4 Results

4.4.1 Inflammation in 6-OHDA-lesioned, LSP1-2111-treated rats

Representative images of the Iba1 stain in the lesioned and intact SNc of partially lesioned rats treated with LSP1-2111 (an mGluR4 agonist) or vehicle are shown in Figure 4.3. There is a clear increase in Iba1 stained cells in the lesioned SNc, though differences between groups are less obvious. Iba1 staining appears quite faint, with some nuclear staining in the background. This was not considered to be an issue as manual counting was employed in the analysis of these images.

Throughout the SNc, there was a considerable increase in Iba1-postive cell number as a result of lesion (Figure 4.4a). However, there was no significant difference in the number of Iba1-positive inflammatory cells in the lesioned nigra between vehicle and LSP1-2111 treated groups (Figure 4.4a).

In the caudal SNc, there was a significant inflammatory effect of the lesion measured through number of Iba1-positive cells ($p = 0.028$), but no effect of LSP1-2111 treatment ($p = 0.092$) or interaction between variables ($p = 0.58$) in a 2-way ANOVA. Sidak's multiple comparisons post-test did not reveal any differences between intact and lesioned nigra for specific groups. This was also true in the mid SNc, where there was a stronger effect of lesioning ($p = 0.0015$) on inflammation but no effect of LSP1-2111 treatment ($p = 0.32$) in a 2-way ANOVA.

In the rostral SNc, there was also a significant effect of lesion ($p < 0.0001$) and no overt effect of LSP1-2111 treatment ($p = 0.15$), however a Sidak's post-test revealed that there was a significant increase in Iba1-positive cells in the lesioned SNc only in vehicle and 1mg/kg LSP1-2111 treatment groups ($p < 0.05$), and not in the 10mg/kg LSP1-2111 group. The greatest change in Iba1-positive cell number between lesioned and intact SNc also occurs in the rostral SNc - and this appears to drive the main overall increase.

This situation of the greatest lesion effect and the greatest drug effect both occurring in the rostral SNc mirrors what was seen with TH cell loss in the SNc of these animals when the neuroprotective effect was examined in Chapter 3.

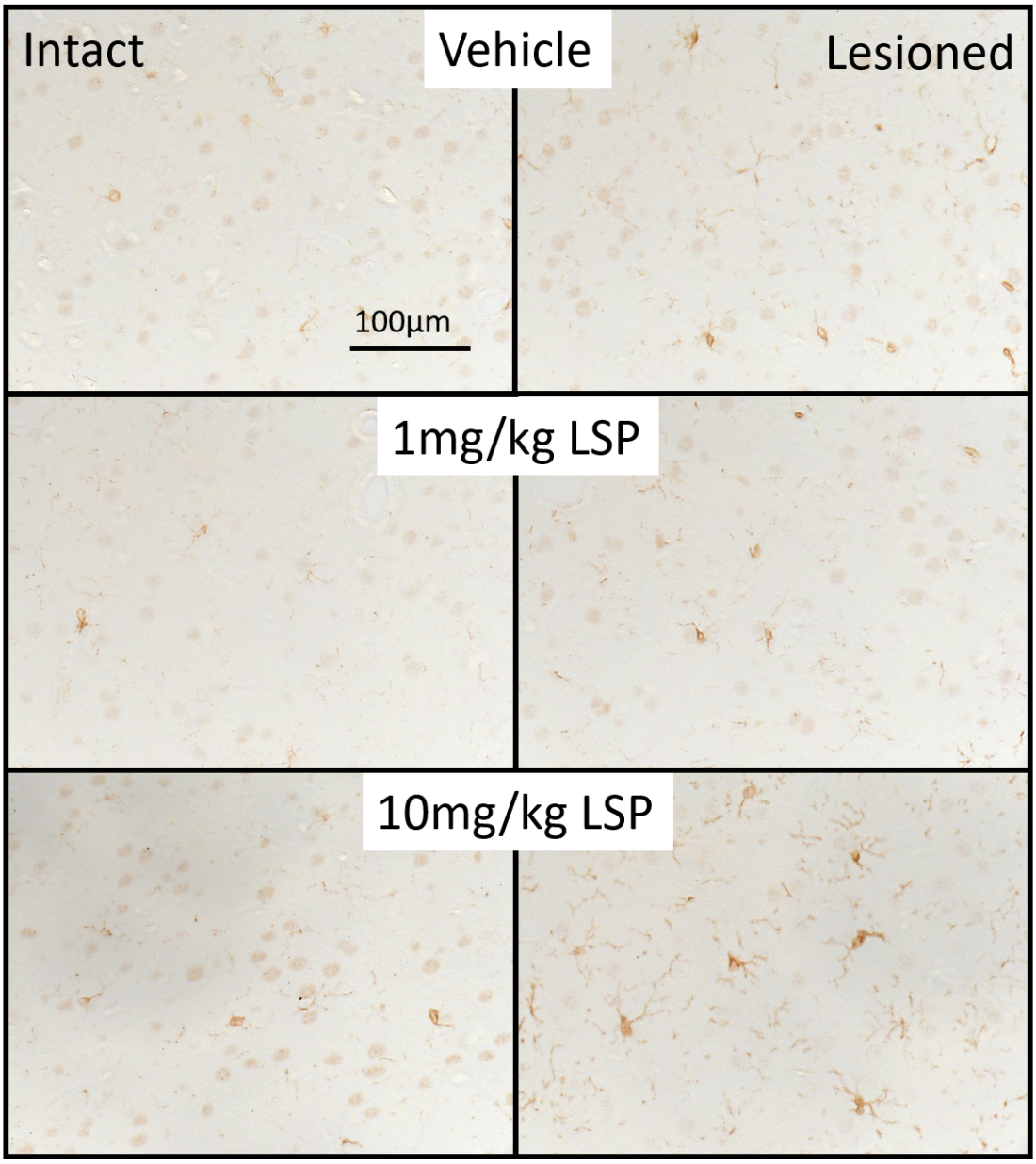

Figure 4.3: Representative images of Iba1 staining in the intact and lesioned rostral SNc 13 days post-lesion in animals dosed with vehicle or 1 or 10mg/kg LSP1-2111.

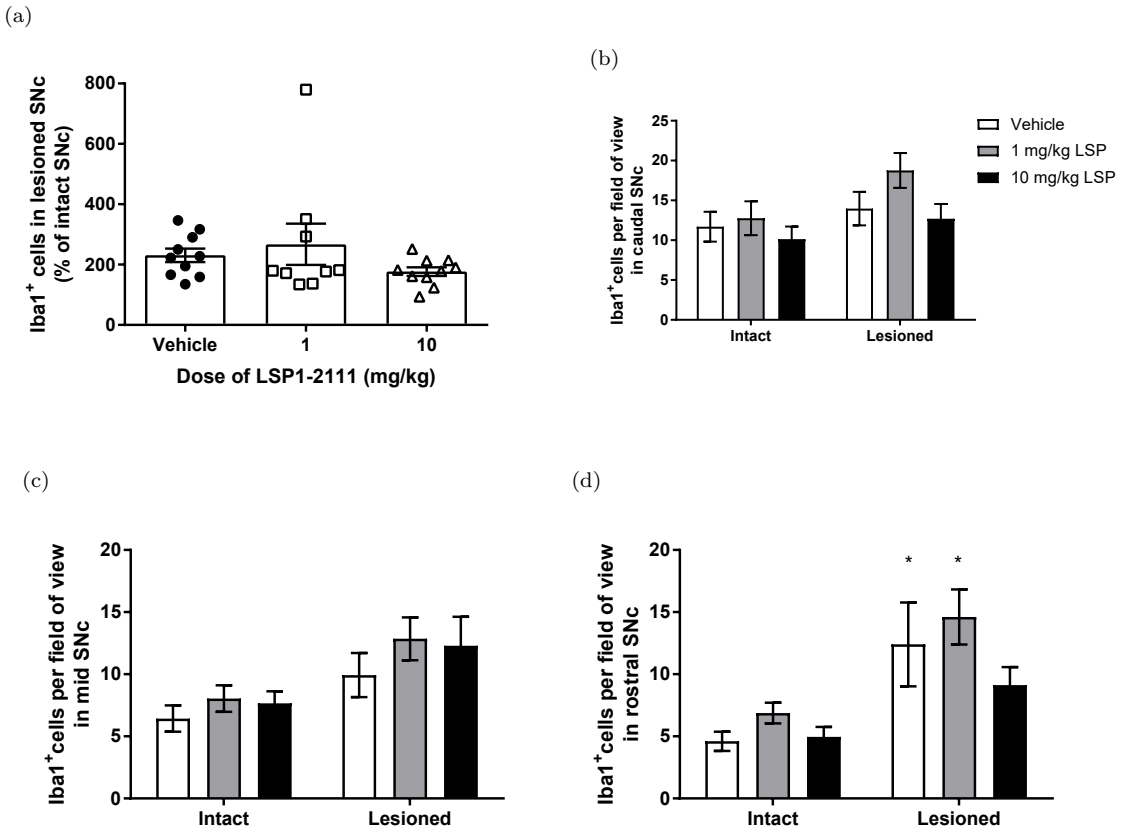

Figure 4.4: Iba1-positive cells per field of view in lesioned and intact rostral SNc of animals treated with LSP1-2111 or vehicle. a) Average numbers of Iba1-positive cells throughout the whole lesioned SNc as a percentage of the intact SNc. b) Raw counts of Iba1-positive cells in the intact and lesioned caudal, c) mid and d) rostral SNc. * = $p < 0.05$ compared to intact SNc in 2-way ANOVA with Sidak's post-test. For all, data are mean ± standard error of the mean (S.E.M.) and n=9-10 per group.

Iba1-positive cells were also counted in the striatum using images representative of each of the four quadrants (DM, DL, VL, VM) and at each of the three levels (caudal, mid and rostral) while taking care to avoid the central glial scar around the site of injection. Figure 4.5 shows representative images of Iba1 staining in intact and lesioned dorsotalteral, rostral striatum. The increase in Iba1-positive cells is evident in the lesioned hemisphere compared to the intact hemisphere of animals in all groups, though there does not appear to be a strong effect of drug.

When taken as an overall average (Figure 4.6a), there was no significant difference in Iba1 increases in lesioned striata between groups in a 1-way ANOVA ($p = 0.45$). The Iba1 response overall in the lesioned striatum of vehicle-treated animals was $269.9\% \pm 28.1$ of the intact striatum. In the lesioned striatum of animals in the 1mg/kg LSP1-2111, the response was $231.8\% \pm 23.0$ and in the 10m/kg LSP1-2111 group the response was $278.1\% \pm 30.1$.

In light of the neuroprotective study showing effects in some quadrants of the striatum (and not others), the inflammatory response was analysed further through examination of the number of Iba1-positive cells apparent per field of view (20x objective) at each level and quadrants of the striatum. At the caudal level, there was a significant effect of lesion and treatment ($p < 0.0001$), but not of quadrant ($p = 0.073$) and no interaction between variables ($p = 0.98$) in a 2-way ANOVA (Figure 4.4b). Sidak's post-test revealed that there were significantly more Iba1-positive cells in the lesioned DM quadrant than the intact equivalent in the vehicle treated animals but not in either LSP1-2111 group. In the DL quadrant, there was also a significant increase in Iba1 cells in the lesioned hemisphere compared to the intact in vehicle and 10mg/kg animals.

In the mid and rostral levels of the striatum (Figures 4.4c and 4.4d), 2-way ANOVAs found a significant effect of lesion and treatment ($p < 0.0001$) and quadrant ($p < 0.0001$) and an interaction between variables ($p = 0.032$). At these levels of the striatum, DL tissue from animals in all groups showed a significant increase in Iba1 positive cells in the lesioned hemisphere compared to the intact hemisphere. There were no differences in Iba1 cell counts between lesioned and intact hemispheres in the other quadrants and no further effect of treatment was elucidated in the post hoc test.

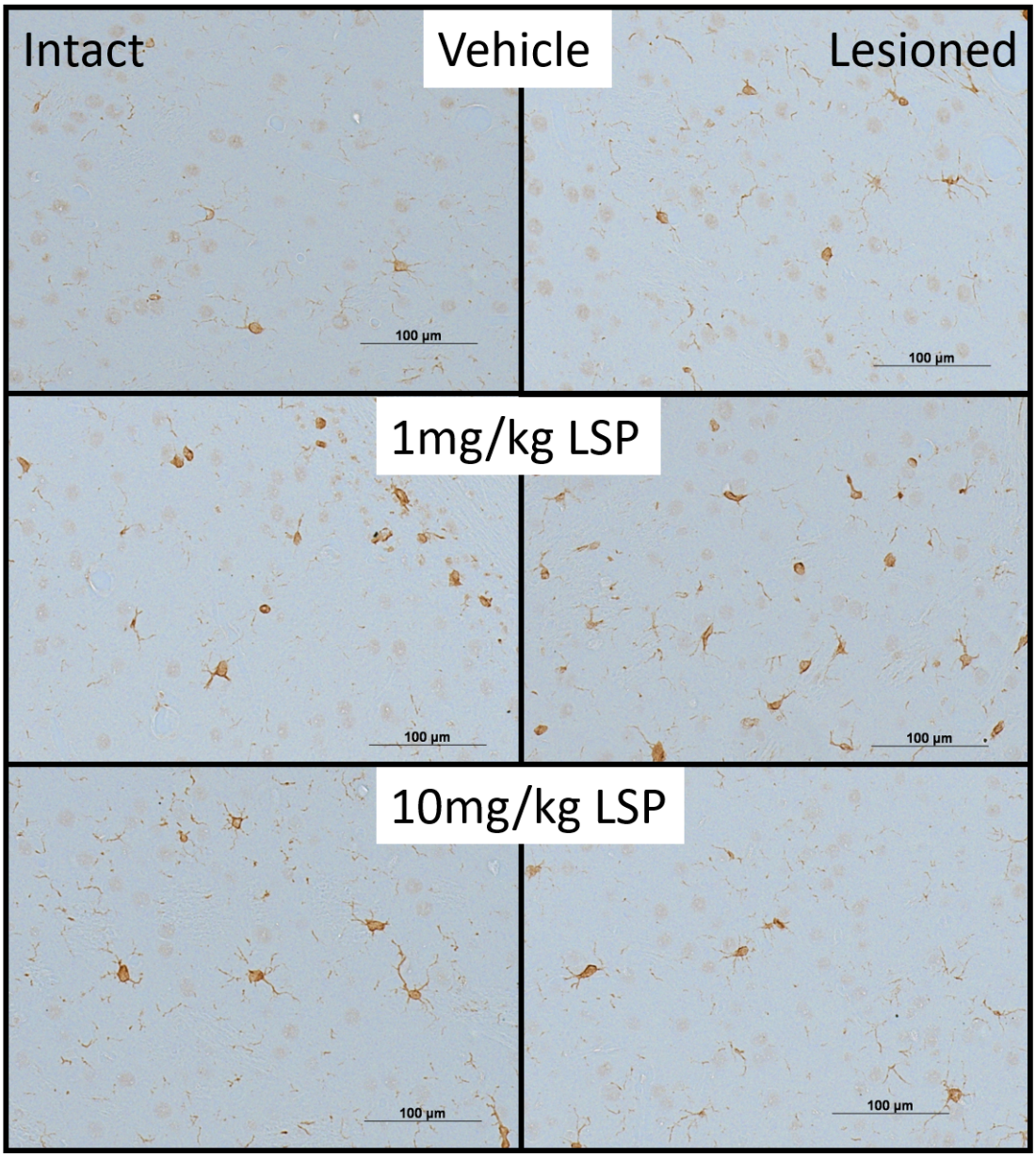

Figure 4.5: Representative images of Iba1 staining in the intact and lesioned rostral dorsolateral striatum 13 days post-lesion in animals dosed with vehicle or 1 or 10mg/kg LSP1-2111.

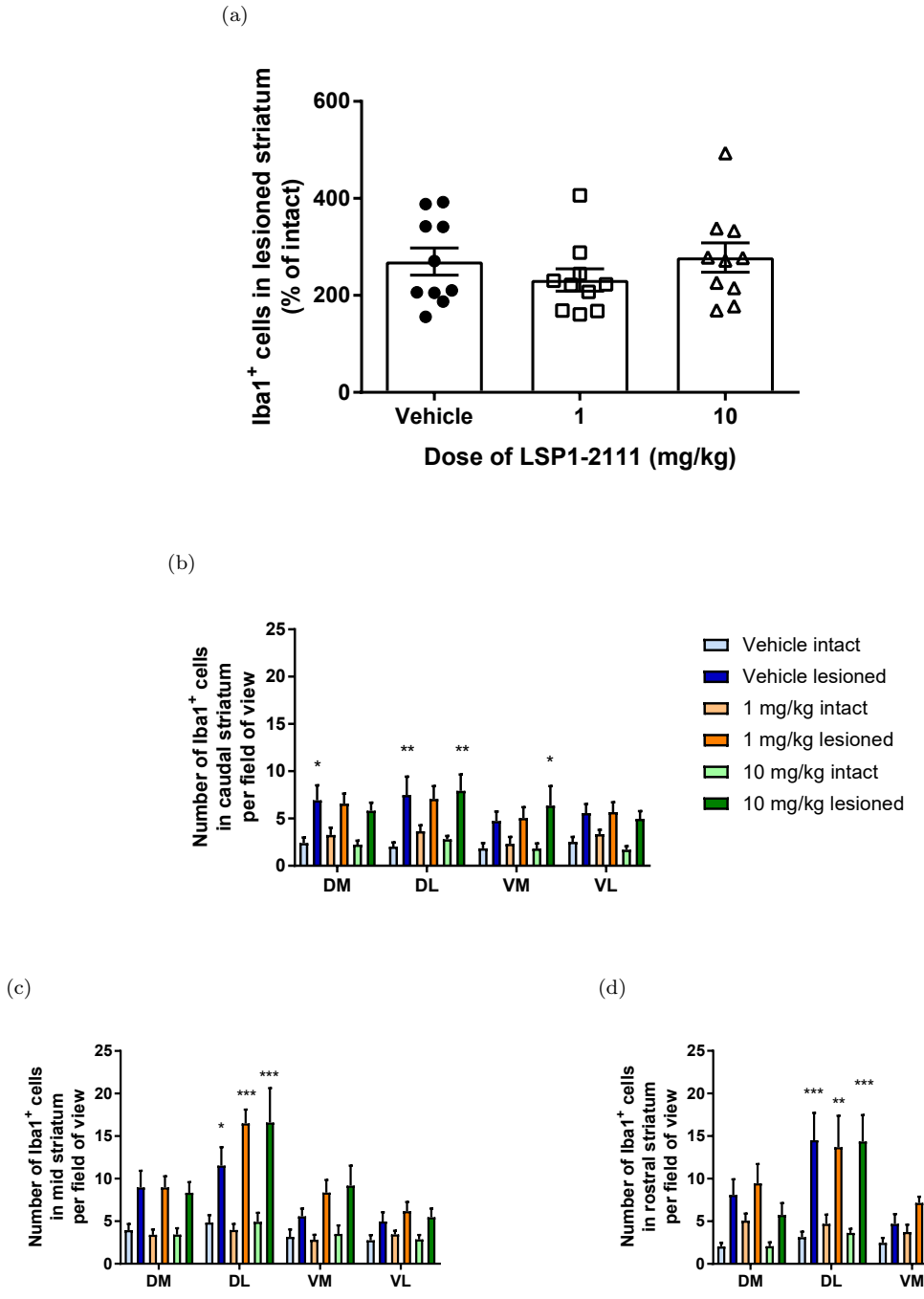

Figure 4.6: Counts of Iba1-positive microglia and monocytes were conducted in representative images of each quadrant of lesioned and intact striatum of animals treated with LSP1-2111 or vehicle. a) Overall increase in Iba1-positive cells throughout the striatum. b) Raw numbers of Iba1-positive cells in the lesioned and intact caudal, c) mid and d) rostral striatum. * = $p < 0.05$, ** = $p < 0.01$, *** = $p < 0.001$ in 2-way ANOVA with Sidak's post-test. For all, data are mean ± S.E.M. and n=9-10 per group. DM, dorsomedial; DL, dorsolateral; VL, ventrolateral; VM, ventromedial.

GFAP stain density was assessed in the SNc in order to ascertain the effect of lesion and LSP1-2111 treatment on astrocytes. Representative images of the GFAP stain obatined in these sections iare shown in Figure 4.7. Due to the thinness of the sections, few whole cells were observed in each image, though a large number of seemingly unconnected processes were. For this reason, densitometry was seen to be a more appropriate method of analysis than counting of individual cells as was performed for Iba1-positive cells.

When the GFAP stain density was averaged over all levels of the SNc (in Figure 4.8a), there was no significant difference between treatment groups ($p = 0.125$ in a 1-way ANOVA). Nevertheless, there was a non-significant, LSP1-2111-mediated decrease in GFAP stain density compared with the lesioned SNc of vehicle-treated animals.

There were no significant differences in GFAP stain density between the treatment groups when the individual caudal (Figure 4.8b, $p = 0.54$), mid (Figure 4.8c, $p = 0.078$) or rostral (where neuroprotection was seen in these animals, Figure 4.8d, $p = 0.49$) levels of the SNc were examined.

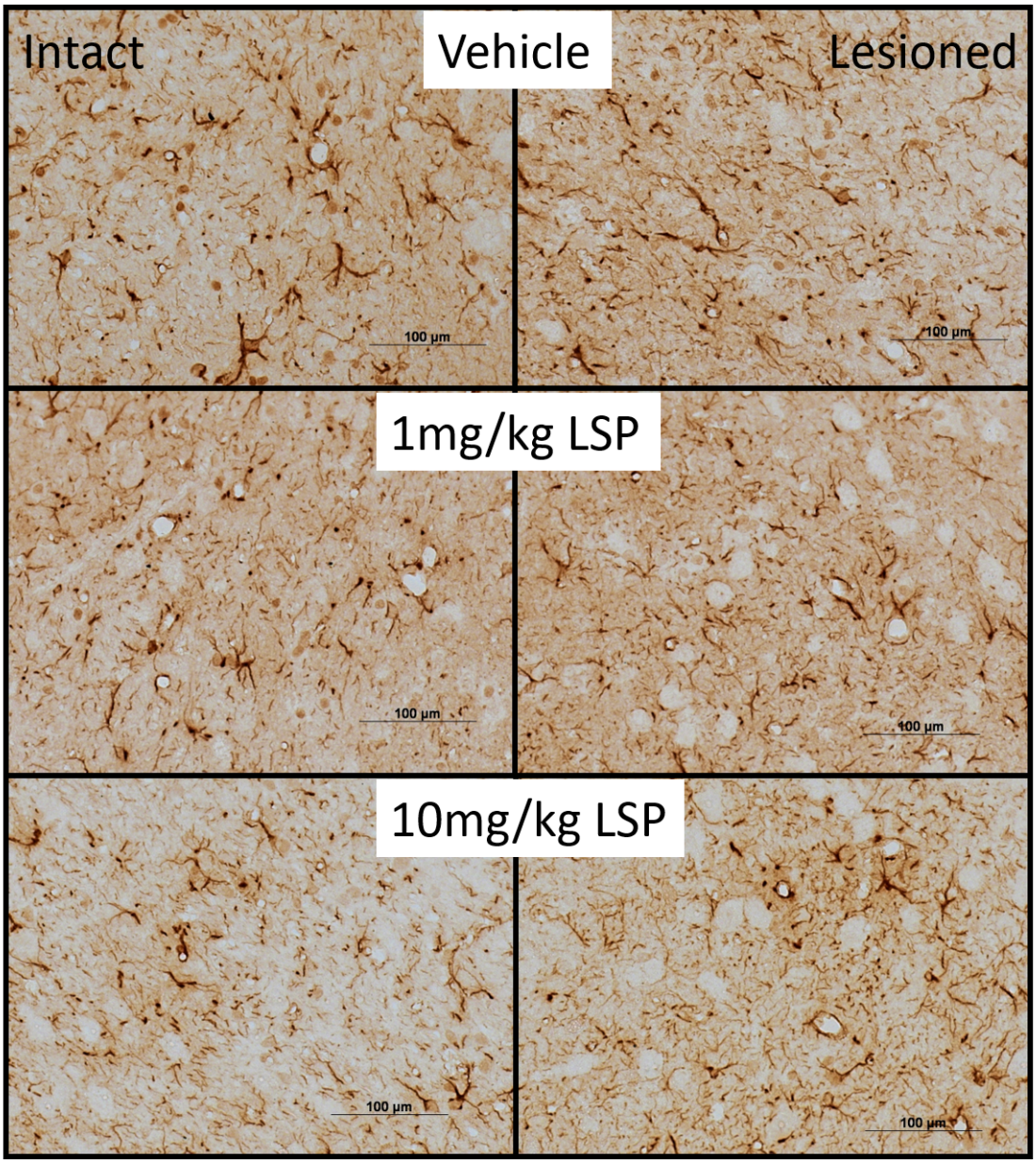

Figure 4.7: Representative images of GFAP staining in the intact and lesioned SNc 13 days post-lesion in animals dosed with vehicle or 1 or 10mg/kg LSP1-2111.

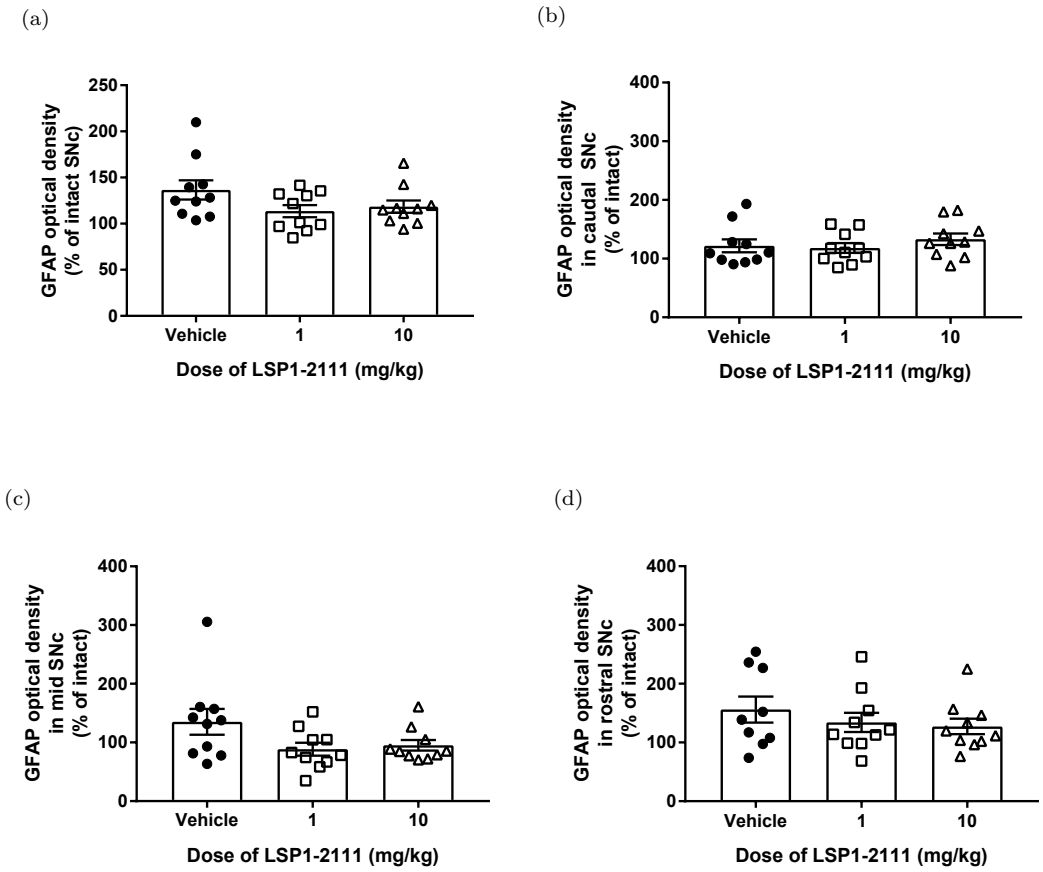

Figure 4.8: GFAP stain density in lesioned SNc as a percentage of intact SNc in animals treated with LSP1-2111 or saline. a) GFAP density in all caudal-rostral levels of a representative image of the centre of the lesioned SNc as a percentage of the intact SNc. b) Densitometry was conducted in the caudal, c) mid and d) rostral SNc. $n = 10$ for all groups and data are mean±S.E.M..

GFAP levels were assessed using densitometry of the GFAP stain in the lesioned striatum compared to the corresponding area in the intact striatum. Stain density was examined in the areas of each striatal quadrant which were not affected by the formation of an astrocytic scar in order to ascertain the role of astrocytes in the inflammatory response to 6-OHDA rather than mechanical damage as a result of the injection. This glial scar is easy to see in the image shown in Figure 4.9a. The staining can be observed as very low background with dense points visible where GFAP-positive cells are heavily stained, especially surrounding the site of injection.

Overall, and indeed throughout the individual levels of the striatum, there was no effect of treatment ($p = 0.95$ in 1-way ANOVA, Figure 4.9b). In vehicle-treated animals there was a minor increase in GFAP in the lesioned striatum to 109.6%$\pm$0.66 of the intact striatum. In the 1mg/kg and 10mg/kg LSP1-2111 treatment group these figures were very similar - 110%$\pm$1.2 and 109.6%$\pm$1.1 respectively.

When the GFAP stain density values were examined by quadrant and level, no difference in GFAP values between regions or treatment groups was evident.

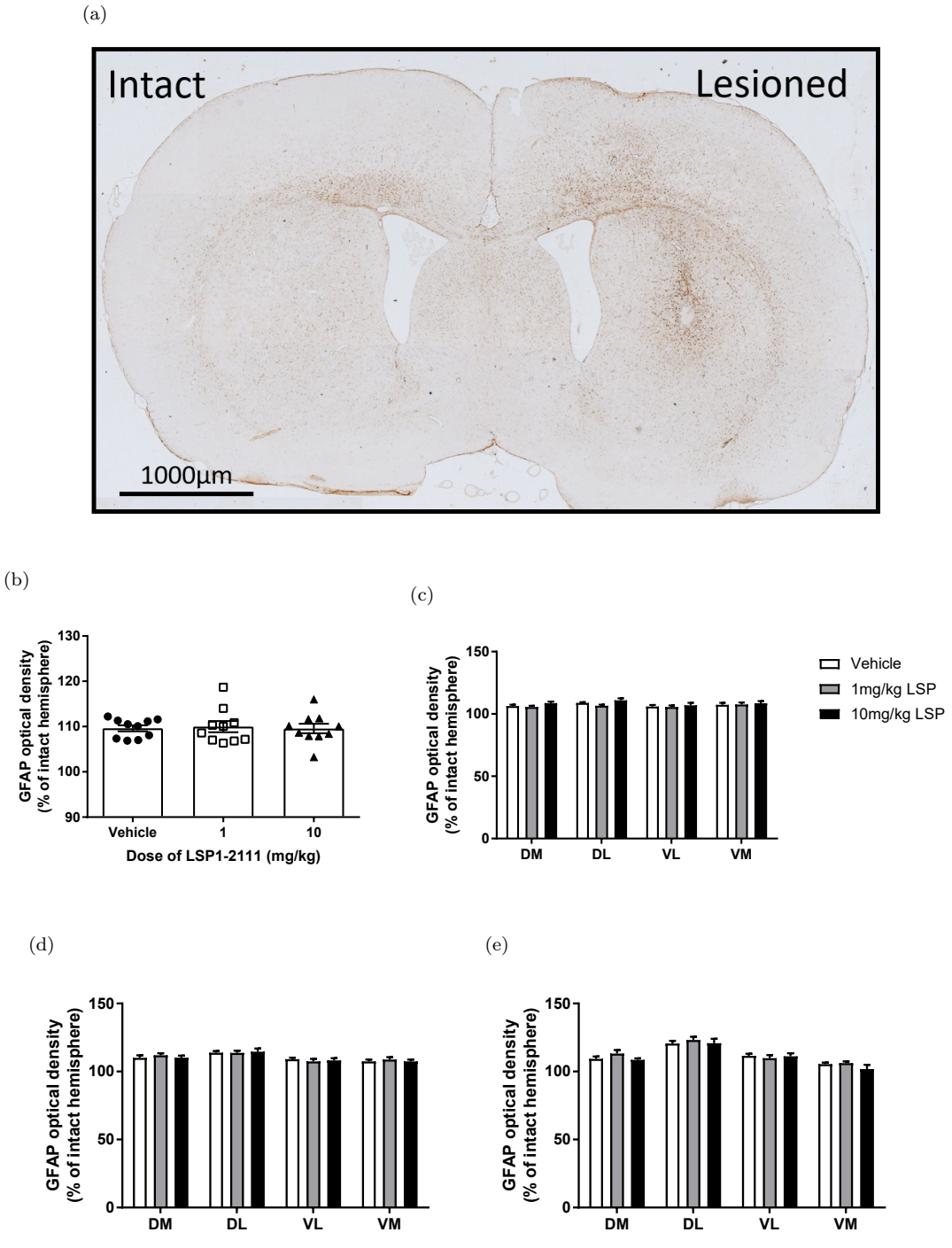

Figure 4.9: GFAP-positive astrocytosis in lesioned and intact striatum. b) Overall increase in GFAP-positive cells throughout the lesioned striatum as a percentage of the intact striatum. c) GFAP densitometry broken down by quadrant in the caudal, d) mid and e) rostral lesioned striatum as a percentage of intact. For all, data are mean ± S.E.M. and n=9-10 per group. DM, dorsomedial; DL, dorsolateral; VL, ventrolateral; VM, ventromedial.

4.4.2 Time course of inflammation following 6-OHDA lesion

The time course study examined the development of the partial lesion over time compared to sham animals using immunohistochemistry and western blotting - no behavioural tests were undertaken.

Two animals died during surgery, possibly as a result of overheating following a failure in the air conditioning.

4.4.2.1 Histological characterisation of lesion

Figure 4.10a shows a representative image of the SNc of sham and 6-OHDA-lesioned animals stained for TH at 7 days post-surgery. Although the difference between images is not striking, the lesioned side of the SNc in 6-OHDA-lesioned animals does appear thinner than the corresponding SNc in sham animals.

There was a significant loss of TH-positive cells in the rostral SNc at day 7 post-lesion only ($p < 0.05$ compared to sham), with an average of 63 $\pm$ 11 cells remaining in the lesioned SNc of 6-OHDA animals and 100 $\pm$ 9 cells in the lesioned SNc of shams (Figure 4.10b). In the initial 2-way ANOVA for cell count values, there was a significant effect of lesioning ($p = 0.016$), no effect of time ($p = 0.52$) and no interaction between variables ($p = 0.14$). A Sidak's post-test revealed that a significant reduction of TH-positive cells was present in the lesioned SNc only of 6-OHDA-treated animals at day 7 post-lesion.

When comparing cell loss as a percentage of intact SNc, there was a significant effect of time ($p = 0.0069$) and a significant effect of lesioning ($p = 0.018$, Figure 4.10c). At days 2 and 3 post-lesion, there was no significant difference between TH-positive cell numbers in the intact and lesioned SNc of sham or 6-OHDA-lesioned animals. By day 4, a modest but significant loss of TH-positive cells could be observed in the lesioned SNc of 6-OHDA-lesioned animals ($86.1\% \pm 4.9$ cells remaining). This lesion was larger by day 7 post-lesion ($58.0\% \pm 6.8$ of intact).

(a)

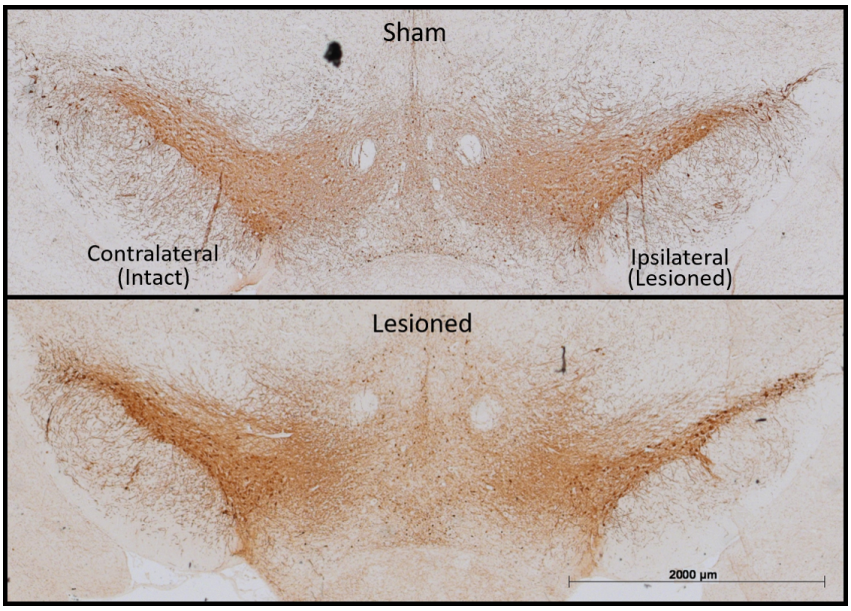

(b)

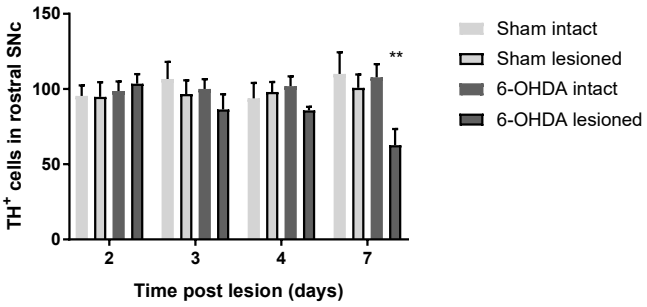

(c)

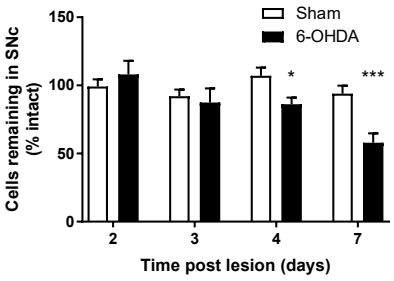

Figure 4.10: TH-positive cell loss over time in the lesioned, rostral SNc of 6-OHDA-lesioned animals. a) Representative image of sham and lesioned SNc, 7 days post surgery. b) Raw numbers of TH-positive cells remaining in intact and lesioned SNc. ** = $p < 0.01$ in 2-way ANOVA with Sidak's post-test. compared intact SNc in lesioned animals. c) Cells in lesioned SNc expressed as a percentage of intact SNc cell numbers. * = $p < 0.05$, *** = $p < 0.001$ compared to sham at the same time point by unpaired t-test. Data are mean ± S.E.M. and n=4-5 per group.

4.4.2.2 Histological characterisation of inflammatory reponse to lesioning

Iba1-positive cells were characterised through a number of different methods from high-magnification (20x) images of immunohistochemical staining (Figure 4.11a). The images in Figure 4.11a from tissue taken at 7 days post-lesion show densely stained Iba1-positive cell bodies with a number of processes varying in length and branching. Many 'disembodied' processes appear in the background of the images as a result of the sectioning process cutting through cells. There appears no obvious difference in the number or morphology of cells between sham and 6-OHDA-lesioned SNc in these images, and this is borne out in the analysis.

A 2-way ANOVA revealed no significant differences in the number of Iba1-positive cells in lesioned or intact SNc between groups at any time point (Figure 4.11b). Further analyses also failed to pick out any differences in activation states of Iba1-positive cells in the SNc between sham and 6-OHDA-lesioned animals at any time point (Figure 4.11c, 4.11d and 4.11e). In these additional analyses, activated microglia were expected to present with a higher density of Iba1 stain and a larger soma size (Kozlowski & Weimer 2012).

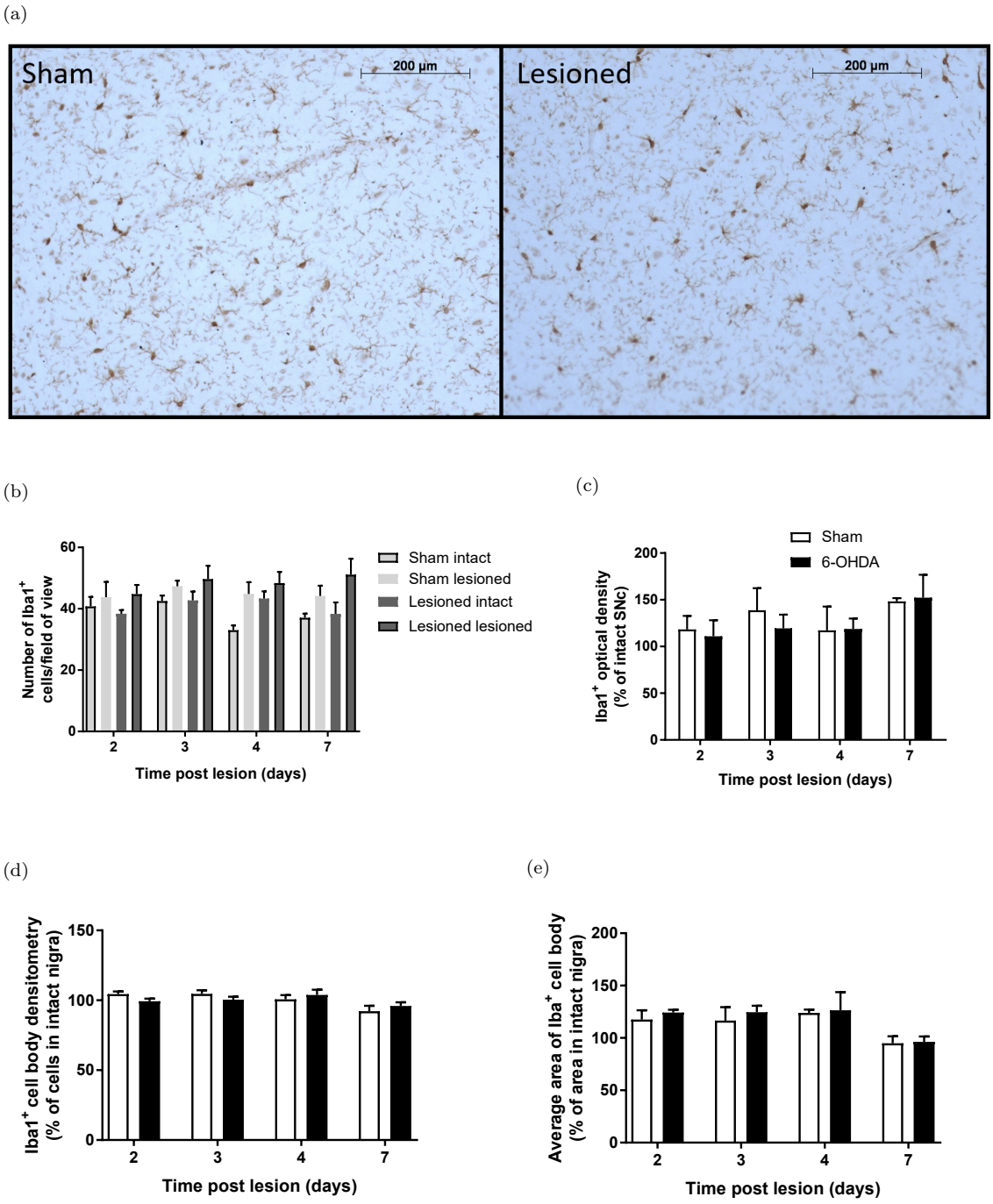

Figure 4.11: Quantitative analysis of Iba1-positive cells in the SNc data after sham- or 6-OHDA-lesion. a) Representative 20x images of Iba1 staining in a central, representative region of sham and lesioned SNc, 7 days post lesion. b) The average number of Iba1 cells per field of view in SNc sections. c) Optical density of Iba1 stain in a representative field of view in rostral SNc. d) Densitometry of Iba1 stain in cell bodies of microglia stain in rostral SNc. e) Average area of Iba1-positive microglial cell body in rostral SNc. Data are mean ± S.E.M. and n=4-5 per group.

GFAP-positive cells in SNc were characterised by two methods - high magnification (20x) cell counts of a representative, central area of the SNc (Figure 4.12 depicts 40x images) and densitometries of the GFAP stain in those same images. The representative images shown in Figure 4.12 show low background staining, a multitude of 'disembodied' processes from astrocytes in tissue adjoining the imaged section, and some full astrocytes with characteristic branching. The image from the 6-OHDA-lesioned SNc appears to show a greater number or density of GFAP stained cells and processes than does the image from the sham SNc.

Densitometric analysis showed no significant difference in nigral GFAP-positive cell number between sham and 6-OHDA groups in unpaired t-tests (Figure 4.13a).

When GFAP stain was quantified through a high-magnification automated cell count (Figure 4.13b), there was no significant difference between 6-OHDA and sham animals. The trend in this data towards an increased number of GFAP-positive cells in the 6-OHDA, as compared to the sham animals, at day 3 may appear at odds with the densitometry data shown in Figure 4.13a. This semblance of disparity between data is likely caused by the non-specificity of densitometric analysis - while the cell count process is programmed to only use data from cells (or patterns) over a certain size, the densitometric analysis uses the entire image. This means that dirt on the slide or processes from cells cut off the image will be used alongside whole cells. The increased density of stain in sham slides on day 3 therefore represents a greater concentration of partial cells ('disembodied' processes which have been separated from the cell through sectioning) compared to whole or large cell fragments in the 6-OHDA images.

The average number of branches per cell (Figure 4.13c) and average branch length (Figure 4.13d) were also calculated using ImageJ software but no differences between sham and 6-OHDA-lesioned animals, or lesioned animals over time, were found.

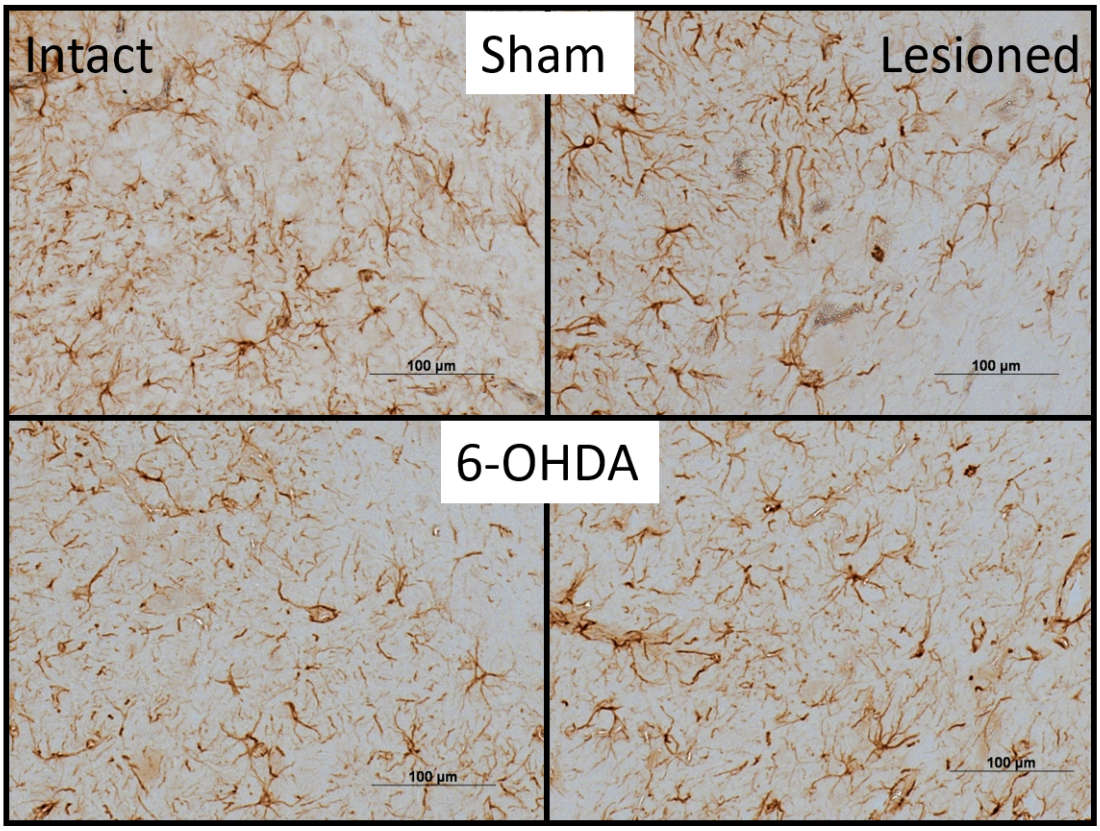

Figure 4.12: Representative 40x images of GFAP staining in the lesioned SNc of 6-OHDA-lesioned and sham animals 7 days post-lesion

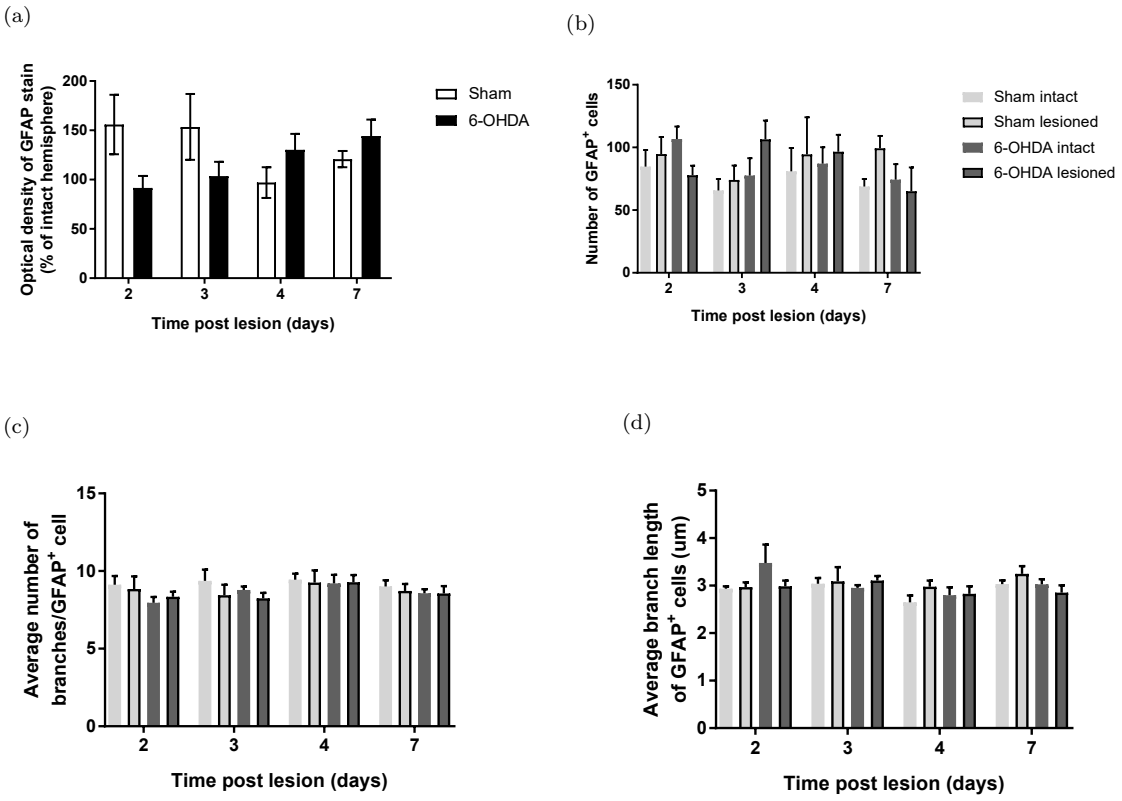

Figure 4.13: Alterations in GFAP expression in the SNc over time after lesioning. a) Changes in the numbers of GFAP-positive cells in the lesioned and intact SNc over time. b) Optical density of GFAP staining in the 6-OHDA-lesioned SNc and intact SNc. c) Average number of branches per GFAP-positive cell in the lesioned and intact SNc of 6-OHDA and sham animals. d) Average length of branches of GFAP-positive cells in lesioned and intact SNc of 6-OHDA and sham animals. Data are mean ± S.E.M. and n=4-5 per group.

4.4.2.3 Lesion characterisation by western blot

Western blotting was used to examine differences over time and between 6-OHDA and sham groups in TH and GFAP (an example blot is shown in 4.14a).

Blotting was able to differentiate between TH-content of striata from animals in sham and 6-OHDA groups ($p = 0.0005$), but there was no significant effect of time ($p = 0.41$) and no interaction of variables ($p = 0.16$) (Figure 4.14b). At day 2 post-lesion there was no difference in TH levels in 6-OHDA-lesioned striata (as a percentage of intact striata) between sham and lesioned animals, with shams having an average of $91.0\% \pm 7.3$ TH remaining and lesioned animals having $82.9\% \pm 20.5$. By day 3 post-lesion, there was a significant difference between striatal TH in 6-OHDA-lesioned and sham animals as sham lesioned striata maintained 97.9 ± 5.5 of intact TH but 6-OHDA-lesioned striata fell to $41.8\% \pm 7.3$ of intact ($p < 0.01$). While sham TH values remained consistent at days 4 and 7 post-lesion, there was more variation in 6-OHDA-lesioned TH values at day 7.

There was no significant difference between lesioned and sham groups in striatal GFAP expression, though both groups had measurably higher GFAP expression in the 6-OHDA-lesioned striatum than the intact striatum and the 6-OHDA group trended towards having a higher expression than shams (Figure 4.14c).

(a)

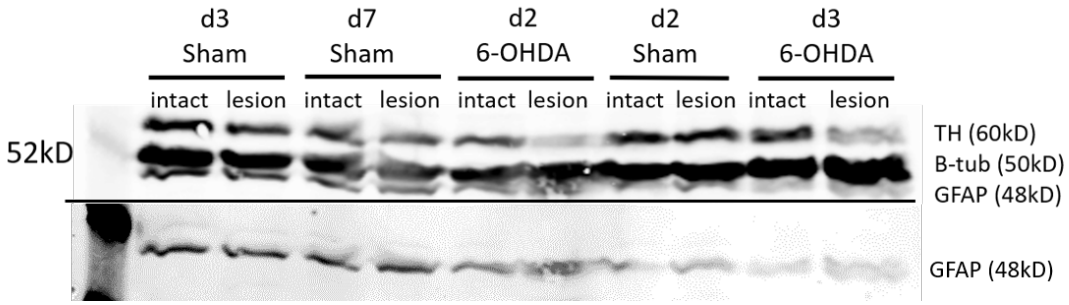

(b)

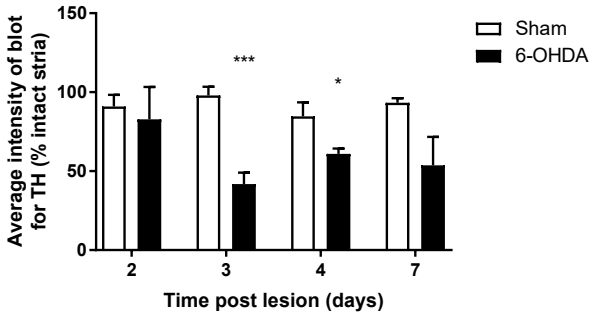

(c)

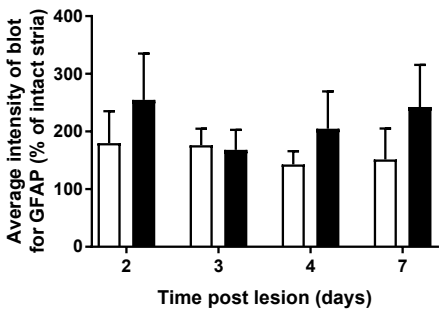

Figure 4.14: Measurement of tissue content of proteins in lesioned and intact striata in lesioned and sham animals by western blot. a) Sample image of a western blot showing bands for TH and β-tubulin. GFAP is also shown separately for clarity of bands. b) Blot intensity of protein bands labelled for TH in sham and lesioned animals over time (lesioned striatal TH intensity as a percentage of intact). * = $p < 0.05$, *** = $p < 0.001$ vs sham in unpaired t-test. c) Blot intensity of protein bands labelled for GFAP in sham and lesioned animals over time (lesioned striatal GFAP intensity as a percentage of intact). Data are mean ± S.E.M. and n=4-5 per group.

4.4.3 Cytokines in inflammatory responses

4.4.3.1 Evidence of lesion

Animals were examined through the cylinder test prior to the last dose of LSP1-2111 or vehicle in order to ascertain the presence of a nigrostriatal lesion affecting motor function. The cylinder data confirms that, in the group of 20 animals which underwent lesioning and dosing in this cohort, there was a significant effect of lesion ($p < 0.0001$), but not of treatment ($p = 0.33$), as was seen in the neuroprotection study performed in Chapter 3. Vehicle treated animals used their intact paw $53.5\% \pm 1.6$ of the time in the baseline test and $43.1\% \pm 2.2$ post-lesion, while LSP1-2111-treated animals' performance fell from $51.2\% \pm 1.9$ at baseline to $41.0\% \pm 2.8$ post-lesion. The groups appear incomplete in this data as some animals failed to meet the inclusion criteria of ≥ 10 touches with either paw and so are not presented in Figure 4.15

From this cohort, only 10 animals (5 per group) with complete cylinder data were taken forward for further examination of cytokine expression as per initial intentions - these are depicted as red points in Figure 4.15. In this reduced cohort, there remained a significant effect of lesioning but not of treatment, as in the full group - thus demonstrating a reliable lesion effect throughout.

In the smaller cohort taken forward for cytokine studies (red data points), these figures were similar: vehicle treated animals' performance in the cylinder test fell from $58.8\% \pm 1.2$ use of the contralateral paw at baseline to $42.8\% \pm 3.$ post-lesion. LSP1-2111 treated animals used their contalateral paw $51.8\% \pm 3.4$ of the time at baseline and $35.1\% \pm 2.6$ post-lesion.

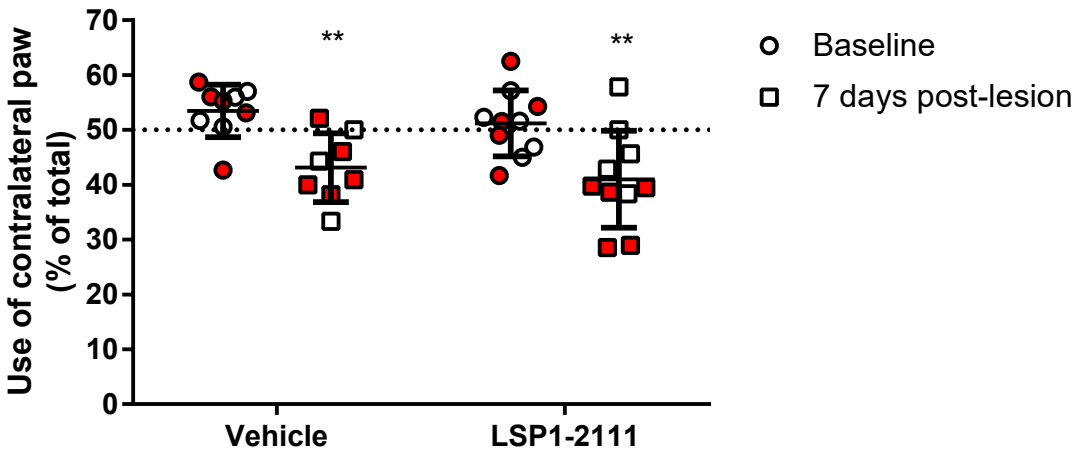

Figure 4.15: Animals were exposed to the cylinder test prior to lesioning and again at 7 days post-lesion in order to measure the motor asymmetry effected by the lesion. Points in red are data from those animals used for further cytokine studies in this chapter. In statistical tests performed on data data points, ** = $p < 0.01$ in a 2-way ANOVA with Sidak's multiple comparisons test. $n = 8 - 10$ per group (reduced group sizes are due to a lack of participation by some animals in the behavioural test) and data are mean±S.E.M..

An ELISA for TH content of the striatum was also undertaken with the intention of confirming a lesion. However, surprisingly this ELISA showed no effect of lesion ($p = 0.35$) and no effect of treatment ($p = 0.81$), with no interactions between variables ($p = 0.52$) (Figure 4.16). This may reflect poor performance of the ELISA rather than a lack of lesion, and will be discussed further in the discussion of this chapter.

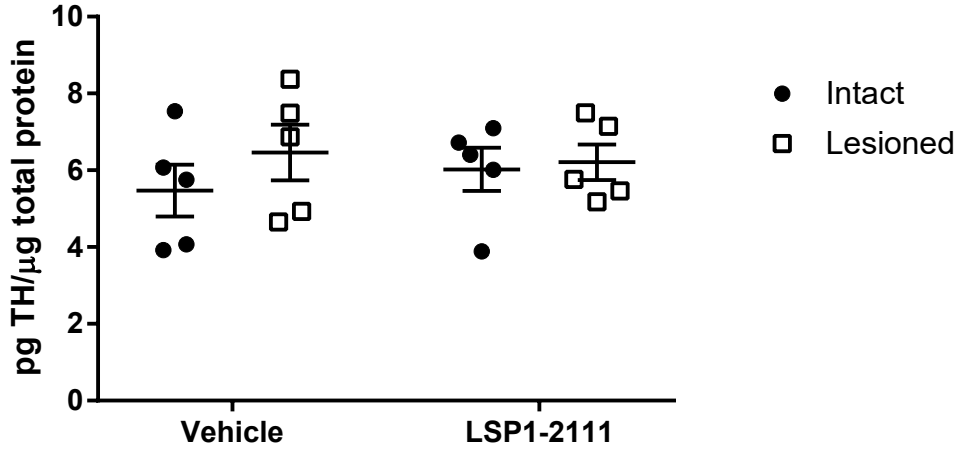

Figure 4.16: An ELISA for TH in striatal tissue from lesioned and unlesioned hemispheres of rats treated with either saline (vehicle) or LSP1-2111. $n = 5$ per group and data are mean±S.E.M..

4.4.3.2 Cytokine arrays

Cytokine arrays were conducted on VM and striatal tissue in order to obtain an overview of inflammatory activity in the brains of unilaterally, partially lesioned animals treated with vehicle or 10mg/kg LSP1-2111 at day 7 post-lesion (Figure 4.17). In both cases, a small number of cytokines showed expression levels considerably higher than the majority of the cytokines tested. These cytokines are displayed on a separate graph in order to preserve visibility of differences in expression of the lower-level cytokines.

In the VM, when cytokines were examined individually, CXCL7 ($p < 0.01$), IFNγ ($p < 0.05$) and LIX/CXCL5 ($p < 0.05$) showed a significant difference between groups in a Kruskal-Wallis test. However, a post hoc Dunn's multiple comparisons test was only able to find a significant difference between intact and lesioned VM from LSP1-2111-treated animals for CXCL7 ($p = 0.020$, Figure 4.18). These data were tested using a non-parametric test as they were found to be non-normally distributed.

Despite the paucity of significant differences in cytokine expression in lesioned/intact VM from vehicle/LSP1-2111 treated animals, there is a general trend towards an increase in expression of cytokine in lesioned tissue. Furthermore, a number of cytokines appear to show a trend towards a reduced expression in lesioned VM from LSP1-2111-treated animals compared to the vehicle counterparts.

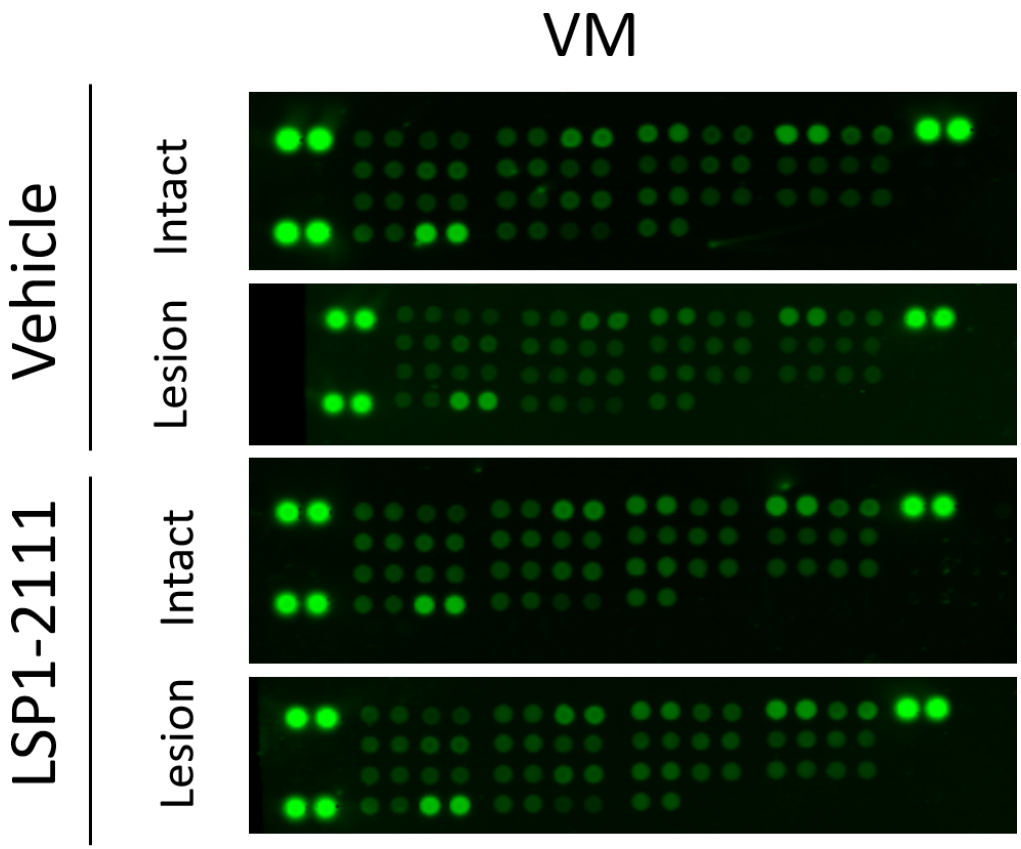

Figure 4.17: Representative images of cytokine arrays performed on VM tissue from the lesioned and intact hemispheres of vehicle- or LSP1-2111-treated animals.

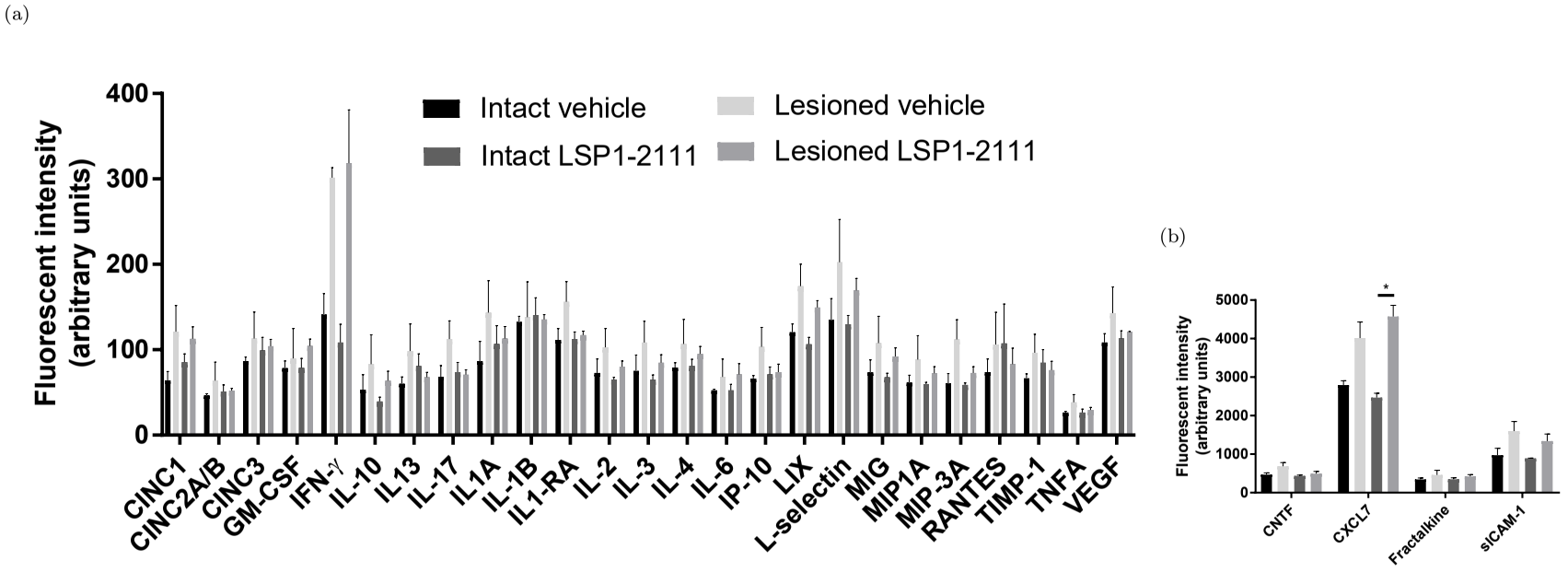

Figure 4.18: Cytokine arrays performed on tissue from the 6-OHDA-lesioned and intact VM of animals treated with vehicle or LSP1-2111, 7 days post-lesion lesion. Bars are the average data from duplicate array spots and pooled tissue from each group was used on the array. Technical replicates were normalised to positive control spots on each array. Error bars represent the S.E.M. between technical replicates. * = $p < 0.05$ in a Dunn's multiple comparisons test.

Arrays were also performed on striatal tissue from the same animals (Figure 4.19). In striatal tissue, IL-13 was the only cytokine to show significantly altered expression in a Kruskal-Wallis test ($p < 0.01$), with no further differences between individual groups evident in Dunn's multiple comparisons test (Figure 4.20). The trend towards an increase in expression in lesioned tissue and decrease in tissue from LSP1-2111-treated animals which was noted in VM tissue is much less evident in the striatum.

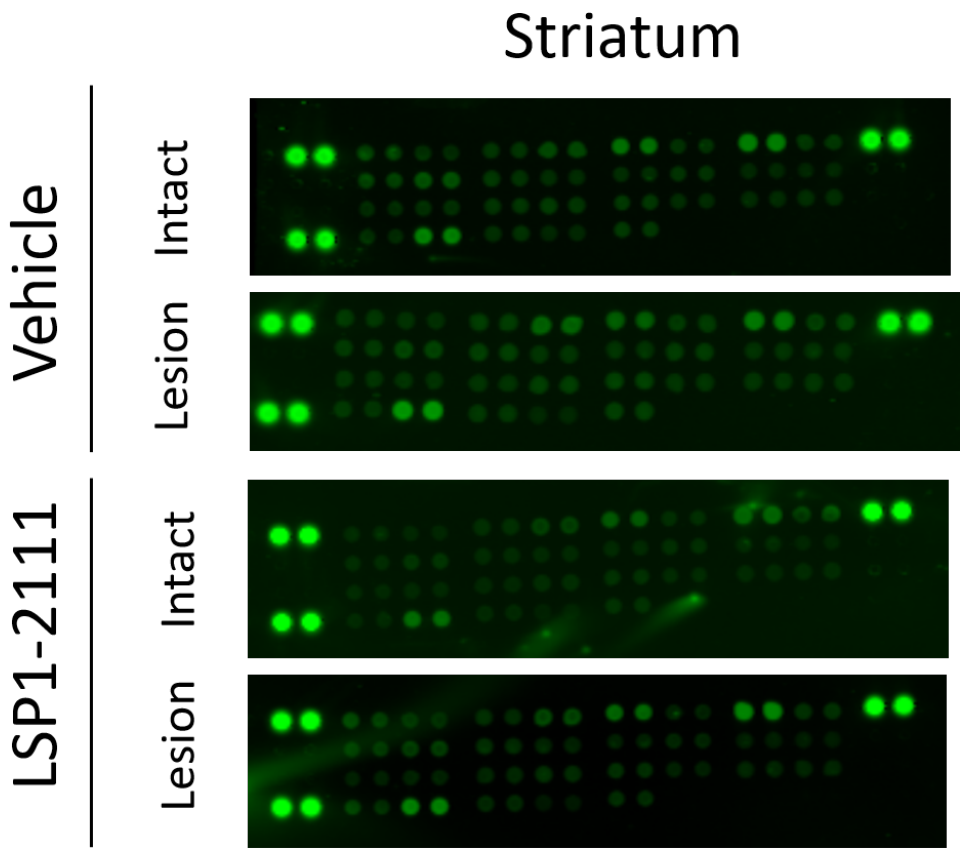

Figure 4.19: Representative images of cytokine arrays performed on striatal tissue from the lesioned and intact hemispheres of vehicle- or LSP1-2111-treated animals.

(a)

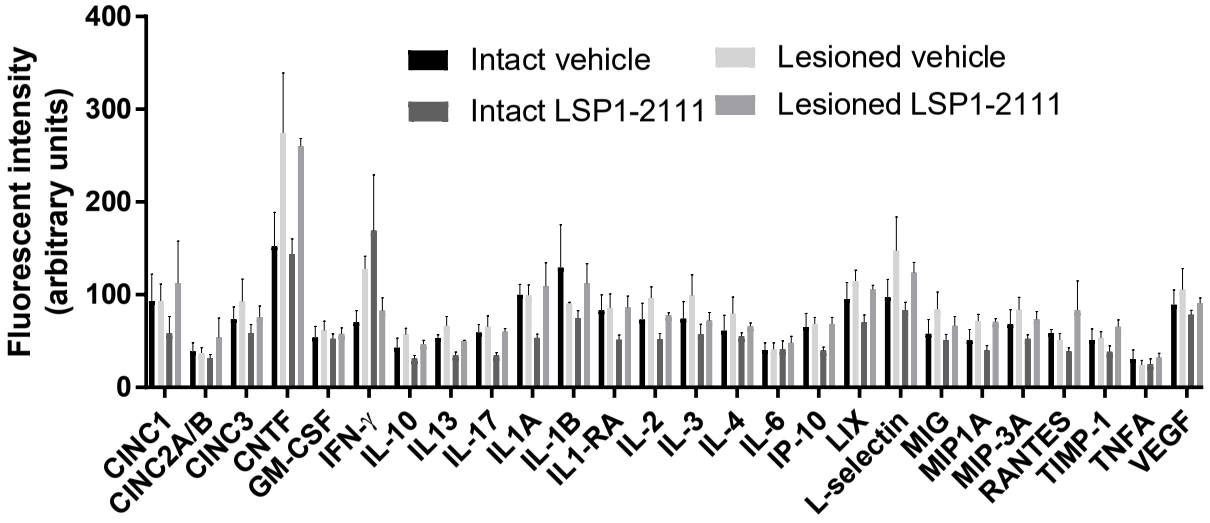

(b)

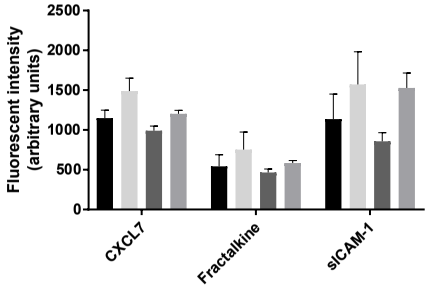

Figure 4.20: Cytokine arrays performed on tissue from the 6-OHDA-lesioned and intact VM of animals treated with vehicle or LSP1-2111, 7 days post-lesion lesion. Bars are the average data from duplicate array spots and pooled tissue from each group was used on the array. Technical replicates were normalised to positive control spots on each array. Error bars represent the S.E.M. between technical replicates.

The cytokines chosen for further examination by ELISA are displayed in Figure 4.21 in order to better display trends towards lesion and drug effects. MIP1α and IP10 in the VM, and CXCL7 in the striatum were chosen for their functional effects as reported in the literature and size of lesion and drug effect apparent in the cytokine array. CXCL7 in the VM was examined due to the large, significant effect of lesion in the LSP1-2111 treated animals in order to validate the cytokine array approach.

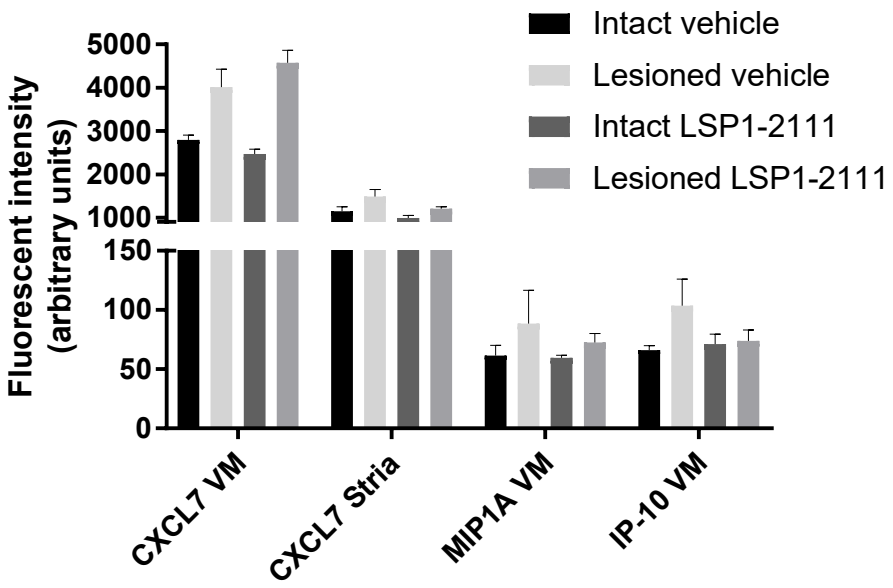

Figure 4.21: A graph showing data on targets chosen from cytokine arrays which display trends towards lesion and drug effects and were chosen for further analysis using ELISAs. These data were extracted from Figures 4.18 and 4.20.

4.4.3.3 Detection of cytokine concentration by ELISA

CXCL7 in the VM was chosen to be analysed by ELISA due to the large and significant effect of lesion apparent in this cytokine in the array. This ELISA was therefore conducted in order to validate the cytokine array approach. In this ELISA there was no significant effect of treatment ($p = 0.97$) or of lesion ($p = 0.055$) and no interaction between variables ($p = 0.76$) in a 2-way ANOVA (Figure 4.22). Despite this, there was a trend towards an increase in CXCL7 in samples of lesioned VM compared to unlesioned VM, though a large variation in the concentration in lesioned VM from LSP1-2111-treated animals.

Intact tissue from vehicle-treated animals showed a CXCL7 concentration of 116.3 ± 20.3pg/μg of total protein, compared with a concentration of 189.8 ± 47.5 in lesioned vehicle-treated animals. Similarly, in LSP1-2111-treated animals, the concentration of CXCL7 was 102.0 ± 21.3pg/μg total protein in intact VM tissue and 201.3 ± 62.0pg/μg total protein in lesioned VM.

Although no significant difference was found in this ELISA, the pattern of expression maps very well to the cytokine arrays - thus validating the approach taken here.

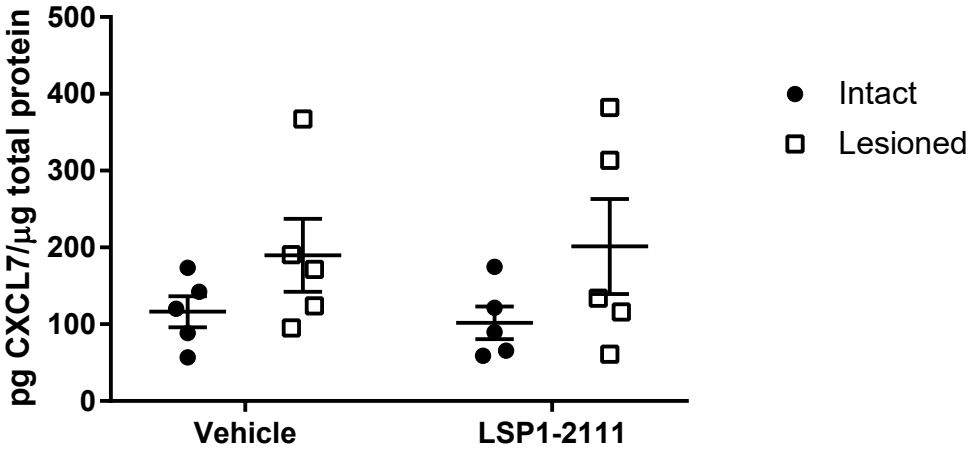

Figure 4.22: An ELISA for CXCL7 was undertaken on lesioned and intact VM tissue from rats treated with LSP1-2111 or saline (vehicle). $n = 5$ per group and data are mean±S.E.M..

Very low levels of MIP1α were detected in the ELISA to examine cytokine concentration in VM tissue. This may limit the validity of the comparison between the ELISA and the initial cytokine array. The expression of MIP1α observed in this ELISA does not map onto the original cytokine array.

There was no significant effect of treatment ($p = 0.50$) or of lesion ($p = 0.087$) and no interaction between variables ($p = 0.89$) in a 2-way ANOVA examining the effect of these variables on MIP1α concentration in the supernatant of homogenised tissue (Figure 4.23).

There was a trend towards a reduction in MIP1α in tissue from the lesioned hemisphere compared to the intact hemisphere. In real numerical terms, this represents a very small difference though, due to the low concentrations overall the difference between lesioned and intact tissue in both treatment groups appears fairly large.

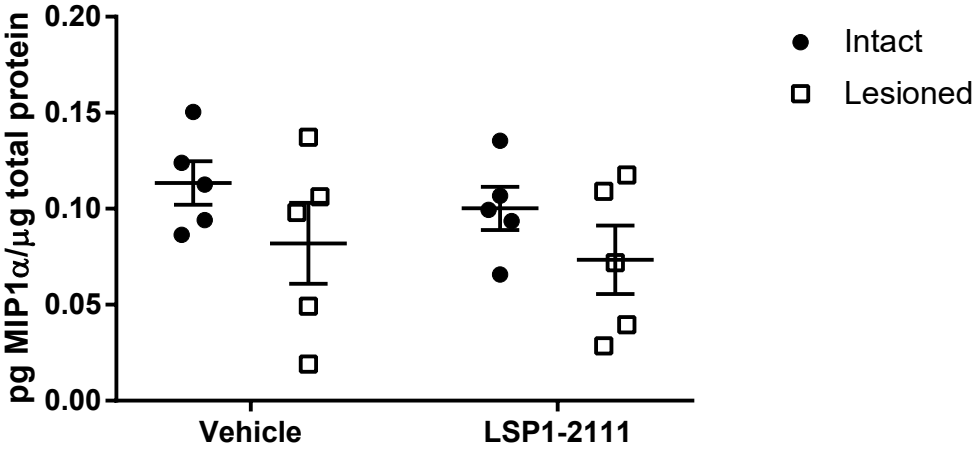

Figure 4.23: An ELISA for MIP1α was undertaken on lesioned and intact VM tissue from rats treated with LSP1-2111 or saline (vehicle). $n = 5$ per group and data are mean$\pm$S.E.M..

As with MIP1α, the concentration of IP10 observed in this ELISA is very low and calls into question the validity of the comparison between the values seen here and those recorded following the cytokine array. Although the expression of IP10 in tissue from vehicle-treated animals and the intact VM from LSP1-2111-treated animals maps well to the array, the IP10 in the VM of LSP1-2111-treated animals appears much higher in the ELISA than in the array.

An ELISA to detect IP10 found a significant effect of lesion ($p < 0.0001$) though no significant effect of treatment ($p = 0.22$) and there was no interaction between variables ($p = 0.063$) in a 2-way ANOVA (Figure 4.24). Sidak's post-test showed a further significant effect of lesioning specifically in the LSP1-2111-treated group ($p = 0.0002$). In this group, the concentration of IP10 in intact VM was 0.048 ± 0.0071pg/μg total protein compared with 0.13 ± 0.015pg/μg total protein in the lesioned VM.

The difference in IP10 concentration in tissue between lesioned and unlesioned VM in the vehicle-treated group was not significant, though did approach significance ($p = 0.053$).

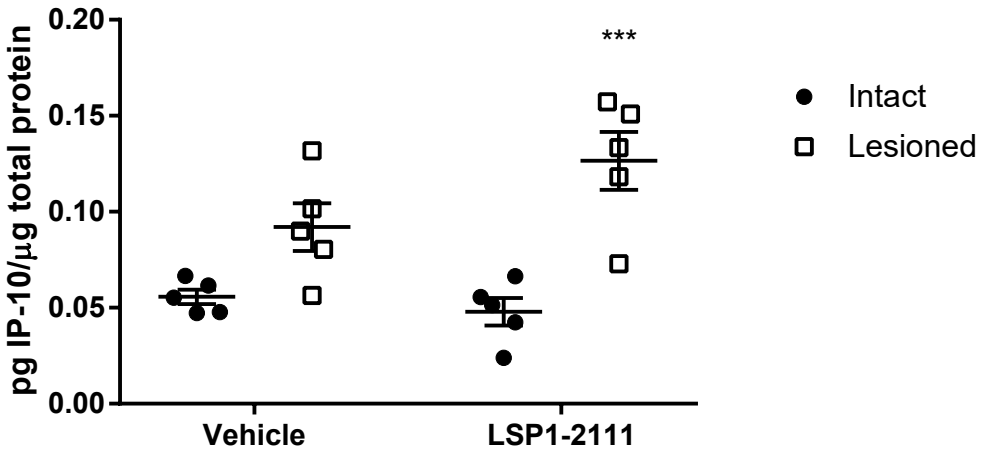

Figure 4.24: An ELISA for IP10 was undertaken on lesioned and intact VM tissue from rats treated with LSP1-2111 or saline (vehicle). ***= $p < 0.001$ compared with intact VM of the same treatment group in a 2-way ANOVA with Sidak's post-test. $n = 5$ per group and data are mean±S.E.M..

Concentration of CXCL7 in the striatal tissue is considerably higher than in the IP10 and MIP1α ELISAs, though the expression does not map well onto that suggested by the cytokine array. There appears to be a lot of variation in the concentration of CXCL7 between different animals, which may reflect individual differences or some inaccuracy within the ELISA.

There was no significant effect of treatment ($p = 0.56$) or lesioning ($p = 0.20$) and no interaction between variables ($p = 0.68$) on CXCL7 concentration in striatal tissue by a 2-way ANOVA (Figure 4.25). As in the MIP1α ELISA, there was a non-significant trend towards a reduction in CXCL7 in lesioned tissue compared with intact tissue, though a large variation in data.

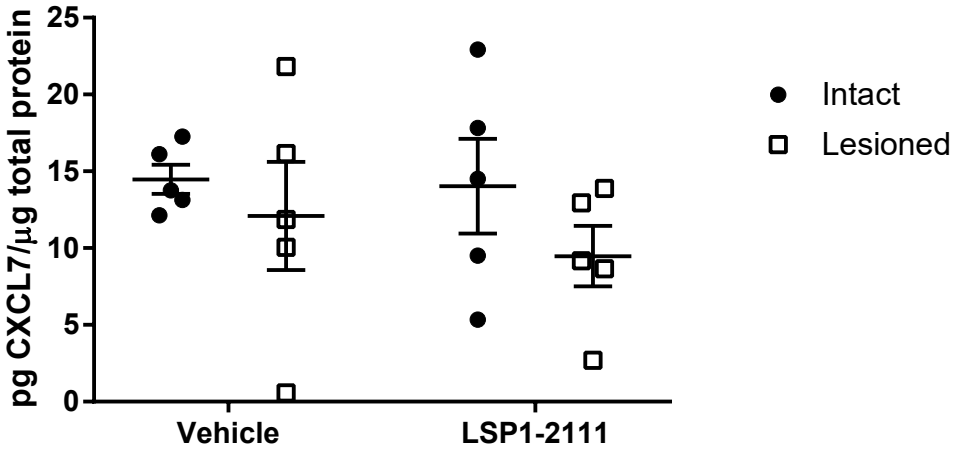

Figure 4.25: An ELISA for CXCL7 was undertaken on lesioned and intact striatal tissue from rats treated with LSP1-2111 or saline (vehicle). $n = 5$ per group and data are mean±S.E.M..

4.4.4 LSP1-2111-mediated transcriptional changes

8 naïve animals were given subcutaneous LSP1-2111 at 10mg/kg or saline vehicle ($n = 4$). Of these animals, 3 from each group were chosen on the basis of their RNA yield for transcriptional analysis.

Principal component analysis was carried out in order to examine the similarity of the transcriptomic profiles within and between groups. This provides an early, simple and qualitative method to determine whether samples from one one group are sufficiently similar to be called a population, and whether samples from different groups are sufficiently different to be from different populations.

In the case of the current data presented in Figure 4.26, it is apparent that samples from VM have a similar transcriptomic profile to each other (due to their clustering in a single area of the graph). Similarly, samples from the striatum have a similar transcriptomic profile and cluster around one point, but striatal and VM profiles are very different from each other.

The greater distance between VM samples in the principal component analysis (Figure 4.26) likely reflects the difficulty of obtaining a clean dissection of the SNc within the VM in comparison to the ease of reliably dissecting out striatum alone - thus giving rise to more variability of tissue types within a VM sample and providing a slightly more diverse transcriptomic profile. That these VM samples may still be grouped along one axis from any field of view shows that they are still sufficiently similar to warrant their further comparisons as one class using data averaged from the three samples.

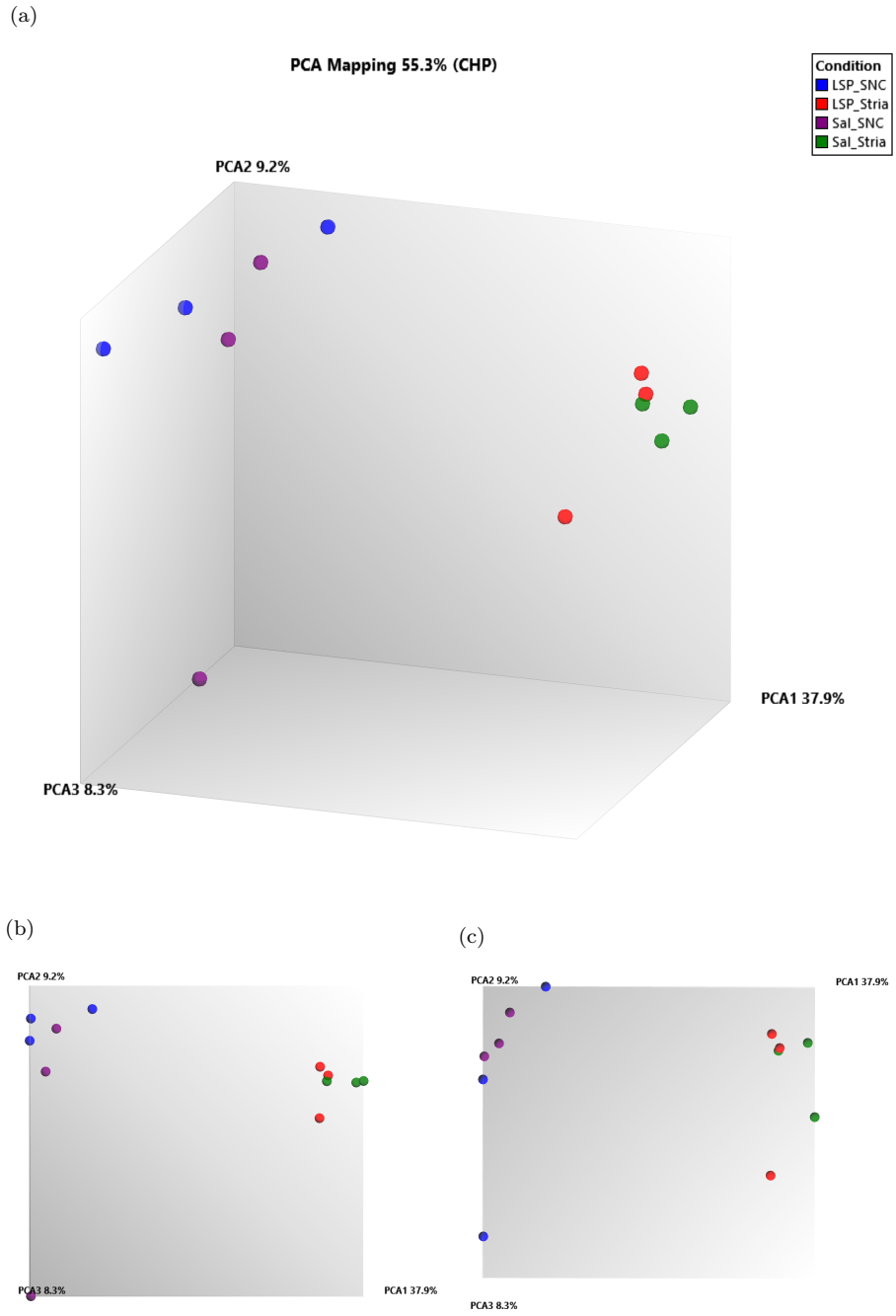

Figure 4.26: Graphs displaying the principal component analysis of samples used for the GeneChip array. Grouping when viewed from any angle and along any axis represents a similarity of the samples in 3d space. Images b and c display graph a from alternative points of view to better enable understanding of data displayed in a 3D format, via a 2D depiction. Blue spots represent the transcriptomic profile of VM tissue from LSP1-2111-treated animals, red dots represent striatal tissue from LSP1-2111-treated animals, purple represents VM from vehicle-treated animals and green represents striatal tissue from vehicle-treated animals.

In the VM, a total of 903 sequences including 495 genes were significantly up- or downregulated following administration of LSP1-2111. However, after correction for a false discovery rate, none of these genes had a p-value of less than 0.05. The application of correction for false discovery in these circumstances is contentious (Pawitan et al. 2005), however, and so for the purposes of the analysis of these data all genes which were regulated by LSP1-2111 with $p < 0.05$ will be considered as significant. These genes are listed in full in the appendix (digital file appended to this thesis). The use of correction for false discovery rate will be further examined in the discussion of this chapter.

A volcano plot was generated in order to show the propertion of sequence hits which met the inclusion criteria in VM tissue (Figure 4.27). Each spot on this graph represents a gene which was regulated in VM tissue by systemic administration of LSP1-2111 3 hours prior to the dissection and their position on the x-axis represents the fold-change of that regulation. Inclusion criteria for genes of interest were set at $\geq$ 2-fold up or downregulation by LSP1-2111 and a significance value of $p < 0.05$ - which is displayed on the y-axis here in the form of -$\log_{10}p$. Red spots on this plot denote genes which met this inclusion criteria and were upregulated by LSP1-2111 (608 genes) while green spots represent genes which met the inclusion criteria and were downregulated (295).

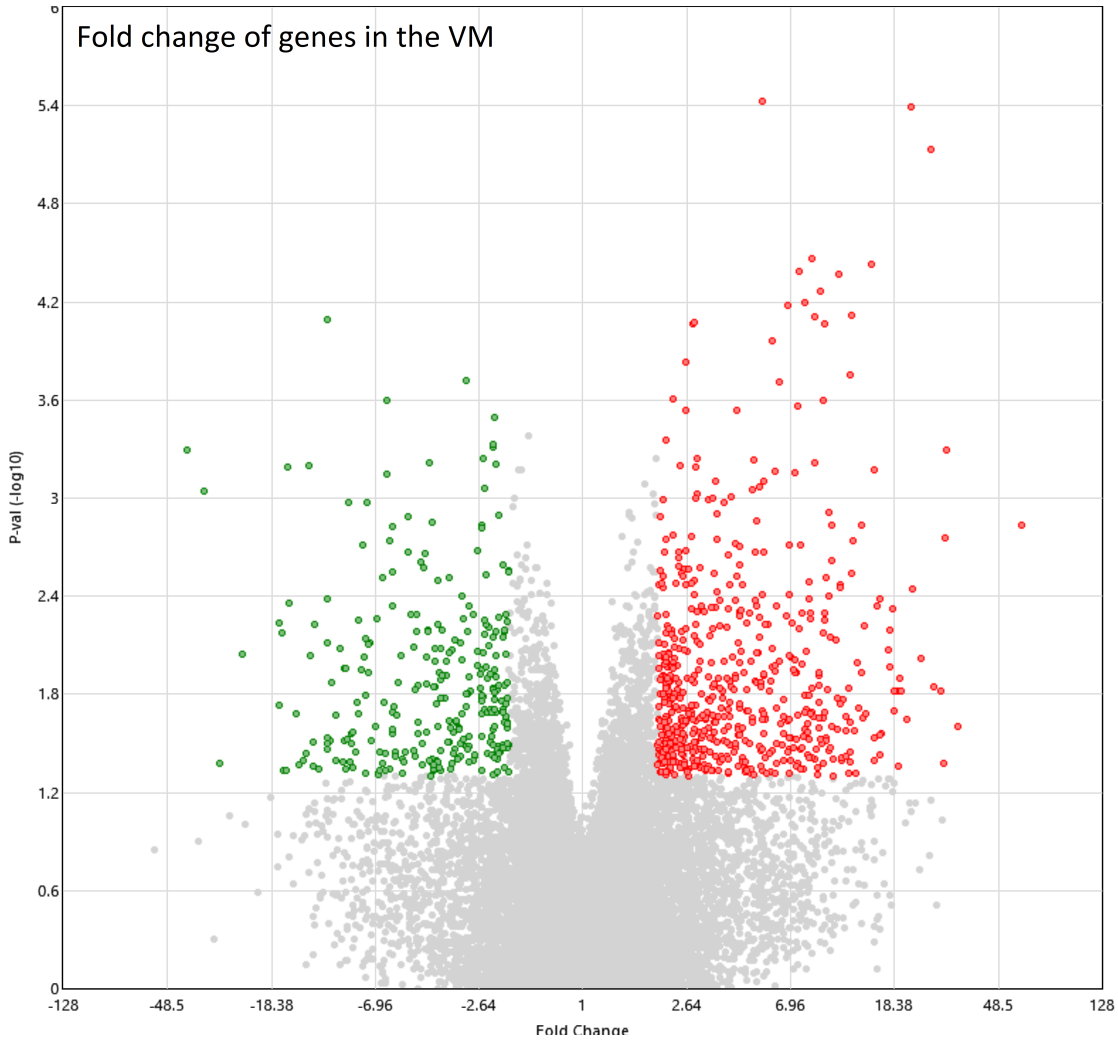

Figure 4.27: A volcano plot of gene regulation in the VM. The highlighted areas of the graph display data which met the inclusion criteria of $\geq$ 2-fold up- or down-regulation (red spots represent upregulation and green represent downregulation) and a p-value of < 0.05. Data are the average regulation occuring in 3 tissue samples for each group.

The genes which were significantly regulated by LSP1-2111 were also subject to cluster analysis using Transcriptome Analysis Console software. Genes were grouped by hierarchical clustering based on their expression in VM tissue from vehicle-treated animals and the direction and strength of their regulation by LSP1-2111. This hierarchical cluster data were then manually subdivided into 5 'major' clusters using the 3rd and 4th branch points of the initial analysis as displayed in Figure 4.28. These clusters were then examined for groups of genes and pathways which were regulated in a specific way by LSP1-2111.

In the cluster data presented in Figure 4.28, a blue colour represents genes which had low expression and a red colour denotes genes with high expression. The intensity of the colour describes the extremeness of the gene expression (intense blue shows a gene had very low expression, intense red shows very high expression and a pale or white gene has medium expression). By this gradient scheme:

- Cluster 1 in the VM tissue analysis contains genes whose expression was low in vehicle-treated animals and increased by LSP1-2111.
- Cluster 2 contains genes with medium expression in VM tissue from vehicle-treated animals but whose expression was decreased by LSP1-2111.
- Cluster 3 contains genes with low expression in both vehicle-treated and LSP1-2111-treated animals.
- Genes in cluster 4 had moderately high expression in both vehicle-treated and LSP1-2111-treated animals.
- Cluster 5 contains genes with middling high or low expression in the VM of vehicle-treated animals and which were oppositely regulated by LSP1-2111 (genes with medium-high expression were decreased and genes with medium-low expression were increased).

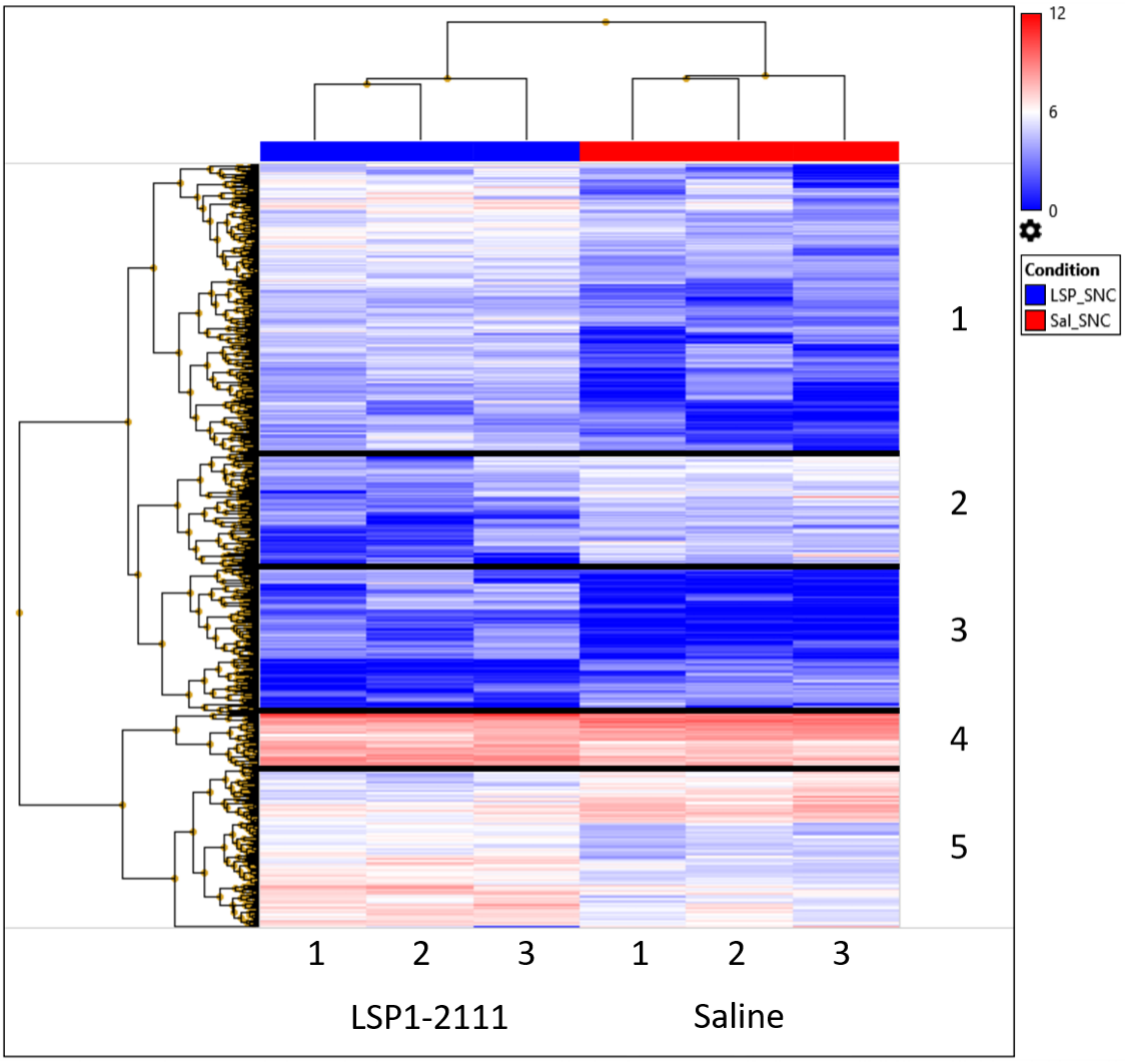

Figure 4.28: Image shows clustering of genes in the VM which were significantly regulated by a single administration of LSP1-2111 in naïve animals. Data were split into 5 main clusters using the 3rd and 4th branch point as the seperation between visual clusters. These 5 clusters are labelled along the right hand side of the image, with animal number and treatment identifier along the bottom.

Pathway analysis was performed using the Trancriptome Analysis Console software in tandem with Wikipathways - the TAC software matched genes which have been significantly regulated by LSP1-2111 with known pathways characterised on the WikiPathways database. In this instance, pathway analysis was performed on genes grouped within each cluster to find broad functions of all clusters. The pathways recognised by WikiPathways containing ≥ 2 significantly regulated genes are tablulated for each cluster in the VM (Table 4.5, p.236). Although all pathways were calculated using only sequences with significant regulation by LSP1-2111 compared to vehicle, the only full pathway which appeared significantly regulated in the VM was the TNF-alpha/NFκB signalling pathway ($p = 0.047$). A list of all pathways regulated by LSP1-2111 in the VM is shown in Table 4.6, p.242.

In the VM, clusters show some crossover in function - with Class A GPCRs, MAPK signalling and focal adhesion, amongst others, being regulated by genes split over at least 2 clusters. Cluster 1, which contains genes with somewhat low expression further downregulated by LSP1-2111, shows pathways involved in inflammation (B cell signalling) and G-protein function. In particular, the downregulation of BCL2L11, a pro-apoptotic protein in the BCL2 family is of interest.

Cluster 2 contains genes with low expression in tissue from vehicle-treated animals which was increased by LSP1-2111. Only two pathways are associated with this cluster, one of which, adipogenesis, is not considered to be relevant to the potential of LSP1-2111 to provide neuroprotection. The other pathway concerns the regulation of class A G-protein coupled receptors (GPCRs). The class A GPCR regulation pathways contains DRD4, the D_2-like dopamine receptor D_4, a potential target in levodopa-induced dyskinesia (LID) treatments (Jankovic & Aguilar 2008), which may be of therapeutic relevance to PD and the antiparkinsonian potential of LSP1-2111.

Cluster 3 shows genes with low expression which is often, but not always, further decreased by LSP1-2111. Pathways in this cluster show a predominant anti-inflammatory and anti-oxidative stress theme, with genes involved in focal adhesion and nuclear factor, erythroid-derived 2, like 2 (NF2EL2) pathways being upregulated following LSP1-2111. Protein kinase D is also significantly upregulated in LSP1-2111 VM. Phosphorylation or overexpression of protein kinase D has been shown to promote survival of dopaminergic cells following 6-OHDA lesioning (Asaithambi et al. 2014).

Cluster 4 predominantly shows genes with high expression which are somewhat upregulated by LSP1-2111 administration, with associated pathways on a theme of cytoskeletal reorganisation

- including regulation of actin cytoskeleton, focal adhesion and MAPK signalling. Examination of these pathways shows that CAV2 (caveolin2, involved in signal transduction and apoptosis), RRAS (Ras-related protein, involved in angiogenesis and regeneration) and PLA2G4B (Phospholipase A2 Group IVB, a mediator of mitochondrial and endosomal function) are all upregulated by LSP1-2111.

Cluster 5 contains genes with medium expression levels that have been either slightly up- or slightly downregulated in pathways on a theme of inflammation - including IL-2 signalling and spinal cord injuries. In this cluster, the voltage-dependent R-type calcium ion channel encoded by CACNA1E is significantly upregulated and NOS1 (encoding nitric oxide synthase, implicated in neurotoxicity in PD (Gatto et al. 2000)) is significantly downregulated by LSP1-2111.

Table 4.5: Cluster analysis in VM tissue			
1	2	3	4
B Cell Receptor Signalling Pathway	*Adipogenesis	*Adipogenesis	EGFR1 Signalling Pathway
*Calcium Regulation in the Cardiac Cell	GPCRs, Class A Rhodopsin-like	Complement and Coagulation Cascades	Focal Adhesion
Complement and Coagulation Cascades		Focal Adhesion	MAPK Signalling Pathway
EGFR1 Signalling Pathway	5	Nuclear factor, erythroid-derived 2, like 2 signaling pathway	Regulation of Actin Cytoskeleton
G Protein Signalling Pathways	*Calcium Regulation in the Cardiac Cell	Striated Muscle Contraction	
GPCRs, Class A Rhodopsin-like	IL-2 Signalling Pathway		
GPCRs (other)	MAPK Signalling Pathway		
Monoamine GPCRs	*Myometrial Relaxation and Contraction Pathways		
Senescence and Autophagy	Nuclear Receptors		
Wnt Signalling Pathway	Spinal Cord Injury		

Table 4.5: Table of pathways regulated in each cluster from analysis of VM tissue. * indicates pathways which are likely irrelevant for neuronal function.

Overleaf, Table 4.6 lists all pathways recognised by the Transcriptome Analysis Console and WikiPathways to be regulated by LSP1-2111 in naïve animals. These pathways are ordered by their p-value and are listed beside the genes which they contain that were significantly regulated by LSP1-2111. This table spans to p.242. Accompanying this information in the Appendix is a full list of genes and unnamed transcripts which were regulated in the VM by LSP1-2111.

Pathway (SNc)	Up List	Down List	p-value
TNF-alpha NF-kB Signaling Pathway	Rpl30		0.047
GPCRs, Class C Metabotropic glutamate, pheromone	Casr,Gabbr1		0.079
Monoamine GPCRs	Adrb3,Drd4	Chrm1	0.084
Nuclear Receptors	Thrb,Nr5a1	Nr4a1	0.12
Polyol pathway	Akr1b1		0.12
Complement and Coagulation Cascades	Cfh,Plaur,Serpinf2	Masp2	0.13
Blood Clotting Cascade	Serpinf2,Fga		0.13
Catecholamine synthesis		Dbh	0.15
IL-7 Signaling Pathway	Il7r,Stam2	Bcl2l11	0.16
PKA-HCG-Glycogen Syntase	Cyp2b3	Phka1	0.17
mRNA Processing		Clp1	0.19
T Cell Receptor Signaling Pathway		Cish	0.20
EPO Receptor Signaling	Epor	Cish	0.20
Cytokines and Inflammatory Response	Cxcl3,RT1-Db1		0.21
Calcium Regulation in the Cardiac Cell	Cacna1e,Atp2b3,Rgs14,Prkd1,Adrb3,Gjb5	Chrm1	0.22
Non-homologous end joining	Xrcc4		0.23
Ovarian Infertility Genes	Nr5a1	Prlr	0.24
Insulin Signaling	Rps6ka3,Trib3		0.25
GPCRs, Class A Rhodopsin-like	Ccr4,Cxcr5,Drd4,Adora2a,Gpr68,Adrb3	Gpr173,Tbxa2r,Chrm1,Gpr83	0.26
Spinal Cord Injury	Vcan	Nr4a1,Nos1,Epha4,Sema6a	0.26

Pathway (SNc)	Up List	Down List	p-value
Nucleotide GPCRs	Adora2a		0.30
GPCRs, Other	Gpr176,Adora2a,Drd4	Gpr83	0.30
Adipogenesis	Lep,Trib3,Egr2	Ucp1,Prlr,Klf15	0.31
Striated Muscle Contraction	Neb	Actc1	0.31
Metapathway biotransformation	Cyp1a1,Cyp8b1		0.33
TGF-beta Receptor Signaling Pathway	Cdk6	Nup214	0.33
Serotonin and anxiety		Arc	0.34
Fatty Acid Omega Oxidation	Cyp1a1		0.34
Estrogen metabolism	Cyp1a1		0.36
Toll-like receptor signaling pathway		Cxcl9	0.37
Electron Transport Chain		Ucp1	0.38
Integrin-mediated cell adhesion	Cav2		0.38
Biogenic Amine Synthesis		Dbh	0.38
The effect of glucocorticoids on target gene expression	Rras		0.38
Fructose Metabolism in Proximal Tubules	Akr1b1		0.44
Small Ligand GPCRs		Tbxa2r	0.44
Statin Pathway	Apoc2		0.46
Nuclear factor, erythroid-derived 2, like 2 signaling pathway	Rras,Prkd1	Acta2,Actc1	0.47
Hypertrophy Model	Nr4a3		0.47

Pathway	Up List	Down List	p-value
Urea cycle and metabolism of amino groups	Ckm		0.47
GPCRs, Class B Secretin-like	Calcrl		0.51
Cholesterol metabolism	Apoc2		0.52
Apoptosis		Bcl2l11	0.52
G Protein Signaling Pathways	Gna15,Rras,Prkd1,Akap4		0.54
ATM Signaling Pathway	Cdk6		0.55
Signal Transduction of S1P Receptor	Racgap1		0.55
TNF-alpha and mucus production in lung epythelium	Muc5ac		0.56
Genetic alterations of lung cancer		Egfr	0.58
Oxidative Stress	Cyp1a1		0.58
One Carbon Metabolism	Mthfr		0.58
MAPK Cascade	Rras		0.60
Folic Acid Network	Mthfr		0.60
Inflammatory Response Pathway	Il5ra		0.62
Regulation of Actin Cytoskeleton	Rras	Egfr,Chrm1	0.63
B Cell Receptor Signaling Pathway	Prkd1,Cdk6	Bcl2l11	0.64
ErbB signaling pathway	Ereg	Egfr	0.66
Tryptophan metabolism	Haao,Cyp1a1		0.66
Wnt Signaling Pathway	Prkd1	Fzd5	0.70
α6-β4 Integrin Signaling Pathway		Egfr	0.72

Pathway	Up List	Down List	p-value
G1 to S cell cycle control	Cdk6		0.73
IL-5 Signaling Pathway	Il5ra		0.73
Cell cycle	Bub1b,Cdk6,Mad2l1		0.76
Wnt Signaling Pathway and Pluripotency	Racgap1,Prkd1	Fzd5	0.77
Senescence and Autophagy	Cdk6,Cxcl3		0.77
Wnt Signaling Pathway NetPath	Nr5a1	Fzd5	0.78
Myometrial Relaxation and Contraction Pathways	Rgs14,Guca2b,Prkd1	Nos1,Actc1	0.81
Focal Adhesion	Cav2	Hgf,Ibsp,Egfr,Kdr	0.84
MAPK Signaling Pathway	Rps6ka3,Rasgrp1,Rras,Pla2g4b,Cacna1e	Egfr,Nr4a1	1
EGFR1 Signaling Pathway	Prkd1,Rps6ka3,Elf3,Cav2	Egfr	1
Androgen Receptor Signaling Pathway	Svil,Nr5a1	Egfr	1
IL-3 Signaling Pathway	Fcer2	Cish,Bcl2l11	1
IL-2 Signaling Pathway	Stam2	Cish	1
Cytoplasmic Ribosomal Proteins	Rps6ka3,Rpl30		1
Delta-Notch Signaling Pathway	Fhl1	Egfr	1
PI3K-AKT-NFKB pathway		Egfr,Pfkfb2	1
Kit Receptor Signaling Pathway	Epor	Cish	1
Peptide GPCRs	Ccr4,Cxcr5		1
Signaling of Hepatocyte Growth Factor Receptor		Hgf	1

Pathway	Up List	Down List	p-value
Cardiovascular Signaling	Racgap1		1
Insulin induced PI3K-Akt and MAPK in hepatocytes		Pfkfb2	1
Id Signaling Pathway	Myf6		1
Hexoses metabolism in proximal tubules	Akr1b1		1
Renin - Angiotensin System		Mme	1
PKC-SCP2	Pla2g4b		1
Glycogen Metabolism		Phka1	1
Nuclear receptors in lipid metabolism and toxicity	Cyp8b1		1
Selenium Micronutrient Network	Mthfr		1
Selenium metabolism Selenoproteins	Rpl30		1
Type II interferon signaling (IFNG)		Cxcl9	1
Oxidative phosphorylation	ND4		1
Hypothetical Network for Drug Addiction	Drd4		1

Table 4.6: Pathway analysis of genes up- or downregulated more than 2-fold in the VM 3 hours following a single systemic administration of LSP1-2111 in otherwise naïve rats. Analysis was carried out using Transcriptome Analysis Console software (Thermo Fisher Scientific, USA). Pathways are presented in order of significance - from smallest to largest p-value.

The same analyses were also conducted on transcriptomic profiles of striatal tissue in order to compare tissue from vehicle-treated animals to that of LSP1-2111-treated animals.

In the striatum, 624 sequences including 398 genes were significantly up- or downregulated following administration of LSP1-2111. However, after correction for a false discovery rate, only two of these genes had a p-value of less than 0.05: PIP5KL1 (phosphatidylinositol-4-phosphate 5-kinase-like 1, 10.43 fold downregulated, $p = 0.0091$) and CTSJ (cathepsin J, 13.04 fold downregulated, $p = 0.0091$). PIP5KL1 may act as a scaffold protein for the localisation of PI_4P kinases for the eventual generation of PI(3,4,5)P3. Cathepsin J is also known as cathepsin C or dipeptidyl-peptidase 1. Despite an increasingly well-characterised role in neutrophil activation, cathepsin J has not yet been associated with Parkinson's disease (Guarino et al. 2017). All genes which met the initial criteria of $p < 0.05$ and $\geq$ 2-fold regulated by LSP1-2111 are considered in this thesis however, and a full list of these genes is given in the appendix (in a digital file appended to the thesis).

A volcano plot was generated in order to show the proportion of sequence hits which met the inclusion criteria in striatal tissue (Figure 4.29). As in the the volcano plot generated to display transcriptomic results for the VM tissue, each spot on this graph represents a gene which was regulated in striatal tissue by systemic administration of LSP1-2111 3 hours prior to the dissection and their position on the x-axis represents the fold-change of that regulation. Red spots on this plot denote genes which met this inclusion criteria and were upregulated by LSP1-2111 (234 genes) while green spots represent genes which met the inclusion criteria and were downregulated (390 genes).

Figure 4.29: A volcano plot of gene regulation in the striatum 3 hours following a single, systemic administration of LSP1-2111 compared with saline-treated animals. The highlighted areas of the graph display data which met the inclusion criteria of $\geq$ 2-fold up- or down-regulation and a p-value of < 0.05. Data are the average regulation occuring in 3 tissue samples for each group.

In the cluster data presented in Figure 4.30, individual genes were again clustered by expression changes and this hierarchical data were split into 5 major clusters using the same branch point criteria (division at the 3rd or 4th branch point, manually). In the striatum, these clusters represented:

- Cluster 1 - genes whose expression was very low in vehicle-treated animals and increased by LSP1-2111.
- Cluster 2 - genes with medium expression in striatal tissue from vehicle-treated animals and whose expression was decreased to very low levels by LSP1-2111.
- Cluster 3 - genes with moderately high expression in both vehicle-treated animals whose expression was somewhat increased in LSP1-2111-treated animals.
- Cluster 4 - genes with medium expression in the striatum of vehicle-treated animals which were decreased in tissue from LSP1-2111-treated animals.
- Cluster 5 - genes with medium expression in the striatum of vehicle-treated animals which were oppositely regulated by LSP1-2111 (genes with medium-high expression were decreased and genes with medium-low expression were increased).

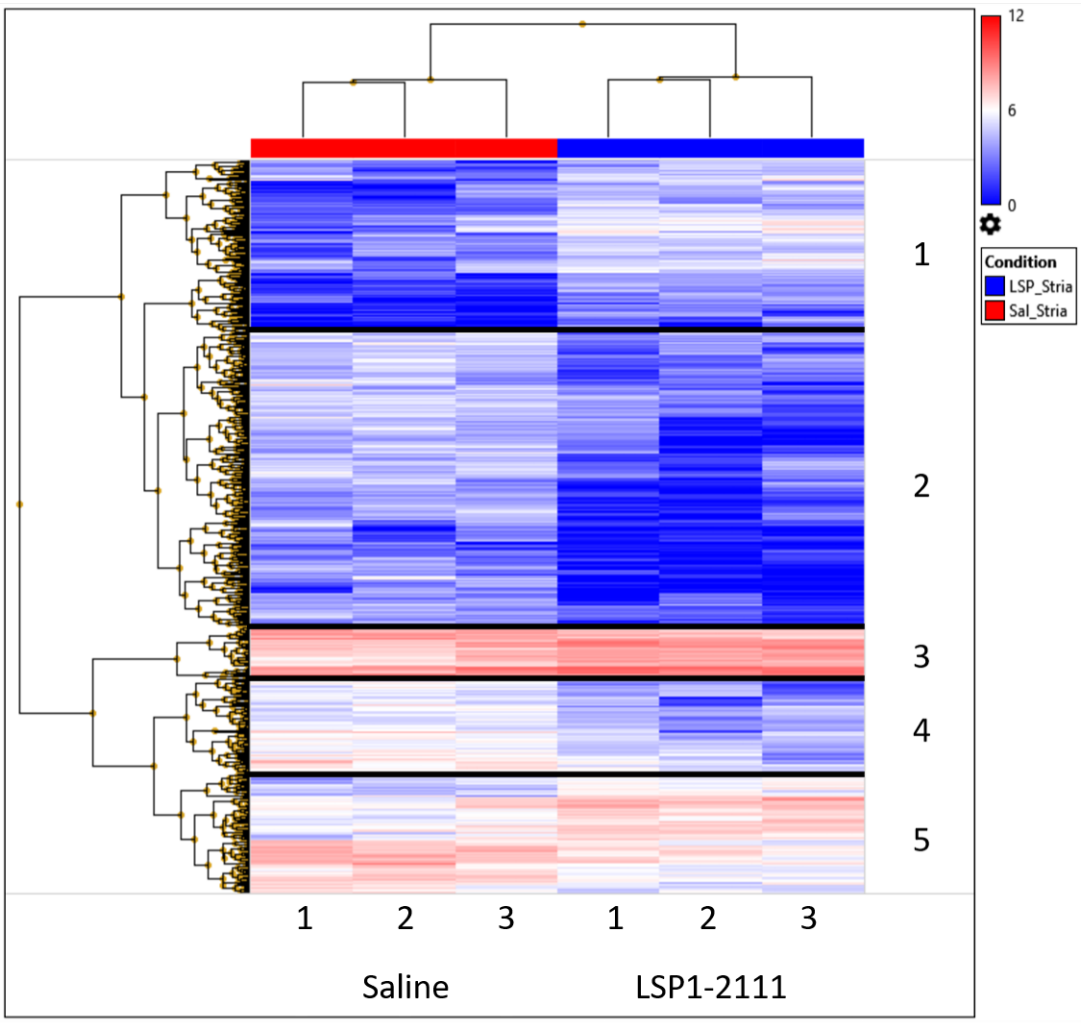

Figure 4.30: Image shows clustering of genes in the striatum which were significantly regulated by a single administration of LSP1-2111 in naïve animals. Data were split into 5 main clusters using the 3rd and 4th branch point as the seperation between visual clusters. These 5 clusters are labelled along the right hand side of the image, with animal number and treatment identifier along the bottom.

Clusters were also used to guide pathway analysis in the striatum (Table 4.7, p.249). Again, there were some pathways which occurred in multiple clusters including focal adhesion and NF2EL2. The only pathway to be significantly altered following LSP1-2111 treatment was adipogenesis ($p < 0.048$). A full list of pathways regulated by LSP1-2111 in the striatum is given in Table 4.8, p.256.

Cluster 1 in the striatal tissue contained genes which had very low expression in vehicle-treated animals which have been upregulated in LSP1-2111-treated animals. The pathways involved in this cluster appear to relate to cell activity - including genes involved with cell cycle control and sensescence/autophagy alongside others. Notable genes significantly more highly expressed following LSP1-2111 treatment in this cluster include CDK2 (cyclin-dependent kinase 2) and TGFB1 (TGFβ1), which has been shown to be beneficial in preclinical models of PD (Tesseur et al. 2017).

Genes in cluster 2 have low expression in vehicle-treated animals and are further suppressed following LSP1-2111 treatment. As in cluster 3 in the VM analysis, there are regulated pathways in this cluster concerned with inflammation, reduction of oxidative stress and cytoskeletal reorganisation. Gene expression of IL-2 and PIK3R2 (Phosphatidylinositol 3-kinase regulatory subunit beta, part of PI3K which is involved in the regulation of many pathways including autophagy) are downregulated, alongside FGF23. Fibroblast growth factor 23 is responsible for the suppression of metabolic activation of vitamin D, which is inversely correlated with PD (Wang, Evatt, Maldonado, Perry, Ritchie, Beecham, Martin, Haines, Pericak-Vance, Vance & Scott 2015).

Genes in cluster 3 showed high expression in vehicle and increased expression following LSP1-2111-treatment. In this cluster, SQSTM1, encoding sequestosome 1 - a ubiquitin-binding, autophagosome cargo protein, is significantly upregulated.

Cluster 4 is comprised of genes with medium expression levels in vehicle-treated animals which has been predominantly decreased following LSP1-2111-treatment. Key genes with decreased expression which fall into this cluster include WNT4, which regulates hormone release, and WNT5a - implicated in inflammation in cancers, rheumatoid arthritis and tuberculosis. Wnt signalling is widely thought to play a key role in development and degeneration and is considered important to PD and therapeutic efficacy in PD (reviewed in Arenas (2014)).

As with cluster 2 in the VM data, cluster 5 in the striatum seems largely comprised of pathways which have no obvious relevance to a potential neuroprotective or antiparkinsonian effect

of LSP1-2111 including adipogenesis, endochondral ossification and myometrial regulation. The TGFβ pathway however, containing the significantly upregulated genes TGFB1 and LIF, shows more promise. TGFB1, although shown to be upregulated in the cerebrospinal fluid of PD patients (Vawter et al. 1996), is thought to have neurotrophic and neuroprotective functions (Tesseur & Wyss-Coray 2006). Likewise, LIF has been shown to be increased in the brains of PD patients (Soilu-Hänninen et al. 2010) but may also have a crucial role in neuroprotection in the 6-OHDA-lesioned mouse (Liu, Peng, Zang & Zhang 2013) and in other models of multiple sclerosis (Slaets et al. 2010).

Table 4.7: Cluster analysis in striatal tissue		
1	2	3
*Adipogenesis	GPCRs, Class A Rhodopsin-like	$\alpha 6 - \beta 4$ Integrin Signalling Pathway
CDKN1A-EGF-CREB	IL-2 Signalling Pathway	Focal Adhesion
Delta-Notch Signalling Pathway	Biotransformation	Nuclear factor, erythroid-derived 2, like 2 signaling pathway
G1 to S cell cycle control	Nuclear factor, erythroid-derived 2, like 2 signaling pathway	
GPCRs (other)	Regulation of Actin Cytoskeleton	
Senescence and Autophagy	Spinal Cord Injury	
4	5	
*Adipogenesis	*Adipogenesis	
Focal Adhesion	Androgen Receptor Signalling Pathway	
Wnt Signalling Pathway	Cell cycle	
Wnt Signalling Pathway and Pluripotency	*Endochondral Ossification	
	*Myometrial Relaxation and Contraction Pathways	
	TGF Beta Signalling Pathway	

Table 4.7: Table of pathways regulated in each cluster from analysis of striatal tissue. * indicates pathways which are likely irrelevant for neuronal function.

All pathways containing genes which were significantly regulated in the striatum by LSP1-2111 are listed in Table 4.8. This table spans until p.256. A list detailing all genes and trasncripts signficantly regulated in the striatum by LSP1-2111 can also be found in the Appendix.

Pathway	Up List	Down List	p-value
Adipogenesis	Lif,Tgfb1,Scd1,Sp1,Pnpla3	Gata3,Irs1	0.048
G1 to S cell cycle control	Cdk2,Creb3l3,Cdc25a	Cdc45	0.086
Selenium metabolism Selenoproteins	Sp1,Gpx2	Fabp1	0.090
Glutathione metabolism	Gpx2	Gstm3	0.098
GPCRs, Class B Secretin-like		Gcgr,Pth2r	0.11
IL-2 Signaling Pathway		Il2,Pik3r2,Irs1,Cish	0.12
GPCRs, Other	Gpr143,Cxcr3,Smo	Drd4	0.12
EPO Receptor Signaling		Cish,Irs1	0.14
Fatty Acid Beta Oxidation 2	Acads		0.14
Cytokines and Inflammatory Response (BioCarta)	Tgfb1	Il2	0.15
Genetic alterations of lung cancer	Tgfb1,Cdk2		0.15
Delta-Notch Signaling Pathway	Dll4,Cdk2	Pik3r2,Maml2	0.15
p53 signal pathway	Cdk2,Perp		0.18
Inflammatory Response Pathway	Lamc1	Il2	0.18
Prostaglandin Synthesis and Regulation		Prl,Ptger3	0.18
Fatty Acid Beta Oxidation 3	Acads		0.19
Phase I biotransformations, non P450	Pon1		0.19

Pathway	Up List	Down List	p-value
Type II interferon signaling (IFNG)	Tap1,Cxcl9		0.21
α6-β4 Integrin Signaling Pathway	Lamc1	Pik3r2,Irs1	0.23
G13 Signaling Pathway	Myl1	Pik3r2	0.23
Irinotecan Pathway	Bche		0.28
Cell cycle	Cdk2,Cdc25a,Tgfb1	Bub1b	0.29
Glycolysis and Gluconeogenesis	Pklr	Ldhal6b	0.29
MAPK Signaling Pathway	Tgfb1,Cacna1g	Fgf23	0.30
Spinal Cord Injury	Cdk2,Tgfb1	Il2,Nox4	0.33
Complement Activation, Classical Pathway	C6		0.34
Mitochondrial LC-Fatty Acid Beta-Oxidation	Acads		0.34
Id Signaling Pathway	Cdk2	Irs1	0.3
Small Ligand GPCRs		Ptger3	0.37
TGF Beta Signaling Pathway	Tgfb1,Lif		0.37
Statin Pathway		Apoc3	0.39
Nuclear factor, erythroid-derived 2, like 2 signaling pathway	Gpx2,Akr1b10,Sqstm1	Pik3r2,Gstm3	0.40
Blood Clotting Cascade		Fga	0.40
Mitochondrial Gene Expression	Sp1		0.40

Pathway	Up List	Down List	p-value
TGF-beta Receptor Signaling Pathway	Tgfb1,Sp1,Cdk2,Cdc25a	Pik3r2	0.42
Hedgehog Signaling Pathway	Smo		0.43
Fatty Acid Biosynthesis	Scd1		0.43
B Cell Receptor Signaling Pathway	Cdk2	Pik3r2	0.44
IL-9 Signaling Pathway		Irs1	0.46
ATM Signaling Pathway	Cdk2		0.47
PI3K-AKT-NFKB pathway	Tap1	Irs1,Pfkfb2	0.48
TNF-alpha and mucus production in lung epythelium	Sp1		0.49
Oxidative Stress	Sp1		0.50
Wnt Signaling Pathway and Pluripotency		Wnt4,Nkd2,Wnt5a	0.52
Electron Transport Chain		Ucp3	0.52
IL-6 Signaling Pathway		Pik3r2	0.52
Folic Acid Network	Gpx2		0.53
Hypothetical Network for Drug Addiction		Drd4	0.55
Beta Oxidation Meta Pathway	Acads		0.56
Selenium Micronutrient Network	Gpx2		0.56
Monoamine GPCRs		Drd4	0.57
Fatty Acid Beta Oxidation	Acads		0.58
Calcium Regulation in the Cardiac Cell		Slc8a1,Atp1a4	0.59

Pathway	Up List	Down List	p-value
Metapathway biotransformation	Sult1b1	Gstm3	0.59
Insulin induced PI3K-Akt and MAPK in hepatocytes		Pfkfb2	0.59
Myometrial Relaxation and Contraction Pathways	Sp1	Slc8a1	0.59
Striated Muscle Contraction	Myl1		0.60
Insulin Signaling	Enpp1,Cblc	Irs1,Pik3r2,Ppp1r3a	0.61
Cardiovascular Signaling		Pgf	0.62
Nuclear Receptors		Nr2f6	0.62
Retinol metabolism		Cd36	0.62
EGFR1 Signaling Pathway	Cblc,Sp1	Pik3r2	0.63
Wnt Signaling Pathway		Wnt4,Wnt5a	0.66
Endochondral Ossification	Enpp1,Tgfb1		0.67
IL-4 Signaling Pathway		Irs1,Pik3r2	0.67
Kit Receptor Signaling Pathway		Pik3r2,Cish	0.69
Peptide GPCRs	Cxcr3	Cckar	0.69
Estrogen signaling	Sp1	Polr2i	0.70
Apoptosis	Prf1		0.73
G Protein Signaling Pathways	Gna14		0.73
Senescence and Autophagy	Tgfb1,Sqstm1,Cdk2		0.75

Pathway	Up List	Down List	p-value
T Cell Receptor Signaling Pathway		Pik3r2,Cish	0.78
Regulation of Actin Cytoskeleton	Myl1	Fgf23,Pik3r2,Mylk	0.79
Focal Adhesion	Lamc1	Pgf,Itgb7,Pik3r2,Mylk	0.82
GPCRs, Class A Rhodopsin-like	Cxcr3	Drd4,Ptger3,F2rl2,Cckar,Opn1mw	0.83
CDKN1A-EGF-CREB	Hbe2,Creb3l3	Polr2i	1
Integrin-mediated cell adhesion		Pik3r2,Itgb7	1
Androgen Receptor Signaling Pathway	Sp1	Plagl1	1
Wnt Signaling Pathway NetPath		Wnt4,Wnt5a	1
IL-3 Signaling Pathway		Pik3r2,Cish	1
PKA-HCG-Glycogen Syntase	Pklr	Pfkfb3	1
Toll-like receptor signaling pathway	Cxcl9	Pik3r2	1
p53 pathway	Cdk2		1
Complement and Coagulation Cascades	C6		1
Eukaryotic Transcription Initiation		Polr2i	1
DNA Replication	Cdk2		1
IL-5 Signaling Pathway		Pik3r2	1
Hexoses metabolism in proximal tubules	Pklr		1

Pathway	Up List	Down List	p-value
Relationship between glutathione and NADPH	Pklr		1
PKC-SCP2		Nox4	1
D-Glucose-Ins1-Rxra	Creb3l3		1
ErbB signaling pathway	Cblc		1
IL-7 Signaling Pathway		Irs1	1

Table 4.8: Pathway analysis of genes up- or downregulated more than 2-fold in the striatum 3 hours following a single systemic administration of LSP1-2111 in otherwise naïve rats. Analysis was carried out using Transcriptome Analysis Console software (Thermo Fisher Scientific, USA). Pathways are presented in order of significance - from smallest to largest p-value.

4.5 Discussion

4.5.1 Inflammation in 6-OHDA-lesioned, LSP1-2111-treated rats

In Chapter 3, LSP1-2111, an mGluR4 agonist, was found to mediate neuroprotection in 6-OHDA-lesioned rats. Tissue was taken from these animals to characterise the inflammatory changes seen in these animals (13 days post-lesion) and to examine the effect of LSP1-2111 on these changes. Here, it was found that LSP1-2111 mediated some subtle changes to inflammatory cells as measured through histology on these sections.

4.5.1.1 Microglia

Inflammatory changes mediated by LSP1-2111 in the present study are difficult to discern using histology alone. In the present study, there is a large increase in the number of Iba1-positive cells in the lesioned striatum compared to the intact striatum. This increase does not appear to be impacted reliably by the administration of LSP1-2111 despite local trends towards a reduction in the dorsal, caudal striatum of animals given 1 or 10mg/kg LSP1-2111. These measures have large error values which may also serve to mask any small LSP1-2111-mediated reductions in inflammation.

In the lesioned SNc, levels of Iba1-positive cells are also increased though to a lesser degree than in the striatum. Again, there is no significant effect of LSP1-2111 when compared directly with vehicle, but there are some more subtle hints of an anti-inflammatory effect. Overall, and despite high error (primarily in the 1mg/kg LSP1-2111 group), there is an apparent trend towards a reduction of Iba1-positive cell numbers in response to LSP1-2111. More specifically, in the lesioned, rostral SNc there is significantly higher Iba1 positivity in both vehicle and 1mg/kg LSP1-2111 groups but not in the 10mg/kg group. This reduction to non-significance of the microgliosis in the rostral SNc of 10mg/kg animals may partially underlie the observed protection in the same area as described in Chapter 3. This concordance supports the relationship between inflammation and neurodegeneration, and that reducing or halting one may impact significantly on the other. Ideally, these findings would be confirmed with the use of another marker - perhaps OX42 as used by Walsh et al. (2011).

4.5.1.2 Astrocytes

GFAP was measured in the striatum by densitometry as a proxy for astrogliosis. There were very minimal increases in GFAP expression, which was primarily visible as a glial scar around the needle tract, and no difference in astrogliosis between groups. This modest increase in GFAP is in line with findings in the time course study (where no significant astrogliosis was found in the striatum by 7 days) and with Walsh et al. (2011) (who found a comparable increase of 120%, which in their case was found to be significant). There was a slight increase in the density of GFAP stain in the SNc which was again in line with the findings of Walsh et al. (2011) who saw a lesioned SNc GFAP density of approximately 110% at 14 days post-lesion, though was not significant. In the mid and, to a lesser extent, the rostral SNc, there appeared a trend towards a reduction of GFAP stain density with LSP1-2111 treatment, however this did not reach significance. This trend was mirrored in the overall average data throughout the SNc.

Given the documented expression of mGluR4 on both reactive astrocytes (Geurts et al. 2005) and activated microglia (Taylor et al. 2003), the modest effect of activation by LSP1-2111 seen in the present study is surprising. The initial hypothesis was that the histological time point of 2 weeks post-lesion had missed the peak of inflammatory activity provoked by 6-OHDA lesion. By this relatively late stage, any reduction in inflammatory activity during the development of the lesion may have ceased due to the 7 day washout of the drug. For this reason, the time course study was conceived and conducted in order to fully characterise the acute inflammatory response to lesioning and to enable better understanding of the potential impact of an mGluR4 agonist during this period. The findings of the time course study suggest that, in reality, it is not the case that the first 7 days post-lesion house particularly high inflammatory activity compared to the 2 week time point used in this study. This suggests that either LSP1-2111 had stronger effects on inflammation earlier in the process which were lost to observation as a result of the washout period, or that LSP1-2111 does not have the same anti-inflammatory properties that VU0155041 had in the hands of Betts et al. (2012). This is likely a result of the intracerebral injection of VU0155041 by Betts et al. (2012) as compared to the subcutaneous administration of LSP1-2111 used here.

At this point, is important to note that LSP1-2111 may have anti-inflammatory effects via these cells beyond simply reducing expression of a cell surface marker or numbers of local inflammatory cells. Both microglia and astrocytes are hypothesised to have a spectrum of phenotypes similar to those documented in macrophages - from a highly pro-inflammatory M1 phenotype to an

anti-inflammatory M2 phenotype (Michelucci et al. 2009, Simpson et al. 2010, Nash et al. 2011). Indeed, pan-agonists of group III mGluRs have been shown to reduce the neurotoxicity of microglia exposed to pro-inflammatory stimuli (Taylor et al. 2003). This experiment neatly exposits the idea that a group III mGluR agonist, or perhaps an mGluR4-specific agonist such as LSP1-2111, may impact positively upon the secretory profile of immune cells - an aspect of inflammation which is not tested by a purely histological approach as was taken here. This concept was subsequently examined by the study using arrays and ELISAs to examine the cytokine profile of lesioned and intact tissue.

4.5.2 Time course of inflammation following 6-OHDA lesion

As described previously, the aim of the time course study was to detail the lesion development and progression of inflammation in the first 7 days after lesioning in order to better understand the potential anti-inflammatory effect of LSP1-2111 in this period when dosing had occurred in the protection study (Chapter 3). The time course study detailed here is not the first to examine the time line of inflammatory changes with a terminal lesion, though no other studies use similar co-ordinates or concentrations of 6-OHDA in rats (and therefore the similarity of these studies to the present study must be questioned at each comparison). In particular, a study by Walsh et al. (2011), using 28μg 6-OHDA and examining histology at 6 hours and 1, 3 and 14 days post-lesion in rats, provides a helpful comparison for the present study and for the inflammatory markers measured following LSP1-2111 administration (Table 4.9). Notably, there are quite marked variations between these studies, models and outcomes, which makes drawing firm conclusions on a time course difficult.

Table 4.9: Partial lesion time course studies

	Current	Walsh et al. (2011)	Stott & Barker (2014)
Model	12μg intrastriatal rat	28μg intrastriatal rat	10μg intrastriatal mouse
Striatal TH loss	3 days	3 days	3 hours
Striatal astrocytes	not by 7 days (GFAP)	3 days (GFAP)	-
Striatal microglia	-	3 days (CD11b/OX42)	-
Nigral TH loss	7 days	14 days	9 days
Nigral astrocytes	not by 7 days (GFAP)	not by 14 days (GFAP)	9 days (GFAP)
Nigral microglia	not by 7 days (Iba1)	3 days (CD11b/OX42)	9 days (CD11b/OX42)

Table 4.9: Time course study data and comparisons with similar studies in the literature.

4.5.2.1 Dopaminergic cells and terminals

Measurement of TH-positive cell counts in the nigra is a method that is standard across the three studies compared in Table 4.9. The studies yield similar results in these measurements, accounting for the selection of different time points, despite differences in the models utilised. Additionally, the nigral cell death in this study, at day 7 (63±11 cells remaining in the lesioned SNc, 63% of intact), is comparable to that seen after 2 weeks in the characterisation study of Chapter 2 (59 ± 7 cells remaining, 68.3% of intact) and in the vehicle-treated animals of the LSP1-2111 study in Chapter 3 (79 ± 10 cells remaining, 56.9% of intact). This suggests that cell death in the SNc is almost complete by day 7 in the current model. Stott & Barker (2014) show a reduction in TH-positive nigral cell diameter by 3 days post-lesion, suggesting that although cell death is not complete until around 1 week following a terminal lesion, apoptosis may initiate sooner and lead to a slower decline than is seen in more traditional axonal lesions.

Furthermore, the time difference between significant TH loss in striatum and cell loss in the SNc suggests that 6-OHDA does not work from the cell body forwards (anterograde degeneration), but rather from the site of injection in the terminals backwards (retrograde degeneration). The high variation seen in the TH day 2 post lesion western blot might also suggest that this was the time threshold for degeneration - especially as this was shortly followed by such a large reduction at day 3. This hypothesis is also backed up by the studies of Walsh et al. (2011) and Stott & Barker (2014) as shown in Table 4.9. The significant striatal TH loss first occurring at day 3 post-lesion in the present study maps well with the findings by Walsh et al. (2011) of significant terminal loss at the same time point, though the loss noted by Stott & Barker (2014) occurring at 3 hours post lesion vastly outstips both studies.

In the present study, significance of TH-positive terminal loss in the striatum is lost by day 7 post-lesion. This is most likely due to variability in the data, or 'noise', rather than due to terminal repair since the S.E.M. of these data increased at this time point compared to those at days 3 and 4 post-lesion.

4.5.2.2 Astrocytes

GFAP in the lesioned SNc shows a trend towards an increase over time when measured by densitometry. This trend may indicate that apoptosis of TH cells is linked with astrogliosis in the SNc. Stott & Barker (2014) see significant nigral astrogliosis only by 9 days post-lesion and Walsh et al.

(2011) do not find significant increases in nigral GFAP during their 2 week time course. In the SNc, any potential increase seen is not likely due to mechanical damage as the injection site was in the striatum. Instead, it is more likely linked with the apoptosis of TH-positive cells. Average branch number, junction number and branch length were also measured in GFAP-positive astrocytes in order to discern whether a phenotypic change indicative of differential activation states took place. No significant difference between groups or time points was noted for any of these additional measurements.

In the striatum, however, western blotting showed that sham animals' lesioned striatum had GFAP levels of 180% of the intact striatum on day 2 post lesion, while lesioned animals had levels of 255% at the same time point. Given the elevated measures of GFAP in sham striata, it seems reasonable to expect that mechanical damage plays some role in causing inflammation. However, taking this into account, GFAP levels in lesioned striata are higher yet, showing that injection of 6-OHDA causes additional inflammation over the measured period on top of measurable mechanical damage from the surgery. That the difference between GFAP levels in the striata of sham and lesioned groups is not significant is an indicator that western blotting may not have been as accurate as necessary to tease apart this response - this can be seen in the large error bars in Figure 4.14c.

In the LSP1-2111 neuroprotection study, GFAP levels in the lesioned striatum were measured at 109.6% of the intact striatum in vehicle-treated animals at day 14 post-lesion. If the results gathered by western blot are reliable in the time course study then this measurement represents a decline in GFAP levels from day 7 to day 14. This may well be an artifact arising from the measurement of whole striatal values (including the glial scar) in the time course measurements, while the GFAP measurements in the histological analysis of the LSP1-2111 study examined areas of the striatum not affected by the scar.

Overall, there was no significant effect of lesioning on nigral or striatal astrocytes apparent over the first week post-lesion evident in this study, and no difference in the number or phenotype of GFAP-positive cells between vehicle and LSP1-2111 groups at 13 days post-lesion. It may therefore be concluded that LSP1-2111 treatment had no effect on astrocyte number in this study, or that any effect that LSP1-2111 had on astrocyte number over the course of dosing (in the first 7 days post-lesion) was incidental to the development of the lesion or neuroprotection.

4.5.2.3 Microglia

As microglia change phenotype from ramified (resting) to activated, several potentially measurable parameters change too. Ramified microglia have long, highly branched processes and a small cell body which expresses Iba1 lightly. In contrast, in activated microglia, the processes are withdrawn and become thicker and less branched, while the cell body increases in size and expresses Iba1 more highly (Davis et al. 1994, Kozlowski & Weimer 2012). In this study, the optical density of Iba1 was measured both in the cell bodies of individual cells and also in the overall image to attempt to capture this upregulation of Iba1 expression. Numbers of Iba1 cells of any morphology were counted in order to account for increased chemotaxis to the site of degeneration. Finally, cell body area was also measured to examine differences in morphology in cells which may be ramified compared to those which were more activated.

In this study, no differences in Iba1 cell number, image optical density, cell body area or cell body densitometry were seen in the SNc at any time up to 7 days post lesion. By this time point, Iba1-positive cells in the lesioned hemisphere are 134.2% of the intact hemisphere. In the LSP1-2111 neuroprotection study, the nigral Iba1 response following partial, striatal lesion is found to be higher by 14 days post-lesion, reaching 222.5% of intact nigra in vehicle-treated animals. This longer time to microgliosis corresponds to the findings of Stott & Barker (2014) - who found significantly shorter microglial branch lengths only after 9 days post-lesion, through the use of the OX42 marker - but not the findings of Walsh et al. (2011), who found significant nigral OX42 volume increases by 3 days post lesion. The minor decrease in Iba1 soma size and cell body stain density seen by day 7 in the present study as compared with earlier time points may, however, suggest a reduced activation state of microglia in both sham and 6-OHDA-lesioned SNc.

Striatal microgliosis was unfortunately not measured in this study due to repeated problems with compatibility of the primary anti-Iba1 antibody with western blotting wherein no bands were observed at any titration of the antibody or at different densities of gel.

These differences in observed microgliosis following lesion may demonstrate the perils of attempting to compare results obtained using different markers to collect information on one cell type. The marker used in the present study for staining microglia (Iba1) also labels peripheral monocytes which may infiltrate the CNS through the damaged blood-brain barrier. Although these cell types may be distingushed by eye (monocytes are round but microglia, even when activated, still have stubby processes), a confident distinction requires either significant expertise or machine

learning to effect. Alternative histological markers may instead be used to differentiate cells with a higher degree of certainty. In the Walsh et al. (2011) and Stott & Barker (2014) studies, CD11b was used as an alternative to Iba1, though CD11b may be expressed on more cell types than Iba1. Ideally, to be sure of the identity of a cell, multiple labels would be used in methods such as immunofluorescence or fluorescence-activated cell sorting (FACS) to refine populations until the only remaining candidate expressing all markers is the cell type of interest. However, these techniques are not always compatible with other endpoints within a study which may require different tissue treatments.

In conclusion, the time course study found that the first 7 days post-lesion did not house particularly strong inflammatory activity compared to the 2 week time point used to examine the neuroprotective efficacy of LSP1-2111. This suggests that the findings of the study into the anti-inflammatory properties of LSP1-2111 2 weeks following lesioning and after a washout period of 6 days may reflect honestly on the anti-inflammatory activity of the compound during the dosing period. This would suggest that the observed reduction of Iba1-positive cells (microglia or monocytes) in the rostral SNc may have been key to the neuroprotection which was measured in the same region in Chapter 3.

4.5.2.4 Potential further histological studies for characterisation of lesion and LSP1-2111 effect

In light of the findings of the time course study and comparisons in the literature, a number of potential areas for improvements or additions in the characterisation of the lesion development are also evident.

Firstly, although nigral cell death and dopaminergic terminal loss appear complete by the latest time point studied here (7 days post-lesion), the inflammatory response may evolve further over time. Additional time points at 10, 14 and 21 days post-lesion would have been valuable in assessing this in order to form a clearer picture of the events surrounding the 2-week time point used in the neuroprotection studies. In reality however, the animal numbers required to extend the study further would have made these additions difficult.

In addition to extending the time course, the methods of *ex vivo* examination of tissue could also be improved. Antibodies long used and well characterised in the lab proved difficult to adapt to western blotting (in the case of Iba1). For GFAP, which worked reliably with western blotting,

low overall protein expression translated to light bands which resulted in high variation. This error masked any change likely to be seen either between groups or over time. Although the use of western blotting in this study provided an valuable opportunity to become familiar with a new technique, continuing to use immunohistochemistry for interrogation of markers in the striatum may have provided a more familiar and reliable basis for the examination of these changes.

Antibodies against additional markers were selected on the basis of their likelihood to be altered by 6-OHDA and/or compounds acting on mGluR4, but failed to show reliable results in work-up either with paraffin-embedded SNc sections or homogenised striatal tissue.

- An anti-OX-6 antibody (ab23990, Abcam, UK - against major histocompatibility complex class II) was chosen for labelling antigen presenting cells in order to further examine the cells involved in the inflammatory response to 6-OHDA, but showed no efficacy in either method. OX-6 binding was used by Marinova-Mutafchieva et al. (2009) as a proxy for marking activated microglia and was found to increase following 6-OHDA-lesioning.

- An antibody against glutamate transporter 1 (GLT1, also known as excitatory amino acid transporter 2 - EAAT2) (sc-365634, Santa Cruz Biotechnology, USA) appeared to work well in paraffin-embedded sections (Figure 4.31). However, contrary to EAAT2's high expression on astrocytes (Lehre et al. 1995), the stain appeared neuronal rather than glial and so was deemed unreliable. Reduced expression of GLT1/EAAT2 has been associated with neurodegenerative disorders (Chung et al. 2008) and, given the nature of neuroprotective treatments examined in this project, measurement of EAAT2 expression may have been interesting.

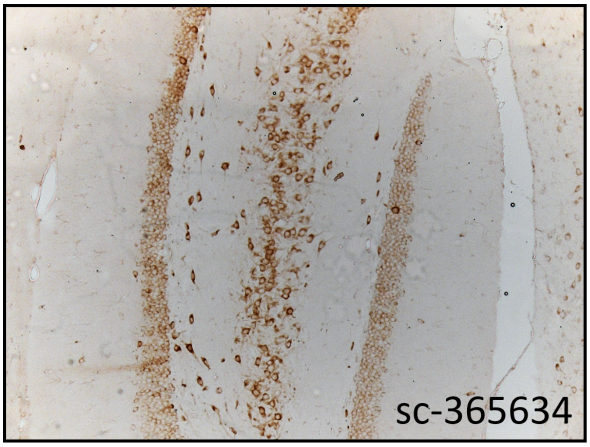

Figure 4.31: Representative picture of DAB staining with a GLT1 antibody in rat hippocampus. Staining appears neuronal (localised to cell bodies, though not nuclei) rather than glial.

- Antibodies against mGluR4 were also investigated for the purpose of understanding the effect of sub-chronic agonists on internalisation and expression of mGluR4 in future studies. Multiple antibodies were assessed with paraffin-embedded sections (ab77988, ab184302, ab189032, Abcam, UK; M388-74F, United States Biological, USA) each at a number of dilutions (though with only n=1) but none showed any promise. Staining in sagittal sections of rat brain tissue including the cerebellum was compared to expression databases Human Protein Atlas (Uhlen et al. 2015) and GENSAT (Heintz & Gerfen n.d.). According to these databases, mGluR4 protein expression is high in Purkinje cells in the cerebellum but low or absent in the granule and molecular layers. In the instances of the mGluR4 antibodies ab184302 and ab189032 there was high background staining in the molecular layer and low staining in the Purkinje cells. In the instance of ab77988, an mGluR2/4 antibody, Purkinje cells were preferentially picked out alongside high background staining. Given the lack of selectivity of the antibody, however, it was not deemed useful for the purpose of further characterisation (Figure 4.32).

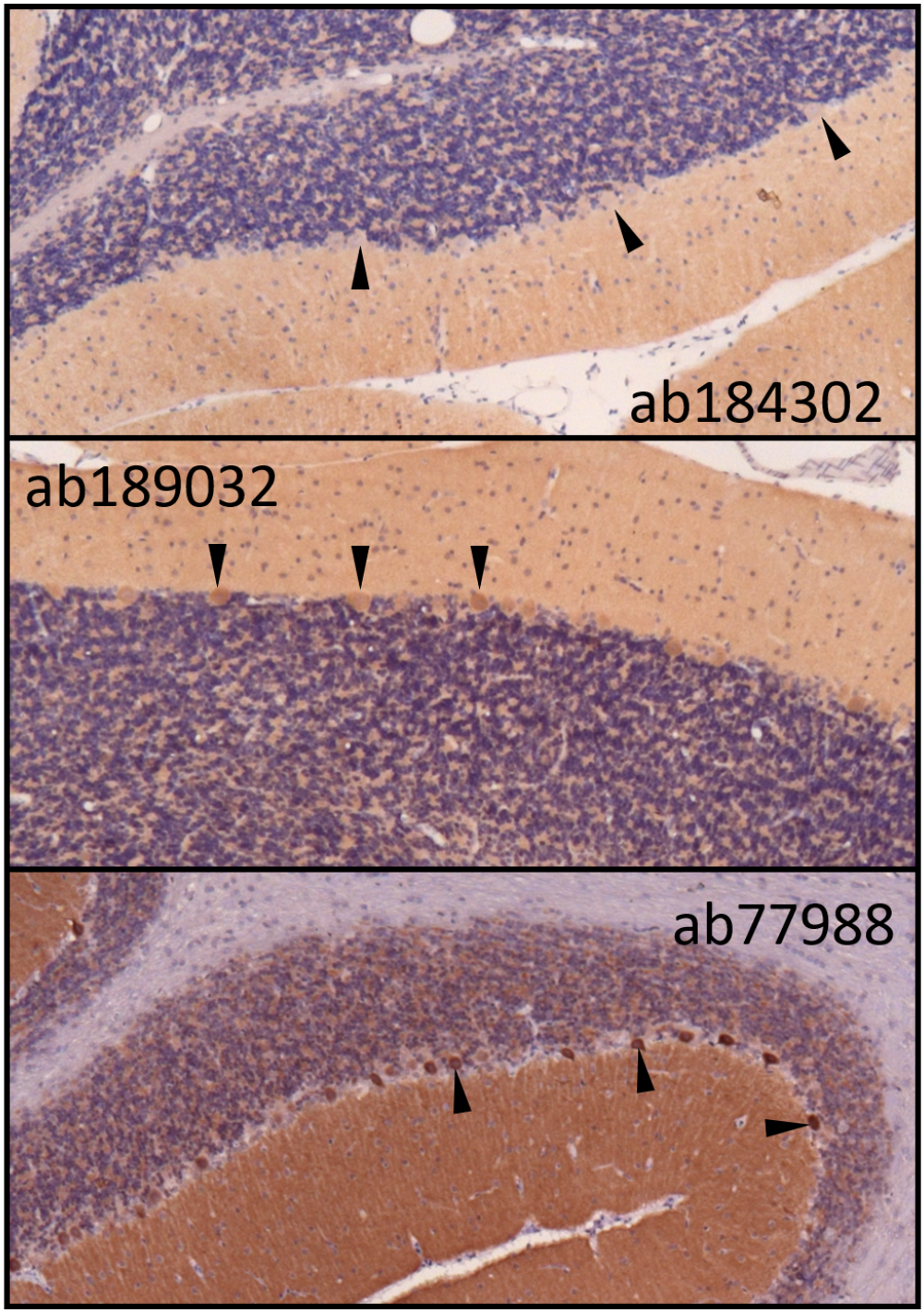

Figure 4.32: Representative pictures of DAB staining with mGluR4 antibodies and Cresyl Violet staining of neuronal cytoplasm (Nissl substance) in the granule layer. Black arrow heads indicate Purkinje cells at the interface of the molecular and granule layers.

4.5.3 Cytokines in inflammatory responses

It is widely recognised that changes in inflammatory cell number is not the only mechanism by which inflammatory state can change. Indeed, alterations in activation state, phenotype and secretory profile of astrocytes and microglia have been shown to be important in neuroprotection and neurodegeneration by a number of groups (Taylor et al. 2003, Michelucci et al. 2009, Simpson et al. 2010). This study was conducted in order to examine fine changes in inflammatory profile of brain tissue in animals which had undergone and unilateral lesion and sub-chronic treatment with either vehicle or LSP1-2111. In general, the experiments in this study tended to show a reliable, if small, trend towards an effect of lesion alongside a smaller (if present) trend towards a change with LSP1-2111 treatment.

4.5.3.1 Evidence of lesion

Because of the need to prepare tissue for cytokine arrays, it was not possible to gauge lesion size by TH immunohistochemistry as before. Instead, an ELISA for TH was used with striatal tissue homogenate. The ELISA for striatal TH showed no significant difference in content between lesioned and intact, vehicle and LSP1-2111-treated tissue. Rather than proving no lesion or neuroprotective effect, this is likely to indicate some failing in the analytical process (discussed below). TH protein levels shown by the ELISA in this chapter appear to be 10- or 100-fold lower than striatal TH quantifications reported elsewhere in the literature - undertaken through the use of quantitative immunoblotting assays - which may suggest a weakness in the ELISA or tissue preparation protocols (Salvatore et al. 2004, Pruett & Salvatore 2013, Salvatore et al. 2016). In all previous studies, the vast majority of animals were successfully lesioned and there were no alterations in the protocol prior to lesioning for the present study. In addition, animals showed a significant deficit in the cylinder test and so there is reason to believe in a reliable lesion effect in this study too.

The neuroprotective effect of LSP1-2111 in the present study is more difficult to be sure of, despite its demonstration in Chapter 3. Even if LSP1-2111 were not protective in this study, at the least, based on the GeneChip data, it may be expected that the sub-chronic administration of LSP1-2111 induced some transcriptional changes. Any effects on cytokine expression in LSP1-2111-treated animals not apparent in the vehicle group may therefore be understood to result from LSP1-2111 administration and be a potential contributor towards a theorised LSP1-2111-mediated protection even if that protection is not proven in this case.

There are a number of potential reasons why the TH ELISA presented in the current study may not reflect the reality of conditions in the striatum.

- Method of sample preparation.

  For these series of ELISAs, tissue was fresh dissected, snap frozen, homogenised, centrifuged and the supernatant removed for analysis in biochemical assays. Thus, the assays were performed solely on the soluble fraction of tissue homogenates and not the insoluble fraction. If TH predominantly remained in the insoluble pellet following centrifugation, this may explain low TH concentrations in the ELISA and little difference between groups. In opposition of this theory, Yamamoto Ki et al. (2001) find that TH remained primarily in the soluble fraction of homogenised Portulaca grandiflora, though it may be the case that TH from this plant is of a different structure than mammalian TH. Indeed, Haavik et al. (1988) used a complex elution and purification protocol to eventually discover TH in the post-centrifugation pellet, rather than supernatant, of bovine adrenal medulla tissue, more likely to have high homology with rat TH.

- Composition of striatum.

  By composition, the striatum is primarily gamma-aminobutyric acid (GABA)-ergic alongside some cholinergic neurons. Dopamine is contained in terminals only, with no dopaminergic cell bodies present in the striatum. It may, therefore, be possible that dopaminergic terminals containing TH are too small a component of the striatal tissue to be reliably measured in a homogenate. This seems difficult to credit, given the plain evidence of TH in immunohistochemical studies. Kim et al. (2014) show in an examination of neurotransmitter levels in brain regions of the mouse that dopamine is, by some margin, the most highly expressed neurotransmitter in the striatum. However, Salvatore & Pruett (2012) show that there is much more dopamine per ng of TH in the terminal field of the striatum (with approximately 2.5pmol dopamine per ng TH) than in the SNc where there is approximately 0.5pmol dopamine per ng TH. This difference in expression between dopamine and TH may therefore explain how the striatum can be highly dopaminergic and yet express low levels of TH. In this case, an assay for dopamine would seem to have provided a more accurate read of lesion size. However, extracellular dopamine concentrations have been shown to remain high in the striatum of lesioned animals (Robinson & Whishaw 1988), and so this approach may also not have been suitable.

- Location of lesion.

  In all previous studies in this thesis where immunohistochemical analysis of the striatum has taken place, the lesion has been located in the dorsal-mid striatum. As this study used a different method of anaylsis based on dissection of individual regions, an incomplete dissection may result in a distorted view of the region. In this case, if the relatively intact ventral striatum had been removed preferentially in the dissection then the TH ELISA may appear to show an unlesioned striatum. However, it is perhaps unlikely that only the ventral striatum could have been removed in all of the dissections in this study and therefore this is less likely than the other reasons to account for the lack of apparent striatal TH reduction in the ELISA.

Lesion effect was also confirmed through a behavioural test. Animals were taken from a larger cohort where all animals were subject to the cylinder test to prove an effect of lesion. In the whole group data, both vehicle and LSP1-2111-treated animals had a significant motor deficit compared to their baseline, thus giving reassuring evidence of a lesion effect. This apparent lack of functional protection in tests of spontaneous motor function was also seen in the neuroprotection study in Chapter 3 and does not preclude a neuroprotective effect of LSP1-2111 administration.

Ideally, the amphetamine-induced rotation test, which showed a significant effect of LSP1-2111 treatment in Chapter 3, would have been used with these animals to confirm an effect of lesion and treatment. In the present study, the amphetamine test was not used in order to avoid any potential resulting alteration of cytokine expression (for example, Shanks et al. (2012) demonstrated that amphetamine can have a significant effect on the secretory profile of BV2 microglia). Furthermore, in the neuroprotection study, the amphetamine-induced rotation test was conducted at day 11 post-lesion in order to allow for a drug washout period. In the present study, animals were culled at day 7 without any washout period and so an amphetamine-induced rotation test would have had to have been conducted while the animals were on drug. This would not, therefore, have been directly comparable to the results of the study in Chapter 3 due to any potential acute effects of LSP1-2111 on rotational behaviour.

4.5.3.2 Cytokine arrays

In the cytokine arrays, there appeared an effect of lesion and an effect of treatment for many cytokines in both the striatum and VM. In reality, few of these changes were shown to be significant following a Kruskal-Wallis test likely to due to high variance between technical replicates. This

may have arisen in part because the cytokine arrays have no standard curve and so the expression of each cytokine must be expressed relative to other cytokines on the array, or relative to the same cytokine on another array. As each array may only be used with one sample (washed over the array completely rather than confined to a well as in an ELISA), the comparison between arrays (or samples) adds another potential source of variability.

Nevetheless, the arrays provided a number of candidate cytokines which appeared altered by both lesion and LSP1-2111. These candidates were examined in the literature for their relevance to PD and neuroinflammation or neuroprotection and three promising nominees assayed by ELISA. One cytokine with significantly different expression between groups (CXCL7 in the VM) was also chosen to validate the array through the use of an ELISA. These choices were limited by limited tissue availability. TNFα and IL-2 were also examined in a small number of samples via ELISA but the tissue homogenates used were found to contain insufficient levels of each cytokine for analysis. Additional cytokine analysis will not be pursued in similar samples due to the remarkably low levels found in the samples analysed in this study.

4.5.3.3 CXCL7

CXCL7 has been shown to bind to CXCR2 (IL-8R β) and sulfated glycosaminoglycans as a monomer or as a dimer with nanomolar efficacy (Brown, Sepuru & Rajarathnam 2017, Brown, Joseph, Sawant & Rajarathnam 2017). When released from activated platelets, CXCL7 plays an important role in the recruitment of neutrophils, the synthesis of extracellular matrix and plasminogen activator and in glucose metabolism (Castor et al. 1983, 1985). CXCL7 has also been shown to prevent the scavenging of pro-inflammatory cytokines in a host response to a bacterial infection (Mei et al. 2013) - indicating a potentially important but unexplored role in neuroinflammation following blood-brain barrier dysruption. The elevated levels of CXCL7 in the lesioned VM tissue therefore likely represents an inflammatory response and the reduction of pro-inflammatory scavenging.

In this study, CXCL7 expression in the VM was studied in order to validate the cytokine array, which predicted increased expression in tissue from the lesioned hemisphere in both vehicle-treated and LSP1-2111-treated animals. This was reflected in the ELISA, though the trend towards an effect was only approaching significance ($p = 0.055$). This validates the principle of using the array to predict hits for follow up via a different method (in this case, ELISA), and supports the cytokine array (at least in cases where cytokine expression is high). This also provides further

evidence, if needed, of a true lesion in these animals in contrast to the TH ELISA.

In the striatum, CXCL7 showed the opposite trend to that suggested by the array - CXCL7 concentration appeared reduced in the lesioned tissue from both vehicle and LSP1-2111-treated animals in comparison to the intact tissue. This inversion in expression is puzzling, and may be related to the availability of neutrophils (expressing CXCR2 and therefore able to 'mop up' CXCL7) to respond to the signal in the striatum, as a result of the blood-brain barrier dysruption, as compared to the lack of availability in the VM. This may facilitate a negative feedback in the striatum which does not exist in the VM and thus explain the reduced CXCL7 in striatal lesioned tissue and increased expression in VM lesioned tissue. This may be mediated by the SOCS or STAT pathways as reviewed in Greenhalgh & Hilton (2001).

The reasons for the differences in CXCL7 expression measured by the cytokine array and by ELISA in the striatum are also unclear. As the ELISA is fully quantitative, as opposed to the semi-quantitative array and, as each sample may be compared in one plate in the ELISA, it seems reasonable to conclude that the ELISA is more likely an accurate representation of the tissue environment in the case of the striatum. Concentrations of CXCL7 in the striatum were less than half those seen in the VM as measured by the cytokine array and approximately 10 times less as measured by ELISA. These low concentrations may explain the apparent dissonance between the two assays.

In the GeneChip microarray, there were significant increases in CXCL7 transcription in both the striatum (7.09 fold) and VM (4.29 fold) following a single 10mg/kg dose of LSP1-2111 in otherwise naïve animals. It is difficult to extrapolate this response to lesioned animals or animals given LSP1-2111 over an extended period of time, but this finding reinforces that LSP1-2111 is capable of mediating changes in expression of the CXCL7 gene - further validating the cytokine array and casting doubt on the results of the ELISA which showed only trends towards a change with lesion and not with treatment.

4.5.3.4 MIP1α

MIP1α, also known as CCL3, has been shown to bind receptors C-C chemokine receptor 1 (CCR1), 4 and 5 which are primarily located on T cells and neutrophils (Reichel et al. 2006, Yoshie & Matsushima 2015). In PD patients, MIP1α is found to be upregulated in the periphery compared with healthy controls (Reale et al. 2009). The functions of MIP1α that are likely relevant in these

PD populations are in chemotactic mobilisation of monocytes, macrophages, microglia, dendritic cells and lymphocytes into tissues (De Buck et al. 2013, Wang et al. 2013, Li et al. 2014).

While MIP1α can be induced from activated macrophages and microglia (Kohno et al. 2014), Kalkonde et al. (2007) have also shown that astrocytes can release MIP1α in mice treated with MPTP and, furthermore, the dopaminergic neurons of the SNc also seem to express MIP1α consitutively. The predicted loss of nigral dopaminergic neurons, combined with no increase in nigral astrocytes or microglia as shown in the LSP1-2111 inflammation and time course studies, as a result of the 6-OHDA lesioning may go some way to explaining a reduction of MIP1α in lesioned tissue.

In this study, MIP1α was predicted by the cytokine array to increase in the lesioned VM of vehicle-treated animals but not in LSP1-2111-treated animals. An ELISA showed that, in fact, MIP1α was decreased in the lesioned VM of both vehicle and LSP1-2111-treated animals compared to the intact VM. That the concentrations of MIP1α in the samples were so low may explain the inaccuracy of the cytokine array data compared with the fully quntitative ELISA.

Although MIP1α has been shown to have a very low EC50 at CCR1 in radioligand membrane binding preparations, the predicted EC50 value of 0.029+0.009nM (Chou et al. 2002) remains approximately 5 times higher than the changes in concentration between intact and lesioned VM of approximately 0.05pg/μg protein (6.4pM). A calcium mobilisation assay puts the EC50 of MIP1α even higher, at 0.1nM (Chou et al. 2002), meaning that the apparent reduction in MIP1α in lesioned tissue may not be functionally relevant.

4.5.3.5 IP10

IP10, also known as CXCL10, is secreted by a number of inflammatory cell types (including monocytes and endothelial cells) in response to IFNγ (Basset et al. 2015) and binds to the C-X-C motif chemokine receptor CXCR3 located on T cells, dendritic cells and natural killer (NK) cells (Oghumu et al. 2015). IP10 is thought to have a number of actions once bound including inhibition of angiogenesis, monocyte chemoattractant and T/NK cell activation (Angiolillo et al. 1995, Dufour et al. 2002).

In a PD population, IP10 upregulation was correlated with cognitive deficits (Rocha et al. 2014) though the average expression in plasma (approximately 1600pg/ml) did not differ from that in

healthy controls. IP10 has also been shown to play a role in leukocyte entry into brain tissue during neuroinflammation (McKimmie & Michlmayr 2014). As the presence of T and B cells was not measured in the present studies, it is impossible to confirm whether this potentially IP10-driven effect was present in the lesioned VM to a different degree than the intact VM - though such information may help to suggest whether the change in IP10 expression was functionally significant. Cognitive studies conducted in Chapter 5 of this thesis, however, show that the animals lesioned through the protocol used here do not appear to show cognitive deficit, and so IP10 upregulation is unlikely to be directly associated with such symptoms in this model and at these concentrations.

In the ELISAs of the present study, IP10 was found to be increased in lesioned VM tissue compared to intact tissue in both treatment groups - this increase was significant in LSP1-2111-treated animals. By comparison, the cytokine array predicted that IP10 would be increased in the lesioned VM tissue of vehicle-treated animals, though also that this would be lessened in LSP1-2111-treated animals.

Similarly, in a transcriptomic study of 6-OHDA-lesioned rats, Kanaan et al. (2015) found that IP10 transcription was significantly upregulated in the VM at weeks 1 (3.02 fold) and 2 (4.02 fold) post-lesion - the time point at which the tissue used in the present study was taken. This correlates well with the approximate 2.5-fold upregulation suggested by the ELISA in the lesioned VM of LSP1-2111-treated animals. The GeneChip study undertaken as part of the work presented here did not find any upregulation of IP10 following a single dose of LSP1-2111 so this may represent either an interaction between lesion and LSP1-2111 or a specific effect of longer-term LSP1-2111 administration.

Heise et al. (2005) reported the EC50 of IP10 to be 7nM for radioligand binding to CXCR3-CHO membranes. Clearly, this is a binding effect rather than an effect attached to functional downstream signalling, which may be significantly different. Nevertheless, the 7nM figure is far in excess of the concentration observed in lesioned VM from LSP1-2111-treated animals here, which is 11.5pM. This evidence, alongside the values recorded in the plasma of PD patients and healthy controls (Rocha et al. 2014), may indicate that the observed change in IP10 concentration as a result of lesion is unlikely to have resulted in any functional effects.

In summary, little in the way of inflammatory changes with potential functional effects in a whole organism was seen through the cytokine array and ELISA approach to understanding the

secretory profile of inflammatory cells in the 6-OHDA-lesioned rat. The initial cytokine arrays, in particular for the VM tissue seemed to show a promising general trend towards an increase in pro-inflammatory cytokine expression in lesioned tissue compared to intact tissue, with a reduction in expression in lesioned tissue from LSP1-2111-treated animals. Apart from the ELISA examining CXCL7 expression in the VM, the subsequent ELISAs did not seem to mirror the changes seen in the initial arrays, calling into question the validity of the assays.

4.5.4 LSP1-2111-mediated transcriptional changes

Although some subtle anti-inflammatory effect was recorded previously in this chapter, the size of the effect does not seem large enough to be solely responsible for the neuroprotection seen in Chapter 3. This study set out to discover other potential actions of LSP1-2111 which may underlie the neuroprotective effect seen previously. Indeed, through the GeneChip study, some alternative explanations for this effect have become apparent.

The GeneChip array highlighted differences in individual gene expression regulation and in the regulation of pathways in the VM and striatum following a single administration of LSP1-2111. Pathway analysis indicated multiple pathways and genes through which a protective effect could be indicated in both the VM and striatal tissue samples. These include the IL-2 and complement signalling pathways and G-protein (specifically, monoamine G-protein) signalling pathways. These data express the potential involvement of multiple protective mechanisms in the antiparkinsonian activity of LSP1-2111, and may help to explain why a single inflammatory or gene expression change does not stand out in the analysis of LSP1-2111-treated animal tissue.

There appears no consensus on the optimal way to analyse large microarray datasets such as those generated in this study through the application of GeneChip. While examination of individual genes with significant regulation risks the least loss of data, it can result in an unmanageable number of hits to piece together and make understanding the global effects of a treatment almost impossible. Pathway analysis allows a more top-down approach with a higher understanding of changes occurring in the tissue, but also loses information on many of the individual genes which may not yet be integrated into the online pathway databases (Moran et al. 2006). Nevetheless, pathway analysis gives higher consensus between microarray studies and a useful overview platform for further analysis (Oerton & Bender 2017).

Likewise, there is no true consensus over the application of a false discovery rate correction in small-scale microarray studies and so its importance has not been overemphasised in the present study. Some groups consider that application of a false discovery rate correction in order to reduce to possibility of false positive discoveries can result in an unacceptably high false negative rate (Pawitan et al. 2005). Indeed, in the application of a false discovery correction to this data, the number of sequences which are significantly (and over 2 fold) regulated by LSP1-2111 falls from 1469 in the two tissues (excluding duplicates significantly regulated in both tissues) to 2.

Although it may seem surprising that a compound marketed to fulfill a specific function (such as LSP1-2111 is an mGluR4 agonist) could regulate so many as 495 genes in one tissue, it is possible that these all reflect changes downstream of receptor activation. To put this number into perspective, Kanaan et al. (2015) found 1331 genes significantly regulated in the VM of intrastiatal 6-OHDA-lesioned rats at any time post-lesion from 1 to 16 weeks. Sárvári et al. (2016) found 497 genes significantly (and $\geq$2 fold) regulated in the hippocampus of ovariectomised rats following treatment with estradiol, an estrogen receptor agonist. Burgdorf et al. (2015) found 486 genes with significantly altered transcription in the rat medial prefrontal cortex (mPFC) following administration of an N-Methyl-D-aspartate (NMDA) receptor modulator even following application of a false discovery rate protocol. Given these comparisons, application of an automated false discovery rate protocol which reduced the 495 genes regulated in the VM by LSP1-2111 in this study to 0 certainly does not seem fitting.

Ideally, some further work would be done to reinforce and validate this microarray approach. Firstly, a number of the pathways suggested through pathway analysis using the Transcriptome Analysis Console and Wikipathways - such as adipogenesis, calcium regulation in the cardiac cell and endochondral ossification, would appear to be incompatible with, or irrelevant to, a neuronal sample. For this reason, a reliable method of neuronal correction in order to remove these seemingly impossible hits may help to reduce the numbers of hits for each sample and thereby increase the number of significant hits following correction for false discovery rate. However, no such method has been detailed in the literature at this point and so its application was not attempted here.

Secondly, it is good practice to validate significant hits following microarray analysis through polymerase chain reaction (PCR) experiments. In this instance, there were too many genes with highly-altered expression to consider validation through this method. Instead, the intention in this case is to use the GeneChip data presented here to inform probe choice for a Luminex Multiplex Assay (Thermo Fisher, USA). Such an assay, limited to 50 targets, will give more data on a smaller number of targets and lower the false discovery rate. Tissue for this assay will come from unilaterally lesioned, LSP1-2111-treated animals in order to further examine the interaction between lesion and treatment. Genes with expression that appears significantly altered in the multiplex assay would then be validated through PCR.

Finally, it should be acknowledged that many uncharacterised expressed sequence tags (ESTs) were discovered as part of this study, some of which were among the most highly up- or downreg-

ulated sequences in the dataset. Although there is currently no reliable way to characterise these ESTs, more sequences are characterised regularly and microarray analysis databases updated with the new findings. Therefore, re-analysis of the GeneChip data file in months or years to come could yield new data on the transcriptional changes mediated by LSP1-2111 in naïve animals.

When examined without the application of a false discovery rate protocol and with only the current knowledge of ESTs, the data provided by the GeneChip assay present ample avenues to pursue for potential effects of acute administration of LSP1-2111 which may underpin the neuroprotective efficacy of the compound and would not necessarily impact upon the number or phenotype of inflammatory cells in the region. In the short term, it seems most pressing to further investigate some of the most exciting data gained from this assay using follow up assays in order to verify the changes (such as PCR). Some examples of these data include the changes in expression of Bcl2l11, protein kinase D, nitric oxide synthase 1 and TGFβ1.

4.6 Summary and conclusions

In summary - the partial lesion model developed in Chapter 2 and used for the neuroprotective studies in Chapter 3 was further characterised here for its inflammatory components. Nigral cell death was found to be relatively slow with significant loss by 4 days which was completed by 7 days. Terminal loss in the striatum was achieved more quickly, with a complete lesion formed by 3 days post-lesion. Nigral inflammation underlying the formation of this lesion was mild, with no significant inflammation in the lesioned hemisphere compared to the intact between 2 and 7 days. Through comparison to Iba1 measurements in the SNc of vehicle-treated animals in the LSP1-2111 study, it would seem that microgliosis continues to grow past the 7 day time point.

The trend towards a reduction in Iba1-positive cells also in the rostral region of the SNc provides a hint about one possible mechanism of mGluR4-mediated neuroprotection. Cytokine arrays, though not ELISAs, also suggest some subtle effect of LSP1-2111 on the secretory profile of inflammatory cells of the VM and striata in lesioned animals which may contribute to an altered inflammatory profile.

The potential of group III mGluR agonists to reduce nigral glutamate has been demonstrated by Austin et al. (2010) through intracranial application. Such an action of LSP1-2111 was not explored in this thesis but a reduction of glutamate release would seem highly likely given the evidence both *in vivo* (Austin et al. 2010) and *in vitro* (Broadstock et al. 2012) for mGluR4 activation producing this effect. The concept that this reduction in glutamate, alongside anti-inflammatory effects of activating mGluR4, could be neuroprotective was shown by Betts et al. (2012). The impact of this effect through a systemically available compound having activity in particular in the rostral SNc is detailed here and shows promise for future, non-dopaminergic, neuroprotective treatments of PD.

The anti-inflammatory effect revealed by Betts et al. (2012) was not robustly evident in the present studies so an anti-inflammatory action of LSP1-2111 may not fully explain the neuroprotective efficacy of the drug. Thus other potential mechanisms of action of LSP1-2111 were explored through a GeneChip assay, which revealed a great many gene transcripts with significantly altered expression after a single dose of LSP1-2111. Although these data need to be followed up through alternative assays such as PCR in order to confirm the effect, many of the genes significantly altered by a single dose of LSP1-2111 can be tied to neurodegeneration and neuroprotection. In particular, protein kinase D (Asaithambi et al. 2014) has shown evidence in 6-OHDA models of

being neuroprotective, and was upregulated by LSP1-2111. These myriad transcriptional changes are likely to contribute further to the neuroprotective mechanisms of LSP1-2111 beyond a simple reduction in immune cell number or cytokine concentration.

5 Characterisation of motor and non-motor signs of Parkinsonism in a rat bilateral partial lesion model

5.1 Introduction

5.1.1 Burden of non-motor symptoms on those with Parkinson's disease

The non-motor symptoms of Parkinson's disease (PD), such as sleep disturbance, cognitive impairment and neuropsychiatric issues, were originally characterised by James Parkinson in 1817 alongside his accounts of the motor features (republished as Parkinson (2002)). After that point, however, non-motor symptoms became under-recognised and under-diagnosed, despite being no less important in affecting the quality of life of the PD patient (Shulman et al. 2002). Today, self-rating scales for the burden of non-motor symptoms on an individual are being developed to help solve this problem and aid in diagnosis of non-motor symptoms (Martinez-Martin et al. 2009).

The range of non-motor features of PD is broad and can vary widely from person to person, with some clinical subtypes of PD becoming evident from studies grouping together types of non-motor symptom (Sauerbier et al. 2016). Some symptoms, such as anxiety, depression, rapid eye movement (REM)-sleep behaviour disorder and olfactory deficits are commonly associated with the prodromal stages of PD, while cognitive impairment is more often seen in the advanced stages of the disease (Galati & Di Giovanni 2010). Below, the common non-motor features of PD will be separated into groups and each discussed briefly. Where a feature has been examined in one or more of the animal models of PD, this will also be reviewed.

5.1.1.1 Sensory features

Olfactory deficits

Hyposmia or anosmia are common features of early PD, and may be produced through an accumulation of Lewy bodies in the olfactory bulb as early as Braak stage 1, before pathology affects the nigrostriatal pathway (Braak et al. 2003). As many as 90% of PD patients display deficits including odour detection, identification and differentiation in the prodromal phase of the disease and, alongside other symptoms, this can be used retrospectively as a reliable test of the onset of PD (Bohnen et al. 2008).

Changes in olfaction have also been noted in some rodent models of PD, but not in others. In keep-

ing with the suggestion that, in PD, olfactory deficits may arise from α-synuclein deposits in the olfactory bulb, Fleming et al. (2008) find that hyposmia is present in mice overexpressing human α-synuclein. Alternatively, systemic administration of 1-methyl-4-phenyl-1,2,3,6-tetrahydropyridine (MPTP) has been shown to significantly and selectively decrease noradrenaline (NA), but not dopamine, in the olfactory bulb in male mice (Dluzen 1992). This likely indicates a failure in the cognitive processing of an odour (such as emotional associations or memory), rather than impairments in the functioning of the olfactory bulb in odour detection. This is consistent with evidence that noradrenergic signalling in the olfactory bulb is important for social recognition in mating behaviour (Brennan et al. 1990) but that noradrenergic and dopaminergic lesioning of the olfactory bulb with 6-hydroxydopamine (6-OHDA) does not impair detection of odours (Doty et al. 1988). Similarly, Royet et al. (1983) find that intra-olfactory 6-OHDA does not cause anosmia, but does alter neophobia and feeding behaviour normally dictated by scent.

Vision

Poor visual acuity and blurred colour vision are also common sensory features of PD, and are largely unresponsive to drug treatment. Problems with vision relating to PD may arise from neurotransmitter changes in the retina or motor impairments such as altered eye movements or blinking, and may predict the development of visual hallucinations later in the disease process (Matsui et al. 2006). *In vivo*, MPTP-treated cynomolgus monkeys have been shown to develop altered visual fields, as in PD (Ghilardi et al. 1988). Alterations in the retina and visual-evoked potentials have also been observed in rat models (Esteve-Rudd et al. 2011, Aras et al. 2014).

Pain

Chronic pain occurs in up to 80% of PD patients, and is associated with more severe motor complications and depressive symptoms than in those with no pain (Nègre-Pagès et al. 2008, Beiske et al. 2009). Pain in PD arises from two main sources - musculoskeletal pain associated with stiffness or dystonia and centrally-mediated pain which is a result of PD-related neurodegeneration. Pain may also either be neuropathic (arising from nerve damage) or nociceptive (arising from tissue damage) in nature.

The basal ganglia, in particular the dorsal striatum, has been shown to play an important role in pain processing and agonists of group III mGluRs applied in the dorsal striatum have been shown to reduce pain in chronic pain rat models (Rossi et al. 2014, Marabese et al. 2018). In PD, the loss of dopaminergic innervation to the dorsal striatum can be sufficient to induce a state of chronic pain which increases in the L-3,4-dihydroxyphenylalanine (L-DOPA) 'off' state and reduces in

the 'on' state (Gerdelat-Mas et al. 2007). The provision of L-DOPA and dopamine agonists does not remove pain in PD altogether, however, suggesting additional roles of other systems. The periaqueductal grey, locus coeruleus, subcoeruleus and various nuclei within the thalamus and hypothalamus are affected by Lewy bodies by Braak stage 4 (Braak et al. 2000, 2003). These nuclei are central to pain processing and their combined dysregulation and disruption in PD underlie the chronic pain phenotype and make finding specific treatments challenging.

In vivo, mechanical and thermal hyperalgesia have been demonstrated in MPTP-treated mice and in 6-OHDA-lesioned rats (Park et al. 2015, Tadaiesky et al. 2008).

5.1.1.2 Neuropsychiatric features

Anxiety and depressive disorders have a higher prevalence in PD populations than general populations and more frequently coexist (Nuti et al. 2004). The existence of these disorders in PD may arise as a psychological reaction to the state of having Parkinson's, or as a result of neurobiological changes during neurodegeneration. They may also predict a worse outcome for the patient including greater disability, reduced quality of life and greater risk of mortality (Brown et al. 2011). Anxious and depressive symptoms can be difficult to separate, and it has been hypothesised that they arise from the same neurobiological changes in both PD and non-PD patients (Nuti et al. 2004, Barlow & Campbell 2000). It should be noted that many neuropsychiatric disorders, such as anxiety and depression, can be broken into subgroups which display quite different symptoms and that reporting of these features both in PD patients and in animal models will vary widely depending on what symptoms are measured and how that measurement is quantified.

Anxiety

Symptoms of anxiety in PD reduce with effective treatment (either L-DOPA or deep brain stimulation) and increase with 'off' periods of L-DOPA treatment and motor fluctuations (Storch et al. 2013). These observations could indicate either that anxiety is a psychological reaction to disability or that it has an underlying dopaminergic component. In support of a neurodegenerative pathology hypothesis, anxiety is often seen in the prodromal phase of the disease, before the onset of motor symptoms (Shiba et al. 2000). Remy et al. (2005) used positron emission tomography (PET) imaging to examine the basis for anxiety in PD. They found that binding of the catecholaminergic ligand, ^{11}C-RTI-32, in a number limbic regions (including the left striatum, left locus coeruleus, bilateral thalamus and bilateral amygdala) was inversely correlated with anxiety. Apathy, however, was only negatively correlated with binding in the striatum. This finding implies

that anxiety in PD has a different neurochemical basis than does apathy.

Remy et al. (2005) were only able to differentiate anxiety from depression using PET imaging in the left amygdala, where ^{11}C-RTI-32 binding is reduced in PD patients with anxiety but not in those with depression, and the right locus coeruleus, where ^{11}C-RTI-32 binding is only reduced in PD patients with depression.

In vivo, Tadaiesky et al. (2008) show that bilateral 6-OHDA lesions can cause measurable anxiety in rats, and that this anxiety is correlated with changes in dopamine and NA in the striatum and medial prefrontal cortex (mPFC). In addition, anxiety was also seen in genetic mouse models of PD and in α-synuclein injection and overexpression models (Zhu et al. 2007, Taylor et al. 2009, Campos et al. 2013).

Depression

Similarly to anxiety, depression in PD may be a psychological reaction to disability or it may arise from neurobiological changes underlying PD itself. Depression in PD is only partially responsive to dopaminergic therapies, suggesting that there is at least some non-dopaminergic, neurological basis of depression in PD (Even & Weintraub 2012). Remy et al. (2005) found that ^{11}C-RTI-32 binding was reduced in the limbic system of patients with PD and depression but not in those with PD but not depression. Furthermore, Kostic et al. (2010) show that people with PD-depression have a reduced mass of white matter in the corticolimbic, dopaminergic reward pathway compared to those with PD but without depression.

Depression in the general populace is often linked with 5-hydroxytryptamine (5-HT) availability, rather than reductions in dopamine, and accordingly treated with selective serotonin reuptake inhibitors (SSRIs). Although the serotonergic raphe nucleus is affected early on in PD, reduced serotonin transporter availability in the raphe was found to be associated with a tremor-dominant phenotype and not significantly correlated with depressive symptoms (Qamhawi et al. 2015). Indeed, SSRI treatment may be less effective in treating PD-associated depression than depression in those without PD and instead, the noradrenergic tricyclic antidepressant (TCA) treatments are preferred in PD cases (Menza et al. 2009, Liu, Dong, Wang, Su, Yan & Sun 2013). This is likely to relate to greater changes in noradrenergic nuclei (such as the locus coeruleus) in those presenting with PD-depression (Frisina et al. 2009).

Depressive and anhedonic behaviours have been seen in animal models of PD including the 6-

OHDA-lesioned rat and vesicular monoamine transporter 2 (VMAT2)-deficient mouse correlated with dopaminergic, noradrenergic and serotonergic changes (Tadaiesky et al. 2008, Taylor et al. 2009).

Apathy

Apathy often co-exists with depression, but either may be present without the other and are both correlated with different aspects of PD, suggesting that the neurobiologies may be different (Oguru et al. 2010). Apathy has been recognised in a large percentage of PD patients, up to 65% by some estimates (Pedersen et al. 2009, Oguru et al. 2010). In PD, apathy has been variously attributed to functioning of the limbic system, to atrophy of the left nucleus accumbens (NAc) and to atrophy of the cingulate and inferior frontal gyri (Remy et al. 2005, Carriere et al. 2014). Measurable apathy has been linked to worse outcomes such as more severe dementia, deterioration of executive function and motor function (Pedersen et al. 2009).

Apathy, anedonia and depression are particularly difficult to differentiate in animal studies, which may unknowingly test behaviour encompassing two or three symptoms. Nevertheless, Tian et al. (2015) attempt to study apathy in MPTP-treated non-human primates and correlate apathetic behaviour with dopaminergic dysfunction in the ventral tegmental area (VTA), NAc and insular cortex.

Cognition

Cognitive decline is associated with either the late stages of PD, or an alternative diagnosis such as Parkinson's disease dementia (PDD), with as many as 83% of 20 year survivors showing cognitive impairment in the mini mental state exam, the clinical dementia rating and the Boston naming test (Hely et al. 2008). Cases of PD where cognitive impairment occurs as an early symptom (onset of dementia < 1 year following onset of motor symptoms) are diagnosed as dementia with Lewy bodies (DLB) (Aarsland et al. 2004).

Cognitive impairment in PD is another non-motor symptom whose underlying cause lies outside of the dopaminergic deficit that is central to the disease. Bohnen et al. (2003) find that there is a severe, cortical cholinergic deficit in PD patients with dementia when compared with PD patients without dementia or even with Alzheimer's disease (AD) patients. The severity of dementia in PD patients also correlates with Lewy pathology in the CA2 region of the hippocampus (Churchyard & Lees 1997). These pathologies hint at the reason why typical dopaminergic therapies for PD do not improve cognitive issues.

Mild cognitive impairment (MCI) may occur in the early stages of PD and exist as a separate entity to the more severe dementia seen in PDD (Kehagia et al. 2013). The MCI seen early in the disease process has been dubbed 'frontostriatal' and seems to arise from dopaminergic, rather than cholinergic deficits (Mattay et al. 2002). This evidence supports the hypothesis that MCI in PD is a distinct symptom rather than an early appearance of more severe, cholinergic dementia in PDD.

These distinct types of cognitive impairment are difficult to distinguish *in vivo*, but deficits have been seen in a number of animal models. Lesions caused by 6-OHDA or MPTP have been shown to cause cognitive impairment in rats and mice (Tadaiesky et al. 2008, Yabuki et al. 2014), though this is sensitive to the lesioning and testing paradigms (Fifel et al. 2013). Genetic models have also shown a propensity towards development of cognitive impairment at late stages, though the pathology underlying these changes in cognition seems variable - with one study finding hippocampal synuclein pathology and another finding cholinergic deficits in the cortex but no changes in the hippocampus (Masliah et al. 2011, Magen et al. 2012). Similar cholinergic deficits are seen in non-human primates treated with MPTP and are akin to those found in the early stages of PD (Decamp & Schneider 2004).

Psychosis

Hallucinations and psychosis are predicted by a number of variables largely relating to severity of PD, duration and dose of L-DOPA (which may in themselves be related), cognitive decline and depression (Svetel et al. 2012). It has previously been noted that reducing dopamine therapies and or giving clozapine (an atypical antipsychotic, antagonist at D_3, D_4 and 5-HT_2 receptors) reduced the incidence of hallucinations (The Parkinson's Study Group 1999). In addition to dopamine medication, PD itself may lead to hallucinations through Lewy pathology in the amygdala and cortex (Papapetropoulos et al. 2006).

Psychosis is difficult to model in animals as it cannot be proven that any behavioural changes seen are as a result of hallucination. However, Visanji et al. (2006) show psychosis-like behaviours in MPTP-treated non-human primates which respond to antipsychotic treatment.

5.1.1.3 Sleep features

REM sleep behaviour disorder (RBD) is characterised by the exhibition of violent motor behaviours during the REM phase of sleep, when muscle tone is inhibited in healthy individuals. RBD has been considered to be a strong predictor of early-stage PD since Schenck et al. (1996) discovered that a high proportion of males diagnosed with RBD went on to develop PD years later. Sixel-Döring et al. (2014) reinforce this discovery by showing that, in 51% of a cohort of newly diagnosed and unmedicated PD patients who had not been diagnosed with RBD, REM behavioural events could be measured - much higher than the 15% of healthy controls. This shows that RBD may still be underrecognised, and could therefore be an even better predictor of future develoment of PD than is currently understood.

Normal sleep is controlled by the ascending reticular activating system, including the VTA, substantia nigra pars compacta (SNc), locus coeruleus, raphe nuclei, hypothalamic nuclei, pedunculopontine nucleus and thalamus (Schwartz & Kilduff 2015). Multiple neurotransmitters are represented in this system, including dopamine, NA and 5-HT which are all affected in Parkinson's. Dopamine agonists may cause excessive sleepiness, and sleep disorders such as narcolepsy can be treated using dopamine active transporter (DAT) blockers (Schapira 2000). This implies that the dopaminergic therapies used to treat PD, in addition to RBD which occurs as a result of PD, may be causing some of the excessive daytime sleepiness that is common to PD patients.

Disturbance in REM sleep has also been noted in animal models. α-synuclein accumulation in the brainstem of genetically-modified mice, mirroring that seen in the early stages of PD, caused sleep dysfunction (Braak et al. 2003, McDowell et al. 2018). Furthermore, MPTP- and 6-OHDA-lesioned rodents and monkeys show evidence of REM disturbance and RBD (Lima et al. 2007, Verhave et al. 2011, McDowell et al. 2018).

5.1.1.4 Autonomic features

Bladder

Increased frequency and urgency of urination (micturition) and nocturia are all associated with PD, mediated through detrusor hyperreflexia. Unlike many other non-motor symptoms, degeneration of the basal ganglia is thought to directly underpin bladder hyper-reflexia in PD, with D1 and D2 receptor mediated output from the basal ganglia having opposing actions on micturition (Seki et al. 2001).

The primary evidence for the role of dopamine in micturition has arisen from *in vivo* models of Parkinson's. Rats lesioned using 6-OHDA and non-human primates lesioned with MPTP show hyperreflexia which can be reversed by infusing D1, but not D2, agonists into the basal ganglia (Yoshimura et al. 1998, 2003). Evidence from MPTP-treated primates shows that alterations in contractility of the bladder detrusor in PD and PD models may be a result of adaptive changes resulting from the loss of dopaminergic input (Pritchard et al. 2017). For this reason, common dopamine agonist treatments of PD, which largely act at the D2 receptor, are not suitable for reducing bladder hyperreflexia. Other, non-dopaminergic regions of the brain also play a role in micturition, including the pontine micturition centre, hypothalamus and frontal cortex, and these may provide alternative targets for the treatments of bladder dysfunction in PD (Sakakibara et al. 2008).

Gastrointestinal tract

There are many gastrointestinal (GI) symptoms which occur prior to and alongside the motor symptoms of PD, including constipation, slowed gastric emptying, difficulty swallowing (dysphagia) and excessive salivation. In PD and other synucleinopathies, there is α-synuclein and Lewy body pathology throughout the central nervous system (CNS), periperal nervous system (PNS) and GI tract. This pathology is so reliably associated with early stage PD that it has been proposed as a diagnostic feature (Gelpi et al. 2014). At the forefront of tissues featuring this pathology and likely to be involved in GI changes, the dorsal motor nucleus of the vagus - which asserts autonomic control of the bowel and is affected in the early stages of disease - is likely to be key (Greene 2014). In addition to the presence of Lewy bodies, there is likely to be a dopaminergic component to GI dysfunction in PD shown by improvement of symptoms after intrajejunal administration of levodopa (Honig et al. 2009).

In vivo, reduced GI motility (Colucci et al. 2012, Noorian et al. 2012), delayed gastric emptying (Karasawa et al. 2014) and constipation (Hallett et al. 2012) can be provoked in PD lesion or genetic models. The pathology underlying GI changes in these models is conflicting and this is likely due to differences in the implementation of the model - where 6-OHDA involves an intracranial infusion of toxin, MPTP is administered systemically. Irrespective of the model, none saw differences in the dorsal motor nucleus of the vagus.

5.1.2 Models of Parkinson's disease which include non-motor symptoms

As discussed in the general introduction, there are a wide variety of animal models of Parkinson's, which are primarily characterised based on the motor symptoms or pathology associated with each. The utility of the primary, mammalian models of PD for the study of non-motor symptoms is tabulated below (Table 5.1 - 5.3). Certain symptoms in some models have a wealth of evidence behind them and, in these cases, only a subset of the references are provided. However, an attempt has been made to show references for as many symptoms and models as have been characterised, including recording instances where a symptom has been examined and found not to be present.

Necessarily, models have been grouped under umbrella terms. For example - not all (or any) of the 6-OHDA, MPTP or rotenone studies referenced here have used the same protocol as the others, and this is likely to account for some of the variation in symptoms observed.

For this study, a bilateral 6-OHDA lesion at co-ordinates previously used in this thesis was selected. This was due to ease of application as a result of prior expertise and a potentially wide range of symptoms accessible through 6-OHDA (as in the evidence presented below). The lesion was carried out bilaterally in order to account for lateralisation of function in the mPFC, NAc and amygdala (Sullivan et al. 2009, 2014, Carriere et al. 2014).

Table 5.1: Sensory non-motor symptoms in commonly used mammalian models of Parkinson's disease

Model	Hyposmia/Anosmia	Vision	Pain
Reserpine			Liu et al. (2014)*
Haloperidol			
6-OHDA	Bonito-Oliva et al. (2014) Tadaiesky et al. (2008) ⋄		Gómez-Paz et al. (2017)
MPTP rodent	Prediger et al. (2006)	Aras et al. (2014)	Park et al. (2015)
MPTP primate	Miwa et al. (2004)	Ghilardi et al. (1988)	
Rotenone		Esteve-Rudd et al. (2011)	
α-synuclein injection/ overexpression	Zhang et al. (2015)		
DJ-1 knockout			
Parkin knockout			
VMAT2 knockdown	Taylor et al. (2009)		
PITX3 knockdown			

Table 5.1: Table displaying references for studies examining sensory symptoms in commonly-used mammalian models of PD. ⋄ denotes studies finding that a symptom does not appear. * denotes an area where a symptom has been characterised but through the use of a test compromised by undiscussed motor impairments.

Table 5.2: Psychiatric non-motor symptoms in commonly used mammalian models of Parkinson's disease

Model	Anxiety	Depression	Cognition	Psychosis
Reserpine		Liu et al. (2014)*	Santos et al. (2013)	
Haloperidol			Hutchings et al. (2013)*	
6-OHDA	Bonito-Oliva et al. (2014) Tadaiesky et al. (2008)	Bonito-Oliva et al. (2014) Tadaiesky et al. (2008) Chiu et al. (2015) Chen et al. (2011) ⋄	Tadaiesky et al. (2008) Evenden et al. (1989) Chiu et al. (2015) ⋄ Chen et al. (2011) ⋄	
MPTP rodent	Shin et al. (2014)	Santiago et al. (2010) Moretti et al. (2015)	Prediger et al. (2006) Da Cunha et al. (2001) Fifel et al. (2013) ⋄	
MPTP primate			Schneider & Pope-Coleman (1995) Fernandez-Ruiz et al. (1995)	Visanji et al. (2006)
Rotenone	Gokul & Muralidhara (2014)	Santiago et al. (2010)	Perez-Pardo et al. (2017)	
α-synuclein injection/ overexpression	↓ Yamakado et al. (2012) ↓ Oaks et al. (2013)	Caudal et al. (2015) Oaks et al. (2013) ⋄	Magen et al. (2015)	
DJ-1 knockout			Pham et al. (2010)	
Parkin knockout	Zhu et al. (2007)		Zhu et al. (2007)	
VMAT2 knockdown	Taylor et al. (2009)	Taylor et al. (2009)		
PITX3 knockdown			Ardayfio et al. (2008)	

Table 5.2: Table displaying references for studies examining psychiatric symptoms in commonly-used mammalian models of PD. ⋄ following a reference denotes a study finding that a symptom does not appear. * denotes an area where a symptom has been characterised but through the use of a test potentially compromised by untested motor impairments. ↓ shows a symptom changing in the opposite way to that expected based on the symptomatology discussed previously.

Table 5.3: Sleep and autonomic symptoms in commonly used mammalian models of Parkinson's disease			
Model	Sleep	Bladder	GI
Reserpine			
Haloperidol			
6-OHDA	Vo et al. (2014)	Mitra et al. (2015) Yoshimura et al. (2003)	Karasawa et al. (2014), Blandini et al. (2009) Colucci et al. (2012)
MPTP rodent	Lima et al. (2007), Fifel et al. (2013) ⋄		Natale et al. (2010)
MPTP primate	Fifel et al. (2014), Verhave et al. (2011)	Yoshimura et al. (1998)	
Rotenone	Yi et al. (2007)		Greene et al. (2009)
α-synuclein injection/ overexpression	McDowell et al. (2018)	Hamill et al. (2012)	Noorian et al. (2012), Hallett et al. (2012)
DJ-1 knockout			
Parkin knockout			
VMAT2 knockdown	Taylor et al. (2009)		Taylor et al. (2009)
PITX3 knockdown			

Table 5.3: Table displaying references for studies examining sleep and autonomic symptoms in commonly-used mammalian models of PD. ⋄ denotes studies finding that a symptom does not appear. * denotes an area where a symptom has been characterised but through the use of a test compromised by undiscussed motor impairments.

5.2 Hypothesis and aims

The non-motor symptoms of PD, though increasingly recognised, are still inadequately understood and ineffectively treated (Zesiewicz et al. 2010). This is likely due to the complexity of the underlying neurobiology of symptoms such as depression and anxiety, and uncertainty as to whether these mechanisms are different when associated with PD (Even & Weintraub 2012). Producing models of non-motor symptoms of Parkinsonism in animals can aid understanding of the underlying mechanism of the disease and also allow for the development of better therapeutics.

The aim of this study was to examine a bilateral, partial 6-OHDA lesion model in rats (at the same co-ordinates as used previously for a unilateral lesion) for typical non-motor symptoms of PD. Once characterised *in vivo*, we also aimed to ascertain the neurological basis for the symptoms which emerged using immunohistochemistry. This study was undertaken with the aim of developing one model for use in the exploration of both motor and non-motor aspects of Parkinsonism.

Previous studies examining non-motor symptoms in bilateral, partial lesions have been conducted. The study described here aims to increase knowledge gained from previous literature and improve upon the methods. For example, while there is an excellent range of behavioural tests in the study conducted by Tadaiesky et al. (2008), the lesion on which the model is based is created low in the ventral striatum, with the DV co-ordinate of the 6-OHDA injection at dura -7.2mm. The present study characterises a lesion created at -5.5mm from skull surface (approximately -4.5 to -5mm from dura), which creates a dorsal-mid striatal lesion more representative of the dorsal striatal-related deficits seen in PD (Voorn et al. 2004). Furthermore, a number of the non-motor symptoms found to be present by Tadaiesky et al. (2008), in particular anhedonia, are likely to occur from direct damage to the NAc and ventral striatum (Voorn et al. 2004). Other studies with a more dorsal, bilateral lesion (Chen et al. 2014, Silva et al. 2016), have a limited number of tests in their battery with which to characterise the model. As shown in the present study, conducting multiple tests for one symptom can be useful in order to inform interpretation of the results. This study expands on previous works in order to create a more fully characterised, more valid model of early stage PD.

We hypothesise that the implementation of a bilateral, partial 6-OHDA lesion at co-ordinates used previously will create both motor (e.g. akinesia, postural instability) and non-motor (e.g. anxiety, anedonia, cognitive impairment) symptoms of Parkinson's in a rat model. These symptoms will be measurable through well-characterised, non-invasive behavioural tests and may be accompanied by changes in monoaminer-

gic transmission in relevant brain regions.

5.3 Materials and Methods

All procedures were performed in accordance with the U.K. Animals (Scientific Procedures) Act, 1986.

5.3.1 Implementation of lesion

20 male Sprague-Dawley (SD) rats (225-275g, Harlan, UK) were maintained on a 12 hour light-dark cycle in a temperature and humidity controlled room with *ad libitum* access to dry chow and tap water. Rats were given at least 7 days to acclimate to the unit prior to lesioning.

Animals were pseudorandomised to 6-OHDA or sham (saline) conditions through the use of a random number generator (Haahr 1998) and the experimenter was blinded to the treatments by a third party. In this way, animals were grouped by 'A' and 'B' rather than sham and lesion, in order to enable regrouping for cage allocation without unblinding. The study was not unblinded until immunohistochemical analysis was completed.

Implementation of the lesion was accomplished similarly to those in previous chapters. Briefly, animals were induced to anaesthesia using 5% isoflurane and the top of the head shaved and swabbed with 0.4% w/v chlorhexidine gluconate (dilution of Hibiscrub, Mölnlycke UK). Viscotears liquid gel (Alcon, Switzerland) was applied to the eyes to prevent drying or damage and the skull was exposed once the animal was appropriately situated within the ear bars and anaesthetic maintenance nose cone. Stereotaxic lesioning took place with the animals under inhaled isofluorane anaesthesia (2% maintenance). Lesions were made using 12μg 6-OHDA in 3μl 0.2% sodium ascorbate, or sodium ascorbate alone (n=10 per group), at AP +0.2mm, ML $\pm$3mm from bregma and -5.5mm from skull surface, with the incisor bar set at -3.3mm (adapted from Przedborski et al. (1995)) (Figure 5.1). The infusions took place at a speed of 1μl/minute and the needle was left in place for a further 3 minutes following infusion to prevent reflux of 6-OHDA. Following withdrawal of the needle, the incision was cleaned with sterile gauze swabs and sutured using coated Vicryl sutures with a 3-0 gauge needle (Ethicon Inc, USA). Animals were given 0.01mg/kg buprenorphine (Vetergesic, Ceva Health Care Ltd, France) via subcutaneous (s.c.) injection with 5ml/kg sterile saline for rehydration and management of post-operative pain, and housed in a heating cabinet at 25°C overnight. All animals were then weighed daily and rehydrated with subcutaneous saline as necessary until their pre-surgery weight was regained. Rats were allowed to recover for a minimum of 6 days prior to behavioural testing.

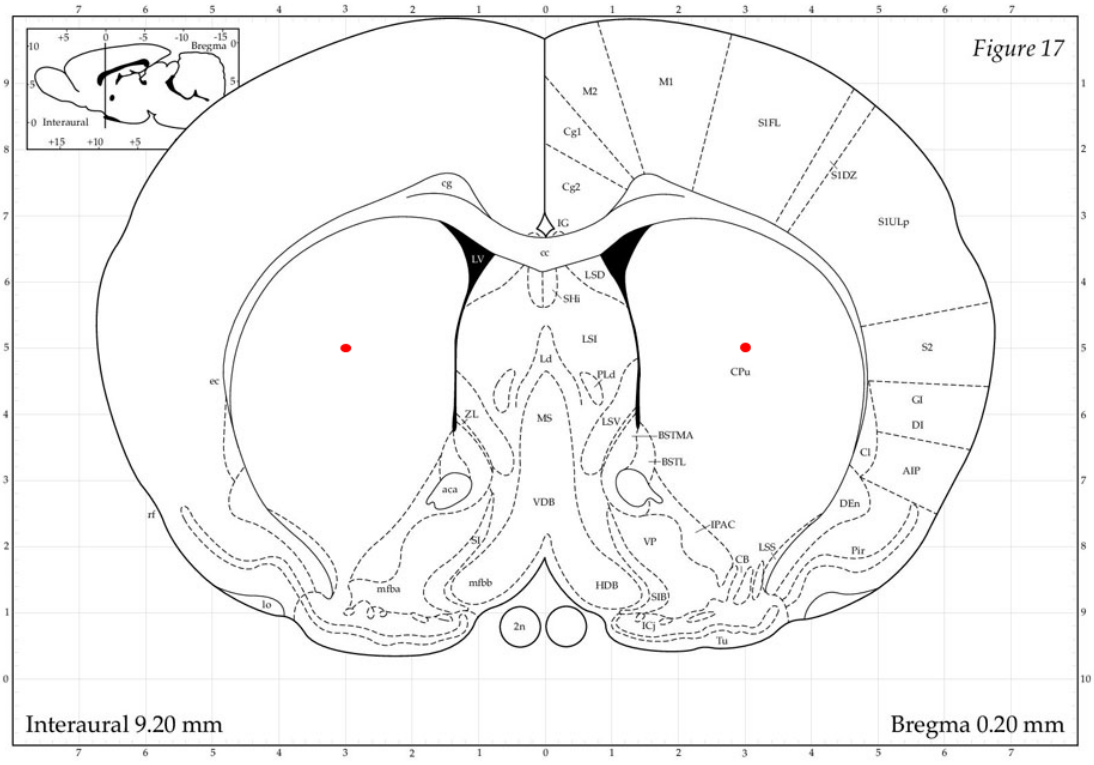

Figure 5.1: Site of bilateral lesion visualised on atlas plate from Paxinos & Watson (1986).

5.3.2 Behavioural characterisation of lesion

Behavioural tests were carried out during the light cycle, between the hours of 7am and 7pm, with the exception of the sucrose preference test which was necessarily continued for a full period of 72 hours. On the fourth day post-lesion, animals were recaged in pairs with another animal from the same original cage and surgical condition. The testing schedule is displayed in Table 5.4, with a key to abbreviations in the legend, followed by a full description of each test.

Table 5.4: Behavioural testing schedule						
Week	Day					
	1	2	3	4	5	6
-1			ARR training	ARR training	ARR training & HP baseline	
0	**Lesioning**				Pair and recage	
1	ARR	OF & SRT	SRT 24hr	HP		
2	MB	SP training	SP			
3	ARR & EPM	OF & SRT	SRT 24hr	HP		
4				SP training	SP	
5			ARR			
6	MWM					**Perfuse & dissect**

Table 5.4: Behavioural testing schedule. Note that each 'week' is comprised of 6 days for simplicity of presentation. Blank space denotes days on which no behavioural tests took place. On any day with multiple behavioural tests, the tests were undertaken in order of least to most invasive and are displayed in the appropriate order. A break of $\geq$2 hours was included between each test. ARR, accelerating rotarod; EPM, elevated plus maze; HP, hotplate test; MB, marble burying test; MWM, Morris water maze; OF, open field arena; SP, sucrose preference test; SRT, social recognition test.

5.3.3 Motor behaviour

5.3.3.1 Accelerating rotorod

Accelerating rotarod (47700, Ugo Basile, Italy) was undertaken on weeks 1, 3 and 5 as a method of ascertaining the effect of the lesion on motor ability. The rotarod speed was set to 4 revolutions/min at the start of the task, accelerating to 40 revolutions/min over the test period (5 minutes) as in Walker et al. (2001). Rats were trained on the rotarod prior to 6-OHDA lesioning until they consistently achieved a fall latency of $\geq$90 seconds, at which point baseline latencies were taken. At the end of the test period, any animals remaining on the rotarod were removed and assigned the maximum latency of 300 s. Any animals attempting to turn (to face backwards) on the rotarod were corrected throughout, and if an animal stopped running and revolved with the rod for $\geq$2 full rotations, they were removed and considered to have fallen at that point. At each time point, tests were run in duplicate with a minimum of 30 minutes and a maximum of 45 minutes between the two trials. The average of the two scores was used for statistical analysis.

5.3.4 Pain behaviour

5.3.4.1 Hot plate

The hot plate test was used to assess a potential effect of the bilateral, partial lesion on thermal hyperalgesia. Rats were placed on a hot plate (35100, Ugo Basile, Italy) pre-heated to, and maintained at, 52°C. Latency to lick, flick or stamp one of the hind paws, or to perform an escape response (e.g. a jump or climb) was recorded (Espejo & Mir 1993). A cutoff limit of 40 seconds (maximal possible latency to pain response) was used to prevent tissue damage. Rats were tested at baseline 3 days prior to lesion surgery and then at 1 and 3 weeks post-lesion.

5.3.5 Anxiety behaviour

5.3.5.1 Open field arena

The open field arena was utilised at weeks 1 and 3 in order to measure activity during free exploration for the purpose of assessing both locomotor behaviour and anxiety. This test was carried out under bright lighting conditions in order to enhance the anxiogenic effect of the open arena. The apparatus was made of varnished plywood and had a floor of $1m^2$ and 40cm walls. A grid was drawn on the floor of the arena separating the space into 25 squares of 20×20cm each (Figure 5.2). The animal to be tested was placed in the central square of the open field (x), and the number of lines crossed (as an approximation of distance) and number of rearings were recorded for the duration of the 5 minute testing period. A line-cross was counted when all four paws had crossed. Vertical exploratory behaviour was recorded when an animal lifted both forepaws off the ground but did not groom. For the measurement of anxious behavioural traits, the time spent in the central 9 squares of the apparatus compared to the time in the squares at the perimeter was also recorded starting at the point at which the animal left the central area on placement (Hazim et al. 2014). This test was chosen for its simplicity and versatility, and adapted from Tadaiesky et al. (2008).

o	o	o	o	o
o	-	-	-	o
o	-	x	-	o
o	-	-	-	o
o	o	o	o	o

Figure 5.2: Layout of open field arena grid. For the purposes of the anxiety measurements, perimeter squares are marked o, central squares are marked - and x. Placement square for starting the task is marked x.

5.3.5.2 Marble burying test

Marble burying behaviour has been used as a correlate of anxiolytic activity of various compounds (Njung'e & Handley 1991), where a reduction in the number of marbles buried in a set period is correlated with anxiolytic efficacy, and an increase in burying correlated with stress. It is not yet well enough understood to be called a true test of anxiety however it is quick, uninvasive and simple to carry out. The test was used effectively by Slawinska et al. (2013) in characterising the anxiolytic properties of (1S, 2R)-N1-(3,4-dichlorophenyl)-cyclohexane-1,2-dicarboxamide (Lu AF21934) in mice. A similar protocol was adapted by Schneider & Popik (2007) for use with rats and this was the protocol followed here, performed on week 2. Rats were tested individually in their home cage which contained their usual bedding, to approximately 5cm depth. Ten identical red marbles, 2.2 cm in diameter, were arranged in rows in one half of the cage. Testing was conducted for a 10-min period under dim light and windows were covered with blackout blinds to remove the variable of daylight intensity. After a 10 minute exposure to the marbles, rats were removed and the buried marbles were counted. The number of marbles that were $\geq 50\%$ buried, and the subset of those that were $\geq 80\%$ buried were counted and recorded.

5.3.5.3 Elevated plus maze

The elevated plus maze is another well-characterised test for anxiety in both rats and mice (Tadaiesky et al. 2008). It relies on the conflict between eagerness to explore a novel environment and a preference for enclosed, dimly lit spaces rather than exposed, brightly lit areas. In this study, the plus maze was only performed once, at week 3, due to its susceptibility to unreliable retest results (Schneider et al. 2011).

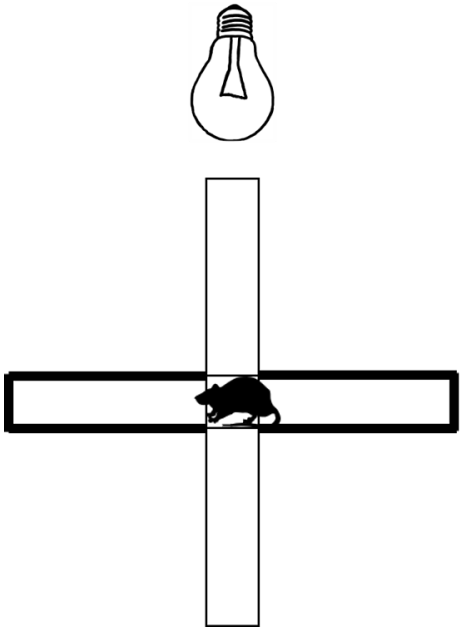

Figure 5.3: An arial view of the elevated plus maze. Arms outlined in bold represent the closed, or walled, arms of the maze while the others are open arms.

The plus maze consisted of a wooden structure elevated to 50cm above floor level. A pair of "open" arms (50cm long by 10cm wide) and a pair of "closed" arms (50 by 10cm with 40cm high walls), were arranged such that each was opposite its identical partner and at right angles to the other pair - forming a + shape parallel to the floor - with a central 10cm by 10cm platform connecting them all (Figure 5.3). Experiments were performed under dim light conditions with a single light shining through the length of the open arms such that it didn't brighten the closed arms. At the start of the trial, the rat was placed on the central platform facing a closed arm. After each 5 minute test, the maze was carefully cleaned with Anistel to prevent previous trials from influencing future ones. The time spent by each animal in open and closed arms, and the number of entries into each type of arm was recorded. The latter was evaluated in order to account for the possibility of a reduction in locomotor activity due to the motor effects of the lesion. An entry into any zone was counted when all four paws had crossed the threshold.

5.3.6 Anhedonic behaviour

5.3.6.1 Sucrose preference test

The sucrose preference test is a well-characterised test of anhedonia or mild stress in rodents. A rodent which has undergone chronic mild stress will not show increased intake of highly palatable substances such as sucrose solution, while a 'control' animal will show a significant preference for the sucrose solution over standard drinking water. This lack of preference can be rectified through treatment with antidepressants, suggesting that anhedonia is a true cause (Katz 1982).

The protocol for this test was adapted from Tadaiesky et al. (2008) for use with dual-housed (same-group) rats and performed at weeks 2 and 4. During the 24 hour training period, rats were acclimated to having two drinking bottles - one on each side of the cage - each containing tap water. Before and after the training period, these bottles were weighed in order to check that they were both being utilised. For the 48 hour testing period, one of the tap water bottles was randomly substituted with 0.8% sucrose solution. Both bottles were weighed before being presented to the rats and the contents recorded. At the mid point of the test period, the two bottles were swapped in order to account for possible side bias. 24 hours later, the bottles were removed and the final weight recorded.

The weights of tap water and sucrose solution were divided by 2 to approximate the volume intake of each rat in the cage, and each was represented in the final analysis.

5.3.7 Cognition

5.3.7.1 Social recognition test

The social recognition test is a test of short- and medium-term social memory, testing olfactory, motivational and cognitive aspects of Parkinsonism. Used here, the protocol was adapted from Tadaiesky et al. (2008) and informed by Mathiasen & DiCamillo (2010) for its suitability for use on rats housed in pairs rather than singly housed.

As detailed at the start of this section, lesioned and sham rats were recaged in pairs following surgery with a familiar cage mate which was in the same treatment group. Rats were tested after a minimum of 3 days of habituation to their new environment to reduce any anxiogenic effects of recaging. The social recognition test was performed at weeks 1 and 3.

An addendum to the protocol was devised to reduce the possibility of fighting between test animals and juveniles. In the event of any sign of aggression during the social recognition test, the trial was to be stopped and the animals separated. If no injuries were sustained and the trial was at a re-introduction phase then the rats were to be re-introduced under close observation. If the trial was at the stage of first introduction then an alternative juvenile was to be used. Implementation of this protocol was not necessary during this study.

The social recognition test consisted of three successive presentations of an unfamiliar male juvenile (defined as being 4 weeks old $\pm$ 1 week) rat. Adult rats were habituated to the observation room for 30 minutes, then placed into individual, perspex, test chambers ($20 \times 30 \times 40cm - h \times w \times l$) with a mesh lid and habituated for a further 30 minutes. The unfamiliar juvenile was then placed into the chamber with the lesioned adult. The time spent by the adult in investigating the juvenile (by sniffing, force-grooming, following or pawing - summarised in Figure 5.4b. Pawing is not pictured but was defined as repeated light touches by the test animal anywhere on the juvenile.) was recorded. Any interactions initiated by the juvenile were not counted. At the end of the first presentation, the juvenile was removed and returned to its home cage during the delay period. After 30 minutes, the rats were re-introduced for a further 5 minute test and the same behaviours recorded. 24 hours following training, adult rats were re-habituated to the observation room for 30 minutes then re-exposed to the same juvenile (after 30 minutes habituation to the test chamber) and interaction scored for a further 5 minutes to assess longer term social recognition (summarised in Figure 5.4a).

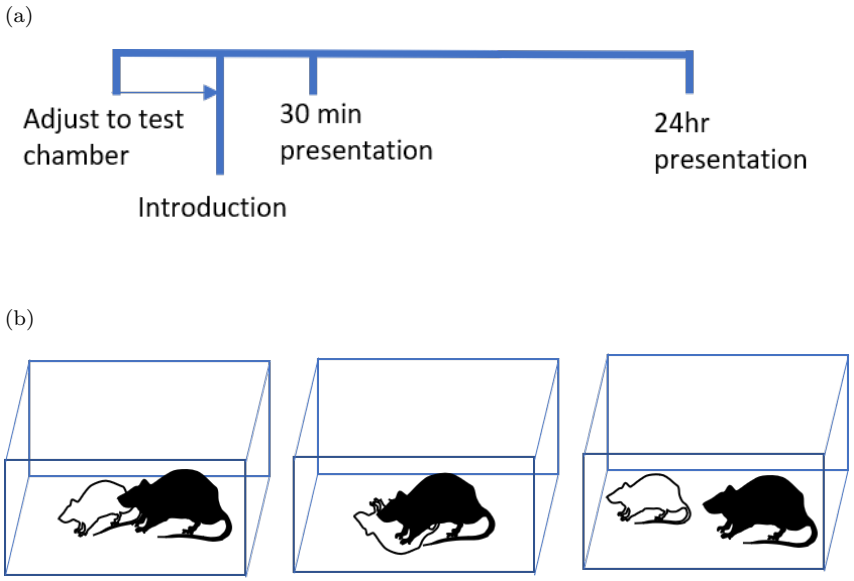

Figure 5.4: Social recognition test. a) Timeline displaying habituation of adult, lesioned rat to test chamber, immediately followed by a 5 minute introduction to the juvenile. 30 minute and 24hr reintroduction of the same juvenile were used to measure investigative behaviours. b) Diagram of behaviours relevant to the social recognition test. Juvenile animal in white and adult test animal in black. This diagram represents sniffing, force-grooming and following respectively.

Recognition was gauged by the length of time in which the adult rat investigated the juvenile. Less time spent investigating through any of the means listed above was taken to imply that the adult recognised the juvenile from a previous presentation.

5.3.7.2 Morris water maze

A version of the Morris water maze test was used here to assess cognitive ability and spatial acquisition, which typically decline in the later stages of PD (Kempster et al. 2010), rather than the earlier stages modelled here. Similar bilateral partial models have picked up cognitive deficits with maze tasks (Tadaiesky et al. 2008) and so it was important to thoroughly test this attribute in order to rule out its potential effects on other tasks. The protocol was advised by the spatial acquisition protocol outlined in Vorhees & Williams (2006), with a potential for a cued version of the task being implemented if necessary to further dissect any deficit seen in the spatial learning task.

A pool 1.8m in diameter and 38cm deep was filled to a 30cm depth with tap water and allowed to adjust to room temperature (19-22°C) overnight. A closed-circuit recording camera responsive only to infrared light was suspended from the ceiling directly above the pool and an infrared light source was placed close to the pool. One small lamp was directed at the wall to provide diffuse, dim lighting. Windows were covered with blackout blinds to remove the variable of light intensities on different days. A transparent platform with a rough surface was positioned in the north-west section of the pool roughly equidistant from the side and the centre. The platform was submerged to 1.5cm below the surface.

Training periods took place each day from 7am-12pm for 4 days. Training periods began by introducing the rat to the pool, facing the pool wall, whereupon the experimenter retreated to a fixed position in order to serve as a cue. Starting positions were named north, east, south and west and were equally spaced around the rim of the pool (Figure 5.5 for a diagram of the setup). Rats were tested from each of the 4 starting positions on each training day with a minimum time of 15 minutes between starts. Once placed in the pool, the rat was given 90 seconds to mount the submerged platform and wait for retrieval. Retrieval took place approximately 10 seconds after the rat mounted the platform to allow time for the animal to learn the location of the platform based on distal cues in fixed positions within the testing room (e.g. the experimenter, a computer, a bench with infrared light source and a window covered with blackout blinds). If the rat did not find the platform in the allotted 90 seconds, they were led to the platform by the experimenter. If the animal located the platform but did not mount, or mounted but immediately left, they were guided back the platform until they waited for retrieval (10 seconds) in order to teach that the platform was the correct escape from the pool.

Analysis of the training sessions included average latency to mounting the platform, average distance swum before mounting the platform and average swim speed. These metrics were plotted against time to in order to show learning speed which may be reduced in cognitively impaired animals.

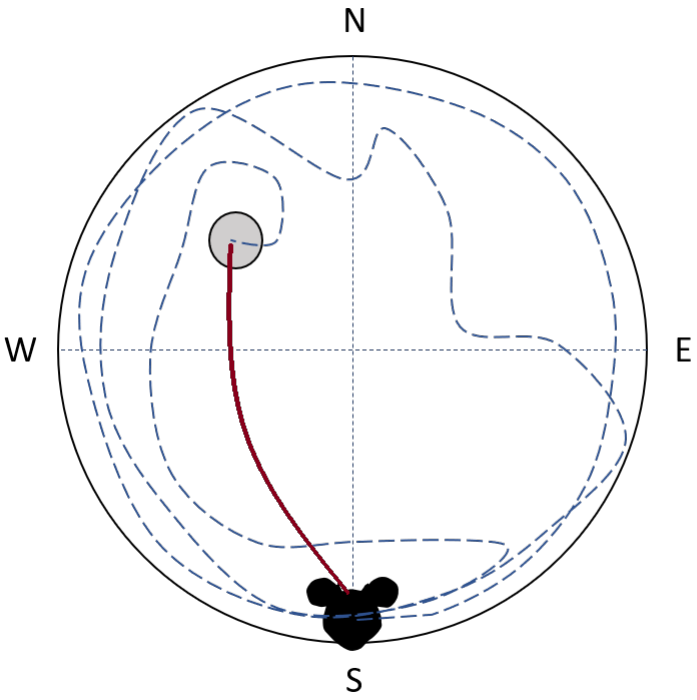

Figure 5.5: A setup of the Morris water maze in which the platform (grey circle) is located in the north-west quadrant and the rat has been placed at the south position for training. The dashed blue line represents a route to the platform which may have been taken by an animal which does not know the location of the platform well. The solid red line is representative of a late-training route for an animal which has learned the location of the platform.

12 hours following the final training period, a probe trial was run. The trial consisted of a 90 second swim period in the same pool following removal of the platform, from a single starting point which was chosen at random. Analysis of the probe trial included time spent in the quadrant that previously contained the platform and latency to enter that quadrant. The probe trial assessed how well the rat had learned the location of the platform and its persistence in finding it again.

Videos were analysed for the aforementioned parameters in a post hoc fashion, using Ethovision XT tracking software (Noldus Information Technology). This was verified with a manual computation of the time-to-platform and time-in-quadrant analyses.

5.3.8 Histological characterisation of lesion

The SNc and striatum were analysed for tyrosine hydroxylase (TH)-positive cell and terminal loss, respectively, in order to quantify lesion size. Behavioural outcomes were used to inform which brain areas were chosen for subsequent histological evaluation. Where a non-motor symptom was observed, the nuclei thought to be associated with development or expression of that symptom were further explored. On these grounds, the retrorubral field (RRF), VTA and the locus coeruleus were examined for alterations in TH expression - reflective of the monoaminergic nature of these nuclei. Further exploration of the pathways was carried out where differences in the numbers of cell bodies in these regions were present.

On week 6, rats were given an overdose (200mg via intraperitoneal (i.p.) injection) of sodium pentobarbital (Euthatal. Merial Animal Health Ltd, UK) and perfused as detailed in Chapter 2. After removal from the animal, the whole brains were hemisected and processed as individual hemispheres. Tissue was then prepared for histology as in Chapter 2, sectioned sagittally at 7μm and stained with (1:750 rabbit polyclonal anti-tyrosine hydroxylase antibody (AB152, Merck Millipore, Canada). Sagittal sectioning was chosen for this study in order to enable visualisation of full pathways in a single section.

The data from 3 sections was averaged to represent each region for each animal. Each section was imaged at 10x or 4x using an Axioskop camera and Nikon microscope for cell counts or a Canon DSLR camera with a macro lens for densitometry. Cell counts and densitometry image analysis were both conducted using ImageJ image processing software as described in Chapter 2, and statistical tests were conducted using GraphPad Prism 7.

5.3.9 Statistical analysis

All data were tested for normality using the D'Agostino and Pearson omnibus normality test prior to undergoing any tests for significant differences between groups. Where sham and lesion groups were compared over a series of tests, or at different points in time, a 2-way ANOVA was used, with Sidak's post-test where appropriate. The outcome of the ANOVA is stated in results sections. Where sham and lesioned animals were compared within a single test or time point, a Mann-Whitney test was used for data not normally distributed, and an unpaired t-test where data were normally distributed. For all, data are shown either as individual data points for each animal, or as mean $\pm$ standard error of the mean (S.E.M.), and p-values are stated for all comparisons.

5.4 Results

5.4.1 Behavioural characterisation of lesion

5.4.1.1 Accelerating rotarod

Performance on the accelerating rotarod was quantified using latency to fall. Overall, lesioned animals showed a reduced latency to fall compared to sham animals, and this reduced latency was stable by 3 weeks post-lesion (Figure 5.6).

At baseline, individuals in the two treatment groups performed comparably, with rats to be sham-lesioned having an average latency to fall of 265±23 seconds and rats to be 6-OHDA-lesioned having an average latency of 234±23 seconds. By 1 week post lesion, 6-OHDA animals' average latency was non-significantly lower than shams ($p > 0.05$; Sidak's post-test). At 3 weeks post lesion, latency had fallen to its minimum in the 6-OHDA animals, 104±20 seconds ($p < 0.01$; Sidak's post test compared to shams), or 44% of baseline. This was sustained at 5 weeks post lesion.

Sham-lesioned animals' latency to fall reduced steadily over the 5 week period and, by week 5, was also significantly decreased compared to baseline ($p < 0.05$; Sidak's post-test), though this was to a lesser degree than 6-OHDA-lesioned rats.

In the repeated measures 2-way ANOVA comparing latency to fall between lesion conditions and over time, there was an interaction between variables ($p = 0.03$), a main effect of time ($p < 0.0001$) and a main effect of lesion ($p = 0.04$).

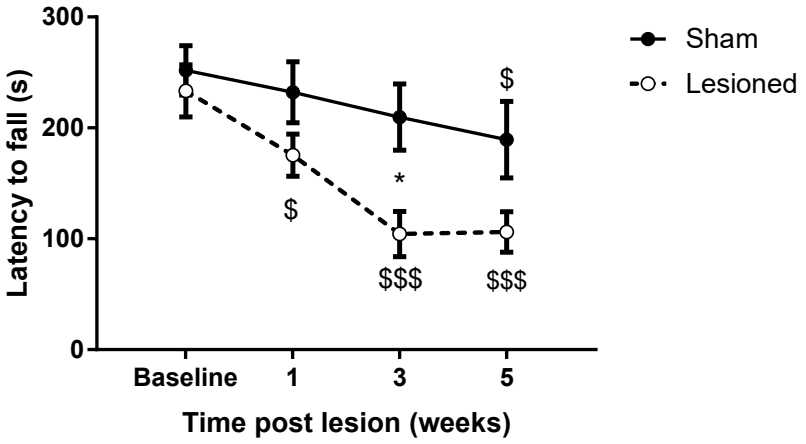

Figure 5.6: Average latency to fall (to a maximum of 300 seconds) from accelerating rotarod compared over time between bilaterally 6-OHDA-lesioned and sham animals. Data are mean ± S.E.M.. * = $p < 0.05$ to sham; $ = $p < 0.05$, $$$ = $p < 0.001$ compared to baseline in a repeated measures 2-way ANOVA with Sidak's post-test. n=10 per group.

5.4.2 Characterisation of pain behaviour

5.4.2.1 Hot plate

Development of hyperalgesia as a result of bilateral, partial 6-OHDA lesioning was quantified through use of the hot plate test. The latency to the display of a pain behaviour (as defined in the methods) was quantified at weeks 1 and 3 and compared with baseline values. The measured latencies did not differ significantly from the baseline values of 12.8±1 second for sham-lesioned animals and 12.1±1.2 seconds for 6-OHDA-lesioned animals (repeated measures 2-way ANOVA, Figure 5.7).

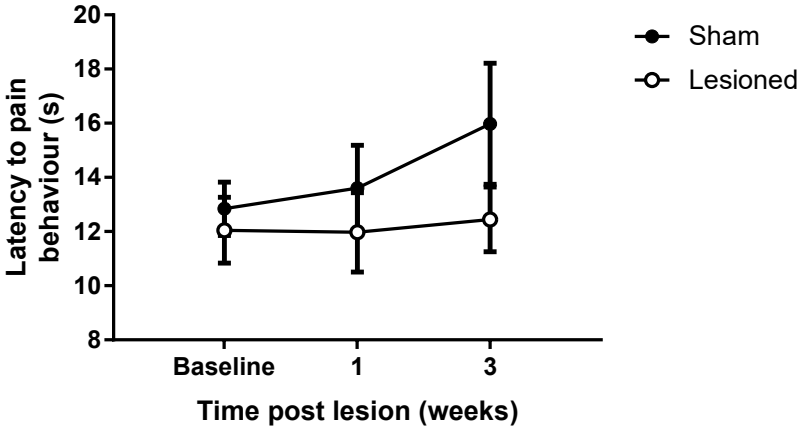

Figure 5.7: Average latency to pain response on hot plate (to a maximum of 40 seconds) compared over time between bilaterally 6-OHDA-lesioned and sham animals. Data are mean ± S.E.M.. n=10 per group.

5.4.3 Characterisation of anxiety behaviour

5.4.3.1 Open field arena

The open field test was performed as a dual measure of both motor performance and anxiety. Figure 5.8a shows the data representing the motor component of the test. At week 1, the average number of line crosses performed by sham rats was 157±20, while the 6-OHDA-lesioned rats performed 135±12. This was not significantly different ($p > 0.05$; Mann-Whitney test). At week 3, line crosses from both groups had fallen, again with no significant difference between groups.

Figure 5.8b shows the time spent in the centre of the arena, used to quantify anxiety in a brightly-lit and novel environment as detailed in the methods. At week 1, the sham-lesioned animals spent an average of 9.5±3.3 seconds in the centre, while the 6-OHDA-lesioned rats spent only 4.1 ± 1.1 seconds. This difference was not significant ($p >$0.05; Mann-Whitney test). Similarly to line-crosses, the time in the centre at week 3 for both groups was much reduced in comparison to week 1 values, with no significant difference between sham and lesioned animals' times.

Figure 5.8c quantifies rearing - another type of exploratory behaviour which may be used to interrogate anxiety in rodents. At week 1, the average count of rearing in sham-lesioned rats was 22±3, while the average in 6-OHDA-lesioned rats was 11 ± 2. This was a significant reduction ($p < 0.01$; Sidak's post-test following repeated measures 2-way ANOVA) of 50%. There was no effect of interaction in the ANOVA ($p = 0.25$), but main effects of lesion ($p = 0.01$) and time after lesion ($p = 0.0002$). By week 3, rearing behaviours in both groups were reduced and there was no significant difference remaining.

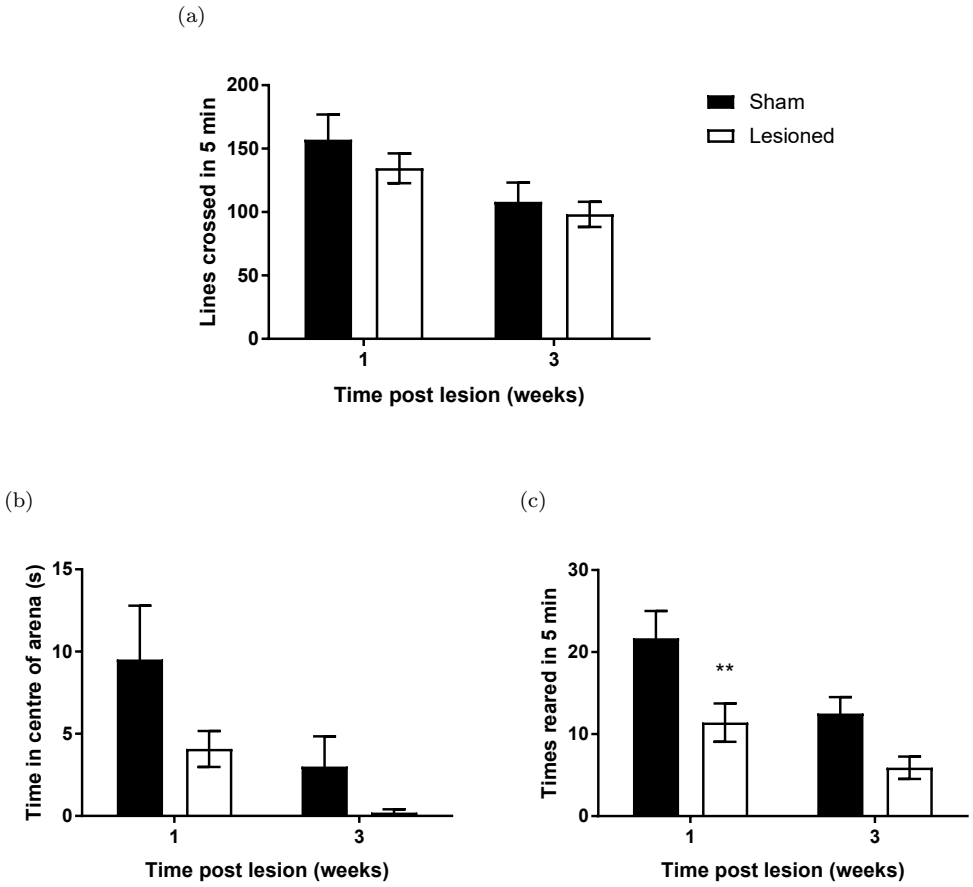

Figure 5.8: Open field free exploration. a) Number of lines crossed during exploration. b) Amount of time spent in the centre of the open field. c) Counts of rearing behaviour during exploration. ** = $p < 0.01$ compared to sham lesions; repeated measures 2-way ANOVA with Sidak's post-test. For all, data are mean ± S.E.M. and n=10 per group.

5.4.3.2 Marble burying test

There was no significant difference in the numbers of marbles buried to any depth between the two groups ($p > 0.05$; unpaired t-test and Mann-Whitney test, Figure 5.9).

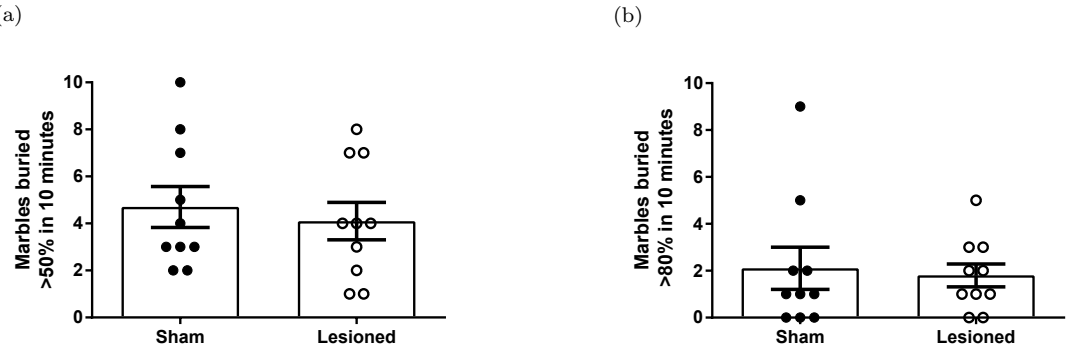

Figure 5.9: Graphs showing average numbers, and individual values for each animals, of marbles buried by sham and bilaterally, 6-OHDA-lesioned rats. For both, data are mean ± S.E.M. and n=10 per group.

5.4.3.3 Elevated plus maze

The elevated plus maze task was used as a well characterised test of anxiety in rats (Pellow et al. 1985). There was no significant difference in the total number of entries into any arm between the two groups ($p > 0.05$; unpaired t-test), 17±1 entries by sham animals compared with 16±1 entries by 6-OHDA-lesioned animals (Figure 5.10a). In contrast, 6-OHDA-lesioned animals performed significantly fewer open arm entries than sham-lesioned rats ($p < 0.05$; Unpaired t-test), 3±1 entries compared with 6±1 performed by sham animals (Figure 5.10b).

Lesioned animals also spent less time in the open arms of the plus maze than sham animals, with an average of 55.7±18 seconds compared to the sham average of 73.4±16 seconds, though this was not significant ($p > 0.05$; Unpaired t-test)(Figure 5.10c).

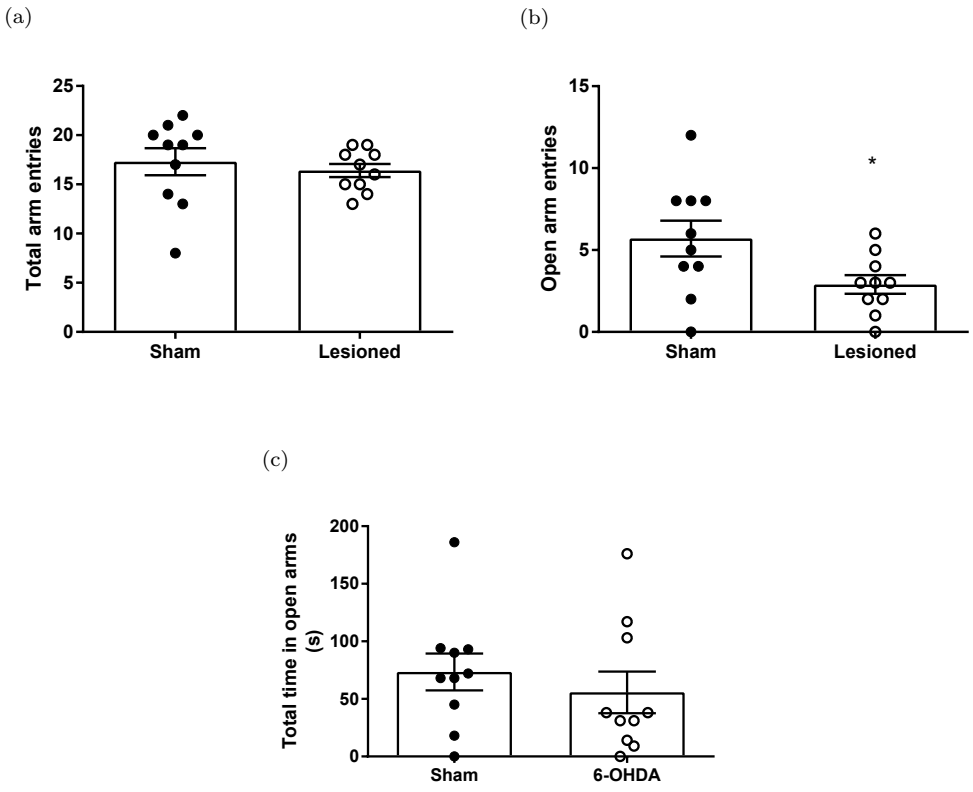

Figure 5.10: Exploration of the elevated plus maze by bilaterally, 6-OHDA-lesioned animals or shams, 3 weeks post-lesion. a) Total number of entries into any arm (open or closed) over the 5 minute exploration period. b) Total number of entries into open arms only. c) Average time spent in open arms of plus maze (maximum of 300s). * = $p < 0.05$; unpaired t-test. For all, data are mean ± S.E.M. and n=10 per group.

5.4.4 Characterisation of anhedonic behaviour

5.4.4.1 Sucrose preference test

The sucrose preference test was carried out in order to assess anhedonia in lesioned and sham-lesioned rats. Training periods are included in the graphs in order to display comparabale intake of normal drinking water between the two groups. In this test, at week 2 post-lesion, lesioned animals consumed significantly more sucrose solution than did sham animals in a 48 hour testing period, with shams consuming 97.0±3.7ml and lesioned animals consuming 117.4±7.7ml (Figure 5.11a). A repeated measures 2-way ANOVA revealed a main effect of lesioning ($p = 0.03$), an effect of drinking solution type ($p < 0.0001$) and interaction between the variables ($p = 0.005$).

During the week 2 48 test period, consumption of water dropped considerably compared to intake in the training period. Consumption of sucrose was considerably higher than water intake in both groups.

In week 4 there was no significant difference between sham animals and lesioned animals in preference for sucrose solution, with sham animals consuming 80.9±5ml over 48 hours and 6-OHDA animals consuming 84.2±7.3ml (Figure 5.11b). A similar trend in consumption of sucrose and water over the 48 hour test period was seen at week 4 as at week 2, with consumption of water being much lower for both groups than in the training period, and consumption of sucrose being much higher. However, consumption of sucrose solution was lower than at week 2. The 2-way ANOVA revealed no effect of interaction ($p = 0.8$) and a main effect of drinking solution type ($p < 0.0001$) but no effect of lesioning ($p = 0.8$).

(a) Week 2 post lesion

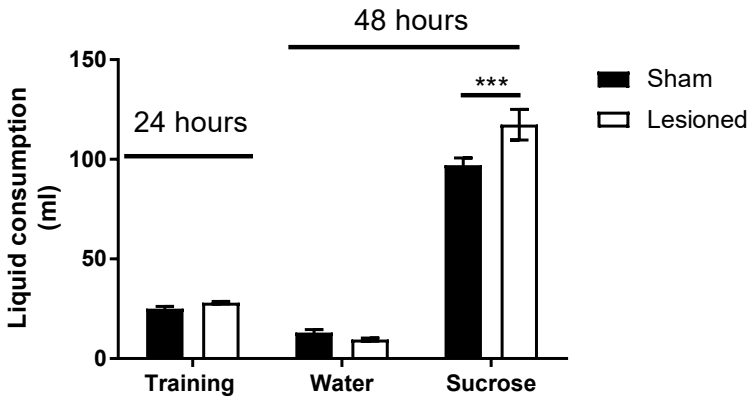

(b) Week 4 post lesion

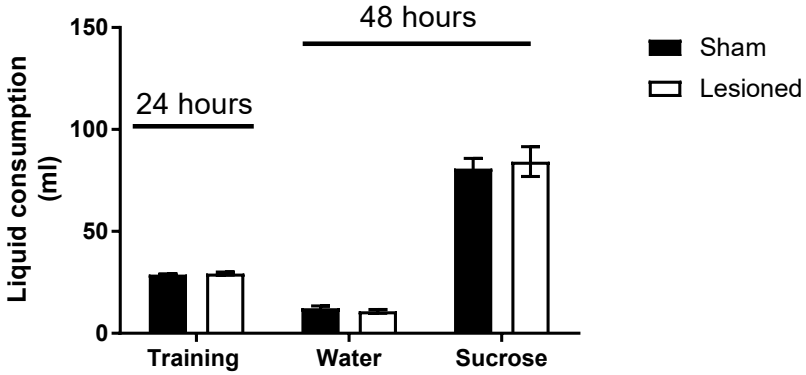

Figure 5.11: Graphs showing average consumption of water and sucrose during 24hr training period and subsequent 48hr test period by sham and bilaterally, 6-OHDA-lesioned rats. For both, individual data points are plotted and line shows mean whle bars show S.E.M.. n=10 per group (refer to methods for more information on groupings). *** = $p < 0.001$ 6-OHDA compared with sham; 2-way ANOVA with Sidak's post-test.

5.4.5 Characterisation of cognition

5.4.5.1 Social recognition test

The social recognition test was used here as a test of social memory. At week 1, lesioned animals spent significantly less time investigating the juveniles than did the shams (Figure 5.12a). At baseline, the 6-OHDA-lesioned rats spent an average of 20% less time (159±10 seconds, compared with 200±12 seconds) investigating the juvenile than the shams did, though this difference was not significant. Time spent investigating was significantly reduced in both groups compared to baseline at the 30 minute reintroduction to 83±11 seconds in the lesioned animals and 142±17 seconds in the shams ($p < 0.05$ and $p < 0.001$ respectively). Lesioned animals spent significantly less time investigating the juvenile than shams at this timepoint ($p < 0.01$). At the final 24 hour time point, lesioned animals continued to show significantly less investigatory behaviour than shams (63% of average sham investigation, $p < 0.001$), though the time spent investigating was no longer significantly lower than at the first introduction. There was no effect of interaction in the repeated measures 2-way ANOVA ($p = 0.6$), but a main effect of lesion and time point of presentation of the juvenile ($p < 0.0001$).

At 3 weeks post lesion, lesioned animals interacted less with the juvenile than shams did at every time point including baseline (Figure 5.12b). At baseline, lesioned animals spent significantly less time with the juveniles than did the shams, spending an average of 152.8±11.7s, while shams spent 215.7±16.1s ($p < 0.05$). There was no significant difference between lesioned and sham animals at either the 30 minute or 24 hour reintroduction. However, both groups spent significantly less time investigating the juvenile at these reintroductions than at the first presentation. There was a main effect of lesion ($p = 0.01$) and time of presentation of the juvenile ($p < 0.0001$), but no interaction between variables ($p = 0.6$) in the repeated measures 2-way ANOVA.

(a) Week 1 post lesion

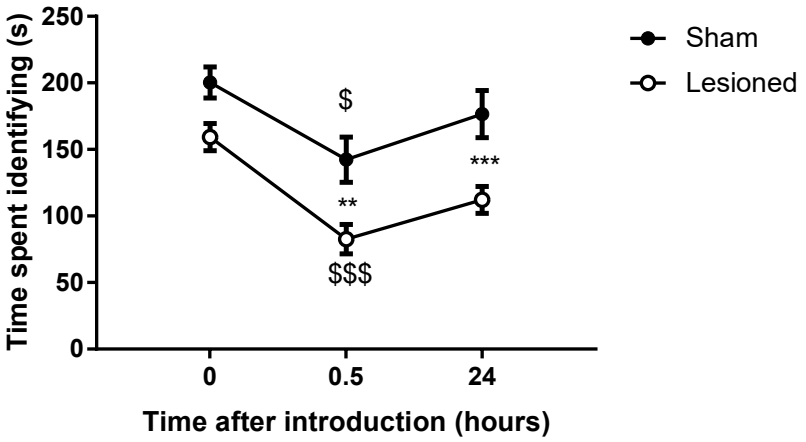

(b) Week 3 post lesion

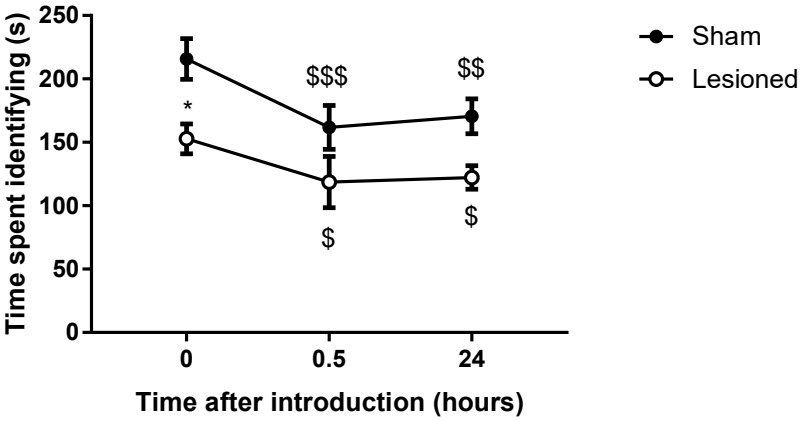

Figure 5.12: Graphs showing average time spent investigating an unknown juvenile rat by bilaterally lesioned or sham lesioned rats in the social recognition test on first presentation and subsequent reintroductions. \$ = $p < 0.05$, \$\$ = $p < 0.01$, \$\$\$ = $p < 0.001$ against relevant baseline and * = $p < 0.05$, ** = $p < 0.01$ and *** = $p < 0.001$ against sham control in 2-way ANOVA with Sidak's post-test. For both, data are mean ± S.E.M. and n=10 per group.

5.4.5.2 Morris water maze

The Morris water maze was used here as a test of spatial learning and memory which can be controlled for motor impairment. Figure 5.13a shows that animals from both groups learned the location of the platform at a similar rate. On day 1, sham animals took 46.7±5.7s to locate the platform. In general, the trial duration reduced with each exposure on consecutive days, falling to 9.3±1.6s on day 5. This learning trend was not significantly different in lesioned animals. The 2-way ANOVA revealed no main effect of lesioning ($p = 0.6$), a main effect of training day ($p < 0.0001$) and no interaction between variables ($p = 0.8$).

Data in Figure 5.13b corresponds with this finding, and shows no significant difference between sham and lesioned animals in the distance swum in order to reach the platform. Distance to platform fell at a similar rate to the latency to platform (or trial duration), predicting that the velocity of the two groups on any given day would be similar. The 2-way ANOVA revealed no main effect of lesioning ($p = 0.9$), a main effect of training day ($p < 0.0001$) and no interaction between variables ($p = 0.9$).

Figure 5.13c shows that there was no significant difference in the average velocity of 6-OHDA-lesioned animals compared with shams at any time point ($p > 0.05$; 2-way ANOVA), though the velocities of both groups varied over the 5 days of training. The highest average velocity of sham rats was 35.7±1.0cm/s on day 4, and 32.9±0.8cm/s for lesioned rats on day 1, while the lowest velocity for both groups was on day 5, with sham animals achieving 24.3±1.2cm/s and lesioned animals 19.6±1cm/s. The 2-way ANOVA revealed no main effect of lesioning ($p = 0.1$), a main effect of training day ($p < 0.0001$) and no interaction between variables ($p = 0.1$).

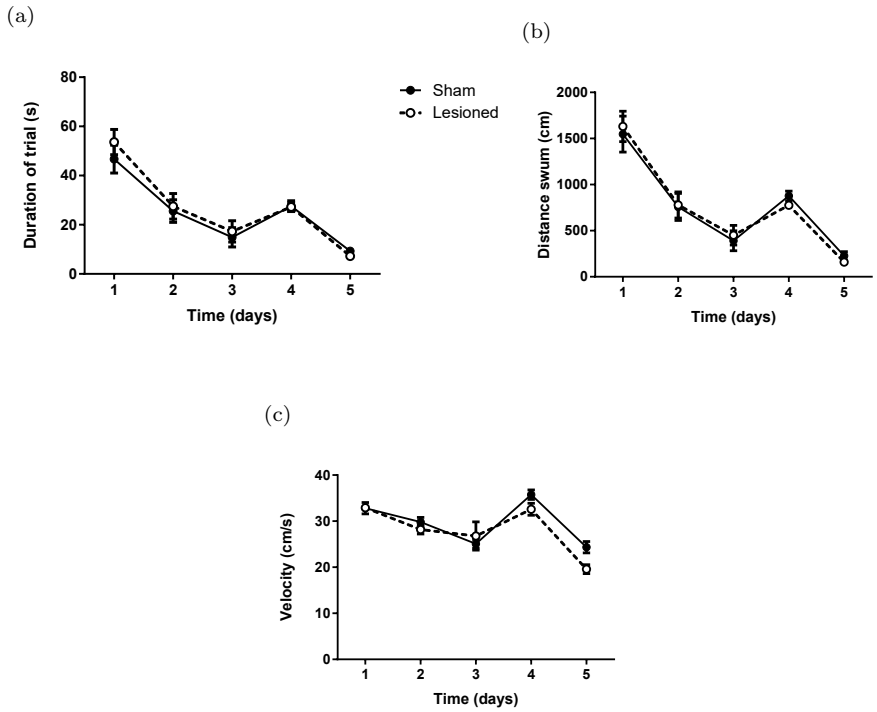

Figure 5.13: Progression of learning by bilaterally, 6-OHDA-lesioned rats and shams during consecutive training sessions in the Morris water maze. a) Average latency to platform during training sessions (maximum 90 seconds). b) Average distance to reach platform in training sessions. c) Average velocity of swimming during training sessions. For all, data are mean±S.E.M. and n=10 per group.

The memory component of the Morris water maze task was tested by the probe trial (Figure 5.14), which took place 12 hours after the last training session. Lesioned animals did not spend a significantly different length of time in the correct quadrant compared to shams ($p > 0.05$; Unpaired t-test) (Figure5.14a). Lesioned animals were also not significantly slower to enter the quadrant zone than shams ($p > 0.05$; unpaired t-test, Figure5.14b).

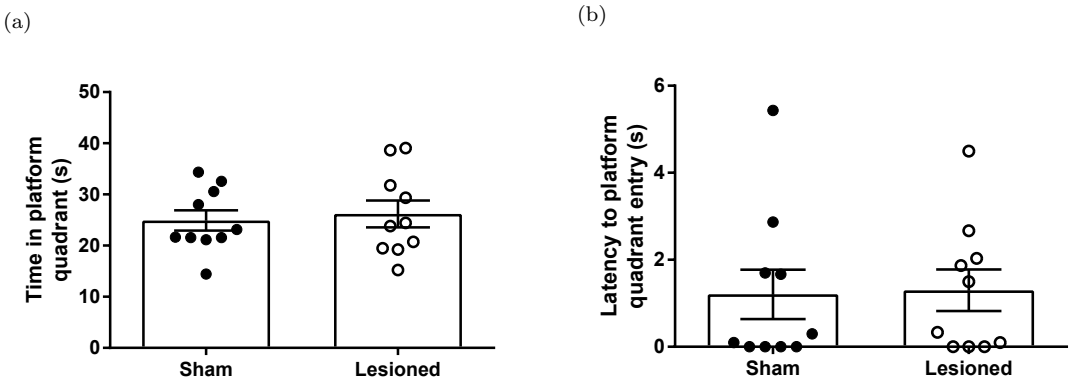

Figure 5.14: Data collected during the 90 second Morris water maze probe trial on 6-OHDA-lesioned animals or shams which had learned the task over the previous 5 days. a) The time spent by each animal in the quadrant which previously contained the platform. b) The latency of each animal to the platform-containing quadrant. Data are mean ± S.E.M.. n=10 per group.

5.4.6 Histological characterisation of lesion

In order to confirm the presence of a bilateral nigrostriatal lesion in 6-OHDA rats, and the absence in sham rats, TH expression was measured in the nigrostriatal tract. Representative images are shown in Figure 5.15a and 5.15b. A clear loss of 3,3'-diaminobenzidine (DAB) staining of TH can be seen in both images in the striatum, medial forebrain bundle (MFB) and SNc, comprising the entire nigrostriatal tract.

In the striatum, 6-OHDA-lesioned rats had a significant 44% reduction in TH compared to shams in the left striatum, and a significant 50% reduction in TH in the right hemisphere. In Figure 5.15c these data are displayed as the overall average TH densitometry for the combined left and right striata of each individual. Again, a significant lesion was confirmed ($p < 0.001$; unpaired t-test).

There was also significant TH-positive cell loss in the SNc, with an average of 15 ± 3 cells per sagittal section in the left SNc of 6-OHDA animals and 40 ± 5 cells per section in the left SNc of shams (a 62% reduction). In the right SNc, 6-OHDA rats had an average of 11 ± 3 cells remaining and shams had 37 ± 3 (a 70% reduction). The presentation in Figure 5.15d combines hemispheres to give a significant overall lesion ($p < 0.001$; Mann-Whitney test). Overall n-numbers are reduced in SNc cell counts due to a lack of suitable sections for analysis.

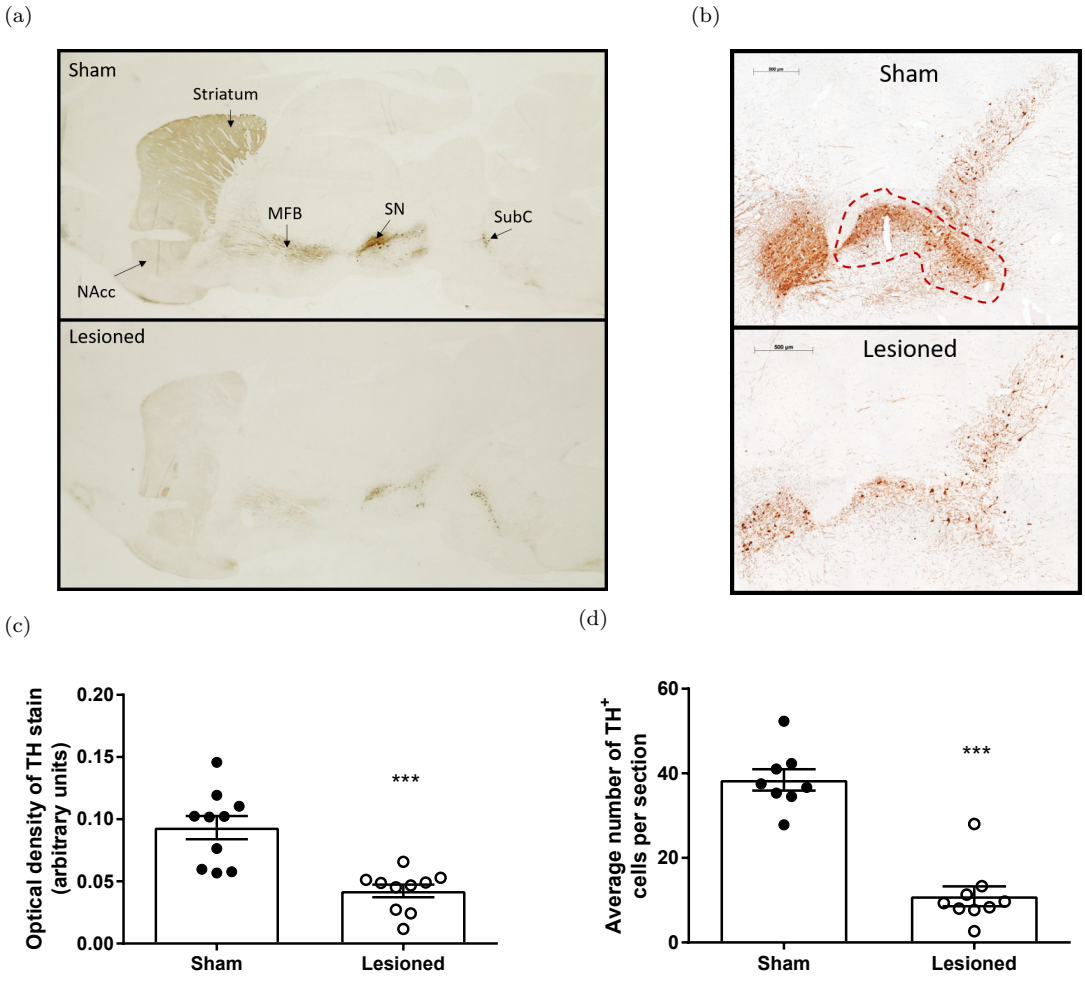

Figure 5.15: Data from TH staining of the A9 nigrostriatal pathway. a) Representative images of TH staining in full sagittal sections at approximately 1.9mm lateral from the midline (Paxinos & Watson 1986). NAcc, nucleus accumbens; MFB, medial forebrain bundle; SN, substantia nigra; SubC, subcoeruleus. b) A view of the midbrain dopaminergic cell groups with the SNc circled in red. c) Densitometry of TH stain in striatum. d) Average number of TH-positive cells in the SNc. Graphs give an average of left and right hemispheres for each animal. Data are displayed as mean ± S.E.M.. n = 10 per group for striatum and n = 8-9 per group for SNc. *** = $p < 0.001$; upaired t-test in c) and Mann-Whitney test in d).

5.4.7 Histological exploration of behavioural phenotype

Alongside the A9 dopaminergic pathway (the nigrostriatal pathway), the A10 dopaminergic pathway projects from the midbrain VTA to the NAc, also known as the ventral striatum, and also to the mPFC. Due to the proximity of the A10 pathway to the lesioned areas in the striatum, and its involvement in reward processing (Richardson & Gratton 1996), TH staining in this region was used to quantify any changes which may describe behavioural alterations in this study such as those seen in sucrose preference.

Figure 5.16a shows representative images of the midbrain in sagittal sections, stained for TH with the VTA highlighted. There is an obvious reduction in staining in lesioned animals compared to sham animals. Representative images in Figure 5.16b show much less evidence of lesioning on TH expression in the NAc.

There was a significant loss of TH-positive cells in the VTA, where sham animals had an average of 49±5 cells per section and 6-OHDA animals had a 47% reduction to 26±5 cells per section ($p < 0.05$, Figure 5.16c). This loss of cell bodies in the VTA did not have a significant impact on terminals in the NAc however, where TH-staining in lesioned animals was not reduced compared to shams (Figure 5.16d).

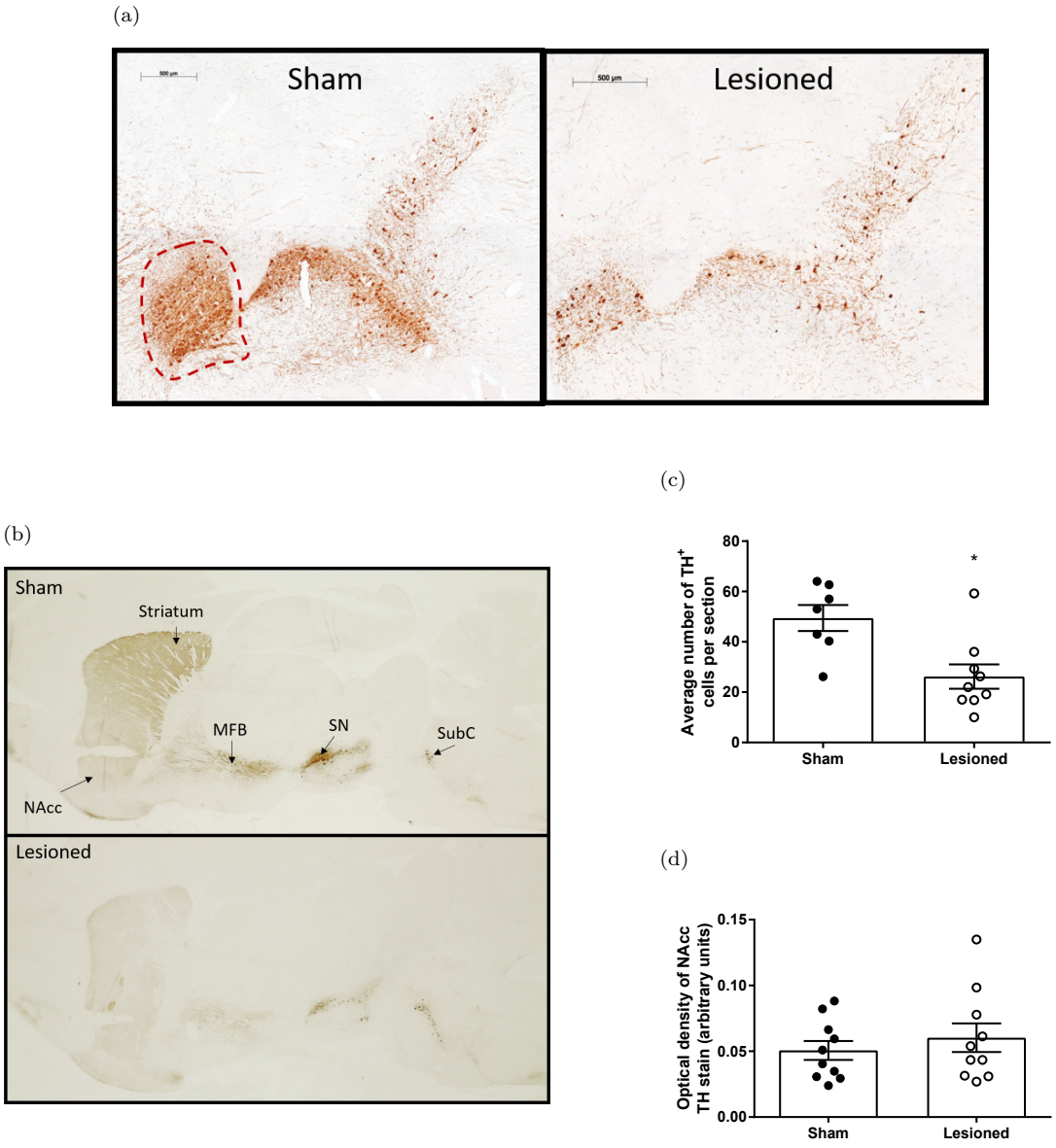

Figure 5.16: Data from TH staining of the A10 dopaminergic pathway. a) Representative images of the midbrain dopaminergic nuclei with the VTA circled in red. b) Representative images of sagittal sections showing the NAc stained for TH. c) Average number of cells remaining in VTA d) Optical density of TH stain in NAc. Graphs give an average of left and right hemispheres for each animal. Data are displayed as mean ± S.E.M.. n = 7-10 per group for all. * = $p < 0.05$; Mann-Whitney test.

The mPFC was also studied as an output region of the VTA. Images in 5.17a show TH staining in a few, dispersed fibres in the mPFC. There was a 55% reduction in TH terminals in the mPFC, though this was not significant due to high variation (Figure 5.17b). Overall *n*-umbers are reduced due to a lack of sections suitable for analysis.

(a)

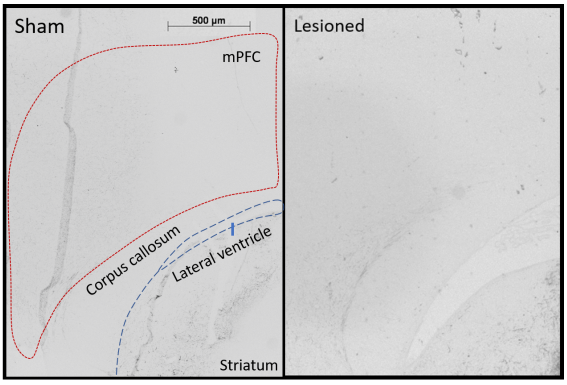

(b)

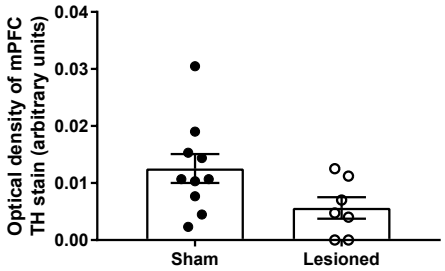

Figure 5.17: Data from TH staining of the A10 dopaminergic pathway mPFC. a) Representative images of the mPFC with neighbouring structures labelled in order to aid definition. b) Optical density of TH stain in the mPFC. Graph gives an average of left and right hemispheres for each animal. Data are displayed as mean ± S.E.M.. n = 7-10 per group.

The final major midbrain dopaminergic structure is the RRF, or the A8 dopaminergic cell-group (Figure 5.18a). In this study, the RRF suffered losses comparable to those in the SNc and the VTA, with a significant ($p = 0.006$ in Mann-Whitney test) 40% reduction in TH-positive cell bodies in lesioned animals compared to shams (12±2 cells per section in lesioned rats compared with 20±2 cells per section in shams, Figure 5.18b). Numbers in each group are reduced as a result of a lack of suitable sections for analysis.

Deutch et al. (1988) found, through the use of anterograde tracing, that the RRF projects to a number of regions including the striatum, NAc, olfactory tubercles, amygdala and areas of the hippocampus. TH staining of the basolateral amygdala (BLA) was examined as part of this study but no stain was present. Central amygdaloid nuclei were unfortunately unavailable for analysis due to the limitations of sectioning. As no cognitive impairment was recorded (Figure 5.14a), the hippocampus was not examined for TH-positive cell loss.

(a)

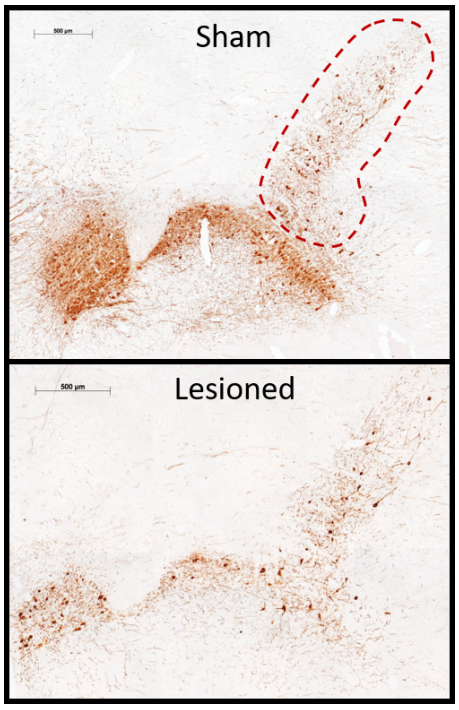

(b)

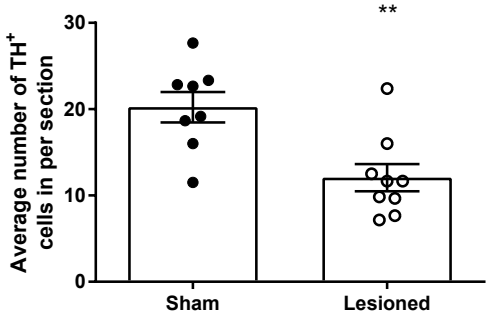

Figure 5.18: Data from the TH staining of the A8 dopaminergic pathway. a) Representative images of the midbrain dopaminergic nuclei with the RRF circled in red. b) Average number of cells remaining in RRF per section. Data are displayed as mean ± S.E.M.. n = 8-9 per group for all. ** = $p < 0.01$; Mann-Whitney test.

The locus coeruleus and subcoeruleus are part of the reticular activating system, with key functions in sleep and wakefulness and the control of stress via inputs to the basolateral amygdala, amongst others (McCall et al. 2017).

The locus coeruleus and subcoeruleus are noradrenergic nuclei and, as such, contain TH. Here, we found that bilateral, partial lesions of the nigrostriatal pathway did not affect the number of cells in the locus coeruleus (Figure 5.19b) or the subcoeruleus (Figure 5.19c). In the locus coeruleus there were an average of 44±5 cells per section in lesioned animals and 46±3 in sham animals. In the sections of subcoeruleus there was an average of 11±1 cells in lesioned animals and 9±2 in sham animals. Further exploration of noradrenergic pathways in the brain and spinal cord was not undertaken due to the lack of difference in locus coeruleus or subcoeruleus cell numbers between 6-OHDA and sham animals. Numbers in each group are reduced as a result of a lack of suitable sections.

(a)

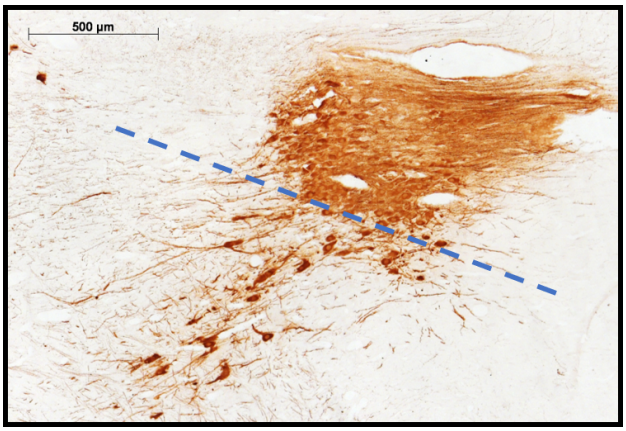

(b)

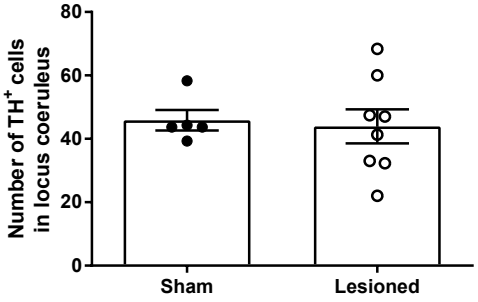

(c)

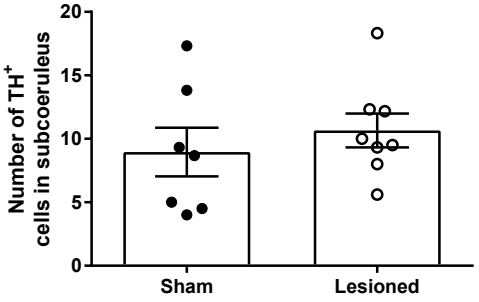

Figure 5.19: Data from TH staining of the locus coeruleus and subcoeruleus. a) Representative image of the locus coeruleus above the dashed line, with the subcoeruleus below the dashed line. b) Average number of cells in locus coeruleus. c) Average number of cells in subcoeruleus. Graphs give an average of left and right hemispheres for each animal. Data are displayed as mean ± S.E.M.. n = 5-10 per group for both.

5.5 Discussion

This study sought to interrogate the bilateral partial lesion model of Parkinson's in rats, and establish its future suitability for examining the effects of compounds on both the motor and non-motor symptoms of Parkinson's.

5.5.1 Confirmation of lesion

Using TH immunohisttochemistry, a bilateral, partial lesion was confirmed in lesioned animals with no sign of TH loss in the striatum of sham animals. The 47% reduction in striatal TH-positive staining in the striatum and 66% reduction in the SNc seen here are difficult to compare to other studies presented in this thesis or in the literature as they appear to utilize coronal sectioning without exception, as opposed to the sagittal sections used here. This means that there cannot be a direct comparison of lesion size by cell count or densitometry since the structures quantified are viewed from a different axis and so, subsequently, each field of view will present a different numbers of cells per section. This makes it likely that the seemingly larger lesion achieved here is a misleading effect of observing the lesion sagittallly, rather than coronally.

In this study, sagittal sections were used to enable the visualisation of a number of structures (or one whole pathway) in any one section of brain tissue. As a bilateral, rather than unilateral lesion was used, it was not considered to be necessary to compare lateral stuctures at the same cordo-rostral level as was the case in previous studies presented in this thesis. However, inexperience with viewing familiar structures from this alternative axis made obtaining sections representing lateral structures at the same medio-lateral level challenging. The effects of this can be seen in uneven n numbers for histology and in higher variability than expected.

5.5.1.1 Motor deficit

Tests used to assess motor deficit in the present study necessarily differed from those used in previous studies discussed in this thesis due to the nature of the bilateral lesion. The cylinder and stepping tests used previously compare the performance of one of the animal's paws to the other in an effort to assess a unilateral reduction in performance. Similarly, the amphetamine-induced rotations test examines the asymmetry of striatal dopamine via motor output of the contralateral and ipsilateral paws. In the present study, new motor tests which do not rely on asymmetry of dopamine or motor performance were utilised.

The accelerating rotarod was a reliable test of motor performance in bilaterally lesioned rats, easily differentiating lesioned animals from sham. Based on rotarod performance, the lesion seemed to grow in size over the initial two weeks post-surgery, reaching a stable maximum by three weeks post-lesion. This correlates well with the data obtained by Sauer & Oertel (1994), who used a similar set of co-ordinates for their lesion which reached a maximum at 2 weeks post-lesion. The information on motor disability obtained through application of the rotarod test is valuable in assessing the time course of lesion development in these bilaterally-lesioned animals. The histology in this study is performed at only one time point, at 6 weeks post-lesion, but the stabilisation of the rotarod motor phenotype provides a hint that the lesion size may reach its maximum between 1 and 3 weeks post-lesion. This suggests that the bilateral lesion may take longer to mature than its unilateral counterpart, characterised in Chapters 2 and 4, which appears full and stable by 7 days.

Here, we also noted that sham-lesioned animals also show a slight, but still significant, decline in performance over time (between baseline and week 5 only). This may be due to normal ageing of the animals over the 5-week period of the study. Shoji et al. (2016) show that performance on the accelerating rotarod test is negatively correlated with age, even showing a significant decline in latency to fall between 2-3 month and 4-5 month-old C57/Bl6J mice. McFadyen et al. (2003) also show that, in some strains of mouse, body length and body weight are significantly negatively correlated with rotarod performance. Due to the age of the rats when lesioning surgery was performed, weight gain over the course of the study is likely to have been a factor in the decline of the perfomance of the sham group over time. Despite this, rotarod seems likely to be a reliable test of motor function in bilaterally-lesion animals and is able to differentiate animals based on lesion size (Monville et al. 2006), making it suitable for examining functional improvements following symptomatic treatments.

5.5.2 Characterisation of pain behaviour

5.5.2.1 Hot plate

In this study, the hot plate did not provide a means to differentiate lesioned and sham animals using thermal hyperalgesia, though by week 3, sham animals were starting to show an increased latency to pain response. This may be due to the fact that animals were not habituated to the apparatus at room temperature before exposure at a noxious heat. Initially low thermal thresholds may have resulted from the animal feeling stress at being placed in a new environment, compounded by the heat sensation. In a future study, it would be interesting to see if habituation

to the hot plate prior to testing increased the baseline latencies to pain behaviours.

The onset of thermal hyperalgesia, if it occurs at all in PD, is likely to be later onset than many other non-motor symptoms, with patients only being significantly affected by this type of pain after > 10 years post-diagnosis, or at a Unified Parkinson's Disease Rating Scale score of > 30 (Mylius et al. 2011). The hot plate therefore may not have been the most appropriate test of hyperalgesia for use in this model. A test of mechanical, rather than thermal hyperalgesia, such as the Von Frey test, could have been used since mechanical hyperalgesia is much more common amongst PD patients (Ha & Jankovic 2012). However, other groups have found evidence that both fully and partially 6-OHDA lesioned rats may develop both mechanical and thermal hyperalgesia (da Rocha et al. 2013, Wang et al. 2017). da Rocha et al. (2013) used 55°C as the cutoff temperature for their test of thermal hyperalgesia. This higher temperature may have been more effective at differentiating animals with thermal hyperalgesia than the 52°C used here. In their study, Wang et al. (2017) use a heat source derived from light, and describe the stimulus in terms of intensity rather than °C, which makes their methodology difficult to compare to this study utilising a hot plate.

5.5.3 Characterisation of anxiety behaviour

Previous studies have highlighted the importance of using multiple tests to measure anxiety in rodents (Clément et al. 2009), as there is no one simple test of anxiety which has been shown to measure all aspects of this complex phenomenon. Sudakov et al. (2013) showed that there was no correlation between anxiety parameters in the open field arena, the elevated plus maze and the Vogel conflict test - three widely-used measures on anxiety. In the study discussed here, there was no significant difference between lesioned and sham animals in the length of time spent in the centre of the arena but, as evinced by the literature, it cannot be concluded from this alone that there was no difference in anxiety. Indeed, the data from the elevated plus maze test, discussed below, supports an anxiogenic effect of 6-OHDA lesioning.

5.5.3.1 Open field arena

The open field test was able to differentiate lesioned animals from sham only in rearing behaviour, and not horizontal exploratory behaviour (measured here using line crossings as a proxy for distance travelled) or time spent in the centre of the arena. Willard et al. (2015) use a multi-injection mouse 6-OHDA model to show that distance travelled in the open field is not a very sensitive mea-

sure of striatal dopamine loss, with significant deficits occurring only at 75% reduction. They also show that rearing in mice is more linearly related to dopamine depletion, especially in the dorsolateral striatum. Though they do not discuss whether the alterations in exploratory behaviour are purely due to motor deficit, or whether they believe that there is an emotional component to the rearing behaviour, the findings of Willard et al. (2015) perfectly describe the open field behaviour observed in this study, where the average striatal lesion size was 55%.

Bai et al. (2017) use the same outcome of reduced rearing behaviour in the open field as a measure of depression or anhedonia in rat stress models. They found that vertical activity of the rats was best correlated with increased D1 and decreased D2-4 dopamine receptor and DAT expression levels in the dorsal striatum, all changes induced by stressors rather than lesions. This alternative interpretation of rearing behaviour shows its potential to be impacted by a variety of interventions and, consequently, the difficulty of fully interpreting its meaning. In this study, reduced rearing behaviour may therefore reflect 'depression', anxiety or motor deficit - or components of all three.

At week 3, both groups of animals performed fewer behaviours of all kinds in the open field, though the relative difference between groups was maintained. This reduction in behaviour with repetition of the test could be explained by the observation of Bolivar et al. (2000) that some strains of mouse habituate quickly on re-exposure to the same open field layout, and that this habituation presents as a reduction in activity. If used in a future study, therefore, more attempt must be made to differentiate open field exposures. This could be achieved by retesting in a different room, using different odours to mask the same setting on retest or, as in Bolivar et al. (2000), altering the texture of the open field floor panel.

5.5.3.2 Marble burying test

The marble burying test was not able to differentiate lesioned and sham animals. Despite initially being characterised as a test of novelty-induced anxiety and used to interrogate the effects of anxiolytic compounds (Jimenez-Gomez et al. 2011), there is some question of what behaviour the marble burying test actually measures. Thomas et al. (2009) suggests that marble burying behaviour is a correlate of genetic background in mice and is more suitable as a measure of repetitive digging behaviour. They find that neither multiple exposure to the marbles nor removal of the marbles alters digging behaviour in strains which are predisposed to burying marbles. This finding suggests that the marble burying test is not a reliable test of anxiety, though may be correlated with anxiolytic effects of some, but not all, compounds.

5.5.3.3 Elevated plus maze

In the elevated plus maze, lesioned animals performed significantly fewer open-arm entries than did sham animals. A possible effect of motor deficit on the exploration of the lesioned animals was measured by summing the total number of entries into any zone of the plus maze and, in this measure, lesioned animals did not differ from shams. It follows that, for the purposes of this test, it can be accepted that any difference in performance was not due to motor impairment as a result of the lesion and, instead, due to a different anxiety state. High variation prevented the emergence of a significant reduction in time spent in the open arms by the lesioned animals, though a trend in this direction is evident.

Chen et al. (2011) find that, after the application of a similarly sized and placed bilateral 6-OHDA lesion, the firing rate of neurons in the BLA is reduced and they propose this as the mechanism by which a nigrostriatal, and mesolimbic, lesion can cause anxiety. The BLA is known to be innervated by dopaminergic projections from the VTA, and fear behaviour can be increased or decreased through pharmacological manipulation of this pathway alone (de Oliveira et al. 2011). In addition, the VTA is likely to signal to the BLA via the mPFC. Wang et al. (2009) show that a full lesion of the nigrostriatal pathway causes an increase in the activity excitatory glutamatergic outputs from the mPFC and shift in the signalling pattern to burst-firing. This increased excitatory output activates gamma-aminobutyric acid (GABA)ergic interneurons in the BLA, thus decreasing the firing rate of the BLA (Hübner et al. 2014). This is summarised in Figure 5.20.

Here, there was no TH staining seen in the BLA, but a non-significant reduction in TH-positive fibres in the mPFC and a significant reduction in cell numbers in the VTA. Based on the evidence above, this may suggest that a reduction in dopaminergic innervation of the mPFC is sufficient to cause a reduction in activity in the BLA via increased firing of GABAergic interneurons without a reduction in TH-positive terminals from the VTA in the BLA. This proposed reduction of activity may well underlie the anxiety responses measured in the elevated plus maze test, however further studies are warranted to fully explore this theory.

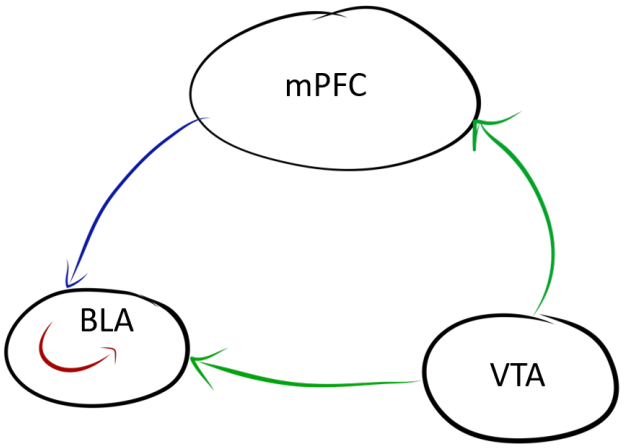

Figure 5.20: Diagram depicting the hypothesised anxiety pathways linking the VTA, mPFC and BLA. The green arrows represent dopaminergic signalling, the red arrow represents GABA-ergic signalling and the blue arrow represents glutamatergic signalling.

5.5.4 Characterisation of anhedonic behaviour

5.5.4.1 Sucrose preference test

The expected outcome of the sucrose preference test is that animals displaying anhedonic or depressive behaviours will consume less sucrose solution than 'normal' /healthy rats. This has been widely shown in studies examining a variety of conditions, including in 6-OHDA-lesioned animals (Tadaiesky et al. 2008). Unexpectedly, the sucrose preference test used here distinguished lesioned and sham animals at week 2 through lesioned animals having a significantly higher sucrose intake than the sham group. This finding demonstrates that anhedonia and depression are more complex than is possible to examine through the use of a reductionist test such as sucrose preference.

Indeed, Bai et al. (2017) describe depression as a multi-component disorder, where not all subjects with depression may co-present with anhedonia; different methods of induction of a depressive state can result in different depressive phenotypes and highly heterogeneous regulation of dopamine receptors and transporters throughout the mesocorticolimbic pathway. The study correlated sucrose preference with increased expression of D3, D5, and DAT protein in the VTA, and with reduced expression of D2-4, and DAT in the NAc (Bai et al. 2017).

In the same study, Bai et al. (2017) used modified receptor expression and behavioural test correlations to associate the trait of anhedonia with dysfunction of the VTA-NAc pathway; passive coping behavior with dysfunction of the VTA to mPFC and amygdala; and reduced exploratory interest with the VTA to mPFC and striatum. Given that, in the present study, no reduction in

TH was measured in the NAc, this may explain why the sucrose preference test for anhedonia did not reveal a decrease in sucrose consumption while, with a more ventral lesion affecting the NAc, the study by Tadaiesky et al. (2008) did. However, with this evidence, the certain involvement of the VTA and the striatum, and the hints of mPFC terminal reductions can be used to explain the appearance of reduced exploratory behaviour (in the elevated plus maze) and reduced social interest (in the social recognition test).

Although these previous findings serve as an explanation for the lack of decreased sucrose preference seen in this study, the significant increase in sucrose intake has yet to be addressed. Waraczynski & Perkins (2000) show that a temporary inactivation of the RRF causes an increase in the frequency of MFB self-stimulation required for a rewarding effect in animals with a 6-OHDA full, unilateral lesion.

If sucrose consumption may be similarly taken as a rewarding behaviour, it stands to reason that a RRF lesion, such as that which was found in the 6-OHDA-lesioned animals in the present study, may similarly increase sucrose preference in the same way that MFB self-stimulation was increased. The increase in sucrose preference seen in the present study may therefore have resulted from lesioned animals seeking to 'compensate' for the reduced reward pathway activity by seeking reward (i.e. sucrose solution) to a greater extent. This has been shown to be true anecdotally in PD patients experiencing increased craving for sugary foods [1].

It may be taken from this evidence that, in future studies undertaking to characterise the depressive or anhedonic phentoype of the bilateral, partial lesion model, multiple tests should be used in order to gain a full understanding of the phenotype. This is similar to the conclusion in the case of the characterisation of anxiety in the same cohort. In this case, any additional tests would need to be chosen carefully in order to take into account potential motor and cognitive deficits. The forced swim test (Porsolt et al. 1978) could be considered a reasonable option as it requires no real learning period and motor swimming ability has been tested (and found to be intact) in the water maze. However, the forced swim test has been much criticised in its own right as a valid test of depression or despair (Molendijk & de Kloet 2015).

[1] https://healthunlocked.com/parkinsonsmovement/posts/699879/have-your-sweet-cravings-gone-through-the-roof-like-mine

5.5.5 Characterisation of cognition

5.5.5.1 Social Recognition Test

At week 1 in the social recognition test, both sham and lesion groups spent significantly less time investigating the juvenile 30 minutes post-introduction, showing their recognition of the animal. Interestingly, lesioned animals spent significantly less time at this time point investigating than did the sham animals. At 24 hours post-introduction, the time spent investigating the juvenile was not significantly less than at the introduction itself. This demonstrates that by 24 hours, both sham and lesion groups have forgotten the juvenile sufficiently to spend a similar amount of time investigating. At this time point too, the lesioned group spent significantly less time investigating than the sham animals. These reduced interactions by the lesioned animals are not indicative of changes in social memory - as they follow the same pattern as the sham group. Rather, they may be indicative of reduced social reward upon interaction. Gunaydin et al. (2014) investigated the mechanism of social reward through optogenetic control of both VTA and NAc in mice, and showed that increased stimulation of either of these areas predicts increased social interaction, and similarly that social interaction predicts increased activity of the pathway. As we have shown that the lesioned animals used in this study have a significant VTA lesion, this may provide the evidence to explain the reduced drive for social interaction apparent in the lesioned rats.

By week 3 post-lesion, both groups spent less time interacting with the juvenile on re-introduction than at the initial introduction. This again shows no social memory deficit in the lesioned animals, though the reduced desire to interact is evident at all time points and is significant at the introduction.

The reduced interaction at 24 hours post-introduction in week 3 is contrary to one study which suggests that social recognition is a short-term memory which may only be observed for $\leq$ 2hours following the initial introduction (Ferguson et al. 2002), but in agreement with others which suggest a longer duration of social memory of up to 1 week (Kogan et al. 2000). The difference in methodology between these studies is likely to be key to the difference in their findings. If rodents are group-housed, as the mice are in Kogan et al. (2000), they have a much longer duration of social memory than was shown in Ferguson et al. (2002) where rats were singly housed for the duration of the study. In the study discussed here, rats were housed in pairs which may explain their ability to recall the juvenile 24 hours after the first exposure.

5.5.5.2 Morris water maze

In this study, Morris water maze readouts suggested that lesioned animals experienced no cognitive decline. This is likely due to the smaller size, and more dorsal placement, of the lesion used in this study compared to that of Tadaiesky et al. (2008), where cognitive impairment was present in lesioned animals (Chen et al. 2011). As this study set out to find an early-stage lesion model of PD, it is appropriate that later stage symptoms such as cognitive impairment are not present.

The version of the Morris water maze used here was a commonly-used method which assesses spatial acquisition and memory, while the version used by Tadaiesky et al. (2008) is a simpler, cued version of the same task. This cued water maze assesses similar abilities to the spatial acquisition version, but uses a platform with a visible cue attached and randomises the starting position of the animal and also the position of the platform. By doing so, the cued version removes the need for subjects to rely on distal cues to form a mental map of the maze, but still tests understanding of the platform as the route of escape. It is thought that if an animal cannot perform well in the cued version of the task, then they are unlikely to be able to perform in the spatial acquisition version; though the reverse is not necessarily true (Vorhees & Williams 2006). For this reason it seems unlikely that, had the cued version been used in place of the acquisition version, this cohort would have performed differently.

Here, certain parameters (i.e. time to platform during acquisition, and time in platform quadrant during the probe trial) were quantified both manually and also with the help of behavioural tracking software. These two forms of measurement gave results which correlated well. Due to variation between videos, a fixed length of 2 seconds after placement in the pool was clipped from each measurement of time to platform/quadrant to reduce error caused by the presence of the experimenter in-frame. This has resulted in some measurements of 0.0s to platform or quadrant where animals took < 2 seconds to reach the platform. However, due to the utility of the swim velocity and distance to platform measurements (which can only be measured by tracking), in ascertaining the effect of motor deficit, the results from the automated software are presented here rather than those of the manual analysis.

One further source of variation affecting these data are the time at which the test was performed. Throughout the acquisition period, duration of trial, swim distance and swim velocity all show a downward trend, with the exception of the 4th day. On this day, animals were exposed to the maze approximately 1 hour earlier than on other days (as a result of other commitments), pushing the

test into the 7pm-7am dark phase. This may explain why performance on this day seems altered with respect to the trend in acquisition. In any future studies, it would be important to avoid any potential variance in the time of the test, especially around the times of light-dark phase switches.

5.5.5.3 Further behavioural characterisation

In future studies making use of the non-motor symptoms this model has to offer, there would be some value in adding tests for a few other symptoms not studied here.

- Sleep disturbance - Vo et al. (2014) discovered that full, unilaterally 6-OHDA lesioned rats suffer from REM sleep behaviour disorder similar to that which PD patients face. The lesioned rats in their study experienced higher wakefulness in the dark phase, and lower wakefulness in the light phase than control animals. It would be interesting to extend this finding into a partial lesion model to further characterise the changes to sleep behaviour caused by a smaller, bilateral dopaminergic lesion.

- Constipation - Blandini et al. (2009) found that gut motility was significantly reduced in full, unilaterally 6-OHDA lesioned rats. Underlying this and as a result of the lesion, nitrergic neuron number was significantly reduced in areas of the gastrointestinal tract. This shows that a midbrain dopamine deficit can have far-reaching consequences for other organ systems within an organism and would be interesting to examine alongside the presently characterised non-motor symptoms.

- Bladder dysfunction - Mitra et al. (2015) evaluated the contractility of the bladder detrusor muscle from 6-OHDA full, unilaterally lesioned rats, finding a significant increase in contractility. This finding suggests that bladder dysfunction, such as that seen in PD patients, may be centrally mediated. It would be interesting to see whether the increase in bladder contractility seen in fully-lesioned animals is also present in partially-lesioned ones.

5.5.5.4 Further histological characterisation

In addition to the primary dopaminergic and noradrenergic nuclei, an examination of the serotonergic nucleus, the dorsal raphe nucleus (DRN) could have been useful in interpreting the neurological basis of the non-motor symptoms measured here. Prinz et al. (2013) show that 6-OHDA lesioning can cause plasticity of 5-HT cells after injection into the striatum. The group observed

increased firing activity in the dorsal raphe nucleus through *in vitro* slice electrophysiology. Had the dorsal raphe nucleus been available for evaluation in the present study, it is possible that changes such as alterations to firing activity would not be picked up by immunohistochemistry alone. Indeed, Miguelez et al. (2011) find that 6-OHDA administration in rats reduces the firing rate of the locus coeruleus and its relationship to the firing of the DRN. This finding brings to light the possibility that finer changes, such as firing rate alterations, may have been present in a number of structures examined where larger changes, such as overt cell or terminal loss, were not.

5.6 Summary and conclusions

This study set out to characterise the motor and non-motor changes accompanying a bilateral, partial striatal lesion in rats. A variety of behavioural tests were used to characterise behaviour, grouped to test symptoms of PD such as anxiety, cognitive decline and anhedonia. Histological characterisation of brain areas relevant to observed behavioural changes was carried out in order to better understand the origins of the non-motor symptoms.

In PD, deficits in serotonergic and noradrenergic signalling, in addition to dopamine deficits, likely underpin non-motor symptoms (Politis & Niccolini 2015, Espay et al. 2014). The present study, along with evidence from the literature, shows that a partial, bilateral 6-OHDA model of PD in rats can display both motor and non-motor symptoms. The lesion, though implemented solely in the dopaminergic nigrostriatal tract, can have far-reaching effects on other nuclei, and even peripheral organ systems. The exact assortment of symptoms presented by lesioned animals depends strongly on the precise position, size and stage of development of the lesion itself and, as such, reports vary widely with differences in protocol.

The group of non-motor symptoms demonstrated here - anxiety, reduced exploratory interest and reduced social reward - match those seen by those in the early stages of PD (Galati & Di Giovanni 2010). The precise natures of the symptoms seen here have not yet been fully elucidated, with the outcome of any one test having a number of different potential causes (e.g. reduced rearing behaviour in open field arena is reported variously as due to motor deficit, anhedonia and anxiety). Further examination of the depressive- and anxiety-like symptoms should be undertaken before this model is used with pharmacological interventions in order to properly assess their efficacy against these non-motor symptoms. This will ensure that the correct conclusions about drug efficacy are drawn from study outcomes, and each behaviour is correctly attributed to a symptom.

A well characterised rodent model of PD which reliably displays the motor and non-motor symptoms of the early stages of PD would also improve the translatability and validity of future *in vivo* research in the field. Furthermore, this type of model represents a refinement of older, full, unilateral lesion models. The bilateral, partial lesion model displaying non-motor symptoms has the potential to reduce the number of animals required for PD research - if a single cohort of animals can be used to display multiple antiparkinsonian effects of one potential therapeutic option through the application of non-invasive behavioural tests then fewer pre-clinical studies will be required to assess the potential beneficial effects to patients. Furthermore, the understanding of

the non-motor symptoms of PD in animal models may aid out understanding of the pathophysiology of the non-motor symptoms of PD.

Overall, with some further characterisation, this model may prove suitable for use in studies of pharmacological intervention in PD to examine efficacy holistically, rather than on motor symptoms alone. This approach can lead to refinements in pre-clinical research and also improved interventions in PD, opening the way for the development of drugs to treat PD in its entirety.

6 General discussion

Parkinson's disease (PD) is a neurodegenerative disease which has a great impact on the quality of life of those who are affected by it. PD impairs motor ability by causing rigidity, bradykinesia, tremor and postural instability - increasing the likelihood of falls and impairing the ability of PD patients to lead independent lives. Not only this, but PD also causes severe non-motor symptoms such as sleep problems, depression, anxiety and chronic pain; which may be equally debilitating as motor symptoms.

Current treatments for PD confer temporary relief of symptoms but are limited by severe side effects and a lack of disease modifying activity. A treatment which slows or halts the course of PD is highly sought after in order to improve the quality of the lives of PD patients. However, thus far, no neuroprotective therapies have been licensed for PD, despite many such compounds being explored in preclinical models. To this end, this thesis explores the potential of metabotropic glutamate receptor 4 (mGluR4) targeting compounds to provide neuroprotection and other potential benefits in preclinical models of PD.

mGluR4 is distributed at key locations on synapses of the basal ganglia which become overactive in the PD brain as a result of the loss of dopaminergic tone following neurodegeneration. Upon activation, mGluR4, which is primarily located presynaptically, reduces the release of neurotransmitter at the synapse. In the PD brain, this has the effect of normalising the transmission at those synapses, and therefore the motor function of the whole organism. Indeed, previous studies undertaken in this group indicate that metabotropic glutamate receptors (mGluRs) and, in particular mGluR4, may be of benefit in providing both symptomatic and neuroprotective efficacy in animal models of PD through this mechanism (Austin et al. 2010, Betts et al. 2012, Broadstock et al. 2012).

Until now the beneficial effects of targeting mGluR4 have been shown in this group following intracranial administration of a positive allosteric modulator (PAM) with allosteric agonist activity (an 'ago-PAM'), VU0155041. Although effective, this method of administration is not suitable for translation to clinical trials and, instead, a more easily accessible route of administration would be required. An earlier paper by Battaglia et al. (2006) supports neuroprotective efficacy of mGluR4 modulation being retained if an mGluR4 PAM is systemically administered. However, this paper used an unusual dosing paradigm in which the PAM, N-phenyl-7-(hydroxyimino)cyclopropa[b]-chromen-1a-carboxamide (PHCCC), was administered only once - prior to the administration of

the 1-methyl-4-phenyl-1,2,3,6-tetrahydropyridine (MPTP) by which the PD model was induced. When an alternative PAM was administered sub-chronically systemically to rats during the development of a 6-hydroxydopamine (6-OHDA) full lesion by Finlay (2014), such protection was not observed.

One possible reason for the difference in outcome between these two studies was thought to have been the difference in PD models used. While Battaglia et al. (2006) utilized an MPTP model resulting in a partial loss of dopaminergic cells and terminals in the substantia nigra pars compacta (SNc) and striatum, Finlay (2014) used a 6-OHDA full lesion model resulting in unilateral, total destruction of the dopaminergic nigrostriatal pathway. These findings necessitated the follow-up studies detailed in this thesis in order to truly ascertain the effectiveness of systemically-administered mGluR4 compounds in providing neuroprotection in a partial lesion, 6-OHDA rat model.

To this end, one of the main aims of this thesis was to fully characterise unilateral and bilateral partial 6-OHDA lesion rat models of PD for motor and non-motor symptoms of early stage Parkinson's. Once characterised, the unilateral partial lesion model was to be used in fulfilling the second aim of this thesis: 'To explore the neuroprotective potential of systemically administered mGluR4 activating compounds'.

6.0.1 Neuroprotective, therapeutic potential of mGluR4 in PD models

Hypothesis: Activation of mGluR4 via systemically administered compounds will provide neuroprotection in a mild, partial lesion rat model of early stage Parkinson's.

The comparison between the present neuroprotection studies and the study of the neuroprotective efficacy of (1S, 2R)-N1-(3,4-dichlorophenyl)-cyclohexane-1,2-dicarboxamide (Lu AF21934) in a full lesion (Finlay 2014), in addition to the availability of pharmacokinetic data demonstrates that, while the systemically administered PAM is capable of crossing the blood brain barrier and achieving reasonable concentrations in brain tissue, it does not have the ability to provide neuroprotection in a 6-OHDA partial lesion rat model. This may be as a result of the intricacies of the intracellular signalling pathway activated by the PAM or as a result of an insufficiency of endogenous agonist at the site of the receptors (as discussed in Chapter 3). Both of these potential reasons for the failure of Lu AF21934 to provide neuroprotection are addressed by the use of an orthosteric or allosteric agonist such as (2S)-2-amino-4-(hydroxy(hydroxy(4-hydroxy-3-

methoxy-5-nitrophenyl)methyl)phosphoryl)butanoic acid (LSP1-2111) (used here) or VU0155041 (used previously by Betts et al. (2012)). Indeed, this is realised in the efficacy of each of these compounds in comparison to Lu AF21934 (Betts et al. 2012, Finlay 2014).

In stark contrast, this thesis shows for the first time that systemic administration of an mGluR4 agonist, LSP1-2111, but not a PAM, Lu AF21934, provided neuroprotection in the early-stage model of PD characterised in Chapter 2. Significant preservation of tyrosine hydroxylase (TH)-positive cells was observed in the SNc of LSP1-2111-treated animals. This was accompanied by a non-significant trend towards preservation of TH-positive fibres in the striatum.

In terms of mGluR4-mediated neuroprotection, therefore, this thesis contrasts the existing body of evidence suggesting that PAMs have more antiparkinsonian potential than do agonists (Battaglia et al. 2006, Bennouar et al. 2013, Iderberg et al. 2015). It may seem surprising that an agonist, with the capability of activating a receptor in an 'unrefined' manner with no regard for the neurochemistry of the surrounding tissue, shows more efficacy than a PAM, touted to be perfect for the treatment of central nervous system (CNS) disorders due to their ability to subtly modulate neuronal activity under certain conditions - particularly as the body of evidence in the literature supports a PAM over an agonist in the case of mGluR4 in PD. However, in terms of translatability to the human disorder, the weight of evidence supports an agonist. This may be because allosteric modulators are a relatively new concept in pharmacology compared with orthosteric agonists and antagonists. The range of actions a compound may achieve following allosteric binding is still being investigated.

Given the lack of translation in past neuroprotection clinical trials, if an agonist is to succeed in progressing to clinical trials it is questionable whether this preclinical potential will be realised. This problems with translation of neuroprotective compounds from preclinical trials to registered treatments likely reflects issues with the design of clinical trials. Trials on treatments for neurodegenerative diseases such as PD or Alzheimer's disease are often run with a view to observing acute, symptomatic changes in patients with advanced disease and severe symptoms. This is not always the best approach to observe symptomatic efficacy, much less disease modifying efficacy. In order to fully test the ability of drugs to modify the course of a disease, patients must be recruited early, before symptoms and degeneration become severe - a point which was recognised even in 1817 by James Parkinson himself (Parkinson 2002). Further, in order to recruit such patients, a strong battery of biomarkers must be recognised and reliably tested in order to be sure of a PD population rather than a heterogeneous mix of patents displaying some early symptoms such as

anosmia and REM sleep behaviour disorder (RBD) but who may not go on to develop full PD.

The question of heterogeneity even with the group of early (or late) PD patients is also an important point to address. Currently there is something of a drive to rename PD to Parkinson's spectrum disorder or Parkinson's syndrome in recognition of the fact that individuals with PD often have very different experiences of the disease - suffering different disease progressions and different groups of symptoms. It may be the case that PD serves as an umbrella term for some subtly different diseases which may have different underlying pathology. If this were indeed the case, it could mean that subtypes of PD respond differently to different treatments. By grouping PD patients of all types together in clinical trials, data from subpopulations which respond better or worse to different treatments could be averaged to find no effect - meaning the failure of drugs which could be beneficial in certain circumstances. In order for this potential pitfall to be avoided in future trials assessing symptomatic or neuroprotective treatments, more research must be done into the stratification of PD subtypes and into biomarkers allowing their early identification.

Future studies to build on the evidence in this thesis for mGluR4 agonists for neuroprotective treatments in PD should:

- Assess at least one more mGluR4 agonist (perhaps the more potent LSP4-2022) in order to conclude that the neuroprotective effect is an on-target, mGluR4 effect rather than a quirk of a single compound. Alternatively or additionally, a the neuroprotective effect of an mGluR4 agonist co-administered with an mGluR4 antagonist could be assessed. Should the neuroprotective effect be blocked in such a paradigm this would suggest that the effect is driven by mGluR4 alone.

- Assess an mGluR4 compound in an alternative preclinical model - LSP1-2111 or the second test compound should be trialled in additional models of PD to ensure that the effect seen in these studies is not peculiar to the 6-OHDA model. Ideally, a secondary model would utilise a toxin or mutation which has a different mechanism of action to 6-OHDA - such as rotenone. However, given the variability of most rotenone models characterised thus far, MPTP-treated mice or marmosets may serve as a better option.

- Assess the ability of LSP1-2111 to modulate glutamate release from the subthalamic nucleus (STN) in intact organisms - this could provide further understanding of the neuroprotection shown here. Previous studies in this group have shown that a pan-group III mGluR agonist delivered intracranially can have this effect (Broadstock et al. 2012). Electrophysiology studies on isolated brain slices have shown the same inhibitory effect with Lu AF21934 on

corticostriatal synapses (Gubellini et al. 2014). Whether these effects hold true in 6-OHDA-lesioned animals with systemically delivered LSP1-2111 may improve our understanding of the neuroprotective effect seen here.

Certainly, this thesis shows that, although administration of LSP1-2111 provided only modest neuroprotection in the partial lesion, 6-OHDA rat model of PD, this mGluR4 agonist was much more capable of conferring neuroprotection than was the PAM. Judging solely by this neuroprotection data, it seems that the mGluR4 agonist approach may be well worth pursuing.

One consideration that must be taken into account prior to the extrapolation of these findings to long-term administration, as would necessarily be the case in the relief of symptoms of PD patients, is the potential consequence of long-term administration of an agonist compound. The dyskinesia side effect of L-3,4-dihydroxyphenylalanine (L-DOPA) emerges after a number of years of daily treatment and, while the animals in the present study were pre-primed to express levodopa-induced dyskinesia (LID) following a single administration of L-DOPA, this is not necessarily to say that the same animals would also show effects of LSP1-2111 after a single dose. In the short to medium term, administration of an agonist of any kind may well result in receptor desensitisation, depending upon the signalling cascade preferred by the agonist and the mechanism of desensitsation of that particular receptor. In the longer term, such chronic stimulation, or desensitisation, of receptors may result in a change in expression at the cell surface. This could serve to downregulate the proportion of receptors at the cell surface such that, even at full receptor occupancy, a low signal is produced - as in opioid receptor desensitisation and the production of tolerance (Stafford et al. 2001). Instead, short term desensitization could result in the long term upregulation of receptors thereby increasing sensitivity - as has been observed with nicotinic $\alpha 4\beta 2$ receptors (Fenster et al. 1999). Furthermore, and as is the case with LID, chronic administration may result in pathological plasticity of certain neuronal areas resulting in side effects which irrevocably build in severity over time.

Clearly, further studies into the potential for, and effects of, LSP1-2111-mediated mGluR4 downreguation must be carried out in order to better understand this effect. Such studies could be carried out *ex vivo* on tissue from animals dosed chronically with the compound given the provision of a functional and reliable antibody against mGluR4 (though sadly one such antibody could not be found for the present studies). Alternatively, *in vitro* binding and activation assays may provide an easy and cheap first glance into this problem.

6.0.2 Mechanisms underlying LSP1-2111-mediated neuroprotection

Hypothesis: Any neuroprotection provided by mGluR4 activating compounds in the aforementioned model will have some anti-inflammatory component.

In previous studies examining the neuroprotective efficacy of mGluR4 activating compounds, intracranial administration of VU0155041 was found to significantly reduce ionized calcium-binding adaptor molecule 1 (Iba1) levels in the lesioned SNc (Betts et al. 2012). As VU0155041 is an agoPAM and was delivered directly above the site of lesion, it is difficult to directly compare the VU0155041-mediated neuroprotective effect observed by Betts et al. (2012) to that mediated by systemically-delivered, orthosteric agonist, LSP1-2111. It may be the case that direct administration of an mGluR4-activating compound to the site of the lesion enables a more targeted anti-inflammatory effect than does systemic administration. Potential alternative mechanisms of action were not examined in the study by Betts et al. (2012) and so further comparisons in neuroprotective mechanisms of the two compounds and studies - such as the induced transcriptional profile - are impossible.

The mechanisms underlying mGluR4-mediated neuroprotection in these animals, including an anti-inflammatory effect, were examined (Chapter 4 in this thesis). From the perspective of finding an anti-inflammatory effect of LSP1-2111 administration, the most promising evidence came in the form of a reduction of Iba1 staining in the rostral SNc - the region where neuroprotection was strongest. It is unclear whether the anti-inflammatory effect here drove the neuroprotection or whether the reduction of inflammation was due to the reduced apoptosis in this area as a result of neuroprotection. Certainly, *in vitro* evidence from the literature seems to suggest that this effect could work either way around (Witting et al. 2002, Taylor et al. 2003).

If inflammation drives apoptosis in the 6-OHDA rat model then, from the small size of the effect observed here, it seems unlikely that LSP1-2111 has a sufficient effect on inflammation alone in this model to underlie significant neuroprotection. If these events occur the other way around and neuroprotection by LSP1-2111 drives a reduction in Iba1 at the site of protection then the cause of protection is not explained by the reduction in inflammation. Whichever the order of events, the results of the histology on inflammatory markers suggest that there are more mechanisms behind the neuroprotective effect than a simple reduction in microglial numbers. This is not to rule out an anti-inflammatory effect of LSP1-2111 underlying neuroprotection, but to suggest more subtle modulations - such as an altered secretory profile or activation state of inflammatory cells - if such

an effect does indeed exist.

These potential additional inflammatory changes mediated by 6-OHDA lesioning and LSP1-2111 treatment were examined through cytokine arrays which suggested hints of a drug effect alongside a strong lesion effect. Some promising results from these initial arrays were followed up using enzyme-linked immunosorbent assays (ELISAs) on 3 individual cytokines. In these ELISAs, although a trend towards an effect of lesion was seen in all cases, no effect of LSP1-2111 treatment on cytokine expression was evident in analysis. In part due to effect sizes and in part due to the disparity between the results of these assays, the cytokine studies detailed in Chapter 4 failed to provide any more real insight into an anti-inflammatory effect of LSP1-2111 in lesioned animals.

In order to explore all other potential actions of LSP1-2111, a microarray examining whole genome transcriptional changes was undertaken on tissue from animals which had been given a single dose of LSP1-2111 (with no lesion) 3 hours prior to dissection. Although the findings of this microarray cannot be directly applied to the LSP1-2111 neuroprotection study due to the lack of chronic dosing or a lesion, the data still suggest a number of interesting mechanisms by which LSP1-2111 may act in a naïve animal and which may be relevant to a neuroprotective effect if sustained in lesioned animals dosed multiple times. Notable amongst these suggestions were genes involved in modulation of tumour necrosis factor α (TNFα) and IL-2 signalling pathways (following an anti-inflammatory thread), reduction of the pro-apoptoic protein 'Bcl-2 interacting mediator of cell death' (BCL2L11) and the increase of protein kinase D and dopamine receptor D4. These last individual genes hint at interesting, and hitherto unconsidered, mechanisms of action of mGluR4 activation (or at least LSP1-2111 administration) involving protein trafficking, reactive oxygen species (ROS) reduction and interference with transcription factor translocation.

Whether the majority of these genes are regulated as a true effect of mGluR4 activation or as an off-target effect of LSP1-2111 specifically needs to be considered in future studies. Such studies could examine the transcriptional profile of animals treated with an alternative mGluR4 agonist (such as LSP4-2022), examine the transcriptional profile of LSP1-2111 itself in an mGluR4-knockout animal or examine the profile of an mGluR4 agonist co-administered with an mGluR4 antagonist. Such data would then be cross referenced with the data produced by the present GeneChip study.

If the majority of genes regulated by LSP1-2111 were unable to be confirmed by these methods then this would suggest that there may be a large off-target effect of LSP1-2111. This in itself could still be useful in presenting some alternative pathways to neuroprotection other than going

via mGluR4 activation. Whether the genes and pathways shown to be regulated by LSP1-2111 here result from mGluR4 activation or from off-target effects, these data provide a multitude of new considerations for targets for neuroprotection in PD models and ultimately PD. Understanding of these potential new targets or implications of mGluR4 activation may, in time, add more routes to success in the search for neuroprotective therapies in PD.

6.0.3 Symptomatic, therapeutic potential of mGluR4 in PD models

An additional study presented in this thesis examined the effect of a single dose of LSP1-2111 alone and in combination with L-DOPA on MPTP-treated marmosets with LID. The present study represents this first of its kind detailed in the literature where an mGluR4 agonist has been administered systemically to a non-human primate. LSP1-2111 did not appear to have an effect on the emergence of LID in these primed animals (confirming the findings of Iderberg et al. (2015) in a rat model), a synergistic effect with L-DOPA in reducing motor disability or in increasing locomotor activity. However, and perhaps most importantly, a single administration of LSP1-2111 alone was able to reduce motor disability without causing any symptoms of dyskinesia.

This finding neatly links with a study reported in the literature wherein L-2-amino-4-phosphonobutyrate (L-AP4), a group III mGluR agonist, and (+/-)-cis-2-(3,5-dichlorphenylcarbamoyl)cyclohexanecarboxylic acid (VU0155041), the mGluR4 agoPAM, were microinjected into the putamen or external globus pallidus (GPe) of MPTP-treated rhesus macaques and electrophysiological recordings were taken (Bogenpohl et al. 2013). This study found that L-AP4, but not VU0155041, was capable of increasing the firing rate of these two structures in MPTP-treated macaques - suggestive of an antiparkinsonian effect of agonist activation of at least one group III mGluR. The present study builds considerably on the findings of the study by Bogenpohl et al. (2013). Although the Bogenpohl et al. (2013) study may seem to suggest that mGluR4 activation is not relevant to a potentially antiparkinsonian effect of firing rate alteration in the GPe and striatum, their use of an mGluR4 specific ago-PAM versus a pan group III agonist to demonstrate this finding leaves the evidence open to interpretation. As this thesis finds in the neuroprotection studies, beneficial effects of agonist activity at mGluR4 cannot necessarily be generalised to PAM activity. Thus, the positive effects of the pan group III agonist found by Bogenpohl et al. (2013) may still be driven by agonism at mGluR4, even while allosteric activation of mGluR4 does not have similar benefits.

The present study therefore builds on, and is complemented by, the study of Bogenpohl et al.

(2013) by suggesting that activation of mGluR4 may well be capable of causing these alterations in firing, but perhaps that an orthosteric agonist is required to do so where an agoPAM is too subtle. Furthermore, the present study shows that such an effect may be brought about following systemic administration rather than intracranial microinjection and, key, that such administration may have behavioural consequences above and beyond simple electrophysiological alterations. These findings represent important advances into our understanding of the potential for mGluR4 activating compounds to modulate basal ganglia function following systemic administration. These findings are particularly exciting in a non-human primate model which is considerably more translatable than the standard rodent models.

An additional aim of the present study into mGluR4 agonism in the MPTP-treated marmoset was to characterise the L-DOPA-sparing efficacy and antidyskinetic potential of LSP1-2111. In this respect, the results of the present study conflict with the findings of Charvin et al. (2018), Le Poul et al. (2012) and Bennouar et al. (2013), who show a LID-reducing effect of an mGluR4 activation by a PAM. However, the finding here that mGluR4 activation has no effect on LID is more in line with the findings of Finlay (2014) and Iderberg et al. (2015), suggesting limited potential for mGluR4 PAMs and agonists for reducing established LID. This is somewhat disturbing in light of the recent entrance of the mGluR4 PAM, Foliglurax, entering clinical trials for the treatment of established LID in PD patients (Charvin et al. 2017). Indeed, the trial will be of interest to all groups involved in working on mGluR4 as it represents the first mGluR4 activating compound of any class to enter man and, depending upon the soundness of its design and the choice of appliction, may provide a lot of information about the translatability of this approach.

In all, the present study provided a new and exciting perspective on the ability of a systemically delivered mGluR4 agonist to provide an antiparkinsonian effect in a well established non-human primate model of PD. The finding that this antiparkinsonian effect is not accompanied by dyskinesia in primed is doubly exciting and may forecast a new future for the symptomatic treatment of PD.

6.0.4 Model development and non-motor symptoms

Hypothesis: Implementing an early-stage model bilaterally will demonstrate both motor and non-motor symptoms of PD which will be measurable with simple behavioural tests.

The serious impact of the non-motor symptoms of PD on the quality of life of PD patients is being increasingly well recognised by charities and researchers. Despite this and because of traditional

research models, much of the preclinical work on antiparkinsonian therapeutics undertaken in models which solely display (or are only examined for) the motor signs of PD. One aim of this thesis was to examine a bilateral version of the unilateral, partial, 6-OHDA lesion model described in Chapter 2 for non-motor symptoms of PD in order to characterise a holistic model of early stage PD - including mild-moderate cell death, mild motor symptoms and some non-motor symptoms.

Although similar models have been created by other groups, the reports of these models seem to suggest either a somewhat inappropriate lesion placement or a dearth of suitable tests of non-motor symptoms. For example, although Tadaiesky et al. (2008) characterise their model well, using a large number of non-motor tests against a good range of symptoms, they utilise a lesion in the ventral striatum of the rat. Such a lesion is not representative of early stage PD terminal loss and, alone, could be predicted to, and indeed does, give rise to non-motor symptoms of PD which tend to appear at late stages of the disease - such as cognitive impairment - making it inaccurate as a model of early stage PD. Alternative publications which use a lesion placement appropriate to degeneration in early PD - in the dorsal striatum - tend to use few tests and so give an incomplete picture of the PD characteristics of their model (Chen et al. 2014, Silva et al. 2016). The study in this thesis therefore fills a gap in the literature left between these publications which are, by turns, detailed in nature or relatively accurate representations of early PD, though rarely both.

The results presented here show that the 6-OHDA partial lesion model characterised in Chapter 2, when applied bilaterally, can indeed give rise to both the motor and non-motor signs commonly seen in PD. Furthermore, the animals appear to show specifically those non-motor symptoms which are characteristic of the early stages of PD, such as anxiety and craving, over those more closely associated with later stage PD, such as cognitive decline. The motor symptoms accompanying the emergence of these non-motor symptoms seem both progressive, worsening over a period of 3 weeks, and subtle, able to be picked out using a complex test of motor endurance and co-ordination (the rotarod), but not in a crude test of exploratory ability and drive (line crossing in the open field arena).

In both motor and non-motor aspects then, the bilateral, partial 6-OHDA-lesioned rat has good face validity as a model of early stage PD. The added benefit of the relatively slow progression of motor symptoms (stable by 3 weeks post-lesion) allows a window of opportunity for the initiation of potential therapeutic treatment starting after the administration of 6-OHDA but before serious cell death occurs. This type of treatment regimen is more realistic than pre-loading animals with a potential therapeutic compound before lesioning and so would provide a more translational test.

The progress made in this thesis towards the production of a more holistic model of PD also opens up the option to examine the effect of one therapeutic intervention on multiple aspects of PD simultaneously. mGluR4 modulation has already been investigated for its potential therapeutic effect in animal models of anxiety, depression and psychosis (Slawinska et al. 2013, Wierońska et al. 2013, Wieronska et al. 2015). Although the origin of PD-related anxiety and depression is not yet well understood, that Lu AF21934 and LSP1-2111 have shown potential therapeutic effect in these conditions in animal models unrelated to PD (Slawinska et al. 2013) shows hope that they may also have a beneficial effect in PD-anxiety.

Given the promise of the model shown in this thesis in only one study, it would be prudent to interrogate the model with alternative tests for anxiety, depression and pain to ensure that these symptoms are shown and correctly interpreted by the experimenter. Having confirmed the presence of these non-motor symptoms, a reasonable next step would be to examine the acute effects of LSP1-2111 in the bilateral lesion model in order to cement a role for mGluR4 and its modulation in the emergence and treatment of non-motor symptoms in PD.

6.0.5 Concluding remarks

In conclusion, the results presented in this thesis support mGluR4 as a therapeutic target in PD both as an agent of neuroprotection and symptomatic benefit. Specifically, agonism of mGluR4 (though not positive allosteric modulation) is beneficial in both a rat 6-OHDA lesion model and a non-human primate MPTP model.

The mechanism behind the neuroprotective and antiparkinsonian potential of LSP1-2111 apppears complex, showing some signs of a mild anti-inflammatory effect in the 6-OHDA rat, a potential action of normalisation of basal ganglia signalling in the MPTP-treated marmoset and myriad additional potential routes of action through a transcriptomic array. This last will take time to truly unravel and understand, and may prove to provide any number of other potential routes into disease modification in Parkinson's. The evidence shown in this thesis can form a promising foundation of further studies which further examine the details of mGluR4 activation in PD models and, in the future, potentially, a disease-modifying therapeutic intervention in PD.

References

Aarsland, D., Ballard, C. G. & Halliday, G. (2004), 'Are Parkinson's Disease with dementia and Dementia with lewy Bodies the Same Entity?', *J. Geriatr. Psychiatry Neurol.* **17**(3), 137–145.

Abbott, R. D., Ross, G. W., Petrovitch, H., Tanner, C. M., Davis, D. G., Masaki, K. H., Launer, L. J., Curb, J. D. & White, L. R. (2007), 'Bowel movement frequency in late-life and incidental Lewy bodies', *Mov. Disord.* **22**(11), 1581–1586.

Adams-Carr, K. L., Bestwick, J. P., Shribman, S., Lees, A., Schrag, A. & Noyce, A. J. (2016), 'Constipation preceding Parkinson's disease: a systematic review and meta-analysis', *J. Neurol. Neurosurg. Psychiatry* **87**(7), 710–716.

Addy, C., Assaid, C., Hreniuk, D., Stroh, M., Xu, Y., Herring, W. J., Ellenbogen, A., Jinnah, H. A., Kirby, L., Leibowitz, M. T., Stewart, R. M., Tarsy, D., Tetrud, J., Stoch, S. A., Gottesdiener, K. & Wagner, J. (2009), 'Single-Dose Administration of MK-0657, an NR2B-Selective NMDA Antagonist, Does Not Result in Clinically Meaningful Improvement in Motor Function in Patients With Moderate Parkinson's Disease', *J. Clin. Pharmacol.* **49**(7), 856–864.

Aguiar, A. S., Tristão, F. S. M., Amar, M., Chevarin, C., Lanfumey, L., Mongeau, R., Corti, O., Prediger, R. D. & Raisman-Vozari, R. (2013), 'Parkin-Knockout Mice did not Display Increased Vulnerability to Intranasal Administration of 1-Methyl-4-phenyl-1,2,3,6-tetrahydropyridine (MPTP)', *Neurotox. Res.* **24**(2), 280–287.

Aguirre, J. A., Kehr, J., Yoshitake, T., Liu, F.-L., Rivera, A., Fernandez-Espinola, S., Andbjer, B., Leo, G., Medhurst, A. D., Agnati, L. F. & Fuxe, K. (2005), 'Protection but maintained dysfunction of nigral dopaminergic nerve cell bodies and striatal dopaminergic terminals in MPTP-lesioned mice after acute treatment with the mGluR5 antagonist MPEP', *Brain Res.* **1033**(2), 216–220.

Ahlskog, J. E. & Muenter, M. D. (2001), 'Frequency of levodopa-related dyskinesias and motor fluctuations as estimated from the cumulative literature.', *Mov. Disord.* **16**(3), 448–58.

Aizman, O., Brismar, H., Uhlén, P., Zettergren, E., Levey, A. I., Forssberg, H., Greengard, P. & Aperia, A. (2000), 'Anatomical and physiological evidence for D1 and D2 dopamine receptor colocalization in neostriatal neurons', *Nat. Neurosci.* **3**(3), 226–230.

Akiyama, H. & McGeer, P. L. (1989), 'Microglial response to 6-hydroxydopamine-induced substantia nigra lesions.', *Brain Res.* **489**(2), 247–53.

Alagarsamy, S., Phillips, M., Pappas, T. & Johnson, K. M. (1997), 'Dopamine neurotoxicity in cortical neurons.', *Drug Alcohol Depend.* **48**(2), 105–11.

Alakurtti, K., Johansson, J. J., Tuokkola, T., Någren, K. & Rinne, J. O. (2013), 'Rostrocaudal gradients of dopamine D2/3 receptor binding in striatal subregions measured with [11C]raclopride and high-resolution positron emission tomography', *Neuroimage* **82**, 252–259.

Alam, M. & Schmidt, W. (2002), 'Rotenone destroys dopaminergic neurons and induces parkinsonian symptoms in rats', *Behav. Brain Res.* **136**(1), 317–324.

Albin, R. L., Young, A. B. & Penney, J. B. (1989), 'The functional anatomy of basal ganglia disorders', *Trends Neurosci.* **12**(10), 366–375.

Alsaad, A. M. S., Zordoky, B. N. M., El-Sherbeni, A. A. & El-Kadi, A. O. S. (2012), 'Chronic Doxorubicin Cardiotoxicity Modulates Cardiac Cytochrome P450-Mediated Arachidonic Acid Metabolism in Rats', *Drug Metab. Dispos.* **40**(11), 2126–2135.

Alvarez-Fischer, D., Henze, C., Strenzke, C., Westrich, J., Ferger, B., Höglinger, G. U., Oertel, W. H. & Hartmann, A. (2008), 'Characterization of the striatal 6-OHDA model of Parkinson's disease in wild type and α-synuclein-deleted mice', *Exp. Neurol.* **210**(1), 182–193.

Alvarez, L., Macias, R., Pavon, N., Lopez, G., Rodriguez-Oroz, M. C., Rodriguez, R., Alvarez, M., Pedroso, I., Teijeiro, J., Fernandez, R., Casabona, E., Salazar, S., Maragoto, C., Carballo, M., Garcia, I., Guridi, J., Juncos, J. L., DeLong, M. R. & Obeso, J. A. (2009), 'Therapeutic efficacy of unilateral subthalamotomy in Parkinson's disease: results in 89 patients followed for up to 36 months', *J. Neurol. Neurosurg. Psychiatry* **80**(9), 979–985.

Ambrosi, G., Armentero, M.-T., Levandis, G., Bramanti, P., Nappi, G. & Blandini, F. (2010), 'Effects of early and delayed treatment with an mGluR5 antagonist on motor impairment, nigrostriatal damage and neuroinflammation in a rodent model of Parkinson's disease', *Brain Res. Bull.* **82**(1-2), 29–38.

Ambrosi, G., Cerri, S. & Blandini, F. (2014), 'A further update on the role of excitotoxicity in the pathogenesis of Parkinson's disease', *J. Neural Transm.* **121**(8), 849–859.

An, L.-L., Mehta, P., Xu, L., Turman, S., Reimer, T., Naiman, B., Connor, J., Sanjuan, M., Kolbeck, R. & Fung, M. (2014), 'Complement C5a potentiates uric acid crystal-induced IL-1β production', *Eur. J. Immunol.* **44**(12), 3669–3679.

Anderson, C. M. & Swanson, R. A. (2000), 'Astrocyte glutamate transport: review of properties, regulation, and physiological functions.', *Glia* **32**(1), 1–14.

Anderson, V. C., Burchiel, K. J., Hogarth, P., Favre, J. & Hammerstad, J. P. (2005), 'Pallidal vs Subthalamic Nucleus Deep Brain Stimulation in Parkinson Disease', *Arch. Neurol.* **62**(4), 554.

Andres-Mateos, E., Mejias, R., Sasaki, M., Li, X., Lin, B. M., Biskup, S., Zhang, L., Banerjee, R., Thomas, B., Yang, L., Liu, G., Beal, M. F., Huso, D. L., Dawson, T. M. & Dawson, V. L. (2009), 'Unexpected Lack of Hypersensitivity in LRRK2 Knock-Out Mice to MPTP (1-Methyl-4-Phenyl-1,2,3,6-Tetrahydropyridine)', *J. Neurosci.* **29**(50), 15846–15850.

Angiolillo, A. L., Sgadari, C., Taub, D. D., Liao, F., Farber, J. M., Maheshwari, S., Kleinman, H. K., Reaman, G. H. & Tosato, G. (1995), 'Human interferon-inducible protein 10 is a potent inhibitor of angiogenesis in vivo.', *J. Exp. Med.* **182**(1), 155–62.

Anichtchik, O., Diekmann, H., Fleming, A., Roach, A., Goldsmith, P. & Rubinsztein, D. C. (2008), 'Loss of PINK1 function affects development and results in neurodegeneration in zebrafish.', *J. Neurosci.* **28**(33), 8199–207.

Anichtchik, O. V., Kaslin, J., Peitsaro, N., Scheinin, M. & Panula, P. (2004), 'Neurochemical and behavioural changes in zebrafish Danio rerio after systemic administration of 6-hydroxydopamine and 1-methyl-4-phenyl-1,2,3,6-tetrahydropyridine.', *J. Neurochem.* **88**(2), 443–53.

Appelmelk, B. J., Negrini, R., Moran, A. P. & Kuipers, E. J. (1997), 'Molecular mimicry between Helicobacter pylori and the host', *Trends Microbiol.* **5**(2), 70–73.

Aras, S., Tanriover, G., Aslan, M., Yargicoglu, P. & Agar, A. (2014), 'The role of nitric oxide on visual-evoked potentials in MPTP-induced Parkinsonism in mice', *Neurochem. Int.* **72**, 48–57.

Ardayfio, P., Moon, J., Leung, K. K. A., Youn-Hwang, D. & Kim, K.-S. (2008), 'Impaired learning and memory in Pitx3 deficient aphakia mice: A genetic model for striatum-dependent cognitive symptoms in Parkinson's disease', *Neurobiol. Dis.* **31**(3), 406–412.

Arenas, E. (2014), 'Wnt signaling in midbrain dopaminergic neuron development and regenerative medicine for Parkinson's disease', *J. Mol. Cell Biol.* **6**(1), 42–53.

Armentero, M.-T., Fancellu, R., Nappi, G., Bramanti, P. & Blandini, F. (2006), 'Prolonged blockade of NMDA or mGluR5 glutamate receptors reduces nigrostriatal degeneration while inducing selective metabolic changes in the basal ganglia circuitry in a rodent model of Parkinson's disease', *Neurobiol. Dis.* **22**(1), 1–9.

Asaithambi, A., Ay, M., Jin, H., Gosh, A., Anantharam, V., Kanthasamy, A. & Kanthasamy, A. G. (2014), 'Protein Kinase D1 (PKD1) Phosphorylation Promotes Dopaminergic Neuronal Survival during 6-OHDA-Induced Oxidative Stress', *PLoS One* **9**(5), e96947.

Aubin, N., Curet, O., Deffois, A. & Carter, C. (1998), 'Aspirin and salicylate protect against MPTP-induced dopamine depletion in mice.', *J. Neurochem.* **71**(4), 1635–42.

Austin, P. J., Betts, M. J., Broadstock, M., O'Neill, M. J., Mitchell, S. N. & Duty, S. (2010), 'Symptomatic and neuroprotective effects following activation of nigral group III metabotropic glutamate receptors in rodent models of Parkinson's disease', *Br J Pharmacol* **160**(7), 1741–1753.

Avet-Rochex, A., Carvajal, N., Christoforou, C. P., Yeung, K., Maierbrugger, K. T., Hobbs, C., Lalli, G., Cagin, U., Plachot, C., McNeill, H. & Bateman, J. M. (2014), 'Unkempt Is Negatively Regulated by mTOR and Uncouples Neuronal Differentiation from Growth Control', *PLoS Genet.* **10**(9), e1004624.

Bai, M., Zhu, X., Zhang, L., Zhang, Y., Xue, L., Wang, Y., Zhong, M. & Zhang, X. (2017), 'Divergent anomaly in mesocorticolimbic dopaminergic circuits might be associated with different depressive behaviors, an animal study', *Brain Behav.* **7**(10), e00808.

Baker, S. N., Olivier, E. & Lemon, R. N. (1997), 'Coherent oscillations in monkey motor cortex and hand muscle EMG show task-dependent modulation', *J. Physiol.* **501**(1), 225–241.

Bargmann, C. I. (1998), 'Neurobiology of the Caenorhabditis elegans genome.', *Science* **282**(5396), 2028–33.

Barlow, D. H. & Campbell, L. A. (2000), 'Mixed anxiety-depression and its implications for models of mood and anxiety disorders', *Compr. Psychiatry* **41**(2), 55–60.

Baron, M. S., Vitek, J. L., Green, J., Kaneoke, Y., Hashimoto, T., Turner, R. S., Woodard, J. L., Delong, M. R., Bakay, R. A. E., Cole, S. A. & McDonald, W. M. (1996), 'Treatment of advanced Parkinson's disease by posterior GPi pallidotomy: 1-year results of a pilot study', *Ann. Neurol.* **40**(3), 355–366.

Barrett, M. J., Wylie, S. A., Harrison, M. B. & Wooten, G. F. (2011), 'Handedness and motor symptom asymmetry in Parkinson's disease.', *J. Neurol. Neurosurg. Psychiatry* **82**(10), 1122–4.

Barry, M. & Feely, J. (1990), 'Enzyme induction and inhibition', *Pharmacol. Ther.* **48**(1), 71–94.

Basset, L., Chevalier, S., Danger, Y., Arshad, M. I., Piquet-Pellorce, C., Gascan, H. & Samson, M. (2015), 'Interleukin-27 and IFNγ regulate the expression of CXCL9, CXCL10, and CXCL11 in hepatitis', *J. Mol. Med.* **93**(12), 1355–1367.

Battaglia, G., Busceti, C. L., Molinaro, G., Biagioni, F., Storto, M., Fornai, F., Nicoletti, F. & Bruno, V. (2004), 'Endogenous Activation of mGlu5 Metabotropic Glutamate Receptors Contributes to the Development of Nigro-Striatal Damage Induced by 1-Methyl-4-Phenyl-1,2,3,6-Tetrahydropyridine in Mice', *J. Neurosci.* **24**(4), 828–835.

Battaglia, G., Busceti, C. L., Molinaro, G., Biagioni, F., Traficante, A., Nicoletti, F. & Bruno, V. (2006), 'Pharmacological activation of mGlu4 metabotropic glutamate receptors reduces nigrostriatal degeneration in mice treated with 1-methyl-4-phenyl-1,2,3,6-tetrahydropyridine', *J Neurosci* **26**(27), 7222–7229.

Battaglia, G., Busceti, C. L., Pontarelli, F., Biagioni, F., Fornai, F., Paparelli, A., Bruno, V., Ruggieri, S. & Nicoletti, F. (2003), 'Protective role of group-II metabotropic glutamate receptors against nigro-striatal degeneration induced by 1-methyl-4-phenyl-1,2,3,6-tetrahydropyridine in mice.', *Neuropharmacology* **45**(2), 155–66.

Battaglia, G., Molinaro, G., Riozzi, B., Storto, M., Busceti, C. L., Spinsanti, P., Bucci, D., Di Liberto, V., Mudò, G., Corti, C., Corsi, M., Nicoletti, F., Belluardo, N. & Bruno, V. (2009), 'Activation of mGlu3 receptors stimulates the production of GDNF in striatal neurons.', *PLoS One* **4**(8), e6591.

Beal, M. F., Oakes, D., Shoulson, I., Henchcliffe, C., Galpern, W. R., Haas, R., Juncos, J. L., Nutt, J. G., Voss, T. S., Ravina, B., Shults, C. M., Helles, K., Snively, V., Lew, M. F., Griebner, B., Watts, A., Gao, S., Pourcher, E., Bond, L., Kompoliti, K., Agarwal, P., Sia, C., Jog, M., Cole, L., Sultana, M., Kurlan, R., Richard, I., Deeley, C., Waters, C. H., Figueroa, A., Arkun, A., Brodsky, M., Ondo, W. G., Hunter, C. B., Jimenez-Shahed, J., Palao, A., Miyasaki, J. M., So, J., Tetrud, J., Reys, L., Smith, K., Singer, C., Blenke, A., Russell, D. S., Cotto, C., Friedman, J. H., Lannon, M., Zhang, L., Drasby, E., Kumar, R., Subramanian, T., Ford, D. S., Grimes, D. A., Cote, D., Conway, J., Siderowf, A. D., Evatt, M. L., Sommerfeld, B., Lieberman, A. N., Okun, M. S., Rodriguez, R. L., Merritt, S., Swartz, C. L., Martin, W. R. W., King, P., Stover, N., Guthrie, S., Watts, R. L., Ahmed, A., Fernandez, H. H., Winters, A., Mari, Z., Dawson, T. M., Dunlop, B., Feigin, A. S., Shannon, B., Nirenberg, M. J., Ogg, M., Ellias, S. A., Thomas, C.-A., Frei, K., Bodis-Wollner, I., Glazman, S., Mayer, T., Hauser, R. A., Pahwa, R., Langhammer, A., Ranawaya, R., Derwent, L., Sethi, K. D., Farrow, B., Prakash, R., Litvan, I., Robinson, A., Sahay, A., Gartner, M., Hinson, V. K., Markind, S., Pelikan, M., Perlmutter, J. S., Hartlein, J., Molho, E., Evans, S., Adler, C. H., Duffy, A., Lind, M., Elmer, L., Davis, K., Spears, J., Wilson, S., Leehey, M. A., Hermanowicz, N., Niswonger, S., Shill, H. A., Obradov, S., Rajput, A., Cowper, M., Lessig, S., Song, D., Fontaine, D., Zadikoff, C., Williams, K., Blindauer, K. A., Bergholte, J., Propsom, C. S., Stacy, M. A., Field, J., Mihaila, D., Chilton,

M., Uc, E. Y., Sieren, J., Simon, D. K., Kraics, L., Silver, A., Boyd, J. T., Hamill, R. W., Ingvoldstad, C., Young, J., Thomas, K., Kostyk, S. K., Wojcieszek, J., Pfeiffer, R. F., Panisset, M., Beland, M., Reich, S. G., Cines, M., Zappala, N., Rivest, J., Zweig, R., Lumina, L. P., Hilliard, C. L., Grill, S., Kellermann, M., Tuite, P., Rolandelli, S., Kang, U. J., Young, J., Rao, J., Cook, M. M., Severt, L., Boyar, K. & Boyar, K. (2014), 'A Randomized Clinical Trial of High-Dosage Coenzyme Q10 in Early Parkinson Disease', *JAMA Neurol.* **71**(5), 543.

Becker, C., Jick, S. S. & Meier, C. R. (2011), 'NSAID use and risk of Parkinson disease: a population-based case-control study', *Eur. J. Neurol.* **18**(11), 1336–1342.

Beckstead, R. M., Domesick, V. B. & Nauta, W. J. (1979), 'Efferent connections of the substantia nigra and ventral tegmental area in the rat', *Brain Res.* **175**(2), 191–217.

Beiske, A. G., Loge, J. H., Rønningen, A. & Svensson, E. (2009), 'Pain in Parkinson's disease: Prevalence and characteristics', *Pain* **141**(1), 173–177.

Bendor, J. T., Logan, T. P. & Edwards, R. H. (2013), 'The function of α-synuclein.', *Neuron* **79**(6), 1044–66.

Bennouar, K. E., Uberti, M. A., Melon, C., Bacolod, M. D., Jimenez, H. N., Cajina, M., Goff, L. K. L., Doller, D. & Gubellini, P. (2013), 'Synergy between L-DOPA and a novel positive allosteric modulator of metabotropic glutamate receptor 4: Implications for Parkinson's disease treatment and dyskinesia', *Neuropharmacology* **66**, 158–169.

Betarbet, R., Sherer, T. B., MacKenzie, G., Garcia-Osuna, M., Panov, A. V. & Greenamyre, J. T. (2000), 'Chronic systemic pesticide exposure reproduces features of Parkinson's disease', *Nat. Neurosci.* **3**(12), 1301–1306.

Betts, M. J., O'Neill, M. J. & Duty, S. (2012), 'Allosteric modulation of the group III mGlu4 receptor provides functional neuroprotection in the 6-hydroxydopamine rat model of Parkinson's disease', *Br J Pharmacol* **166**(8), 2317–2330.

Bezard, E., Gross, C. E. & Brotchie, J. M. (2003), 'Presymptomatic compensation in Parkinson's disease is not dopamine-mediated', *Trends Neurosci.* **26**(4), 215–221.

Biedler, J. L., Roffler-Tarlov, S., Schachner, M. & Freedman, L. S. (1978), 'Multiple neurotransmitter synthesis by human neuroblastoma cell lines and clones.', *Cancer Res.* **38**(11 Pt 1), 3751–7.

Biggs, C. S., Fowler, L. J., Whitton, P. S. & Starr, M. S. (1997), 'Extracellular levels of glutamate and aspartate in the entopeduncular nucleus of the rat determined by microdialysis: regulation by striatal dopamine D2 receptors via the indirect striatal output pathway?', *Brain Res.* **753**(1), 163–75.

Birkmayer, W. & Hornykiewicz, O. (1961), '[The L-3,4-dioxyphenylalanine (DOPA)-effect in Parkinson-akinesia].', *Wien. Klin. Wochenschr.* **73**, 787–8.

Blandini, F., Balestra, B., Levandis, G., Cervio, M., Greco, R., Tassorelli, C., Colucci, M., Faniglione, M., Bazzini, E., Nappi, G., Clavenzani, P., Vigneri, S., De Giorgio, R. & Tonini, M. (2009), 'Functional and neurochemical changes of the gastrointestinal tract in a rodent model of Parkinson's disease', *Neurosci Lett* **467**(3), 203–207.

Blum-Degen, D., Müller, T., Kuhn, W., Gerlach, M., Przuntek, H. & Riederer, P. (1995), 'Interleukin-1 beta and interleukin-6 are elevated in the cerebrospinal fluid of Alzheimer's and de novo Parkinson's disease patients.', *Neurosci. Lett.* **202**(1-2), 17–20.

Bogenpohl, J., Galvan, A., Hu, X., Wichmann, T. & Smith, Y. (2013), 'Metabotropic glutamate receptor 4 in the basal ganglia of parkinsonian monkeys: ultrastructural localization and electrophysiological effects of activation in the striatopallidal complex.', *Neuropharmacology* **66**, 242–52.

Bohnen, N. I., Kaufer, D. I., Ivanco, L. S., Lopresti, B., Koeppe, R. A., Davis, J. G., Mathis, C. A., Moore, R. Y. & DeKosky, S. T. (2003), 'Cortical Cholinergic Function Is More Severely Affected in Parkinsonian Dementia Than in Alzheimer Disease', *Arch. Neurol.* **60**(12), 1745.

Bohnen, N. I., Studenski, S. A., Constantine, G. M. & Moore, R. Y. (2008), 'Diagnostic performance of clinical motor and non-motor tests of Parkinson disease: a matched case-control study', *Eur. J. Neurol.* **15**(7), 685–691.

Bolivar, V. J., Caldarone, B. J., Reilly, A. A. & Flaherty, L. (2000), 'Habituation of Activity in an Open Field: A Survey of Inbred Strains and F1 Hybrids', *Behav. Genet.* **30**(4), 285–293.

Bonito-Oliva, A., Masini, D. & Fisone, G. (2014), 'A mouse model of non-motor symptoms in Parkinson's disease: focus on pharmacological interventions targeting affective dysfunctions.', *Front. Behav. Neurosci.* **8**, 290.

Borgohain, R., Szasz, J., Stanzione, P., Meshram, C., Bhatt, M., Chirilineau, D., Stocchi, F., Lucini, V., Giuliani, R., Forrest, E., Rice, P., Anand, R. & Study 016 Investigators (2014), 'Randomized trial of safinamide add-on to levodopa in Parkinson's disease with motor fluctuations', *Mov. Disord.* **29**(2), 229–237.

Bosch, C., Mailly, P., Degos, B., Deniau, J.-M. & Venance, L. (2012), 'Preservation of the hyperdirect pathway of basal ganglia in a rodent brain slice.', *Neuroscience* **215**, 31–41.

Boshoff, E., Fletcher, E. & Duty, S. (2018), 'Fibroblast growth factor 20 is protective towards dopaminergic neurons in vivo in a paracrine manner', *Neuropharmacology* **137**, 156–163.

Braak, H., de Vos, R. A., Bohl, J. & Del Tredici, K. (2006), 'Gastric α-synuclein immunoreactive inclusions in Meissner's and Auerbach's plexuses in cases staged for Parkinson's disease-related brain pathology', *Neurosci. Lett.* **396**(1), 67–72.

Braak, H., Del Tredici, K., Rüb, U., de Vos, R. A. I., Jansen Steur, E. N. H. & Braak, E. (2003), 'Staging of brain pathology related to sporadic Parkinson's disease.', *Neurobiol. Aging* **24**(2), 197–211.

Braak, H., Rüb, U., Sandmann-Keil, D., Gai, W. P., de Vos, R. A., Jansen Steur, E. N., Arai, K. & Braak, E. (2000), 'Parkinson's disease: affection of brain stem nuclei controlling premotor and motor neurons of the somatomotor system.', *Acta Neuropathol.* **99**(5), 489–95.

Braungart, E., Gerlach, M., Riederer, P., Baumeister, R. & Hoener, M. C. (2004), 'Caenorhabditis elegans MPP+ Model of Parkinson's Disease for High-Throughput Drug Screenings', *Neurodegener. Dis.* **1**(4-5), 175–183.

Brennan, P., Kaba, H. & Keverne, E. B. (1990), 'Olfactory recognition: a simple memory system.', *Science* **250**(4985), 1223–6.

Bretaud, S., Lee, S. & Guo, S. (2004), 'Sensitivity of zebrafish to environmental toxins implicated in Parkinson's disease', *Neurotoxicol. Teratol.* **26**(6), 857–864.

Breysse, N., Baunez, C., Spooren, W., Gasparini, F. & Amalric, M. (2002), 'Chronic but not acute treatment with a metabotropic glutamate 5 receptor antagonist reverses the akinetic deficits in a rat model of parkinsonism.', *J. Neurosci.* **22**(13), 5669–78.

Broadstock, M., Austin, P. J., Betts, M. J. & Duty, S. (2012), 'Antiparkinsonian potential of targeting group III metabotropic glutamate receptor subtypes in the rodent substantia nigra pars reticulata', *Br J Pharmacol* **165**(4b), 1034–1045.

Brocco, M., Dekeyne, A., Veiga, S., Girardon, S. & Millan, M. J. (2002), 'Induction of hyperlocomotion in mice exposed to a novel environment by inhibition of serotonin reuptake: A pharmacological characterization of diverse classes of antidepressant agents', *Pharmacol. Biochem. Behav.* **71**(4), 667–680.

Brooks, J., Ding, J., Simon-Sanchez, J., Paisan-Ruiz, C., Singleton, A. B. & Scholz, S. W. (2009), 'Parkin and PINK1 mutations in early-onset Parkinson's disease: comprehensive screening in publicly available cases and control', *J. Med. Genet.* **46**(6), 375–381.

Brown, A. J., Joseph, P. R. B., Sawant, K. V. & Rajarathnam, K. (2017), 'Chemokine CXCL7 Heterodimers: Structural Insights, CXCR2 Receptor Function, and Glycosaminoglycan Interactions.', *Int. J. Mol. Sci.* **18**(4).

Brown, A. J., Sepuru, K. M. & Rajarathnam, K. (2017), 'Structural Basis of Native CXCL7 Monomer Binding to CXCR2 Receptor N-Domain and Glycosaminoglycan Heparin.', *Int. J. Mol. Sci.* **18**(3).

Brown, L. L., Smith, D. M. & Goldbloom, L. M. (1998), 'Organizing principles of cortical integration in the rat neostriatum: corticostriate map of the body surface is an ordered lattice of curved laminae and radial points.', *J. Comp. Neurol.* **392**(4), 468–88.

Brown, R. G., Landau, S., Hindle, J. V., Playfer, J., Samuel, M., Wilson, K. C., Hurt, C. S., Anderson, R. J., Carnell, J., Dickinson, L., Gibson, G., van Schaick, R., Sellwood, K., Thomas, B. A., Burn, D. J. & PROMS-PD Study Group (2011), 'Depression and anxiety related subtypes in Parkinson's disease', *J. Neurol. Neurosurg. Psychiatry* **82**(7), 803–809.

Brücke, T., Asenbaum, S., Pirker, W., Djamshidian, S., Wenger, S., Wöber, C., Müller, C. & Podreka, I. (1997), 'Measurement of the dopaminergic degeneration in Parkinson's disease with [123I] beta-CIT and SPECT. Correlation with clinical findings and comparison with multiple system atrophy and progressive supranuclear palsy.', *J. Neural Transm. Suppl.* **50**, 9–24.

Brüggemann, N., Mitterer, M., Lanthaler, A. J., Djarmati, A., Hagenah, J., Wiegers, K., Winkler, S., Pawlack, H., Lohnau, T., Pramstaller, P. P., Klein, C. & Lohmann, K. (2009), 'Frequency of heterozygous Parkin mutations in healthy subjects: Need for careful prospective follow-up examination of mutation carriers', *Parkinsonism Relat. Disord.* **15**(6), 425–429.

Burgdorf, J., Kroes, R. A., Zhang, X.-l., Gross, A. L., Schmidt, M., Weiss, C., Disterhoft, J. F., Burch, R. M., Stanton, P. K. & Moskal, J. R. (2015), 'Rapastinel (GLYX-13) has therapeutic potential for the treatment of post-traumatic stress disorder: Characterization of a NMDA receptor-mediated metaplasticity process in the medial prefrontal cortex of rats', *Behav. Brain Res.* **294**, 177–185.

Burns, R. S., Chiueh, C. C., Markey, S. P., Ebert, M. H., Jacobowitz, D. M. & Kopin, I. J. (1983), 'A primate model of parkinsonism: selective destruction of dopaminergic neurons in the pars compacta of the substantia nigra by N-methyl-4-phenyl-1,2,3,6-tetrahydropyridine.', *Proc. Natl. Acad. Sci. U. S. A.* **80**(14), 4546–50.

Burns, T. C., Li, M. D., Mehta, S., Awad, A. J. & Morgan, A. A. (2015), 'Mouse models rarely mimic the transcriptome of human neurodegenerative diseases: A systematic bioinformatics-based critique of preclinical models', *Eur. J. Pharmacol.* **759**, 101–117.

Byrnes, K. R., Stoica, B., Loane, D. J., Riccio, A., Davis, M. I. & Faden, A. I. (2009),

'Metabotropic glutamate receptor 5 activation inhibits microglial associated inflammation and neurotoxicity', *Glia* **57**(5), 550–560.

Cagni, P., Melo, G. C., de Jesus, A. G. & Barros, M. (2014), 'Cannabinoid type-1 receptor ligands, alone or in combination with cocaine, affect vigilance-related behaviors of marmoset monkeys', *Brain Res.* **1550**, 27–35.

Cajina, M., Nattini, M., Song, D., Smagin, G., Jorgensen, E. B., Chandrasena, G., Bundgaard, C., Toft, D. B., Huang, X., Acher, F. & Doller, D. (2014), 'Qualification of LSP1-2111 as a Brain Penetrant Group III Metabotropic Glutamate Receptor Orthosteric Agonist', *ACS Med Chem Lett* **5**(2), 119–123.

Calabresi, P., Maj, R., Pisani, A., Mercuri, N. B. & Bernardi, G. (1992), 'Long-term synaptic depression in the striatum: physiological and pharmacological characterization.', *J. Neurosci.* **12**(11), 4224–33.

Campos, F. L., Carvalho, M. M., Cristovão, A. C., Je, G., Baltazar, G., Salgado, A. J., Kim, Y.-S. & Sousa, N. (2013), 'Rodent models of Parkinson's disease: beyond the motor symptomatology', *Front. Behav. Neurosci.* **7**, 175.

Cannon, J. R., Tapias, V., Na, H. M., Honick, A. S., Drolet, R. E. & Greenamyre, J. T. (2009), 'A highly reproducible rotenone model of Parkinson's disease.', *Neurobiol. Dis.* **34**(2), 279–90.

Cantuti-Castelvetri, I., Keller-McGandy, C., Bouzou, B., Asteris, G., Clark, T. W., Frosch, M. P. & Standaert, D. G. (2007), 'Effects of gender on nigral gene expression and parkinson disease', *Neurobiol. Dis.* **26**(3), 606–614.

Cao, S., Gelwix, C. C., Caldwell, K. A. & Caldwell, G. A. (2005), 'Torsin-mediated protection from cellular stress in the dopaminergic neurons of Caenorhabditis elegans.', *J. Neurosci.* **25**(15), 3801–12.

Caraci, F., Molinaro, G., Battaglia, G., Giuffrida, M. L., Riozzi, B., Traficante, A., Bruno, V., Cannella, M., Merlo, S., Wang, X., Heinz, B. A., Nisenbaum, E. S., Britton, T. C., Drago, F., Sortino, M. A., Copani, A. & Nicoletti, F. (2011), 'Targeting Group II Metabotropic Glutamate (mGlu) Receptors for the Treatment of Psychosis Associated with Alzheimer's Disease: Selective Activation of mGlu2 Receptors Amplifies -Amyloid Toxicity in Cultured Neurons, Whereas Dual Activation of mGlu2 and mG', *Mol. Pharmacol.* **79**(3), 618–626.

Carmine Belin, A., Westerlund, M., Sydow, O., Lundströmer, K., Håkansson, A., Nissbrandt, H., Olson, L. & Galter, D. (2006), 'Leucine-rich repeat kinase 2 (LRRK2) mutations in a Swedish Parkinson cohort and a healthy nonagenarian', *Mov. Disord.* **21**(10), 1731–1734.

Carrasco, E. & Werner, P. (2002), 'Selective destruction of dopaminergic neurons by low concentrations of 6-OHDA and MPP+: protection by acetylsalicylic acid (aspirin)', *Parkinsonism Relat. Disord.* **8**(6), 407–411.

Carriere, N., Besson, P., Dujardin, K., Duhamel, A., Defebvre, L., Delmaire, C. & Devos, D. (2014), 'Apathy in Parkinson's disease is associated with nucleus accumbens atrophy: A magnetic resonance imaging shape analysis', *Mov. Disord.* **29**(7), 897–903.

Carta, M., Carlsson, T., Kirik, D. & Bjorklund, A. (2007), 'Dopamine released from 5-HT terminals is the cause of L-DOPA-induced dyskinesia in parkinsonian rats', *Brain* **130**(7), 1819–1833.

Castor, C. W., Furlong, A. M. & Carter-Su, C. (1985), 'Connective tissue activation: stimulation of glucose transport by connective tissue activating peptide III', *Biochemistry* **24**(7), 1762–1767.

Castor, C. W., Miller, J. W. & Walz, D. A. (1983), 'Structural and biological characteristics of connective tissue activating peptide (CTAP-III), a major human platelet-derived growth factor.', *Proc. Natl. Acad. Sci. U. S. A.* **80**(3), 765–9.

Caudal, D., Alvarsson, A., Björklund, A. & Svenningsson, P. (2015), 'Depressive-like phenotype induced by AAV-mediated overexpression of human α-synuclein in midbrain dopaminergic neurons', *Exp. Neurol.* **273**, 243–252.

Chan, H., Paur, H., Vernon, A. C., Zabarsky, V., Datla, K. P., Croucher, M. J. & Dexter, D. T. (2010), 'Neuroprotection and Functional Recovery Associated with Decreased Microglial Activation Following Selective Activation of mGluR2/3 Receptors in a Rodent Model of Parkinson's Disease', *Park. Dis* **2010**.

Charvin, D., Di Paolo, T., Bezard, E., Gregoire, L., Takano, A., Duvey, G., Pioli, E., Halldin, C., Medori, R. & Conquet, F. (2018), 'An mGlu4-Positive Allosteric Modulator Alleviates Parkinsonism in Primates', *Mov. Disord.* .

Charvin, D., Pomel, V., Ortiz, M., Frauli, M., Scheffler, S., Steinberg, E., Baron, L., Deshons, L., Rudigier, R., Thiarc, D., Morice, C., Manteau, B., Mayer, S., Graham, D., Giethlen, B., Brugger, N., Hédou, G., Conquet, F. & Schann, S. (2017), 'Discovery, Structure–Activity Relationship, and Antiparkinsonian Effect of a Potent and Brain-Penetrant Chemical Series of Positive Allosteric Modulators of Metabotropic Glutamate Receptor 4', *J. Med. Chem.* **60**(20), 8515–8537.

Chauhan, N. B., Siegel, G. J. & Lee, J. M. (2001), 'Depletion of glial cell line-derived neurotrophic factor in substantia nigra neurons of Parkinson's disease brain.', *J. Chem. Neuroanat.* **21**(4), 277–88.

Chen, H., Zhang, S. M., Hernan, M. A., Schwarzschild, M. A., Willett, W. C., Colditz, G. A., Speizer, F. E. & Ascherio, A. (2003), 'Nonsteroidal anti-inflammatory drugs and the risk of Parkinson disease', *Arch Neurol* **60**.

Chen, J. F., Xu, K., Petzer, J. P., Staal, R., Xu, Y. H., Beilstein, M., Sonsalla, P. K., Castagnoli, K., Castagnoli, N. & Schwarzschild, M. A. (2001), 'Neuroprotection by caffeine and A(2A) adenosine receptor inactivation in a model of Parkinson's disease.', *J. Neurosci.* **21**(10), RC143.

Chen, L., Deltheil, T., Turle-Lorenzo, N., Liberge, M., Rosier, C., Watabe, I., Sreng, L., Amalric, M. & Mourre, C. (2014), 'SK channel blockade reverses cognitive and motor deficits induced by nigrostriatal dopamine lesions in rats', *Int J Neuropsychopharmacol* **17**(8), 1295–1306.

Chen, L., Liu, J., Zhang, Q. J., Feng, J. J., Gui, Z. H., Ali, U., Wang, Y., Fan, L. L., Hou, C. & Wang, T. (2011), 'Alterations of emotion, cognition and firing activity of the basolateral nucleus of the amygdala after partial bilateral lesions of the nigrostriatal pathway in rats', *Brain Res. Bull.* **85**(6), 329–338.

Chesselet, M.-F. (2008), 'In vivo alpha-synuclein overexpression in rodents: A useful model of Parkinson's disease?', *Exp. Neurol.* **209**(1), 22–27.

Chien, W.-L., Lee, T.-R., Hung, S.-Y., Kang, K.-H., Wu, R.-M., Lee, M.-J. & Fu, W.-M. (2013), 'Increase of oxidative stress by a novel PINK1 mutation, P209A', *Free Radic. Biol. Med.* **58**, 160–169.

Chiu, W.-H., Depboylu, C., Hermanns, G., Maurer, L., Windolph, A., Oertel, W. H., Ries, V. & Höglinger, G. U. (2015), 'Long-term treatment with L-DOPA or pramipexole affects adult neurogenesis and corresponding non-motor behavior in a mouse model of Parkinson's disease.', *Neuropharmacology* **95**, 367–76.

Chiueh, C. C., Markey, S. P., Burns, R. S., Johannessen, J. N., Pert, A. & Kopin, I. J. (1984), 'Neurochemical and behavioral effects of systemic and intranigral administration of N-methyl-4-phenyl-1,2,3,6-tetrahydropyridine in the rat.', *Eur. J. Pharmacol.* **100**(2), 189–94.

Choi, I., Kim, J., Jeong, H.-K., Kim, B., Jou, I., Park, S. M., Chen, L., Kang, U.-J., Zhuang, X. & Joe, E.-h. (2013), 'Pink1 deficiency attenuates astrocyte proliferation through mitochondrial dysfunction, reduced akt and increased p38 mapk activation, and downregulation of egfr', *Glia* **61**(5), 800–812.

Choi, J. Y., Kim, C. H., Jeon, T. J., Cho, W. G., Lee, J. S., Lee, S. J., Choi, T. H., Kim, B. S., Yi, C. H., Seo, Y., Yi, D. I., Han, S. J., Lee, M., Kim, D. G., Lee, J. D., An, G. & Ryu, Y. H.

(2012), 'Evaluation of dopamine transporters and D2 receptors in hemiparkinsonian rat brains in vivo using consecutive PET scans of [18F]FPCIT and [18F]fallypride', *Appl. Radiat. Isot.* **70**(12), 2689–2694.

Chou, C.-C., Fine, J. S., Pugliese-Sivo, C., Gonsiorek, W., Davies, L., Deno, G., Petro, M., Schwarz, M., Zavodny, P. J. & Hipkin, R. W. (2002), 'Pharmacological characterization of the chemokine receptor, hCCR1 in a stable transfectant and differentiated HL-60 cells: antagonism of hCCR1 activation by MIP-1β', *Br. J. Pharmacol.* **137**(5), 663–675.

Chu, H.-Y., McIver, E. L., Kovaleski, R. F., Atherton, J. F. & Bevan, M. D. (2017), 'Loss of Hyperdirect Pathway Cortico-Subthalamic Inputs Following Degeneration of Midbrain Dopamine Neurons', *Neuron* **95**(6), 1306–1318.e5.

Chung, E., Chen, L., Chan, Y. & Yung, K. (2008), 'Downregulation of glial glutamate transporters after dopamine denervation in the striatum of 6-hydroxydopamine-lesioned rats', *J. Comp. Neurol.* **511**(4), 421–437.

Churchyard, A. & Lees, A. J. (1997), 'The relationship between dementia and direct involvement of the hippocampus and amygdala in Parkinson's disease.', *Neurology* **49**(6), 1570–6.

Clément, Y., Le Guisquet, A.-M., Venault, P., Chapouthier, G. & Belzung, C. (2009), 'Pharmacological Alterations of Anxious Behaviour in Mice Depending on Both Strain and the Behavioural Situation', *PLoS One* **4**(11), e7745.

Çoban, A., Hanagasi, H. A., Karamursel, S. & Barlas, O. (2009), 'Comparison of unilateral pallidotomy and subthalamotomy findings in advanced idiopathic Parkinson's disease', *Br. J. Neurosurg.* **23**(1), 23–29.

Colpaert, F. C. (1987), 'Pharmacological characteristics of tremor, rigidity and hypokinesia induced by reserpine in rat.', *Neuropharmacology* **26**(9), 1431–40.

Colucci, M., Cervio, M., Faniglione, M., De Angelis, S., Pajoro, M., Levandis, G., Tassorelli, C., Blandini, F., Feletti, F., De Giorgio, R., Dellabianca, A., Tonini, S. & Tonini, M. (2012), 'Intestinal dysmotility and enteric neurochemical changes in a Parkinson's disease rat model', *Auton. Neurosci.* **169**(2), 77–86.

Corti, C., Aldegheri, L., Somogyi, P. & Ferraguti, F. (2002), 'Distribution and synaptic localisation of the metabotropic glutamate receptor 4 (mGluR4) in the rodent CNS', *Neuroscience* **110**(3), 403–420.

Corti, C., Battaglia, G., Molinaro, G., Riozzi, B., Pittaluga, A., Corsi, M., Mugnaini, M., Nicoletti, F. & Bruno, V. (2007), 'The Use of Knock-Out Mice Unravels Distinct Roles for mGlu2 and mGlu3 Metabotropic Glutamate Receptors in Mechanisms of Neurodegeneration/Neuroprotection', *J. Neurosci.* **27**(31), 8297–8308.

Costall, B., Domeney, A. M., Naylor, R. J. & Tyers, M. B. (1987), 'Effects of the 5-HT3 receptor antagonist, GR38032F, on raised dopaminergic activity in the mesolimbic system of the rat and marmoset brain.', *Br. J. Pharmacol.* **92**(4), 881–94.

Coulom, H. & Birman, S. (2004), 'Chronic Exposure to Rotenone Models Sporadic Parkinson's Disease in Drosophila melanogaster', *J. Neurosci.* **24**(48), 10993–10998.

Creese, I., Burt, D. R. & Snyder, S. H. (1975), 'Dopamine receptor binding: Differentiation of agonist and antagonist states with 3H-dopamine and 3H-haloperidol', *Life Sci.* **17**(6), 993–1001.

Crosby, N. J., Deane, K. & Clarke, C. E. (2003), 'Amantadine for dyskinesia in Parkinson's disease', *Cochrane Database Syst. Rev.* (2), CD003467.

Cuomo, D., Martella, G., Barabino, E., Platania, P., Vita, D., Madeo, G., Selvam, C., Goudet, C., Oueslati, N., Pin, J.-P., Acher, F., Pisani, A., Beurrier, C., Melon, C., Kerkerian-Le Goff, L. & Gubellini, P. (2009), 'Metabotropic glutamate receptor subtype 4 selectively modulates both glutamate and GABA transmission in the striatum: implications for Parkinson's disease treatment', *J. Neurochem.* **109**(4), 1096–1105.

Curtin, K., Fleckenstein, A. E., Robison, R. J., Crookston, M. J., Smith, K. R. & Hanson, G. R. (2015), 'Methamphetamine/amphetamine abuse and risk of Parkinson's disease in Utah: A population-based assessment', *Drug Alcohol Depend.* **146**, 30–38.

Da Cunha, C., Gevaerd, M. S., Vital, M. A., Miyoshi, E., Andreatini, R., Silveira, R., Takahashi, R. N. & Canteras, N. S. (2001), 'Memory disruption in rats with nigral lesions induced by MPTP: a model for early Parkinson's disease amnesia.', *Behav. Brain Res.* **124**(1), 9–18.

da Rocha, J. T., Pinton, S., Gai, B. M. & Nogueira, C. W. (2013), 'Diphenyl Diselenide Reduces Mechanical and Thermal Nociceptive Behavioral Responses After Unilateral Intrastriatal Administration of 6-Hydroxydopamine in Rats', *Biol. Trace Elem. Res.* **154**(3), 372–378.

Dahlström, A., Wigander, A., Lundmark, K., Gottfries, C. G., Carvey, P. M. & McRae, A. (1990), 'Investigations on auto-antibodies in Alzheimer's and Parkinson's diseases, using defined neuronal cultures.', *J. Neural Transm. Suppl.* **29**, 195–206.

Damier, P., Hirsch, E. C., Agid, Y. & Graybiel, A. M. (1999), 'The substantia nigra of the human brain', *Brain* **122**(8), 1437–1448.

Damier, P., Hirsch, E. C., Zhang, P., Agid, Y. & Javoy-Agid, F. (1993), 'Glutathione peroxidase, glial cells and Parkinson's disease.', *Neuroscience* **52**(1), 1–6.

Davis, E., Foster, T. & Thomas, W. (1994), 'Cellular forms and functions of brain microglia', *Brain Res. Bull.* **34**(1), 73–78.

Davis, G. C., Williams, A. C., Markey, S. P., Ebert, M. H., Caine, E. D., Reichert, C. M. & Kopin, I. J. (1979), 'Chronic Parkinsonism secondary to intravenous injection of meperidine analogues.', *Psychiatry Res.* **1**(3), 249–54.

Dawson, L., Chadha, A., Megalou, M. & Duty, S. (2000), 'The group II metabotropic glutamate receptor agonist, DCG-IV, alleviates akinesia following intranigral or intraventricular administration in the reserpine-treated rat.', *Br. J. Pharmacol.* **129**(3), 541–6.

De Buck, M., Gouwy, M., Proost, P., Struyf, S. & Van Damme, J. (2013), 'Identification and characterization of MIP-1α/CCL3 isoform 2 from bovine serum as a potent monocyte/dendritic cell chemoattractant', *Biochem. Pharmacol.* **85**(6), 789–797.

de Oliveira, A. R., Reimer, A. E., de Macedo, C. E. A., de Carvalho, M. C., Silva, M. A. d. S. & Brandão, M. L. (2011), 'Conditioned fear is modulated by D2 receptor pathway connecting the ventral tegmental area and basolateral amygdala', *Neurobiol. Learn. Mem.* **95**(1), 37–45.

de Rijk, M. C., Launer, L. J., Berger, K., Breteler, M. M., Dartigues, J. F., Baldereschi, M., Fratiglioni, L., Lobo, A., Martinez-Lage, J., Trenkwalder, C. & Hofman, A. (2000), 'Prevalence of Parkinson's disease in Europe: A collaborative study of population-based cohorts. Neurologic Diseases in the Elderly Research Group.', *Neurology* **54**(11 Suppl 5), S21–3.

de Rijk, M. C., Tzourio, C., Breteler, M. M., Dartigues, J. F., Amaducci, L., Lopez-Pousa, S., Manubens-Bertran, J. M., Alpérovitch, A. & Rocca, W. A. (1997), 'Prevalence of parkinsonism and Parkinson's disease in Europe: the EUROPARKINSON Collaborative Study. European Community Concerted Action on the Epidemiology of Parkinson's disease.', *J. Neurol. Neurosurg. Psychiatry* **62**(1), 10–5.

Decamp, E. & Schneider, J. S. (2004), 'Attention and executive function deficits in chronic low-dose MPTP-treated non-human primates', *Eur. J. Neurosci.* **20**(5), 1371–1378.

Deeks, E. D. (2015), 'Safinamide: First Global Approval', *Drugs* **75**(6), 705–711.

Dekundy, A., Pietraszek, M., Schaefer, D., Cenci, M. A. & Danysz, W. (2006), 'Effects of group I metabotropic glutamate receptors blockade in experimental models of Parkinson's disease', *Brain Res. Bull.* **69**(3), 318–326.

DeLong, M. R. (1990), 'Primate models of movement disorders of basal ganglia origin', *Trends Neurosci.* **13**(7), 281–285.

Deniau, J. M., Menetrey, A. & Charpier, S. (1996), 'The lamellar organization of the rat substantia nigra pars reticulata: segregated patterns of striatal afferents and relationship to the topography of corticostriatal projections.', *Neuroscience* **73**(3), 761–81.

Derkinderen, P., Shannon, K. M. & Brundin, P. (2014), 'Gut feelings about smoking and coffee in Parkinson's disease.', *Mov. Disord.* **29**(8), 976–9.

Deutch, A. Y., Goldstein, M., Baldino, F. & Roth, R. H. (1988), 'Telencephalic projections of the A8 dopamine cell group.', *Ann. N. Y. Acad. Sci.* **537**, 27–50.

Di Fonzo, A., Tassorelli, C., De Mari, M., Chien, H. F., Ferreira, J., Rohé, C. F., Riboldazzi, G., Antonini, A., Albani, G., Mauro, A., Marconi, R., Abbruzzese, G., Lopiano, L., Fincati, E., Guidi, M., Marini, P., Stocchi, F., Onofrj, M., Toni, V., Tinazzi, M., Fabbrini, G., Lamberti, P., Vanacore, N., Meco, G., Leitner, P., Uitti, R. J., Wszolek, Z. K., Gasser, T., Simons, E. J., Breedveld, G. J., Goldwurm, S., Pezzoli, G., Sampaio, C., Barbosa, E., Martignoni, E., Oostra, B. A., Bonifati, V. & Italian Parkinson's Genetics Network (2006), 'Comprehensive analysis of the LRRK2 gene in sixty families with Parkinson's disease', *Eur. J. Hum. Genet.* **14**(3), 322–331.

Dias, V., Junn, E. & Mouradian, M. M. (2013), 'The role of oxidative stress in Parkinson's disease.', *J. Parkinsons. Dis.* **3**(4), 461–91.

Djaldetti, R., Yust-Katz, S., Kolianov, V., Melamed, E. & Dabby, R. (2007), 'The effect of duloxetine on primary pain symptoms in Parkinson disease.', *Clin. Neuropharmacol.* **30**(4), 201–5.

Dluzen, D. E. (1992), '1-Methyl-4-phenyl-1,2,3,6-tetrahydropyridine (MPTP) reduces norepinephrine concentrations in the olfactory bulbs of male mice', *Brain Res.* **586**(1), 144–147.

Dominguez-Meijide, A., Rodriguez-Perez, A. I., Diaz-Ruiz, C., Guerra, M. J. & Labandeira-Garcia, J. L. (2017), 'Dopamine modulates astroglial and microglial activity via glial renin-angiotensin system in cultures', *Brain. Behav. Immun.* **62**, 277–290.

Doty, R. L., Ferguson-Segall, M., Lucki, I. & Kreider, M. (1988), 'Effects of intrabulbar injections of 6-hydroxydopamine on ethyl acetate odor detection in castrate and non-castrate male rats.', *Brain Res.* **444**(1), 95–103.

Doumazane, E., Scholler, P., Zwier, J. M., Trinquet, E., Rondard, P. & Pin, J.-P. (2011), 'A new approach to analyze cell surface protein complexes reveals specific heterodimeric metabotropic glutamate receptors', *FASEB J.* **25**(1), 66–77.

Drolet, R. E., Cannon, J. R., Montero, L. & Greenamyre, J. T. (2009), 'Chronic rotenone exposure reproduces Parkinson's disease gastrointestinal neuropathology', *Neurobiol. Dis.* **36**(1), 96–102.

Dufour, J. H., Dziejman, M., Liu, M. T., Leung, J. H., Lane, T. E. & Luster, A. D. (2002), 'IFN-gamma-inducible protein 10 (IP-10; CXCL10)-deficient mice reveal a role for IP-10 in effector T cell generation and trafficking.', *J. Immunol.* **168**(7), 3195–204.

Duke, D. C., Moran, L. B., Pearce, R. K. B. & Graeber, M. B. (2007), 'The medial and lateral substantia nigra in Parkinson's disease: mRNA profiles associated with higher brain tissue vulnerability', *Neurogenetics* **8**(2), 83–94.

Duty, S. & Jenner, P. (2011), 'Animal models of Parkinson's disease: a source of novel treatments and clues to the cause of the disease', *Br J Pharmacol* **164**(4), 1357–1391.

Ellegård, R., Crisci, E., Burgener, A., Sjöwall, C., Birse, K., Westmacott, G., Hinkula, J., Lifson, J. D. & Larsson, M. (2014), 'Complement Opsonization of HIV-1 Results in Decreased Antiviral and Inflammatory Responses in Immature Dendritic Cells via CR3', *J. Immunol.* **193**(9), 4590–4601.

Emmrich, J. V., Hornik, T. C., Neher, J. J. & Brown, G. C. (2013), 'Rotenone induces neuronal death by microglial phagocytosis of neurons', *FEBS J.* **280**(20), 5030–5038.

Engele, J. & Bohn, M. C. (1991), 'The neurotrophic effects of fibroblast growth factors on dopaminergic neurons in vitro are mediated by mesencephalic glia.', *J. Neurosci.* **11**(10), 3070–8.

Eslamboli, A., Georgievska, B., Ridley, R. M., Baker, H. F., Muzyczka, N., Burger, C., Mandel, R. J., Annett, L. & Kirik, D. (2005), 'Continuous Low-Level Glial Cell Line-Derived Neurotrophic Factor Delivery Using Recombinant Adeno-Associated Viral Vectors Provides Neuroprotection and Induces Behavioral Recovery in a Primate Model of Parkinson's Disease', *J. Neurosci.* **25**(4), 769–777.

Espay, A. J., LeWitt, P. A. & Kaufmann, H. (2014), 'Norepinephrine deficiency in Parkinson's disease: The case for noradrenergic enhancement', *Mov. Disord.* **29**(14), 1710–1719.

Espejo, E. F. & Mir, D. (1993), 'Structure of the rat's behaviour in the hot plate test', *Behav Brain Res* **56**(2), 171–176.

Esteve-Rudd, J., Fernández-Sánchez, L., Lax, P., De Juan, E., Martín-Nieto, J. & Cuenca, N. (2011), 'Rotenone induces degeneration of photoreceptors and impairs the dopaminergic system in the rat retina', *Neurobiol. Dis.* **44**(1), 102–115.

Evans, A. H., Lawrence, A. D., Potts, J., MacGregor, L., Katzenschlager, R., Shaw, K., Zijlmans, J. & Lees, A. J. (2005), 'Relationship between impulsive sensation seeking traits, smoking, alcohol and caffeine intake, and Parkinson's disease', *J. Neurol. Neurosurg. Psychiatry* **77**(3), 317–321.

Even, C. & Weintraub, D. (2012), 'Is depression in Parkinson's Disease (PD) a specific entity?', *J. Affect. Disord.* **139**(2), 103–112.

Evenden, J. L., Marston, H. M., Jones, G. H., Giardini, V., Lenard, L., Everitt, B. J. & Robbins, T. W. (1989), 'Effects of excitotoxic lesions of the substantia innominata, ventral and dorsal globus pallidus on visual discrimination acquisition, performance and reversal in the rat.', *Behav. Brain Res.* **32**(2), 129–49.

Fang, F., Chen, H., Feldman, A. L., Kamel, F., Ye, W. & Wirdefeldt, K. (2012), 'Head injury and Parkinson's disease: A population-based study', *Mov. Disord.* **27**(13), 1632–1635.

Feany, M. B. & Bender, W. W. (2000), 'A Drosophila model of Parkinson's disease', *Nature* **404**(6776), 394–398.

Fearnley, J. M. & Lees, A. J. (1991), 'Ageing and Parkinson's Disease: Substantia Nigra Regional Selectivity', *Brain* **114**(5), 2283–2301.

Feng, C.-W., Wen, Z.-H., Huang, S.-Y., Hung, H.-C., Chen, C.-H., Yang, S.-N., Chen, N.-F., Wang, H.-M., Hsiao, C.-D. & Chen, W.-F. (2014), 'Effects of 6-Hydroxydopamine Exposure on Motor Activity and Biochemical Expression in Zebrafish (Danio Rerio) Larvae', *Zebrafish* **11**(3), 227–239.

Fenster, C. P., Whitworth, T. L., Sheffield, E. B., Quick, M. W. & Lester, R. A. (1999), 'Upregulation of surface alpha4beta2 nicotinic receptors is initiated by receptor desensitization after chronic exposure to nicotine.', *J. Neurosci.* **19**(12), 4804–14.

Ferger, B., Teismann, P., Earl, C., Kuschinsky, K. & Oertel, W. (1999), 'Salicylate protects against MPTP-induced impairments in dopaminergic neurotransmission at the striatal and nigral level in mice', *Naunyn. Schmiedebergs. Arch. Pharmacol.* **360**(3), 256–261.

Ferguson, J. N., Young, L. J. & Insel, T. R. (2002), 'The Neuroendocrine Basis of Social Recognition', *Front. Neuroendocrinol.* **23**(2), 200–224.

Fernandez-Ruiz, J., Doudet, D. J. & Aigner, T. G. (1995), 'Long-term cognitive impairment in MPTP-treated rhesus monkeys.', *Neuroreport* **7**(1), 102–4.

Fifel, K., Dkhissi-Benyahya, O. & Cooper, H. M. (2013), 'Lack of long-term changes in circadian, locomotor, and cognitive functions in acute and chronic MPTP (1-methyl-4-phenyl-1,2,3,6-tetrahydropyridine) mouse models of parkinson's disease', *Chronobiol. Int.* **30**(6), 741–755.

Fifel, K., Vezoli, J., Dzahini, K., Claustrat, B., Leviel, V., Kennedy, H., Procyk, E., Dkhissi-Benyahya, O., Gronfier, C. & Cooper, H. M. (2014), 'Alteration of daily and circadian rhythms following dopamine depletion in MPTP treated non-human primates.', *PLoS One* **9**(1), e86240.

Finehout, E. J., Franck, Z. & Lee, K. H. (2005), 'Complement protein isoforms in CSF as possible biomarkers for neurodegenerative disease.', *Dis. Markers* **21**(2), 93–101.

Finlay, C. J. (2014), Investigating group III metabotropic glutamate receptors as novel therapeutic targets in Parkinson's disease and Levodopa-induced dyskinesia - Research Portal, King's College, London, PhD thesis, King's College London.

Fisher, R., Lincoln, L., Jackson, M. J., Abbate, V., Jenner, P., Hider, R., Lees, A. & Rose, S. (2018), 'The effect of Banisteriopsis caapi (B. caapi) on the motor deficits in the MPTP-treated common marmoset model of Parkinson's disease', *Phyther. Res.* **32**(4), 678–687.

Fleming, S. M., Tetreault, N. A., Mulligan, C. K., Hutson, C. B., Masliah, E. & Chesselet, M.-F. (2008), 'Olfactory deficits in mice overexpressing human wildtype alpha-synuclein.', *Eur. J. Neurosci.* **28**(2), 247–56.

Flinn, L., Bretaud, S., Lo, C., Ingham, P. W. & Bandmann, O. (2008), 'Zebrafish as a new animal model for movement disorders', *J. Neurochem.* **106**(5), 1991–1997.

Foster, H. D. & Hoffer, A. (2004), 'The two faces of L-DOPA: benefits and adverse side effects in the treatment of Encephalitis lethargica, Parkinson's disease, multiple sclerosis and amyotrophic lateral sclerosis', *Med. Hypotheses* **62**(2), 177–181.

Fox, S. H., Katzenschlager, R., Lim, S.-Y., Ravina, B., Seppi, K., Coelho, M., Poewe, W., Rascol, O., Goetz, C. G. & Sampaio, C. (2011), 'The Movement Disorder Society Evidence-Based Medicine Review Update: Treatments for the motor symptoms of Parkinson's disease', *Mov. Disord.* **26**(S3), S2–S41.

Freire, C. & Koifman, S. (2012), 'Pesticide exposure and Parkinson's disease: Epidemiological evidence of association', *Neurotoxicology* **33**(5), 947–971.

Frisina, P. G., Haroutunian, V. & Libow, L. S. (2009), 'The neuropathological basis for depression in Parkinson's disease', *Parkinsonism Relat. Disord.* **15**(2), 144–148.

Fu, R.-H., Harn, H.-J., Liu, S.-P., Chen, C.-S., Chang, W.-L., Chen, Y.-M., Huang, J.-E., Li, R.-J., Tsai, S.-Y., Hung, H.-S., Shyu, W.-C., Lin, S.-Z. & Wang, Y.-C. (2014), 'n-Butylidenephthalide Protects against Dopaminergic Neuron Degeneration and α-Synuclein Accumulation in Caenorhabditis elegans Models of Parkinson's Disease', *PLoS One* **9**(1), e85305.

Fukushima, K., Kobuchi, S., Mizuhara, K., Aoyama, H., Takada, K. & Sugioka, N. (2013), 'Time-Dependent Interaction of Ritonavir in Chronic Use: The Power Balance Between Inhibition and Induction of P-Glycoprotein and Cytochrome P450 3A', *J. Pharm. Sci.* **102**(6), 2044–2055.

Gage, G. J., Stoetzner, C. R., Wiltschko, A. B. & Berke, J. D. (2010), 'Selective activation of striatal fast-spiking interneurons during choice execution.', *Neuron* **67**(3), 466–79.

Gainetdinov, R. R., Fumagalli, F., Jones, S. R. & Caron, M. G. (1997), 'Dopamine transporter is required for in vivo MPTP neurotoxicity: evidence from mice lacking the transporter.', *J. Neurochem.* **69**(3), 1322–5.

Galasko, D. (2017), 'Lewy Body Disorders.', *Neurol. Clin.* **35**(2), 325–338.

Galati, S. & Di Giovanni, G. (2010), 'Neuroprotection in Parkinson's Disease: a Realistic Goal?', *CNS Neurosci. Ther.* **16**(6), 327–329.

Galeffi, F., Bianchi, L., Bolam, J. P. & Della Corte, L. (2003), 'The effect of 6-hydroxydopamine lesions on the release of amino acids in the direct and indirect pathways of the basal ganglia: a dual microdialysis probe analysis.', *Eur. J. Neurosci.* **18**(4), 856–68.

Galter, D., Pernold, K., Yoshitake, T., Lindqvist, E., Hoffer, B., Kehr, J., Larsson, N.-G. & Olson, L. (2010), 'MitoPark mice mirror the slow progression of key symptoms and L-DOPA response in Parkinson's disease', *Genes, Brain Behav.* **9**(2), 173–181.

Galvan, A. & Wichmann, T. (2008), 'Pathophysiology of Parkinsonism', *Clin. Neurophysiol.* **119**(7), 1459–1474.

Gangarossa, G., Espallergues, J., Mailly, P., De Bundel, D., de Kerchove d'Exaerde, A., Hervé, D., Girault, J.-A., Valjent, E. & Krieger, P. (2013), 'Spatial distribution of D1R- and D2R-expressing medium-sized spiny neurons differs along the rostro-caudal axis of the mouse dorsal striatum.', *Front. Neural Circuits* **7**, 124.

Gao, H.-M., Hong, J.-S., Zhang, W. & Liu, B. (2002), 'Distinct role for microglia in rotenone-induced degeneration of dopaminergic neurons.', *J. Neurosci.* **22**(3), 782–90.

Gao, X., Chen, H., Schwarzschild, M. A. & Ascherio, A. (2011), 'Use of ibuprofen and risk of Parkinson disease.', *Neurology* **76**(10), 863–9.

Gardoni, F., Picconi, B., Ghiglieri, V., Polli, F., Bagetta, V., Bernardi, G., Cattabeni, F., Di Luca, M. & Calabresi, P. (2006), 'A critical interaction between NR2B and MAGUK in L-DOPA induced dyskinesia.', *J Neurosci* **26**(11), 2914–22.

Gatto, E. M., Riobó, N. A., Carreras, M., Cherñavsky, A., Rubio, A., Satz, M. & Poderoso, J. J. (2000), 'Overexpression of Neutrophil Neuronal Nitric Oxide Synthase in Parkinson's Disease', *Nitric Oxide* **4**(5), 534–539.

Gelpi, E., Navarro-Otano, J., Tolosa, E., Gaig, C., Compta, Y., Rey, M. J., Martí, M. J., Hernández, I., Valldeoriola, F., Reñé, R. & Ribalta, T. (2014), 'Multiple organ involvement by alpha-synuclein pathology in Lewy body disorders', *Mov. Disord.* **29**(8), 1010–1018.

Gerdelat-Mas, A., Simonetta-Moreau, M., Thalamas, C., Ory-Magne, F., Slaoui, T., Rascol, O. & Brefel-Courbon, C. (2007), 'Levodopa raises objective pain threshold in Parkinson's disease: a RIII reflex study', *J. Neurol. Neurosurg. & Psychiatry* **78**(10), 1140–1142.

Geurts, J. J. G., Wolswijk, G., Bö, L., Redeker, S., Ramkema, M., Troost, D. & Aronica, E. (2005), 'Expression patterns of Group III metabotropic glutamate receptors mGluR4 and mGluR8 in multiple sclerosis lesions.', *J. Neuroimmunol.* **158**(1-2), 182–90.

Ghilardi, M. F., Bodis-Wollner, I., Onofrj, M. C., Marx, M. S. & Glover, A. A. (1988), 'Spatial frequency-dependent abnormalities of the pattern electroretinogram and visual evoked potentials in a parkinsonian monkey model.', *Brain* **111 (Pt 1**, 131–49.

Giasson, B. I., Duda, J. E., Quinn, S. M., Zhang, B., Trojanowski, J. Q. & Lee, V. M.-Y. (2002), 'Neuronal alpha-synucleinopathy with severe movement disorder in mice expressing A53T human alpha-synuclein.', *Neuron* **34**(4), 521–33.

Gill, S. S., Patel, N. K., Hotton, G. R., O'Sullivan, K., McCarter, R., Bunnage, M., Brooks, D. J., Svendsen, C. N. & Heywood, P. (2003), 'Direct brain infusion of glial cell line–derived neurotrophic factor in Parkinson disease', *Nat. Med.* **9**(5), 589–595.

Glinka, Y. Y. & Youdim, M. B. (1995), 'Inhibition of mitochondrial complexes I and IV by 6-hydroxydopamine.', *Eur. J. Pharmacol.* **292**(3-4), 329–32.

Godbout, J. P. & Johnson, R. W. (2006), 'Age and Neuroinflammation: A Lifetime of Psychoneuroimmune Consequences', *Neurol. Clin.* **24**(3), 521–538.

Gokul, K. & Muralidhara (2014), 'Oral Supplements of Aqueous Extract of Tomato Seeds Alleviate Motor Abnormality, Oxidative Impairments and Neurotoxicity Induced by Rotenone in Mice: Relevance to Parkinson's Disease', *Neurochem. Res.* **39**(7), 1382–1394.

Goldin, E. (2010), 'Gaucher disease and parkinsonism, a molecular link theory', *Mol. Genet. Metab.* **101**(4), 307–310.

Goldstein, J. M., Barnett, A. & Malick, J. B. (1975), 'The evaluation of anti-parkinson drugs on reserpine-induced rigidity in rats', *Eur. J. Pharmacol.* **33**(1), 183–188.

Gómez-Paz, A., Drucker-Colín, R., Milán-Aldaco, D., Palomero-Rivero, M. & Ambriz-Tututi, M. (2017), 'Intrastriatal chromospheres' transplant reduces nociception in hemiparkinsonian rats', *Neuroscience* .

Gómez-Suaga, P., Fdez, E., Fernández, B., Martínez-Salvador, M., Blanca Ramírez, M., Madero-Pérez, J., Rivero-Ríos, P., Fuentes, J. & Hilfiker, S. (2014), 'Novel insights into the neurobiology underlying LRRK2-linked Parkinson's disease', *Neuropharmacology* **85**, 45–56.

Gomeza, J., Joly, C., Kuhn, R., Knöpfel, T., Bockaert, J. & Pin, J. P. (1996), 'The second intracellular loop of metabotropic glutamate receptor 1 cooperates with the other intracellular domains to control coupling to G-proteins.', *J. Biol. Chem.* **271**(4), 2199–205.

Gomide, V. G., Bibancos, T. & Chadi, G. (2005), 'DOPAMINE CELL MORPHOLOGY AND GLIAL CELL HYPERTROPHY AND PROCESS BRANCHING IN THE NIGROSTRIATAL SYSTEM AFTER STRIATAL 6-OHDA ANALYZED BY SPECIFIC STEROLOGICAL TOOLS', *Int. J. Neurosci.* **115**(4), 557–582.

Graham, W., Robertson, R., Sambrook, M. & Crossman, A. (1990), 'Injection of excitatory amino acid antagonists into the medial pallidal segment of a 1-methyl-4-phenyl-1,2,3,6-tetrahydropyridine (MPTP) treated primate reverses motor symptoms of parkinsonism', *Life Sci.* **47**(18), PL91–PL97.

Gravius, A., Dekundy, A., Nagel, J., Morè, L., Pietraszek, M. & Danysz, W. (2008), 'Investigation on tolerance development to subchronic blockade of mGluR5 in models of learning, anxiety, and levodopa-induced dyskinesia in rats', *J. Neural Transm.* **115**(12), 1609–1619.

Greene, J. G. (2014), 'Causes and Consequences of Degeneration of the Dorsal Motor Nucleus of the Vagus Nerve in Parkinson's Disease', *Antioxid. Redox Signal.* **21**(4), 649–667.

Greene, J. G., Noorian, A. R. & Srinivasan, S. (2009), 'Delayed gastric emptying and enteric nervous system dysfunction in the rotenone model of Parkinson's disease', *Exp. Neurol.* **218**(1), 154–161.

Greenhalgh, C. J. & Hilton, D. J. (2001), 'Negative regulation of cytokine signaling.', *J. Leukoc. Biol.* **70**(3), 348–56.

Grünblatt, E., Mandel, S., Maor, G. & Youdim, M. B. (2001), 'Gene expression analysis in N-methyl-4-phenyl-1,2,3,6-tetrahydropyridine mice model of Parkinson's disease using cDNA microarray: effect of R-apomorphine.', *J. Neurochem.* **78**(1), 1–12.

Guarino, C., Hamon, Y., Croix, C., Lamort, A.-S., Dallet-Choisy, S., Marchand-Adam, S., Lesner, A., Baranek, T., Viaud-Massuard, M.-C., Lauritzen, C., Pedersen, J., Heuzé-Vourc'h, N., Si-Tahar, M., Fıratlı, E., Jenne, D. E., Gauthier, F., Horwitz, M. S., Borregaard, N. & Korkmaz, B. (2017), 'Prolonged pharmacological inhibition of cathepsin C results in elimination of neutrophil serine proteases', *Biochem. Pharmacol.* **131**, 52–67.

Gubellini, P., Melon, C., Dale, E., Doller, D. & Kerkerian-Le Goff, L. (2014), 'Distinct effects of mGlu4 receptor positive allosteric modulators at corticostriatal vs. striatopallidal synapses may differentially contribute to their antiparkinsonian action', *Neuropharmacology* **85**, 166–177.

Gunaydin, L. A., Grosenick, L., Finkelstein, J. C., Kauvar, I. V., Fenno, L. E., Adhikari, A., Lammel, S., Mirzabekov, J. J., Airan, R. D., Zalocusky, K. A., Tye, K. M., Anikeeva, P., Malenka, R. C. & Deisseroth, K. (2014), 'Natural Neural Projection Dynamics Underlying Social Behavior', *Cell* **157**(7), 1535–1551.

Guo, M. (2012), 'Drosophila as a model to study mitochondrial dysfunction in Parkinson's disease.', *Cold Spring Harb. Perspect. Med.* **2**(11), a009944.

Gupta, D. K., Hang, X., Liu, R., Hasan, A. & Feng, Z. (2016), 'Levodopa-Induced Motor and Dopamine Receptor Changes in Caenorhabditis elegans Overexpressing Human Alpha-Synuclein.', *Neurodegener. Dis.* **16**(3-4), 179–83.

Ha, A. D. & Jankovic, J. (2012), 'Pain in Parkinson's disease', *Mov. Disord.* **27**(4), 485–491.

Haahr, M. (1998), 'RANDOM.ORG - True Random Number Service'.

Haavik, J., Andersson, K. K., Petersson, L. & Flatmark, T. (1988), 'Soluble tyrosine hydroxylase (tyrosine 3-monooxygenase) from bovine adrenal medulla: Large-scale purification and physicochemical properties', *Biochim. Biophys. Acta - Protein Struct. Mol. Enzymol.* **953**, 142–156.

Håkansson, A., Westberg, L., Nilsson, S., Buervenich, S., Carmine, A., Holmberg, B., Sydow, O., Olson, L., Johnels, B., Eriksson, E. & Nissbrandt, H. (2005), 'Interaction of polymorphisms in the genes encoding interleukin-6 and estrogen receptor beta on the susceptibility to Parkinson's disease', *Am. J. Med. Genet. Part B Neuropsychiatr. Genet.* **133B**(1), 88–92.

Hallett, P. J., McLean, J. R., Kartunen, A., Langston, J. W. & Isacson, O. (2012), 'Alpha-synuclein overexpressing transgenic mice show internal organ pathology and autonomic deficits', *Neurobiol. Dis.* **47**(2), 258–267.

Hallett, P. J. & Standaert, D. G. (2004), 'Rationale for and use of NMDA receptor antagonists in Parkinson's disease', *Pharmacol. Ther.* **102**(2), 155–174.

Hamamichi, S., Rivas, R. N., Knight, A. L., Cao, S., Caldwell, K. A. & Caldwell, G. A. (2008), 'Hypothesis-based RNAi screening identifies neuroprotective genes in a Parkinson's disease model.', *Proc. Natl. Acad. Sci. U. S. A.* **105**(2), 728–33.

Hamill, R. W., Tompkins, J. D., Girard, B. M., Kershen, R. T., Parsons, R. L. & Vizzard, M. A. (2012), 'Autonomic dysfunction and plasticity in micturition reflexes in human α-synuclein mice.', *Dev. Neurobiol.* **72**(6), 918–36.

Hanaway, J., McConnell, J. A. & Netsky, M. G. (1970), 'Cytoarchitecture of the substantia nigra in the rat', *Am. J. Anat.* **129**(4), 417–437.

Hånell, A. & Marklund, N. (2014), 'Structured evaluation of rodent behavioral tests used in drug discovery research.', *Front. Behav. Neurosci.* **8**, 252.

Hanrott, K., Gudmunsen, L., O'Neill, M. J. & Wonnacott, S. (2006), '6-hydroxydopamine-induced apoptosis is mediated via extracellular auto-oxidation and caspase 3-dependent activation of protein kinase Cdelta.', *J. Biol. Chem.* **281**(9), 5373–82.

Hardman, C. D., Henderson, J. M., Finkelstein, D. I., Horne, M. K., Paxinos, G. & Halliday, G. M. (2002), 'Comparison of the basal ganglia in rats, marmosets, macaques, baboons, and humans: volume and neuronal number for the output, internal relay, and striatal modulating nuclei.', *J. Comp. Neurol.* **445**(3), 238–55.

Harms, A. S., Barnum, C. J., Ruhn, K. A., Varghese, S., Treviño, I., Blesch, A. & Tansey, M. G. (2011), 'Delayed dominant-negative TNF gene therapy halts progressive loss of nigral dopaminergic neurons in a rat model of Parkinson's disease.', *Mol. Ther.* **19**(1), 46–52.

Harris, M. A., Shen, H., Marion, S. A., Tsui, J. K. C. & Teschke, K. (2013), 'Head injuries and Parkinson's disease in a case-control study', *Occup. Environ. Med.* **70**(12), 839–844.

Hauser, M. A., Li, Y.-J., Xu, H., Noureddine, M. A., Shao, Y. S., Gullans, S. R., Scherzer, C. R., Jensen, R. V., McLaurin, A. C., Gibson, J. R., Scott, B. L., Jewett, R. M., Stenger, J. E., Schmechel, D. E., Hulette, C. M. & Vance, J. M. (2005), 'Expression Profiling of Substantia Nigra in Parkinson Disease, Progressive Supranuclear Palsy, and Frontotemporal Dementia With Parkinsonism', *Arch. Neurol.* **62**(6), 917–21.

Hazim, A. I., Ramanathan, S., Parthasarathy, S., Muzaimi, M. & Mansor, S. M. (2014), 'Anxiolytic-like effects of mitragynine in the open-field and elevated plus-maze tests in rats', *J. Physiol. Sci.* **64**(3), 161–169.

Hefti, F., Melamed, E. & Wurtman, R. J. (1980), 'Partial lesions of the dopaminergic nigrostriatal system in rat brain: biochemical characterization', *Brain Res* **195**(1), 123–137.

Heikkila, R. E., Hess, A. & Duvoisin, R. C. (1984), 'Dopaminergic neurotoxicity of 1-methyl-4-phenyl-1,2,5,6-tetrahydropyridine in mice.', *Science* **224**(4656), 1451–3.

Heikkila, R. E., Manzino, L., Cabbat, F. S. & Duvoisin, R. C. (1984), 'Protection against the dopaminergic neurotoxicity of 1-methyl-4-phenyl-1,2,5,6-tetrahydropyridine by monoamine oxidase inhibitors.', *Nature* **311**(5985), 467–9.

Heikkila, R. E., Nicklas, W. J., Vyas, I. & Duvoisin, R. C. (1985), 'Dopaminergic toxicity of rotenone and the 1-methyl-4-phenylpyridinium ion after their stereotaxic administration to rats: Implication for the mechanism of 1-methyl-4-phenyl-1,2,3,6-tetrahydropyridine toxicity', *Neurosci. Lett.* **62**(3), 389–394.

Heintz, N. & Gerfen, C. (n.d.), 'GENSAT Brain Atlas of gene expression in EGFP Transgenic Mice'.

Heinz, S., Freyberger, A., Lawrenz, B., Schladt, L., Schmuck, G. & Ellinger-Ziegelbauer, H. (2017), 'Mechanistic Investigations of the Mitochondrial Complex I Inhibitor Rotenone in the Context of Pharmacological and Safety Evaluation', *Sci. Rep.* **7**, 45465.

Heise, C. E., Pahuja, A., Hudson, S. C., Mistry, M. S., Putnam, A. L., Gross, M. M., Gottlieb, P. A., Wade, W. S., Kiankarimi, M., Schwarz, D., Crowe, P., Zlotnik, A. & Alleva, D. G. (2005), 'Pharmacological Characterization of CXC Chemokine Receptor 3 Ligands and a Small Molecule Antagonist', *J. Pharmacol. Exp. Ther.* **313**(3), 1263–1271.

Hely, M. A., Morris, J. G., Reid, W. G. & Trafficante, R. (2005), 'Sydney multicenter study of Parkinson's disease: Non-L-dopa-responsive problems dominate at 15 years', *Mov. Disord.* **20**(2), 190–199.

Hely, M. A., Reid, W. G., Adena, M. A., Halliday, G. M. & Morris, J. G. (2008), 'The Sydney multicenter study of Parkinson's disease: The inevitability of dementia at 20 years', *Mov. Disord.* **23**(6), 837–844.

Hernandez-Baltazar, D., Mendoza-Garrido, M. E. & Martinez-Fong, D. (2013), 'Activation of GSK-3β and caspase-3 occurs in Nigral dopamine neurons during the development of apoptosis activated by a striatal injection of 6-hydroxydopamine.', *PLoS One* **8**(8), e70951.

Hernandez-Lopez, S., Tkatch, T., Perez-Garci, E., Galarraga, E., Bargas, J., Hamm, H. & Surmeier, D. J. (2000), 'D2 dopamine receptors in striatal medium spiny neurons reduce L-type Ca2+ currents and excitability via a novel PLC[beta]1-IP3-calcineurin-signaling cascade.', *J. Neurosci.* **20**(24), 8987–95.

Herrera, A., Castaño, A., Venero, J., Cano, J. & Machado, A. (2000), 'The Single Intranigral Injection of LPS as a New Model for Studying the Selective Effects of Inflammatory Reactions on Dopaminergic System', *Neurobiol. Dis.* **7**(4), 429–447.

Heusinkveld, H. J. & Westerink, R. H. (2017), 'Comparison of different in vitro cell models for the assessment of pesticide-induced dopaminergic neurotoxicity', *Toxicol. Vitr.* **45**, 81–88.

Hibell, A. D., Kidd, E. J., Chessell, I. P., Humphrey, P. P. & Michel, A. D. (2000), 'Apparent species differences in the kinetic properties of P2X(7) receptors.', *Br. J. Pharmacol.* **130**(1), 167–73.

Hilker, R., Portman, A., Voges, J., Staal, M., Burghaus, L., van Laar, T., Koulousakis, A., Maguire, R., Pruim, J., de Jong, B. M., Herholz, K., Sturm, V., Heiss, W. & Leenders, K. (2005), 'Disease progression continues in patients with advanced Parkinson's disease and effective subthalamic nucleus stimulation', *J Neurol Neurosurg Psychiatry* **76**(9), 1217–1221.

Hirsch, D. B., Steiner, J. P., Dawson, T. M., Mammen, A., Hayek, E. & Snyder, S. H. (1993), 'Neurotransmitter release regulated by nitric oxide in PC-12 cells and brain synaptosomes.', *Curr. Biol.* **3**(11), 749–54.

Hoehn, M. M. & Yahr, M. D. (1967), 'Parkinsonism: onset, progression and mortality.', *Neurology* **17**(5), 427–42.

Hoekstra, J. G., Cook, T. J., Stewart, T., Mattison, H., Dreisbach, M. T., Hoffer, Z. S. & Zhang, J. (2015), 'Astrocytic Dynamin-Like Protein 1 Regulates Neuronal Protection against Excitotoxicity in Parkinson Disease', *Am. J. Pathol.* **185**(2), 536–549.

Hollerman, J. R. & Grace, A. A. (1992), 'Subthalamic nucleus cell firing in the 6-OHDA-treated rat: basal activity and response to haloperidol.', *Brain Res.* **590**(1-2), 291–9.

Holloway, R. G., Shoulson, I., Fahn, S., Kieburtz, K., Lang, A., Marek, K., McDermott, M., Seibyl, J., Weiner, W., Musch, B., Kamp, C., Welsh, M., Shinaman, A., Pahwa, R., Barclay, L., Hubble, J., LeWitt, P., Miyasaki, J., Suchowersky, O., Stacy, M., Russell, D. S., Ford, B., Hammerstad, J., Riley, D., Standaert, D., Wooten, F., Factor, S., Jankovic, J., Atassi, F., Kurlan, R., Panisset, M., Rajput, A., Rodnitzky, R., Shults, C., Petsinger, G., Waters, C.,

Pfeiffer, R., Biglan, K., Borchert, L., Montgomery, A., Sutherland, L., Weeks, C., DeAngelis, M., Sime, E., Wood, S., Pantella, C., Harrigan, M., Fussell, B., Dillon, S., Alexander-Brown, B., Rainey, P., Tennis, M., Rost-Ruffner, E., Brown, D., Evans, S., Berry, D., Hall, J., Shirley, T., Dobson, J., Fontaine, D., Pfeiffer, B., Brocht, A., Bennett, S., Daigneault, S., Hodgeman, K., O'Connell, C., Ross, T., Richard, K., Watts, A. & Parkinson Study Group (2004), 'Pramipexole vs Levodopa as Initial Treatment for Parkinson Disease', *Arch. Neurol.* **61**(7), 1044–53.

Honig, H., Antonini, A., Martinez-Martin, P., Forgacs, I., Faye, G. C., Fox, T., Fox, K., Mancini, F., Canesi, M., Odin, P. & Chaudhuri, K. R. (2009), 'Intrajejunal levodopa infusion in Parkinson's disease: A pilot multicenter study of effects on nonmotor symptoms and quality of life', *Mov. Disord.* **24**(10), 1468–1474.

Hoozemans, J., van Haastert, E., Eikelenboom, P., de Vos, R., Rozemuller, J. & Scheper, W. (2007), 'Activation of the unfolded protein response in Parkinson's disease', *Biochem. Biophys. Res. Commun.* **354**(3), 707–711.

Hsieh, M.-H., Ho, S.-C., Yeh, K.-Y., Pawlak, C. R., Chang, H.-M., Ho, Y.-J., Lai, T.-J. & Wu, F.-Y. (2012), 'Blockade of metabotropic glutamate receptors inhibits cognition and neurodegeneration in an MPTP-induced Parkinson's disease rat model', *Pharmacol. Biochem. Behav.* **102**(1), 64–71.

Hübner, C., Bosch, D., Gall, A., Lüthi, A. & Ehrlich, I. (2014), 'Ex vivo dissection of optogenetically activated mPFC and hippocampal inputs to neurons in the basolateral amygdala: implications for fear and emotional memory', *Front. Behav. Neurosci.* **8**, 64.

Hudson, J. L., van Horne, C. G., Strömberg, I., Brock, S., Clayton, J., Masserano, J., Hoffer, B. J. & Gerhardt, G. A. (1993), 'Correlation of apomorphine- and amphetamine-induced turning with nigrostriatal dopamine content in unilateral 6-hydroxydopamine lesioned rats', *Brain Res* **626**(1–2), 167–174.

Huganir, R. L. & Nicoll, R. A. (2013), 'AMPARs and Synaptic Plasticity: The Last 25 Years', *Neuron* **80**(3), 704–717.

Hüls, S., Högen, T., Vassallo, N., Danzer, K. M., Hengerer, B., Giese, A. & Herms, J. (2011), 'AMPA-receptor-mediated excitatory synaptic transmission is enhanced by iron-induced α-synuclein oligomers', *J. Neurochem.* **117**(5), 868–878.

Hutchings, E. J., Waller, J. L. & Terry, A. V. (2013), 'Differential Long-Term Effects of Haloperidol and Risperidone on the Acquisition and Performance of Tasks of Spatial Working and Short-Term Memory and Sustained Attention in Rats', *J. Pharmacol. Exp. Ther.* **347**(3), 547–556.

Iderberg, H., Francardo, V. & Pioli, E. (2012), 'Animal models of l-DOPA–induced dyskinesia: an update on the current options', *Neuroscience* **211**, 13–27.

Iderberg, H., Maslava, N., Thompson, A. D., Bubser, M., Niswender, C. M., Hopkins, C. R., Lindsley, C. W., Conn, P. J., Jones, C. K. & Cenci, M. A. (2015), 'Pharmacological stimulation of metabotropic glutamate receptor type 4 in a rat model of Parkinson's disease and l-DOPA-induced dyskinesia: Comparison between a positive allosteric modulator and an orthosteric agonist', *Neuropharmacology* **95**, 121–129.

Imai, Y., Soda, M. & Takahashi, R. (2000), 'Parkin suppresses unfolded protein stress-induced cell death through its E3 ubiquitin-protein ligase activity.', *J. Biol. Chem.* **275**(46), 35661–4.

Imamura, K., Hishikawa, N., Sawada, M., Nagatsu, T., Yoshida, M. & Hashizume, Y. (2003), 'Distribution of major histocompatibility complex class II-positive microglia and cytokine profile of Parkinson's disease brains', *Acta Neuropathol.* **106**(6), 518–526.

Iravani, M. M., Leung, C. C. M., Sadeghian, M., Haddon, C. O., Rose, S. & Jenner, P. (2005), 'The acute and the long-term effects of nigral lipopolysaccharide administration on dopaminergic dysfunction and glial cell activation', *Eur. J. Neurosci.* **22**(2), 317–330.

Iravani, M. M., Sadeghian, M., Leung, C. C., Jenner, P. & Rose, S. (2012), 'Lipopolysaccharide-induced nigral inflammation leads to increased IL-1β tissue content and expression of astrocytic glial cell line-derived neurotrophic factor', *Neurosci. Lett.* **510**(2), 138–142.

Iravani, M. M., Sadeghian, M., Leung, C. C., Tel, B. C., Rose, S., Schapira, A. H. & Jenner, P. (2008), 'Continuous subcutaneous infusion of pramipexole protects against lipopolysaccharide-induced dopaminergic cell death without affecting the inflammatory response', *Exp. Neurol.* **212**(2), 522–531.

Iravani, M. M., Sadeghian, M., Rose, S. & Jenner, P. (2014), 'Loss of locus coeruleus noradrenergic neurons alters the inflammatory response to LPS in substantia nigra but does not affect nigral cell loss', *J. Neural Transm.* **121**(12), 1493–1505.

Ishikawa, K.-I., Motoi, Y., Mizuno, Y., Kubo, S.-I. & Hattori, N. (2014), 'Effects of donepezil dose escalation in Parkinson's patients with dementia receiving long-term donepezil treatment: an exploratory study', *Psychogeriatrics* **14**(2), 93–100.

Iskhakova, L. & Smith, Y. (2016), 'mGluR4-containing corticostriatal terminals: synaptic interactions with direct and indirect pathway neurons in mice', *Brain Struct. Funct.* **221**(9), 4589–4599.

Iyer, J., Wang, Q., Le, T., Pizzo, L., Grönke, S., Ambegaokar, S. S., Imai, Y., Srivastava, A., Troisí, B. L., Mardon, G., Artero, R., Jackson, G. R., Isaacs, A. M., Partridge, L., Lu, B., Kumar, J. P. & Girirajan, S. (2016), 'Quantitative Assessment of Eye Phenotypes for Functional Genetic Studies Using Drosophila melanogaster.', *G3 (Bethesda).* **6**(5), 1427–37.

Jackson-Lewis, V. & Przedborski, S. (2007), 'Protocol for the MPTP mouse model of Parkinson's disease', *Nat. Protoc.* **2**(1), 141–151.

Jafari, S., Etminan, M., Aminzadeh, F. & Samii, A. (2013), 'Head injury and risk of Parkinson disease: A systematic review and meta-analysis', *Mov. Disord.* **28**(9), 1222–1229.

Jankovic, J. & Aguilar, L. G. (2008), 'Current approaches to the treatment of Parkinson's disease.', *Neuropsychiatr. Dis. Treat.* **4**(4), 743–57.

Jansen, R. L. M., Brogan, B., Whitworth, A. J. & Okello, E. J. (2014), 'Effects of Five Ayurvedic Herbs on Locomotor Behaviour in a Drosophila melanogaster Parkinson's Disease Model', *Phyther. Res.* **28**(12), 1789–1795.

Jellinger, K. A. (1991), 'Pathology of Parkinson's disease. Changes other than the nigrostriatal pathway.', *Mol. Chem. Neuropathol.* **14**(3), 153–97.

Jellinger, K. A. (2004), 'Lewy body-related alpha-synucleinopathy in the aged human brain', *J. Neural Transm.* **111**(10-11), 1219–1235.

Jemnitz, K., Veres, Z., Monostory, K., Kóbori, L. & Vereczkey, L. (2008), 'Interspecies differences in acetaminophen sensitivity of human, rat, and mouse primary hepatocytes', *Toxicol. Vitr.* **22**(4), 961–967.

Jimenez-Gomez, C., Osentoski, A. & Woods, J. H. (2011), 'Pharmacological evaluation of the adequacy of marble burying as an animal model of compulsion and/or anxiety', *Behav. Pharmacol.* **22**(7), 711–713.

Jin, H., Kanthasamy, A., Ghosh, A., Anantharam, V., Kalyanaraman, B. & Kanthasamy, A. G. (2014), 'Mitochondria-targeted antioxidants for treatment of Parkinson's disease: Preclinical and clinical outcomes', *Biochim. Biophys. Acta - Mol. Basis Dis.* **1842**(8), 1282–1294.

Johannessen, J. N., Chiueh, C. C., Burns, R. S. & Markey, S. P. (1985), 'IV. Differences in the metabolism of MPTP in the rodent and primate parallel differences in sensitivity to its neurotoxic effects', *Life Sci.* **36**(3), 219–224.

Johnston, L. C., Jackson, M. J., Rose, S., McCreary, A. C. & Jenner, P. (2010), 'Pardoprunox reverses motor deficits but induces only mild dyskinesia in MPTP-treated common marmosets', *Mov. Disord.* **25**(13), 2059–2066.

Joyce, J. N., Davis, R. E. & Van Hartesveldt, C. (1981), 'Behavioral effects of unilateral dopamine injection into dorsal or ventral striatum.', *Eur. J. Pharmacol.* **72**(1), 1–10.

Kalkonde, Y. V., Morgan, W. W., Sigala, J., Maffi, S. K., Condello, C., Kuziel, W., Ahuja, S. S. & Ahuja, S. K. (2007), 'Chemokines in the MPTP model of Parkinson's disease: Absence of CCL2 and its receptor CCR2 does not protect against striatal neurodegeneration', *Brain Res.* **1128**(1), 1–11.

Kammermeier, P. J. (2012), 'Functional and pharmacological characteristics of metabotropic glutamate receptors 2/4 heterodimers', *Mol Pharmacol* **82**(3), 438–447.

Kammermeier, P. J., Davis, M. I. & Ikeda, S. R. (2003), 'Specificity of metabotropic glutamate receptor 2 coupling to G proteins.', *Mol. Pharmacol.* **63**(1), 183–91.

Kanaan, N. M., Collier, T. J., Cole-Strauss, A., Grabinski, T., Mattingly, Z. R., Winn, M. E., Steece-Collier, K., Sortwell, C. E., Manfredsson, F. P. & Lipton, J. W. (2015), 'The longitudinal transcriptomic response of the substantia nigra to intrastriatal 6-hydroxydopamine reveals significant upregulation of regeneration-associated genes.', *PLoS One* **10**(5), e0127768.

Kanazawa, I., Marshall, G. R. & Kelly, J. S. (1976), 'Afferents to the rat substantia nigra studied with horseradish peroxidase, with special reference to fibres from the subthalamic nucleus', *Brain Res.* **115**(3), 485–491.

Kandiah, N., Pai, M.-C., Senanarong, V., Looi, I., Ampil, E., Park, K. W., Karanam, A. K. & Christopher, S. (2017), 'Rivastigmine: the advantages of dual inhibition of acetylcholinesterase and butyrylcholinesterase and its role in subcortical vascular dementia and Parkinson's disease dementia', *Clin. Interv. Aging* **Volume 12**, 697–707.

Kanthasamy, A. G., Kanthasamy, A., Matsumoto, R. R., Vu, T. Q. & Truong, D. D. (1997), 'Neuroprotective effects of the strychnine-insensitive glycine site NMDA antagonist (R)-HA-966 in an experimental model of Parkinson's disease.', *Brain Res.* **759**(1), 1–8.

Karasawa, H., Pietra, C., Giuliano, C., Garcia-Rubio, S., Xu, X., Yakabi, S., Taché, Y. & Wang, L. (2014), 'New ghrelin agonist, HM01 alleviates constipation and L-dopa-delayed gastric emptying in 6-hydroxydopamine rat model of Parkinson's disease', *Neurogastroenterol. Motil.* **26**(12), 1771–1782.

Kataoka, H., Sawa, N., Sugie, K. & Ueno, S. (2014), 'Can dopamine agonists trigger tactile hallucinations in patients with Parkinson's disease?', *J. Neurol. Sci.* **347**(1-2), 361–363.

Katz, R. J. (1982), 'Animal model of depression: Pharmacological sensitivity of a hedonic deficit', *Pharmacol. Biochem. Behav.* **16**(6), 965–968.

Kehagia, A. A., Barker, R. A. & Robbins, T. W. (2013), 'Cognitive impairment in Parkinson's disease: the dual syndrome hypothesis.', *Neurodegener. Dis.* **11**(2), 79–92.

Kempster, P. A., O'Sullivan, S. S., Holton, J. L., Revesz, T. & Lees, A. J. (2010), 'Relationships between age and late progression of Parkinson's disease: a clinico-pathological study', *Brain* **133**(6), 1755–1762.

Kenborg, L., Rugbjerg, K., Lee, P.-C., Ravnskjær, L., Christensen, J., Ritz, B. & Lassen, C. F. (2015), 'Head injury and risk for Parkinson disease: results from a Danish case-control study.', *Neurology* **84**(11), 1098–103.

Kennelly, P. J. & Krebs, E. G. (1991), 'Consensus sequences as substrate specificity determinants for protein kinases and protein phosphatases.', *J. Biol. Chem.* **266**(24), 15555–8.

Kim, K., Kim, S.-H., Kim, J., Kim, H. & Yim, J. (2012), 'Glutathione S -Transferase Omega 1 Activity Is Sufficient to Suppress Neurodegeneration in a Drosophila Model of Parkinson Disease', *J. Biol. Chem.* **287**(9), 6628–6641.

Kim, T.-H., Choi, J., Kim, H.-G. & Kim, H. R. (2014), 'Quantification of neurotransmitters in mouse brain tissue by using liquid chromatography coupled electrospray tandem mass spectrometry.', *J. Anal. Methods Chem.* **2014**, 506870.

Kirik, D., Rosenblad, C. & Björklund, A. (1998), 'Characterization of Behavioral and Neurodegenerative Changes Following Partial Lesions of the Nigrostriatal Dopamine System Induced by Intrastriatal 6-Hydroxydopamine in the Rat', *Exp. Neurol.* **152**(2), 259–277.

Kitada, T., Asakawa, S., Hattori, N., Matsumine, H., Yamamura, Y., Minoshima, S., Yokochi, M., Mizuno, Y. & Shimizu, N. (1998), 'Mutations in the parkin gene cause autosomal recessive juvenile parkinsonism', *Nature* **392**(6676), 605–608.

Kiyohara, C. & Kusuhara, S. (2011), 'Cigarette smoking and Parkinson's disease: a meta-analysis.', *Fukuoka Igaku Zasshi* **102**(8), 254–65.

Klassen, B., Lyons, M. K. & Evidente, V. G. H. (2011), 'Bilateral globus pallidus internus deep brain stimulation in parkinson's disease with periodic limb movement disorder', *Turk. Neurosurg.* **23**(1), 104–6.

Klegeris, A., Pelech, S., Giasson, B. I., Maguire, J., Zhang, H., McGeer, E. G. & McGeer, P. L. (2008), 'α-Synuclein activates stress signaling protein kinases in THP-1 cells and microglia', *Neurobiol. Aging* **29**(5), 739–752.

Klein, C. & Westenberger, A. (2012), 'Genetics of Parkinson's disease.', *Cold Spring Harb. Perspect. Med.* **2**(1), a008888.

Klintworth, H., Garden, G. & Xia, Z. (2009), 'Rotenone and paraquat do not directly activate microglia or induce inflammatory cytokine release.', *Neurosci. Lett.* **462**(1), 1–5.

Klockgether, T. & Turski, L. (1990), 'NMDA antagonists potentiate antiparkinsonian actions ofL-dopa in monoamine-depleted rats', *Ann. Neurol.* **28**(4), 539–546.

Klockgether, T., Turski, L., Honoré, T., Zhang, Z., Gash, D. M., Kurlan, R. & Greenamyre, J. T. (1991), 'The AMPA receptor antagonist NBQX has antiparkinsonian effects in monoamine-depleted rats and MPTP-treated monkeys', *Ann. Neurol.* **30**(5), 717–723.

Kobayashi, T., Araki, T., Itoyama, Y., Takeshita, M., Ohta, T. & Oshima, Y. (1997), 'Effects of L-dopa and bromocriptine on haloperidol-induced motor deficits in mice.', *Life Sci.* **61**(26), 2529–38.

Kogan, J. H., Franklandand, P. W. & Silva, A. J. (2000), 'Long-term memory underlying hippocampus-dependent social recognition in mice', *Hippocampus* **10**(1), 47–56.

Koh, I. Y. Y., Lindquist, W. B., Zito, K., Nimchinsky, E. A. & Svoboda, K. (2002), 'An Image Analysis Algorithm for Dendritic Spines', *Neural Comput.* **14**(6), 1283–1310.

Kohno, H., Maeda, T., Perusek, L., Pearlman, E. & Maeda, A. (2014), 'CCL3 Production by Microglial Cells Modulates Disease Severity in Murine Models of Retinal Degeneration', *J. Immunol.* **192**(8), 3816–3827.

Konitsiotis, S., Blanchet, P. J., Verhagen, L., Lamers, E. & Chase, T. N. (2000), 'AMPA receptor blockade improves levodopa-induced dyskinesia in MPTP monkeys.', *Neurology* **54**(8), 1589–95.

Kordower, J. H., Olanow, C. W., Dodiya, H. B., Chu, Y., Beach, T. G., Adler, C. H., Halliday, G. M. & Bartus, R. T. (2013), 'Disease duration and the integrity of the nigrostriatal system in Parkinson's disease', *Brain* **136**(8), 2419–2431.

Kortekaas, R., Leenders, K. L., van Oostrom, J. C. H., Vaalburg, W., Bart, J., Willemsen, A. T. M. & Hendrikse, N. H. (2005), 'Blood-brain barrier dysfunction in parkinsonian midbrain in vivo', *Ann. Neurol.* **57**(2), 176–179.

Kostic, V. S., Agosta, F., Petrovic, I., Galantucci, S., Spica, V., Jecmenica-Lukic, M. & Filippi, M. (2010), 'Regional patterns of brain tissue loss associated with depression in Parkinson disease', *Neurology* **75**(10), 857–863.

Kozlowski, C. & Weimer, R. M. (2012), 'An automated method to quantify microglia morphology and application to monitor activation state longitudinally in vivo.', *PLoS One* **7**(2), e31814.

Kravitz, A. V., Freeze, B. S., Parker, P. R. L., Kay, K., Thwin, M. T., Deisseroth, K. & Kreitzer, A. C. (2010), 'Regulation of parkinsonian motor behaviours by optogenetic control of basal ganglia circuitry', *Nature* **466**(7306), 622–626.

Krishna, A., Biryukov, M., Trefois, C., Antony, P. M., Hussong, R., Lin, J., Heinäniemi, M., Glusman, G., Köglsberger, S., Boyd, O., van den Berg, B. H., Linke, D., Huang, D., Wang, K., Hood, L., Tholey, A., Schneider, R., Galas, D. J., Balling, R. & May, P. (2014), 'Systems genomics evaluation of the SH-SY5Y neuroblastoma cell line as a model for Parkinson's disease', *BMC Genomics* **15**(1), 1154.

Kulkarni, S. K., Bishnoi, M. & Chopra, K. (2009), 'In vivo microdialysis studies of striatal level of neurotransmitters after haloperidol and chlorpromazine administration.', *Indian J. Exp. Biol.* **47**(2), 91–7.

Kupsch, A., Löschmann, P. A., Sauer, H., Arnold, G., Renner, P., Pufal, D., Burg, M., Wachtel, H., ten Bruggencate, G. & Oertel, W. H. (1992), 'Do NMDA receptor antagonists protect against MPTP-toxicity? Biochemical and immunocytochemical analyses in black mice.', *Brain Res.* **592**(1-2), 74–83.

Kurkowska-Jastrzębska, I., Wrońska, A., Kohutnicka, M., Członkowski, A. & Członkowska, A. (1999), 'The Inflammatory Reaction Following 1-Methyl-4-phenyl-1,2,3,6-tetrahydropyridine Intoxication in Mouse', *Exp. Neurol.* **156**(1), 50–61.

Lai, C.-T. & Yu, P. H. (1997), 'Dopamine- and l-β-3,4-dihydroxyphenylalanine hydrochloriDe (l-Dopa)-induced cytotoxicity towards catecholaminergic neuroblastoma SH-SY5Y Cells: Effects of oxidative stress and antioxidative factors', *Biochem. Pharmacol.* **53**(3), 363–372.

Lam, C. S., Korzh, V. & Strahle, U. (2005), 'Zebrafish embryos are susceptible to the dopaminergic neurotoxin MPTP', *Eur. J. Neurosci.* **21**(6), 1758–1762.

Lang, A. E., Gill, S., Patel, N. K., Lozano, A., Nutt, J. G., Penn, R., Brooks, D. J., Hotton, G., Moro, E., Heywood, P., Brodsky, M. A., Burchiel, K., Kelly, P., Dalvi, A., Scott, B., Stacy, M., Turner, D., Wooten, V. G. F., Elias, W. J., Laws, E. R., Dhawan, V., Stoessl, A. J., Matcham,

J., Coffey, R. J. & Traub, M. (2006), 'Randomized controlled trial of intraputamenal glial cell line-derived neurotrophic factor infusion in Parkinson disease', *Ann. Neurol.* **59**(3), 459–466.

Langston, J. W., Ballard, P., Tetrud, J. W. & Irwin, I. (1983), 'Chronic Parkinsonism in humans due to a product of meperidine-analog synthesis', *Science (80-.).* **219**(4587), 979–980.

Le Moine, C. & Bloch, B. (1995), 'D1 and D2 dopamine receptor gene expression in the rat striatum: Sensitive cRNA probes demonstrate prominent segregation of D1 and D2 mRNAS in distinct neuronal populations of the dorsal and ventral striatum', *J. Comp. Neurol.* **355**(3), 418–426.

Le Poul, E., Bolea, C., Girard, F., Poli, S., Charvin, D., Campo, B., Bortoli, J., Bessif, A., Luo, B., Koser, A. J., Hodge, L. M., Smith, K. M., DiLella, A. G., Liverton, N., Hess, F., Browne, S. E. & Reynolds, I. J. (2012), 'A Potent and Selective Metabotropic Glutamate Receptor 4 Positive Allosteric Modulator Improves Movement in Rodent Models of Parkinson's Disease', *J. Pharmacol. Exp. Ther.* **343**(1), 167–177.

Lebouvier, T., Tasselli, M., Paillusson, S., Pouclet, H., Neunlist, M. & Derkinderen, P. (2010), 'Biopsable Neural Tissues: Toward New Biomarkers for Parkinson's Disease?', *Front. Psychiatry* **1**.

Ledesma, J. C., Miquel, M., Pascual, M., Guerri, C. & Aragon, C. M. (2014), 'Induction of brain cytochrome P450 2E1 boosts the locomotor-stimulating effects of ethanol in mice', *Neuropharmacology* **85**, 36–44.

Lehre, K. P., Levy, L. M., Ottersen, O. P., Storm-Mathisen, J. & Danbolt, N. C. (1995), 'Differential expression of two glial glutamate transporters in the rat brain: quantitative and immunocytochemical observations.', *J. Neurosci.* **15**(3 Pt 1), 1835–53.

Lei, Q., Jones, M. B., Talley, E. M., Schrier, A. D., McIntire, W. E., Garrison, J. C. & Bayliss, D. A. (2000), 'Activation and inhibition of G protein-coupled inwardly rectifying potassium (Kir3) channels by G protein beta gamma subunits.', *Proc. Natl. Acad. Sci. U. S. A.* **97**(17), 9771–6.

Lesnick, T. G., Papapetropoulos, S., Mash, D. C., Ffrench-Mullen, J., Shehadeh, L., de Andrade, M., Henley, J. R., Rocca, W. A., Ahlskog, J. E. & Maraganore, D. M. (2007), 'A Genomic Pathway Approach to a Complex Disease: Axon Guidance and Parkinson Disease', *PLoS Genet.* **3**(6), e98.

Levey, A. I., Hersch, S. M., Rye, D. B., Sunahara, R. K., Niznik, H. B., Kitt, C. A., Price, D. L., Maggio, R., Brann, M. R. & Ciliax, B. J. (1993), 'Localization of D1 and D2 dopamine receptors in brain with subtype-specific antibodies.', *Proc. Natl. Acad. Sci. U. S. A.* **90**(19), 8861–5.

Li, J., Yang, J., Zhao, P., Li, S., Zhang, R., Zhang, X., Liu, D. & Zhang, B. (2012), 'Neuromelanin enhances the toxicity of α-synuclein in SK-N-SH cells', *J. Neural Transm.* **119**(6), 685–691.

Li, N., Ragheb, K., Lawler, G., Sturgis, J., Rajwa, B., Melendez, J. A. & Robinson, J. P. (2003), 'Mitochondrial complex I inhibitor rotenone induces apoptosis through enhancing mitochondrial reactive oxygen species production.', *J. Biol. Chem.* **278**(10), 8516–25.

Li, X., Li, W., Liu, G., Shen, X. & Tang, Y. (2015), 'Association between cigarette smoking and Parkinson's disease: A meta-analysis', *Arch. Gerontol. Geriatr.* **61**(3), 510–516.

Li, Y., Zheng, Y., Yang, L., Wang, Q., Bi, E., Li, T., Lu, Y., Qian, J., Zhang, M., Yang, M., Yi, Q. & Cai, Z. (2014), 'Chemokines CCL14 and CCL3 Facilitate Monocytes/Macrophage Infiltration in Multiple Myeloma Bone Marrow', *Blood* **124**(21).

Lima, M. M., Andersen, M. L., Reksidler, A. B., Vital, M. A. & Tufik, S. (2007), 'The Role of the Substantia Nigra Pars Compacta in Regulating Sleep Patterns in Rats', *PLoS One* **2**(6), e513.

Limousin, P., Krack, P., Pollak, P., Benazzouz, A., Ardouin, C., Hoffmann, D. & Benabid, A.-L. (1998), 'Electrical Stimulation of the Subthalamic Nucleus in Advanced Parkinson's Disease', *N. Engl. J. Med.* **339**(16), 1105–1111.

Limousin, P., Pollak, P., Benazzouz, A., Hoffmann, D., Le Bas, J. F., Broussolle, E., Perret, J. E. & Benabid, A. L. (1995), 'Effect of parkinsonian signs and symptoms of bilateral subthalamic nucleus stimulation.', *Lancet (London, England)* **345**(8942), 91–5.

Lin, C.-H., You, J.-R., Wei, K.-C. & Gean, P.-W. (2014), 'Stimulating ERK/PI3K/NFκB signaling pathways upon activation of mGluR2/3 restores OGD-induced impairment in glutamate clearance in astrocytes', *Eur. J. Neurosci.* **39**(1), 83–96.

Lin, X., Parisiadou, L., Gu, X.-L., Wang, L., Shim, H., Sun, L., Xie, C., Long, C.-X., Yang, W.-J., Ding, J., Chen, Z. Z., Gallant, P. E., Tao-Cheng, J.-H., Rudow, G., Troncoso, J. C., Liu, Z., Li, Z. & Cai, H. (2009), 'Leucine-rich repeat kinase 2 regulates the progression of neuropathology induced by Parkinson's-disease-related mutant alpha-synuclein.', *Neuron* **64**(6), 807–27.

Lintas, A., Silkis, I. G., Albéri, L. & Villa, A. E. (2012), 'Dopamine deficiency increases synchronized activity in the rat subthalamic nucleus', *Brain Res.* **1434**, 142–151.

Little, S. & Brown, P. (2014), 'The functional role of beta oscillations in Parkinson's disease.', *Parkinsonism Relat. Disord.* **20 Suppl 1**, S44–8.

Liu, J., Banskota, A., Critchley, A., Hafting, J. & Prithiviraj, B. (2015), 'Neuroprotective Effects of the Cultivated Chondrus crispus in a C. elegans Model of Parkinson's Disease', *Mar. Drugs* **13**(4), 2250–2266.

Liu, J., Dong, J., Wang, L., Su, Y., Yan, P. & Sun, S. (2013), 'Comparative efficacy and acceptability of antidepressants in Parkinson's disease: a network meta-analysis.', *PLoS One* **8**(10), e76651.

Liu, J., Wang, M.-W., Gu, P., Ma, Q.-Y., Wang, Y.-Y., Geng, Y., Yuan, Z.-Y., Cui, D.-S., Zhang, Z.-X., Ma, L., Zhang, B.-H., Zhou, M.-G. & Zhu, A.-P. (2010), 'Microglial activation and age-related dopaminergic neurodegeneration in MPTP-treated SAMP8 mice', *Brain Res.* **1345**, 213–220.

Liu, S.-b., Zhao, R., Li, X.-s., Guo, H.-j., Tian, Z., Zhang, N., Gao, G.-d. & Zhao, M.-g. (2014), 'Attenuation of Reserpine-Induced Pain/Depression Dyad by Gentiopicroside Through Down-regulation of GluN2B Receptors in the Amygdala of Mice', *NeuroMolecular Med.* **16**(2), 350–359.

Liu, Y., Peng, M., Zang, D. & Zhang, B. (2013), 'Leukemia inhibitory factor promotes nestin-positive cells, and increases gp130 levels in the Parkinson disease mouse model of 6-hydroxydopamine.', *Neurosciences (Riyadh).* **18**(4), 363–70.

Lopez, S., Bonito-Oliva, A., Pallottino, S., Acher, F. & Fisone, G. (2011), 'Activation of metabotropic glutamate 4 receptors decreases L-DOPA-induced dyskinesia in a mouse model of Parkinson's disease.', *J. Parkinsons. Dis.* **1**(4), 339–46.

Lopez, S., Jouve, L., Turle-Lorenzo, N., Kerkerian-LeGoff, L., Salin, P. & Amalric, M. (2012), 'Antiparkinsonian action of a selective group III mGlu receptor agonist is associated with reversal of subthalamonigral overactivity', *Neurobiol. Dis.* **46**(1), 69–77.

Lorrain, D. S., Schaffhauser, H., Campbell, U. C., Baccei, C. S., Correa, L. D., Rowe, B., Rodriguez, D. E., Anderson, J. J., Varney, M. A., Pinkerton, A. B., Vernier, J.-M. & Bristow, L. J. (2003), 'Group II mGlu receptor activation suppresses norepinephrine release in the ventral hippocampus and locomotor responses to acute ketamine challenge.', *Neuropsychopharmacology* **28**(9), 1622–32.

Löschmann, P.-A., De Groote, C., Smith, L., Wüllner, U., Fischer, G., Kemp, J. A., Jenner, P. & Klockgether, T. (2004), 'Antiparkinsonian activity of Ro 25-6981, a NR2B subunit specific

NMDA receptor antagonist, in animal models of Parkinson's disease', *Exp. Neurol.* **187**(1), 86–93.

Löschmann, P.-A., Smith, L. A., Lange, K. W., Jähnig, P., Jenner, P. & Marsden, C. D. (1992), 'Motor activity following the administration of selective D-1 and D-2 dopaminergic drugs to MPTP-treated common marmosets', *Psychopharmacology (Berl).* **109**(1-2), 49–56.

Lu, Y., Zhang, X., Zhao, L., Yang, C., Pan, L., Li, C., Liu, K., Bai, G., Gao, H. & Yan, Z. (2018), 'Metabolic Disturbances in the Striatum and Substantia Nigra in the Onset and Progression of MPTP-Induced Parkinsonism Model', *Front. Neurosci.* **12**, 90.

Lui, H., Zhang, J., Makinson, S. R., Cahill, M. K., Kelley, K. W., Huang, H.-Y., Shang, Y., Oldham, M. C., Martens, L. H., Gao, F., Coppola, G., Sloan, S. A., Hsieh, C. L., Kim, C. C., Bigio, E. H., Weintraub, S., Mesulam, M.-M., Rademakers, R., Mackenzie, I. R., Seeley, W. W., Karydas, A., Miller, B. L., Borroni, B., Ghidoni, R., Farese, R. V., Paz, J. T., Barres, B. A. & Huang, E. J. (2016), 'Progranulin Deficiency Promotes Circuit-Specific Synaptic Pruning by Microglia via Complement Activation', *Cell* **165**(4), 921–935.

Luquin, M., Obeso, J., Laguna, J., Guillén, J. & Martínez-Lage, J. (1993), 'The AMPA receptor antagonist NBQX does not alter the motor response induced by selective dopamine agonists in MPTP-treated monkeys', *Eur. J. Pharmacol.* **235**(2-3), 297–300.

Luquin, M., Saldise, L., Guillen, J., Belzunegui, S., Sansebastian, W., Izal, A., Garrido, P. & Vazquez, M. (2006), 'Does increased excitatory drive from the subthalamic nucleus contribute to dopaminergic neuronal death in Parkinson's disease?', *Exp. Neurol.* **201**(2), 407–415.

Luthman, J., Bolioli, B., Tsutsumi, T., Verhofstad, A. & Jonsson, G. (1987), 'Sprouting of striatal serotonin nerve terminals following selective lesions of nigro-striatal dopamine neurons in neonatal rat.', *Brain Res. Bull.* **19**(2), 269–74.

Lynch, M. R. & Carey, R. J. (1989), 'Amphetamine-induced rotation reveals post 6-OHDA lesion neurochemical reorganization', *Behav. Brain Res.* **32**(1), 69–74.

MacInnes, N. & Duty, S. (2008), 'Group III metabotropic glutamate receptors act as heteroreceptors modulating evoked GABA release in the globus pallidus in vivo', *Eur. J. Pharmacol.* **580**(1–2), 95–99.

MacInnes, N., Messenger, M. J. & Duty, S. (2004), 'Activation of group III metabotropic glutamate receptors in selected regions of the basal ganglia alleviates akinesia in the reserpine-treated rat', *Br J Pharmacol* **141**(1), 15–22.

Magen, I., Fleming, S. M., Zhu, C., Garcia, E. C., Cardiff, K. M., Dinh, D., De La Rosa, K., Sanchez, M., Torres, E. R., Masliah, E., David Jentsch, J. & Chesselet, M.-F. (2012), 'Cognitive deficits in a mouse model of pre-manifest Parkinson's disease', *Eur. J. Neurosci.* **35**(6), 870–882.

Magen, I., Torres, E. R., Dinh, D., Chung, A., Masliah, E. & Chesselet, M.-F. (2015), 'Social Cognition Impairments in Mice Overexpressing Alpha-Synuclein Under the Thy1 Promoter, a Model of Pre-manifest Parkinson's Disease', *J. Parkinsons. Dis.* **5**(3), 669–680.

Maggio, R., Riva, M., Vaglini, F., Fornai, F., Molteni, R., Armogida, M., Racagni, G. & Corsini, G. U. (1998), 'Nicotine prevents experimental parkinsonism in rodents and induces striatal increase of neurotrophic factors.', *J. Neurochem.* **71**(6), 2439–46.

Makar, T. K., Nedergaard, M., Preuss, A., Gelbard, A. S., Perumal, A. S. & Cooper, A. J. (1994), 'Vitamin E, ascorbate, glutathione, glutathione disulfide, and enzymes of glutathione metabolism in cultures of chick astrocytes and neurons: evidence that astrocytes play an important role in antioxidative processes in the brain.', *J. Neurochem.* **62**(1), 45–53.

Mallet, N., Ballion, B., Le Moine, C. & Gonon, F. (2006), 'Cortical inputs and GABA interneurons imbalance projection neurons in the striatum of parkinsonian rats.', *J. Neurosci.* **26**(14), 3875–84.

Marabese, I., Boccella, S., Iannotta, M., Luongo, L., de Novellis, V., Guida, F., Serra, N., Farina, A., Maione, S. & Palazzo, E. (2018), 'Metabotropic glutamate receptor subtype 7 in the dorsal striatum oppositely modulates pain in sham and neuropathic rats', *Neuropharmacology* .

Marin, C., Bonastre, M., Mengod, G., Cortés, R. & Rodríguez-Oroz, M. (2015), 'From unilateral to bilateral parkinsonism: Effects of lateralization on dyskinesias and associated molecular mechanisms', *Neuropharmacology* **97**, 365–375.

Marino, M. J., Williams, D. L., O'Brien, J. A., Valenti, O., McDonald, T. P., Clements, M. K., Wang, R., DiLella, A. G., Hess, J. F., Kinney, G. G. & Conn, P. J. (2003), 'Allosteric modulation of group III metabotropic glutamate receptor 4: A potential approach to Parkinson's disease treatment', *Proc. Natl. Acad. Sci.* **100**(23), 13668–13673.

Marinova-Mutafchieva, L., Sadeghian, M., Broom, L., Davis, J. B., Medhurst, A. D. & Dexter, D. T. (2009), 'Relationship between microglial activation and dopaminergic neuronal loss in the substantia nigra: a time course study in a 6-hydroxydopamine model of Parkinson's disease', *J. Neurochem.* **110**(3), 966–975.

Martin, L. J., Pan, Y., Price, A. C., Sterling, W., Copeland, N. G., Jenkins, N. A., Price, D. L. & Lee, M. K. (2006), 'Parkinson's Disease -Synuclein Transgenic Mice Develop Neuronal Mitochondrial Degeneration and Cell Death', *J. Neurosci.* **26**(1), 41–50.

Martinez, B. A., Petersen, D. A., Gaeta, A. L., Stanley, S. P., Caldwell, G. A. & Caldwell, K. A. (2017), 'Dysregulation of the Mitochondrial Unfolded Protein Response Induces Non-Apoptotic Dopaminergic Neurodegeneration in C. elegans Models of Parkinson's Disease', *J. Neurosci.* **37**(46), 11085–11100.

Martinez-Martin, P., Rodriguez-Blazquez, C., Abe, K., Bhattacharyya, K. B., Bloem, B. R., Carod-Artal, F. J., Prakash, R., Esselink, R., Falup-Pecurariu, C., Gallardo, M., Mir, P., Naidu, Y., Nicoletti, A., Sethi, K., Tsuboi, Y., van Hilten, J. J., Visser, M., Zappia, M. & Chaudhuri, K. R. (2009), 'International study on the psychometric attributes of the Non-Motor Symptoms Scale in Parkinson disease', *Neurology* **73**(19), 1584–1591.

Masilamoni, G. J., Bogenpohl, J. W., Alagille, D., Delevich, K., Tamagnan, G., Votaw, J. R., Wichmann, T. & Smith, Y. (2011), 'Metabotropic glutamate receptor 5 antagonist protects dopaminergic and noradrenergic neurons from degeneration in MPTP-treated monkeys.', *Brain* **134**(Pt 7), 2057–73.

Masliah, E., Rockenstein, E., Mante, M., Crews, L., Spencer, B., Adame, A., Patrick, C., Trejo, M., Ubhi, K., Rohn, T. T., Mueller-Steiner, S., Seubert, P., Barbour, R., McConlogue, L., Buttini, M., Games, D. & Schenk, D. (2011), 'Passive Immunization Reduces Behavioral and Neuropathological Deficits in an Alpha-Synuclein Transgenic Model of Lewy Body Disease', *PLoS One* **6**(4), e19338.

Masuda-Suzukake, M., Nonaka, T., Hosokawa, M., Oikawa, T., Arai, T., Akiyama, H., Mann, D. M. A. & Hasegawa, M. (2013), 'Prion-like spreading of pathological α-synuclein in brain', *Brain* **136**(4), 1128–1138.

Mathiasen, J. R. & DiCamillo, A. (2010), 'Social recognition assay in the rat', *Curr Protoc Neurosci* **Chapter 8**, Unit 8 5I.

Matsuda, W., Furuta, T., Nakamura, K. C., Hioki, H., Fujiyama, F., Arai, R. & Kaneko, T. (2009), 'Single Nigrostriatal Dopaminergic Neurons Form Widely Spread and Highly Dense Axonal Arborizations in the Neostriatum', *J. Neurosci.* **29**(2), 444–453.

Matsui, H., Udaka, F., Tamura, A., Oda, M., Kubori, T., Nishinaka, K. & Kameyama, M. (2006), 'Impaired Visual Acuity as a Risk Factor for Visual Hallucinations in Parkinson's Disease', *J. Geriatr. Psychiatry Neurol.* **19**(1), 36–40.

Mattay, V. S., Tessitore, A., Callicott, J. H., Bertolino, A., Goldberg, T. E., Chase, T. N., Hyde, T. M. & Weinberger, D. R. (2002), 'Dopaminergic modulation of cortical function in patients with Parkinson's disease.', *Ann. Neurol.* **51**(2), 156–64.

Maurin, Y., Banrezes, B., Menetrey, A., Mailly, P. & Deniau, J. M. (1999), 'Three-dimensional distribution of nigrostriatal neurons in the rat: relation to the topography of striatonigral projections', *Neuroscience* **91**(3), 891–909.

McCall, J. G., Siuda, E. R., Bhatti, D. L., Lawson, L. A., McElligott, Z. A., Stuber, G. D. & Bruchas, M. R. (2017), 'Locus coeruleus to basolateral amygdala noradrenergic projections promote anxiety-like behavior.', *Elife* **6**.

McDowell, K. A., Shin, D., Roos, K. P. & Chesselet, M.-F. (2018), 'Sleep Dysfunction and EEG Alterations in Mice Overexpressing Alpha-Synuclein', *J. Parkinsons. Dis.* **4**(3), 531–539.

McFadyen, M. P., Kusek, G., Bolivar, V. J. & Flaherty, L. (2003), 'Differences among eight inbred strains of mice in motor ability and motor learning on a rotorod', *Genes, Brain Behav.* **2**(4), 214–219.

McFarland, N. R. & Haber, S. N. (2002), 'Thalamic relay nuclei of the basal ganglia form both reciprocal and nonreciprocal cortical connections, linking multiple frontal cortical areas.', *J. Neurosci.* **22**(18), 8117–32.

McGeer, P. L., Itagaki, S., Akiyama, H. & McGeer, E. G. (1988), 'Rate of cell death in parkinsonism indicates active neuropathological process', *Ann. Neurol.* **24**(4), 574–576.

McGeer, P. L., Itagaki, S., Boyes, B. E. & McGeer, E. G. (1988), 'Reactive microglia are positive for HLA-DR in the substantia nigra of Parkinson's and Alzheimer's disease brains.', *Neurology* **38**(8), 1285–91.

McGeer, P. L. & McGeer, E. G. (2004), 'Inflammation and neurodegeneration in Parkinson's disease', *Parkinsonism Relat. Disord.* **10**, S3–S7.

McGeer, P. L., Schwab, C., Parent, A. & Doudet, D. (2003), 'Presence of reactive microglia in monkey substantia nigra years after 1-methyl-4-phenyl-1,2,3,6-tetrahydropyridine administration', *Ann Neurol* **54**.

McGeer, P. L., Yasojima, K. & McGeer, E. G. (2002), 'Association of interleukin-1 beta polymorphisms with idiopathic Parkinson's disease.', *Neurosci. Lett.* **326**(1), 67–9.

McGeorge, A. J. & Faull, R. L. (1989), 'The organization of the projection from the cerebral cortex to the striatum in the rat.', *Neuroscience* **29**(3), 503–37.

McKimmie, C. & Michlmayr, D. (2014), 'Role of CXCL10 in central nervous system inflammation', *Int. J. Interf. Cytokine Mediat. Res.* **6**, 1.

McNaught, K. S. & Jenner, P. (1999), 'Altered glial function causes neuronal death and increases neuronal susceptibility to 1-methyl-4-phenylpyridinium- and 6-hydroxydopamine-induced toxicity in astrocytic/ventral mesencephalic co-cultures.', *J. Neurochem.* **73**(6), 2469–76.

McNaught, K. S. & Jenner, P. (2000), 'Extracellular accumulation of nitric oxide, hydrogen peroxide, and glutamate in astrocytic cultures following glutathione depletion, complex I inhibition, and/or lipopolysaccharide-induced activation.', *Biochem. Pharmacol.* **60**(7), 979–88.

McNaught, K. S. P. & Olanow, C. W. (2003), 'Proteolytic stress: A unifying concept for the etiopathogenesis of Parkinson's disease', *Ann. Neurol.* **53**(S3), S73–S86.

Mead, E. L., Mosley, A., Eaton, S., Dobson, L., Heales, S. J. & Pocock, J. M. (2012), 'Microglial neurotransmitter receptors trigger superoxide production in microglia; consequences for microglial-neuronal interactions', *J. Neurochem.* **121**(2), 287–301.

Meeuwsen, S., Persoon-Deen, C., Bsibsi, M., Ravid, R. & Noort, J. M. V. (2003), 'Cytokine, chemokine and growth factor gene profiling of cultured human astrocytes after exposure to proinflammatory stimuli', *Glia* **43**(3), 243–253.

Mei, J., Kowalska, M. A., Dai, N., Liu, Y., Hudock, K., Jeyaseelan, S., Lee, J., Guttentag, S., Poncz, M. & Worthen, G. S. (2013), 'Platelet CXCL7 and CXCL4 inhibit chemokine scavenging and improve innate immunity to bacterial infection (P1317)', *J. Immunol.* **190**(1 Supplement).

Mela, F., Marti, M., Dekundy, A., Danysz, W., Morari, M. & Cenci, M. A. (2007), 'Antagonism of metabotropic glutamate receptor type 5 attenuates l-DOPA-induced dyskinesia and its molecular and neurochemical correlates in a rat model of Parkinson?s disease', *J. Neurochem.* **101**(2), 483–497.

Melamed, E., Rosenthal, J., Globus, M., Cohen, O. & Uzzan, A. (1985), 'Suppression of MPTP-induced dopaminergic neurotoxicity in mice by nomifensine and L-DOPA.', *Brain Res.* **342**(2), 401–4.

Mena, M. A. & García de Yébenes, J. (2008), 'Glial Cells as Players in Parkinsonism: The "Good," the "Bad," and the "Mysterious" Glia', *Neurosci.* **14**(6), 544–560.

Menza, M., Dobkin, R. D., Marin, H., Mark, M. H., Gara, M., Buyske, S., Bienfait, K. & Dicke, A. (2009), 'A controlled trial of antidepressants in patients with Parkinson disease and depression', *Neurology* **72**(10), 886–892.

Meredith, G. E., Totterdell, S., Petroske, E., Santa Cruz, K., Callison, R. C. & Lau, Y.-S. (2002), 'Lysosomal malfunction accompanies alpha-synuclein aggregation in a progressive mouse model of Parkinson's disease.', *Brain Res.* **956**(1), 156–65.

Messenger, M. J., Dawson, L. G. & Duty, S. (2002), 'Changes in metabotropic glutamate receptor 1-8 gene expression in the rodent basal ganglia motor loop following lesion of the nigrostriatal tract.', *Neuropharmacology* **43**(2), 261–71.

Michelucci, A., Heurtaux, T., Grandbarbe, L., Morga, E. & Heuschling, P. (2009), 'Characterization of the microglial phenotype under specific pro-inflammatory and anti-inflammatory conditions: Effects of oligomeric and fibrillar amyloid-β', *J. Neuroimmunol.* **210**(1-2), 3–12.

Miguelez, C., Grandoso, L. & Ugedo, L. (2011), 'Locus coeruleus and dorsal raphe neuron activity and response to acute antidepressant administration in a rat model of Parkinson's disease', *Int. J. Neuropsychopharmacol.* **14**(02), 187–200.

Miklossy, J., Doudet, D., Schwab, C., Yu, S., McGeer, E. & McGeer, P. (2006), 'Role of ICAM-1 in persisting inflammation in Parkinson disease and MPTP monkeys', *Exp. Neurol.* **197**(2), 275–283.

Milber, J. M., Noorigian, J. V., Morley, J. F., Petrovitch, H., White, L., Ross, G. W. & Duda, J. E. (2012), 'Lewy pathology is not the first sign of degeneration in vulnerable neurons in Parkinson disease', *Neurology* **79**(24), 2307–2314.

Miller, C. T., Freiwald, W. A., Leopold, D. A., Mitchell, J. F., Silva, A. C. & Wang, X. (2016), 'Marmosets: A Neuroscientific Model of Human Social Behavior.', *Neuron* **90**(2), 219–33.

Miller, D. B., Ali, S. F., O'Callaghan, J. P. & Laws, S. C. (1998), 'The impact of gender and estrogen on striatal dopaminergic neurotoxicity.', *Ann. N. Y. Acad. Sci.* **844**, 153–65.

Miller, D. W., Hague, S. M., Clarimon, J., Baptista, M., Gwinn-Hardy, K., Cookson, M. R. & Singleton, A. B. (2004), 'Alpha-synuclein in blood and brain from familial Parkinson disease with SNCA locus triplication.', *Neurology* **62**(10), 1835–8.

Miller, R. M. & Federoff, H. J. (2005), 'Altered Gene Expression Profiles Reveal Similarities and Differences Between Parkinson Disease and Model Systems', *Neurosci.* **11**(6), 539–549.

Mitra, R., Aronsson, P., Winder, M., Tobin, G., Bergquist, F. & Carlsson, T. (2015), 'Local Change in Urinary Bladder Contractility Following CNS Dopamine Denervation in the 6-OHDA Rat Model of Parkinson's Disease', *J. Parkinsons. Dis.* **5**(2), 301–311.

Mitsumoto, A. & Nakagawa, Y. (2001), 'DJ-1 is an indicator for endogenous reactive oxygen species elicited by endotoxin.', *Free Radic. Res.* **35**(6), 885–93.

Miwa, T., Watanabe, A., Mitsumoto, Y., Furukawa, M., Fukushima, N. & Moriizumi, T. (2004), 'Olfactory impairment and parkinson's disease-like symptoms observed in the common marmoset following administration of 1-methyl-4-phenyl-1,2,3,6-tetrahydropyridine', *Acta Otolaryngol.* **124**(0), 80–84.

Miyake, Y., Fukushima, W., Tanaka, K., Sasaki, S., Kiyohara, C., Tsuboi, Y., Yamada, T., Oeda, T., Miki, T., Kawamura, N., Sakae, N., Fukuyama, H., Hirota, Y., Nagai, M. & Fukuoka Kinki Parkinson's Disease Study Group (2011), 'Dietary intake of antioxidant vitamins and risk of Parkinson's disease: a case-control study in Japan', *Eur. J. Neurol.* **18**(1), 106–113.

Mizoguchi, K., Yuzurihara, M., Ishige, A., Sasaki, H. & Tabira, T. (2002), 'Chronic stress impairs rotarod performance in rats: implications for depressive state', *Pharmacol. Biochem. Behav.* **71**(1-2), 79–84.

Mizuno, Y., Kondo, T. & Japanese Istradefylline Study Group (2013), 'Adenosine A 2A receptor antagonist istradefylline reduces daily OFF time in Parkinson's disease', *Mov. Disord.* **28**(8), 1138–1141.

Mogi, M., Harada, M., Riederer, P., Narabayashi, H., Fujita, K. & Nagatsu, T. (1994), 'Tumor necrosis factor-alpha (TNF-alpha) increases both in the brain and in the cerebrospinal fluid from parkinsonian patients.', *Neurosci. Lett.* **165**(1-2), 208–10.

Mogi, M., Kondo, T., Mizuno, Y. & Nagatsu, T. (2007), 'p53 protein, interferon-γ, and NF-κB levels are elevated in the parkinsonian brain', *Neurosci. Lett.* **414**(1), 94–97.

Mogi, M., Togari, A., Kondo, T., Mizuno, Y., Komure, O., Kuno, S., Ichinose, H. & Nagatsu, T. (1999), 'Brain-derived growth factor and nerve growth factor concentrations are decreased in the substantia nigra in Parkinson's disease.', *Neurosci. Lett.* **270**(1), 45–8.

Moidunny, S., Matos, M., Wesseling, E., Banerjee, S., Volsky, D. J., Cunha, R. A., Agostinho, P., Boddeke, H. W. & Roy, S. (2016), 'Oncostatin M promotes excitotoxicity by inhibiting glutamate uptake in astrocytes: implications in HIV-associated neurotoxicity', *J. Neuroinflammation* **13**(1), 144.

Molendijk, M. L. & de Kloet, E. R. (2015), 'Immobility in the forced swim test is adaptive and does not reflect depression', *Psychoneuroendocrinology* **62**, 389–391.

Mong, J. A., Kurzweil, R. L., Davis, A. M., Rocca, M. S. & Mccarthy, M. M. (1996), 'Evidence for Sexual Differentiation of Glia in Rat Brain', *Horm. Behav.* **30**(4), 553–562.

Monti, D. A., Zabrecky, G., Kremens, D., Liang, T.-W., Wintering, N. A., Cai, J., Wei, X., Bazzan, A. J., Zhong, L., Bowen, B., Intenzo, C. M., Iacovitti, L. & Newberg, A. B. (2016), 'N-Acetyl Cysteine May Support Dopamine Neurons in Parkinson's Disease: Preliminary Clinical and Cell Line Data', *PLoS One* **11**(6), e0157602.

Monville, C., Torres, E. M. & Dunnett, S. B. (2006), 'Comparison of incremental and accelerating protocols of the rotarod test for the assessment of motor deficits in the 6-OHDA model', *J. Neurosci. Methods* **158**(2), 219–223.

Moran, L. B., Duke, D. C., Deprez, M., Dexter, D. T., Pearce, R. K. B. & Graeber, M. B. (2006), 'Whole genome expression profiling of the medial and lateral substantia nigra in Parkinson's disease', *Neurogenetics* **7**(1), 1–11.

Moreau, C., Delval, A., Tiffreau, V., Defebvre, L., Dujardin, K., Duhamel, A., Petyt, G., Hossein-Foucher, C., Blum, D., Sablonniere, B., Schraen, S., Allorge, D., Destee, A., Bordet, R. & Devos, D. (2013), 'Memantine for axial signs in Parkinson's disease: a randomised, double-blind, placebo-controlled pilot study', *J. Neurol. Neurosurg. Psychiatry* **84**(5), 552–555.

Moretti, M., Neis, V. B., Matheus, F. C., Cunha, M. P., Rosa, P. B., Ribeiro, C. M., Rodrigues, A. L. S. & Prediger, R. D. (2015), 'Effects of Agmatine on Depressive-Like Behavior Induced by Intracerebroventricular Administration of 1-Methyl-4-phenylpyridinium (MPP+)', *Neurotox. Res.* **28**(3), 222–231.

Morin, N., Morissette, M., Grégoire, L., Gomez-Mancilla, B., Gasparini, F. & Di Paolo, T. (2013), 'Chronic treatment with MPEP, an mGlu5 receptor antagonist, normalizes basal ganglia glutamate neurotransmission in l-DOPA-treated parkinsonian monkeys', *Neuropharmacology* **73**, 216–231.

Müller, T., Blum-Degen, D., Przuntek, H. & Kuhn, W. (1998), 'Interleukin-6 levels in cerebrospinal fluid inversely correlate to severity of Parkinson's disease.', *Acta Neurol. Scand.* **98**(2), 142–4.

Murphy, K. E., Gysbers, A. M., Abbott, S. K., Tayebi, N., Kim, W. S., Sidransky, E., Cooper, A., Garner, B. & Halliday, G. M. (2014), 'Reduced glucocerebrosidase is associated with increased α-synuclein in sporadic Parkinson's disease', *Brain* **137**(3), 834–848.

Murray, T. K., Messenger, M. J., Ward, M. A., Woodhouse, S., Osborne, D. J., Duty, S. & O'Neill, M. J. (2002), 'Evaluation of the mGluR2/3 agonist LY379268 in rodent models of Parkinson's disease.', *Pharmacol. Biochem. Behav.* **73**(2), 455–66.

Mylius, V., Brebbermann, J., Dohmann, H., Engau, I., Oertel, W. H. & Möller, J. C. (2011), 'Pain sensitivity and clinical progression in Parkinson's disease', *Mov. Disord.* **26**(12), 2220–2225.

Mythri, R. B., Venkateshappa, C., Harish, G., Mahadevan, A., Muthane, U. B., Yasha, T. C., Srinivas Bharath, M. M. & Shankar, S. K. (2011), 'Evaluation of Markers of Oxidative Stress, Antioxidant Function and Astrocytic Proliferation in the Striatum and Frontal Cortex of Parkinson's Disease Brains', *Neurochem. Res.* **36**(8), 1452–1463.

Nagatsu, T. & Sawada, M. (2005), 'Inflammatory process in Parkinson's disease: role for cytokines.', *Curr. Pharm. Des.* **11**(8), 999–1016.

Nam, J. H., Park, E. S., Won, S.-Y., Lee, Y. A., Kim, K. I., Jeong, J. Y., Baek, J. Y., Cho, E. J., Jin, M., Chung, Y. C., Lee, B. D., Kim, S. H., Kim, E.-G., Byun, K., Lee, B., Woo, D. H., Lee, C. J., Kim, S. R., Bok, E., Kim, Y.-S., Ahn, T.-B., Ko, H. W., Brahmachari, S., Pletinkova, O., Troconso, J. C., Dawson, V. L., Dawson, T. M. & Jin, B. K. (2015), 'TRPV1 on astrocytes rescues nigral dopamine neurons in Parkinson's disease via CNTF', *Brain* **138**(12), 3610–3622.

Nambu, A., Tokuno, H. & Takada, M. (2002), 'Functional significance of the cortico-subthalamopallidal 'hyperdirect' pathway.', *Neurosci. Res.* **43**(2), 111–7.

Nash, B., Ioannidou, K. & Barnett, S. C. (2011), 'Astrocyte phenotypes and their relationship to myelination.', *J. Anat.* **219**(1), 44–52.

Nash, J. E., Hill, M. P. & Brotchie, J. M. (1999), 'Antiparkinsonian Actions of Blockade of NR2B-Containing NMDA Receptors in the Reserpine-Treated Rat', *Exp. Neurol.* **155**(1), 42–48.

Natale, G., Kastsiushenka, O., Fulceri, F., Ruggieri, S., Paparelli, A. & Fornai, F. (2010), 'MPTP-induced parkinsonism extends to a subclass of TH-positive neurons in the gut', *Brain Res.* **1355**, 195–206.

Navarro, J. A., Heßner, S., Yenisetti, S. C., Bayersdorfer, F., Zhang, L., Voigt, A., Schneuwly, S. & Botella, J. A. (2014), 'Analysis of dopaminergic neuronal dysfunction in genetic and toxin-induced models of Parkinson's disease in Drosophila', *J. Neurochem.* **131**(3), 369–382.

Nègre-Pagès, L., Regragui, W., Bouhassira, D., Grandjean, H., Rascol, O. & DoPaMiP Study Group (2008), 'Chronic pain in Parkinson's disease: The cross-sectional French DoPaMiP survey', *Mov. Disord.* **23**(10), 1361–1369.

Nemani, V. M., Lu, W., Berge, V., Nakamura, K., Onoa, B., Lee, M. K., Chaudhry, F. A., Nicoll, R. A. & Edwards, R. H. (2010), 'Increased Expression of α-Synuclein Reduces Neurotransmitter Release by Inhibiting Synaptic Vesicle Reclustering after Endocytosis', *Neuron* **65**(1), 66–79.

Neudorfer, O., Giladi, N., Elstein, D., Abrahamov, A., Turezkite, T., Aghai, E., Reches, A., Bembi, B. & Zimran, A. (1996), 'Occurrence of Parkinson's syndrome in type I Gaucher disease.', *QJM* **89**(9), 691–4.

Neumann, J., Bras, J., Deas, E., O'Sullivan, S. S., Parkkinen, L., Lachmann, R. H., Li, A., Holton, J., Guerreiro, R., Paudel, R., Segarane, B., Singleton, A., Lees, A., Hardy, J., Houlden, H., Revesz, T. & Wood, N. W. (2009), 'Glucocerebrosidase mutations in clinical and pathologically proven Parkinson's disease', *Brain* **132**(7), 1783–1794.

Nichols, W. C., Pankratz, N., Marek, D. K., Pauciulo, M. W., Elsaesser, V. E., Halter, C. A., Rudolph, A., Wojcieszek, J., Pfeiffer, R. F., Foroud, T. & Parkinson Study Group-PROGENI Investigators (2009), 'Mutations in GBA are associated with familial Parkinson disease susceptibility and age at onset', *Neurology* **72**(4), 310–316.

Nicoletti, F., Bruno, V., Ngomba, R. T., Gradini, R. & Battaglia, G. (2015), 'Metabotropic glutamate receptors as drug targets: what's new?', *Curr. Opin. Pharmacol.* **20**, 89–94.

Nielsen, H. H., Qiu, J., Friis, S., Wermuth, L. & Ritz, B. (2012), 'Treatment for Helicobacter pylori infection and risk of parkinson's disease in Denmark', *Eur. J. Neurol.* **19**(6), 864–869.

Niranjan, R. (2014), 'The Role of Inflammatory and Oxidative Stress Mechanisms in the Pathogenesis of Parkinson's Disease: Focus on Astrocytes', *Mol. Neurobiol.* **49**(1), 28–38.

Nishi, A., Kuroiwa, M. & Shuto, T. (2011), 'Mechanisms for the modulation of dopamine d(1) receptor signaling in striatal neurons.', *Front. Neuroanat.* **5**, 43.

Nissen, T., Newman, E. J., Grosset, K., Daghem, M., Pal, G., Stewart, M., Odin, P., Macphee, G. J. & Grosset, D. G. (2012), 'Duration of l-dopa and dopamine agonist monotherapy in Parkinson's disease', *Scott. Med. J.* **57**(4), 217–220.

Niswender, C. M., Johnson, K. A., Weaver, C. D., Jones, C. K., Xiang, Z., Luo, Q., Rodriguez, A. L., Marlo, J. E., de Paulis, T., Thompson, A. D., Days, E. L., Nalywajko, T., Austin, C. A., Williams, M. B., Ayala, J. E., Williams, R., Lindsley, C. W. & Conn, P. J. (2008), 'Discovery, characterization, and antiparkinsonian effect of novel positive allosteric modulators of metabotropic glutamate receptor 4.', *Mol. Pharmacol.* **74**(5), 1345–58.

Njung'e, K. & Handley, S. L. (1991), 'Effects of 5-HT uptake inhibitors, agonists and antagonists on the burying of harmless objects by mice; a putative test for anxiolytic agents.', *Br. J. Pharmacol.* **104**(1), 105–12.

Noorian, A. R., Rha, J., Annerino, D. M., Bernhard, D., Taylor, G. M. & Greene, J. G. (2012), 'Alpha-synuclein transgenic mice display age-related slowing of gastrointestinal motility associated with transgene expression in the vagal system', *Neurobiol. Dis.* **48**(1), 9–19.

Norazit, A., Meedeniya, A. C., Nguyen, M. N. & Mackay-Sim, A. (2010), 'Progressive loss of dopaminergic neurons induced by unilateral rotenone infusion into the medial forebrain bundle', *Brain Res.* **1360**, 119–129.

Noyce, A. J., Bestwick, J. P., Silveira-Moriyama, L., Hawkes, C. H., Giovannoni, G., Lees, A. J. & Schrag, A. (2012), 'Meta-analysis of early nonmotor features and risk factors for Parkinson disease', *Ann. Neurol.* **72**(6), 893–901.

Noyce, A. J., Lees, A. J. & Schrag, A.-E. (2016), 'The prediagnostic phase of Parkinson's disease.', *J. Neurol. Neurosurg. Psychiatry* **87**(8), 871–8.

Nuti, A., Ceravolo, R., Piccinni, A., Dell'Agnello, G., Bellini, G., Gambaccini, G., Rossi, C., Logi, C., Dell'Osso, L. & Bonuccelli, U. (2004), 'Psychiatric comorbidity in a population of Parkinson's disease patients', *Eur. J. Neurol.* **11**(5), 315–320.

Nuytemans, K., Theuns, J., Cruts, M. & Van Broeckhoven, C. (2010), 'Genetic etiology of Parkinson disease associated with mutations in the SNCA, PARK2, PINK1, PARK7, and LRRK2 genes: a mutation update', *Hum. Mutat.* **31**(7), 763–780.

Oaks, A. W., Frankfurt, M., Finkelstein, D. I. & Sidhu, A. (2013), 'Age-dependent effects of A53T alpha-synuclein on behavior and dopaminergic function.', *PLoS One* **8**(4), e60378.

Oerton, E. & Bender, A. (2017), 'Concordance analysis of microarray studies identifies representative gene expression changes in Parkinson's disease: a comparison of 33 human and animal studies', *BMC Neurol.* **17**(1), 58.

Ogawa, N., Hirose, Y., Ohara, S., Ono, T. & Watanabe, Y. (1985), 'A simple quantitative bradykinesia test in MPTP-treated mice.', *Res. Commun. Chem. Pathol. Pharmacol.* **50**(3), 435–41.

Oghumu, S., Terrazas, C. A., Varikuti, S., Kimble, J., Vadia, S., Yu, L., Seveau, S. & Satoskar, A. R. (2015), 'CXCR3 expression defines a novel subset of innate CD8 + T cells that enhance immunity against bacterial infection and cancer upon stimulation with IL-15', *FASEB J.* **29**(3), 1019–1028.

Oguru, M., Tachibana, H., Toda, K., Okuda, B. & Oka, N. (2010), 'Apathy and Depression in Parkinson Disease', *J. Geriatr. Psychiatry Neurol.* **23**(1), 35–41.

Ohnuki, T., Nakamura, A., Okuyama, S. & Nakamura, S. (2010), 'Gene expression profiling in progressively MPTP-lesioned macaques reveals molecular pathways associated with sporadic Parkinson's disease', *Brain Res.* **1346**, 26–42.

Oldham, W. M. & Hamm, H. E. (2008), 'Heterotrimeric G protein activation by G-protein-coupled receptors', *Nat. Rev. Mol. Cell Biol.* **9**(1), 60–71.

Olds, M., Jacques, D. & Kopyov, O. (2006), 'Relation between rotation in the 6-OHDA lesioned rat and dopamine loss in striatal and substantia nigra subregions', *Synapse* **59**(8), 532–544.

Olgiati, S., Thomas, A., Quadri, M., Breedveld, G. J., Graafland, J., Eussen, H., Douben, H., de Klein, A., Onofrj, M. & Bonifati, V. (2015), 'Early-onset parkinsonism caused by alpha-synuclein gene triplication: Clinical and genetic findings in a novel family', *Parkinsonism Relat. Disord.* **21**(8), 981–986.

Oliveras-Salvá, M., Macchi, F., Coessens, V., Deleersnijder, A., Gérard, M., Van der Perren, A., Van den Haute, C. & Baekelandt, V. (2014), 'Alpha-synuclein-induced neurodegeneration is exacerbated in PINK1 knockout mice', *Neurobiol. Aging* **35**(11), 2625–2636.

Olsson, M., Nikkhah, G., Bentlage, C. & Bjorklund, A. (1995), 'Forelimb akinesia in the rat Parkinson model: differential effects of dopamine agonists and nigral transplants as assessed by a new stepping test', *J Neurosci* **15**(5 Pt 2), 3863–3875.

Osellame, L. D., Blacker, T. S. & Duchen, M. R. (2012), 'Cellular and molecular mechanisms of mitochondrial function.', *Best Pract. Res. Clin. Endocrinol. Metab.* **26**(6), 711–23.

Ossola, B., Schendzielorz, N., Chen, S.-H., Bird, G. S., Tuominen, R. K., Männistö, P. T. & Hong, J.-S. (2011), 'Amantadine protects dopamine neurons by a dual action: Reducing activation of microglia and inducing expression of GNDF in astroglia', *Neuropharmacology* **61**(4), 574–582.

Ossowska, K., Konieczny, J., Wolfarth, S., Wierońska, J. & Pilc, A. (2001), 'Blockade of the metabotropic glutamate receptor subtype 5 (mGluR5) produces antiparkinsonian-like effects in rats.', *Neuropharmacology* **41**(4), 413–20.

Oyagi, A., Oida, Y., Hara, H., Izuta, H., Shimazawa, M., Matsunaga, N., Adachi, T. & Hara, H. (2008), 'Protective effects of SUN N8075, a novel agent with antioxidant properties, in in vitro and in vivo models of Parkinson's disease', *Brain Res.* **1214**, 169–176.

Pacelli, C., Giguère, N., Bourque, M.-J., Lévesque, M., Slack, R. S. & Trudeau, L.-É. (2015), 'Elevated Mitochondrial Bioenergetics and Axonal Arborization Size Are Key Contributors to the Vulnerability of Dopamine Neurons', *Curr. Biol.* **25**(18), 2349–2360.

Pahwa, R., Tanner, C. M., Hauser, R. A., Isaacson, S. H., Nausieda, P. A., Truong, D. D., Agarwal, P., Hull, K. L., Lyons, K. E., Johnson, R. & Stempien, M. J. (2017), 'ADS-5102 (Amantadine) Extended-Release Capsules for Levodopa-Induced Dyskinesia in Parkinson Disease (EASE LID Study): A Randomized Clinical Trial.', *JAMA Neurol.* **74**(8), 941–949.

Paille, V., Picconi, B., Bagetta, V., Ghiglieri, V., Sgobio, C., Di Filippo, M., Viscomi, M. T., Giampa, C., Fusco, F. R., Gardoni, F., Bernardi, G., Greengard, P., Di Luca, M. & Calabresi, P. (2010), 'Distinct Levels of Dopamine Denervation Differentially Alter Striatal Synaptic Plasticity and NMDA Receptor Subunit Composition', *J. Neurosci.* **30**(42), 14182–14193.

Pakkenberg, B., Møller, A., Gundersen, H. J., Mouritzen Dam, A. & Pakkenberg, H. (1991), 'The absolute number of nerve cells in substantia nigra in normal subjects and in patients with Parkinson's disease estimated with an unbiased stereological method.', *J. Neurol. Neurosurg. Psychiatry* **54**(1), 30–3.

Pakkenberg, H. & Pakkenberg, B. (1996), 'No clinical progression in a non-addict MPTP-patient in a 20-year period.', *Parkinsonism Relat. Disord.* **2**(2), 107.

Papageorgiou, I. E., Lewen, A., Galow, L. V., Cesetti, T., Scheffel, J., Regen, T., Hanisch, U.-K. & Kann, O. (2016), 'TLR4-activated microglia require IFN-γ to induce severe neuronal dysfunction and death in situ', *Proc. Natl. Acad. Sci.* **113**(1), 212–217.

Papapetropoulos, S., McCorquodale, D. S., Gonzalez, J., Jean-Gilles, L. & Mash, D. C. (2006), 'Cortical and amygdalar Lewy body burden in Parkinson's disease patients with visual hallucinations', *Parkinsonism Relat. Disord.* **12**(4), 253–256.

Parent, A. & Hazrati, L. N. (1995), 'Functional anatomy of the basal ganglia. II. The place of subthalamic nucleus and external pallidum in basal ganglia circuitry.', *Brain Res. Brain Res. Rev.* **20**(1), 128–54.

Parent, M. & Parent, A. (2006), Relationship between axonal collateralization and neuronal degeneration in basal ganglia, *in* 'Park. Dis. Relat. Disord.', Springer Vienna, pp. 85–88.

Park, B., Yang, J., Yun, N., Choe, K.-M., Jin, B. K. & Oh, Y. J. (2010), 'Proteomic analysis of expression and protein interactions in a 6-hydroxydopamine-induced rat brain lesion model', *Neurochem. Int.* **57**(1), 16–32.

Park, J., Lim, C.-S., Seo, H., Park, C.-A., Zhuo, M., Kaang, B.-K. & Lee, K. (2015), 'Pain perception in acute model mice of Parkinson's disease induced by 1-methyl-4-phenyl-1,2,3,6-tetrahydropyridine (MPTP).', *Mol. Pain* **11**, 28.

Parkinson, J. (2002), 'An Essay on the Shaking Palsy. 1817.', *J. Neuropsychiatry Clin. Neurosci.* **14**(2), 223–236.

Patel, A. J. & Gray, C. W. (1993), Neurotrophic Factors Produced by Astrocytes involved in the Regulation of Cholinergic Neurons in the Central Nervous System, *in* 'Biol. Pathol. Astrocyte-Neuron Interact.', Springer US, Boston, MA, pp. 103–115.

Paumier, K. L., Luk, K. C., Manfredsson, F. P., Kanaan, N. M., Lipton, J. W., Collier, T. J., Steece-Collier, K., Kemp, C. J., Celano, S., Schulz, E., Sandoval, I. M., Fleming, S., Dirr, E., Polinski, N. K., Trojanowski, J. Q., Lee, V. M. & Sortwell, C. E. (2015), 'Intrastriatal injection of pre-formed mouse α-synuclein fibrils into rats triggers α-synuclein pathology and bilateral nigrostriatal degeneration.', *Neurobiol. Dis.* **82**, 185–199.

Pawitan, Y., Michiels, S., Koscielny, S., Gusnanto, A. & Ploner, A. (2005), 'False discovery rate, sensitivity and sample size for microarray studies', *Bioinformatics* **21**(13), 3017–3024.

Paxinos, G. & Watson, C. (1986), *The Rat Brain in Stereotaxic Coordinates*, 2 edn, Academic Press, San Diego.

Pedersen, K. F., Alves, G., Aarsland, D. & Larsen, J. P. (2009), 'Occurrence and risk factors for apathy in Parkinson disease: a 4-year prospective longitudinal study.', *J. Neurol. Neurosurg. Psychiatry* **80**(11), 1279–82.

Pellow, S., Chopin, P., File, S. E. & Briley, M. (1985), 'Validation of open:closed arm entries in an elevated plus-maze as a measure of anxiety in the rat.', *J. Neurosci. Methods* **14**(3), 149–67.

Pelvig, D., Pakkenberg, H., Stark, A. & Pakkenberg, B. (2008), 'Neocortical glial cell numbers in human brains', *Neurobiol. Aging* **29**(11), 1754–1762.

Perea, G., Navarrete, M. & Araque, A. (2009), 'Tripartite synapses: astrocytes process and control synaptic information', *Trends Neurosci.* **32**(8), 421–431.

Perez, F. A. & Palmiter, R. D. (2005), 'Parkin-deficient mice are not a robust model of parkinsonism', *Proc. Natl. Acad. Sci.* **102**(6), 2174–2179.

Perez-Pardo, P., de Jong, E. M., Broersen, L. M., van Wijk, N., Attali, A., Garssen, J. & Kraneveld, A. D. (2017), 'Promising Effects of Neurorestorative Diets on Motor, Cognitive, and Gastrointestinal Dysfunction after Symptom Development in a Mouse Model of Parkinson's Disease.', *Front. Aging Neurosci.* **9**, 57.

Perry, T. L. & Yong, V. W. (1986), 'Idiopathic Parkinson's disease, progressive supranuclear palsy and glutathione metabolism in the substantia nigra of patients.', *Neurosci. Lett.* **67**(3), 269–74.

Peterson, L. J. & Flood, P. M. (2012), 'Oxidative stress and microglial cells in Parkinson's disease.', *Mediators Inflamm.* **2012**, 401264.

Petrovitch, H., Abbott, R. D., Ross, G. W., Nelson, J., Masaki, K. H., Tanner, C. M., Launer, L. J. & White, L. R. (2009), 'Bowel movement frequency in late-life and substantia nigra neuron density at death', *Mov. Disord.* **24**(3), 371–376.

Pham, T. T., Giesert, F., Röthig, A., Floss, T., Kallnik, M., Weindl, K., Hölter, S. M., Ahting, U., Prokisch, H., Becker, L., Klopstock, T., Hrabé de Angelis, M., Beyer, K., Görner, K., Kahle, P. J., Vogt Weisenhorn, D. M. & Wurst, W. (2010), 'DJ-1-deficient mice show less TH-positive neurons in the ventral tegmental area and exhibit non-motoric behavioural impairments', *Genes, Brain Behav.* **9**(3), 305–317.

Philips, T. & Rothstein, J. D. (2017), 'Oligodendroglia: metabolic supporters of neurons.', *J. Clin. Invest.* **127**(9), 3271–3280.
URL: *http://www.ncbi.nlm.nih.gov/pubmed/28862639 http://www.pubmedcentral.nih.gov/articlerender.fcgi?a*

Picconi, B. & Calabresi, P. (2014), 'Targeting metabotropic glutamate receptors as a new strategy against levodopa-induced dyskinesia in Parkinson's disease?', *Mov. Disord.* **29**(6), 715–719.

Pienaar, I. S., Götz, J. & Feany, M. B. (2010), 'Parkinson's disease: Insights from non-traditional model organisms', *Prog. Neurobiol.* **92**(4), 558–571.

Piggott, M., Marshall, E., Thomas, N., Lloyd, S., Court, J., Jaros, E., Costa, D., Perry, R. & Perry, E. (1999), 'Dopaminergic activities in the human striatum: rostrocaudal gradients of uptake sites and of D1 and D2 but not of D3 receptor binding or dopamine', *Neuroscience* **90**(2), 433–445.

Pisani, A., Calabresi, P., Centonze, D. & Bernardi, G. (1997), 'Activation of group III metabotropic glutamate receptors depresses glutamatergic transmission at corticostriatal synapse.', *Neuropharmacology* **36**(6), 845–51.

Politis, M. & Niccolini, F. (2015), 'Serotonin in Parkinson's disease', *Behav. Brain Res.* **277**, 136–145.

Politis, M., Wu, K., Loane, C., Brooks, D. J., Kiferle, L., Turkheimer, F. E., Bain, P., Molloy, S. & Piccini, P. (2014), 'Serotonergic mechanisms responsible for levodopa-induced dyskinesias in Parkinson's disease patients', *J. Clin. Invest.* **124**(3), 1340–1349.

Polymeropoulos, M. H., Higgins, J. J., Golbe, L. I., Johnson, W. G., Ide, S. E., Di Iorio, G., Sanges, G., Stenroos, E. S., Pho, L. T., Schaffer, A. A., Lazzarini, A. M., Nussbaum, R. L. &

Duvoisin, R. C. (1996), 'Mapping of a gene for Parkinson's disease to chromosome 4q21-q23.', *Science* **274**(5290), 1197–9.

Polymeropoulos, M. H., Lavedan, C., Leroy, E., Ide, S. E., Dehejia, A., Dutra, A., Pike, B., Root, H., Rubenstein, J., Boyer, R., Stenroos, E. S., Chandrasekharappa, S., Athanassiadou, A., Papapetropoulos, T., Johnson, W. G., Lazzarini, A. M., Duvoisin, R. C., Di Iorio, G., Golbe, L. I. & Nussbaum, R. L. (1997), 'Mutation in the alpha-synuclein gene identified in families with Parkinson's disease.', *Science (80-.).* **276**(5321), 2045–2047.

Ponnazhagan, R., Harms, A. S., Thome, A. D., Jurkuvenaite, A., Gogliotti, R., Niswender, C. M., Conn, P. J. & Standaert, D. G. (2016), 'The Metabotropic Glutamate Receptor 4 Positive Allosteric Modulator ADX88178 Inhibits Inflammatory Responses in Primary Microglia', *J. Neuroimmune Pharmacol.* **11**(2), 231–237.

Popova, D., Karlsson, J. & Jacobsson, S. O. P. (2017), 'Comparison of neurons derived from mouse P19, rat PC12 and human SH-SY5Y cells in the assessment of chemical- and toxin-induced neurotoxicity.', *BMC Pharmacol. Toxicol.* **18**(1), 42.

Porsolt, R. D., Anton, G., Blavet, N. & Jalfre, M. (1978), 'Behavioural despair in rats: a new model sensitive to antidepressant treatments.', *Eur. J. Pharmacol.* **47**(4), 379–91.

Prediger, R., Batista, L., Medeiros, R., Pandolfo, P., Florio, J. & Takahashi, R. (2006), 'The risk is in the air: Intranasal administration of MPTP to rats reproducing clinical features of Parkinson's disease', *Exp. Neurol.* **202**(2), 391–403.

Prinz, A., Selesnew, L.-M., Liss, B., Roeper, J. & Carlsson, T. (2013), 'Increased excitability in serotonin neurons in the dorsal raphe nucleus in the 6-OHDA mouse model of Parkinson's disease', *Exp. Neurol.* **248**, 236–245.

Pritchard, S., Jackson, M. J., Hikima, A., Lione, L., Benham, C. D., Chaudhuri, K. R., Rose, S., Jenner, P. & Iravani, M. M. (2017), 'Altered detrusor contractility in MPTP-treated common marmosets with bladder hyperreflexia', *PLoS One* **12**(5), e0175797.

Pruett, B. S. & Salvatore, M. F. (2013), 'Nigral GFRα1 infusion in aged rats increases locomotor activity, nigral tyrosine hydroxylase, and dopamine content in synchronicity.', *Mol. Neurobiol.* **47**(3), 988–99.

Przedborski, S., Leviver, M., Jiang, H., Ferreira, M., Jackson-Lewis, V., Donaldson, D. & Togasaki, D. M. (1995), 'Dose-dependent lesions of the dopaminergic nigrostriatal pathway induced by intrastriatal injection of 6-hydroxydopamine', *Neuroscience* **67**(3), 631–647.

Qamhawi, Z., Towey, D., Shah, B., Pagano, G., Seibyl, J., Marek, K., Borghammer, P., Brooks, D. J. & Pavese, N. (2015), 'Clinical correlates of raphe serotonergic dysfunction in early Parkinson's disease', *Brain* **138**(10), 2964–2973.

Qin, L., Wu, X., Block, M. L., Liu, Y., Breese, G. R., Hong, J.-S., Knapp, D. J. & Crews, F. T. (2007), 'Systemic LPS Causes Chronic Neuroinflammation and Progressive Neurodegeneration', *Glia* **55**(5), 453–462.

Quik, M., Chen, L., Parameswaran, N., Xie, X., Langston, J. W. & McCallum, S. E. (2006), 'Chronic Oral Nicotine Normalizes Dopaminergic Function and Synaptic Plasticity in 1-Methyl-4-Phenyl-1,2,3,6-Tetrahydropyridine-Lesioned Primates', *J. Neurosci.* **26**(17), 4681–4689.

Quinn, E. J., Blumenfeld, Z., Velisar, A., Koop, M. M., Shreve, L. A., Trager, M. H., Hill, B. C., Kilbane, C., Henderson, J. M. & Brontë-Stewart, H. (2015), 'Beta oscillations in freely moving Parkinson's subjects are attenuated during deep brain stimulation', *Mov. Disord.* **30**(13), 1750–1758.

Quirk, J. C. & Nisenbaum, E. S. (2002), 'LY404187: a novel positive allosteric modulator of AMPA receptors.', *CNS Drug Rev.* **8**(3), 255–82.

Rascol, O., Brooks, D. J., Korczyn, A. D., De Deyn, P. P., Clarke, C. E. & Lang, A. E. (2000), 'A Five-Year Study of the Incidence of Dyskinesia in Patients with Early Parkinson's Disease Who Were Treated with Ropinirole or Levodopa', *N. Engl. J. Med.* **342**(20), 1484–1491.

Rascol, O., Fox, S., Gasparini, F., Kenney, C., Di Paolo, T. & Gomez-Mancilla, B. (2014), 'Use of metabotropic glutamate 5-receptor antagonists for treatment of levodopa-induced dyskinesias', *Parkinsonism Relat. Disord.* **20**(9), 947–956.

Ray, A., Martinez, B. A., Berkowitz, L. A., Caldwell, G. A. & Caldwell, K. A. (2014), 'Mitochondrial dysfunction, oxidative stress and neurodegeneration elicited by a bacterial metabolite in a C. elegans Parkinson's model', *Cell Death Dis.* **5**(1), e984–e984.

Reale, M., Iarlori, C., Thomas, A., Gambi, D., Perfetti, B., Di Nicola, M. & Onofrj, M. (2009), 'Peripheral cytokines profile in Parkinson's disease', *Brain. Behav. Immun.* **23**(1), 55–63.

Redgrave, P. & Mitchell, I. (1982), 'Functional validation of projection topography in the nigrostriatal dopamine system.', *Neuroscience* **7**(4), 885–94.

Reichel, C. A., Khandoga, A., Anders, H.-J., Schlöndorff, D., Luckow, B. & Krombach, F. (2006), 'Chemokine receptors Ccr1, Ccr2, and Ccr5 mediate neutrophil migration to postischemic tissue', *J. Leukoc. Biol.* **79**(1), 114–122.

Reijnders, J. S., Ehrt, U., Weber, W. E., Aarsland, D. & Leentjens, A. F. (2008), 'A systematic review of prevalence studies of depression in Parkinson's disease', *Mov. Disord.* **23**(2), 183–189.

Remple, M. S., Bradenham, C. H., Kao, C. C., Charles, P. D., Neimat, J. S. & Konrad, P. E. (2011), 'Subthalamic nucleus neuronal firing rate increases with Parkinson's disease progression', *Mov. Disord.* **26**(9), 1657–1662.

Remy, P., Doder, M., Lees, A., Turjanski, N. & Brooks, D. (2005), 'Depression in Parkinson's disease: loss of dopamine and noradrenaline innervation in the limbic system', *Brain* **128**(6), 1314–1322.

Rial, D., Castro, A. A., Machado, N., Garção, P., Gonçalves, F. Q., Silva, H. B., Tomé, Â. R., Köfalvi, A., Corti, O., Raisman-Vozari, R., Cunha, R. A. & Prediger, R. D. (2014), 'Behavioral Phenotyping of Parkin-Deficient Mice: Looking for Early Preclinical Features of Parkinson's Disease', *PLoS One* **9**(12), e114216.

Richardson, N. R. & Gratton, A. (1996), 'Behavior-relevant changes in nucleus accumbens dopamine transmission elicited by food reinforcement: an electrochemical study in rat.', *J. Neurosci.* **16**(24), 8160–9.

Riess, O., Krüger, R. & Schulz, J. B. (2002), 'Spectrum of phenotypes and genotypes in Parkinson's disease', *J. Neurol.* **249**(0), 1–1.

Rijnboutt, S., Aerts, H. M., Geuze, H. J., Tager, J. M. & Strous, G. J. (1991), 'Mannose 6-phosphate-independent membrane association of cathepsin D, glucocerebrosidase, and sphingolipid-activating protein in HepG2 cells.', *J. Biol. Chem.* **266**(8), 4862–8.

Rink, E. & Wullimann, M. F. (2001), 'The teleostean (zebrafish) dopaminergic system ascending to the subpallium (striatum) is located in the basal diencephalon (posterior tuberculum)', *Brain Res.* **889**(1-2), 316–330.

Robbins, T. W. & Everitt, B. J. (1992), 'Functions of dopamine in the dorsal and ventral striatum', *Semin. Neurosci.* **4**(2), 119–127.

Robinson, T. E. & Whishaw, I. Q. (1988), 'Normalization of extracellular dopamine in striatum following recovery from a partial unilateral 6-OHDA lesion of the substantia nigra: a microdialysis study in freely moving rats', *Brain Res* **450**(1–2), 209–224.

Robledo, P. & Feger, J. (1991), 'Acute monoaminergic depletion in the rat potentiates the excitatory effect of the subthalamic nucleus in the substantia nigra pars reticulata but not in the pallidal complex.', *J. Neural Transm. Gen. Sect.* **86**(2), 115–26.

Rocha, N. P., Scalzo, P. L., Barbosa, I. G., Souza, M. S., Morato, I. B., Vieira, E. L. M., Christo, P. P., Teixeira, A. L. & Reis, H. J. (2014), 'Cognitive Status Correlates with CXCL10/IP-10 Levels in Parkinson's Disease.', *Parkinsons. Dis.* **2014**, 903796.

Rockenstein, E., Mallory, M., Hashimoto, M., Song, D., Shults, C. W., Lang, I. & Masliah, E. (2002), 'Differential neuropathological alterations in transgenic mice expressing ?-synuclein from the platelet-derived growth factor and Thy-1 promoters', *J. Neurosci. Res.* **68**(5), 568–578.

Rodriguez, M. C., Obeso, J. A. & Olanow, C. W. (1998), 'Subthalamic nucleus-mediated excitotoxicity in Parkinson's disease: a target for neuroprotection.', *Ann. Neurol.* **44**(3 Suppl 1), S175–88.

Roedter, A., Winkler, C., Samii, M., Walter, G. F., Brandis, A. & Nikkhah, G. (2001), 'Comparison of unilateral and bilateral intrastriatal 6-hydroxydopamine-induced axon terminal lesions: Evidence for interhemispheric functional coupling of the two nigrostriatal pathways', *J. Comp. Neurol.* **432**(2), 217–229.

Roome, R. B. & Vanderluit, J. L. (2015), 'Paw-Dragging: a Novel, Sensitive Analysis of the Mouse Cylinder Test', *J. Vis. Exp.* (98), e52701.

Ross, G. W. & Petrovitch, H. (2001), 'Current evidence for neuroprotective effects of nicotine and caffeine against Parkinson's disease.', *Drugs Aging* **18**(11), 797–806.

Ross, O. A., O'Neill, C., Rea, I., Lynch, T., Gosal, D., Wallace, A., Curran, M. D., Middleton, D. & Gibson, J. (2004), 'Functional promoter region polymorphism of the proinflammatory chemokine IL-8 gene associates with Parkinson's disease in the Irish', *Hum. Immunol.* **65**(4), 340–346.

Rossi, F., Marabese, I., De Chiaro, M., Boccella, S., Luongo, L., Guida, F., De Gregorio, D., Giordano, C., de Novellis, V., Palazzo, E. & Maione, S. (2014), 'Dorsal striatum metabotropic glutamate receptor 8 affects nocifensive responses and rostral ventromedial medulla cell activity in neuropathic pain conditions', *J. Neurophysiol.* **111**(11), 2196–2209.

Rouse, S. T., Marino, M. J., Bradley, S. R., Awad, H., Wittmann, M. & Conn, P. J. (2000), 'Distribution and roles of metabotropic glutamate receptors in the basal ganglia motor circuit: implications for treatment of Parkinson's disease and related disorders.', *Pharmacol. Ther.* **88**(3), 427–35.

Roy, A., Ghosh, A., Jana, A., Liu, X., Brahmachari, S., Gendelman, H. E. & Pahan, K. (2012), 'Sodium Phenylbutyrate Controls Neuroinflammatory and Antioxidant Activities and Protects Dopaminergic Neurons in Mouse Models of Parkinson's Disease', *PLoS One* **7**(6), e38113.

Royet, J. P., Gervais, R. & Araneda, S. (1983), 'Effect of local 6-OHDA and 5,6-DHT injections into the rat olfactory bulb on neophobia and learned aversion to a novel food.', *Behav. Brain Res.* **10**(2-3), 297–309.

Rylander, D., Recchia, A., Mela, F., Dekundy, A., Danysz, W. & Cenci, M. A. (2009), 'Pharmacological modulation of glutamate transmission in a rat model of L-DOPA-induced dyskinesia: effects on motor behavior and striatal nuclear signaling', *J Pharmacol Exp Ther* **330**(1), 227–235.

Ryu, E. J., Harding, H. P., Angelastro, J. M., Vitolo, O. V., Ron, D. & Greene, L. A. (2002), 'Endoplasmic reticulum stress and the unfolded protein response in cellular models of Parkinson's disease.', *J. Neurosci.* **22**(24), 10690–8.

Sachs, C. & Jonsson, G. (1975), 'Mechanisms of action of 6-hydroxydopamine', *Biochem. Pharmacol.* **24**(1), 1–8.

Sadeghian, M., Mullali, G., Pocock, J. M., Piers, T., Roach, A. & Smith, K. J. (2016), 'Neuroprotection by safinamide in the 6-hydroxydopamine model of Parkinson's disease', *Neuropathol. Appl. Neurobiol.* **42**(5), 423–435.

Saha, K., Sambo, D., Richardson, B. D., Lin, L. M., Butler, B., Villarroel, L. & Khoshbouei, H. (2014), 'Intracellular Methamphetamine Prevents the Dopamine-induced Enhancement of Neuronal Firing', *J. Biol. Chem.* **289**(32), 22246–22257.

Sahli, Z. T. & Tarazi, F. I. (2018), 'Pimavanserin: novel pharmacotherapy for Parkinson's disease psychosis', *Expert Opin. Drug Discov.* **13**(1), 103–110.

Sakai, K. & Gash, D. M. (1994), 'Effect of bilateral 6-OHDA lesions of the substantia nigra on locomotor activity in the rat.', *Brain Res.* **633**(1-2), 144–50.

Sakakibara, R., Uchiyama, T., Yamanishi, T., Shirai, K. & Hattori, T. (2008), 'Bladder and bowel dysfunction in Parkinson's disease', *J. Neural Transm.* **115**(3), 443–460.

Salois, G. & Smith, J. S. (2016), 'Housing Complexity Alters GFAP-Immunoreactive Astrocyte Morphology in the Rat Dentate Gyrus', *Neural Plast.* **2016**, 1–11.

Salt, T. E. & Eaton, S. A. (1995), 'Distinct presynaptic metabotropic receptors for L-AP4 and CCG1 on GABAergic terminals: pharmacological evidence using novel alpha-methyl derivative mGluR antagonists, MAP4 and MCCG, in the rat thalamus in vivo.', *Neuroscience* **65**(1), 5–13.

Salvatore, M. F., Calipari, E. S. & Jones, S. R. (2016), 'Regulation of Tyrosine Hydroxylase Expression and Phosphorylation in Dopamine Transporter-Deficient Mice.', *ACS Chem. Neurosci.* **7**(7), 941–51.

Salvatore, M. F. & Pruett, B. S. (2012), 'Dichotomy of tyrosine hydroxylase and dopamine regulation between somatodendritic and terminal field areas of nigrostriatal and mesoaccumbens pathways.', *PLoS One* **7**(1), e29867.

Salvatore, M. F., Zhang, J.-L., Large, D. M., Wilson, P. E., Gash, C. R., Thomas, T. C., Haycock, J. W., Bing, G., Stanford, J. A., Gash, D. M. & Gerhardt, G. A. (2004), 'Striatal GDNF administration increases tyrosine hydroxylase phosphorylation in the rat striatum and substantia nigra', *J. Neurochem.* **90**(1), 245–254.

Santiago, R. M., Barbieiro, J., Lima, M. M., Dombrowski, P. A., Andreatini, R. & Vital, M. A. (2010), 'Depressive-like behaviors alterations induced by intranigral MPTP, 6-OHDA, LPS and rotenone models of Parkinson's disease are predominantly associated with serotonin and dopamine', *Prog. Neuro-Psychopharmacology Biol. Psychiatry* **34**(6), 1104–1114.

Santos, J. R., Cunha, J. A., Dierschnabel, A. L., Campêlo, C. L., Leão, A. H., Silva, A. F., Engelberth, R. C., Izídio, G. S., Cavalcante, J. S., Abílio, V. C., Ribeiro, A. M. & Silva, R. H. (2013), 'Cognitive, motor and tyrosine hydroxylase temporal impairment in a model of parkinsonism induced by reserpine', *Behav. Brain Res.* **253**, 68–77.

Sárvári, M., Kalló, I., Hrabovszky, E., Solymosi, N., Rodolosse, A. & Liposits, Z. (2016), 'Long-Term Estrogen Receptor Beta Agonist Treatment Modifies the Hippocampal Transcriptome in Middle-Aged Ovariectomized Rats', *Front. Cell. Neurosci.* **10**, 149.

Sauer, H. & Oertel, W. H. (1994), 'Progressive degeneration of nigrostriatal dopamine neurons following intrastriatal terminal lesions with 6-hydroxydopamine: a combined retrograde tracing and immunocytochemical study in the rat', *Neuroscience* **59**.

Sauerbier, A., Jenner, P., Todorova, A. & Chaudhuri, K. R. (2016), 'Non motor subtypes and Parkinson's disease', *Parkinsonism Relat. Disord.* **22**, S41–S46.

Saugstad, J. A., Kinzie, J. M., Shinohara, M. M., Segerson, T. P. & Westbrook, G. L. (1997), 'Cloning and expression of rat metabotropic glutamate receptor 8 reveals a distinct pharmacological profile.', *Mol. Pharmacol.* **51**(1), 119–25.

Savica, R., Carlin, J. M., Grossardt, B. R., Bower, J. H., Ahlskog, J. E., Maraganore, D. M., Bharucha, A. E. & Rocca, W. A. (2009), 'Medical records documentation of constipation preceding Parkinson disease: A case-control study', *Neurology* **73**(21), 1752–1758.

Savica, R., Parisi, J. E., Wold, L. E., Josephs, K. A. & Ahlskog, J. E. (2012), 'High School Football and Risk of Neurodegeneration: A Community-Based Study', *Mayo Clin. Proc.* **87**(4), 335–340.

Schallert, T., Fleming, S. M., Leasure, J., Tillerson, J. L. & Bland, S. T. (2000), 'CNS plasticity and assessment of forelimb sensorimotor outcome in unilateral rat models of stroke, cortical ablation, parkinsonism and spinal cord injury', *Neuropharmacology* **39**(5), 777–787.

Schapira, A. H. (2000), 'Sleep attacks (sleep episodes) with pergolide', *Lancet* **355**(9212), 1332–1333.

Schapira, A. H. (2015), 'Glucocerebrosidase and Parkinson disease: Recent advances', *Mol. Cell. Neurosci.* **66**(Pt A), 37–42.

Schell, G. R. & Strick, P. L. (1984), 'The origin of thalamic inputs to the arcuate premotor and supplementary motor areas.', *J. Neurosci.* **4**(2), 539–60.

Schenck, C. H., Bundlie, S. R. & Mahowald, M. W. (1996), 'Delayed emergence of a parkinsonian disorder in 38% of 29 older men initially diagnosed with idiopathic rapid eye movement sleep behaviour disorder.', *Neurology* **46**(2), 388–93.

Schneeberger, A., Mandler, M., Mattner, F. & Schmidt, W. (2012), 'Vaccination for Parkinson's disease', *Parkinsonism Relat. Disord.* **18**, S11–S13.

Schneider, J. S. & Pope-Coleman, A. (1995), 'Cognitive deficits precede motor deficits in a slowly progressing model of parkinsonism in the monkey.', *Neurodegeneration* **4**(3), 245–55.

Schneider, P., Ho, Y.-J., Spanagel, R. & Pawlak, C. (2011), 'A Novel Elevated Plus-Maze Procedure to Avoid the One-Trial Tolerance Problem', *Front. Behav. Neurosci.* **5**, 43.

Schneider, T. & Popik, P. (2007), 'Attenuation of estrous cycle-dependent marble burying in female rats by acute treatment with progesterone and antidepressants', *Psychoneuroendocrinology* **32**(6), 651–659.

Schuldiner, S., Liu, Y. & Edwards, R. H. (1993), 'Reserpine binding to a vesicular amine transporter expressed in Chinese hamster ovary fibroblasts.', *J. Biol. Chem.* **268**(1), 29–34.

Schulz-Schaeffer, W. J. (2015), 'Is Cell Death Primary or Secondary in the Pathophysiology of Idiopathic Parkinson's Disease?', *Biomolecules* **5**(3), 1467–79.

Schwab, R. S., England, A. C., Poskanzer, D. C. & Young, R. R. (1969), 'Amantadine in the Treatment of Parkinson's Disease', *JAMA J. Am. Med. Assoc.* **208**(7), 1168.

Schwartz, M. D. & Kilduff, T. S. (2015), 'The Neurobiology of Sleep and Wakefulness', *Psychiatr. Clin. North Am.* **38**(4), 615–644.

Seki, S., Igawa, Y., Kaidoh, K., Ishizuka, O., Nishizawa, O. & Andersson, K. E. (2001), 'Role of dopamine D1 and D2 receptors in the micturition reflex in conscious rats.', *Neurourol. Urodyn.* **20**(1), 105–13.

Shamoto-Nagai, M., Maruyama, W., Kato, Y., Isobe, K.-i., Tanaka, M., Naoi, M. & Osawa, T. (2003), 'An inhibitor of mitochondrial complex I, rotenone, inactivates proteasome by oxidative modification and induces aggregation of oxidized proteins in SH-SY5Y cells', *J. Neurosci. Res.* **74**(4), 589–597.

Shanks, R. A., Anderson, J. R., Taylor, J. R. & Lloyd, S. A. (2012), 'Amphetamine and Methamphetamine Have a Direct and Differential Effect on BV2 Microglia Cells', *Bull. Exp. Biol. Med.* **154**(2), 228–232.

Sherer, T. B., Betarbet, R., Kim, J. H. & Greenamyre, J. T. (2003), 'Selective microglial activation in the rat rotenone model of Parkinson's disease.', *Neurosci. Lett.* **341**(2), 87–90.

Shi, Z., Lu, Z., Zhao, Y., Wang, Y., Zhao-Wilson, X., Guan, P., Duan, X., Chang, Y.-Z. & Zhao, B. (2013), 'Neuroprotective effects of aqueous extracts of Uncaria tomentosa: Insights from 6-OHDA induced cell damage and transgenic Caenorhabditis elegans model', *Neurochem. Int.* **62**(7), 940–947.

Shiba, M., Bower, J. H., Maraganore, D. M., McDonnell, S. K., Peterson, B. J., Ahlskog, J. E., Schaid, D. J. & Rocca, W. A. (2000), 'Anxiety disorders and depressive disorders preceding Parkinson's disease: a case-control study.', *Mov. Disord.* **15**(4), 669–77.

Shigemoto, R., Kinoshita, A., Wada, E., Nomura, S., Ohishi, H., Takada, M., Flor, P. J., Neki, A., Abe, T., Nakanishi, S. & Mizuno, N. (1997), 'Differential presynaptic localization of metabotropic glutamate receptor subtypes in the rat hippocampus.', *J. Neurosci.* **17**(19), 7503–22.

Shimo, Y. & Wichmann, T. (2009), 'Neuronal activity in the subthalamic nucleus modulates the release of dopamine in the monkey striatum', *Eur. J. Neurosci.* **29**(1), 104–113.

Shimoji, M., Zhang, L., Mandir, A. S., Dawson, V. L. & Dawson, T. M. (2005), 'Absence of inclusion body formation in the MPTP mouse model of Parkinson's disease', *Mol. Brain Res.* **134**(1), 103–108.

Shin, H.-W. & Chung, S. J. (2012), 'Drug-induced parkinsonism.', *J. Clin. Neurol.* **8**(1), 15–21.

Shin, K. S., Zhao, T. T., Choi, H. S., Hwang, B. Y., Lee, C. K. & Lee, M. K. (2014), 'Effects of gypenosides on anxiety disorders in MPTP-lesioned mouse model of Parkinson's disease', *Brain Res.* **1567**, 57–65.

Shoji, H., Takao, K., Hattori, S. & Miyakawa, T. (2016), 'Age-related changes in behavior in C57BL/6J mice from young adulthood to middle age.', *Mol. Brain* **9**, 11.

Shulman, L., Taback, R., Rabinstein, A. & Weiner, W. (2002), 'Non-recognition of depression and other non-motor symptoms in Parkinson's disease', *Parkinsonism Relat. Disord.* **8**(3), 193–197.

Silva, T. P., Poli, A., Hara, D. B. & Takahashi, R. N. (2016), 'Time course study of microglial and behavioral alterations induced by 6-hydroxydopamine in rats', *Neurosci Lett* **622**, 83–87.

Simpson, J. E., Ince, P. G., Lace, G., Forster, G., Shaw, P. J., Matthews, F., Savva, G., Brayne, C., Wharton, S. B. & MRC Cognitive Function and Ageing Neuropathology Study Group (2010), 'Astrocyte phenotype in relation to Alzheimer-type pathology in the ageing brain.', *Neurobiol. Aging* **31**(4), 578–90.

Sixel-Döring, F., Trautmann, E., Mollenhauer, B. & Trenkwalder, C. (2014), 'Rapid Eye Movement Sleep Behavioral Events: A New Marker for Neurodegeneration in Early Parkinson Disease?', *Sleep* **37**(3), 431–438.

Slaets, H., Hendriks, J. J., Stinissen, P., Kilpatrick, T. J. & Hellings, N. (2010), 'Therapeutic potential of LIF in multiple sclerosis', *Trends Mol. Med.* **16**(11), 493–500.

Slawinska, A., Wieronska, J. M., Stachowicz, K., Palucha-Poniewiera, A., Uberti, M. A., Bacolod, M. A., Doller, D. & Pilc, A. (2013), 'Anxiolytic- but not antidepressant-like activity of Lu AF21934, a novel, selective positive allosteric modulator of the mGlu(4) receptor', *Neuropharmacology* **66**, 225–235.

Slenter, D. N., Kutmon, M., Hanspers, K., Riutta, A., Windsor, J., Nunes, N., Mélius, J., Cirillo, E., Coort, S. L., Digles, D., Ehrhart, F., Giesbertz, P., Kalafati, M., Martens, M., Miller, R., Nishida, K., Rieswijk, L., Waagmeester, A., Eijssen, L. M. T., Evelo, C. T., Pico, A. R. & Willighagen, E. L. (2018), 'WikiPathways: a multifaceted pathway database bridging metabolomics to other omics research', *Nucleic Acids Res.* **46**(D1), D661–D667.

Smith, L. A., Jackson, M. J., Al-Barghouthy, G. & Jenner, P. (2002), 'The actions of a D-1 agonist in MPTP treated primates show dependence on both D-1 and D-2 receptor function and tolerance on repeated administration', *J. Neural Transm.* **109**(2), 123–140.

Sofic, E., Lange, K. W., Jellinger, K. & Riederer, P. (1992), 'Reduced and oxidized glutathione in the substantia nigra of patients with Parkinson's disease.', *Neurosci. Lett.* **142**(2), 128–30.

Soilu-Hänninen, M., Broberg, E., Röyttä, M., Mattila, P., Rinne, J. & Hukkanen, V. (2010), 'Expression of LIF and LIF receptor beta in Alzheimer's and Parkinson's diseases.', *Acta Neurol. Scand.* **121**(1), 44–50.

Solomon, G. (2018), 'Chronic traumatic encephalopathy in sports: a historical and narrative review', *Dev. Neuropsychol.* **43**(4), 279–311.

Son, O.-L., Kim, H.-T., Ji, M.-H., Yoo, K.-W., Rhee, M. & Kim, C.-H. (2003), 'Cloning and expression analysis of a Parkinson's disease gene, uch-L1, and its promoter in zebrafish', *Biochem. Biophys. Res. Commun.* **312**(3), 601–607.

Spinelli, K. J., Taylor, J. K., Osterberg, V. R., Churchill, M. J., Pollock, E., Moore, C., Meshul, C. K. & Unni, V. K. (2014), 'Presynaptic Alpha-Synuclein Aggregation in a Mouse Model of Parkinson's Disease', *J. Neurosci.* **34**(6), 2037–2050.

Spinelli, S., Pennanen, L., Dettling, A. C., Feldon, J., Higgins, G. A. & Pryce, C. R. (2004), 'Performance of the marmoset monkey on computerized tasks of attention and working memory', *Cogn. Brain Res.* **19**(2), 123–137.

Stafford, K., Gomes, A. B., Shen, J. & Yoburn, B. C. (2001), 'mu-Opioid receptor downregulation contributes to opioid tolerance in vivo.', *Pharmacol. Biochem. Behav.* **69**(1-2), 233–7.

Steece-Collier, K., Chambers, L. K., Jaw-Tsai, S. S., Menniti, F. S. & Greenamyre, J. (2000), 'Antiparkinsonian Actions of CP-101,606, an Antagonist of NR2B Subunit-Containing N-Methyl-d-Aspartate Receptors', *Exp. Neurol.* **163**(1), 239–243.

Steger, M., Tonelli, F., Ito, G., Davies, P., Trost, M., Vetter, M., Wachter, S., Lorentzen, E., Duddy, G., Wilson, S., Baptista, M. A., Fiske, B. K., Fell, M. J., Morrow, J. A., Reith, A. D., Alessi, D. R. & Mann, M. (2016), 'Phosphoproteomics reveals that Parkinson's disease kinase LRRK2 regulates a subset of Rab GTPases', *Elife* **5**.

Stocchi, F. & Olanow, C. W. (2004), 'Continuous dopaminergic stimulation in early and advanced Parkinson's disease.', *Neurology* **62**(1 Suppl 1), S56–63.

Storch, A., Schneider, C. B., Wolz, M., Sturwald, Y., Nebe, A., Odin, P., Mahler, A., Fuchs, G., Jost, W. H., Chaudhuri, K. R., Koch, R., Reichmann, H. & Ebersbach, G. (2013), 'Nonmotor fluctuations in Parkinson disease: Severity and correlation with motor complications', *Neurology* **80**(9), 800–809.

Stott, S. R. W. & Barker, R. A. (2014), 'Time course of dopamine neuron loss and glial response in the 6-OHDA striatal mouse model of Parkinson's disease', *Eur. J. Neurosci.* **39**(6), 1042–1056.

Stranger, B. E., Nica, A. C., Forrest, M. S., Dimas, A., Bird, C. P., Beazley, C., Ingle, C. E., Dunning, M., Flicek, P., Koller, D., Montgomery, S., Tavaré, S., Deloukas, P. & Dermitzakis, E. T. (2007), 'Population genomics of human gene expression', *Nat. Genet.* **39**(10), 1217–1224.

Su, X., Maguire-Zeiss, K. A., Giuliano, R., Prifti, L., Venkatesh, K. & Federoff, H. J. (2008), 'Synuclein activates microglia in a model of Parkinson's disease', *Neurobiol. Aging* **29**(11), 1690–1701.

Sudakov, S. K., Nazarova, G. A., Alekseeva, E. V. & Bashkatova, V. G. (2013), 'Estimation of the Level of Anxiety in Rats: Differences in Results of Open-Field Test, Elevated Plus-Maze Test, and Vogel's Conflict Test', *Bull. Exp. Biol. Med.* **155**(3), 295–297.

Sullivan, R., Dufresne, M., Siontas, D., Chehab, S., Townsend, J. & Laplante, F. (2014), 'Meso-cortical dopamine depletion and anxiety-related behavior in the rat: Sex and hemisphere differences', *Prog. Neuro-Psychopharmacology Biol. Psychiatry* **54**, 59–66.

Sullivan, R. M., Duchesne, A., Hussain, D., Waldron, J. & Laplante, F. (2009), 'Effects of unilateral amygdala dopamine depletion on behaviour in the elevated plus maze: Role of sex, hemisphere and retesting', *Behav Brain Res* **205**(1), 115–122.

Sullivan, R. M. & Szechtman, H. (1994), 'Left/right nigrostriatal asymmetry in susceptibility to neurotoxic dopamine depletion with 6-hydroxydopamine in rats.', *Neurosci. Lett.* **170**(1), 83–6.

Sulston, J., Dew, M. & Brenner, S. (1975), 'Dopaminergic neurons in the nematodeCaenorhabditis elegans', *J. Comp. Neurol.* **163**(2), 215–226.

Sun, L., Shen, R., Agnihotri, S. K., Chen, Y., Huang, Z. & Büeler, H. (2018), 'Lack of PINK1 alters glia innate immune responses and enhances inflammation-induced, nitric oxide-mediated neuron death', *Sci. Rep.* **8**(1), 383.

Sun, Y., Olson, R., Horning, M., Armstrong, N., Mayer, M. & Gouaux, E. (2002), 'Mechanism of glutamate receptor desensitization', *Nature* **417**(6886), 245–253.

Surmeier, D. J., Guzman, J. N., Sanchez-Padilla, J. & Goldberg, J. A. (2011), 'The Origins of Oxidant Stress in Parkinson's Disease and Therapeutic Strategies', *Antioxid. Redox Signal.* **14**(7), 1289–1301.

Sutherland, G. T., Matigian, N. A., Chalk, A. M., Anderson, M. J., Silburn, P. A., Mackay-Sim, A., Wells, C. A. & Mellick, G. D. (2009), 'A Cross-Study Transcriptional Analysis of Parkinson's Disease', *PLoS One* **4**(3), e4955.

Svetel, M., Smiljković, T., Pekmezović, T. & Kostić, V. (2012), 'Hallucinations in Parkinson's disease: cross-sectional study', *Acta Neurol. Belg.* **112**(1), 33–37.

Tadaiesky, M. T., Dombrowski, P. A., Figueiredo, C. P., Cargnin-Ferreira, E., Da Cunha, C. & Takahashi, R. N. (2008), 'Emotional, cognitive and neurochemical alterations in a premotor stage model of Parkinson's disease', *Neuroscience* **156**(4), 830–840.

Takuma, K., Baba, A. & Matsuda, T. (2004), 'Astrocyte apoptosis: implications for neuroprotection', *Prog. Neurobiol.* **72**(2), 111–127.

Talati, R., Reinhart, K., Baker, W., White, C. M. & Coleman, C. I. (2009), 'Pharmacologic treatment of advanced Parkinson's disease: A meta-analysis of COMT inhibitors and MAO-B inhibitors', *Parkinsonism Relat. Disord.* **15**(7), 500–505.

Tanaka, H., Kannari, K., Maeda, T., Tomiyama, M., Suda, T. & Matsunaga, M. (1999), 'Role of serotonergic neurons in L-DOPA-derived extracellular dopamine in the striatum of 6-OHDA-lesioned rats.', *Neuroreport* **10**(3), 631–4.

Tansey, M. G., McCoy, M. K. & Frank-Cannon, T. C. (2007), 'Neuroinflammatory mechanisms in Parkinson's disease: Potential environmental triggers, pathways, and targets for early therapeutic intervention', *Exp. Neurol.* **208**(1), 1–25.

Tarassishin, L., Suh, H.-S. & Lee, S. C. (2014), 'LPS and IL-1 differentially activate mouse and human astrocytes: Role of CD14', *Glia* **62**(6), 999–1013.

Tavassoly, O. & Lee, J. S. (2012), 'Methamphetamine binds to α-synuclein and causes a conformational change which can be detected by nanopore analysis', *FEBS Lett.* **586**(19), 3222–3228.

Taylor, D. L., Diemel, L. T., Cuzner, M. L. & Pocock, J. M. (2002), 'Activation of group II metabotropic glutamate receptors underlies microglial reactivity and neurotoxicity following stimulation with chromogranin A, a peptide up-regulated in Alzheimer's disease', *J. Neurochem.* **82**(5), 1179–1191.

Taylor, D. L., Diemel, L. T. & Pocock, J. M. (2003), 'Activation of microglial group III metabotropic glutamate receptors protects neurons against microglial neurotoxicity.', *J. Neurosci.* **23**(6), 2150–60.

Taylor, T. N., Caudle, W. M., Shepherd, K. R., Noorian, A., Jackson, C. R., Iuvone, P. M., Weinshenker, D., Greene, J. G. & Miller, G. W. (2009), 'Nonmotor Symptoms of Parkinson's Disease Revealed in an Animal Model with Reduced Monoamine Storage Capacity', *J. Neurosci.* **29**(25), 8103–8113.

Teixeira, F. G., Gago, M. F., Marques, P., Moreira, P. S., Magalhães, R., Sousa, N. & Salgado, A. J. (2018), 'Safinamide: a new hope for Parkinson's disease?', *Drug Discov. Today* **23**(3), 736–744.

Tesseur, I., Nguyen, A., Chang, B., Li, L., Woodling, N. S., Wyss-Coray, T. & Luo, J. (2017), 'Deficiency in Neuronal TGF-β Signaling Leads to Nigrostriatal Degeneration and Activation of TGF-β Signaling Protects against MPTP Neurotoxicity in Mice', *J. Neurosci.* **37**(17), 4584–4592.

Tesseur, I. & Wyss-Coray, T. (2006), 'A role for TGF-beta signaling in neurodegeneration: evidence from genetically engineered models.', *Curr. Alzheimer Res.* **3**(5), 505–13.

Testa, C. M., Standaert, D. G., Young, A. B. & Penney Jr., J. B. (1994), 'Metabotropic glutamate receptor mRNA expression in the basal ganglia of the rat', *J Neurosci* **14**(5 Pt 2), 3005–3018.

Thakur, P. & Nehru, B. (2015), 'Inhibition of Neuroinflammation and Mitochondrial Dysfunctions by Carbenoxolone in the Rotenone Model of Parkinson's Disease', *Mol. Neurobiol.* **51**(1), 209–219.

The Parkinson's Study Group (1999), 'Low-Dose Clozapine for the Treatment of Drug-Induced Psychosis in Parkinson's Disease', *N. Engl. J. Med.* **340**(10), 757–763.

Theodore, S., Cao, S., McLean, P. J. & Standaert, D. G. (2008), 'Targeted Overexpression of Human α-Synuclein Triggers Microglial Activation and an Adaptive Immune Response in a Mouse Model of Parkinson Disease', *J. Neuropathol. Exp. Neurol.* **67**(12), 1149–1158.

Thomas, A., Burant, A., Bui, N., Graham, D., Yuva-Paylor, L. A. & Paylor, R. (2009), 'Marble burying reflects a repetitive and perseverative behavior more than novelty-induced anxiety.', *Psychopharmacology (Berl).* **204**(2), 361–73.

Thompson, A. J., Scholz, S. W., Singleton, A. B., Hardwick, A., McFarland, N. R. & Okun, M. S. (2013), 'Variability in clinical phenotypes of heterozygous and homozygous cases of Parkin-related Parkinson's disease', *Int. J. Neurosci.* **123**(12), 847–849.

Thrash, B., Karuppagounder, S. S., Uthayathas, S., Suppiramaniam, V. & Dhanasekaran, M. (2010), 'Neurotoxic Effects of Methamphetamine', *Neurochem. Res.* **35**(1), 171–179.

Tian, L., Xia, Y., Flores, H. P., Campbell, M. C., Moerlein, S. M. & Perlmutter, J. S. (2015), 'Neuroimaging Analysis of the Dopamine Basis for Apathetic Behaviors in an MPTP-Lesioned Primate Model', *PLoS One* **10**(7), e0132064.

Tison, F., Keywood, C., Wakefield, M., Durif, F., Corvol, J.-C., Eggert, K., Lew, M., Isaacson, S., Bezard, E., Poli, S.-M., Goetz, C. G., Trenkwalder, C. & Rascol, O. (2016), 'A Phase 2A Trial of the Novel mGluR5-Negative Allosteric Modulator Dipraglurant for Levodopa-Induced Dyskinesia in Parkinson's Disease', *Mov. Disord.* **31**(9), 1373–1380.

Tofaris, G. K., Garcia Reitböck, P., Humby, T., Lambourne, S. L., O'Connell, M., Ghetti, B., Gossage, H., Emson, P. C., Wilkinson, L. S., Goedert, M. & Spillantini, M. G. (2006), 'Pathological Changes in Dopaminergic Nerve Cells of the Substantia Nigra and Olfactory Bulb in Mice Transgenic for Truncated Human -Synuclein(1-120): Implications for Lewy Body Disorders', *J. Neurosci.* **26**(15), 3942–3950.

Tompkins, M. M. & Hill, W. D. (1997), 'Contribution of somal Lewy bodies to neuronal death.', *Brain Res.* **775**(1-2), 24–9.

Török, N., Majláth, Z., Szalárdy, L. & Vécsei, L. (2016), 'Investigational α-synuclein aggregation inhibitors: hope for Parkinson's disease', *Expert Opin. Investig. Drugs* **25**(11), 1281–1294.

Trenkwalder, C., Chaudhuri, K. R., Martinez-Martin, P., Rascol, O., Ehret, R., Vališ, M., Sátori, M., Krygowska-Wajs, A., Marti, M. J., Reimer, K., Oksche, A., Lomax, M., DeCesare, J., Hopp, M. & study group, P. (2015), 'Prolonged-release oxycodone–naloxone for treatment of severe pain in patients with Parkinson's disease (PANDA): a double-blind, randomised, placebo-controlled trial', *Lancet Neurol.* **14**(12), 1161–1170.

Triantafilou, K., Hughes, T. R., Triantafilou, M. & Morgan, B. P. (2013), 'The complement membrane attack complex triggers intracellular Ca2+ fluxes leading to NLRP3 inflammasome activation', *J. Cell Sci.* **126**(13), 2903–2913.

Trinh, K., Andrews, L., Krause, J., Hanak, T., Lee, D., Gelb, M. & Pallanck, L. (2010), 'Decaffeinated Coffee and Nicotine-Free Tobacco Provide Neuroprotection in Drosophila Models of Parkinson's Disease through an NRF2-Dependent Mechanism', *J. Neurosci.* **30**(16), 5525–5532.

Tsika, E., Glauser, L., Moser, R., Fiser, A., Daniel, G., Sheerin, U.-M., Lees, A., Troncoso, J. C., Lewis, P. A., Bandopadhyay, R., Schneider, B. L. & Moore, D. J. (2014), 'Parkinson's disease-linked mutations in VPS35 induce dopaminergic neurodegeneration', *Hum. Mol. Genet.* **23**(17), 4621–4638.

Turski, L., Bressler, K., Jürgen Rettig, K., Löschmann, P.-A. & Wachtel, H. (1991), 'Protection of substantia nigra from MPP+ neurotoxicity by N-methyl-D-aspartate antagonists', *Nature* **349**(6308), 414–418.

Uhlen, M., Fagerberg, L., Hallstrom, B. M., Lindskog, C., Oksvold, P., Mardinoglu, A., Sivertsson, A., Kampf, C., Sjostedt, E., Asplund, A., Olsson, I., Edlund, K., Lundberg, E., Navani, S., Szigyarto, C. A.-K., Odeberg, J., Djureinovic, D., Takanen, J. O., Hober, S., Alm, T., Edqvist, P.-H., Berling, H., Tegel, H., Mulder, J., Rockberg, J., Nilsson, P., Schwenk, J. M., Hamsten, M., von Feilitzen, K., Forsberg, M., Persson, L., Johansson, F., Zwahlen, M., von Heijne, G., Nielsen, J. & Ponten, F. (2015), 'Tissue-based map of the human proteome', *Science (80-.).* **347**(6220), 1260419–1260419.

Ungerstedt, U. (1968), '6-Hydroxy-dopamine induced degeneration of central monoamine neurons.', *Eur. J. Pharmacol.* **5**(1), 107–10.

Urra, H., Dufey, E., Lisbona, F., Rojas-Rivera, D. & Hetz, C. (2013), 'When ER stress reaches a dead end', *Biochim. Biophys. Acta - Mol. Cell Res.* **1833**(12), 3507–3517.

Valença, G. T., Glass, P. G., Negreiros, N. N., Duarte, M. B., Ventura, L. M., Mueller, M. & Oliveira-Filho, J. (2013), 'Past smoking and current dopamine agonist use show an independent and dose-dependent association with impulse control disorders in Parkinson's disease', *Parkinsonism Relat. Disord.* **19**(7), 698–700.

Valente, E. M., Bentivoglio, A. R., Dixon, P. H., Ferraris, A., Ialongo, T., Frontali, M., Albanese, A. & Wood, N. W. (2001), 'Localization of a novel locus for autosomal recessive early-onset parkinsonism, PARK6, on human chromosome 1p35-p36.', *Am. J. Hum. Genet.* **68**(4), 895–900.

Valenti, O., Mannaioni, G., Seabrook, G. R., Conn, P. J. & Marino, M. J. (2005), 'Group III metabotropic glutamate-receptor-mediated modulation of excitatory transmission in rodent substantia nigra pars compacta dopamine neurons', *J Pharmacol Exp Ther* **313**(3), 1296–1304.

Valenti, O., Marino, M. J., Wittmann, M., Lis, E., DiLella, A. G., Kinney, G. G. & Conn, P. J. (2003), 'Group III metabotropic glutamate receptor-mediated modulation of the striatopallidal synapse.', *J. Neurosci.* **23**(18), 7218–26.

van Duijn, C., Dekker, M., Bonifati, V., Galjaard, R., Houwing-Duistermaat, J., Snijders, P., Testers, L., Breedveld, G., Horstink, M., Sandkuijl, L., van Swieten, J., Oostra, B. & Heutink, P. (2001), 'PARK7, a Novel Locus for Autosomal Recessive Early-Onset Parkinsonism, on Chromosome 1p36', *Am. J. Hum. Genet.* **69**(3), 629–634.

Vanzulli, I. & Butt, A. M. (2015), 'mGluR5 protect astrocytes from ischemic damage in postnatal CNS white matter', *Cell Calcium* **58**(5), 423–430.

Vawter, M. P., Dillon-Carter, O., Tourtellotte, W., Carvey, P. & Freed, W. J. (1996), 'TGFβ1 and TGFβ2 Concentrations Are Elevated in Parkinson's Disease in Ventricular Cerebrospinal Fluid', *Exp. Neurol.* **142**(2), 313–322.

Verhave, P. S., Jongsma, M. J., Van den Berg, R. M., Vis, J. C., Vanwersch, R. A., Smit, A. B., Van Someren, E. J. & Philippens, I. H. (2011), 'REM sleep behavior disorder in the marmoset MPTP model of early Parkinson disease.', *Sleep* **34**(8), 1119–1125.

Vernon, A. C., Palmer, S., Datla, K. P., Zbarsky, V., Croucher, M. J. & Dexter, D. T. (2005), 'Neuroprotective effects of metabotropic glutamate receptor ligands in a 6-hydroxydopamine rodent model of Parkinson's disease', *Eur. J. Neurosci.* **22**(7), 1799–1806.

Visanji, N. P., Gomez-Ramirez, J., Johnston, T. H., Pires, D., Voon, V., Brotchie, J. M. & Fox, S. H. (2006), 'Pharmacological characterization of psychosis-like behavior in the MPTP-lesioned nonhuman primate model of Parkinson's disease', *Mov. Disord.* **21**(11), 1879–1891.

Vo, Q., Gilmour, T. P., Venkiteswaran, K., Fang, J. & Subramanian, T. (2014), 'Polysomnographic Features of Sleep Disturbances and REM Sleep Behavior Disorder in the Unilateral 6-OHDA Lesioned Hemiparkinsonian Rat.', *Parkinsons. Dis.* **2014**, 852965.

von Wrangel, C., Schwabe, K., John, N., Krauss, J. K. & Alam, M. (2015), 'The rotenone-induced rat model of Parkinson's disease: Behavioral and electrophysiological findings', *Behav. Brain Res.* **279**, 52–61.

Voorn, P., Vanderschuren, L. J. M. J., Groenewegen, H. J., Robbins, T. W. & Pennartz, C. M. A. (2004), 'Putting a spin on the dorsal-ventral divide of the striatum.', *Trends Neurosci.* **27**(8), 468–74.

Vorhees, C. V. & Williams, M. T. (2006), 'Morris water maze: procedures for assessing spatial and related forms of learning and memory', *Nat Protoc* **1**(2), 848–858.

Wakabayashi, K., Tanji, K., Mori, F. & Takahashi, H. (2007), 'The Lewy body in Parkinson's disease: molecules implicated in the formation and degradation of alpha-synuclein aggregates.', *Neuropathology* **27**(5), 494–506.

Walker, K., Bowes, M., Panesar, M., Davis, A., Gentry, C., Kesingland, A., Gasparini, F., Spooren, W., Stoehr, N., Pagano, A., Flor, P. J., Vranesic, I., Lingenhoehl, K., Johnson, E. C., Varney, M., Urban, L. & Kuhn, R. (2001), 'Metabotropic glutamate receptor subtype 5 (mGlu5) and nociceptive function: I. Selective blockade of mGlu5 receptors in models of acute, persistent and chronic pain', *Neuropharmacology* **40**(1), 1–9.

Walsh, S., Finn, D. & Dowd, E. (2011), 'Time-course of nigrostriatal neurodegeneration and neuroinflammation in the 6-hydroxydopamine-induced axonal and terminal lesion models of Parkinson's disease in the rat', *Neuroscience* **175**, 251–261.

Wang, C., Lu, R., Ouyang, X., Ho, M. W. L., Chia, W., Yu, F. & Lim, K.-L. (2007), 'Drosophila Overexpressing Parkin R275W Mutant Exhibits Dopaminergic Neuron Degeneration and Mitochondrial Abnormalities', *J. Neurosci.* **27**(32), 8563–8570.

Wang, C.-T., Mao, C.-J., Zhang, X.-Q., Zhang, C.-Y., Lv, D.-J., Yang, Y.-P., Xia, K.-L., Liu, J.-Y., Wang, F., Hu, L.-F., Xu, G.-Y. & Liu, C.-F. (2017), 'Attenuation of hyperalgesia responses via the modulation of 5-hydroxytryptamine signalings in the rostral ventromedial medulla and spinal cord in a 6-hydroxydopamine-induced rat model of Parkinson's disease.', *Mol. Pain* **13**, 1744806917691525.

Wang, J., Tian, Y., Phillips, K. L. E., Chiverton, N., Haddock, G., Bunning, R. A., Cross, A. K., Shapiro, I. M., Le Maitre, C. L. & Risbud, M. V. (2013), 'Tumor necrosis factor α- and interleukin-1β-dependent induction of CCL3 expression by nucleus pulposus cells promotes macrophage migration through CCR1', *Arthritis Rheum.* **65**(3), 832–842.

Wang, J., Yang, Q. X., Sun, X., Vesek, J., Mosher, Z., Vasavada, M., Chu, J., Kanekar, S., Shivkumar, V., Venkiteswaran, K. & Subramanian, T. (2015), 'MRI evaluation of asymmetry of nigrostriatal damage in the early stage of early-onset Parkinson's disease', *Parkinsonism Relat. Disord.* **21**(6), 590–596.

Wang, L., Das, U., Scott, D. A., Tang, Y., McLean, P. J. & Roy, S. (2014), 'α-Synuclein Multimers Cluster Synaptic Vesicles and Attenuate Recycling', *Curr. Biol.* **24**(19), 2319–2326.

Wang, L., Evatt, M. L., Maldonado, L. G., Perry, W. R., Ritchie, J. C., Beecham, G. W., Martin, E. R., Haines, J. L., Pericak-Vance, M. A., Vance, J. M. & Scott, W. K. (2015), 'Vitamin D from different sources is inversely associated with Parkinson disease', *Mov. Disord.* **30**(4), 560–566.

Wang, S., Zhang, Q., Liu, J., Wu, Z., Ali, U., Wang, Y., Chen, L. & Gui, Z. (2009), 'The firing activity of pyramidal neurons in medial prefrontal cortex and their response to 5-hydroxytryptamine-1A receptor stimulation in a rat model of Parkinson's disease', *Neuroscience* **162**(4), 1091–1100.

Wang, W., Wang, X., Fujioka, H., Hoppel, C., Whone, A. L., Caldwell, M. A., Cullen, P. J., Liu, J. & Zhu, X. (2016), 'Parkinson's disease–associated mutant VPS35 causes mitochondrial dysfunction by recycling DLP1 complexes', *Nat. Med.* **22**(1), 54–63.

Wang, X.-F., Li, S., Chou, A. P. & Bronstein, J. M. (2006), 'Inhibitory effects of pesticides on proteasome activity: Implication in Parkinson's disease', *Neurobiol. Dis.* **23**(1), 198–205.

Waraczynski, M. & Perkins, M. (2000), 'Temporary inactivation of the retrorubral fields decreases the rewarding effect of medial forebrain bundle stimulation.', *Brain Res.* **885**(2), 154–65.

Weeks, A. M., Harms, J. E., Partin, K. M. & Benveniste, M. (2014), 'Functional insight into development of positive allosteric modulators of AMPA receptors.', *Neuropharmacology* **85**, 57–66.

Wierońska, J. M., Acher, F. C., Sławińska, A., Gruca, P., Łasoń-Tyburkiewicz, M., Papp, M. & Pilc, A. (2013), 'The antipsychotic-like effects of the mGlu group III orthosteric agonist, LSP1-2111, involves 5-HT1A signalling', *Psychopharmacology (Berl).* **227**(4), 711–725.

Wieronska, J. M., Slawinska, A., Lason-Tyburkiewicz, M., Gruca, P., Papp, M., Zorn, S. H., Doller, D., Kleczek, N., Noworyta-Sokolowska, K., Golembiowska, K. & Pilc, A. (2015), 'The antipsychotic-like effects in rodents of the positive allosteric modulator Lu AF21934 involve 5-HT1A receptor signaling: mechanistic studies', *Psychopharmacol.* **232**(1), 259–273.

Willard, A. M., Bouchard, R. S. & Gittis, A. H. (2015), 'Differential degradation of motor deficits during gradual dopamine depletion with 6-hydroxydopamine in mice.', *Neuroscience* **301**, 254–67.

Willner, P. (1986), 'Validation criteria for animal models of human mental disorders: Learned helplessness as a paradigm case', *Prog. Neuro-Psychopharmacology Biol. Psychiatry* **10**(6), 677–690.

Willoughby, L. F., Schlosser, T., Manning, S. A., Parisot, J. P., Street, I. P., Richardson, H. E., Humbert, P. O. & Brumby, A. M. (2013), 'An in vivo large-scale chemical screening platform using Drosophila for anti-cancer drug discovery.', *Dis. Model. Mech.* **6**(2), 521–9.

Wilms, H., Rosenstiel, P., Sievers, J., Deuschl, G., Zecca, L. & Lucius, R. (2003), 'Activation of microglia by human neuromelanin is NF-κB dependent and involves p38 mitogen-activated protein kinase: implications for Parkinson's disease', *FASEB J.* **17**(3), 500–502.

Wilson, A. G., Symons, J. A., McDowell, T. L., McDevitt, H. O. & Duff, G. W. (1997), 'Effects of a polymorphism in the human tumor necrosis factor alpha promoter on transcriptional activation.', *Proc. Natl. Acad. Sci. U. S. A.* **94**(7), 3195–9.

Wilson, B., Slater, H., Kikuchi, Y., Milne, A. E., Marslen-Wilson, W. D., Smith, K. & Petkov, C. I. (2013), 'Auditory Artificial Grammar Learning in Macaque and Marmoset Monkeys', *J. Neurosci.* **33**(48), 18825–18835.

Witting, A., Müller, P., Herrmann, A., Kettenmann, H. & Nolte, C. (2002), 'Phagocytic Clearance of Apoptotic Neurons by Microglia/Brain Macrophages In Vitro', *J. Neurochem.* **75**(3), 1060–1070.

Wroblewska, B., Santi, M. R. & Neale, J. H. (1998), 'N-acetylaspartylglutamate activates cyclic AMP-coupled metabotropic glutamate receptors in cerebellar astrocytes.', *Glia* **24**(2), 172–9.

Wu, H.-M., Tzeng, N.-S., Qian, L., Wei, S.-J., Hu, X., Chen, S.-H., Rawls, S. M., Flood, P., Hong, J.-S. & Lu, R.-B. (2009), 'Novel Neuroprotective Mechanisms of Memantine: Increase in Neurotrophic Factor Release from Astroglia and Anti-Inflammation by Preventing Microglial Activation', *Neuropsychopharmacology* **34**(10), 2344–2357.

Wu, J. & Kaufman, R. J. (2006), 'From acute ER stress to physiological roles of the Unfolded Protein Response', *Cell Death Differ.* **13**(3), 374–384.

Wu, W. Y.-Y., Kang, K.-H., Chen, S. L.-S., Chiu, S. Y.-H., Yen, A. M.-F., Fann, J. C.-Y., Su, C.-W., Liu, H.-C., Lee, C.-Z., Fu, W.-M., Chen, H.-H. & Liou, H.-H. (2015), 'Hepatitis C virus infection: a risk factor for Parkinson's disease', *J. Viral Hepat.* **22**(10), 784–791.

Xi, Y., Ryan, J., Noble, S., Yu, M., Yilbas, A. E. & Ekker, M. (2010), 'Impaired dopaminergic neuron development and locomotor function in zebrafish with loss of pink1 function', *Eur. J. Neurosci.* **31**(4), 623–633.

Xi, Z.-X., Baker, D. A., Shen, H., Carson, D. S. & Kalivas, P. W. (2002), 'Group II metabotropic glutamate receptors modulate extracellular glutamate in the nucleus accumbens.', *J. Pharmacol. Exp. Ther.* **300**(1), 162–71.

Xiong, H., Wang, D., Chen, L., Choo, Y. S., Ma, H., Tang, C., Xia, K., Jiang, W., Ronai, Z., Zhuang, X. & Zhang, Z. (2009), 'Parkin, PINK1, and DJ-1 form a ubiquitin E3 ligase complex promoting unfolded protein degradation', *J. Clin. Invest.* **119**(3), 650–660.

Xu, X., Li, D., He, Q., Gao, J., Chen, B. & Xie, A. (2011), 'Interleukin-18 promoter polymorphisms and risk of Parkinson's disease in a Han Chinese population', *Brain Res.* **1381**, 90–94.

Yabuki, Y., Ohizumi, Y., Yokosuka, A., Mimaki, Y. & Fukunaga, K. (2014), 'Nobiletin treatment improves motor and cognitive deficits seen in MPTP-induced Parkinson model mice', *Neuroscience* **259**, 126–141.

Yamada, T., McGeer, P. L. & McGeer, E. G. (1992), 'Lewy bodies in Parkinson's disease are recognized by antibodies to complement proteins.', *Acta Neuropathol.* **84**(1), 100–4.

Yamakado, H., Moriwaki, Y., Yamasaki, N., Miyakawa, T., Kurisu, J., Uemura, K., Inoue, H., Takahashi, M. & Takahashi, R. (2012), 'α-Synuclein BAC transgenic mice as a model for Parkinson's disease manifested decreased anxiety-like behavior and hyperlocomotion', *Neurosci. Res.* **73**(2), 173–177.

Yamamoto Ki, Kobayashi, N., Yoshitama, K., Teramoto, S. & Komamine, A. (2001), 'Isolation and purification of tyrosine hydroxylase from callus cultures of Portulaca grandiflora.', *Plant Cell Physiol.* **42**(9), 969–75.

Yan, Y., Ng, L. F., Ng, L. T., Choi, K. B., Gruber, J., Bettiol, A. A. & Thakor, N. V. (2014), 'A continuous-flow C. elegans sorting system with integrated optical fiber detection and laminar flow switching.', *Lab Chip* **14**(20), 4000–6.

Yasuda, Y., Shimoda, T., Uno, K., Tateishi, N., Furuya, S., Yagi, K., Suzuki, K. & Fujita, S. (2008), 'The effects of MPTP on the activation of microglia/astrocytes and cytokine/chemokine levels in different mice strains', *J. Neuroimmunol.* **204**(1-2), 43–51.

Yi, P.-L., Tsai, C.-H., Lu, M.-K., Liu, H.-J., Chen, Y.-C. & Chang, F.-C. (2007), 'Interleukin-1beta mediates sleep alteration in rats with rotenone-induced parkinsonism.', *Sleep* **30**(4), 413–25.

Yoshie, O. & Matsushima, K. (2015), 'CCR4 and its ligands: from bench to bedside', *Int. Immunol.* **27**(1), 11–20.

Yoshimura, N., Kuno, S., Chancellor, M. B., Groat, W. C. & Seki, S. (2003), 'Dopaminergic mechanisms underlying bladder hyperactivity in rats with a unilateral 6-hydroxydopamine (6-OHDA) lesion of the nigrostriatal pathway', *Br. J. Pharmacol.* **139**(8), 1425–1432.

Yoshimura, N., Mizuta, E., Yoshida, O. & Kuno, S. (1998), 'Therapeutic effects of dopamine D1/D2 receptor agonists on detrusor hyperreflexia in 1-methyl-4-phenyl-1,2,3,6-tetrahydropyridine-lesioned parkinsonian cynomolgus monkeys.', *J. Pharmacol. Exp. Ther.* **286**(1), 228–33.

Yoshioka, Y., Sugino, Y., Tozawa, A., Yamamuro, A., Kasai, A., Ishimaru, Y. & Maeda, S. (2016), 'Dopamine inhibits lipopolysaccharide-induced nitric oxide production through the formation of dopamine quinone in murine microglia BV-2 cells', *J. Pharmacol. Sci.* **130**(2), 51–59.

Zeng, B.-Y., Iravani, M. M., Jackson, M. J., Rose, S., Parent, A. & Jenner, P. (2010), 'Morphological changes in serotoninergic neurites in the striatum and globus pallidus in levodopa primed MPTP treated common marmosets with dyskinesia', *Neurobiol. Dis.* **40**(3), 599–607.

Zesiewicz, T. A., Sullivan, K. L., Arnulf, I., Chaudhuri, K. R., Morgan, J. C., Gronseth, G. S., Miyasaki, J., Iverson, D. J., Weiner, W. J. & Quality Standards Subcommittee of the American Academy of Neurology (2010), 'Practice Parameter: Treatment of nonmotor symptoms of Parkinson disease: Report of the Quality Standards Subcommittee of the American Academy of Neurology', *Neurology* **74**(11), 924–931.

Zhang, S., Xiao, Q. & Le, W. (2015), 'Olfactory Dysfunction and Neurotransmitter Disturbance in Olfactory Bulb of Transgenic Mice Expressing Human A53T Mutant α-Synuclein', *PLoS One* **10**(3), e0119928.

Zhang, Y., James, M., Middleton, F. A. & Davis, R. L. (2005), 'Transcriptional analysis of multiple brain regions in Parkinson's disease supports the involvement of specific protein processing, energy metabolism, and signaling pathways, and suggests novel disease mechanisms', *Am. J. Med. Genet. Part B Neuropsychiatr. Genet.* **137B**(1), 5–16.

Zhang, Y., Meredith, G. E., Mendoza-Elias, N., Rademacher, D. J., Tseng, K. Y. & Steece-Collier, K. (2013), 'Aberrant Restoration of Spines and their Synapses in L-DOPA-Induced Dyskinesia: Involvement of Corticostriatal but Not Thalamostriatal Synapses', *J. Neurosci.* **33**(28), 11655–11667.

Zheng, M., Gorelenkova, O., Yang, J. & Feng, Z. (2012), 'A liquid phase based C. elegans behavioral analysis system identifies motor activity loss in a nematode Parkinson's disease model', *J. Neurosci. Methods* **204**(2), 234–237.

Zhou, F., Yao, H.-H., Wu, J.-Y., Yang, Y.-J., Ding, J.-H., Zhang, J. & Hu, G. (2006), 'Activation of Group II/III metabotropic glutamate receptors attenuates LPS-induced astroglial neurotoxicity via promoting glutamate uptake', *J. Neurosci. Res.* **84**(2), 268–277.

Zhu, X.-R., Maskri, L., Herold, C., Bader, V., Stichel, C. C., Güntürkün, O. & Lübbert, H. (2007), 'Non-motor behavioural impairments in parkin-deficient mice', *Eur. J. Neurosci.* **26**(7), 1902–1911.

Zuddas, A., Vaglini, F., Fornai, F., Fascetti, F., Saginario, A. & Corsini, G. U. (1992), 'Pharmacologic modulation of MPTP toxicity: MK 801 in prevention of dopaminergic cell death in monkeys and mice.', *Ann. N. Y. Acad. Sci.* **648**, 268–71.

Table of transcript regulation for individual genes by LSP1-2111 compared to saline in the striatum of otherwise naïve animals.

ID	LSP Stria Avg (log2)	Sal Stria Avg (log2)	Fold Change	P-val	FDR P-val	Gene Symbol	Description
1393672_at	4.93	0	30.4	0.0015	0.9662	Hmcn1	hemicentin 1
1391123_at	6.56	1.87	25.78	0.0001	0.3815		
1385816_at	4.56	0.13	21.54	0.0162	0.9962	Fam72a	family with sequence similarity 72, member A
1370033_at	4.26	0	19.09	0.0072	0.9962	Myl1	myosin, light chain 1
1385419_at	5.34	1.13	18.49	0.0416	0.9962	Gpr143	G protein-coupled receptor 143
1381240_at	5.97	1.93	16.46	0.0032	0.9962		
1397971_at	4.51	0.49	16.22	0.0229	0.9962		
1381643_at	6.53	2.54	15.91	0.0466	0.9962		
1387011_at	6.31	2.35	15.53	0.004	0.9962	Lcn2	lipocalin 2
1397087_at	4.94	1.04	14.94	0.0283	0.9962	LOC102554579	uncharacterized LOC102554579
1394740_at	4.2	0.31	14.88	0.002	0.9962		
1384726_at	4.78	0.9	14.72	0.0064	0.9962		
1394780_at	6.59	2.76	14.22	0.0497	0.9962		
1387725_at	4.4	0.62	13.72	0.048	0.9962	Gulo	gulonolactone (L-) oxidase
1385396_at	3.76	0	13.51	0.0106	0.9962		
1390249_at	5.91	2.17	13.31	0.0007	0.9032	RGD1305464	similar to human chromosome 15 open reading frame 39
1398273_at	5.71	2	13.15	0.0067	0.9962	Efna1	ephrin A1
1370632_at	3.85	0.14	13.09	0.028	0.9962	Obp2b	odorant binding protein 2B
1381079_at	3.63	0	12.42	0.0233	0.9962	Bnc1	basonuclin 1
1394259_at	5.18	1.59	12.01	0.0001	0.3815	Cldn15	claudin 15
1376958_at	4.27	0.77	11.35	0.0201	0.9962	LOC100911107; RGD1562844	leukocyte elastase inhibitor A-like; similar to serine (or cysteine) proteinase inhibitor, clade B, member 9

ID	LSP Stria Avg (log2)	Sal Stria Avg (log2)	Fold Change	P-val	FDR P-val	Gene Symbol	Description
1390975_at	3.66	0.16	11.33	0.0086	0.9962	LOC100912248	uncharacterized LOC100912248
1387605_at	4.46	0.98	11.09	0.0279	0.9962	Casp12	caspase 12
1394646_at	3.91	0.46	10.98	0.017	0.9962		
1398199_at	4.13	0.69	10.84	0.0352	0.9962		
1385303_at	3.38	0	10.4	0.0474	0.9962		
1381707_at	3.3	0	9.87	0.0461	0.9962		
1369558_at	4.58	1.35	9.43	0.0215	0.9962	Inhbc	inhibin beta C
1397330_at	4.64	1.42	9.3	0.0219	0.9962		
1380181_at	4.95	1.78	8.96	0.0109	0.9962	Lhx4	LIM homeobox 4
1397198_at	3.71	0.55	8.94	0.0016	0.9962	LOC100912510	uncharacterized LOC100912510
1395600_at	5.82	2.71	8.62	0.0496	0.9962	Ccdc117	coiled-coil domain containing 117
1391737_at	5.02	2.02	7.96	1.04E-05	0.0809	Ncf4	neutrophil cytosolic factor 4
1369347_s_at	4.98	2.02	7.79	0.0245	0.9962	Prom2	prominin 2
1392022_at	4.26	1.32	7.66	0.0431	0.9962		
1369295_at	4.06	1.13	7.63	0.0055	0.9962	Pgc	progastricsin (pepsinogen C)
1378364_at	6.24	3.31	7.62	0.0006	0.9032	Zfp668	zinc finger protein 668
1384580_at	4.16	1.23	7.62	0.0237	0.9962	C6	complement component 6
1369189_at	2.87	0	7.32	0.0124	0.9962	Npy4r	neuropeptide Y receptor Y4
1381580_at	4.2	1.35	7.21	0.0008	0.9032	Trex2	three prime repair exonuclease 2
1394464_at	4.78	1.95	7.14	0.0197	0.9962	LOC100912450; LOC100912609; RGD1560652	uncharacterized LOC100912450; uncharacterized LOC100912609; RGD1560652
1383203_at	4.92	2.09	7.11	0.0181	0.9962	Bpifa5	BPI fold containing family A, member 5
1370636_at	3.44	0.62	7.09	0.0329	0.9962	Ppbp	pro-platelet basic protein (chemokine (C-X-C motif) ligand 7)
1374070_at	3.76	0.95	7	0.0207	0.9962	Gpx2	glutathione peroxidase 2

ID	LSP Stria Avg (log2)	Sal Stria Avg (log2)	Fold Change	P-val	FDR P-val	Gene Symbol	Description
1396217_at	4.6	1.8	6.99	0.0337	0.9962	Ap1s2	adaptor-related protein complex 1, sigma 2 subunit
1392751_at	3.09	0.31	6.86	0.0128	0.9962	Fndc3c1	fibronectin type III domain containing 3C1
1396293_at	3.64	0.91	6.61	0.0014	0.9555		
1385225_at	4.73	2.01	6.58	0.0124	0.9962	Spatc1	spermatogenesis and centriole associated 1
1381657_at	5.5	2.79	6.54	0.0408	0.9962		
1370227_at	3.15	0.46	6.48	0.0023	0.9962	Prl8a7	prolactin family 8, subfamily a, member 7
1379790_at	5.62	2.93	6.44	0.0169	0.9962	Dll4	delta-like 4 (Drosophila)
1378168_at	6.44	3.77	6.36	0.0051	0.9962	Fam101b	family with sequence similarity 101, member B
1385172_at	4.51	1.86	6.3	0.0083	0.9962		
1396778_at	2.65	0	6.29	0.0252	0.9962		
1384796_at	3.79	1.15	6.26	0.0067	0.9962	Ebf2	early B-cell factor 2
1396818_at	4.59	1.97	6.14	0.041	0.9962		
1368651_at	4.43	1.82	6.09	0.0387	0.9962	Pklr	pyruvate kinase, liver and RBC
1373544_at	3.83	1.28	5.89	0.0406	0.9962	Cxcl9	chemokine (C-X-C motif) ligand 9
1391226_at	3.84	1.29	5.84	0.0184	0.9962	Rasgrf2	RAS protein-specific guanine nucleotide-releasing factor 2
1380139_at	4.87	2.35	5.71	7.12E-05	0.3159	St3gal1	ST3 beta-galactoside alpha-2,3-sialyltransferase 1
1390581_at	5.55	3.04	5.68	0.0036	0.9962	LOC103691977	uncharacterized LOC103691977
1394915_at	3.87	1.38	5.63	0.0339	0.9962		
1370560_at	4.81	2.37	5.41	0.0227	0.9962	Zfp689	zinc finger protein 689
1377592_at	2.42	0	5.35	0.0487	0.9962	Zfpm2	zinc finger protein, multitype 2

ID	LSP Stria Avg (log2)	Sal Stria Avg (log2)	Fold Change	P-val	FDR P-val	Gene Symbol	Description
1387314_at	2.39	0	5.24	0.0267	0.9962	Sult1b1	sulfotransferase family, cytosolic, 1B, member 1
1397299_at	3.65	1.27	5.23	0.0195	0.9962		
1373674_at	5.26	2.87	5.22	0.0221	0.9962	Mfap5	microfibrillar associated protein 5
1390195_at	3.98	1.6	5.21	0.0024	0.9962	Psd4	pleckstrin and Sec7 domain containing 4
1368804_at	4.13	1.78	5.07	0.0288	0.9962	Lif	leukemia inhibitory factor
1387313_at	5.04	2.7	5.07	0.0334	0.9962	Myoc	myocilin, trabecular meshwork inducible glucocorticoid response
1368498_a_at	3.9	1.57	5.03	0.03	0.9962	Slc21a4	kidney specific organic anion transporter
1391483_at	5.37	3.05	5	0.0253	0.9962	Creb3l3	cAMP responsive element binding protein 3-like 3
1371220_at	5.06	2.75	4.97	0.0454	0.9962	Sqstm1	sequestosome 1
1398104_at	2.3	0	4.92	0.0435	0.9962		
1369835_at	4.46	2.17	4.88	0.0187	0.9962	Omp	olfactory marker protein
1371264_at	4.03	1.74	4.88	0.0454	0.9962	Hbe2	hemoglobin, epsilon 2
1371075_at	3.62	1.36	4.8	0.0019	0.9962	Myh13	myosin, heavy chain 13, skeletal muscle
1371628_at	3.24	0.99	4.77	0.0388	0.9962	Ceacam11	carcinoembryonic antigen-related cell adhesion molecule 11
1389808_at	7.68	5.43	4.76	0.0011	0.9032	Prcd	progressive rod-cone degeneration
1377894_at	5.29	3.05	4.73	0.0233	0.9962		
1391835_at	3.98	1.74	4.72	0.0405	0.9962	Baz1a	bromodomain adjacent to zinc finger domain, 1A
1369530_at	4.12	1.92E+00	4.57	0.0168	0.9962	Isl2	ISL LIM homeobox 2
1380258_at	4.26	2.07	4.55	0.0012	0.9422		
1391326_at	3.38	1.21	4.48	0.0095	0.9962	Hoxb5	homeo box B5

ID	LSP Stria Avg (log2)	Sal Stria Avg (log2)	Fold Change	P-val	FDR P-val	Gene Symbol	Description
1379766_at	5.53	3.37	4.46	0.0018	0.9962		
1376271_at	3.96	1.81	4.46	0.043	0.9962	Tmem167a	transmembrane protein 167A
1378443_at	3.62	1.48	4.43	0.0076	0.9962	Slamf9	SLAM family member 9
1375683_at	6.46	4.32	4.41	0.0353	0.9962	Cdc25a	cell division cycle 25A
1375356_at	4.4	2.3	4.28	0.0135	0.9962	RGD1310262	hypothetical LOC304650
1389707_at	7.15	5.1	4.15	0.0288	0.9962		
1396875_at	4.82	2.77	4.14	0.0385	0.9962		
1380013_at	5.49	3.44	4.13	0.0075	0.9962	Pnpla3	patatin-like phospholipase domain containing 3
1390938_at	4.19	2.14	4.11	0.0191	0.9962	Arhgap28	Rho GTPase activating protein 28
1375133_at	4.96	2.93	4.08	0.0343	0.9962	Scarf2	scavenger receptor class F, member 2
1395849_at	2.83	0.82	4.04	0.0078	0.9962		
1370765_at	3.02	1.01	4.04	0.0276	0.9962	Gzmf	granzyme F
1389712_at	4.09	2.11	3.95	0.0073	0.9962	Ebf3	early B-cell factor 3
1393272_at	2.55	0.62	3.83	0.046	0.9962		
1368461_at	7.87	5.94	3.81	0.0297	0.9962	Slc22a8	solute carrier family 22 (organic anion transporter), member 8
1382815_at	5.71	3.78	3.8	0.0199	0.9962		
1378613_at	2.58	0.66	3.79	0.0399	0.9962		
1393825_at	4.51	2.59	3.77	0.042	0.9962	Gna14	guanine nucleotide binding protein, alpha 14
1375103_at	2.15	0.25	3.75	0.0045	0.9962		
1368775_at	8.2	6.31	3.73	0.0095	0.9962	Giot1	gonadotropin inducible ovarian transcription factor 1
1392303_at	5.68	3.79	3.7	0.0261	0.9962	Morc2	MORC family CW-type zinc finger 2
1379100_at	7.39	5.51	3.7	0.0324	0.9962	Elmsan1	ELM2 and Myb/SANT-like domain containing 1
1375949_at	4.31	2.43	3.69	0.0187	0.9962		

ID	LSP Stria Avg (log2)	Sal Stria Avg (log2)	Fold Change	P-val	FDR P-val	Gene Symbol	Description
1381055_at	5.45	3.56	3.69	0.0352	0.9962		
1370082_at	6.25	4.38	3.65	0.0055	0.9962	Tgfb1	transforming growth factor, beta 1
1382896_at	3.89	2.02	3.64	0.0103	0.9962		
1370508_a_at	4.96	3.11	3.6	0.0018	0.9962	Cacna1g	calcium channel, voltage-dependent, T type, alpha 1G subunit
1382412_at	6.08	4.23	3.6	0.0146	0.9962		
1375109_at	4.81	2.97	3.58	0.0176	0.9962		
1386543_at	4.64	2.82	3.54	0.0222	0.9962	Fbxl8	F-box and leucine-rich repeat protein 8
1387831_at	4.78	2.96	3.53	0.016	0.9962	Xcl1	chemokine (C motif) ligand 1
1394889_at	6.21	4.39	3.53	0.028	0.9962	Dapk2	death-associated protein kinase 2
1384415_at	5.55	3.73	3.53	0.0389	0.9962	Sox7	SRY (sex determining region Y)-box 7
1378889_at	4.73	2.91	3.53	0.0404	0.9962		
1369348_at	1.82	0	3.53	0.0432	0.9962	Trpm8	transient receptor potential cation channel, subfamily M, member 8
1375092_at	4.92	3.1	3.52	0.0251	0.9962	Myo18b	myosin XVIIIb
1368733_at	4.34	2.52	3.52	0.0254	0.9962	Sult1e1	sulfotransferase family 1E, estrogen-preferring, member 1
1378907_at	7	5.18E+00	3.51	0.0107	0.9962	Kank2	KN motif and ankyrin repeat domains 2
1368192_at	4.51	2.71E+00	3.47	0.0348	0.9962	Cxcr3	chemokine (C-X-C motif) receptor 3
1367703_at	3.88	2.09	3.46	0.0385	0.9962	Crygd; Cryge	crystallin, gamma D; crystallin, gamma E
1373302_at	7.87	6.1	3.42	0.0089	0.9962	Acer2	alkaline ceramidase 2
1392852_at	4.88	3.11	3.41	0.0296	0.9962	Smoc1	SPARC related modular calcium binding 1
1382173_at	4.8	3.03	3.41	0.0371	0.9962		
1394995_at	4.55	2.8	3.37	0.0497	0.9962		

ID	LSP Stria Avg (log2)	Sal Stria Avg (log2)	Fold Change	P-val	FDR P-val	Gene Symbol	Description
1375759_at	5.01	3.26	3.36	0.0182	0.9962		
1368316_at	3.63	1.9	3.33	0.0368	0.9962	Aqp8	aquaporin 8
1382185_at	6.44	4.72	3.3	0.0139	0.9962	C1qtnf2	C1q and tumor necrosis factor related protein 2
1388149_at	5.86	4.14	3.3	0.022	0.9962	Tap1	transporter 1, ATP-binding cassette, sub-family B (MDR/TAP)
1378225_at	6.31	4.6	3.28	0.02	0.9962		
1392680_at	6.16	4.46	3.27	0.0031	0.9962		
1376012_at	2.57	0.89	3.2	0.0279	0.9962	RGD1564419	similar to hypothetical gene supported by BC025338
1394140_at	5.1	3.43	3.2	0.0349	0.9962	Krt31	keratin 31, type I
1384492_at	3.62	1.96	3.17	0.0179	0.9962		
1396582_at	4.96	3.3	3.16	0.0052	0.9962		
1394421_at	6.44	4.82	3.07	0.0084	0.9962		
1396233_at	6.17	4.56	3.05	0.0437	0.9962	Arsk	arylsulfatase family, member K
1394320_at	5.61	4.01	3.04	0.0412	0.9962	Cdk2	cyclin dependent kinase 2
1389255_at	7.97	6.39	3	0.0254	0.9962	Cdh5	cadherin 5
1394753_at	1.86	0.3	2.94	0.0432	0.9962	Lsmem2	leucine-rich single-pass membrane protein 2
1385139_at	4.31	2.78	2.9	0.0089	0.9962	Fam221a	family with sequence similarity 221, member A
1382527_at	7.51	5.98	2.89	0.0039	0.9962	Plcxd2	phosphatidylinositol-specific phospholipase C, X domain containing 2
1391083_at	6.77	5.25	2.88	0.0256	0.9962	Arhgap22	Rho GTPase activating protein 22
1393419_at	7.83	6.31	2.87	0.0011	0.9032	Rcbtb2	regulator of chromosome condensation (RCC1) and BTB (POZ) domain containing protein 2

ID	LSP Stria Avg (log2)	Sal Stria Avg (log2)	Fold Change	P-val	FDR P-val	Gene Symbol	Description
1378423_at	4.29	2.77	2.87	0.0214	0.9962	Nmrk2	nicotinamide riboside kinase 2
1381369_at	7.56	6.08	2.79	0.0049	0.9962	Lgi3	leucine-rich repeat LGI family, member 3
1378830_at	5.04	3.56	2.78	0.0033	0.9962	Irs4	insulin receptor substrate 4
1391981_at	5.47	3.99	2.78	0.0034	0.9962		
1387027_a_at	7.79	6.32	2.77	0.0276	0.9962	Lgals9	lectin, galactoside-binding, soluble, 9
1392631_at	7.63	6.17	2.76	0.0328	0.9962	Sp1	Sp1 transcription factor
1377027_at	5.91	4.44	2.76	0.0393	0.9962		
1396557_at	5.23	3.77	2.74	0.0131	0.9962		
1384073_at	8.47	7.04	2.7	0.0096	0.9962	Adhfe1	alcohol dehydrogenase, iron containing, 1
1374955_at	6.34	4.92	2.68	0.0481	0.9962		
1377589_at	4.74	3.32	2.67	0.0481	0.9962		
1380277_at	5.2	3.82	2.61	0.0129	0.9962	Rad51ap1	RAD51 associated protein 1
1381007_at	5.89	4.51	2.59	0.043	0.9962		
1390024_at	9.35	8	2.55	0.0028	0.9962	Clec2g	C-type lectin domain family 2, member G
1397943_at	7.35	6	2.55	0.0389	0.9962	LOC103692950	uncharacterized LOC103692950
1388302_x_at	1.87	0.54	2.52	0.0211	0.9962	Andpro	androgen regulated protein
1392197_at	4.77	3.44	2.52	0.0226	0.9962		
1394440_at	8.68	7.34	2.52	0.0285	0.9962	Tnpo1	transportin 1
1397249_at	2.3	0.98	2.5	0.0071	0.9962	LOC103693656; LOC103693657	uncharacterized LOC103693656; uncharacterized LOC103693657
1375388_at	6.93	5.6	2.5	0.0184	0.9962		
1393891_at	5.02	3.7	2.49	0.0044	0.9962	Col8a1	collagen, type VIII, alpha 1
1390496_at	6.92	5.61	2.49	0.0329	0.9962	Elfn2	extracellular leucine-rich repeat and fibronectin type III domain containing 2

ID	LSP Stria Avg (log2)	Sal Stria Avg (log2)	Fold Change	P-val	FDR P-val	Gene Symbol	Description
1369235_at	7.74	6.43	2.47	0.0188	0.9962	Unc5b	unc-5 netrin receptor B
1370355_at	8.66	7.36	2.45	0.0001	0.3815	Scd1	stearoyl-Coenzyme A desaturase 1
1394804_at	3.14	1.86	2.44	0.0172	0.9962		
1376932_at	5.9	4.63	2.41	0.0256	0.9962	Cysrt1	cysteine-rich tail protein 1
1394871_at	8.19	6.92	2.41	0.0479	0.9962		
1391630_at	5.3	4.04	2.4	0.0176	0.9962	Tbx18	T-box18
1383533_at	8.01	6.74	2.4	0.0357	0.9962	LOC102551140	REST corepressor 3-like
1377112_at	3.34	2.07	2.4	0.0391	0.9962	Cda; LOC100909857	cytidine deaminase; cytidine deaminase-like
1373434_at	9	7.75	2.37	0.0059	0.9962		
1378550_at	5.3	4.05	2.37	0.0462	0.9962	Cblc	Cbl proto-oncogene C, E3 ubiquitin protein ligase
1372423_at	6.61	5.37	2.36	0.0339	0.9962	Perp	PERP, TP53 apoptosis effector
1389332_at	9.53	8.29	2.36	0.049	0.9962	Ptprb	protein tyrosine phosphatase, receptor type, B
1372481_at	9.75	8.52	2.35	0.0083	0.9962		
1391211_at	8.16	6.93	2.35	0.0157	0.9962	Atp11c	ATPase, class VI, type 11C
1380444_at	5.39	4.15	2.35	0.0195	0.9962	Ucma	upper zone of growth plate and cartilage matrix associated
1381629_at	5.62	4.4	2.33	0.0325	0.9962		
1382197_at	5.17	3.96	2.32	0.0274	0.9962	Rhod	ras homolog family member D
1393227_at	8.68	7.48	2.3	0.0082	0.9962		
1381245_at	7.28	6.08	2.3	0.0244	0.9962		
1392386_at	8.56	7.36	2.29	0.0159	0.9962		
1386739_at	5.43	4.24	2.29	0.0448	0.9962	Etv4	ets variant 4
1381305_at	8.28	7.11	2.26	0.0262	0.9962	RGD1308428	similar to RIKEN cDNA 4931406P16
1380640_at	6.82	5.65	2.26	0.0326	0.9962		
1374819_at	6.95	5.79	2.24	0.0359	0.9962	Tmem201	transmembrane protein 201

ID	LSP Stria Avg (log2)	Sal Stria Avg (log2)	Fold Change	P-val	FDR P-val	Gene Symbol	Description
1376378_at	7.12	5.96	2.23	0.0003	0.5392		
1369332_a_at	8.79	7.63	2.23	0.0072	0.9962	Rims1	regulating synaptic membrane exocytosis 1
1370993_at	8.28	7.12	2.23	0.0107	0.9962	Lamc1	laminin, gamma 1
1397928_at	7.09	5.93	2.23	0.02	0.9962	RGD1307554	similar to CG16812-PA
1393832_at	7.21	6.05	2.22	0.0048	0.9962	Rbm43	RNA binding motif protein 43
1390754_at	5.36	4.22	2.21	0.0254	0.9962		
1383193_at	7.6	6.46	2.21	0.0361	0.9962	Msrb3	methionine sulfoxide reductase B3
1382398_at	5.05	3.9	2.21	0.0443	0.9962	Shisa3	shisa family member 3
1386628_at	7.09	5.96	2.19	0.0152	0.9962		
1376709_at	7.85	6.72	2.19	0.0314	0.9962	Slc39a8	solute carrier family 39 (zinc transporter), member 8
1380426_at	7.18	6.06	2.18	0.0213	0.9962	Ankrd52	ankyrin repeat domain 52
1394398_at	6.84	5.71	2.18	0.0292	0.9962	LOC100909912	uncharacterized LOC100909912
1370589_at	6.61	5.5	2.17	0.0317	0.9962	Zfp709	zinc finger protein 709
1387547_a_at	7.96	6.84	2.17	0.0321	0.9962	Adgrl4	adhesion G protein-coupled receptor L4
1367828_at	7.91	6.8	2.15	0.0045	0.9962	Acads	acyl-CoA dehydrogenase, C-2 to C-3 short chain
1390415_at	6.09	4.99	2.14	0.0311	0.9962	Trip13	thyroid hormone receptor interactor 13
1391116_at	8.26	7.18	2.11	0.0041	0.9962		
1388539_at	6.65	5.57	2.11	0.0389	0.9962	Pkp2	plakophilin 2
1398149_at	9.4	8.32	2.11	0.0431	0.9962	Sema5a	sema domain, seven thrombospondin repeats (type 1 and type 1-like), transmembrane domain (TM) and short cytoplasmic domain, (semaphorin) 5A

ID	LSP Stria Avg (log2)	Sal Stria Avg (log2)	Fold Change	P-val	FDR P-val	Gene Symbol	Description
1380347_at	8.12	7.05	2.11	0.0448	0.9962	Bche	butyrylcholinesterase
1382799_at	6.91	5.84	2.1	0.0134	0.9962		
1370143_at	6.82	5.75	2.1	0.0401	0.9962	Smo	smoothened, frizzled class receptor
1393911_at	7.43	6.37	2.09	0.0267	0.9962	Sh3bp4	SH3-domain binding protein 4
1393479_at	10.49	9.43	2.09	0.0445	0.9962		
1398119_at	4.53	3.47	2.08	0.0089	0.9962		
1381503_at	9.71	8.65	2.08	0.0254	0.9962		
1388952_at	6.5	5.44	2.08	0.0276	0.9962	Dhrs11	dehydrogenase/reductase (SDR family) member 11
1390512_at	6.71	5.65	2.08	0.0369	0.9962	Asah2	N-acylsphingosine amidohydrolase (non-lysosomal ceramidase) 2
1378577_a_at	5.8	4.74	2.08	0.0466	0.9962	Mzf1	myeloid zinc finger 1
1382034_at	8.3	7.25	2.07	0.0014	0.9555	Akr1b10; Akr1b8; LOC100910708	aldo-keto reductase family 1, member B10 (aldose reductase); aldo-keto reductase family 1, member B8; aldose reductase-related protein 1-like
1378556_at	6.53	5.48	2.07	0.0412	0.9962	Enpp1	ectonucleotide pyrophosphatase/phosphodiesterase 1
1390161_at	8.76	7.72	2.06	0.0092	0.9962	Cyyr1	cysteine/tyrosine-rich 1
1387094_at	8.5	7.45	2.06	0.0122	0.9962	Slco1a2	solute carrier organic anion transporter family, member 1A2
1389011_at	9.17	8.13	2.06	0.028	0.9962	Nsmce2	NSE2/MMS21 homolog, SMC5-SMC6 complex SUMO ligase
1392040_at	6.74	5.7	2.05	0.0378	0.9962	Sass6	SAS-6 centriolar assembly protein
1394277_at	5.04	4.01	2.04	0.0203	0.9962	Borcs7	BLOC-1 related complex subunit 7
1397344_at	1.84	0.82	2.04	0.0279	0.9962	Cmtm8	CKLF-like MARVEL transmembrane domain containing 8

ID	LSP Stria Avg (log2)	Sal Stria Avg (log2)	Fold Change	P-val	FDR P-val	Gene Symbol	Description
1380845_at	6.26	5.23	2.04	0.0282	0.9962	Naalad2	N-acetylated alpha-linked acidic dipeptidase 2
1385061_at	9.65	8.62	2.04	0.0292	0.9962	Tmem229a	transmembrane protein 229A
1374039_at	7.83	6.81	2.02	0.0009	0.9032	Car14	carbonic anhydrase 14
1395277_at	6.87	5.85	2.02	0.005	0.9962		
1382136_at	4.31	5.32	-2.01	0.0191	0.9962	Slc2a9	solute carrier family 2 (facilitated glucose transporter), member 9
1377521_at	5.81	6.82	-2.01	0.0377	0.9962		
1395060_at	6.65	7.67	-2.02	0.0033	0.9962		
1392412_at	4.29	5.31	-2.03	0.0207	0.9962		
1384136_at	7.39	8.41	-2.03	0.0431	0.9962	Osbpl3	oxysterol binding protein-like 3
1378290_at	6.21	7.24	-2.04	0.0039	0.9962	Slc26a6	solute carrier family 26 (anion exchanger), member 6
1384379_at	5.7	6.73	-2.04	0.0476	0.9962		
1398153_at	6.24	7.28	-2.05	0.0035	0.9962		
1385249_at	5.1	6.14	-2.05	0.0382	0.9962	LOC103690134	uncharacterized LOC103690134
1377990_at	7.34	8.38	-2.06	0.043	0.9962	Emsy	EMSY BRCA2-interacting transcriptional repressor
1380036_at	4.08	5.13	-2.07	0.0096	0.9962		
1389894_at	5.25	6.3	-2.07	0.0269	0.9962	Dlc1	DLC1 Rho GTPase activating protein
1387580_at	4.64	5.69E+00	-2.07	0.049	0.9962	Srd5a2	steroid-5-alpha-reductase, alpha polypeptide 2 (3-oxo-5 alpha-steroid delta 4-dehydrogenase alpha 2)
1369461_at	3.23	4.29	-2.08	0.0164	0.9962	Pth2r	parathyroid hormone 2 receptor
1376253_at	8.47	9.52	-2.08	0.0236	0.9962	Ly6h	lymphocyte antigen 6 complex, locus H
1369771_at	5.29	6.35	-2.08	0.0253	0.9962	Irs1	insulin receptor substrate 1
1385652_at	6.79	7.85	-2.08	0.0453	0.9962	Zfp623	zinc finger protein 623

ID	LSP Stria Avg (log2)	Sal Stria Avg (log2)	Fold Change	P-val	FDR P-val	Gene Symbol	Description
1370588_a_at	5.55	6.62	-2.1	0.0299	0.9962	Slc8a1	solute carrier family 8 (sodium/calcium exchanger), member 1
1380395_at	7.05	8.12	-2.1	0.0448	0.9962		
1397871_at	7.11	8.19	-2.11	0.0127	0.9962		
1382091_at	4.31	5.39	-2.11	0.0193	0.9962		
1390608_at	3.5	4.57	-2.11	0.0202	0.9962		
1370722_at	0.8	1.88	-2.11	0.0316	0.9962	Cngb1	cyclic nucleotide gated channel beta 1
1368919_at	4.56	5.64	-2.12	0.024	0.9962	Pgf	placental growth factor
1380154_at	5.5	6.58	-2.12	0.0496	0.9962	Immt	inner membrane protein, mitochondrial
1378286_at	5.6	6.69	-2.13	0.0202	0.9962	Nbeal2	neurobeachin-like 2
1390737_at	4.46	5.55	-2.13	0.0217	0.9962		
1398662_at	4.13	5.22	-2.13	0.0277	0.9962	Fam167a	family with sequence similarity 167, member A
1377135_at	0.58	1.69	-2.15	0.0023	0.9962	LOC102547797	uncharacterized LOC102547797
1394545_at	7.37	8.48	-2.16	0.0262	0.9962	Spire2	spire-type actin nucleation factor 2
1392260_at	8.18	9.29	-2.16	0.0327	0.9962		
1391350_at	4.75	5.87	-2.17	0.0034	0.9962	H2afy2	H2A histone family, member Y2
1393941_at	4.22	5.34	-2.17	0.0102	0.9962	Pon1	paraoxonase 1
1380619_at	4.73	5.85	-2.18	0.0058	0.9962	RGD1305537	similar to RIKEN cDNA 3110001I22
1386619_at	5.52	6.66	-2.2	0.0147	0.9962		
1375008_at	7.53	8.67	-2.2	0.0328	0.9962	Aurkc	aurora kinase C
1382671_at	4.97	6.12	-2.21	0.0165	0.9962		
1377940_at	6.38	7.52	-2.21	0.021	0.9962	Fam101b	family with sequence similarity 101, member B
1391624_at	3.66	4.81	-2.21	0.0219	0.9962	Sec14l3; Sec14l4	SEC14-like lipid binding 3; SEC14-like lipid binding 4

ID	LSP Stria Avg (log2)	Sal Stria Avg (log2)	Fold Change	P-val	FDR P-val	Gene Symbol	Description
1381792_at	5.38	6.52	-2.21	0.0267	0.9962	Mrps15	mitochondrial ribosomal protein S15
1396880_at	3.21	4.35E+00	-2.21	0.0317	0.9962		
1378062_at	6.32	7.46	-2.21	0.04	0.9962		
1393535_at	4.42	5.57	-2.22	0.0069	0.9962		
1382887_at	3.75	4.9	-2.22	0.0313	0.9962		
1392939_at	7.26	8.41	-2.23	0.0004	0.7057	Slc41a3	solute carrier family 41, member 3
1370009_at	3.79	4.94	-2.23	0.0096	0.9962	Apoc3	apolipoprotein C-III
1391118_at	7.44	8.6	-2.24	0.035	0.9962		
1376977_at	4.35	5.51	-2.24	0.0483	0.9962	Ptger3	prostaglandin E receptor 3 (subtype EP3)
1385566_at	5.95	7.13	-2.25	0.0191	0.9962	Akap2	A kinase (PRKA) anchor protein 2
1380112_at	4.86	6.04	-2.26	0.0339	0.9962		
1397492_at	6.5	7.68	-2.27	0.01	0.9962	Lmo7	LIM domain 7
1370624_at	3.73	4.91	-2.27	0.038	0.9962	F2rl2	coagulation factor II (thrombin) receptor-like 2
1369405_a_at	3.12	4.32	-2.29	0.0067	0.9962	Chrnb4	cholinergic receptor, nicotinic, beta 4 (neuronal)
1397376_at	4.08	5.28	-2.29	0.0342	0.9962		
1381146_at	4.83	6.03	-2.3	0.0111	0.9962		
1396270_at	5.2	6.4	-2.3	0.0397	0.9962		
1381334_at	6.82	8.03	-2.31	0.0096	0.9962		
1387293_at	3.29	4.51	-2.33	0.0141	0.9962	Zp2	zona pellucida glycoprotein 2 (sperm receptor)
1375627_at	4.85	6.08	-2.34	0.0343	0.9962	Akirin2	akirin 2
1386872_at	6.47	7.7	-2.35	0.0271	0.9962	Igf2r	insulin-like growth factor 2 receptor
1387157_at	2.27	3.5	-2.35	0.0343	0.9962	Pmfbp1	polyamine modulated factor 1 binding protein 1
1392825_at	2.52	3.77	-2.37	0.0263	0.9962	RGD1559600	RGD1559600

ID	LSP Stria Avg (log2)	Sal Stria Avg (log2)	Fold Change	P-val	FDR P-val	Gene Symbol	Description
1396252_at	6.83	8.07	-2.37	0.0385	0.9962		
1390733_at	5.4	6.65	-2.38	0.0076	0.9962		
1379844_at	1.85	3.12	-2.4	0.0177	0.9962		
1370100_at	7.01	8.28	-2.41	0.0256	0.9962	Pik3r2	phosphoinositide-3-kinase, regulatory subunit 2 (beta)
1380153_at	5.51	6.78	-2.42	0.0157	0.9962		
1387528_at	0.63	1.91	-2.42	0.0403	0.9962	LOC100911854; Mbl2	mannose-binding protein C-like; mannose-binding lectin (protein C) 2
1382666_at	3.26	4.54	-2.43	0.0054	0.9962		
1382147_at	4.9	6.19	-2.43	0.0155	0.9962	Tmem132c	transmembrane protein 132C
1392011_at	4.86	6.14	-2.43	0.0388	0.9962		
1371106_at	3.9	5.2	-2.46	0.049	0.9962	Itgb7	integrin, beta 7
1379686_at	6.33	7.64	-2.48	0.0396	0.9962		
1392270_at	4.4	5.72	-2.49	0.0044	0.9962		
1388846_at	6.05	7.36	-2.49	0.0135	0.9962	Bcl2l12	BCL2-like 12 (proline rich)
1369789_at	4.34	5.66	-2.49	0.0152	0.9962	Glra3	glycine receptor, alpha 3
1384590_at	3.96	5.28	-2.49	0.0249	0.9962		
1368732_at	2.03	3.35	-2.5	0.01	0.9962	LOC103689996; Tap2	antigen peptide transporter 2; transporter 2, ATP-binding cassette, sub-family B (MDR/TAP)
1393821_at	5.35	6.68	-2.51	0.0265	0.9962	Nkain3	Na+/K+ transporting ATPase interacting 3
1388233_at	3.53	4.86	-2.52	0.0107	0.9962	Cish	cytokine inducible SH2-containing protein
1388254_a_at	2.32	3.66	-2.52	0.04	0.9962	RT1-CE5	RT1 class I, locus CE5
1392798_at	4.19	5.54	-2.54	0.0346	0.9962	Pdia2	protein disulfide isomerase family A, member 2
1390329_at	5.64	7	-2.56	0.0238	0.9962	Mfap3	microfibrillar-associated protein 3

ID	LSP Stria Avg (log2)	Sal Stria Avg (log2)	Fold Change	P-val	FDR P-val	Gene Symbol	Description
1378522_at	6.78	8.13	-2.56	0.0315	0.9962		
1376732_at	4.39	5.75	-2.57	0.0321	0.9962	Calr3	calreticulin 3
1380046_at	4.32	5.69	-2.58	0.0187	0.9962	Herc3	HECT and RLD domain containing E3 ubiquitin protein ligase 3
1370580_a_at	0.9	2.27E+00	-2.58	0.0373	0.9962	Cyp2c6v1	cytochrome P450, family 2, subfamily C, polypeptide 6, variant 1
1380949_at	5.24	6.61	-2.58	0.0449	0.9962	Gabra2	gamma-aminobutyric acid (GABA) A receptor, alpha 2
1387441_at	4.53	5.91	-2.59	0.0301	0.9962	Kcnk3	potassium channel, two pore domain subfamily K, member 3
1394843_at	4.45	5.84	-2.6	0.0102	0.9962		
1368491_at	3.12	4.5	-2.6	0.0162	0.9962	Dnase2b	deoxyribonuclease II beta
1391372_at	6.52	7.89	-2.6	0.0261	0.9962		
1396258_at	3.16	4.54	-2.6	0.0288	0.9962	Vps50	VPS50 EARP/GARPII complex subunit
1378783_at	4.53	5.91	-2.6	0.0438	0.9962		
1393200_at	4.12	5.5	-2.6	0.0479	0.9962	Tnfrsf13b	tumor necrosis factor receptor superfamily, member 13B
1396605_at	2.98	4.37	-2.61	0.0268	0.9962	Mov10l1	Mov10 RISC complex RNA helicase like 1
1383853_at	5.49	6.87	-2.61	0.0373	0.9962	Dyrk3	dual-specificity tyrosine-(Y)-phosphorylation regulated kinase 3
1380274_at	4.67	6.05	-2.62	0.0224	0.9962	RGD1560795; Spr	similar to Sepiapterin reductase (SPR); sepiapterin reductase (7,8-dihydrobiopterin:NADP+ oxidoreductase)
1397236_at	5.65	7.04	-2.62	0.0446	0.9962		
1381152_at	4.88	6.29	-2.66	0.0178	0.9962	Ntmt1	N-terminal Xaa-Pro-Lys N-methyltransferase 1

ID	LSP Stria Avg (log2)	Sal Stria Avg (log2)	Fold Change	P-val	FDR P-val	Gene Symbol	Description
1381719_at	6.37	7.79	-2.67	0.0017	0.9962		
1382208_at	6.69	8.11	-2.67	0.0141	0.9962		
1398584_at	0.42	1.85	-2.69	0.0047	0.9962	Krt36	keratin 36, type I
1397117_at	5.58	7.01	-2.69	0.0065	0.9962		
1368641_at	4.6	6.03	-2.69	0.0464	0.9962	Wnt4	wingless-type MMTV integration site family, member 4
1394629_at	5.82	7.26	-2.71	0.0313	0.9962	Katnbl1	katanin p80 subunit B-like 1
1395770_at	4.46	5.91	-2.73	0.0232	0.9962		
1396469_at	3.08	4.53	-2.73	0.0432	0.9962		
1384818_at	6.35	7.82	-2.77	0.0378	0.9962	Mylk	myosin light chain kinase
1396147_at	4.59	6.07	-2.78	0.0011	0.9032		
1370703_at	1.07	2.56	-2.8	0.0137	0.9962	Mrgprf	MAS-related GPR, member F
1395178_at	4.35	5.84	-2.81	0.0036	0.9962		
1379086_at	3.57	5.07	-2.82	0.0337	0.9962		
1387833_at	1.55	3.05	-2.84	0.015	0.9962	Tmprss2	transmembrane protease, serine 2
1376556_at	5.07	6.58	-2.85	0.0165	0.9962		
1387122_at	6.08	7.59	-2.85	0.0387	0.9962	Plagl1	pleiomorphic adenoma gene-like 1
1379908_at	1.64	3.16	-2.86	0.0366	0.9962	Asb4	ankyrin repeat and SOCS box-containing 4
1367792_at	1.71	3.23	-2.87	0.0283	0.9962	Bpifa2	BPI fold containing family A, member 2
1369019_at	3.63	5.16	-2.88	0.0122	0.9962	Chrna5	cholinergic receptor, nicotinic, alpha 5
1396001_at	6.16	7.69E+00	-2.89	0.006	0.9962		
1370522_at	2.73	4.27	-2.91	0.0079	0.9962	Gcgr	glucagon receptor
1369162_at	3	4.54	-2.92	0.0234	0.9962	Gucy2c	guanylate cyclase 2C
1397082_at	3.64	5.19	-2.93	0.0023	0.9962	Pfkfb3	6-phosphofructo-2-kinase/fructose-2,6-biphosphatase 3
1376178_at	5.7	7.25	-2.94	0.0096	0.9962		
1380799_at	6.17	7.73	-2.94	0.0395	0.9962	Grem2	gremlin 2

ID	LSP Stria Avg (log2)	Sal Stria Avg (log2)	Fold Change	P-val	FDR P-val	Gene Symbol	Description
1394976_at	3.83	5.4	-2.96	0.0089	0.9962		
1390359_at	2.95	4.51	-2.96	0.0158	0.9962		
1394628_at	3.73	5.32	-3	0.0164	0.9962		
1369153_at	2.46	4.05	-3.01	0.0392	0.9962	Nphs1	nephrosis 1, congenital, Finnish type (nephrin)
1398136_at	1.83	3.42	-3.02	0.0145	0.9962	RGD1562218	similar to RIKEN cDNA 0610039J04
1389731_at	5.56	7.15	-3.02	0.0163	0.9962		
1384616_at	5.56	7.15	-3.02	0.0374	0.9962	Fkbp15; LOC102556352	FK506 binding protein 15; FK506-binding protein 15-like
1395691_at	2.93	4.54	-3.05	0.0489	0.9962	Klhl22	kelch-like family member 22
1392430_at	3.54	5.15	-3.06	0.0042	0.9962	Clcnkb	chloride channel, voltage-sensitive Kb
1388014_at	2.5	4.12	-3.07	0.0185	0.9962	Obp1f	odorant binding protein I f
1394559_at	4.65	6.26	-3.07	0.0412	0.9962		
1383926_at	3.38	5.01	-3.1	0.0105	0.9962	Bub1b	BUB1 mitotic checkpoint serine/threonine kinase B
1398186_at	4.32	5.97	-3.14	0.0294	0.9962		
1391519_at	3.8	5.47	-3.17	0.0125	0.9962	Fmn1	formin 1
1379888_at	3.2	4.86	-3.17	0.0215	0.9962	LOC100912602	uncharacterized LOC100912602
1373710_at	2.95	4.63	-3.2	0.0044	0.9962	Slc38a4	solute carrier family 38, member 4
1397980_at	4.07	5.74	-3.2	0.0118	0.9962		
1372053_at	2.29	3.96	-3.2	0.0338	0.9962		
1389160_at	5.08	6.78	-3.23	0.0393	0.9962	Ahsp	alpha hemoglobin stabilizing protein
1393504_at	3.49	5.2	-3.25	0.0227	0.9962		
1393259_at	4.06	5.77	-3.27	0.0153	0.9962		
1392432_at	3.98	5.7	-3.31	0.0257	0.9962		
1391059_at	2.09	3.82	-3.32	0.0321	0.9962	Npw	neuropeptide W
1391777_at	2.06	3.8	-3.33	0.0014	0.9555		
1397897_x_at	5.55	7.29	-3.33	0.0055	0.9962	LOC103690718	uncharacterized LOC103690718

ID	LSP Stria Avg (log2)	Sal Stria Avg (log2)	Fold Change	P-val	FDR P-val	Gene Symbol	Description
1368317_at	1.44	3.18	-3.35	0.0395	0.9962	Aqp7	aquaporin 7
1369913_at	0.73	2.49	-3.37	0.0066	0.9962	Opn1mw	opsin 1 (cone pigments), medium-wave-sensitive
1369525_at	4.46	6.24	-3.41	0.0131	0.9962	Gata3	GATA binding protein 3
1368585_at	9.16	10.93	-3.41	0.017	0.9962	Cartpt	CART prepropeptide
1369294_at	2.62	4.42	-3.48	0.0126	0.9962	Bst1	bone marrow stromal cell antigen 1
1381059_at	1.46	3.26	-3.49	0.0028	0.9962		
1389881_at	3.06	4.86	-3.49	0.0176	0.9962		
1391374_at	2.47	4.27	-3.49	0.0489	0.9962	Tacc3	transforming, acidic coiled-coil containing protein 3
1392600_a_at	4.88	6.69	-3.51	0.0354	0.9962	Maml2	mastermind-like transcriptional coactivator 2
1392314_at	4.11	5.92	-3.51	0.0412	0.9962		
1380240_at	3.14	4.95	-3.51	0.0452	0.9962		
1378970_at	2.93	4.76	-3.54	0.0063	0.9962		
1369111_at	3.43	5.26	-3.55	0.0204	0.9962	Fabp1	fatty acid binding protein 1, liver
1375039_x_at	2.22	4.05	-3.56	0.0208	0.9962	Fcgbpl1	Fc fragment of IgG binding protein-like 1
1379158_at	2.51	4.34	-3.56	0.0218	0.9962		
1369413_at	1.04	2.88	-3.57	0.0005	0.7964	Uncx	UNC homeobox
1378327_at	0.37	2.21	-3.58	0.0057	0.9962	Dmrt2	doublesex and mab-3 related transcription factor 2
1398243_at	1.94	3.81	-3.65	0.0368	0.9962	Csrp3	cysteine and glycine-rich protein 3 (cardiac LIM protein)
1390826_at	4.37	6.25	-3.67	0.0148	0.9962	LOC102551963	uncharacterized LOC102551963
1384448_at	2.99	4.87	-3.68	0.0083	0.9962	RGD1565844	similar to RIKEN cDNA 1700045I19
1381125_at	0.94	2.82	-3.69	0.0171	0.9962		
1377372_at	2.36	4.24	-3.7	0.0184	0.9962		

ID	LSP Stria Avg (log2)	Sal Stria Avg (log2)	Fold Change	P-val	FDR P-val	Gene Symbol	Description
1391141_at	3.04	4.93	-3.7	0.0292	0.9962	LOC102551175; LOC102555078	uncharacterized LOC102551175; uncharacterized LOC102555078
1371364_a_at	4.61	6.52	-3.75	0.0154	0.9962	Andpro	androgen regulated protein
1384721_at	0.91	2.83	-3.79	0.0295	0.9962	Sprr2d	small proline-rich protein 2D
1393714_at	3.88	5.82	-3.85	0.0112	0.9962		
1396476_at	2.52	4.47	-3.86	0.0115	0.9962	Rsph10b	radial spoke head 10 homolog B (Chlamydomonas)
1387681_at	3.17	5.12	-3.87	0.0174	0.9962	Ucp3	uncoupling protein 3 (mitochondrial, proton carrier)
1394195_at	0.41	2.37	-3.88	0.0471	0.9962		
1392628_at	1.66	3.62	-3.9	0.0238	0.9962	Ms4a6bl	membrane-spanning 4-domains, subfamily A, member 6B-like
1370380_s_at	3.61	5.57	-3.9	0.0444	0.9962	Nr2f6	nuclear receptor subfamily 2, group F, member 6
1378607_at	4.77	6.74	-3.92	0.0308	0.9962		
1385045_at	2.16	4.12	-3.92	0.0333	0.9962		
1382985_at	2.59	4.56	-3.92	0.0464	0.9962		
1397145_at	4.5	6.49	-3.95	0.0231	0.9962		
1369364_at	2.71	4.7	-3.96	0.0214	0.9962	Atp1a4	ATPase, Na+/K+ transporting, alpha 4 polypeptide
1395187_at	5.2	7.19	-3.97	0.0061	0.9962		
1384575_at	2.92	4.93	-4.04	0.0069	0.9962	LOC102552020	uncharacterized LOC102552020
1385486_at	1.11	3.13	-4.06	0.0119	0.9962	Bnc2	basonuclin 2
1392400_at	2.42	4.45	-4.08	0.0197	0.9962		
1386901_at	3.08	5.12	-4.11	0.0054	0.9962	Cd36; LOC100365047; LOC103690020	CD36 molecule (thrombospondin receptor); scavenger receptor class B, member 2-like; platelet glycoprotein 4-like

ID	LSP Stria Avg (log2)	Sal Stria Avg (log2)	Fold Change	P-val	FDR P-val	Gene Symbol	Description
1390961_at	2.88	4.92	-4.12	0.0446	0.9962	Gp9	glycoprotein IX (platelet)
1390211_at	0.64	2.69	-4.13	0.0135	0.9962	Slc27a3	solute carrier family 27 (fatty acid transporter), member 3
1385781_at	2.57	4.62	-4.15	0.0288	0.9962	Ercc6l	excision repair cross-complementation group 6-like
1385004_at	5.91	7.96	-4.16	0.0134	0.9962		
1370778_at	0	2.06	-4.18	0.0297	0.9962	LOC688489; Mup5	similar to alpha2u globulin; major urinary protein 5
1392327_s_at	5.72	7.8	-4.23	0.0189	0.9962	Krt77	keratin 77, type II
1368579_at	1.3	3.39	-4.24	0.0116	0.9962	Prl2a1	Prolactin family 2, subfamily a, member 1
1397901_at	5.33	7.42	-4.24	0.0466	0.9962		
1391214_at	1.74	3.84	-4.29	0.0112	0.9962	Fam26f	family with sequence similarity 26, member F
1368611_at	2.43	4.54	-4.3	0.0233	0.9962	Grp	gastrin releasing peptide
1395141_at	4.84	6.96	-4.33	0.0256	0.9962	Lrrc3	leucine rich repeat containing 3
1395342_at	4.1	6.22	-4.34	0.0352	0.9962	Ckap4	cytoskeleton-associated protein 4
1375002_at	3.71	5.83	-4.35	0.028	0.9962		
1394533_at	3.83	5.95	-4.36	0.005	0.9962		
1374817_at	4.34	6.47	-4.37	0.0313	0.9962	Wnt5a	wingless-type MMTV integration site family, member 5A
1371156_a_at	2.25	4.39	-4.43	0.0053	0.9962	Glra1	glycine receptor, alpha 1
1383351_at	1.86	4.01	-4.44	0.0102	0.9962		
1370793_at	1.76	3.91	-4.45	0.0093	0.9962		
1384752_at	1.25	3.43	-4.52	0.0103	0.9962	LOC689770	similar to osteoclast inhibitory lectin
1385058_at	0.87	3.04	-4.52	0.0354	0.9962	Cldn8	claudin 8
1369613_at	0	2.18	-4.54	0.0264	0.9962		
1373567_at	3.55	5.75	-4.57	0.0243	0.9962	Tle6	transducin-like enhancer of split 6

ID	LSP Stria Avg (log2)	Sal Stria Avg (log2)	Fold Change	P-val	FDR P-val	Gene Symbol	Description
1391172_at	0.44	2.64	-4.6	0.0002	0.5392	LOC103690947	uncharacterized LOC103690947
1374378_at	1.93	4.13	-4.6	0.0169	0.9962	Arl9	ADP-ribosylation factor-like 9
1369921_at	1.91	4.12	-4.62	0.021	0.9962	Gstm3	glutathione S-transferase mu 3
1371279_at	1.18	3.4	-4.65	0.0085	0.9962	Hist1h2af	histone cluster 1, H2af
1385679_at	1.92	4.14	-4.65	0.0138	0.9962		
1386224_at	2.76	4.98	-4.67	0.0008	0.9032		
1393426_at	2.29	4.55	-4.77	0.0099	0.9962	Pde6a	phosphodiesterase 6A, cGMP-specific, rod, alpha
1391615_at	1.46	3.72	-4.78	0.0044	0.9962	LOC102555788	uncharacterized LOC102555788
1390216_a_at	3.19	5.47	-4.84	0.0205	0.9962		
1382968_at	1.47	3.74	-4.85	0.0166	0.9962		
1396624_at	2	4.29	-4.88	0.0039	0.9962		
1392132_at	2.67	4.96	-4.9	0.0145	0.9962	LOC103690054; Polr2i	DNA-directed RNA polymerase II subunit RPB9; polymerase (RNA) II (DNA directed) polypeptide I
1387477_at	2.36	4.66	-4.91	0.0144	0.9962	Kcnk12	potassium channel, two pore domain subfamily K, member 12
1381566_at	2.55	4.86	-4.95	0.0067	0.9962		
1396900_at	4.41	6.73	-5.02	0.0321	0.9962		
1397559_at	0	2.33	-5.03	0.0325	0.9962	Ppp1r3a	protein phosphatase 1, regulatory subunit 3A
1379502_at	1.6	3.94	-5.07	0.0212	0.9962	C1H19orf84	chromosome 1 open reading frame, human C19orf84
1380461_at	2.59	4.94	-5.1	0.0284	0.9962	LOC102553514	uncharacterized LOC102553514
1372889_at	1.61	3.96	-5.12	0.041	0.9962	Slco2a1	solute carrier organic anion transporter family, member 2a1
1396800_at	2.71	5.07	-5.14	0.0316	0.9962		
1395961_at	0	2.37	-5.16	0.0049	0.9962		

ID	LSP Stria Avg (log2)	Sal Stria Avg (log2)	Fold Change	P-val	FDR P-val	Gene Symbol	Description
1386350_at	0.14	2.52	-5.2	0.034	0.9962		
1381746_at	3.01	5.39	-5.21	0.0263	0.9962		
1393775_at	2.79	5.18	-5.25	0.0217	0.9962	LOC103689949; N4bp3	nedd4 binding protein 3; Nedd4 binding protein 3
1393680_at	3.32	5.72	-5.28	0.0133	0.9962	Cetn1	centrin, EF-hand protein, 1
1378946_at	0.91	3.31	-5.29	0.0446	0.9962		
1387539_at	0.2	2.61	-5.32	0.0279	0.9962	Si	sucrase-isomaltase (alpha-glucosidase)
1376105_at	2.83	5.25	-5.34	0.0119	0.9962	Col14a1	collagen, type XIV, alpha 1
1382695_at	3.34	5.75	-5.34	0.0195	0.9962	Lrrn4cl	LRRN4 C-terminal like
1394385_s_at	2.18	4.64	-5.5	0.0458	0.9962	Drd4	dopamine receptor D4
1380389_at	2.18	4.64	-5.53	0.0261	0.9962		
1389856_at	1.87	4.34	-5.54	0.0349	0.9962	Cgm4; Psg16	carcinoembryonic antigen gene family 4; pregnancy specific glycoprotein 16
1377144_at	1.83	4.31	-5.57	0.0471	0.9962		
1379812_at	2.46	4.95	-5.6	0.022	0.9962	Nnmt	nicotinamide N-methyltransferase
1393768_at	1.4	3.89	-5.61	0.0107	0.9962	Lingo1	leucine rich repeat and Ig domain containing 1
1393560_at	4.65	7.14	-5.63	0.0273	0.9962	LOC680875	similar to dystonin isoform 1
1380442_at	1.86	4.36	-5.63	0.0314	0.9962	Hoxc8	homeobox C8
1380115_at	0.1	2.59	-5.64	0.0307	0.9962		
1379403_at	3.1	5.6	-5.69	0.0235	0.9962		
1385362_at	0.55	3.06	-5.7	0.0066	0.9962		
1396003_at	2.33	4.85	-5.73	0.0288	0.9962		
1375515_at	1.47	4	-5.76	0.0158	0.9962	LOC102553382	uncharacterized LOC102553382
1380988_at	1.35	3.89	-5.84	0.0149	0.9962		
1376474_at	0	2.55	-5.84	0.0281	0.9962	Cdrt4	CMT1A duplicated region transcript 4
1384712_at	1.91	4.46	-5.87	0.0011	0.9032		

ID	LSP Stria Avg (log2)	Sal Stria Avg (log2)	Fold Change	P-val	FDR P-val	Gene Symbol	Description
1375607_at	0.72	3.28	-5.87	0.0497	0.9962	Foxc2	forkhead box C2
1391400_at	2.1	4.66	-5.89	0.014	0.9962	Cplx3	complexin 3
1396597_at	1.02	3.58	-5.9	0.0412	0.9962		
1398077_at	2.02	4.59	-5.93	0.0098	0.9962		
1387303_at	1.93	4.49	-5.93	0.0499	0.9962	Slc22a2	solute carrier family 22 (organic cation transporter), member 2
1377672_at	0	2.57	-5.96	0.0071	0.9962	LOC100910526; Sult1c2	sulfotransferase 1C2-like; sulfotransferase family 1C member 2
1371080_at	1.24	3.81	-5.97	0.0074	0.9962	Klk1c4	kallikrein 1-related peptidase C4
1370401_at	1.1	3.69	-6	0.001	0.9032	Ly6i	lymphocyte antigen 6 complex, locus I
1397801_at	0.9	3.5	-6.05	0.0199	0.9962		
1391457_a_at	2.32	4.93	-6.08	0.0033	0.9962	Irx2	iroquois homeobox 2
1385631_at	0.96	3.6	-6.26	0.0361	0.9962		
1369787_at	1.97	4.62	-6.27	0.0049	0.9962	Cckar	cholecystokinin A receptor
1376976_at	0.62	3.27	-6.31	6.33E-05	0.3159	Sectm1b	secreted and transmembrane 1B
1397252_at	1.76	4.42	-6.31	0.0424	0.9962		
1368751_at	2.53	5.21	-6.4	0.0409	0.9962	Kcns3	potassium voltage-gated channel, modifier subfamily S, member 3
1384650_at	0.36	3.07	-6.56	0.0129	0.9962		
1393871_at	2.09	4.81	-6.59	0.0327	0.9962		
1370096_at	1.34	4.11	-6.84	0.0128	0.9962	Prf1	perforin 1 (pore forming protein)
1369250_at	3.11	5.89	-6.86	0.0062	0.9962	Slc28a1	solute carrier family 28 (concentrative nucleoside transporter), member 1
1369422_at	0.83	3.61	-6.89	0.0079	0.9962	Fap	fibroblast activation protein, alpha
1384700_at	1.69	4.47	-6.89	0.0326	0.9962		
1395670_at	1.91	4.7	-6.9	0.0105	0.9962		

ID	LSP Stria Avg (log2)	Sal Stria Avg (log2)	Fold Change	P-val	FDR P-val	Gene Symbol	Description
1392296_at	1.79	4.58	-6.9	0.0499	0.9962	Gcsam	germinal center-associated, signaling and motility
1368663_at	0.93	3.72	-6.93	0.0022	0.9962	LOC56764	dnaj-like protein
1369503_at	0	2.81	-6.99	0.0305	0.9962	Amy2a3	amylase 2a3
1392318_at	1.2	4.02	-7.03	0.0207	0.9962	Ubald2	UBA-like domain containing 2
1384825_at	1.48	4.29	-7.05	0.0391	0.9962	LOC102550682	carcinoembryonic antigen-related cell adhesion molecule 5-like
1398678_at	0	2.82	-7.07	0.0011	0.9032	Brwd3	bromodomain and WD repeat domain containing 3
1384395_at	1.98	4.8	-7.09	0.0058	0.9962	Ldhal6b	lactate dehydrogenase A-like 6B
1373723_at	1.44	4.27	-7.11	0.0038	0.9962	Gpihbp1	glycosylphosphatidylinositol anchored high density lipoprotein binding protein 1
1379142_at	3.31	6.14	-7.11	0.0398	0.9962		
1382583_at	1.16	4	-7.13	0.003	0.9962		
1371274_at	0	2.85	-7.2	0.0164	0.9962	Cyss	cystatin S
1396454_at	1.99	4.85	-7.27	0.0016	0.9962		
1375317_at	2.27	5.13	-7.29	0.0004	0.7449		
1387839_at	1.38	4.27	-7.39	0.043	0.9962	RT1-N1; RT1-N2	RT1 class Ib, locus N1; RT1 class Ib, locus N2
1396788_at	0	2.9	-7.46	0.001	0.9032	LOC100365542	rCG41957-like
1379961_at	1.48	4.38	-7.46	0.0183	0.9962		
1395788_at	1.17	4.08	-7.5	0.0286	0.9962		
1381372_at	1.54	4.46	-7.59	0.0056	0.9962	Cep76	centrosomal protein 76
1383739_at	1.56	4.53	-7.83	0.0281	0.9962	LOC100909782; LOC100909810	uncharacterized LOC100909782; uncharacterized LOC100909810
1381712_at	0.13	3.12	-7.91	0.0243	0.9962		

ID	LSP Stria Avg (log2)	Sal Stria Avg (log2)	Fold Change	P-val	FDR P-val	Gene Symbol	Description
1389783_s_at	1.42	4.4	-7.92	0.0287	0.9962	Fcgbp; Fcgbpl1	Fc fragment of IgG binding protein; Fc fragment of IgG binding protein-like 1
1398146_at	1.76	4.74	-7.93	0.0081	0.9962		
1391707_at	0.06	3.07	-8.04	0.0002	0.5392		
1396260_at	3.24	6.25	-8.06	0.0197	0.9962		
1388435_at	0.6	3.61	-8.06	0.0245	0.9962	Crygs	crystallin, gamma S
1368746_a_at	0.52	3.53	-8.07	0.0063	0.9962	Atp12a	ATPase, H+/K+ transporting, nongastric, alpha polypeptide
1370992_a_at	0.66	3.69	-8.13	3.36E-05	0.2085	Fga	fibrinogen alpha chain
1398278_at	0.92	3.95	-8.16	0.0063	0.9962	Prl	prolactin
1385120_at	0.7	3.73	-8.19	0.0048	0.9962	Pof1b	premature ovarian failure 1B
1391747_at	2.02	5.06	-8.2	0.0308	0.9962		
1397857_at	1.43	4.47	-8.25	0.0128	0.9962		
1387550_a_at	0.8	3.85	-8.26	0.0234	0.9962	Slc14a2	solute carrier family 14 (urea transporter), member 2
1384805_at	1.99	5.04	-8.29	0.0318	0.9962	Defb24	defensin beta 24
1396158_at	1.33	4.38	-8.3	0.0002	0.5392	Rem1	RAS (RAD and GEM)-like GTP-binding 1
1387648_at	0	3.08	-8.48	0.019	0.9962	Cxcl6	chemokine (C-X-C motif) ligand 6
1398144_at	1.05	4.15	-8.55	0.0241	0.9962		
1396608_at	3.12	6.22	-8.58	0.0014	0.9555		
1397223_at	0.43	3.53	-8.59	0.0387	0.9962		
1369225_at	0.96	4.07	-8.68	0.0109	0.9962	Kng2	kininogen 2
1384660_at	1.54	4.66	-8.74	0.024	0.9962	Nkd2	naked cuticle homolog 2 (Drosophila)
1371143_at	0	3.13	-8.78	0.0303	0.9962	Serpina7	serpin peptidase inhibitor, clade A (alpha-1 antiproteinase, antitrypsin), member 7
1387134_at	0.43	3.58	-8.9	0.0352	0.9962	Slfn4	schlafen 4

ID	LSP Stria Avg (log2)	Sal Stria Avg (log2)	Fold Change	P-val	FDR P-val	Gene Symbol	Description
1385541_at	0	3.16	-8.91	0.0298	0.9962		
1398090_at	1.42	4.58	-8.95	0.0266	0.9962	Klk5	kallikrein related-peptidase 5
1398018_at	2.28	5.44	-8.97	0.0189	0.9962	LOC102553465	uncharacterized LOC102553465
1396429_at	0	3.19	-9.13	0.0249	0.9962		
1391712_at	2.28	5.47	-9.16	0.0432	0.9962	Il22ra1	interleukin 22 receptor, alpha 1
1384338_at	2.5	5.71	-9.21	0.0065	0.9962	Cdc45	cell division cycle 45
1396595_at	2.38	5.59	-9.29	0.0224	0.9962		
1375099_at	2.65	5.87	-9.33	0.0162	0.9962		
1381932_at	1	4.23	-9.34	0.0414	0.9962	Fam46a	family with sequence similarity 46, member A
1385599_at	0	3.25	-9.51	0.0027	0.9962	RSA-14-44	RSA-14-44 protein
1368783_at	1.76	5.01	-9.54	0.0412	0.9962	Icos	inducible T-cell co-stimulator
1395094_at	1.18	4.44	-9.55	0.0212	0.9962		
1390664_at	0.3	3.56	-9.57	0.0339	0.9962	Tmem116	transmembrane protein 116
1387212_at	0.49	3.75	-9.59	0.0175	0.9962	Bhlha15	basic helix-loop-helix family, member a15
1384499_at	1.01	4.28	-9.64	0.0108	0.9962	Acsm1; Acsm2a	acyl-CoA synthetase medium-chain family member 1; acyl-CoA synthetase medium-chain family member 2A
1370647_at	2.3	5.58	-9.71	0.0046	0.9962	Impg2	interphotoreceptor matrix proteoglycan 2
1397739_at	2.57	5.87	-9.82	0.0447	0.9962	Slc25a31	solute carrier family 25 (mitochondrial carrier; adenine nucleotide translocator), member 31
1386383_at	1.96	5.28	-9.99	0.0012	0.9231		
1369595_at	0.62	3.95	-10.03	9.80E-06	0.0809	Fgf23	fibroblast growth factor 23
1381370_at	1.54	4.92	-10.41	0.0006	0.9032		

ID	LSP Stria Avg (log2)	Sal Stria Avg (log2)	Fold Change	P-val	FDR P-val	Gene Symbol	Description
1396389_at	3.13	6.51	-10.43	5.84E-07	0.0091	Pip5kl1	phosphatidylinositol-4-phosphate 5-kinase-like 1
1369585_at	0	3.45	-10.9	0.0336	0.9962	Tore	trispanning orphan
1387974_a_at	0	3.45	-10.95	0.0497	0.9962	Slc21a4	kidney specific organic anion transporter
1387985_a_at	0.51	3.99	-11.16	0.0029	0.9962	Obp3	alpha-2u globulin PGCL4
1380768_at	0	3.5	-11.28	0.0187	0.9962		
1381226_at	1.08	4.6	-11.45	0.0003	0.5392		
1384522_at	2.64	6.17	-11.54	0.013	0.9962	Sytl3	synaptotagmin-like 3
1381337_at	0.93	4.46	-11.58	0.013	0.9962		
1386230_at	0.01	3.54	-11.61	0.0434	0.9962		
1370013_at	0.51	4.06	-11.73	0.0148	0.9962	Cnga1	cyclic nucleotide gated channel alpha 1
1385251_at	0.09	3.64	-11.75	0.0011	0.9032	Fam110c	family with sequence similarity 110, member C
1381409_at	0.72	4.3	-11.96	0.0065	0.9962		
1386292_at	0	3.59	-12	0.007	0.9962		
1393508_at	0.25	3.85	-12.12	0.0321	0.9962	Nox4	NADPH oxidase 4
1394141_at	0.02	3.63	-12.21	0.0296	0.9962		
1392780_at	0.62	4.23	-12.21	0.0399	0.9962	Nxf7	nuclear RNA export factor 7
1398201_at	0	3.64	-12.46	0.0025	0.9962		
1391504_at	0.14	3.79	-12.57	0.0238	0.9962		
1378636_at	1.37	5.02	-12.58	0.0051	0.9962	Chmp4b	charged multivesicular body protein 4B
1388124_at	0.01	3.72	-13.04	5.21E-07	0.0091	Ctsj	cathepsin J
1393061_at	0.82	4.52	-13.04	0.0448	0.9962	Ttc36	tetratricopeptide repeat domain 36
1368996_at	0.19	3.91	-13.13	0.0043	0.9962	Ceacam3	carcinoembryonic antigen-related cell adhesion molecule 3

ID	LSP Stria Avg (log2)	Sal Stria Avg (log2)	Fold Change	P-val	FDR P-val	Gene Symbol	Description
1398200_at	0.22	3.94	-13.18	0.0209	0.9962		
1396553_at	0.69	4.44	-13.45	0.0008	0.9032		
1377275_at	0.95	4.72	-13.68	0.035	0.9962	Art1	ADP-ribosyltransferase 1
1369509_a_at	0.08	3.86	-13.74	0.032	0.9962	A1bg	alpha-1-B glycoprotein
1380085_at	0.04	3.86	-14.07	0.0045	0.9962	LOC102546489	uncharacterized LOC102546489
1368762_at	0.44	4.3	-14.45	0.0382	0.9962	Ubd	ubiquitin D
1369918_at	0.38	4.27	-14.78	0.0008	0.9032	Klrh1	killer cell lectin-like receptor subfamily H, member 1
1391734_at	0	3.98	-15.73	0.0261	0.9962		
1387234_at	0	3.98	-15.77	0.0061	0.9962	Azgp1	alpha-2-glycoprotein 1, zinc-binding
1381942_at	0.05	4.14	-16.98	0.0016	0.9962	Hic1	hypermethylated in cancer 1
1382652_at	0.2	4.28	-17	0.0238	0.9962	Il27ra	interleukin 27 receptor, alpha
1388018_at	0.31	4.4	-17.02	0.0286	0.9962	Sele	selectin E
1377716_at	0.05	4.19	-17.68	0.0376	0.9962	Tfap2b	transcription factor AP-2 beta
1385701_at	1.37	5.53	-17.89	0.0112	0.9962	Ahnak2	AHNAK nucleoprotein 2
1398320_at	0.1	4.3	-18.39	0.0174	0.9962	Pfkfb2	6-phosphofructo-2-kinase/fructose-2,6-biphosphatase 2
1389966_at	0.73	4.94	-18.44	0.0062	0.9962	Col6a3	collagen, type VI, alpha 3
1380885_at	0.6	4.84	-18.88	0.0144	0.9962		
1385034_at	0	4.26	-19.2	0.0062	0.9962	Lhx9	LIM homeobox 9
1379712_at	0.23	4.52	-19.56	0.0289	0.9962		
1395055_at	0.15	4.52	-20.71	0.0238	0.9962	Tmem26	transmembrane protein 26
1391150_at	0	4.4	-21.06	0.0094	0.9962		
1380574_at	0	4.48	-22.24	0.0095	0.9962		
1390724_at	1.05	5.62	-23.79	0.0494	0.9962		
1380047_at	0.05	4.67	-24.73	0.0061	0.9962		
1398082_at	0	4.96	-31.03	0.0037	0.9962		
1369596_at	0.14	5.46	-40.07	0.0322	0.9962	Il2	interleukin 2

Table of transcript regulation for individual genes by LSP1-2111 compared to saline in the VM of otherwise naïve animals.

ID	LSP VM Avg (log2)	Sal VM Avg (log2)	Fold Change	P-val	FDR P-val	Gene Symbol	Description
1397646_at	6.15	0.24	60.14	1.50E-03	5.30E-01	LOC103691824	uncharacterized LOC103691824
1395897_at	5.05	0	33.21	2.47E-02	7.87E-01		
1382999_at	5.69	0.79	29.83	5.00E-04	4.33E-01	Art2b	ADP-ribosyltransferase 2b
1384317_at	4.89	0	29.55	1.80E-03	5.91E-01		
1394408_at	4.86	0	28.96	4.15E-02	7.97E-01	RGD1563692	similar to hypothetical protein FLJ22671
1395830_at	4.82	0	28.15	1.52E-02	7.34E-01		
1382450_at	4.73	0	26.54	1.42E-02	7.33E-01		
1398739_at	4.69	0	25.87	7.30E-06	7.56E-02		
1390166_at	4.55	0	23.48	9.60E-03	7.03E-01		
1396573_at	4.44	0.00E+00	21.7	3.60E-03	6.58E-01		
1396476_at	5.69	1.28	21.35	4.05E-06	6.29E-02	Rsph10b	radial spoke head 10 homolog B (Chlamydomonas)
1396636_at	4.37	0	20.73	2.23E-02	7.74E-01		
1377718_at	4.6	0.31	19.55	1.52E-02	7.34E-01	Fancb	Fanconi anemia, complementation group B
1396576_at	4.27	0	19.27	1.25E-02	7.17E-01		
1398747_at	4.48	0.22	19.14	4.34E-02	8.00E-01		
1376287_at	4.27	0.02	19.1	1.52E-02	7.35E-01	Capn13	calpain 13
1387269_s_at	4.33	0.13	18.28	2.01E-02	7.73E-01	Plaur	plasminogen activator, urokinase receptor
1382370_at	5.29	1.1	18.27	1.51E-02	7.34E-01	Ccnf	cyclin F
1368995_at	5.39	1.22	18.07	4.70E-03	6.58E-01	Ralgapa1	Ral GTPase activating protein, alpha subunit 1 (catalytic)
1375941_at	6.07	1.93	17.67	1.09E-02	7.05E-01	Baiap2l1	BAI1-associated protein 2-like 1

ID	LSP VM Avg (log2)	Sal VM Avg (log2)	Fold Change	P-val	FDR P-val	Gene Symbol	Description
1393206_at	4.14	0	17.58	6.40E-03	6.58E-01	Esrp1	epithelial splicing regulatory protein 1
1381212_at	4.59	0.47	17.39	8.50E-03	6.99E-01		
1381430_at	4.02	0	16.28	2.75E-02	7.87E-01		
1381236_at	4.01	0	16.11	4.10E-03	6.58E-01		
1381889_at	4.01	0	16.09	2.82E-02	7.92E-01	Cdc123	cell division cycle 123
1369225_at	4.01	0	16.09	3.70E-02	7.97E-01	Kng2	kininogen 2
1383323_at	5.3	1.34	15.63	4.60E-03	6.58E-01	Dsn1	DSN1 homolog, MIS12 kinetochore complex component
1390011_at	4.37	0.44	15.22	2.90E-02	7.97E-01		
1377129_at	4.05	0.13	15.21	7.00E-04	4.33E-01	Fbxo39	F-box protein 39
1380362_at	3.96	0.04	15.15	4.06E-02	7.97E-01		
1374810_at	3.89	0	14.85	3.70E-05	1.68E-01		
1394911_at	3.84	0.02	14.1	2.08E-02	7.73E-01	Zc3hav1l	zinc finger CCCH-type, antiviral 1-like
1381964_at	5.33	1.53	13.86	6.00E-03	6.58E-01	Bpifb1	BPI fold containing family B, member 1
1392459_x_at	4.27	0.51	13.62	2.21E-02	7.74E-01		
1397738_at	6.09	2.33	13.56	1.50E-03	5.30E-01		
1388197_at	5.82	2.07	13.53	1.17E-02	7.10E-01	Hoxa4	homeo box A4
1380207_at	3.87	0.15	13.14	1.90E-02	7.73E-01		
1377915_at	3.69	0.01	12.89	1.00E-02	7.03E-01		
1398653_at	3.67	0	12.75	4.79E-02	8.03E-01	Ppp1r42	protein phosphatase 1, regulatory subunit 42
1396697_at	4.07	0.43	12.54	2.64E-02	7.87E-01		
1395210_at	3.64	0	12.43	1.80E-03	5.91E-01	Svil	supervillin
1381724_at	3.63	0	12.36	2.90E-03	6.33E-01		

ID	LSP VM Avg (log2)	Sal VM Avg (log2)	Fold Change	P-val	FDR P-val	Gene Symbol	Description
1390195_at	5.7	2.07	12.34	7.61E-05	1.68E-01	Psd4	pleckstrin and Sec7 domain containing 4
1392694_at	4.04	0.43	12.2	2.00E-04	2.85E-01	Bcl2l15	BCL2-like 15
1380133_at	4.51	0.9	12.15	4.06E-02	7.97E-01	Osr2	odd-skipped related transciption factor 2
1392053_at	4.2	0.6	12.1	3.59E-02	7.97E-01	Mmrn1	multimerin 1
1398163_at	3.89	0.29	12.09	2.36E-02	7.74E-01		
1396887_at	4.13	0.54	11.98	1.44E-02	7.33E-01		
1394666_at	4.01	0.43	11.92	4.82E-02	8.03E-01	Neb	nebulin
1396919_at	3.86	0.31	11.72	3.81E-02	7.97E-01	Wnk1	WNK lysine deficient protein kinase 1
1395933_at	3.54	0	11.63	2.16E-02	7.74E-01		
1391982_at	3.58	0.04	11.63	2.62E-02	7.87E-01		
1385080_s_at	3.5	0	11.31	1.70E-02	7.49E-01	Gsdma	gasdermin A
1393139_at	4.2	0.71	11.22	3.84E-02	7.97E-01	Apoc2	apolipoprotein C-II
1384027_a_at	4.01	0.53	11.22	3.99E-02	7.97E-01		
1398744_at	5.08	1.61	11.11	1.82E-02	7.66E-01		
1385766_at	3.46	0	11.04	3.40E-03	6.41E-01	Als2cr11	amyotrophic lateral sclerosis 2 (juvenile) chromosome region, candidate 11
1392037_at	3.46	0	11	3.50E-03	6.49E-01		
1393579_at	3.46	0	10.97	4.25E-05	1.68E-01	Chrdl1	chordin-like 1
1381473_at	4.97	1.54	10.82	2.59E-02	7.87E-01	Mir351	microRNA 351
1391141_at	3.7	0.27	10.72	1.69E-02	7.49E-01	LOC102551175; LOC102555078	uncharacterized LOC102551175; uncharacterized LOC102555078
1392334_at	4.16	0.76	10.57	7.40E-03	6.80E-01	RT1-Ba	RT1 class II, locus Ba

ID	LSP VM Avg (log2)	Sal VM Avg (log2)	Fold Change	P-val	FDR P-val	Gene Symbol	Description
1393286_at	3.5	0.13	10.34	4.98E-02	8.07E-01	Nr5a1	nuclear receptor subfamily 5, group A, member 1
1385523_at	3.37	0	10.33	3.90E-02	7.97E-01		
1383926_at	4.08	0.72	10.27	2.40E-03	6.33E-01	Bub1b	BUB1 mitotic checkpoint serine/threonine kinase B
1390296_at	3.35	0	10.19	2.49E-02	7.87E-01		
1381059_at	3.34	0	10.14	1.40E-03	5.30E-01		
1389502_at	3.71	0.38	10.11	7.10E-03	6.72E-01		
1391261_at	3.34	0	10.09	3.39E-02	7.97E-01		
1395529_at	4.24	9.20E-01	9.98	1.20E-03	5.09E-01	Eral1	Era-like 12S mitochondrial rRNA chaperone 1
1391541_at	4.91	1.6	9.93	3.90E-03	6.58E-01		
1384625_at	3.31	0	9.91	3.52E-02	7.97E-01	Gtsf1l	gametocyte specific factor 1-like
1396360_at	3.98	0.69	9.82	1.49E-02	7.33E-01	Akr1b1	aldo-keto reductase family 1, member B1 (aldose reductase)
1380945_at	4.12	8.40E-01	9.68	3.03E-02	7.97E-01		
1386383_at	4.5	1.23	9.67	3.00E-03	6.41E-01		
1370425_at	5.7	2.43	9.64	2.94E-02	7.97E-01	LOC102548083; LOC259244; LOC259246	major urinary protein-like; alpha-2u globulin PGCL3; alpha-2u globulin PGCL1
1396084_at	4.49	1.22	9.61	8.66E-05	1.68E-01		
1376550_at	5.39	2.13	9.59	5.00E-03	6.58E-01		
1386503_at	4.63	1.38	9.55	2.03E-02	7.73E-01	Tango2	transport and golgi organization 2 homolog
1392790_at	3.82	0.57	9.52	5.60E-03	6.58E-01		
1380147_at	3.25	0	9.49	3.00E-04	3.28E-01		
1369217_at	4.03	0.79	9.45	6.60E-03	6.58E-01	Nr4a3	nuclear receptor subfamily 4, group A, member 3

ID	LSP VM Avg (log2)	Sal VM Avg (log2)	Fold Change	P-val	FDR P-val	Gene Symbol	Description
1369392_at	5.49	2.25	9.45	4.20E-02	7.97E-01	Akap4	A kinase (PRKA) anchor protein 4
1380010_at	4.67	1.43	9.43	2.21E-02	7.74E-01		
1383518_at	3.87	0.65	9.3	3.15E-02	7.97E-01		
1370610_at	4.12	0.91	9.27	2.22E-02	7.74E-01	Slc34a1	solute carrier family 34 (type II sodium/phosphate cotransporter), member 1
1376976_at	3.2	0	9.21	5.45E-05	1.68E-01	Sectm1b	secreted and transmembrane 1B
1384206_at	3.19	0	9.13	2.98E-02	7.97E-01	Sdr16c5	short chain dehydrogenase/reductase family 16C, member 5
1398018_at	4.1	0.91	9.11	1.17E-02	7.10E-01	LOC102553465	uncharacterized LOC102553465
1397166_at	3.29	0.1	9.11	1.21E-02	7.14E-01	Eps8l1	EPS8-like 1
1379392_at	4.93	1.74	9.1	1.38E-02	7.32E-01	Adprhl1; Grtp1	ADP-ribosylhydrolase like 1; growth hormone regulated TBC protein 1
1382106_at	3.95	0.76	9.1	2.53E-02	7.87E-01		
1385756_at	4.87	1.69	9.07	1.20E-02	7.14E-01	Itih1	inter-alpha trypsin inhibitor, heavy chain 1
1389495_at	4.75	1.57	9.06	1.77E-02	7.59E-01	Lrp2bp	Lrp2 binding protein
1392271_at	4.48	1.3	9.03	2.21E-02	7.74E-01		
1392035_at	3.32	0.15	8.95	4.42E-02	8.03E-01		
1394852_at	4.41	1.26	8.91	4.92E-02	8.06E-01		
1379584_at	3.14	0	8.81	3.42E-02	7.97E-01		
1390608_at	4.55	1.43	8.72	6.00E-04	4.33E-01		
1369587_at	3.66	0.54	8.68	7.78E-05	1.68E-01	Ereg	epiregulin
1378928_at	4.64	1.52	8.67	3.92E-02	7.97E-01		
1387414_at	5.93	2.84	8.55	2.14E-02	7.74E-01	Duox2	dual oxidase 2
1370749_at	3.09	0	8.54	3.44E-05	1.68E-01	Vom1r101	vomeronasal 1 receptor 101
1378943_at	6.04	2.95	8.53	3.84E-02	7.97E-01		

ID	LSP VM Avg (log2)	Sal VM Avg (log2)	Fold Change	P-val	FDR P-val	Gene Symbol	Description
1396607_at	3.08	0	8.48	1.46E-02	7.33E-01		
1383906_at	4.72	1.65	8.44	2.04E-02	7.73E-01	Neurl3	neuralized E3 ubiquitin protein ligase 3
1380749_at	3.48	0.41	8.39	2.06E-02	7.73E-01		
1393814_at	6.34	3.27	8.38	5.10E-03	6.58E-01	Zan	zonadhesin
1388292_at	4.31	1.25	8.34	5.50E-03	6.58E-01		
1393986_at	3.68	0.63	8.31	3.83E-02	7.97E-01	Hmgb4	high-mobility group box 4
1383344_at	3.87	0.82	8.28	4.10E-03	6.58E-01	Bet1l	Bet1 golgi vesicular membrane trafficking protein-like
1396644_at	3.05	0	8.26	3.20E-03	6.41E-01		
1391178_at	4.11	1.07	8.26	1.61E-02	7.41E-01		
1385599_at	3.04	0	8.24	2.95E-02	7.97E-01	RSA-14-44	RSA-14-44 protein
1370269_at	3.68	0.66	8.16	3.69E-02	7.97E-01	Cyp1a1	cytochrome P450, family 1, subfamily a, polypeptide 1
1372858_at	5.88	2.86	8.11	2.39E-02	7.78E-01	Mrln	myoregulin
1397864_at	3.19	0.17	8.11	2.69E-02	7.87E-01		
1397000_at	4.85	1.83	8.1	8.60E-03	6.99E-01		
1393864_at	4.8	1.78	8.09	1.96E-02	7.73E-01	Izumo1r	IZUMO1 receptor, JUNO
1383153_at	3	0	7.98	6.41E-05	1.68E-01	Hoxd4	homeo box D4
1396183_at	3	0	7.98	2.06E-02	7.73E-01	LOC100909810	uncharacterized LOC100909810
1381155_at	4.97	1.98	7.95	1.59E-02	7.37E-01	Tbc1d10c	TBC1 domain family, member 10C
1396898_at	6.28	3.29	7.95	2.61E-02	7.87E-01		
1370634_x_at	4.76	1.8	7.81	4.53E-02	8.03E-01	Cxcl3	chemokine (C-X-C motif) ligand 3
1369869_at	3.69	0.73	7.79	2.84E-02	7.93E-01	Capza3	capping protein (actin filament) muscle Z-line, alpha 3
1396699_at	4.52	1.56	7.78	5.00E-03	6.58E-01		

ID	LSP VM Avg (log2)	Sal VM Avg (log2)	Fold Change	P-val	FDR P-val	Gene Symbol	Description
1387249_at	4.2	1.25	7.73	1.02E-02	7.05E-01	Bik	BCL2-interacting killer (apoptosis-inducing)
1382985_at	4.45	1.5	7.72	3.36E-02	7.97E-01		
1375539_at	4.23	1.3	7.61	1.90E-03	5.92E-01	Tbr1	T-box, brain, 1
1373827_at	2.92	0	7.58	3.40E-02	7.97E-01	Prl7a4	prolactin family 7, subfamily a, member 4
1397833_at	4.57	1.65	7.58	4.57E-02	8.03E-01		
1380083_at	3.89	0.99	7.51	6.20E-03	6.58E-01	Klk10	kallikrein related-peptidase 10
1393529_at	2.9	0	7.48	4.08E-05	1.68E-01		
1368556_at	4.83	1.92	7.48	4.22E-02	7.97E-01	LOC100911507; Vegp2	von Ebner gland protein 2-like; von Ebners gland protein 2
1378596_at	6.65	3.75E+00	7.47	2.11E-02	7.73E-01		
1385640_at	4.89	2	7.4	3.00E-04	3.36E-01	Pcsk9	proprotein convertase subtilisin/kexin type 9
1381885_at	5.26	2.38	7.35	2.95E-02	7.97E-01	Nr6a1	nuclear receptor subfamily 6, group A, member 1
1368706_at	6.34	3.47	7.32	1.18E-02	7.10E-01	Tm4sf4	transmembrane 4 L six family member 4
1370924_at	6.2	3.34	7.3	4.32E-02	7.99E-01	Tcrb	T-cell receptor beta chain
1385858_at	4.04	1.18	7.26	1.16E-02	7.10E-01		
1397320_at	5.36	2.5	7.25	7.00E-04	4.33E-01		
1378195_at	4.16	1.31	7.24	9.70E-03	7.03E-01		
1383046_at	3.18	0.34	7.18	3.37E-02	7.97E-01	Cfh; LOC100361907	complement factor H; complement factor H-related protein B
1394661_at	4.36	1.52	7.17	1.11E-02	7.05E-01		
1390083_at	6.18	3.36	7.05	5.80E-03	6.58E-01		
1369555_at	3.81	1.01	6.98	2.89E-02	7.96E-01	Ccr4	chemokine (C-C motif) receptor 4
1375507_at	4.61	1.82	6.96	9.40E-03	7.03E-01		

ID	LSP VM Avg (log2)	Sal VM Avg (log2)	Fold Change	P-val	FDR P-val	Gene Symbol	Description
1379161_at	3.72	0.93	6.93	4.04E-02	7.97E-01		
1371095_at	3.09	0.3	6.91	2.92E-02	7.97E-01	Kif6	kinesin family member 6
1397159_at	3.89	1.1	6.9	3.90E-03	6.58E-01		
1381346_at	5.55	2.77	6.87	3.42E-02	7.97E-01		
1395072_at	4.94	2.17	6.85	1.90E-03	5.92E-01		
1390975_at	2.78	0	6.85	4.82E-02	8.03E-01	LOC100912248	uncharacterized LOC100912248
1381766_at	4.48	1.71	6.84	2.24E-02	7.74E-01		
1395670_at	5.05	2.27	6.82	9.20E-03	7.02E-01		
1381286_at	3.91	1.14	6.8	6.63E-05	1.68E-01	LOC686143	similar to keratinocytes proline-rich protein
1371248_at	4.49	1.73	6.77	2.30E-02	7.74E-01	Sprr1a	small proline-rich protein 1A
1394750_at	4.47	1.72	6.73	3.60E-02	7.97E-01	Fhl1	four and a half LIM domains 1
1394002_at	3.26	0.52	6.67	5.20E-03	6.58E-01		
1384893_at	4.09	1.38	6.53	2.72E-02	7.87E-01		
1396419_at	4.26	1.56	6.52	1.69E-02	7.49E-01		
1368986_at	7.1	4.4	6.49	2.16E-02	7.74E-01	Slc17a7	solute carrier family 17 (vesicular glutamate transporter), member 7
1377030_at	4.62	1.92	6.47	3.99E-02	7.97E-01		
1394665_at	6	3.31	6.43	3.22E-02	7.97E-01		
1378488_at	4.71	2.05	6.33	2.37E-02	7.76E-01		
1385286_at	3.14	0.49	6.28	2.00E-04	2.86E-01	Elovl3	ELOVL fatty acid elongase 3
1369288_at	4.55	1.91	6.23	9.90E-03	7.03E-01	Pitx1	paired-like homeodomain 1
1391835_at	4.06	1.45	6.12	1.92E-02	7.73E-01	Baz1a	bromodomain adjacent to zinc finger domain, 1A
1385436_at	4.6	2	6.09	4.60E-03	6.58E-01	Tmc4	transmembrane channel-like 4
1396224_at	4.07	1.46	6.09	4.21E-02	7.97E-01		
1381613_at	6.4	3.8	6.07	3.15E-02	7.97E-01		
1385688_at	3.03	0.44	6.03	7.00E-04	4.33E-01		

ID	LSP VM Avg (log2)	Sal VM Avg (log2)	Fold Change	P-val	FDR P-val	Gene Symbol	Description
1380983_at	6.7	4.11	6.03	1.06E-02	7.05E-01		
1394134_at	4.18	1.59	6.02	4.78E-02	8.03E-01	Dock8	dedicator of cytokinesis 8
1379199_at	2.58	0	5.98	1.13E-02	7.08E-01		
1395495_at	4.32	1.77	5.87	1.00E-04	2.00E-01		
1370791_at	6.13	3.57	5.87	3.50E-02	7.97E-01	RatNP-3b	defensin RatNP-3 precursor
1378701_at	4.66	2.11	5.86	1.08E-02	7.05E-01		
1393394_at	5.68	3.14	5.82	8.30E-03	6.99E-01		
1380782_at	4.25	1.71	5.81	1.31E-02	7.24E-01		
1387748_at	2.56	0.02	5.81	4.73E-02	8.03E-01	Lep	leptin
1396976_at	3.23	0.72	5.73	1.51E-02	7.34E-01		
1397782_at	4.41	1.9	5.69	3.63E-02	7.97E-01		
1390732_at	6.45	3.95	5.66	6.00E-03	6.58E-01		
1391657_at	5.58	3.1	5.57	4.84E-02	8.03E-01	Aldh5a1	aldehyde dehydrogenase 5 family, member A1
1392703_at	5.02	2.56	5.5	2.24E-02	7.74E-01	Tbx4	T-box 4
1398138_at	3.32	8.70E-01	5.47	5.90E-03	6.58E-01		
1367626_at	4.51	2.06	5.47	3.88E-02	7.97E-01	Ckm	creatine kinase, muscle
1382505_at	3.4	0.96	5.45	2.19E-02	7.74E-01		
1396785_at	5.4	2.96	5.43	2.10E-02	7.73E-01		
1382804_at	4.59	2.15	5.43	2.73E-02	7.87E-01		
1384881_at	4.91	2.47	5.42	8.00E-04	4.63E-01	Zdhhc19	zinc finger, DHHC-type containing 19
1381172_at	6.07	3.64	5.4	1.21E-02	7.14E-01		
1398069_at	2.43	0	5.38	2.20E-03	6.02E-01		
1396158_at	3.98	1.55	5.38	1.19E-02	7.10E-01	Rem1	RAS (RAD and GEM)-like GTP-binding 1
1393456_at	4.06	1.64	5.36	2.26E-02	7.74E-01		
1375330_at	5.59	3.17	5.35	4.63E-02	8.03E-01		
1383904_at	3.5	1.09	5.32	3.90E-03	6.58E-01	Fgl1	fibrinogen-like 1

ID	LSP VM Avg (log2)	Sal VM Avg (log2)	Fold Change	P-val	FDR P-val	Gene Symbol	Description
1377443_at	4.2	1.79	5.31	3.71E-06	6.29E-02		
1390679_at	2.41	0	5.31	3.45E-02	7.97E-01		
1397903_at	3.97	1.56	5.3	1.43E-02	7.33E-01		
1392751_at	2.41	0	5.3	2.01E-02	7.73E-01	Fndc3c1	fibronectin type III domain containing 3C1
1384831_at	4.29	1.89	5.29	4.35E-02	8.00E-01	Slc7a13	solute carrier family 7 (anionic amino acid transporter), member 13
1397079_at	3.47	1.07	5.28	1.33E-02	7.24E-01		
1368689_at	4.38	1.99	5.27	3.51E-02	7.97E-01	Gjb5	gap junction protein, beta 5
1368338_at	6.43	4.05	5.23	3.29E-02	7.97E-01	Cd52	CD52 molecule
1381949_at	4.65	2.27	5.21	7.00E-03	6.68E-01	Prkd1	protein kinase D1
1390307_at	5.73	3.35	5.19	5.40E-03	6.58E-01	Eml6	echinoderm microtubule associated protein like 6
1391377_at	4.29	1.92	5.18	9.00E-04	4.78E-01		
1379479_at	3.98	1.62	5.12	8.80E-03	6.99E-01	Kif4a	kinesin family member 4A
1395253_at	4.85	2.5	5.09	4.50E-03	6.58E-01	Fam65a	family with sequence similarity 65, member A
1398461_at	4.29	1.95	5.04	1.40E-03	5.25E-01		
1381037_at	5.55	3.22	5.04	8.80E-03	6.99E-01		
1394531_at	2.33	0	5.04	1.34E-02	7.24E-01		
1378450_at	4.96	2.63	5.03	2.10E-03	6.02E-01		
1384614_at	3.42	1.1	5.01	4.20E-03	6.58E-01		
1390970_at	3.33	1.01	5	1.31E-02	7.24E-01		
1379426_at	2.3	0	4.92	4.94E-02	8.07E-01		
1388302_x_at	2.29	0	4.9	6.00E-04	4.33E-01	Andpro	androgen regulated protein
1382606_at	5.08	2.79	4.87	2.22E-02	7.74E-01		
1391617_at	5.72	3.43	4.87	2.32E-02	7.74E-01		

ID	LSP VM Avg (log2)	Sal VM Avg (log2)	Fold Change	P-val	FDR P-val	Gene Symbol	Description
1395729_at	5.83	3.54	4.86	9.00E-04	4.78E-01		
1381641_at	6.17	3.9	4.83	9.90E-03	7.03E-01	Bcas3	breast carcinoma amplified sequence 3
1385438_at	3.93	1.65	4.83	4.57E-02	8.03E-01	ND4	NADH dehydrogenase subunit 4
1368628_at	4.07	1.81	4.81	4.77E-02	8.03E-01	Klk1c2	kallikrein 1-related peptidase C2
1393433_at	5.66	3.4	4.77	3.17E-02	7.97E-01	Egflam	EGF-like, fibronectin type III and laminin G domains
1388252_at	3.53	1.28	4.75	5.10E-03	6.58E-01		
1396397_at	4.34	2.12	4.66	1.99E-02	7.73E-01		
1391626_at	5.64	3.42	4.64	1.48E-02	7.33E-01	Mnd1	meiotic nuclear divisions 1
1376563_at	2.21	0	4.62	4.56E-02	8.03E-01		
1390521_at	6.14	3.94	4.61	5.70E-03	6.58E-01		
1369549_at	4.9	2.7	4.6	2.01E-02	7.73E-01	Klrk1	killer cell lectin-like receptor subfamily K, member 1
1398516_at	4.43	2.23	4.6	4.65E-02	8.03E-01	Golt1a	golgi transport 1A
1370475_at	3.6	1.4	4.58	3.02E-02	7.97E-01	Cyp2b3	cytochrome P450, family 2, subfamily b, polypeptide 3
1395801_at	5.28	3.09	4.58	4.12E-02	7.97E-01	Sdccag8	serologically defined colon cancer antigen 8
1389517_at	7.58	5.4	4.52	4.75E-02	8.03E-01	LOC102552073; LOC681186	uncharacterized LOC102552073; hypothetical protein LOC681186
1374744_at	4.58	2.4	4.51	4.39E-02	8.01E-01		
1379722_at	4.51	2.35	4.49	1.17E-02	7.10E-01	Large	like-glycosyltransferase
1379799_at	4.81	2.66	4.45	3.90E-02	7.97E-01		
1379845_at	3.32	1.17	4.45	4.11E-02	7.97E-01	LOC103690517	uncharacterized LOC103690517
1387833_at	3.31	1.16	4.43	3.40E-03	6.42E-01	Tmprss2	transmembrane protease, serine 2
1380792_at	5.15	3	4.43	2.56E-02	7.87E-01		

ID	LSP VM Avg (log2)	Sal VM Avg (log2)	Fold Change	P-val	FDR P-val	Gene Symbol	Description
1394983_at	4.99	2.87	4.36	4.80E-03	6.58E-01	Ndc80	NDC80 kinetochore complex component
1375111_at	4.97	2.85	4.36	8.70E-03	6.99E-01		
1397287_at	4.87	2.75	4.34	2.81E-02	7.91E-01	Fancd2os	FANCD2 opposite strand
1375409_at	5.6	3.49	4.33	2.60E-03	6.33E-01		
1394384_at	4.93	2.81	4.33	4.90E-03	6.58E-01	Drd4	dopamine receptor D4
1384033_at	2.95	0.83	4.33	1.91E-02	7.73E-01	Vgll2	vestigial-like family member 2
1396605_at	3.48	1.38	4.31	5.30E-03	6.58E-01	Mov10l1	Mov10 RISC complex RNA helicase like 1
1386002_at	7.03	4.92	4.31	1.81E-02	7.66E-01	LOC100910106	zinc finger protein 845-like
1390892_at	6.46	4.36	4.3	1.02E-02	7.04E-01	Depdc1b	DEP domain containing 1B
1391748_at	5.96	3.86	4.29	2.00E-03	5.92E-01		
1370636_at	3.55	1.45	4.29	2.62E-02	7.87E-01	Ppbp	pro-platelet basic protein (chemokine (C-X-C motif) ligand 7)
1387181_at	2.1	0	4.28	2.59E-02	7.87E-01	Myf6	myogenic factor 6
1392225_at	6.07	3.98	4.27	7.70E-03	6.86E-01		
1369154_at	3.36	1.27	4.27	2.49E-02	7.87E-01	Nphs1	nephrosis 1, congenital, Finnish type (nephrin)
1394903_at	5.04	2.94	4.27	4.37E-02	8.00E-01	Tmem179b	transmembrane protein 179B
1394791_at	2.9	0.81	4.25	2.80E-02	7.91E-01		
1396415_at	7.09	5.01	4.23	3.00E-03	6.41E-01		
1393931_at	4.37	2.29	4.22	3.00E-04	3.36E-01	RGD1311447	LOC363276
1391068_at	3.09	1.04	4.17	1.22E-02	7.14E-01	Sfta2	surfactant associated 2
1391717_at	4.49	2.44	4.15	4.20E-03	6.58E-01	LOC103691481	uncharacterized LOC103691481
1393609_at	7.04	4.99	4.14	1.25E-02	7.17E-01		
1380974_at	4.37	2.32	4.14	3.17E-02	7.97E-01		
1374912_at	4.34	2.3	4.13	1.90E-03	5.92E-01	Kif2c	kinesin family member 2C

ID	LSP VM Avg (log2)	Sal VM Avg (log2)	Fold Change	P-val	FDR P-val	Gene Symbol	Description
1370383_s_at	8.2	6.16	4.13	3.33E-02	7.97E-01	RT1-Db1	RT1 class II, locus Db1
1392018_at	3.95	1.9	4.12	1.48E-02	7.33E-01		
1378867_at	5.07	3.05E+00	4.08	3.56E-02	7.97E-01		
1392005_at	6.24	4.23	4.03	9.40E-03	7.03E-01		
1382266_at	7.32	5.32	4	1.00E-03	4.78E-01	Gpr146	G protein-coupled receptor 146
1385079_at	3.9	1.91	3.97	1.43E-02	7.33E-01	Gsdma	gasdermin A
1391644_at	4.14	2.16	3.96	1.32E-02	7.24E-01	Denr	density-regulated protein
1368300_at	7.68	5.7	3.94	2.18E-02	7.74E-01	Adora2a	adenosine A2a receptor
1379189_at	6.66	4.68	3.93	3.40E-03	6.41E-01		
1395722_at	1.98	0	3.93	1.78E-02	7.59E-01		
1387519_at	7.33	5.36	3.92	3.23E-02	7.97E-01	Vamp1	vesicle-associated membrane protein 1
1391362_at	1.96	0	3.9	2.20E-03	6.02E-01		
1377033_at	4.31	2.35	3.9	3.93E-02	7.97E-01	Serpinf2	serpin peptidase inhibitor, clade F (alpha-2 antiplasmin, pigment epithelium derived factor), member 2
1381858_at	6.77	4.81	3.9	4.67E-02	8.03E-01	Trim14	tripartite motif-containing 14
1378060_at	6.2	4.23	3.9	4.80E-02	8.03E-01		
1384280_at	6.2	4.24	3.89	4.70E-03	6.58E-01	Nusap1	nucleolar and spindle associated protein 1
1388090_a_at	5.38	3.42	3.89	1.94E-02	7.73E-01	Epor	erythropoietin receptor
1377734_at	8.27	6.31	3.88	2.47E-02	7.87E-01	RGD1306063	similar to HT021
1392082_a_at	5.1	3.15	3.86	1.27E-02	7.17E-01	Cd7	Cd7 molecule
1369911_at	3.27	1.32	3.85	3.78E-02	7.97E-01	Cxcr5	chemokine (C-X-C motif) receptor 5

ID	LSP VM Avg (log2)	Sal VM Avg (log2)	Fold Change	P-val	FDR P-val	Gene Symbol	Description
1397031_at	5.55	3.61	3.83	6.10E-03	6.58E-01		
1381585_at	4.94	3	3.83	3.10E-02	7.97E-01		
1392732_at	5.3	3.4	3.75	2.14E-02	7.74E-01	Nusap1	nucleolar and spindle associated protein 1
1383990_at	4.21	2.3	3.74	1.10E-03	4.78E-01		
1387999_at	4.66	2.76	3.74	2.63E-02	7.87E-01	Slc18a1	solute carrier family 18 (vesicular monoamine transporter), member 1
1371364_a_at	5.24	3.34	3.72	1.00E-02	7.03E-01	Andpro	androgen regulated protein
1370257_at	4.47	2.58	3.72	3.02E-02	7.97E-01	Pla2g1b	phospholipase A2, group IB, pancreas
1368913_at	1.88	0	3.68	1.68E-02	7.49E-01	Csn2	casein beta
1386416_at	1.88	0	3.67	1.52E-02	7.35E-01	LOC103692328	uncharacterized LOC103692328
1384371_at	5.52	3.64	3.67	3.90E-02	7.97E-01	Tead3	TEA domain family member 3
1387253_at	5.67	3.81	3.63	1.90E-02	7.73E-01	Guca2b	guanylate cyclase activator 2B
1369107_at	3.49	1.63	3.63	3.77E-02	7.97E-01	Sftpa1	surfactant protein A1
1369872_a_at	3.53	1.68	3.61	4.08E-02	7.97E-01	Fcer2	Fc fragment of IgE, low affinity II, receptor for (CD23)
1379181_at	5.06	3.21	3.6	4.20E-03	6.58E-01		
1372147_at	10.95	9.11	3.59	6.00E-03	6.58E-01		
1396767_at	6.72	4.88	3.59	1.44E-02	7.33E-01		
1374802_at	6.61	4.78	3.55	2.18E-02	7.74E-01	Haus4	HAUS augmin-like complex, subunit 4
1386321_s_at	5.02	3.2	3.54	1.27E-02	7.18E-01	Trib3	tribbles pseudokinase 3
1384113_at	5.78	3.96	3.52	4.65E-02	8.03E-01	LOC102552830; LOC103690347	uncharacterized LOC102552830; uncharacterized LOC103690347
1398105_at	5.98	4.17	3.51	3.11E-02	7.97E-01		

ID	LSP VM Avg (log2)	Sal VM Avg (log2)	Fold Change	P-val	FDR P-val	Gene Symbol	Description
1386194_at	6.44	4.63	3.5	1.20E-03	5.09E-01	Fam132a	family with sequence similarity 132, member A
1398046_at	5.39	3.59	3.49	1.80E-03	5.91E-01		
1393533_at	5.35	3.56	3.47	3.70E-03	6.58E-01	LOC100911950	uncharacterized LOC100911950
1395810_at	5.36	3.57	3.46	8.00E-04	4.63E-01		
1376509_at	6.14	4.35	3.46	4.60E-03	6.58E-01		
1393202_a_at	6.03	4.24	3.45	2.33E-02	7.74E-01	Igf2bp3	insulin-like growth factor 2 mRNA binding protein 3
1381660_at	3.44	1.66	3.43	3.81E-02	7.97E-01		
1395024_at	5.97	4.2	3.41	1.38E-02	7.31E-01		
1398284_at	2.08	0.31	3.4	2.90E-03	6.33E-01	Rax	retina and anterior neural fold homeobox
1380246_at	4.4	2.63	3.4	2.36E-02	7.75E-01		
1398687_at	1.77	0	3.4	2.70E-02	7.87E-01	LOC100909941	uncharacterized LOC100909941
1368639_at	4.05	2.3	3.38	6.20E-03	6.58E-01	Kcnip2	Kv channel-interacting protein 2
1381321_at	4.88	3.12	3.37	2.13E-02	7.74E-01		
1389280_at	4.75	3	3.36	1.00E-03	4.78E-01		
1384535_at	7.47	5.73	3.35	1.42E-02	7.33E-01		
1396516_at	4.85	3.1	3.35	4.60E-02	8.03E-01		
1380720_at	5.2	3.46	3.34	1.63E-02	7.48E-01		
1380727_at	2.8	1.07	3.34	2.98E-02	7.97E-01		
1397978_at	4.6	2.87	3.32	4.61E-02	8.03E-01		
1378622_at	5.47	3.75	3.31	4.60E-03	6.58E-01	Cdk6	cyclin-dependent kinase 6
1395882_at	4.2	2.48	3.3	1.02E-02	7.04E-01		
1385603_at	6.36	4.64	3.3	4.59E-02	8.03E-01		
1391729_at	8.45	6.73	3.28	1.72E-02	7.53E-01		
1396873_at	4.3	2.58	3.28	2.91E-02	7.97E-01		

ID	LSP VM Avg (log2)	Sal VM Avg (log2)	Fold Change	P-val	FDR P-val	Gene Symbol	Description
1381398_at	1.75	0.04	3.28	3.59E-02	7.97E-01	LOC689168; LOC689212	similar to Cystatin S precursor (LM protein)
1385479_at	4.36	2.66	3.25	6.90E-03	6.65E-01	Ccdc187	coiled-coil domain containing 187
1375109_at	3.59	1.89	3.24	1.00E-03	4.78E-01		
1378653_at	5.18	3.49	3.24	1.70E-02	7.49E-01	Lrrn4	leucine rich repeat neuronal 4
1378289_at	6.48	4.78	3.24	2.54E-02	7.87E-01	Dcaf6	DDB1 and CUL4 associated factor 6
1378423_at	3.12	1.43	3.21	1.23E-02	7.14E-01	Nmrk2	nicotinamide riboside kinase 2
1378108_at	5.88	4.2	3.21	4.39E-02	8.01E-01		
1381815_at	5.18	3.5	3.2	2.02E-02	7.73E-01		
1397958_at	6.88	5.21	3.18	4.51E-02	8.03E-01	Tagap	T-cell activation RhoGTPase activating protein
1398361_at	6.68	5.02	3.16	4.62E-02	8.03E-01	Arhgap10	Rho GTPase activating protein 10
1387333_at	3.53	1.89	3.13	2.27E-02	7.74E-01	Il5ra	interleukin 5 receptor, alpha
1395091_at	6.29	4.64	3.12	2.21E-02	7.74E-01	Nsmce1	NSE1 homolog, SMC5-SMC6 complex component
1388547_at	6.42	4.78	3.11	2.70E-02	7.87E-01	Cldn4	claudin 4
1384433_at	5.62	3.98	3.11	4.56E-02	8.03E-01		
1369158_at	5.17	3.55	3.09	4.90E-03	6.58E-01	Casr	calcium-sensing receptor
1397117_at	5.98	4.36	3.09	2.63E-02	7.87E-01		
1385507_at	5.6	3.97	3.09	3.39E-02	7.97E-01	Fam109a	family with sequence similarity 109, member A
1393962_at	1.63	0	3.09	4.27E-02	7.97E-01		
1396920_at	3.34	1.72	3.08	2.83E-02	7.92E-01	Gpr176	G protein-coupled receptor 176
1396095_at	8.41	6.79	3.07	2.10E-02	7.73E-01	LOC102550950	uncharacterized LOC102550950
1377435_at	4.86	3.24	3.06	2.11E-02	7.73E-01		
1380944_at	6.93	5.32	3.05	3.78E-02	7.97E-01		
1382442_at	5.98	4.38	3.04	4.60E-03	6.58E-01	Sept6	septin 6
1381474_at	1.6	0	3.03	2.89E-02	7.96E-01	Mbnl3	muscleblind-like splicing regulator 3

ID	LSP VM Avg (log2)	Sal VM Avg (log2)	Fold Change	P-val	FDR P-val	Gene Symbol	Description
1396289_at	8.76	7.17	3.02	1.59E-02	7.37E-01	Mdga1	MAM domain containing glycosylphosphatidylinositol anchor 1
1380676_at	5.85	4.27	3	2.70E-03	6.33E-01		
1374119_at	4.15	2.57	3	2.72E-02	7.87E-01	Elf3	E74-like factor 3
1374373_at	5.7	4.12	2.99	3.39E-02	7.97E-01	Shroom1	shroom family member 1
1377026_a_at	5.73	4.16	2.97	7.90E-03	6.89E-01		
1379198_at	5.48	3.91	2.97	2.21E-02	7.74E-01	Gpatch2	G patch domain containing 2
1378684_at	6.74	5.17	2.97	4.41E-02	8.02E-01	Rem1	RAS (RAD and GEM)-like GTP-binding 1
1388741_at	1.57	0	2.96	1.00E-02	7.03E-01	Cmya5	cardiomyopathy associated 5
1370722_at	2.77	1.21	2.95	1.11E-02	7.05E-01	Cngb1	cyclic nucleotide gated channel beta 1
1378625_at	4.48	2.93	2.94	4.36E-02	8.00E-01		
1387189_at	6.32	4.78	2.92	9.00E-04	4.78E-01	Slc22a3	solute carrier family 22 (organic cation transporter), member 3
1385827_at	3.6	2.06	2.92	3.99E-02	7.97E-01	Clcf1	cardiotrophin-like cytokine factor 1
1396420_at	6.29	4.75	2.9	4.90E-03	6.58E-01		
1396746_at	6.2	4.66	2.89	6.00E-04	4.33E-01		
1376517_at	5.19	3.66	2.89	7.60E-03	6.86E-01	NEWGENE_1595506; Tlx2	T-cell leukemia homeobox 2
1397890_at	5.67	4.14E+00	2.88	6.00E-04	4.33E-01	RGD1564053	similar to hypothetical protein
1374259_at	6.85	5.32	2.88	1.84E-02	7.68E-01	Plag1	pleiomorphic adenoma gene 1
1392740_at	5.14	3.62	2.87	1.00E-03	4.78E-01	Dbt	dihydrolipoamide branched chain transacylase E2

ID	LSP VM Avg (log2)	Sal VM Avg (log2)	Fold Change	P-val	FDR P-val	Gene Symbol	Description
1382852_at	4.31	2.79	2.87	5.90E-03	6.58E-01	March10	membrane-associated ring finger (C3HC4) 10, E3 ubiquitin protein ligase
1384598_at	4.55	3.03	2.86	2.30E-02	7.74E-01	LOC102552654	uncharacterized LOC102552654
1373659_at	8.71	7.19	2.86	3.13E-02	7.97E-01	Smim5	small integral membrane protein 5
1376566_at	6.2	4.69	2.86	3.47E-02	7.97E-01	Ppp1r7	protein phosphatase 1, regulatory subunit 7
1393041_at	7.18	5.67	2.85	3.12E-02	7.97E-01	Smc2	structural maintenance of chromosomes 2
1386530_at	5.83	4.32	2.85	4.37E-02	8.00E-01	Stc1	stanniocalcin 1
1390980_at	4.1	2.59	2.84	1.22E-02	7.14E-01		
1390065_at	4.2	2.7	2.84	3.33E-02	7.97E-01	Kcnv2	potassium channel, voltage-gated modifier subfamily V, member 2
1381092_at	6.25	4.74	2.84	4.15E-02	7.97E-01		
1392282_at	5.51	4	2.84	4.36E-02	8.00E-01		
1381674_at	4.43	2.92	2.83	7.00E-03	6.68E-01		
1379821_at	4.57	3.08	2.82	3.90E-03	6.58E-01	Gpr62	G protein-coupled receptor 62
1389236_at	1.51	0.02	2.82	1.33E-02	7.24E-01	Mybphl	myosin binding protein H-like
1369045_at	7.02	5.53	2.82	2.58E-02	7.87E-01	Rgs14	regulator of G-protein signaling 14
1380448_at	7.91	6.42	2.81	8.43E-05	1.68E-01	Alkbh1	alkB homolog 1, histone H2A dioxygenase
1370619_at	1.86	0.37	2.81	3.20E-03	6.41E-01	Ccl22	chemokine (C-C motif) ligand 22
1382607_at	5.12	3.64	2.8	2.27E-02	7.74E-01		
1378872_at	6.42	4.94	2.79	8.51E-05	1.68E-01		
1389831_at	4.15	2.67	2.79	2.74E-02	7.87E-01		
1373005_at	4.28	2.81	2.79	3.23E-02	7.97E-01	Krtdap	keratinocyte differentiation associated protein

ID	LSP VM Avg (log2)	Sal VM Avg (log2)	Fold Change	P-val	FDR P-val	Gene Symbol	Description
1370423_at	5.92	4.44	2.79	3.49E-02	7.97E-01	Gna15	guanine nucleotide binding protein, alpha 15
1389553_at	6.26	4.78	2.79	3.52E-02	7.97E-01	Clec4a3	C-type lectin domain family 4, member A3
1378951_at	4.92	3.44	2.79	3.56E-02	7.97E-01		
1379531_at	2.12	0.65	2.79	3.94E-02	7.97E-01		
1385612_at	7.04	5.57E+00	2.77	2.22E-02	7.74E-01	Krt71	keratin 71, type II
1392398_at	3.83	2.36	2.77	2.24E-02	7.74E-01		
1378406_at	5.52	4.06	2.76	1.70E-03	5.87E-01	Ttc14	tetratricopeptide repeat domain 14
1385865_at	7.57	6.1	2.76	4.80E-03	6.58E-01	Poc1a	POC1 centriolar protein A
1391192_at	5.26	3.79	2.76	2.11E-02	7.73E-01		
1395639_at	6.34	4.88	2.75	3.30E-03	6.41E-01		
1398035_at	6.62	5.16	2.75	1.28E-02	7.18E-01		
1385426_at	6.52	5.06	2.75	2.03E-02	7.73E-01	Ccdc109b	coiled-coil domain containing 109B
1394537_at	6.12	4.66	2.74	1.85E-02	7.68E-01	Prickle3	prickle homolog 3
1398266_a_at	2.11	0.68	2.7	3.27E-02	7.97E-01	Egr2	early growth response 2
1393200_at	5.51	4.08E+00	2.69	2.70E-03	6.33E-01	Tnfrsf13b	tumor necrosis factor receptor superfamily, member 13B
1394275_at	8.69	7.27	2.69	2.08E-02	7.73E-01	Stard5	StAR-related lipid transfer (START) domain containing 5
1390411_at	5.04	3.62	2.69	4.56E-02	8.03E-01	Cldn19	claudin 19
1378618_at	4.95	3.52	2.68	2.00E-02	7.73E-01		
1392244_at	7.29	5.87	2.67	4.99E-02	8.07E-01		
1378615_at	5.41	4	2.66	1.27E-02	7.17E-01	Brwd1; LOC100911399	bromodomain and WD repeat domain containing 1; bromodomain and WD repeat-containing protein 1-like

ID	LSP VM Avg (log2)	Sal VM Avg (log2)	Fold Change	P-val	FDR P-val	Gene Symbol	Description
1381722_at	3.33	1.92	2.66	4.58E-02	8.03E-01	Plin5	perilipin 5
1398224_at	6.27	4.86	2.66	4.74E-02	8.03E-01		
1377350_at	7.8	6.39	2.65	8.70E-03	6.99E-01	Nsl1	NSL1, MIS12 kinetochore complex component
1397158_at	5.03	3.63	2.64	3.34E-02	7.97E-01		
1396689_at	5.45	4.06	2.62	3.40E-03	6.41E-01		
1380436_at	5.37	3.98	2.62	6.30E-03	6.58E-01	RT1-A1; RT1-A2; RT1-EC2	RT1 class Ia, locus A1; RT1 class Ia, locus A2; RT1 class Ib, locus EC2
1394776_at	5.26	3.88	2.61	1.00E-04	2.55E-01	Adamts6	ADAM metallopeptidase with thrombospondin type 1 motif, 6
1390891_at	3.71	2.32	2.61	2.10E-03	6.02E-01	Kif11	kinesin family member 11
1386325_at	2.7	1.32	2.61	2.32E-02	7.74E-01		
1369372_at	9.11	7.74	2.6	2.35E-02	7.74E-01	Gabbr1	gamma-aminobutyric acid (GABA) B receptor 1
1381670_at	5.25	3.87	2.59	3.00E-04	3.36E-01		
1389948_at	4.04	2.67	2.59	2.70E-03	6.33E-01		
1397138_at	6.41	5.04	2.59	8.50E-03	6.99E-01		
1381431_at	6.42	5.05	2.59	2.86E-02	7.94E-01		
1382501_at	5.75	4.39	2.57	4.08E-02	7.97E-01		
1396217_at	5.1	3.74	2.57	4.30E-02	7.99E-01	Ap1s2	adaptor-related protein complex 1, sigma 2 subunit
1394070_at	4.56	3.2	2.56	1.54E-02	7.37E-01		
1391583_at	8.96	7.61	2.56	2.31E-02	7.74E-01	Carkd	carbohydrate kinase domain containing
1377840_at	6.68	5.33	2.56	3.74E-02	7.97E-01	Ccm2l	cerebral cavernous malformation 2-like
1372852_at	5.63	4.27	2.56	4.32E-02	7.99E-01	Ptprcap	protein tyrosine phosphatase, receptor type, C-associated protein

ID	LSP VM Avg (log2)	Sal VM Avg (log2)	Fold Change	P-val	FDR P-val	Gene Symbol	Description
1393325_at	8.43	7.08	2.55	1.93E-02	7.73E-01	Gtpbp6; LOC100912590	GTP binding protein 6 (putative); putative GTP-binding protein 6-like
1395902_at	5.92	4.57	2.54	3.00E-03	6.41E-01		
1388202_at	5.64	4.29	2.54	7.40E-03	6.80E-01	RT1-EC2	RT1 class Ib, locus EC2
1369648_at	5.48	4.13	2.54	2.42E-02	7.82E-01	Calcrl	calcitonin receptor-like
1392131_at	5.52	4.18	2.54	3.05E-02	7.97E-01	Dsn1; LOC102547986	DSN1 homolog, MIS12 kinetochore complex component; 40S ribosomal protein S2-like
1375578_at	6	4.66	2.54	4.45E-02	8.03E-01		
1391800_at	6.77	5.43	2.53	2.75E-02	7.87E-01		
1370734_a_at	5.19	3.85	2.52	2.29E-02	7.74E-01	Dspp	dentin sialophosphoprotein
1385205_at	6.65	5.32	2.51	2.90E-03	6.33E-01		
1389732_at	7.65	6.32	2.51	6.50E-03	6.58E-01	Dram1	DNA-damage regulated autophagy modulator 1
1376675_at	5.9	4.57	2.51	2.19E-02	7.74E-01	Cd300a	Cd300a molecule
1380668_at	5.8	4.47	2.51	3.66E-02	7.97E-01		
1377515_at	4.76	3.44	2.5	3.05E-02	7.97E-01		
1383432_at	5.56	4.24	2.5	3.18E-02	7.97E-01	Dapl1	death associated protein-like 1
1395486_at	5.91	4.59	2.5	3.40E-02	7.97E-01	Gtf3c1	general transcription factor IIIC, polypeptide 1, alpha
1394915_at	1.55	0.23	2.49	4.44E-02	8.03E-01		
1368625_at	4.7	3.39	2.48	1.54E-02	7.37E-01	Prap1	proline-rich acidic protein 1
1397935_at	4.66	3.35	2.48	2.99E-02	7.97E-01	LOC102551129	uncharacterized LOC102551129
1390935_at	6.37	5.06	2.48	3.25E-02	7.97E-01		
1370671_at	3.2	1.89	2.47	1.58E-02	7.37E-01	Gucy2g	guanylate cyclase 2G
1382945_at	11.08	9.77	2.47	1.68E-02	7.49E-01	Ggact	gamma-glutamylamine cyclotransferase

ID	LSP VM Avg (log2)	Sal VM Avg (log2)	Fold Change	P-val	FDR P-val	Gene Symbol	Description
1382395_at	4.84	3.54	2.47	2.65E-02	7.87E-01	Prrg4	proline rich Gla (G-carboxyglutamic acid) 4 (transmembrane)
1388228_at	5.83	4.53	2.46	6.00E-04	4.33E-01	Mthfr	methylenetetrahydrofolate reductase (NAD(P)H)
1368317_at	3.49	2.19	2.46	4.17E-02	7.97E-01	Aqp7	aquaporin 7
1387442_at	5.76	4.47	2.45	8.30E-03	6.99E-01	Egr4	early growth response 4
1384085_at	4.16	2.86	2.45	1.97E-02	7.73E-01	Gtf2h5	general transcription factor IIH, polypeptide 5
1377544_at	6.18	4.88	2.45	2.67E-02	7.87E-01	Gpr68	G protein-coupled receptor 68
1378726_at	8.69	7.4	2.44	2.10E-03	6.02E-01	Alkbh4	alkB homolog 4, lysine demthylase
1386517_at	5.08	3.8	2.44	2.60E-03	6.33E-01	Rpl30	ribosomal protein L30
1369130_at	10.14	8.86	2.43	2.30E-03	6.19E-01	Rasgrp1	RAS guanyl releasing protein 1 (calcium and DAG-regulated)
1368780_at	4.56	3.28	2.43	1.06E-02	7.05E-01	Adrb3	adrenoceptor beta 3
1373994_at	6.98	5.7	2.43	1.34E-02	7.24E-01	Aplf	aprataxin and PNKP like factor
1384847_at	4.72	3.45	2.4	1.48E-02	7.33E-01	RGD1311745	similar to RIKEN cDNA 1110059G10
1396362_at	5.94	4.67	2.4	2.70E-02	7.87E-01	LOC102550729	zinc finger protein 120-like
1381695_at	4.79	3.53	2.4	2.71E-02	7.87E-01		
1397752_at	6.59	5.33	2.39	3.30E-03	6.41E-01		
1379158_at	4.23	2.98	2.39	2.48E-02	7.87E-01		
1374827_at	8.93	7.67	2.38	1.26E-02	7.17E-01	Ndst2; NEWGENE_1304700	N-deacetylase/N-sulfotransferase (heparan glucosaminyl) 2
1377036_at	6.02	4.77	2.38	1.64E-02	7.48E-01		
1392679_at	5.98	4.73	2.38	1.87E-02	7.72E-01	Zfp787	zinc finger protein 787
1397750_at	8.9	7.65E+00	2.37	3.03E-02	7.97E-01	Rps6ka3	ribosomal protein S6 kinase polypeptide 3
1395221_at	6.84	5.59	2.37	3.39E-02	7.97E-01		

ID	LSP VM Avg (log2)	Sal VM Avg (log2)	Fold Change	P-val	FDR P-val	Gene Symbol	Description
1381910_at	5.58	4.34	2.37	4.07E-02	7.97E-01		
1368492_at	6.06	4.82	2.36	1.92E-02	7.73E-01	Hpgds	hematopoietic prostaglandin D synthase
1390752_at	5.75	4.51	2.35	7.20E-03	6.72E-01		
1379636_at	7.3	6.07	2.35	8.20E-03	6.99E-01	Rmdn2	regulator of microtubule dynamics 2
1382566_at	5.8	4.57	2.35	1.57E-02	7.37E-01	Il7r	interleukin 7 receptor
1376473_at	5.51	4.27	2.35	2.66E-02	7.87E-01		
1375225_at	6.11	4.87	2.35	3.25E-02	7.97E-01		
1377037_at	6.57	5.33	2.35	4.88E-02	8.03E-01	Acot4	acyl-CoA thioesterase 4
1376694_at	6.38	5.16	2.34	9.50E-03	7.03E-01	Lmbr1l	limb development membrane protein 1-like
1392040_at	7.58	6.36	2.33	1.09E-02	7.05E-01	Sass6	SAS-6 centriolar assembly protein
1378460_at	3.66	2.45	2.33	1.65E-02	7.48E-01		
1396966_at	5.33	4.11	2.33	3.73E-02	7.97E-01		
1396927_at	6.29	5.07	2.33	3.86E-02	7.97E-01		
1377150_at	5.77	4.55	2.32	1.01E-02	7.03E-01		
1381939_at	5.76	4.55	2.32	1.07E-02	7.05E-01		
1397967_at	2.95	1.74	2.32	1.68E-02	7.49E-01		
1398239_at	5.94	4.72	2.32	4.10E-02	7.97E-01		
1377321_at	6.92	5.71	2.31	1.70E-03	5.87E-01		
1378520_at	5.97	4.77	2.3	2.00E-04	3.28E-01	Bcl11b	B-cell CLL/lymphoma 11B (zinc finger protein)
1388265_x_at	5.74	4.54	2.3	6.40E-03	6.58E-01	Vcan	versican
1385791_at	5.09	3.89	2.3	6.90E-03	6.63E-01	Vill	villin-like
1391077_at	3.39	2.19	2.3	1.07E-02	7.05E-01	Clspn; LOC100912611	claspin; claspin-like

ID	LSP VM Avg (log2)	Sal VM Avg (log2)	Fold Change	P-val	FDR P-val	Gene Symbol	Description
1388729_at	7.9	6.7	2.29	2.05E-02	7.73E-01	Rras	related RAS viral (r-ras) oncogene homolog
1384010_at	5.01	3.82	2.28	2.60E-02	7.87E-01		
1398569_at	6.53	5.35	2.28	2.87E-02	7.94E-01	LOC100911519; Pidd1	p53-induced protein with a death domain-like; p53-induced death domain protein 1
1380839_at	6.6	5.41	2.28	3.48E-02	7.97E-01		
1382153_at	5.19	4.01	2.27	1.74E-02	7.58E-01	Clec4a	C-type lectin domain family 4, member A
1375982_at	6.91	5.73	2.27	3.83E-02	7.97E-01	Ldb3	LIM domain binding 3
1393261_at	5.97	4.79	2.27	4.48E-02	8.03E-01	LOC102547242	uncharacterized LOC102547242
1386656_at	8.7	7.52	2.26	3.14E-02	7.97E-01	Plppr1	phospholipid phosphatase related 1
1380557_at	6.17	4.99	2.26	3.30E-02	7.97E-01	Bckdha	branched chain ketoacid dehydrogenase E1, alpha polypeptide
1378933_at	5.75	4.58	2.25	1.22E-02	7.14E-01		
1390329_at	5.92	4.75	2.25	1.32E-02	7.24E-01	Mfap3	microfibrillar-associated protein 3
1384851_at	6.08	4.91	2.25	4.59E-02	8.03E-01	Smarcad1	SWI/SNF-related, matrix-associated actin-dependent regulator of chromatin, subfamily a, containing DEAD/H box 1
1397311_at	6.66	5.5	2.24	1.32E-02	7.24E-01		
1376951_at	6.78	5.61	2.24	3.54E-02	7.97E-01	Mad2l1	MAD2 mitotic arrest deficient-like 1 (yeast)
1384556_at	6.06	4.89	2.24	4.19E-02	7.97E-01	Atp10a	ATPase, class V, type 10A
1395277_at	6.01	4.85	2.23	6.30E-03	6.58E-01		
1395554_at	7.54	6.39	2.23	9.00E-03	7.02E-01		
1377516_at	6.63	5.47	2.23	1.51E-02	7.34E-01		

ID	LSP VM Avg (log2)	Sal VM Avg (log2)	Fold Change	P-val	FDR P-val	Gene Symbol	Description
1390376_at	4.99	3.83	2.23	2.29E-02	7.74E-01		
1386733_at	6.24	5.09	2.22	1.82E-02	7.66E-01	Ccdc88a	coiled coil domain containing 88A
1398664_at	6.18	5.03	2.22	2.78E-02	7.87E-01	Gramd3	GRAM domain containing 3
1387633_at	6.04	4.89	2.22	4.54E-02	8.03E-01	Prg2	proteoglycan 2
1381289_at	5.7	4.56	2.21	8.80E-03	6.99E-01	Haus8; LOC100364316	HAUS augmin-like complex, subunit 8; hypothetical LOC100364316
1377056_at	6.09	4.95	2.21	2.19E-02	7.74E-01	LOC103691455	uncharacterized LOC103691455
1396963_at	5.43	4.29	2.21	2.56E-02	7.87E-01		
1398290_at	5.67	4.53	2.21	3.80E-02	7.97E-01	Kcnk13	potassium channel, two pore domain subfamily K, member 13
1369412_a_at	8.31	7.17	2.21	3.93E-02	7.97E-01	Slc19a1	solute carrier family 19 (folate transporter), member 1
1394804_at	2.15	1.01	2.21	4.70E-02	8.03E-01		
1379784_at	8.32	7.18	2.2	6.00E-03	6.58E-01	Pex7	peroxisomal biogenesis factor 7
1395918_at	7.15	6.01	2.2	3.34E-02	7.97E-01	Aldh3b2	aldehyde dehydrogenase 3 family, member B2
1371172_at	6.65	5.52	2.2	3.43E-02	7.97E-01	Atp2b3	ATPase, Ca++ transporting, plasma membrane 3
1390583_at	6.81	5.68	2.19	1.07E-02	7.05E-01		
1398213_at	4.34	3.21	2.19	1.26E-02	7.17E-01		
1387310_at	4.72	3.59	2.19	1.44E-02	7.33E-01	Atp2c2	ATPase, Ca++ transporting, type 2C, member 2
1377080_at	8.08	6.95	2.19	1.57E-02	7.37E-01	Nradd	neurotrophin receptor associated death domain
1393889_x_at	4.36	3.24	2.18	1.36E-02	7.28E-01		
1395126_at	7.94	6.82	2.18	2.57E-02	7.87E-01	Fcrl2	Fc receptor-like 2
1381947_at	4.46	3.33	2.18	2.80E-02	7.91E-01	LOC102556209	uncharacterized LOC102556209

ID	LSP VM Avg (log2)	Sal VM Avg (log2)	Fold Change	P-val	FDR P-val	Gene Symbol	Description
1392150_at	4.7	3.58	2.18	4.09E-02	7.97E-01		
1368773_at	5	3.88	2.17	6.70E-03	6.58E-01	Cenpi	centromere protein I
1397261_at	6.96	5.85	2.17	9.40E-03	7.03E-01		
1392572_at	10.96	9.84	2.17	1.00E-02	7.03E-01	Msi2	musashi RNA-binding protein 2
1384377_at	8.08	6.97	2.17	1.24E-02	7.14E-01	Ddx28	DEAD (Asp-Glu-Ala-Asp) box polypeptide 28
1382433_at	8.15	7.04	2.17	1.45E-02	7.33E-01	Sorcs1	sortilin-related VPS10 domain containing receptor 1
1370992_a_at	2.24	1.12	2.17	3.05E-02	7.97E-01	Fga	fibrinogen alpha chain
1383352_at	8.04	6.92	2.17	3.24E-02	7.97E-01	Ttf1	transcription termination factor, RNA polymerase I
1396591_at	4.44	3.32	2.17	4.68E-02	8.03E-01	Pan2	PAN2 poly(A) specific ribonuclease subunit
1381146_at	5.89	4.77	2.17	4.83E-02	8.03E-01		
1395060_at	6.71	5.6	2.16	4.00E-04	4.33E-01		
1397534_at	9.04	7.93	2.16	1.80E-03	5.91E-01	LOC103695171	uncharacterized LOC103695171
1398442_at	6.92	5.81	2.16	5.20E-03	6.58E-01	LOC690422	hypothetical protein LOC690422
1393526_at	5.05	3.94	2.16	2.15E-02	7.74E-01		
1387337_at	6.32	5.21	2.16	2.71E-02	7.87E-01	Cort	cortistatin
1385139_at	5.19	4.08	2.16	3.15E-02	7.97E-01	Fam221a	family with sequence similarity 221, member A
1398153_at	5.54	4.43	2.16	3.45E-02	7.97E-01		
1370596_a_at	7.3	6.18	2.16	4.72E-02	8.03E-01	Wipf3	WAS/WASL interacting protein family, member 3
1393694_at	7.25	6.14	2.16	4.75E-02	8.03E-01		
1391124_at	1.13	0.01	2.16	4.94E-02	8.07E-01		
1380155_at	6.83	5.73	2.15	7.80E-03	6.88E-01		

ID	LSP VM Avg (log2)	Sal VM Avg (log2)	Fold Change	P-val	FDR P-val	Gene Symbol	Description
1377727_at	6.21	5.1	2.15	1.03E-02	7.05E-01	Baz1a	bromodomain adjacent to zinc finger domain, 1A
1395867_at	6.56	5.46	2.15	1.65E-02	7.48E-01		
1390321_at	4.76	3.66	2.15	2.48E-02	7.87E-01	Mms22l	MMS22-like, DNA repair protein
1368435_at	4.53	3.43	2.15	3.63E-02	7.97E-01	Cyp8b1	cytochrome P450, family 8, subfamily b, polypeptide 1
1395139_at	6.52	5.41	2.15	4.13E-02	7.97E-01	Kif16b	kinesin family member 16B
1389568_at	7	5.9	2.14	9.60E-03	7.03E-01	Calhm2	calcium homeostasis modulator 2
1368794_at	5.7	4.6	2.14	1.78E-02	7.59E-01	Haao	3-hydroxyanthranilate 3,4-dioxygenase
1394743_at	6.36	5.27	2.14	2.26E-02	7.74E-01	LOC100363228; LOC100911379	hypothetical LOC100363228; transmembrane protein C1orf162 homolog
1396272_at	5.85	4.75	2.14	2.34E-02	7.74E-01		
1398250_at	7.13	6.04	2.13	2.10E-03	6.02E-01	Acot1	acyl-CoA thioesterase 1
1375975_at	5.45	4.36	2.13	3.50E-03	6.50E-01	Ankrd26	ankyrin repeat domain 26
1398044_at	6.25	5.16	2.13	1.56E-02	7.37E-01		
1377323_at	6.99	5.9	2.13	1.75E-02	7.59E-01	Pla2g4b	phospholipase A2, group IVB (cytosolic)
1398671_at	5.25	4.15	2.13	1.77E-02	7.59E-01		
1384810_at	7.3	6.22	2.13	3.59E-02	7.97E-01	Stam2	signal transducing adaptor molecule (SH3 domain and ITAM motif) 2
1380585_at	4.66	3.57	2.13	4.02E-02	7.97E-01	NEWGENE_1595506; Tlx2	T-cell leukemia homeobox 2
1384259_at	5.13	4.05	2.12	9.00E-03	7.02E-01	LOC103690014; Racgap1	rac GTPase-activating protein 1-like; Rac GTPase-activating protein 1
1370128_at	6.59	5.5	2.12	3.87E-02	7.97E-01	Hand1	heart and neural crest derivatives expressed 1

ID	LSP VM Avg (log2)	Sal VM Avg (log2)	Fold Change	P-val	FDR P-val	Gene Symbol	Description
1385195_at	6.19	5.11	2.11	1.00E-03	4.78E-01	Fbxl18	F-box and leucine-rich repeat protein 18
1398156_at	5.6	4.52	2.11	3.00E-03	6.41E-01		
1382197_at	5.06	3.99	2.11	1.21E-02	7.14E-01	Rhod	ras homolog family member D
1379798_at	5.39	4.31	2.11	3.84E-02	7.97E-01		
1375681_at	6.09	5.02	2.1	1.24E-02	7.14E-01	Dcaf15	DDB1 and CUL4 associated factor 15
1379602_at	4.32	3.25	2.1	2.49E-02	7.87E-01		
1394832_at	6.76	5.69	2.1	4.16E-02	7.97E-01		
1384046_at	6.94	5.88	2.09	3.30E-03	6.41E-01	Mtfr1	mitochondrial fission regulator 1
1386272_at	5.96	4.89	2.09	2.82E-02	7.92E-01		
1377642_at	8.39	7.32	2.09	4.02E-02	7.97E-01	Cav2	caveolin 2
1383872_at	6.82	5.77	2.08	1.23E-02	7.14E-01	Cacna1e	calcium channel, voltage-dependent, R type, alpha 1E subunit
1389686_at	7.64	6.58	2.08	3.63E-02	7.97E-01	Prkx	protein kinase, X-linked
1384630_at	5.41	4.36	2.08	3.89E-02	7.97E-01		
1382764_at	7.03	5.97	2.08	4.69E-02	8.03E-01		
1378457_at	7.48	6.43	2.07	1.30E-03	5.09E-01	Thrb	thyroid hormone receptor beta
1381880_at	4.06	3.01	2.07	3.54E-02	7.97E-01	LOC102554187	uncharacterized LOC102554187
1371009_at	2.54	1.49	2.06	2.80E-03	6.33E-01	Muc5ac	mucin 5AC, oligomeric mucus/gel-forming
1380074_at	6.01	4.97	2.06	1.59E-02	7.37E-01	Rnls	renalase, FAD-dependent amine oxidase
1378581_at	7.94	6.9	2.06	2.28E-02	7.74E-01	Ccdc62	coiled-coil domain containing 62
1386594_at	6.45	5.42	2.05	1.28E-02	7.18E-01		
1396460_at	8.16	7.13	2.05	2.47E-02	7.87E-01	LOC102556093	uncharacterized LOC102556093
1390609_at	5.71	4.68	2.05	3.64E-02	7.97E-01	Xkr7	XK, Kell blood group complex subunit-related family, member 7
1380616_at	7.68	6.64	2.05	4.75E-02	8.03E-01		

ID	LSP VM Avg (log2)	Sal VM Avg (log2)	Fold Change	P-val	FDR P-val	Gene Symbol	Description
1389516_at	3.09	2.06	2.04	3.40E-03	6.41E-01		
1395545_at	5.95	4.93	2.04	7.70E-03	6.86E-01	Usp13	ubiquitin specific peptidase 13
1384431_at	6.16	5.13	2.04	9.20E-03	7.03E-01	Lca5	Leber congenital amaurosis 5
1390834_at	6.28	5.25	2.04	1.88E-02	7.72E-01	Abcc10	ATP-binding cassette, subfamily C (CFTR/MRP), member 10
1373194_at	9.56	8.53	2.04	2.27E-02	7.74E-01	Lyrm2	LYR motif containing 2
1377031_at	5.36	4.33	2.03	3.39E-02	7.97E-01		
1395137_at	5.09	4.08	2.02	1.11E-02	7.05E-01	Xrcc4	X-ray repair complementing defective repair in Chinese hamster cells 4
1398121_at	4.17	3.16	2.02	3.10E-02	7.97E-01		
1374238_at	3.27	2.26	2.02	3.44E-02	7.97E-01		
1380950_at	6.11	5.1	2.02	3.74E-02	7.97E-01		
1374776_at	7.57	6.56	2.02	4.19E-02	7.97E-01	Vash2	vasohibin 2
1378031_at	8.08	7.07	2.02	4.24E-02	7.97E-01	Dhx37	DEAH (Asp-Glu-Ala-His) box polypeptide 37
1394557_at	5.64	4.63	2.01	3.24E-02	7.97E-01		
1394943_at	8.19	7.19	2	5.20E-03	6.58E-01	Crebzf	CREB/ATF bZIP transcription factor
1385069_at	7.38	8.39	-2	2.80E-03	6.33E-01	Acvr1	activin A receptor, type I
1388951_at	6.17	7.17	-2.01	2.80E-03	6.33E-01	Kmt2b	lysine (K)-specific methyltransferase 2B
1378492_at	8.41	9.41	-2.01	3.26E-02	7.97E-01		
1376856_at	3.83	4.84	-2.01	4.72E-02	8.03E-01	Tti2	TELO2 interacting protein 2
1398233_at	7.55	8.58	-2.03	5.70E-03	6.58E-01		
1385282_at	7.69	8.71	-2.03	1.34E-02	7.24E-01	Nat14	N-acetyltransferase 14
1394433_at	7.51	8.53	-2.03	1.67E-02	7.49E-01	Katnal1; LOC103690050	katanin p60 subunit A-like 1; katanin p60 ATPase-containing subunit A-like 1

ID	LSP VM Avg (log2)	Sal VM Avg (log2)	Fold Change	P-val	FDR P-val	Gene Symbol	Description
1385298_at	5.19	6.21	-2.03	2.41E-02	7.81E-01	Slc26a10	solute carrier family 26, member 10
1391728_at	5.65	6.67	-2.03	3.14E-02	7.97E-01	Mab21l2	mab-21-like 2 (C. elegans)
1385678_at	5.19	6.22	-2.04	2.18E-02	7.74E-01	Polk	polymerase (DNA directed) kappa
1376529_at	5.26	6.29	-2.04	2.35E-02	7.74E-01		
1380202_at	6.76	7.79	-2.04	2.53E-02	7.87E-01	Zfp821	zinc finger protein 821
1390953_at	6.05	7.08	-2.04	3.36E-02	7.97E-01	Zbtb11	zinc finger and BTB domain containing 11
1385864_at	3.78	4.81	-2.05	5.10E-03	6.58E-01	Xpo4	exportin 4
1383370_at	7.91	8.94	-2.05	9.00E-03	7.02E-01	Brinp2	bone morphogenetic protein/retinoic acid inducible neural-specific 2
1381355_at	5.42	6.45	-2.05	1.80E-02	7.62E-01	Mks1	Meckel syndrome, type 1
1373800_at	5.32	6.36	-2.05	2.27E-02	7.74E-01		
1390053_at	5.41	6.46	-2.07	6.40E-03	6.58E-01	Mplkip	M-phase specific PLK1 interacting protein
1397885_at	4.08	5.15	-2.09	4.46E-02	8.03E-01		
1388052_a_at	6.98	8.04	-2.09	4.47E-02	8.03E-01	Kcnq3	potassium channel, voltage-gated KQT-like subfamily Q, member 3
1375308_at	6.96	8.03	-2.1	6.50E-03	6.58E-01	Zfp646	zinc finger protein 646
1379941_at	7.26	8.33	-2.1	1.40E-02	7.33E-01		
1393740_at	3.62	4.69	-2.1	2.03E-02	7.73E-01	Cnksr1	connector enhancer of kinase suppressor of Ras 1
1383945_at	8.03	9.1	-2.1	2.32E-02	7.74E-01	Uck2	uridine-cytidine kinase 2
1381393_at	5.54	6.61	-2.1	3.22E-02	7.97E-01		
1396810_at	3.25	4.33	-2.1	3.33E-02	7.97E-01		
1393551_at	8.22	9.29	-2.11	2.50E-03	6.33E-01	Tstd1	thiosulfate sulfurtransferase (rhodanese)-like domain containing 1

ID	LSP VM Avg (log2)	Sal VM Avg (log2)	Fold Change	P-val	FDR P-val	Gene Symbol	Description
1385760_at	7.25	8.33	-2.11	1.95E-02	7.73E-01	Zbtb42	zinc finger and BTB domain containing 42
1381309_at	7.54	8.63	-2.12	7.10E-03	6.70E-01	Kcnj9	potassium channel, inwardly rectifying subfamily J, member 9
1379835_at	6.31	7.41	-2.14	1.72E-02	7.53E-01		
1394624_at	3.97	5.09	-2.17	3.57E-02	7.97E-01		
1377061_at	8.05	9.19	-2.2	1.30E-03	5.09E-01	Arhgap32	Rho GTPase activating protein 32
1386586_at	5.78	6.92	-2.21	5.40E-03	6.58E-01	Pak1ip1	PAK1 interacting protein 1
1387068_at	5.68	6.82	-2.21	1.39E-02	7.32E-01	Arc	activity-regulated cytoskeleton-associated protein
1380336_at	6.39	7.53	-2.21	3.30E-02	7.97E-01	Irak3	interleukin-1 receptor-associated kinase 3
1397002_at	2.72	3.86	-2.21	3.67E-02	7.97E-01		
1369357_at	6.62	7.77	-2.22	1.47E-02	7.33E-01	Phka1	phosphorylase kinase, alpha 1
1394497_at	8.29	9.43	-2.22	3.91E-02	7.97E-01	Tcf7l2	transcription factor 7-like 2 (T-cell specific, HMG-box)
1384665_at	4.62	5.77	-2.23	3.42E-02	7.97E-01		
1394396_at	5.51	6.67	-2.23	4.76E-02	8.03E-01		
1368357_at	3.73	4.9	-2.24	9.30E-03	7.03E-01	Kcnh4	potassium channel, voltage gated eag related subfamily H, member 4
1368061_at	5.8	6.97	-2.25	6.50E-03	6.58E-01	Kcnh1; Rcor3	potassium channel, voltage gated eag related subfamily H, member 1; REST corepressor 3
1370384_a_at	4.73	5.9	-2.25	4.80E-02	8.03E-01	Prlr	prolactin receptor
1393446_at	4.31	5.49	-2.26	2.04E-02	7.73E-01		
1381476_at	6.08	7.26	-2.26	3.73E-02	7.97E-01	Rnf32	ring finger protein 32

ID	LSP VM Avg (log2)	Sal VM Avg (log2)	Fold Change	P-val	FDR P-val	Gene Symbol	Description
1386935_at	4.72	5.9	-2.26	3.82E-02	7.97E-01	Nr4a1	nuclear receptor subfamily 4, group A, member 1
1368416_at	3.47	4.65	-2.27	6.00E-04	4.33E-01	Ibsp	integrin-binding sialoprotein
1370254_at	5.83	7.01	-2.27	1.25E-02	7.17E-01	Clic5	chloride intracellular channel 5
1369277_at	7.69	8.88	-2.28	3.00E-04	3.59E-01	Mecp2	methyl CpG binding protein 2
1396020_at	7.95	9.14	-2.28	1.54E-02	7.37E-01	Tlk2	tousled-like kinase 2
1396520_at	3.87	5.06	-2.28	1.70E-02	7.49E-01		
1397553_s_at	5.76	6.95	-2.28	1.96E-02	7.73E-01	Prdm2	PR domain containing 2, with ZNF domain
1398188_at	4.01	5.21	-2.29	3.88E-02	7.97E-01		
1397472_at	4.23	5.43	-2.3	1.11E-02	7.05E-01		
1384990_at	4.07	5.27	-2.3	2.47E-02	7.87E-01		
1378628_at	4.82	6.03	-2.31	5.00E-04	4.33E-01		
1380012_at	5.8	7	-2.31	1.49E-02	7.33E-01	Ddx19b	DEAD (Asp-Glu-Ala-As) box polypeptide 19B
1382211_at	5.61	6.82	-2.31	2.59E-02	7.87E-01	Mme	membrane metallo-endopeptidase
1383684_at	3.32	4.53	-2.32	7.00E-03	6.69E-01	Asf1b	anti-silencing function 1B histone chaperone
1385554_at	3.88	5.09	-2.32	3.23E-02	7.97E-01		
1370830_at	7.65	8.86	-2.32	4.88E-02	8.03E-01	Egfr	epidermal growth factor receptor
1378823_at	5.46	6.68	-2.33	5.00E-04	4.33E-01		
1386993_at	6.81	8.03	-2.33	1.46E-02	7.33E-01	Myh7	myosin, heavy chain 7, cardiac muscle, beta
1396798_at	5.59	6.82	-2.34	2.05E-02	7.73E-01		
1385043_at	9.68	10.91	-2.34	2.05E-02	7.73E-01	Inadl	InaD-like (Drosophila)
1375707_at	8.26	9.49	-2.35	2.87E-02	7.94E-01		
1370512_at	7.63	8.87	-2.36	3.07E-02	7.97E-01	Tnrc6b	trinucleotide repeat containing 6B
1397822_at	4.06	5.29	-2.36	3.74E-02	7.97E-01		

ID	LSP VM Avg (log2)	Sal VM Avg (log2)	Fold Change	P-val	FDR P-val	Gene Symbol	Description
1384331_at	6.32	7.57	-2.38	1.96E-02	7.73E-01	Srxn1	sulfiredoxin 1
1382908_at	8.84	10.1	-2.39	1.18E-02	7.10E-01	Epha4	Eph receptor A4
1388233_at	4.71	5.97	-2.41	2.03E-02	7.73E-01	Cish	cytokine inducible SH2-containing protein
1374814_at	6.33	7.6	-2.42	6.20E-03	6.58E-01	Kcng2	potassium channel, voltage gated modifier subfamily G, member 2
1394933_at	4.31	5.58	-2.43	7.90E-03	6.89E-01		
1381182_at	2.9	4.18	-2.44	1.26E-02	7.17E-01		
1380197_at	3.74	5.03	-2.44	3.65E-02	7.97E-01		
1381913_at	3.87	5.16	-2.45	2.05E-02	7.73E-01	Vsig10l	V-set and immunoglobulin domain containing 10 like
1394969_at	5.91	7.21	-2.47	2.90E-03	6.39E-01	Zfp329	zinc finger protein 329
1387033_at	2.01	3.32	-2.48	5.90E-03	6.58E-01	LOC100909612; Ucp1	mitochondrial brown fat uncoupling protein 1-like; uncoupling protein 1 (mitochondrial, proton carrier)
1385230_at	6.48	7.79	-2.48	1.08E-02	7.05E-01	Eogt	EGF domain-specific O-linked N-acetylglucosamine (GlcNAc) transferase
1396626_at	3.95	5.28	-2.5	9.00E-04	4.78E-01		
1382814_at	7.07	8.39	-2.5	5.50E-03	6.58E-01	Tenm3	teneurin transmembrane protein 3
1393967_at	4.6	5.92	-2.5	5.60E-03	6.58E-01		
1378252_at	4.81	6.13	-2.5	1.97E-02	7.73E-01	Chodl	chondrolectin
1380361_at	3.63	4.96	-2.51	6.80E-03	6.63E-01		
1390828_at	7.01	8.36	-2.54	8.80E-03	6.99E-01	Npy1r	neuropeptide Y receptor Y1
1382565_at	6.81	8.16	-2.55	1.65E-02	7.48E-01	Mapk1ip1l	mitogen-activated protein kinase 1 interacting protein 1-like
1392270_at	2.71	4.07	-2.56	6.00E-04	4.33E-01		

ID	LSP VM Avg (log2)	Sal VM Avg (log2)	Fold Change	P-val	FDR P-val	Gene Symbol	Description
1368749_at	4.84	6.2	-2.56	1.50E-03	5.30E-01	Kcns1	potassium voltage-gated channel, modifier subfamily S, member 1
1384612_at	3.19	4.55	-2.56	1.69E-02	7.49E-01	Pomc	proopiomelanocortin
1396392_at	6.77	8.13	-2.57	2.86E-02	7.94E-01		
1376865_at	5.03	6.39	-2.57	4.63E-02	8.03E-01	Onecut2	one cut homeobox 2
1381719_at	4.67	6.04	-2.58	1.50E-03	5.39E-01		
1381000_at	4.87	6.24	-2.58	1.11E-02	7.05E-01		
1397449_at	5.6	6.97	-2.58	1.59E-02	7.37E-01		
1389848_at	3.57	4.94	-2.58	1.70E-02	7.49E-01	Arhgap23	Rho GTPase activating protein 23
1394164_at	4.11	5.47	-2.58	2.07E-02	7.73E-01		
1381246_at	5.02	6.39	-2.58	4.61E-02	8.03E-01	Phf21b	PHD finger protein 21B
1391956_at	3.23	4.6	-2.59	1.75E-02	7.59E-01		
1391893_at	4.65	6.03	-2.61	1.18E-02	7.10E-01	Clp1	cleavage and polyadenylation factor I subunit 1
1383238_at	7.73	9.12	-2.62	1.46E-02	7.33E-01	Qtrt1	queuine tRNA-ribosyltransferase 1
1371224_a_at	6.25	7.67	-2.66	2.10E-03	6.02E-01	Drp2	dystrophin related protein 2
1395982_at	5.8	7.22	-2.67	8.60E-03	6.99E-01	Nup214	nucleoporin 214
1398646_at	4.65	6.07	-2.68	1.05E-02	7.05E-01	Rgs22	regulator of G-protein signaling 22
1382546_at	5.56	6.99	-2.7	1.06E-02	7.05E-01	LOC102551046; LOC102557219; Phf11; Phf11b; Setdb2	PHD finger protein 11-like; PHD finger protein 11; PHD finger protein 11B; SET domain, bifurcated 2
1391874_at	0.79	2.24	-2.74	3.74E-02	7.97E-01		
1388029_at	4.5	5.96	-2.75	3.76E-02	7.97E-01	Zfand4	zinc finger, AN1-type domain 4
1390652_at	7.06	8.52	-2.77	3.81E-02	7.97E-01		
1368825_at	4.96	6.44	-2.79	5.10E-03	6.58E-01	Shox2	short stature homeobox 2
1378647_at	3.74	5.22	-2.8	4.02E-02	7.97E-01	Akip1	A kinase (PRKA) interacting protein 1

ID	LSP VM Avg (log2)	Sal VM Avg (log2)	Fold Change	P-val	FDR P-val	Gene Symbol	Description
1368351_at	2.07	3.59	-2.87	1.51E-02	7.34E-01	Scn10a	sodium channel, voltage-gated, type X, alpha subunit
1382358_at	6.01	7.54	-2.9	2.87E-02	7.94E-01	Sox5	SRY (sex determining region Y)-box 5
1379156_at	4.47	6	-2.9	3.30E-02	7.97E-01		
1385694_at	4.17	5.71	-2.91	4.60E-03	6.58E-01		
1396678_at	4.21	5.75	-2.91	1.24E-02	7.14E-01		
1379927_at	3.91	5.45	-2.91	4.11E-02	7.97E-01		
1378434_at	3.14	4.7	-2.94	6.60E-03	6.58E-01		
1377444_at	4.35	5.91	-2.95	1.57E-02	7.37E-01		
1397673_at	4.83	6.39	-2.95	3.46E-02	7.97E-01		
1383569_at	4.19	5.77	-2.98	1.56E-02	7.37E-01	Pmpcb	peptidase (mitochondrial processing) beta
1369015_at	5.36	6.94	-2.98	3.31E-02	7.97E-01	Nos1	nitric oxide synthase 1, neuronal
1397602_at	5.68	7.26	-2.99	1.90E-02	7.73E-01		
1387402_at	6.34	7.92	-3	2.00E-04	2.86E-01	Myh9; Myh9l1	myosin, heavy chain 9, non-muscle; myosin, heavy chain 9, non-muscle-like 1
1394713_at	4.16	5.77	-3.05	5.50E-03	6.58E-01		
1394843_at	3.28	4.89	-3.05	2.97E-02	7.97E-01		
1375600_at	5.79	7.41	-3.08	9.70E-03	7.03E-01	Pigo	phosphatidylinositol glycan anchor biosynthesis, class O
1396558_at	1.76	3.4	-3.1	2.09E-02	7.73E-01		
1386470_at	5.95	7.59	-3.12	4.00E-03	6.58E-01	Ranbp17	RAN binding protein 17
1371260_at	0	1.64	-3.12	7.60E-03	6.86E-01	Mcpt1; Mcpt2	mast cell protease 1; mast cell protease 2
1386724_at	4.3	5.95	-3.13	3.16E-02	7.97E-01	Lrrc75b	leucine rich repeat containing 75B

ID	LSP VM Avg (log2)	Sal VM Avg (log2)	Fold Change	P-val	FDR P-val	Gene Symbol	Description
1381570_at	3.58	5.23	-3.14	3.79E-02	7.97E-01	Nfkbid	nuclear factor of kappa light polypeptide gene enhancer in B-cells inhibitor, delta
1396229_at	2.67	4.34	-3.17	2.57E-02	7.87E-01		
1386387_at	0.88	2.55	-3.19	2.55E-02	7.87E-01	Sox1	SRY box 1
1391061_at	5.28	6.96	-3.22	3.91E-02	7.97E-01		
1394951_at	3.96	5.66	-3.25	2.32E-02	7.74E-01		
1397936_at	3.39	5.09	-3.27	2.30E-02	7.74E-01	Foxr1	forkhead box R1
1382982_at	3.3	5.02	-3.3	7.30E-03	6.80E-01		
1368107_at	1.18	2.91	-3.33	3.40E-02	7.97E-01	Prl3c1	Prolactin family 3, subfamily c, member 1
1381370_at	1.38	3.13	-3.35	2.67E-02	7.87E-01		
1387699_at	0.43	2.18	-3.37	3.66E-02	7.97E-01	Cnga2; LOC103690077	cyclic nucleotide gated channel alpha 2; cyclic nucleotide-gated olfactory channel-like
1377228_at	2.76	4.53	-3.42	8.40E-03	6.99E-01		
1396547_at	1.7	3.47	-3.42	4.17E-02	7.97E-01		
1396882_at	4.88	6.66	-3.43	2.55E-02	7.87E-01		
1380701_at	4.34	6.13	-3.46	4.50E-02	8.03E-01		
1394861_at	2.99	4.79	-3.48	3.10E-03	6.41E-01		
1397695_at	4.28	6.09	-3.5	8.80E-03	6.99E-01		
1369838_at	3.08	4.89	-3.5	2.32E-02	7.74E-01	Hif3a	hypoxia inducible factor 3, alpha subunit
1369551_at	2.95	4.76	-3.5	3.12E-02	7.97E-01	Gpr173	G-protein coupled receptor 173
1378132_at	3.59	5.41	-3.53	3.11E-02	7.97E-01		
1391945_at	0.26	2.11	-3.6	1.00E-02	7.03E-01		
1382583_at	1.82	3.67	-3.6	1.21E-02	7.14E-01		

ID	LSP VM Avg (log2)	Sal VM Avg (log2)	Fold Change	P-val	FDR P-val	Gene Symbol	Description
1395295_at	1.66	3.53	-3.65	1.66E-02	7.48E-01	Mllt6	myeloid/lymphoid or mixed-lineage leukemia; translocated to, 6
1397171_at	4.73	6.63	-3.71	6.40E-03	6.58E-01	Rnft2	ring finger protein, transmembrane 2
1396281_at	5.25	7.16	-3.75	1.20E-02	7.14E-01	LOC103690403	uncharacterized LOC103690403
1396937_at	2.19	4.1	-3.77	1.66E-02	7.49E-01		
1370471_at	1.25	3.16	-3.78	8.20E-03	6.99E-01	Prl6a1	prolactin family 6, subfamily a, member 1
1375052_at	0.23	2.15	-3.79	3.50E-02	7.97E-01	C2cd4b	C2 calcium-dependent domain containing 4B
1376230_at	3.9	5.82	-3.79	4.66E-02	8.03E-01	Tmem82	transmembrane protein 82
1375227_at	4.93	6.85	-3.8	1.28E-02	7.18E-01		
1381861_x_at	1.17	3.1	-3.82	4.44E-02	8.03E-01	Acta2; Actc1	actin, alpha 2, smooth muscle, aorta; actin, alpha, cardiac muscle 1
1368299_at	7.11	9.05	-3.85	1.16E-02	7.10E-01	Gpr83	G protein-coupled receptor 83
1377886_at	3.15	5.1	-3.86	5.90E-03	6.58E-01	Trim6	tripartite motif containing 6
1385207_at	1.13	3.08	-3.88	3.20E-03	6.41E-01	Prr27	proline rich 27
1376439_at	3.37	5.34	-3.9	2.48E-02	7.87E-01		
1379072_at	3.76	5.73	-3.91	4.09E-02	7.97E-01		
1381884_at	1.51	3.48	-3.92	1.81E-02	7.66E-01		
1375490_at	2.16	4.14	-3.93	4.27E-02	7.97E-01		
1388256_at	1.27	3.25	-3.96	4.04E-02	7.97E-01	RT1-A3	RT1 class I, locus A3
1397593_at	3.05	5.04	-3.98	8.40E-03	6.99E-01		
1386242_at	4.01	6	-3.98	9.90E-03	7.03E-01		
1372936_at	5.07	7.06	-3.98	1.43E-02	7.33E-01	Pcp2	Purkinje cell protein 2
1380756_at	2.67	4.66	-3.98	4.56E-02	8.03E-01		
1373796_at	0.57	2.57	-4	4.13E-02	7.97E-01	LOC103691211	uncharacterized LOC103691211
1383761_at	0	2.01	-4.04	1.43E-02	7.33E-01		

ID	LSP VM Avg (log2)	Sal VM Avg (log2)	Fold Change	P-val	FDR P-val	Gene Symbol	Description
1392628_at	2.89	4.91	-4.05	4.57E-02	8.03E-01	Ms4a6bl	membrane-spanning 4-domains, subfamily A, member 6B-like
1389938_at	3.76	5.78	-4.05	4.63E-02	8.03E-01	Etv6	ets variant 6
1395195_at	2.52	4.55	-4.07	4.31E-02	7.99E-01		
1390349_at	4.97	7	-4.1	1.40E-03	5.27E-01		
1389985_at	4.56	6.6	-4.12	3.95E-02	7.97E-01	Tfe3	transcription factor binding to IGHM enhancer 3
1381093_at	3.76	5.8	-4.13	4.99E-02	8.07E-01		
1381453_at	3.41	5.46	-4.16	4.12E-02	7.97E-01		
1387069_a_at	3	5.07	-4.2	6.00E-04	4.33E-01	Tbxa2r	thromboxane A2 receptor
1382896_at	0.76	2.83	-4.22	4.05E-02	7.97E-01		
1380709_at	1.8	3.9	-4.27	6.30E-03	6.58E-01		
1391174_at	6.12	8.21	-4.27	6.50E-03	6.58E-01		
1381060_at	2.42	4.53	-4.3	1.36E-02	7.28E-01		
1394206_s_at	0	2.11	-4.31	9.40E-03	7.03E-01	LOC103692328	uncharacterized LOC103692328
1375761_at	2.13	4.24	-4.32	2.72E-02	7.87E-01		
1385116_at	0	2.14	-4.4	2.20E-03	6.02E-01	Pcdhb21	protocadherin beta 21
1397099_at	1.14	3.3	-4.46	2.70E-03	6.33E-01		
1381015_at	1.35	3.51	-4.48	3.14E-02	7.97E-01		
1381746_at	3.08	5.25	-4.49	4.29E-02	7.99E-01		
1387701_at	1.19	3.36	-4.53	2.40E-03	6.33E-01	Hgf	hepatocyte growth factor
1391375_at	1.79	4	-4.65	1.40E-02	7.33E-01		
1370681_at	2.21	4.43	-4.67	2.77E-02	7.87E-01	Pacs1	phosphofurin acidic cluster sorting protein 1
1380887_at	4.18	6.4	-4.68	2.35E-02	7.74E-01		
1391248_at	3.24	5.48	-4.72	6.60E-03	6.58E-01		

ID	LSP VM Avg (log2)	Sal VM Avg (log2)	Fold Change	P-val	FDR P-val	Gene Symbol	Description
1397489_at	3.57	5.82	-4.76	5.20E-03	6.58E-01		
1391949_at	0.47	2.73	-4.81	3.79E-02	7.97E-01		
1391615_at	0.66	2.93	-4.82	1.49E-02	7.34E-01	LOC102555788	uncharacterized LOC102555788
1396603_at	2.69	4.97	-4.84	8.10E-03	6.98E-01		
1395959_at	1.32	3.59	-4.85	3.51E-02	7.97E-01		
1374226_at	1.68	4.01	-5.02	5.20E-03	6.58E-01	Col7a1	collagen, type VII, alpha 1
1397116_at	1.9	4.26	-5.14	2.10E-03	6.02E-01		
1397145_at	1.49	3.86	-5.16	1.30E-03	5.09E-01		
1379979_at	1.03	3.43	-5.3	3.58E-02	7.97E-01	LOC102556194	uncharacterized LOC102556194
1380342_at	3.09	5.5	-5.3	4.10E-02	7.97E-01	LOC680885	hypothetical protein LOC680885
1387100_at	1.51	3.94	-5.41	3.93E-02	7.97E-01	Aqp3	aquaporin 3
1377796_at	3.35	5.79	-5.43	4.79E-02	8.03E-01	Fzd5	frizzled class receptor 5
1387736_at	1.39	3.84	-5.47	9.10E-03	7.02E-01	Chrm1	cholinergic receptor, muscarinic 1
1379233_at	1.27	3.76	-5.61	1.35E-02	7.24E-01		
1396928_at	1.78	4.28	-5.68	2.11E-02	7.73E-01		
1387013_at	1.99	4.52	-5.75	3.58E-02	7.97E-01	Tmem27	transmembrane protein 27
1384988_at	1.59	4.12	-5.78	3.78E-02	7.97E-01	Fbxo5	F-box protein 5
1381602_at	3.81	6.35	-5.83	1.88E-02	7.72E-01	Mid1	midline 1
1384631_at	0.44	3.01	-5.91	2.73E-02	7.87E-01		
1398737_at	1.54	4.1	-5.93	2.80E-03	6.33E-01		
1369682_at	0.8	3.37	-5.94	4.60E-03	6.58E-01	Hnf1b	HNF1 homeobox B
1380488_at	1.63	4.21	-5.96	1.50E-03	5.30E-01		
1371098_a_at	0.53	3.1	-5.96	2.03E-02	7.73E-01	Masp2	mannan-binding lectin serine peptidase 2
1386785_a_at	0	2.58	-5.97	2.60E-02	7.87E-01	LOC100911498	uncharacterized LOC100911498
1380315_at	1.9	4.5	-6.07	4.56E-02	8.03E-01	LOC102552820	uncharacterized LOC102552820

ID	LSP VM Avg (log2)	Sal VM Avg (log2)	Fold Change	P-val	FDR P-val	Gene Symbol	Description
1368733_at	0	2.61	-6.12	1.80E-03	5.91E-01	Sult1e1	sulfotransferase family 1E, estrogen-preferring, member 1
1387943_at	1.82	4.45	-6.22	3.00E-04	3.28E-01	Defa5	defensin, alpha 5, Paneth cell-specific
1369348_at	0	2.64	-6.23	7.00E-04	4.33E-01	Trpm8	transient receptor potential cation channel, subfamily M, member 8
1397658_at	2.12	4.78	-6.31	3.64E-02	7.97E-01		
1392825_at	0	2.66	-6.31	4.64E-02	8.03E-01	RGD1559600	RGD1559600
1384140_at	4.38	7.06	-6.42	1.76E-02	7.59E-01		
1397735_at	0.18	2.87	-6.47	3.10E-03	6.41E-01	Bpifb6	BPI fold containing family B, member 6
1378807_at	1.8	4.5	-6.49	4.17E-02	7.97E-01		
1380506_at	1.88	4.62	-6.68	3.54E-02	7.97E-01		
1396806_at	0.41	3.15	-6.7	4.61E-02	8.03E-01	LOC102549483	uncharacterized LOC102549483
1385096_at	0	2.75	-6.74	4.93E-02	8.06E-01		
1376394_at	1.12	3.89	-6.8	4.81E-02	8.03E-01	Clec9a	C-type lectin domain family 9, member A
1385579_at	2.07	4.84	-6.82	5.40E-03	6.58E-01		
1374345_at	2.06	4.85	-6.93	2.50E-02	7.87E-01		
1381694_at	0	2.85	-7.22	3.06E-02	7.97E-01		
1373544_at	1.08	3.96	-7.36	7.70E-03	6.86E-01	Cxcl9	chemokine (C-X-C motif) ligand 9
1396661_at	4.22	7.11	-7.4	1.17E-02	7.10E-01	Ddx19a; Ddx19b	DEAD (Asp-Glu-Ala-Asp) box polypeptide 19a; DEAD (Asp-Glu-Ala-As) box polypeptide 19B
1378341_at	1.02	3.91	-7.42	7.80E-03	6.88E-01	Gabra6	gamma-aminobutyric acid (GABA) A receptor, alpha 6
1378507_at	1.81	4.72	-7.52	1.10E-03	4.78E-01	Dtl	denticleless E3 ubiquitin protein ligase homolog (Drosophila)
1393135_at	2.53	5.45	-7.59	7.20E-03	6.72E-01		

ID	LSP VM Avg (log2)	Sal VM Avg (log2)	Fold Change	P-val	FDR P-val	Gene Symbol	Description
1395097_at	1.87	4.8	-7.62	1.61E-02	7.41E-01		
1373259_at	0.78	3.71	-7.63	4.82E-02	8.03E-01		
1380588_at	1.69	4.63	-7.71	9.40E-03	7.03E-01		
1376405_at	2.45	5.43	-7.88	2.00E-03	5.92E-01		
1370564_at	3.23	6.22	-7.92	1.11E-02	7.05E-01	Dbh	dopamine beta-hydroxylase (dopamine beta-monooxygenase)
1387490_at	1.89	4.92	-8.19	5.60E-03	6.58E-01		
1370592_at	0	3.04	-8.2	2.09E-02	7.73E-01	Glyatl2	glycine-N-acyltransferase-like 2
1398320_at	0.43	3.48	-8.29	1.77E-02	7.59E-01	Pfkfb2	6-phosphofructo-2-kinase/fructose-2,6-biphosphatase 2
1375383_at	0.96	4.03	-8.4	3.56E-02	7.97E-01		
1395881_at	1.82	4.92	-8.55	4.44E-02	8.03E-01		
1398634_at	0	3.11	-8.64	2.70E-02	7.87E-01	Smlr1	small leucine-rich protein 1
1397868_at	0	3.12	-8.68	2.76E-02	7.87E-01	Kdr	kinase insert domain receptor
1368579_at	0.28	3.4	-8.69	3.15E-02	7.97E-01	Prl2a1	Prolactin family 2, subfamily a, member 1
1384800_at	1.62	4.76	-8.84	4.06E-02	7.97E-01	Zic3	Zic family member 3
1392048_at	2.35	5.51	-8.96	1.10E-03	4.78E-01		
1381395_at	1.93	5.12	-9.1	2.95E-02	7.97E-01	Klf15	Kruppel-like factor 15
1394879_at	0.23	3.42	-9.15	4.49E-02	8.03E-01		
1396473_at	0.12	3.32	-9.22	1.09E-02	7.05E-01	LOC102548409	uncharacterized LOC102548409
1378662_at	0	3.21	-9.25	1.09E-02	7.05E-01		
1373360_at	0.87	4.09	-9.31	3.04E-02	7.97E-01		
1386324_at	0	3.25	-9.49	4.12E-02	7.97E-01		
1381848_at	1.43	4.71	-9.7	8.40E-03	6.99E-01		
1380742_at	0.79	4.12	-10.04	2.11E-02	7.73E-01		
1382507_at	0	3.34	-10.11	4.01E-02	7.97E-01	Cd96	CD96 molecule
1375693_at	0	3.38	-10.42	1.34E-02	7.24E-01		

ID	LSP VM Avg (log2)	Sal VM Avg (log2)	Fold Change	P-val	FDR P-val	Gene Symbol	Description
1387338_s_at	0.16	3.57	-10.68	3.05E-02	7.97E-01	Bcl2l11	BCL2-like 11 (apoptosis facilitator)
1395291_at	0.6	4.04	-10.84	4.20E-03	6.58E-01	Golph3l	golgi phosphoprotein 3-like
1396629_at	1.51	4.95	-10.86	3.18E-02	7.97E-01		
1391382_at	0.83	4.27	-10.86	3.41E-02	7.97E-01		
1387819_at	1.91	5.36	-10.92	8.09E-05	1.68E-01	Cela1	chymotrypsin-like elastase family, member 1
1389697_at	1.53	4.98	-10.93	7.70E-03	6.86E-01		
1380378_at	2.22	5.68	-10.98	2.92E-02	7.97E-01	Tmem51	transmembrane protein 51
1396026_at	0	3.57	-11.87	4.55E-02	8.03E-01		
1370641_s_at	1.08	4.69	-12.25	5.90E-03	6.58E-01	Cacna1i	calcium channel, voltage-dependent, T type, alpha 1I subunit
1392583_at	0.15	3.79	-12.5	3.12E-02	7.97E-01	Plin1	perilipin 1
1385607_at	0	3.65	-12.53	4.39E-02	8.01E-01		
1397498_at	0	3.67	-12.72	9.10E-03	7.02E-01		
1375840_at	0.2	3.91	-13.04	6.00E-04	4.33E-01		
1369871_at	0.38	4.11	-13.27	3.66E-02	7.97E-01	Areg	amphiregulin
1378466_at	1.58	5.35	-13.71	3.98E-02	7.97E-01		
1382392_at	0.28	4.1	-14.17	4.27E-02	7.97E-01		
1374354_at	0.17	4.03	-14.55	2.07E-02	7.73E-01	Phf19	PHD finger protein 19
1379530_at	0.04	4	-15.58	4.30E-03	6.58E-01	Eomes	eomesodermin
1378005_at	1.86	5.84	-15.76	6.00E-04	4.33E-01	Sema6a	sema domain, transmembrane domain (TM), and cytoplasmic domain, (semaphorin) 6A
1393542_at	1.2	5.21	-16.07	4.58E-02	8.03E-01	LOC103692581	uncharacterized LOC103692581
1391659_at	0.45	4.48	-16.39	4.67E-02	8.03E-01		
1367552_at	0.09	4.14	-16.56	6.60E-03	6.58E-01	Svs4	seminal vesicle secretory protein 4
1392284_at	0.01	4.11	-17.12	1.85E-02	7.68E-01		

ID	LSP VM Avg (log2)	Sal VM Avg (log2)	Fold Change	P-val	FDR P-val	Gene Symbol	Description
1381498_at	0	4.1	-17.14	5.80E-03	6.58E-01		
1378076_at	0.71	5.3	-24.09	9.00E-03	7.02E-01		
1380777_at	0.01	4.91	-29.84	4.18E-02	7.97E-01		
1394034_at	0.43	5.54	-34.6	9.00E-04	4.78E-01		
1369673_at	0.35	5.69	-40.43	5.00E-04	4.33E-01	P2rx5	purinergic receptor P2X, ligand-gated ion channel, 5